

**Large-scale analysis of kinase inhibitors' target binding kinetics.
Implications for drug discovery?**

Dissertation

zur Erlangung des Doktorgrades
der Naturwissenschaften

vorgelegt beim Fachbereich 14

Biochemie, Chemie und Pharmazie

der Johann Wolfgang Goethe-Universität

in Frankfurt am Main

von

Victoria Georgi

aus Berlin

Frankfurt 2018

(D 30)

**vom Fachbereich 14
der Johann Wolfgang Goethe - Universität als Dissertation angenommen.**

Dekan:
Prof. Dr. Clemens Glaubitz

Gutachter:
Prof. Dr. Stefan Knapp
Prof. Dr. Eugen Proschak
Prof. Dr. Dieter Steinhilber
Prof. Dr. Martin Grinninger

Datum der Disputation:
20.11.2018

Danksagung

Die Erstellung einer Dissertation erfordert neben der Forschungsarbeit, auch Enthusiasmus, Kraft und Nervenstärke. Zum Glück ist man im Leben nie ganz allein. Ich möchte mich an dieser Stelle bei all den lieben Menschen bedanken, die mich auf meinem Weg begleitet und unterstützt haben, ob fachlich oder persönlich.

Mein besonderer Dank gebührt meinem Mentor Dr. Amaury Ernesto Fernández-Montalván, dessen Energie und Begeisterung für die Forschung sehr ansteckend sind. Vielen Dank für jede hilfreiche Anregung und die konstruktive Kritik, aber auch dafür, dass ich mich ausprobieren und frei arbeiten durfte – besser hätte ich mir es nicht wünschen können.

Mein tiefer Dank gilt außerdem meinen Betreuern Prof. Dr. Stefan Knapp und Prof. Dr. Michael Brands, die stets ein offenes Ohr für mich hatten und einen alternativen Blickwinkel in die eine oder andere Fragestellung eröffnen konnten. Vielen Dank für eure wertvollen Ratschläge.

Ein großes Dankeschön geht auch an die AG Fernández und einige Alumni, einerseits für die gute Vorarbeit zum Thema kPCA, andererseits aber auch für den herzlichen Empfang und die Unterstützung im Laboralltag. Hierbei möchte ich insbesondere Dr. Felix Schiele, Benedict-Tilman Berger, Nicole Dittmar, Robert Karmauss und Anne Mattstedt danken.

Vielen Dank an Dr. James D. Vasta und Dr. Matthew B. Robers von Promega für die Durchführung der nanoBRET Experimente nach Wunsch. Die Auswertung dieser Daten haben meine Arbeit sehr bereichert.

Vielen lieben Dank für die tolle Arbeitsatmosphäre bei Bayer und an jede Menge Kollegen, die mich bei den verschiedensten Meilensteinen dieser Arbeit unterstützt und/oder mir ihr Wissen weitergegeben haben. Vielen Dank an Carola Weidner und Simone Grum für ihre Unterstützung bei der Literaturrecherche. Vielen Dank an Dr. Uwe Eberspächer, Elisa Chemik und Dr. Pelin Ayaz für die Produktion und Bereitstellung von Proteinen. Ein ganz großes Dankeschön an Dr. Andreas Steffen, Dr. Paula Marin Zapata und Dr. Hans Briem für die Hilfe und Lehren bei der statistischen Auswertung mithilfe bio- und cheminformatischer Tools. Diesbezüglich möchte ich auch Dr. Djork-Arne Clevert und Lara Kuhnke für die interessanten Diskussionen danken. Ein besonderer Dank gilt auch Dr. Stephan Menz und Dr. Cornelia Preusse für ihre Unterstützung und Betreuung bezüglich der pharmakokinetischen Berechnungen und Simulationen. Außerdem möchte ich dem Patente-Team und insbesondere Dr. Anita Krüger danken, die im Rahmen des Genehmigungsumlaufs fleißig alle Dokumente, wie Abstracts, Vorträge, Poster oder Manuskripte, durchgesehen haben.

Ein herzliches Dankeschön auch an Dr. Anke Müller-Farnow und Dr. Jörg Fanghänel für bereichernde Diskussionen und für euer Verständnis, gerade als es am Ende der Arbeit zeitlich doch etwas knapp wurde.

Diese Dissertation entstand im Rahmen des IMI K4DD („Kinetics for drug discovery“) Projekts *. Die informativen Konsortiumstreffen mitsamt der lehrreichen Seminare und anregenden Debatten werde ich stets in guter Erinnerung behalten. Insbesondere möchte ich Dr. Arne Rufer für seinen leidenschaftlichen Vortrag zu Monte-Carlo-Analysen danken, der mir den Impuls gab dies für die Analyse des Motulsky-Mahan-Modells auszuprobieren. Lieben Dank auch an Dr. Chris de Graaf und Dr. Albert Kooistra für ihre Unterstützung bezüglich der KLIFS Datenbank. Viel Dank auch dafür, dass ich im Rahmen des öffentlichen Endmeetings einen Vortrag halten durfte. Auch möchte ich an dieser Stelle Dr. David C. Swinney und Prof. Dr. Peter J. Tongue für das persönliche positive Feedback und die interessanten Ratschläge danken.

Auch wenn ich sie nie persönlich getroffen habe, möchte hier auch den Herren Harvey Motulsky und Lawrence Mahan danken. Die mathematische Grundlage für die Bindungskinetik-Berechnungen habe ich Ihnen zu verdanken. Zudem danke ich Harvey Motulsky für die durchdachte GraphPad Software sowie für das lehrreiche und detaillierte Benutzerhandbuch.

Es war mir eine sehr große Freude mit euch allen zusammenzuarbeiten und von euch und mit euch zu lernen!

Abschließend möchte ich mich bei meiner Familie und ganz besonders bei meinem Ehemann für den starken emotionalen Rückhalt und die tatkräftige Unterstützung im Alltag bedanken.

* The work was in part supported by the Innovative Medicines Initiative Joint Undertaking (IMI JU) under grant agreement n° [115366], resources of which are composed of financial contribution from the European Union's Seventh Framework Programme (FP7/2007-2013) and EFPIA companies' in kind contribution.

Publikationsliste

Publikationen

Wesentliche Teile der Dissertation sind in den folgenden Manuskripten/Publicationen niedergelegt.

- **Georgi, V.; Schiele, F.; Berger, B.-T.; Steffen, A.; Zapata, P. M.; Briem, H.; Menz, S.; Preusse, C.; Vasta, J. D.; Robers, M. B.; Brands, M.; Knapp, S.; Fernández-Montalván, A. E.:** *“Binding kinetics survey of the drugged kinome”*; *Journal of the American Chemical Society*; 2018; 140 (46): 15774-82
- **Georgi, V.; Dubrovskiy, A.; Steigele, S.; Fernández-Montalván, A. E.:** *“Precision and accuracy of the ‘Motulsky-Mahan’ model for the analysis of kinetic competition association assays”*; manuscript submitted

Erkenntnisse aus dieser Dissertation wurden in den folgenden Manuskripten/Publicationen verwendet. Die Studien wurden in Kollaborationen im Rahmen des IMI K4DD (engl. Kinetics for Drug Discovery) Projekts parallel zum Hauptthema der Doktorarbeit durchgeführt.

- Nederpelt, I.; **Georgi, V.**; Schiele, F.; Nowak-Reppel, K.; Fernández-Montalván, A. E.; I. Jzerman, A. P.; Heitman, L. H.: *“Characterization of 12 GnRH peptide agonists - a kinetic perspective”*; *British Journal of Pharmacology*; 2016; 173 (1): 181-41
- Heroven, C.; **Georgi, V.**; Ganotra, G. K.; Brennan, P.; Wolfreys, F.; Wade, R. C.; Fernández-Montalván, A. E.; Chaikuad, A.; Knapp, S.: *“Halogen-Aromatic π Interactions Modulate Inhibitor Residence Times”*; *Angewandte Chemie*; 2018; 57 (24): 7220-24
Heroven, C.; **Georgi, V.**; Ganotra, G. K.; Brennan, P.; Wolfreys, F.; Wade, R. C.; Fernández-Montalván, A. E.; Chaikuad, A.; Knapp, S.: *“Halogenaromatische π -Wechselwirkungen modulieren die Verweilzeit von Inhibitoren”*; *Angewandte Chemie*; 2018; 130 (24)
- de Witte, W. E. A.; Versfelt, J. W.; Kuzikov, M.; Rolland, S.; **Georgi, V.**; Gribbon, P.; Gul, S.; Huntjens, D.; van der Graaf, P. H.; Danhof, M.; Fernández-Montalván, A. E.; Witt, G.; Lange, E. C. M.: *“In vitro and in silico analysis of the influence of D₂ antagonist target binding kinetics on the cellular response to fluctuating dopamine concentrations”*; *British Journal of Pharmacology*; 2018; accepted article: doi:10.1111/bph.14456
- Bosma, R.; Stoddart, L. A.; **Georgi, V.**; Bouzo-Lorenzo, M.; Bushby, N.; Inkoom, L.; Waring, M. J.; Briddon, S. J.; Vischer, H. F.; Sheppard, R. J.; Fernández-Montalván, A. E.; Hill, S.; Leurs, R.: *“Probe dependency in the determination of ligand binding kinetics at a G protein coupled receptor via competitive association kinetics”*; manuscript in clearance for submission

Das nächst folgende Review basiert auf einer detaillierten Literaturrecherche zum Thema *“Bindungskinetik im Wirkstofffindungsprozess”*, die zu Beginn dieser Dissertation durchgeführt wurde. Ein spezieller Fokus wurde auf unter Arzneimittelforschern diskutierten Struktur-Bindungs-kinetik Beziehungen sowie auf Assay-Technologien gelegt, die derzeit für die bindungskinetische Charakterisierung von niedermolekularen Liganden verwendet werden. Das darauf folgende Review stellt Ergebnisse des IMI-K4DD Projektes vor und kommentiert unter anderem die Verwendung von kPCA.

- **Georgi, V.; Andres, D.; Fernández-Montalván, A. E.; Stegmann, C. M.; Becker, A.; Mueller-Fahrnow, A.:** *“Binding kinetics in drug discovery – A current perspective”*; *Frontiers in Bioscience*; 2017; 22: 21-47
- Schuetz, D. A.; de Witte, W. E. A.; Wong, Y. C.; Knasmueller, B.; Richter, L.; Kokh, D. B.; Sadiq, S. K.; Bosma, R.; Nederpelt, I.; Heitman, L. H.; Segala, E.; Amaral, M.; Guo, D.; Andres, D.; **Georgi, V.**; Stoddart, L. A.; Hill, S.; Cooke, R. M.; De Graaf, C.; Leurs, R.; Frech, M.; Wade, R. C.; de Lange, E. C. M.; I. Jzerman AP; Muller-Fahrnow, A.; Ecker, G. F.: *“Kinetics for Drug Discovery: an industry-driven effort to target drug residence time”*; *Drug Discovery Today*; 22(6): 896-911

Vorträge

Einladung zum Vortrag im Rahmen des offenen K4DD Scientific Meeting "Binding kinetics: Time is of the essence" in Berlin (16.-18. Oktober 2017):

„TR-FRET competition assays for high throughput profiling of drug-target binding kinetics“

Der Abstract wurde für einen Vortrag auf dem EFMC International Symposium of Medical Chemistry 2018 in Ljubljana angenommen (2.-6. September 2018):

„Large-Scale Analysis of Kinase Inhibitors' Target Binding Kinetics and its Implications for Drug Discovery“

Poster Präsentationen

Teilergebnisse und/oder Erkenntnisse dieser Dissertation wurden/werden in den folgenden Präsentationen vorgestellt.

- **Georgi, V.; Berger, B. T.; Schiele, F.; Fernández-Montalván, A. E.:** *„A binding kinetics selectivity panel for high throughput profiling of kinase inhibitors“*; Novalix Conference - Biophysics in Drug Discovery 2015
- **Georgi, V.; Berger, B. T.; Schiele, F.; Fernández-Montalván, A. E.:** *„Large-scale binding kinetics profiling of kinase inhibitors“*; EMTRAIN PhD Workshop 2016
- **Georgi, V.; Berger, B. T.; Schiele, F.; Fernández-Montalván, A. E.:** *„Large-scale binding kinetics profiling of kinase inhibitors – a kinetic perspective for efficacy and safety“*; EMBO conference Cellular signalling and cancer therapy 2016
- Dubrovskiy, A.; **Georgi, V.**; Shatalina, M.; Rolland, S.; Råse, S.; Heyse, S.; Steigele, S.; Fernández-Montalván, A. E.: *“Fast and accurate assessment of binding kinetics in HTS format with the kinetic Probe Competition Assays and Genedata screener“*; verwandte Poster wurden präsentiert auf der 1) European Laboratory Robotics Interest Group (ELRIG) Drug Discovery 2016; 2) 6th Conference of the Society for Laboratory Automation & Screening (SLAS) 2017, und 3) Novalix Conference – Biophysics in Drug Discovery 2017
- Fernández-Montalván, A. E.; **Georgi, V.**; Vasta, J.; Puetter, V.; Glaske, S.; Robers, M. B.; Moenning, U.; Sturz, A.; Lefranc, J.; Ziegelbauer, K.; Brands, M.; Stegmann, C.; Scott, W. J.; Liu, N.: *“High-target binding affinity, long-lasting cellular target engagement, and high-dose intermittent schedule of PI3K inhibitor copanlisib contribute to its potent anti-tumor activity and good safety profile“*; American Association for Cancer Research (AACR) Annual Meeting 2017
- **Georgi, V.; Berger, B. T.; Schiele, F.; Dubrovskiy, A.; Shatalina, M.; Rolland, S.; Bosma, R.; Råse, S.; Heyse, S.; Steigele, S.; Fernández-Montalván, A. E.:** *„Novel approaches for the assessment of data from competitive binding kinetics assays“*; K4DD Scientific Meeting "Binding kinetics: Time is of the essence" 2017
- **Georgi, V.; Berger, B. T.; Schiele, F.; Steffen, A.; Zapata, P. M.; Briem, H.; Menz, S. ; Preusse, C.; Brands, M.; Knapp, S.; E.Fernández-Montalván, A. E.:** *„Binding kinetics survey of the drugged kinome“*; K4DD Scientific Meeting "Binding kinetics: Time is of the essence" 2017
- **Georgi, V.; Berger, B. T.; Schiele, F.; Steffen, A.; Zapata, P. M.; Briem, H.; Menz, S. ; Preusse, C.; Vasta, J. D.; Robers, M. B.; Brands, M.; Knapp, S.; E.Fernández-Montalván, A. E.:** *“High throughput profiling of drug-target binding kinetics – Methodology and Learnings“*; IMI 10th Anniversary Scientific Symposium 2018 (accepted Poster)

Eidesstattliche Erklärung

Ich erkläre hiermit an Eides Statt, dass ich die vorliegende Arbeit selbstständig verfasst und keine anderen als die angegebenen Quellen und Hilfsmittel verwendet habe. Die Grundsätze der guten wissenschaftlichen Praxis habe ich jederzeit beachtet.

Berlin, den 03.08.2018



Victoria Georgi

Es folgt eine kurze und eine ausführliche Zusammenfassung der Dissertation in deutscher Sprache, sowie die Dissertation in englischer Sprache.

Zusammenfassung

Eine Grundvoraussetzung für die pharmakologische Wirkung von Arzneimitteln ist, dass der Wirkstoff an krankheitsrelevante Zielmoleküle (sogenannte Targets) des Patienten bindet. Eine der häufigsten Zielmolekülklassen der pharmazeutischen Industrie sind Kinasen, regulatorische und signalübermittelnde Enzyme, deren Fehlregulation zur Entwicklung einer Vielzahl von Krankheiten, einschließlich Krebs, führen kann. Für die systematische Suche nach potenten und selektiven Wirkstoffkandidaten, die an Zielmoleküle binden, kommen in der Arzneimittelforschung meist Gleichgewichts-basierte Bindungsmaße wie Affinität (K_i , K_D) oder Potenz (IC_{50} , EC_{50}) zum Einsatz. In den letzten Jahren wurde diskutiert, ob dynamische Bindungsparameter, die Assoziationsrate (k_{on}) und die Dissoziationsrate (k_{off}) des Wirkstoffs für das gewünschte Target und für unerwünschte Antitargets, im Vergleich zur Affinität *per se* ($K_D = k_{off} / k_{on}$) besser geeignet sind, um die Entstehung und die Verweildauer des Wirkstoff-(Anti)Target-Komplexes *in vivo* und damit die therapeutische Wirkung und Sicherheit des Arzneimittels vorherzusagen. Es ist noch wenig erforscht, ob und wann Bindungskinetik den pharmazeutischen Effekt im komplexen Zusammenhang mit Pharmakokinetik und Pharmakodynamik beeinflussen kann und wie diese kinetischen Geschwindigkeitskonstanten rational optimiert werden können. Der Mangel an umfangreichen, direkt vergleichbaren Bindungskinetik-Datensätzen ist ein wesentliches Hindernis für ein besseres Verständnis des Themas.

Das Ziel dieser Dissertation ist eine umfassende Analyse der Bindungskinetik- und Affinitätsparameter eines diversen Sets von 270 niedermolekularen Kinaseinhibitoren für eine Reihe pharmakologisch relevanter Kinasen, um die Wichtigkeit der Bindungskinetik für die Arzneimittelforschung einzuschätzen: Anhand der neu generierten Daten soll der Einfluss von physikochemischen Eigenschaften auf Bindungskinetik, sowie die Relevanz von kinetischen Bindungseigenschaften für den klinischen Erfolg von Compounds untersucht werden.

Die umfangreiche Untersuchung wurde durch den kürzlich entwickelten „kinetic Probe Competition Assay“ (kPCA, engl. für kinetischer Sonden-Kompetitions-Test, kPCA) ermöglicht, dessen Evaluierung auf Motulskys und Mahans „Kinetik der kompetitiven Bindungstheorie“ beruht. Monte-Carlo-Analysen, die im Rahmen dieser Dissertation durchgeführt wurden, konnten zu einem besseren theoretischen Verständnis dieser Methode beitragen, lieferten neue Einblicke in ihre Grenzen und erlaubten es, Empfehlungen für das Assaydesign abzuleiten. Es zeigte sich, dass kPCA in der Tat hochdurchsatzfähig und bezüglich Präzision und Genauigkeit mit anderen biochemischen und biophysikalischen Assayformaten vergleichbar ist.

Multivariable lineare Regression zur Beschreibung der gemessenen Kinaseinhibitor-Target Bindungsparameter (k_{on} , k_{off} oder K_D) unter Verwendung von molekularen Eigenschaften und/oder bestimmten Kinase-Inhibitor-Wechselwirkungen als Deskriptoren konnte die Annahme bestätigen, dass

molekulare Eigenschaften von Verbindungen die Bindungskinetik beeinflussen können, und es konnten neue Hypothesen über molekulare Determinanten aufgestellt werden, die bestimmte Bindungseigenschaften hervorrufen könnten. Dies liefert eine rationale Grundlage für folgende Studien zur Untersuchung der Struktur-Bindungskinetik Beziehung. Bemerkenswerterweise konnten die bindungskinetischen Geschwindigkeitskonstanten durch die Modelle besser beschrieben werden als die Affinität.

Die systematische, quantitative Analyse der Inhibitor-Kinase-Bindungskinetikdaten zeigte interessanterweise, dass eine langsame Dissoziationsrate vom Haupttarget ein Merkmal ist, das bei Inhibitoren in fortgeschrittenen klinischen Entwicklungsphasen häufiger auftritt. Außerdem konnte gezeigt werden, dass die Bindungskinetik von Kinaseinhibitoren im Vergleich zur Affinität *per se* besser geeignet ist, um den zeitlichen Verlauf der Zielmolekülbelegung in Zellen zu simulieren. Darüber hinaus führt die Simulation mit einem traditionellen Pharmakokinetik-Modell und einem modifizierten Modell, das zusätzlich die Bindungskinetik der Inhibitoren berücksichtigt, in einigen Fällen zu verschiedenen *in vivo* Kinasebindungs-Zeitprofilen. Es wurde durch Simulationen illustriert, wie das Konzept der kinetischen Selektivität verwendet werden könnte, um dafür zu sorgen, dass ein unter Gleichgewichtsbedingungen unselektiver Inhibitor im offenen *in vivo* System, in dem das thermodynamische Gleichgewicht der Medikament-Target-Bindung nicht immer erreicht wird, selektiver ist.

Die generierten Daten und Modelle dieser Arbeit liefern Hinweise auf die Relevanz der Bindungskinetik in der Wirkstoffforschung und stellen eine wertvolle Ressource für zukünftige Studien auf diesem Gebiet dar.

Schlagwörter: Bindungskinetik, Verweilzeit, Dissoziationsrate, Assoziationsrate, kinetischer Kompetitionsassay, Kinetik der kompetitiven Bindung, Targetbelegung, Struktur-Bindungskinetik Beziehung, Pharmakokinetik, Wirkstofffindung, Kinase, Kinaseinhibitor

Ausführliche Zusammenfassung

Hintergrund

Die pharmakologische Wirkung von Arzneimitteln wird dadurch hervorgerufen, dass der Wirkstoff an krankheitsrelevante Zielmoleküle (sogenannte Targets) des Patienten bindet. In den meisten Fällen sind Wirkstoffe dabei kleine chemische Moleküle (Compounds). Kinasen sind Enzyme und stellen eine der größten Zielmolekülklassen dar. Sie können einen Phosphatrest von Adenosintriphosphat (ATP) auf andere Moleküle (wie Proteine, Lipide, Zucker) übertragen, um deren Verhalten und damit zelluläre Prozesse zu regulieren. Bei Fehlregulation der Kinasen können viele Krankheiten entstehen. Kinaseinhibitoren sind insbesondere für die Krebstherapie relevant. Da sie häufig mit der ATP Bindestelle interagieren, die eine hochkonservierte Region ist, die in allen Kinasen vorzufinden ist, kommt es oft zur Inhibierung mehrerer Kinasen, was zu Sicherheitsproblemen durch Antitarget basierte Toxizität führen kann. Daher ist Selektivität ein wichtiges Optimierungskriterium bei der Entwicklung von Kinaseinhibitoren. Derzeit basiert die Suche nach effektiven und selektiven Wirkstoffen hauptsächlich auf im Gleichgewicht bestimmten Bindungsparametern wie der Affinität oder Potenz. In den letzten Jahren wurde viel diskutiert, ob bindungskinetische Parameter den Blickwinkel auf den therapeutischen Effekt und die Selektivität verändern könnten. Die zugrundeliegende Idee ist, dass die Assoziationsrate (k_{on}) und Dissoziationsrate (k_{off}) im offenen System des Patienten, in welchem sich die Bindung des Wirkstoffs an das zugehörige Zielmolekül nicht immer im thermodynamischen Gleichgewicht befindet, wichtiger sein könnten als die Affinität an sich ($K_D = k_{off} / k_{on}$), und dass eine längere Verweilzeit ($= 1/k_{off}$) am Primärtarget als an Antitargets das Selektivitätsprofil und damit die Sicherheit des Wirkstoffs verbessern kann. Auch die Relevanz der Assoziationsrate für die Entstehung des Wirkstoff-Target-Komplexes steht zur Diskussion. Einige der bisherigen Studien zu diesem Thema deuten auf eine Relevanz der Bindungskinetik hin, andere bezweifeln diese. Noch ist unklar, ob und wann Bindungskinetik im komplexen System Mensch den pharmakologischen Effekt beeinflussen kann. Ein großes Hindernis für ein besseres Verständnis war das Fehlen einer hochdurchsatzgeeigneten Methode zur Bestimmung der Bindungskinetik. Viele Publikationen beruhen daher meist auf Simulationen, wenigen Targets, wenigen Inhibitoren und/oder publikationsbasierter Voreingenommenheit (oft werden nur hoch affine Substanzen untersucht und insbesondere langsame Dissoziationsraten berichtet). Das kürzlich entwickelte „kinetic Probe Competition Assay“ (engl. für kinetischer Sonden-Kompetitions-Test, kPCA) ermöglicht die Ermittlung bindungskinetischer Daten im großen Maßstab. Dabei wird die gleichzeitige kompetitive Bindung von einem Wirkstoffkandidat und einem Akzeptor-markierten Molekül (Sonde, auch Tracer genannt) an ein Donor-markiertes Target zeitlich verfolgt. Bei räumlicher Nähe von durch Licht angeregtem Donor und Akzeptor kommt es zur strahlungsfreien Energieübertragung, was zur messbaren Abnahme der Lichtemission des Donors und Zunahme der Emission des Akzeptors führt. Unter Nutzung der im Vorfeld bestimmten Tracerkinetik können mithilfe des Motulsky-Mahan-Modells, das die kompetitive Bindung mathematisch beschreibt, die k_{on} - und k_{off} -Konstanten des Compound-Target-Komplexes ermittelt werden.

Ziel der Arbeit

In dieser Arbeit sollte unter Verwendung der kPCA Methode die Bindungskinetik eines diversen Sets von 270 niedermolekularen Kinaseinhibitoren für eine Reihe pharmakologisch relevanter Kinasen untersucht und insbesondere im Hinblick auf die Relevanz für die Selektivität analysiert werden. Dafür musste zunächst die Genauigkeit des mathematischen Motulsky-Mahan-Modells im Zusammenspiel mit experimentell erhobenen Daten verstanden werden. Zudem sollte gezeigt werden, dass kPCA tatsächlich hochdurchsatzgeeignet ist und die Ergebnisse quantitativ mit anderen Methoden vergleichbar sind. Die Analyse der neu gewonnenen Daten sollte verschiedene Fragen beantworten: Wie ist die Verteilung der Assoziationsraten und Dissoziationsraten und ist eine lange Verweildauer am Target eine typische Eigenschaft von klinisch erfolgreichen Kinaseinhibitoren? Wie beeinflussen molekulare Eigenschaften der Inhibitoren die Targetbindungskinetik? Kann die Bindungskinetik den zeitlichen Verlauf der Targetbindungsprofile verändern?

Forschungsarbeit und Erkenntnisse

1) Erkenntnisse für die Entwicklung und Auswertung von kinetischen Competitionsassays

Kinetische Competitionsassays werden häufig mit Motulskys und Mahans „Kinetik der kompetitiven Bindung“ Modellgleichung ausgewertet. Im Rahmen dieser Dissertation wurde die Genauigkeit dieser Methode im Parameterraum (also in Abhängigkeit von verschiedenen Einflussfaktoren) mithilfe von Monte-Carlo-Analysen untersucht. Hierbei handelt es sich um die Simulation von tausenden Pseudo-Experimenten mit bekannten Eingabewerten und die Auswertung der Pseudo-Messsignale, wodurch man statistisch aussagekräftige Ergebnisse erhält und die Richtigkeit der erhaltenen Messwerte (deren Übereinstimmung mit dem wahren Wert) genau ermitteln kann.

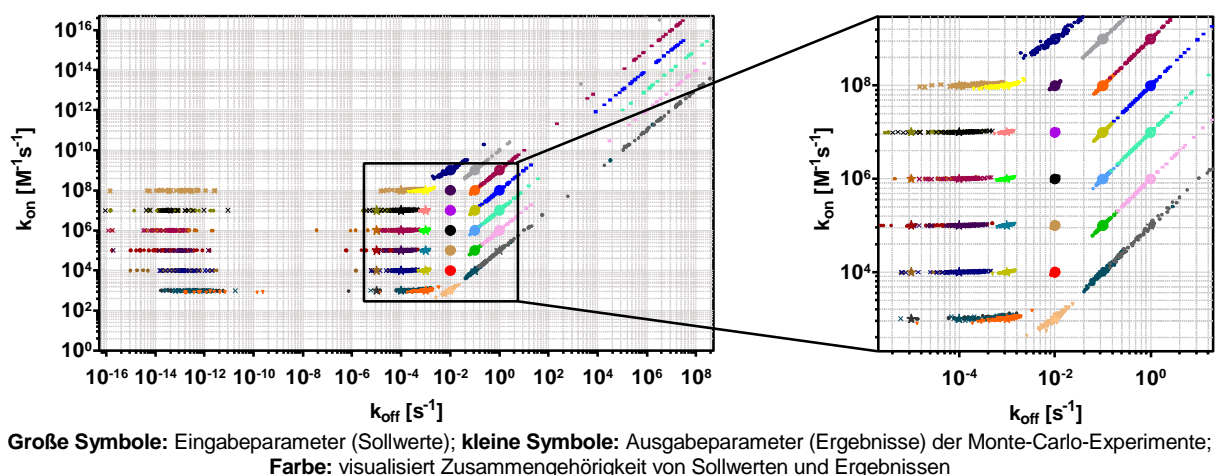


Abb. 1: Präzision und Richtigkeit der mit dem Motulsky-Mahan-Modell ermittelten bindungskinetischen Parameter

Simulation von kPCA Experimenten für Compounds mit verschiedenen bindungskinetischen Eigenschaften und anschließende Auswertung dieser Pseudo-Experimente mit dem Motulsky-Mahan-Modell erlaubt die Analyse der Genauigkeit des Modells. Für die Simulationen wurden genau die gleichen Bedingungen wie im kPCA Experiment verwendet (Compound-Konzentrationen [nM]: 0, 2.5, 25, 250, 2500; Tracerkinetik, -konzentration und Signalrauschen wie in BTK Assay (siehe Seiten 139f, 40f), 40× alle 10 s Signalmessung)

Es wurde entdeckt, dass die Präzision (Streuung der Messwerte) und Richtigkeit der ermittelten Werte insbesondere von der zu messenden Dissoziationsrate der Compounds abhängt (Abbildung 1). Die k_{off} -Grenzen werden dabei vor allem von der Beobachtungszeit und dem Messintervall festgelegt. Die folgenden Faustregeln konnten abgeleitet werden: **1)** Ist die Verweildauer des Compounds am Target länger als das Fünffache der Beobachtungszeit, so kann das Motulsky-Mahan-Modell weder die Dissoziationsrate noch die Affinität korrekt ermitteln, die Assoziationsrate wird aber immer noch mit höchster Präzision und Genauigkeit bestimmt. In diesen Fällen kann also tatsächlich (wie bereits vorgeschlagen, aber nicht allgemein akzeptiert) die k_{off} mithilfe der k_{on} und der im Gleichgewicht bestimmten K_D berechnet werden ($k_{\text{off}} = K_D \times k_{\text{on}}$). Dabei muss aber darauf geachtet werden, dass im Gleichgewichts- bzw. Endpunkt-Assay eine Mindestinkubationszeit von einer halben Verweildauer des Compounds am Target nötig ist, um dessen Affinität annähernd korrekt zu bestimmen (weniger als dreifache Unterschätzung). Außerdem ist bekannt, dass die sogenannte Assay Wall zur Unterschätzung der Affinität führen kann (wenn die Kinasekonzentration größer als das Doppelte der Affinität ist). Es ist also zu vermuten, dass die k_{off} oft unterschätzt wird. Trotzdem liefert diese Variante wesentlich bessere Ergebnisse als das Motulsky-Mahan-Modell, bei dem eine massive Über- und Unterschätzung möglich ist. Für kleinmaßstäbliche Analysen kann alternativ die Beobachtungszeit im Kompetitionsassay erhöht werden. **2)** Ist die Dissoziationsrate des Compounds schneller als die Messfrequenz, so kann das Motulsky-Mahan-Modell weder die Dissoziationsrate noch die Assoziationsrate korrekt ermitteln, die Affinität wird aber immer noch mit höchster Präzision und Genauigkeit bestimmt. Dies zeigt, dass der alleinige Vergleich der im Gleichgewichtsassay und im kinetischen Assay bestimmten Affinitäten nicht ausreicht, um die experimentellen Ergebnisse zu validieren. Eben dies wird aber derzeit sehr häufig ausgeführt. **3)** Die Grenzen für die minimal und maximal bestimmbare Compound-Assoziationsrate werden vor allem durch das Zusammenspiel von Tracer und Compound Affinität und Konzentration vorgegeben. **4)** Auch die Tracerkinetik spielt eine Rolle für die k_{on} - und k_{off} -Grenzen, allerdings eine geringere als die bisher beschriebenen Parameter. Eine schnelle Assoziationsrate des Tracers wirkt sich positiv auf die minimal bestimmbaren Geschwindigkeitskonstanten aus, wohingegen ein zu langsam assoziierender Tracer negative Effekte hat (ähnlich wie starke Messschwankungen). Höhere Tracerkonzentrationen verhalten sich äquivalent zu höheren Tracer-Assoziationsraten. **5)** Zudem wurde deutlich, dass der prozentuale Anteil des erreichten Gleichgewichts der Tracer-Kinase Bindung in der Kontrolle ohne Compound ein weiterer Faktor mit sehr hohem Einfluss auf die Genauigkeit der Methode ist (80% vom Gleichgewicht reichten aus, 25% erlaubten keine korrekte Bestimmung).

Die Richtigkeit der Bindungsparameterbestimmung kann durch experimentelle und konzeptionelle Fehler beeinträchtigt werden. Interessanterweise wurde entdeckt, dass Fehler dabei nie den gleichen Effekt auf schnell und langsam dissoziierende Compounds haben. Es wurde gezeigt, wie Fehler entdeckt werden können und dass die Methode durch die vielen verwendeten Compoundkonzentrationen robust gegenüber kleineren Konzentrationsfehlern ist. Da aber die Korrektheit der

Tracerkonzentration und dessen Bindungskinetikbestimmung eine wichtige Grundvoraussetzung ist, wurden die Limitationen dieser Bestimmung dargelegt, und es wurde eine alternative Methode vorgestellt, die etwas später von Messintervallgrenzen beeinträchtigt wird. Da fluoreszenzbasierte Assays oft mit einem zeitlichen Signalverlust behaftet sind, wurde zuvor eine Möglichkeit eingeführt mit diesem Problem umzugehen, dabei wurde das Motulsky-Mahan-Modell mit einem monoexponentiell abnehmenden Signaldrift Term multipliziert. Hier wurde eine neue Methode vorgestellt, die auf Normalisierung der Signale und des Modells beruht und gezeigt, dass diese mindestens genauso gut funktioniert und langsam dissoziierenden Compounds vermutlich besser gerecht wird (die ermittelten Dissoziationsraten haben besser mit denen aus einem Radioligandenkompetitionsassay übereingestimmt).

II) Der „kinetic Probe Competition Assay“ zur umfangreichen Analyse von Kinase-Inhibitor-Bindungskinetiken

kPCA und das dazugehörige Endpunkt-Assay ePCA wurden für 40 pharmakologisch relevante Kinasen entwickelt. Darunter befinden sich viele Tyrosinkinase, aber auch Vertreter anderer Kinase-Familien (Abbildung 2a) und insgesamt 25 Targets von durch die amerikanische Gesundheitsbehörde FDA (Food and Drug Administration) zugelassenen Kinaseinhibitoren. Unter den 270 Kinaseinhibitoren (davon lagen sechs Inhibitoren in unterschiedlichen Salzformen oder doppelt vor), die mit diesen Assays auf ihre Target-Bindungskinetik und -affinität untersucht wurden, befinden sich präklinische und klinische Wirkstoff-Kandidaten (darunter >90% der FDA Zulassungen, Stand Jan. 2018). Die Erkenntnisse aus den Monte-Carlo-Analysen wurden für die Auswertung der experimentell ermittelten Bindungsparameter angewendet. So wurde eine gute Intra- und Inter-Assay Präzision erreicht, und die Ergebnisse stimmten gut mit denen aus orthogonalen Methoden und vorhandenen Literaturwerten überein. Damit hat sich kPCA tatsächlich als großmaßstabgeeignete Methode bewiesen. Nur 41 der untersuchten Kinase-Inhibitor Paare wurden bereits in der bisher größten Studie zur Bindungskinetik von Kinaseinhibitoren untersucht. Diese Dissertation liefert Informationen über die Bindungskinetik und -affinität von insgesamt 4177 verschiedenen Kinase-Inhibitor Paaren und erlaubt damit eine beispiellos umfangreiche Analyse. Bemerkenswerterweise nehmen im Allgemeinen die Assoziations-, aber nicht die Dissoziationsraten mit zunehmenden Affinitäten zu. Wohingegen unter den potenziell klinisch relevanten höher affinen Interaktionen der Anteil der langsam dissoziierenden Kinase-Inhibitor-Komplexe bei Substanzen in späten klinischen Entwicklungsphasen häufiger auftritt, aber die Verteilung der Assoziationsraten unverändert bleibt (Abbildung 2b). Dabei sind die Dissoziationsraten weit verteilt, und die langsamsten (> 2h Verweildauer) werden für die Haupttargets der FDA zugelassenen Kinaseinhibitoren, aber nicht deren andere Targets beobachtet, was eine Voraussetzung für kinetische Selektivität erfüllt. Obwohl eine langsame Dissoziationsrate damit eine häufig beobachtete Eigenschaft von klinischen Kinaseinhibitoren ist, gibt es trotzdem auch FDA zugelassene Kinaseinhibitoren mit schnellen Dissoziationsraten vom Primärtarget.

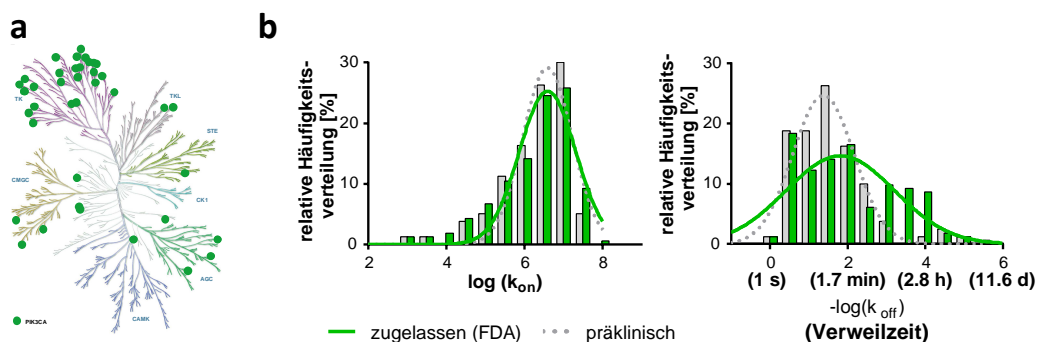


Abb. 2: a) Analyzierte Kinasen und b) Häufigkeitsverteilung der Bindungskinetiken von Kinase-Inhibitor in verschiedenen Phasen der klinischen Entwicklung

Es wurde die Bindung von 270 Kinaseinhibitoren gegen 40 Kinasen untersucht. Insgesamt wurde für 4177 verschiedene Kinase-Inhibitor Paare eine Interaktion beobachtet, wobei für 4014 die Bindungskinetik bestimmt werden konnte. 1029 Kinase-Inhibitor Paare haben eine Affinität $< 10^{-7}$ M. **a)** Darstellung der 40 Kinasen im phylogenetischen Baum des humanen Kinoms. **b)** Häufigkeitsverteilungen von Assoziations- und Dissoziationsraten (und zugehörige Gauss-Verteilung-Fits) für potenziell klinisch relevante Kinase-Interaktionen (Affinität $< 10^{-7}$ M) von Inhibitoren in verschiedenen Phasen der klinischen Entwicklung (Interaktionen von Inhibitoren, die durch FDA zugelassen sind: 166, oder in präklinischer Phase sind: 80) – mehr Details sind im Anhang K zu finden (Figure 55).

III) Der Einfluss struktureller Eigenschaften auf die Bindungskinetik von Kinase-Inhibitor Komplexen

Unter den untersuchten Inhibitoren gibt es verschiedenste Chemotypen, daher sind quantitative Analysen nötig, um darin enthaltene Informationen zu Struktur-Bindungskinetik Beziehungen zu offenbaren. Neben Häufigkeitsverteilungs-Untersuchungen wurden Korrelationsanalysen und multivariable lineare Regression mithilfe eines genetischen Algorithmus, der Modelle nach dem Prinzip der Evolution generiert und die wichtigsten Deskriptoren automatisch auswählt, durchgeführt. Es wurde bereits vermutet, dass Dissoziationsraten von den molekularen Eigenschaften des Compounds und der Kinasekonformation beeinflusst werden. In dieser Dissertation wurden Hinweise gefunden, dass sterische Hinderung (große unflexible Moleküle), Halogen-Interaktionen und konformationelle Änderungen der Kinase (DFG und α C-Helix Konformation) die Bindungskinetik beeinflussen können. Dies gilt aber oft nur für höher affine Interaktionen (mindestens im zweistellig nanomolaren Bereich) und es gibt Ausnahmen für die beobachteten Trends. Spezifische Wechselwirkungen zwischen den Kinaseinhibitoren und Aminosäuren in der Kinasebindungstasche spielen bekannter Weise eine entscheidendere Rolle. Mithilfe des genetischen Algorithmus' konnten auch neue Hypothesen aufgestellt werden, welche Interaktionen für Assoziations- und/oder Dissoziationsraten relevant sein könnten. Darunter waren auffallend viele hydrophobe Wechselwirkungen und oft in der Nähe oder mit Aminosäuren der sogenannten Kinase-Spines (spine: engl. für Rückgrat), was die Spine-Theorie unterstützt. Zusammengefasst wurde eine rationale Grundlage für folgende Studien zur Untersuchung der Struktur-Bindungskinetik Beziehung geschaffen.

Erwähnenswert ist auch die Beobachtung, dass molekulare Eigenschaften mit einer beschleunigenden oder verlangsamen Wirkung auf Assoziationsraten oft einen ähnlichen Effekt auf die Dissoziationsraten haben, wodurch der Effekt auf die Affinität verringert wird, sowie dass die aufgestellten Modelle, die die spezifischen Kinase-Inhibitor Wechselwirkungen als Deskriptoren verwenden, die bindungskinetischen Geschwindigkeitskonstanten besser beschreiben können als die Affinität.

IV) Die Relevanz der Bindungskinetik für den zeitlichen Verlauf der Targetbelegung mit Inhibitoren

Zuletzt wurde der Einfluss der Bindungskinetik von Kinaseinhibitoren auf die Targetbelegung in Zellen untersucht und die Frage adressiert, ob Bindungskinetik im offenen *in vivo* System im Vergleich zum reinen Konzentrations-Affinitäts-Effekt zu verschiedenen zeitlichen Profilen der Targetbelegung führen könnte. Acht Kinasen und fünf möglichst unselektive und klinisch relevante Inhibitoren wurden so ausgewählt, dass insgesamt ein weites Spektrum von verschiedenen Assoziationsraten, Dissoziationsraten und Affinitäten repräsentiert wird. Das intrazelluläre kinetische Bindungsverhalten dieser 40 Kinase-Inhibitor Paare wurde experimentell mithilfe eines NanoBRET Targetbelegungsassays bestimmt. Dabei wurden die Zellen zunächst mit den Inhibitoren vorinkubiert, dann ungebundene Inhibitoren aus dem Medium entfernt und schließlich der zeitliche Verlauf der Abnahme der Targetbelegung mithilfe eines Tracers verfolgt. K_D und k_{off} , jedoch nicht k_{on} einzeln betrachtet korrelierten mit der zeitlichen Abnahme der Targetbelegung in Zellen. Doch für die Interaktion zweier Compounds mit den Kinasen konnte der zeitliche Verlauf der Targetbelegung wesentlich besser simuliert werden, indem die Bindungskinetik berücksichtigt wurde, wohingegen der Konzentrations-Affinitäts-Effekt nicht ausreicht um die Verläufe zu beschreiben (ein Beispiel ist in Abbildung 3 zu sehen). Für die Beschreibung der zeitlichen Targetbelegungsprofile war es dabei notwendig, den Einfluss der Konkurrenz mit ATP und die Permeation der Inhibitoren durch die zelluläre Membran auf die verfügbare freie Target- und Inhibitor-Menge zu berücksichtigen, sowie den Präinkubationsschritt einzubeziehen, um die Targetbelegung zu Beginn des intrazellulären Dissoziationsexperiments zu bestimmen. Insgesamt ist für den zeitlichen Verlauf weder die Affinität, noch die Dissoziationsrate oder Assoziationsrate einzeln betrachtet, sondern das Zusammenspiel aller Faktoren wichtig. Für die drei anderen Compounds spielten weitere unaufgeklärte mikrofarmako-

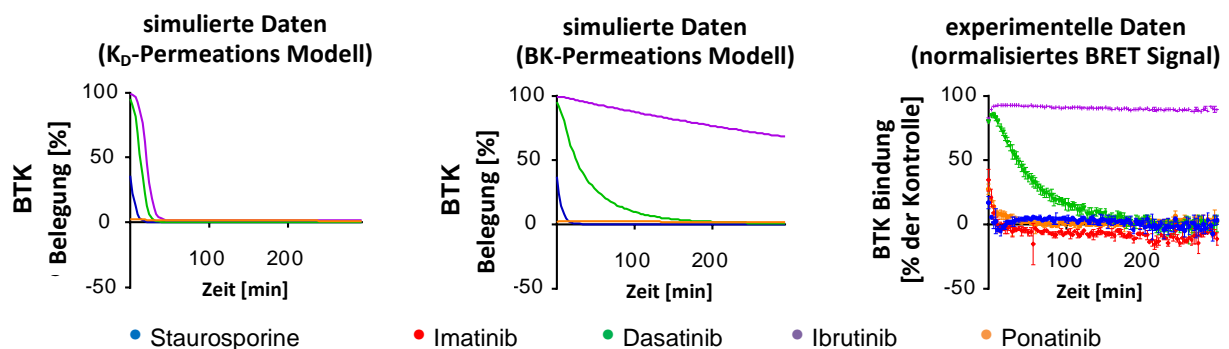


Abb. 3: Simulierter Verlauf der Targetbelegung in Zellen im Vergleich zum experimentell ermittelten Verlauf

Nach Vorinkubation von Zellen mit dem jeweiligen Compound wird das ungebundene Compound durch Medienwechsel entfernt (ausgewaschen) und die Targetbelegung zeitlich aufgelöst verfolgt. Simulation der zeitlichen Abnahme der BTK Belegung mit dem Compound in Zellen unter Berücksichtigung des Konzentrations-Affinitäts-Effekts (Links) beziehungsweise der Bindungskinetik (Mitte) bei sonst identischen Modellen (Berücksichtigung von ATP Konkurrenz und Permeation durch Zellmembran) im Vergleich zu experimentell erhobenen Daten (Rechts). Die zugrundeliegenden Modellgleichungen sind in Anhang I und Details zum Experiment auf Seite 33f zu finden. Da Ibrutinib kovalent an BTK bindet, lange Verweilzeiten im biochemischen Assay aber unterschätzt werden (siehe Monte-Carlo-Analysen), kommt es zu einer leichten Abweichung zwischen Bindungskinetik-basierter Simulation und Realität für Ibrutinib.

kinetische Prozesse eine Rolle (dies könnten z.B. die Interaktion mit Membranen oder aktiver Transport sein). Diese Fälle konnten identifiziert werden, da die Zeitprofile von denen des reinen Permeations-Bindungskinetik-Modells abweichen. Damit unterstützt das Wissen über k_{on} und k_{off} die Interpretierbarkeit von zellulären Experimenten, selbst wenn am Ende unter Berücksichtigung des Einflusses der mikropharmakokinetischen Faktoren auch die Affinität ausreicht um die Targetbelegung zu beschreiben.

Eine weitere wichtige Frage ist, ob Bindungskinetik auch im komplexen Zusammenhang mit der Pharmakokinetik (beschreibt die Freisetzung, Aufnahme, Verteilung, Verstoffwechslung und Ausscheidung von Wirkstoffen im Körper) das Profil der Targetbindung beeinflusst. Unter Nutzung traditioneller pharmakokinetischer Modelle bestimmt insbesondere die Clearance (Maß für Ausscheidung), die mit der Plasmaeliminationsrate beschrieben werden kann, die Abnahme der verfügbaren Wirkstoffkonzentration und damit die Abnahme der Targetbelegung, die über den reinen Konzentrations-Affinitäts-Effekt berechnet wird. Mithilfe einer aus der Literatur bekannten Methode (der sogenannten rate-limiting step approximation) konnten 250 Kinase-Inhibitor Interaktionen identifiziert werden, in denen die Dissoziationsrate (bestimmt die Verweildauer am Target) sowie die Assoziationsrate (kann repetitive Bindung zum Target begünstigen) gemeinsam mit der Plasmaeliminationsrate zur zeitlichen Reduktion der Targetbindung beitragen könnten. Dabei wurde aber unter anderem nicht der potentielle Einfluss der Bindungskinetik auf die Entstehung des Inhibitor-Target Komplexes berücksichtigt. Um den Einfluss auf das gesamte Targetbindungsprofil abzubilden, muss das Wirkstoffkonzentrations-Zeit Profil simuliert werden. Wohingegen frühere Arbeiten den Einfluss der Dissoziationsrate auf Targetbindungsprofile meist untersucht haben, indem bei der Simulation entweder die Assoziationsrate oder die Affinität fixiert und nur die jeweils anderen Parameter variiert wurden, liefert diese Dissertation durch Nutzung echter bindungskinetischer Daten eine größere Vielfalt an verschiedenen k_{on} - k_{off} Kombinationen. Zudem wird in der Literatur meist der Verlauf der Targetinteraktion nur mit dem Konzentrationsprofil verglichen. In dieser Dissertation hingegen demonstriert der bisher meist unberücksichtigte direkte Vergleich mit dem Konzentrations-Affinitäts-Effekt, dass die Bindungskinetik die simulierten Profile beeinflussen kann. Zudem konnte durch Simulation illustriert werden, wie das Zusammenspiel von Affinität, Bindungskinetik und Pharmakokinetik ausgenutzt werden könnte um dafür zu sorgen, dass ein unter Gleichgewichtsbedingungen unselektiver Inhibitor im offenen System des lebenden Organismus selektiver ist (Abbildung 4). Dabei wurde ausgenutzt, dass am Haupttarget eine schnelle Assoziationsrate und eine langsame Dissoziationsrate vorliegen und an anderen Targets eine langsamere k_{on} und/oder schnellere k_{off} beobachtet wird. Würde man dies bereits in der Wirkstofffindung beachten, könnte man eine schnellere Plasmaeliminierung bevorzugen, und zusätzlich durch niedrigere und weniger häufige Dosierung den gewünschten Effekt einstellen. Es sollte erwähnt sein, dass bei diesen Simulationen ein gewöhnliches Zwei-Kompartiment-Modell verwendet wurde und

weder die Konkurrenz mit ATP noch die zusätzliche Kompartimentierung durch die Zelle berücksichtigt wurden, die vermutlich die Relevanz der Bindungskinetik noch verstärken würden (siehe Abbildung 3), wohingegen andere mikropharmakokinetische Effekte (hier insbesondere auch die Synthese- und Degradationsrate des Targets) die Möglichkeit zur Nutzung kinetischer Selektivität ausschließen oder reduzieren können.

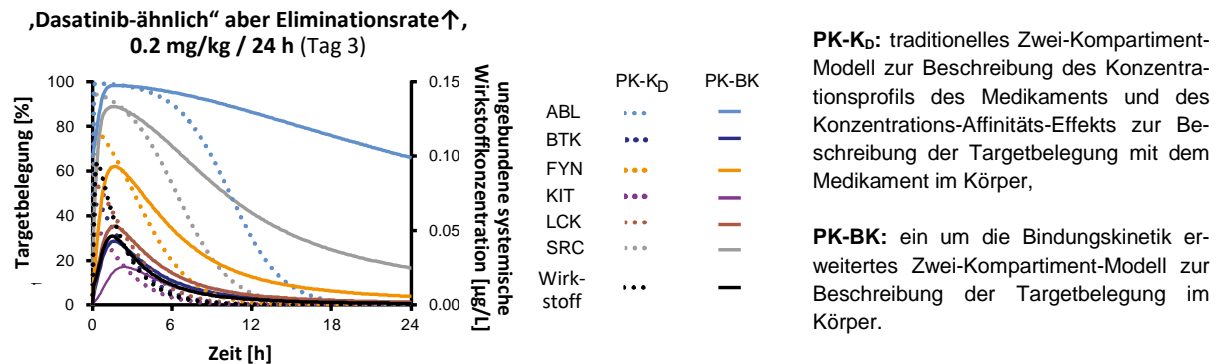


Abb. 4: Vergleich des simulierten Verlaufs der Targetbelegung im Menschen unter Berücksichtigung der Affinität oder der Bindungskinetik

Die Simulation des zeitlichen Verlaufs der Targetbelegung (von Kinasen: ABL, BTK, FYN, KIT, LCK, SRC) mit einem Dasatinib-ähnlichen Compound. Für die Simulationen wurden die experimentell erhobenen Bindungsdaten (Kinetik oder Affinität) von Dasatinib verwendet. Die pharmakokinetischen Parameter wurden anhand von Dasatinib-Konzentrationszeitprofilen abgeschätzt, wobei eine schnellere Interkompartiment- und Plasmaelimination angenommen wurde. Die den Simulationen zugrundeliegenden Modellgleichungen sind in Anhang J zu finden, weitere Informationen in Kapitel 5.4.3.2.

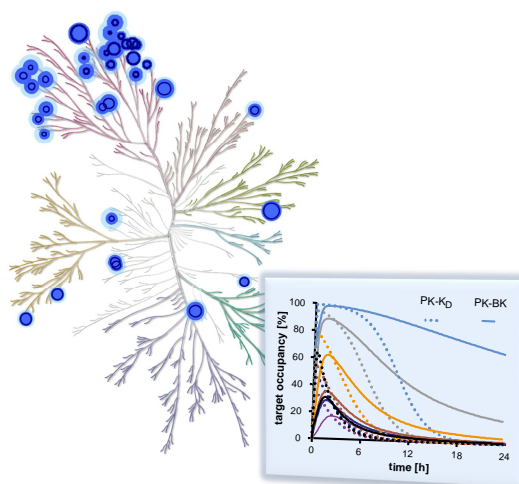
Schlusswort

Zusammengenommen konnte gezeigt werden, dass Assoziations- und Dissoziationsraten tatsächlich wesentliche Informationen enthalten und gemeinsam unter bestimmten Voraussetzungen bessere Prädiktoren und Deskriptoren für die Targetinteraktion sind als die Affinität *per se* und dass sie das zeitliche Selektivitätsprofil beeinflussen können. Der genaue Einfluss auf den pharmakologischen Effekt ist weiterhin von pharmakodynamischen Prozessen (z.B. Reversibilität des beeinflussten Signaltransduktionswegs oder Feedback-Mechanismen) abhängig und sollte zukünftig genauer untersucht werden. Interessanterweise scheint eine langsame Dissoziationsrate vom Haupttarget ein vorteilhaftes Merkmal von Kinaseinhibitoren in fortgeschrittener klinischer Entwicklung zu sein. Im Rahmen dieser Arbeit wird an vielen Stellen deutlich, dass die Bindungskinetik aber eher zusätzlich zur, und nicht an Stelle von der Affinität berücksichtigt werden sollte. Die Ergebnisse stellen darüber hinaus eine wertvolle Ressource für zukünftige Studien auf diesem Gebiet dar.

Dissertation

Large-scale analysis of kinase inhibitors' target binding kinetics. Implications for drug discovery?

2015-2018



submitted by

Victoria Georgi

in partial fulfillment of the requirements for the degree of
„Doktor der Naturwissenschaften“

Contact: Victoria.Georgi@gmx.de

Supervisors: Dr. Amaury Ernesto Fernández-Montalván (Bayer AG),
Prof. Dr. Stefan Knapp (Goethe-University), Prof. Dr. Michael Brands (Bayer AG)

Frankfurt am Main, 2018

Table of Contents

Abbreviations	1
List of Tables.....	2
List of Figures	3
1 Abstract	5
2 Introduction – Current state of knowledge.....	7
2.1 Drug discovery and development.....	7
2.2 Binding kinetic rate constants in drug discovery	11
2.2.1 Background	11
2.2.2 The debate about the importance of binding kinetic rate constants in drug discovery.....	12
2.3 Kinases and their inhibitors: Biological background and disease implications.....	15
3 Aim of the thesis.....	20
4 Material and methods.....	22
4.1 Material	22
4.1.1 Equipment, accessories and consumables	22
4.1.2 Chemicals, buffers, compounds, recombinant proteins and cells.....	23
4.1.3 Software and databases	24
4.2 Experimental Techniques	25
4.2.1 Probe competition assays (PCA) for large scale profiling	25
4.2.2 Surface plasmon resonance (SPR) biosensor-based assay	30
4.2.3 Cellular assay based on bioluminescence resonance energy transfer (BRET)	32
4.3 Computational Techniques and data analysis	34
4.3.1 Model fitting	34
4.3.2 General statistics	38
4.3.3 Monte Carlo simulations for assessment of precision and accuracy.....	39
4.3.4 Distance matrices and clustering technique.....	40
4.3.5 Definition and calculation of physicochemical properties of compounds	41
4.3.6 Multivariable linear regression based on a genetic function approximation algorithm.....	42
4.3.7 Gini scores as metric for selectivity	43
4.3.8 Quantitative systems biology and pharmacokinetics simulations with Copasi	44
5 Results	47
5.1 Assessment of precision and accuracy of binding kinetic parameters determined with kPCA and the ‘kinetics of competitive binding equation’	47
5.1.1 Precision and accuracy within the parameter space for exemplary kPCA setup.....	47
5.1.2 Effect of assay parameters and properties on precision and accuracy	50
5.1.3 Effect of errors on accuracy	61
5.1.4 Limitations of approaches for analysis of kinetics of tracer-target binding	66
5.1.5 The ‘kinetics of competitive binding equation’ and systematic signal decay	68

5.2	Large-scale analysis of kinase inhibitors' target binding kinetics	71
5.2.1	Binding kinetics and affinity profiling of kinase inhibitors.....	71
5.2.2	Validation of determined binding kinetics and affinity data	75
5.2.3	Binding kinetics perspective on kinase-inhibitor interactions.....	78
5.3	Investigation of the influence of structural features on kinase inhibitors' binding kinetics (KI BK)....	83
5.3.1	Effect of molecular properties of kinase inhibitors & conformations of proteins on KI BK.....	83
5.3.2	Effect of kinase-inhibitor interaction fingerprints on KI BK	90
5.4	Evaluation of the effect of kinase inhibitors' binding kinetics on target occupancy profiles.....	95
5.4.1	Target occupancy in intact cells.....	95
5.4.2	Binding kinetics perspective on selectivity	99
5.4.3	Combined effect of pharmacokinetics and binding kinetics on target occupancy	102
6	Discussion	108
6.1	Recommendations for the analysis and design of 'kinetics of competitive binding' experiments ...	109
6.2	Suitability of the 'kinetic probe competition assay' for large-scale binding kinetics profiling	114
6.3	Structural features influencing binding kinetic parameters.....	117
6.4	Binding kinetics impact on target occupancy profiles and pharmacological effects.....	121
6.5	Concluding remarks.....	130
7	References.....	132
7.1	Literature references.....	132
7.2	Collaboration partners and published parts of the thesis	137
Appendix	139
A	Kinase constructs and compounds.....	139
B	Binding kinetic rate constants of tracers and kinase specific assay parameters.....	143
C	„Association then dissociation – two or more concentration of hot” model for determination of tracer binding kinetics	145
D	kPCA traces with signal decrease and their evaluation based on normalization	146
E	Determination of kinase specific assay parameters and kinetic characterization of kPCA probe.....	148
F	Large-scale binding kinetics profiling	153
G	Close derivatives among the inhibitors in the profiling panel.....	156
H	Effect of specific inhibitor-kinase interactions on binding parameters.....	158
I	Model equations for simulations of target occupancy in cells.....	159
J	Model equations for simulations of target occupancy in the <i>in vivo</i> situation	161
K	Effect of binding kinetics on target occupancy and the pharmacological effect.....	162
Supplementary Spreadsheet:	Profiling results – Kinase inhibitors' target binding kinetics and affinities	165
CURRICULUM VITAE.....	220

Abbreviations

ATP	adenosine-5'-triphosphate
AUC	area under the curve
BK	binding kinetics
BP	back pocket (of kinase binding site)
BRET	bioluminescence resonance energy transfer
BSA	bovine serum albumin
BTN	biotin
2D	two dimensional
3D	three dimensional
DFG	amino acid sequence Asp-Phe-Gly (Aspartic Acid-Phenylalanine- Glycine), the DFG motif conformation is a structural feature of kinases
DMSO	dimethyl sulfoxide
DTT	dithiothreitol
ePCA	equilibrium probe competition assays
FDA	or USFDA; Food and Drug Administration – a federal agency of the United States of America
FP	front pocket (of kinase binding site)
GFA	genetic function approximation
HBD	hydrogen bond donor
HBA	hydrogen bond acceptor
HRD	amino acid sequence His-Arg-Asp (Histidine-Arginine-Aspartic Acid), the DFG motif conformation is a structural feature of kinases
HTS	high-throughput screening
IC ₅₀	ligand concentration required for 50% inhibition of the effect in the test system
K _D	equilibrium dissociation constant (a metric for affinity), K _{D eq} and K _{D kin} are the apparent K _D s determined in endpoint and kinetic assays, respectively
KI BK	kinase inhibitors' binding kinetics
KLIFS	KLIFS – a structural kinase-ligand interaction database
k _{on}	rate constant of association of the ligand-target complex
k _{off}	rate constant of dissociation of the ligand-target complex
kPCA	kinetic probe competition assay
MgCl ₂	magnesium chloride
MCS	Monte Carlo simulations
MW	or MolWt, molecular weight
NaCl	sodium chloride
nanoBRET	bioluminescence resonance energy transfer using the extremely bright Nanoluc luciferase as energy donor to increase sensitivity and dynamic range
Na ₃ VO ₄	sodium orthovanadate
PD	pharmacodynamics

PDB	or RCSB PDB, RCSB (Research Collaboratory for Structural Bioinformatics) Protein Data Bank
PDB ID	4-character unique identifier for PDB entries
PK	pharmacokinetics
PK-PD	pharmacokinetics- pharmacodynamics
RT	residence time ($=1/k_{off}$)
rpm	rounds per minute
SPR	surface plasmon resonance
St-Tb	terbium-labeled streptavidin
Tb	terbium
TO	target occupancy
TO _{max}	maximum target occupancy
TPSA	total polar surface area
TR-FRET	time-resolved fluorescence resonance energy transfer
Tris-HCl	tris(hydroxymethyl)aminomethane hydrochloride

List of Tables

Table 1: Percentage of variability of binding data explained by linear models with molecular properties as descriptors	88
Table 2: Percentage of variability of binding data on individual kinases explained by linear models with molecular properties as descriptors	89
Table 3: Percentage of variability of binding data of kinase-compound interactions with known cocrystal structures explained by linear models with molecular properties or KLIFS binding mode information and/or KLIFS interaction fingerprints (IFPs) as descriptors	90

Tables in Appendix:

Table 4: 40 kinases screened using equilibrium and kinetic Probe Competition Assay.....	139
Table 5: 270 compounds screened using equilibrium and kinetic Probe Competition Assay	140
Table 6: Assay conditions for equilibrium and kinetic Probe Competition Assay	143
Table 7: Binding kinetic and affinity parameters of Kinase Tracers (the kPCA probes)	144
Table 8: Determination of kinase specific assay parameters and kinetic characterization of kPCA probe	148
Table 9: Close derivatives among the 270 analyzed compounds screened	156
Table 10: Area under the curve (AUC) and maximal target occupancy (TO _{max}) for the simulated <i>in vivo</i> target occupancy profiles (TO) (as shown in Figure 44).	164

List of Figures

Figure 1 [3]: Overview about the drug discovery process.....	7
Figure 2 [29, 36]: Current hypothesis about the role of binding kinetics for the prediction of the drugs therapeutic effect	12
Figure 3 [37]: Frequency distribution of the biochemical mode of action of 85 FDA approved drugs (2001-2004)	13
Figure 4 [52]: Biological relevance of kinases in core signalling pathways	15
Figure 5 [57]: Phylogenetic trees of the human kinome with main targets of FDA approved small-molecule kinase inhibitors	16
Figure 6 [53]: Schematic representation of structural features of active and inactive kinases.....	18
Figure 7: Workflow of binding kinetic profiling based on kinetic Probe Competition Assay (kPCA)	25
Figure 8: Principle of the kinetic Probe Competition Assay (kPCA)	29
Figure 9: Comparison of experimental kPCA traces versus simulated kPCA traces.....	47
Figure 10: Precision and accuracy of the Motulsky-Mahan model under the conditions in a standard kPCA setup	48
Figure 11: Effect of incubation times in equilibrium binding assays on apparent dissociation constants	50
Figure 12: Effect of longer incubation times on traces of slow dissociating kinase-compound pairs	51
Figure 13: Effect of longer incubation times on precision and accuracy of the Motulsky-Mahan model	52
Figure 14: Effect of measurement intervals on traces of fast dissociating kinase-compound pairs.....	54
Figure 15: Effect of measurement intervals on precision and accuracy of the Motulsky-Mahan model	55
Figure 16: Effect of tracer binding kinetics on traces of fast dissociating kinase-compound pairs	56
Figure 17: Effect of the concentration and the binding kinetics of the tracer on precision and accuracy of the Motulsky-Mahan model.....	57
Figure 18: Combined effect of various parameters on the precision and accuracy of the Motulsky-Mahan model	59
Figure 19: Effect of experiential errors on kPCA traces	62
Figure 20: Effect of experiential errors on the accuracy of the Motulsky-Mahan model.....	63
Figure 21: Effect of conceptual errors on kPCA traces and calculated on- and off-rates	65
Figure 22: Comparison of two approaches for determination of kinetic rate constants of tracer-target binding	67
Figure 23: Comparison of two approaches coping with kPCA traces with systematic signal decay	69
Figure 24: Kinetic characterization of probes – exemplary kinase binding traces.....	71
Figure 25: Overview of the large-scale binding kinetics profiling performed in this thesis	73
Figure 26: Comparison of binding parameters calculated from steady state (ePCA) versus kPCA model fit results	74
Figure 27: Comparison of binding parameters obtained in Run A versus Run B (two independent experiments) ..	76
Figure 28: Comparison of affinity metrics obtained in this thesis versus literature reference values	76
Figure 29: Comparison of binding kinetic parameters obtained with kPCA in this study versus own and literature values measured with SPR	77
Figure 30: Distribution of on-and off-rates of 3230 kinase-inhibitor interactions quantified in this study	79
Figure 31: Kinase-inhibitor interaction maps from steady state and binding kinetics perspective	81
Figure 32 (part 2 of 2): Distributions of binding parameters across compound molecular properties	85
Figure 33: Distribution of binding parameters across kinase conformations	86
Figure 34: Relationships between binding parameters and molecular properties – correlation and linear regression	88

Figure 35: Relationships between binding parameters and specific inhibitor interactions with kinase binding site residues (a) as specified in KLIFS database (b [78])	91
Figure 36: Comparison of imatinib, rebastinib, ponatinib and nilotinib binding to ABL.....	92
Figure 37: kon-koff plot representing the wide-spread distribution of on- and off-rates for 5 compounds binding to 8 kinases that were selected for cellular experiments.	95
Figure 38: NanoBRET™ traces for analysis of the time course of target engagement in intact cells.	96
Figure 39: Comparison of biochemical binding parameters and duration of target binding in the cellular context	96
Figure 40: Reactions and events relevant for simulation of target occupancy.....	97
Figure 41: Simulated time course of target occupancy decline in cells compared to experimental traces.....	98
Figure 42: Influence of binding kinetics on target selectivity.	101
Figure 43: Trends for the effect of residence time on target occupancy and the pharmacological effect.....	103
Figure 44: Comparison of simulations of the time course of <i>in vivo</i> target occupancy with drug from the binding kinetics (PK-BK) versus the affinity perspective (PK-K _D).....	105

Figures in Appendix:

Figure 45: Exemplary kPCA traces influenced by systematic signal decay (a) and their corresponding normalized traces representing the percentage of compound binding (b)	146
Figure 46: Binding kinetics, affinities and concentrations of Kinase Tracers investigated in this thesis	152
Figure 47: Phylogenetic tree of the human kinome with kinases targeted by kPCA compatible tracers.....	153
Figure 48: Binding parameters of 270 kinase inhibitors for individual kinases	153
Figure 49: Comparison of binding kinetic and affinity parameters determined for different salt forms of kinase inhibitors	154
Figure 50: Comparison of binding kinetic and affinity parameters determined for labeled and unlabeled compounds.....	154
Figure 51: Binding parameters of kinase inhibitors in different clinical phases	155
Figure 52: Comparison of binding kinetic and affinity parameters determined for close derivatives among the compounds in the screening panel	157
Figure 53: Relationships between binding parameters and molecular properties and/or specific inhibitor-kinase interactions as specified in KLIFS database	158
Figure 54: Comparison of percent changes in target occupancy ΔTO (30 and 90 min upon compound washout) derived from simulated and experimental traces (as shown in Figure 41)	162
Figure 55: Distribution of kinase-compound binding kinetic rate constants depending on the clinical phase of the kinase inhibitor.....	163

1 Abstract

A necessary requirement for a pharmacological effect is that a drug molecule tightly interacts with its disease relevant target molecule in the patient. Kinases are regulatory, signal transmitting enzymes and are a large protein family that belongs to the most frequent targets of pharmaceutical industry, as deregulation of kinases has been associated with the development of a variety of diseases, including cancer. In drug discovery, equilibrium binding metrics such as the affinity (K_i , K_D) or potency (IC_{50} , EC_{50}) are usually applied for the systematic profiling for potent and selective drug candidates. In recent years, dynamic binding parameters, the drugs association (k_{on}) and dissociation (k_{off}) rates for desired primary-targets and undesired off-targets, were discussed to be better predictors than steady-state affinity *per se* ($K_D = k_{off} / k_{on}$) for the onset and duration of the drug-target complex in the open *in vivo* environment and thereby for the therapeutic effect and safety of the drug. It is yet unclear whether and when the binding kinetics parameters can influence drug action in the complex context of pharmacokinetics and pharmacodynamics and how the kinetic rate constants can be optimized rationally. One major obstacle for providing proof for the hypothesis that drug binding kinetics is of importance for drug action is the generation of large and comparable binding kinetic datasets.

The aim of this thesis was the comprehensive analysis of the binding kinetic and affinity parameters of a diverse spectrum of 270 small-molecule kinase inhibitors against a panel of pharmacologically relevant kinases to study the role played by binding kinetics for drug discovery: The generated dataset was utilized to assess the effect of chemical properties on drug binding kinetics, and to evaluate the impact of kinetic rate constants on the success of compounds in the drug discovery pipeline.

Large scale profiling was made possible by a recently developed “kinetic Probe Competition Assay” (kPCA), whose evaluation is based on Motulsky’s and Mahan’s “kinetics of competitive binding” theory. Monte Carlo analyses performed in this dissertation widened the theoretical knowledge of this theory, provided new insights into its limitations and allowed to derive recommendations about how to best design assays. It was demonstrated that kPCA is indeed high-throughput compatible and that it is comparable to other biochemical and biophysical assay formats in terms of precision and accuracy.

Multivariable linear regression for the description of the determined kinase inhibitors’ target binding characteristics (k_{on} or k_{off} or K_D) using molecular properties and/or particular kinase-inhibitor interactions as descriptors supported the assumption that molecular properties of compounds might affect binding kinetics, generated new hypothesis about molecular determinants influencing binding kinetic parameters and provided a rational basis for following structure-kinetic relationship studies.

Remarkably, the binding kinetic rate constants were better described by the established models than binding affinities.

Interestingly, the systematic, quantitative analysis of kinase inhibitors' target binding kinetics indicated that a slow dissociation rate for the main target is a feature which is more frequently observed in inhibitors that reached approval or late stage clinical testing than in earlier phases of clinical development. In addition, it was demonstrated that binding kinetics of kinase inhibitors is a better predictor for the time course of target engagement in cells as compared to affinity *per se*. Furthermore, in some study cases simulations using a standard pharmacokinetics model and a modified model considering the inhibitors binding kinetics lead to different *in vivo* kinase occupancy time profiles. It was illustrated by simulations how the concept of kinetic selectivity can be applied to turn an unselective compound in equilibrium conditions into a more selective compound in the open *in vivo* situation, where the thermodynamic equilibrium of drug-target binding is not necessarily reached.

Thus the generated data and models provide evidence for the importance of binding kinetics in drug discovery and represent a valuable resource for future studies in this field.

Keywords: Binding kinetics, residence time, off-rate, on-rate, dissociation rate, association rate, kinetic probe competition assay, kinetics of competitive binding model, target engagement, target occupancy, structure-kinetic relationship, pharmacokinetics, drug discovery, kinase, kinase inhibitor

2 Introduction – Current state of knowledge

2.1 Drug discovery and development

Pharmaceutical drugs are used to alleviate, cure or prevent a disease. Drugs can be categorized in biological and chemical substances: Biologics are in most cases therapeutic peptides or proteins, such as insulin (for use in treating diabetes; molecular weight: 5800 g/mol) or antibodies, and are produced in biotechnological processes. Chemically manufactured substances, such as acetyl salicylic acid (inter alia used to treat pain, inflammation and fever; molecular weight: 180 g/mol), are substantially smaller than biologics and account for 90% of the approved drugs [1]. The focus of this work is on small molecules. Therapeutic agents were historically often either serendipitous discoveries or based on trial and error. Nowadays, discovery of new chemical entities walks along a systematic, iterative multi-step approach (Figure 1). The goal is to find a new treatment or an alternative drug with higher efficacy and fewer side effects.

The first important step of the drug discovery process is target discovery, i.e. the identification of proteins or other biomolecules (such as DNA, RNA, lipids) with biological relevance for the disease. In most cases these so-called targets are proteins, in particular enzymes or receptors. Kinases (an enzyme subclass) and G protein-coupled receptors (a receptor class) belong to the most frequent human protein targets of pharmaceutical industry [2]. Depending on whether the target molecule potentially has a negative effect or a positive effect on the course of the disease, the desired treatment strategy could be to inhibit or to stimulate the activity of the target. The modulation of the

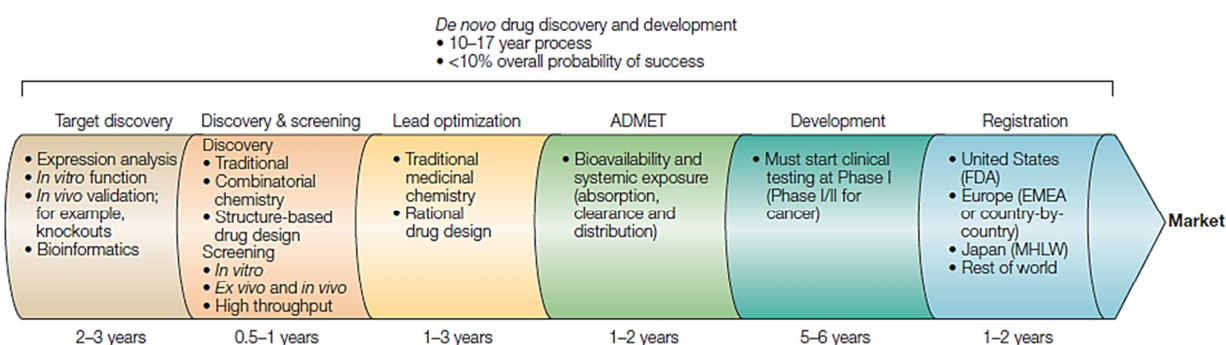


Figure 1 [3]: Overview about the drug discovery process

Target-based drug discovery is a long multi-step process comprising 1) the discovery of target molecules, in most cases proteins, with biological relevance for the disease, 2) the identification of small-molecule compounds modulating the activity of the target in the desired way, 3) the optimization of the identified leads to reach favorable pharmacodynamics (potency, selectivity, efficacy) and pharmacokinetics (absorption, distribution, metabolism, clearance), 4) clinical development to study how the drug candidates interact with the human body. If the drug is safe and effective for the intended indication and superior to alternative treatment, government agencies examine the data and decide to approve or not approve the drug.

target should translate into the desired therapeutic effect under minimal side effects [4]. The next step following target discovery and validation is the lead identification and optimization phase.

The idea of targeted therapeutics is that pharmacological effects can only be induced when a drug is bound to its target. This principle was introduced a century ago by Paul Ehrlich [5, 6]. The goal of the lead identification phase is therefore to identify small molecules binding to the target and to characterize their potency for modulating the target activity. To date, laboratory automation and miniaturized assays (test systems) allow high-throughput screening of comprehensive compound libraries for small molecules with the desired action profile: The libraries of pharmaceutical institutes contain thousands to millions of compounds generated by various methods, such as historical collection or high-throughput chemistry [7]. Besides robotics and liquid handling devices, a further prerequisite for the screening of these large compound collections is the development of miniaturizable and automatable methods for investigation of compound-target binding and the induced effect. These assays must be performed in microtiter plates, with assay volumes of a few microliters to enable high-throughput screening at reasonable costs [7]. Compounds with the desired activity in the screen are tested in secondary assays to confirm the hit [8]. Further tests with lower throughput are conducted for the hits to identify compounds or compound series (with common chemical features) demonstrating desired activity and selectivity for the target molecule [9]. Chemoinformatics tools can help to find cluster of molecules with similar activities and structures [10].

Lead molecules have to meet further criteria, for example chemical optimization potential, purity and stability of compound, non-frequent hitters and promising pharmacokinetic properties (for more information see below) [11]. Initially the hits possess rather weak activities and do not yet possess all properties required for therapeutic use so that optimization is required to attain good drug candidates [7]. The molecular structure of the target protein is studied to find out how the compounds interact with the protein binding pockets. This can be accomplished by X-ray crystallography: X-rays are diffracted at the atoms of the crystallized protein-compound complex and interfere with other scattered X-rays. The resulting diffraction pattern allows calculating the density of electrons and thereby determining the position of atoms and finally to get a 3D image of the protein-compound co-crystal structure [12]. Computational chemistry can utilize this information to prioritize leads by identification of entry points for lead optimization and can even conduct screening of virtual compound libraries to identify new leads [13].

The next step consists in the lead optimization programs, which are iterative processes comprising synthesis of structural analogs and testing of their pharmacokinetic and pharmacological properties. This knowledge can be used to derive structure-activity relationships helping to identify the best drug

candidate [7]. There are several other key optimization and selection criteria: E.g. binding strength and activity on primary targets and off-targets are measures for pharmacodynamics parameters, i.e. for potency, efficacy and selectivity [11]. Selectivity for the intended target protein(s) is important, as harmful adverse events can result from interactions with other proteins [14, 15]. Another factor is the consideration of “drug-likeness” rules which have been deduced from retrospective analysis of marketed drugs [7]. An example is the Lipinski “Rule of Five”: Good oral bioavailability is more likely, if a compound possesses no more than 5 hydrogen bond donors, no more than 10 hydrogen bond acceptors, no more than a molecular weight of 500 g/mol and no more than an octanol-water partition coefficient Log P of 5, whereas the possibility for poor absorption and limited membrane permeability is high if the compound violates two or more of these criteria [16].

Following numerous *in vitro* studies and cell assays, the toxicology and pharmacology of the drug candidates are studied in living organisms (*in vivo*), i.e. animal models are used to determine the rate and extent of the drug candidate’s absorption, distribution, metabolization (chemically modification) and excretion in/from the living organism (pharmacokinetics) and to study how the drug candidate affects the organism (pharmacodynamics) [17]. The pharmacokinetic properties decide if and at which concentration the drug candidate reaches the site of action and how long it stays there. Favorable pharmacokinetics, e.g. high absorption and low clearance (slow elimination / removal), is another important optimization and selection goal during preclinical development [18]. Moreover, pharmacokinetic information is considered together with pharmacodynamics parameters to determine the drug concentration-effect relationship allowing deduction of the dosing regimen (amount and frequency of drug administration) required to achieve the desired concentration-time profile and finally to produce the desired effect [17]. This provides insights into the minimum dose required for the intended therapeutic effect but also into the maximum dose and related adverse events. Adverse reactions can arise from chemical-based, on-target or off-target toxicity: The induction of negative effects on e.g. cellular organelles or membranes by the physicochemical characteristics of the compound is called chemical-based toxicity, adverse events due to the interaction with the intended target is called on-target toxicity and negative effects induced by unselectively and modulation of other targets it is called off-target toxicity [19].

Furthermore, the pharmaceutical formulation, i.e. the combination of the therapeutic agent with other inactive components and their incorporation into tablets, capsules (for oral administration) or liquids (for e.g. intravenous administration), influences the stability, bioavailability and time course of drug release and thereby the concentration-time profile [20].

If a compound can fulfill the requirements of all the mentioned preclinical studies and proved to be tolerable to a sufficient extend in preclinical toxicology-studies, it proceeds with the clinical

development. In the clinical phases it is studied how the drug interacts with the human body: Phase I trials are performed with healthy volunteers (exception: real patients are allowed for late-stage and so far incurable diseases, such as in oncology (cancer) and HIV drug trials) by administering initially low and stepwise increasing doses in order to test the tolerability and to determine the pharmacokinetic properties in the human body, Phase II trials are performed with patients in order to assess if the drug works, if there are adverse events and to determine the optimal therapeutic dosing regimen, and Phase III trials are performed with a larger group of patients in order to proof effectiveness, safety and the benefit compared to the standard treatment (if available) [21]. Then the results from preclinical and clinical studies are summarized and reviewed by government agencies (e.g. Food and Drug Administration (FDA) of the United States) which decide to approve or not approve the drug for therapeutic purposes. Finally the long-term effects of the approved drugs are monitored in the Post Marketing Surveillance trial (Phase IV) [21].

In total the whole drug discovery and development process takes 10-17 years and costs more than \$ 1 billion, whereby about 50% account for the clinical development [22, 23]. Less than 10% of the compounds discovered in the preclinical trials reach the market [23]. In the light of the high attrition rates and high costs in the later stages of the drug discovery process [22, 23], it becomes obvious that the goal is still to learn from failures and successes and to adapt accordingly the selection criteria for lead identification and optimization in the preclinical phase.

2.2 Binding kinetic rate constants in drug discovery

2.2.1 Background

Currently, systematic profiling for potent and selective drug candidates is mainly based on equilibrium binding metrics such as the affinity or potency (in closed biological systems, i.e. according to Copeland *in vitro* systems where thermodynamic equilibrium of drug-target binding can be reached) [14, 24, 25].

The affinity is a measure of the binding strength and can be described by the equilibrium dissociation constant K_D . Assuming a one-step reaction and 1:1 binding (i.e. one drug molecule binds to one target molecule), the equilibrium dissociation constant is the ratio of the binding kinetic rate constants, in other words the quotient of the rates of dissociation (off-rate: k_{off}) and association (on-rate: k_{on}) of the drug-target complex [26], and the K_D can be simply interpreted and determined as it equals the molar concentration of drug required to occupy 50% of the target protein at equilibrium *in vitro* [27] (further information about the dissociation constant and the law of mass action is provided in chapter 4.3.1). A low K_D indicates a high affinity.

Likewise, potency is also determined in equilibrium and is a measure of the drug's biological activity described by the molar concentration of drug required to produce or inhibit 50% of an effect *in vitro* (EC_{50} , IC_{50}) [27]. Additionally, also the drug's concentration in plasma required to evoke 50% of the maximum effect at steady-state conditions *in vivo* is called IC_{50} and EC_{50} . As effects can only be induced when a drug is bound to its target [6, 28], potency depends on both affinity and efficacy (the maximum achievable effect on function at a given concentration).

It should be emphasized that the same affinity can be reached with both a fast on- and off-rate as well as a slow on- and off-rate (since $K_D = k_{off} / k_{on}$). The difference is how quickly the drug-target complexes form and dissociate and therefore how long it takes to reach equilibrium [29]: For a 1-step reaction, equilibrium is reached when the number of binding events per unit time equal the number of dissociation events per unit time. The number of binding events is dependent on both the concentration of the reactants (drug, target) and their kinetic rate constant of association, while the number of dissociation events per unit time is only dependent on the dissociation rate. At very high drug concentrations 100% of the target is bound to the drug in equilibrium, i.e. the target is saturated with the drug. The necessity of a conformational change reduces the rate constants and fast association rates are limited by diffusion [30-33].

For many drug-target interactions a simple one-step binding mode does not apply due to transient or covalent interactions as well as structural changes. In reality, binding is a multi-step process comprising many small conformational adjustments [34]. Nonetheless one-step binding mode is often used as simplified model although it is insufficient to explain how slow off-rates can occur (structural features discussed to influence binding kinetics are introduced in chapter 2.3 - last

paragraph). For explaining slow off-rates can occur, more complex binding mechanism models are frequently used such as **1)** induced fit model, which assumes that the binding is followed by a conformational change in the target (that may trap the drug) which strengthens binding, or **2)** conformational selection, where the target adopts two conformations to which the drug binds with different affinities or the drugs binds to only one of the conformations [35].

2.2.2 The debate about the importance of binding kinetic rate constants in drug discovery

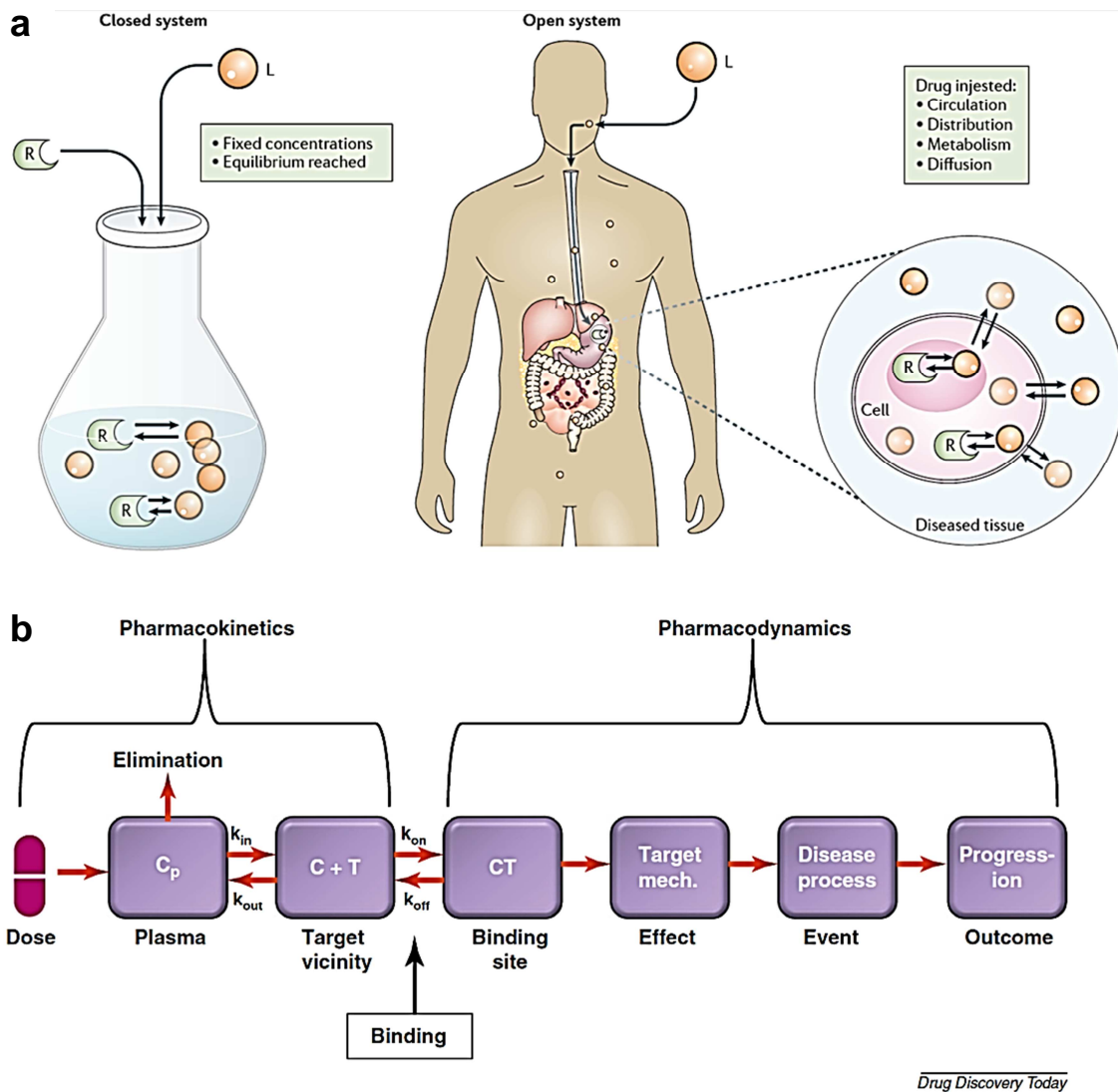


Figure 2 [29, 36]: Current hypothesis about the role of binding kinetics for the prediction of the drugs therapeutic effect

a) In contrast to the *in vitro* test environment, the human body is an open biological system where the thermodynamic equilibrium of drug-target binding is not necessarily reached. Therefore, the dynamic binding parameters, the rates of drug association (k_{on}) and dissociation (k_{off}) from the target, might play a more important role than equilibrium binding metrics such as steady state affinity *per se*.

b) Binding kinetics as link between pharmacokinetics and pharmacodynamics. Conventional steady-state PK-PD (pharmacokinetics-pharmacodynamics) models describing the extent and time course of a drugs pharmacological effect consider the time-dependent resorption, distribution, metabolism and excretion of a compound, but thereby neglect the influence of the binding kinetics on the duration of the drugs effect. The potential impact of binding kinetics on the onset and duration of the drug-target interaction and thereby on the therapeutic effect and safety of the drug is currently a topic of intense debate.

Recently, the impact of binding kinetic rate constants on the onset and duration of the drug-target interaction and thereby on pharmacological properties has become a topic of intense debate [29-31, 36, 37]. The underlying idea is that animal models and ultimately patients are open biological systems, where the thermodynamic equilibrium of drug-target binding is not necessarily reached. Therefore, the dynamic binding parameters, the rates of drug association and dissociation from the target, might play a more important role than steady state affinity *per se* (Figure 2a).

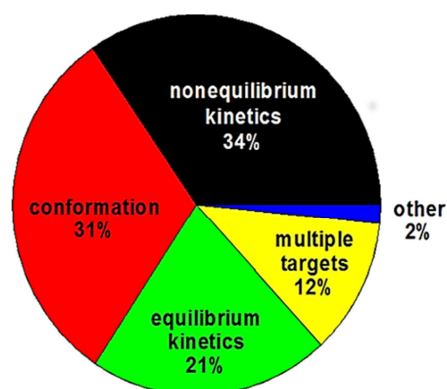


Figure 3 [37]: Frequency distribution of the biochemical mode of action of 85 FDA approved drugs (2001-2004)

The retrospective analysis suggests that in addition to equilibrium binding metrics (e.g. affinity, potency), non-equilibrium binding kinetic rate constants could be valuable criteria during lead discovery and optimization.

Traditionally, binding kinetics was not considered for lead optimization and drug candidate selection. It was assumed that the binding reaction is fast enough to reach equilibrium, especially since pharmacokinetic concentration changes typically take hours [29].

This view was challenged in 2006 by Swinney's retrospective analysis of recently FDA approved drugs revealing that one third of 85 FDA approved drugs interact with their target through non-equilibrium kinetics mechanisms (Figure 3) [37], suggesting that the compounds on- and off-rate can be valuable criteria for drug candidates prioritization, as well as by the introduction of the drug-target residence time concept by Copeland *et al.* [31]. The drug-target residence time concept postulates that consideration of binding kinetic

dissociation rates 1) allows a better prediction of the duration and extent of the pharmacological effect in animal models and the human body (Figure 2b), since slow off-rates sustain the effect even if the drug is removed from the system, and 2) can lead to the identification of medicines with improved safety, owing to kinetic selectivity, i.e. a significantly longer residence times ($RT = 1 / k_{off}$) on their primary targets than on their off-targets, which is thought to mitigate off-target toxicity [31, 38].

Since then slow off-rates received increasing attention (>600 citations of the paper from Copeland *et al.*) and acceptance [36]. The additional importance and consideration of on-rates broadened the drug-target residence time concept [30, 39]. Simulation studies demonstrated that too slow on-rates at low doses will not lead to high target occupancies before the compound is cleared from the system, albeit that effect can be overcome by higher and/or repeated dosing [29, 40]. Furthermore, following dissociation from the target protein, the probability of rebinding to the target protein rather than diffusing away is increased by fast association rates, which also increases the duration of the drug-target interaction [40]. Slow-dissociating compounds are proposed to provide a higher barrier to efflux-mediated resistance [31, 41], and binding kinetic parameters were used to simulate the duration of target occupancy which reflected *in vivo* efficacy [42]. For some indications, a short

duration of effect or fast binding kinetics might be advantageous [43]: e.g. fast on-rates and fast-off rates of antipsychotic drugs are discussed to prevent adverse events caused by on-target-based toxicity [44-46]. In his 10 years retrospective analysis [36], Copeland recently summarized examples where residence time was indeed the better predictor for efficacy or *in vivo* pharmacological activity than affinity.

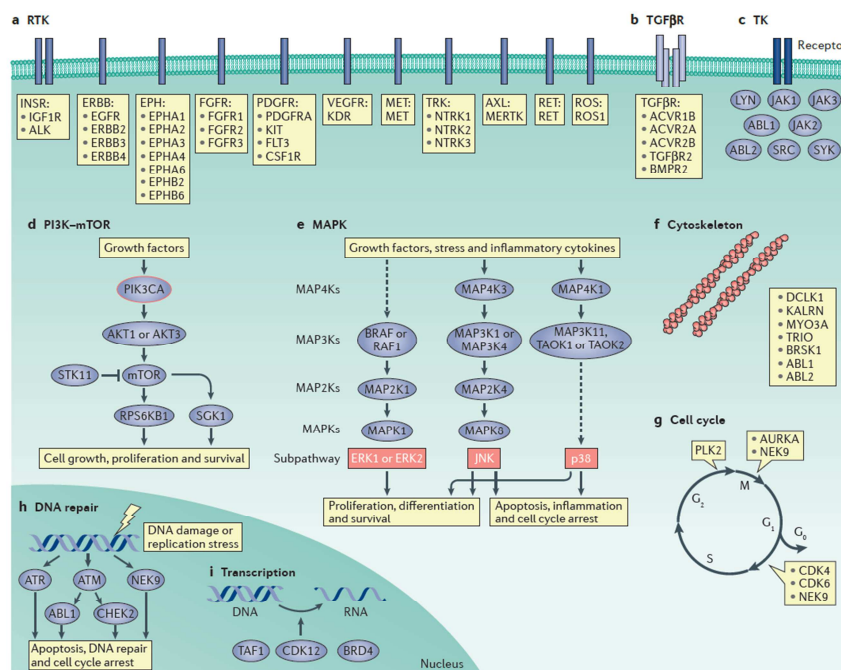
However, despite the increasing awareness, the importance of drug target binding kinetics for drug discovery is still intensely discussed: First open criticism arose in 2013, where Dahl and Akerud pointed out that only few studies consider the combined effect of pharmacokinetics and binding kinetics on the duration of drug action [29]. They propose that the drug's concentration profile, imposed by pharmacokinetics, dictate whether or not the dissociation rate constant can prolong the duration of effect *in vivo*, and suggest usage of the ratio between dissociation and elimination half-lives as predictor if the off-rate might affect the time course of the therapeutic effect [29]. In this respect it is worth mentioning, that recently (2016) Witte *et al.* presented an alternative, more complex, approach which additionally considers the impact of target concentration and rebinding due to on-rates on the duration of effect [39]. Dahl and Akerud further emphasized the relevance of target biology and the biochemical pathway affected by drug action: e.g. target occupancy level required to induce and sustain the desired effect, competition within endogenous ligands (natural substrates / signaling molecules) and target degradation. Nonetheless, they believe that binding kinetics is worth studying and should be considered in addition to rather than instead of equilibrium binding metrics, but call to avoid oversimplification of the highly complex, not yet fully understood topic [29]. Folmer recently (2017) published an article called "Drug target residence time: a misleading concept" [30]. He claims that most of the studies supporting the residence-time concept are based on "rather misleading simulations and arguments" and "examples [47] where compounds are taken out of the pharmacokinetics context" [30]. In other words, he would like to see more mathematical and experimental support for the claim that binding kinetics can lead to pharmacological effects that outlast systemic drug clearance, rather than mere comparisons between kinetic rate constants and affinity. Folmers e.g. reminds the community that target turnover (protein degradation and resynthesis), which typically ranges from a couple of hours to a day [48], can diminish the impact of slow off-rates and of stepwise increase of target occupancy by repeated dosing, so that slow on-rate compounds would have to be provided at high doses to achieve the desired target occupancy level. He highlights that both on-rates and off-rates are important, but concludes that "good-old potency is still one's best bet" [30].

In summary, the potential impact of the consideration of binding kinetics during lead identification and optimization is currently a topic of intense debate, albeit the drug discovery community seems to agree that under certain prerequisites on-rates and/or off-rates can have an impact on the drug's therapeutic effect.

2.3 Kinases and their inhibitors: Biological background and disease implications

Kinases belong to the most important targets of pharmaceutical interest [2]. The large kinase family (also known as human kinome) with >500 members of human protein kinases is involved in key cellular and extracellular pathways and processes [49], and their defective regulation causes a variety of diseases [50].

Endergonic cellular reactions of transport, biosynthesis or motion run at the expense of a universal energy currency, especially the energy rich adenosine-5'-triphosphate (ATP), which is in turn continuously re/generated by respiration (i.e. in particular by oxidative phosphorylation in mitochondria) [51]. Kinases are enzymes which catalyze phosphorylation of lipids, sugars, peptides and proteins by transfer of the gamma phosphate of ATP, and thereby regulate the activity (e.g. many kinases are expressed in the inactive form and can be activated by phosphorylation), binding behavior and/or reactivity of these molecules. Besides their contribution to metabolic pathways (e.g. phosphorylation of glucose during glycolysis), kinases play a pivotal role in many signal transduction pathways regulating inter alia apoptosis (programmed cell death), proliferation (cell growth and division), inflammation and migration (movement of cells) [52] (Figure 4). Thereby, some kinases are catalytic receptors (e.g. for growth factors), others are enzymes downstream of signaling pathways activated by receptors. Mutations, gene amplification, loss of negative regulators and/or



driver kinases to core cellular pathways and processes

- receptor tyrosine kinases (RTKs) to particular RTK families
- act as receptors for specific transforming growth factor- β (TGF β) superfamily members (TGF β Rs)
- Non-receptor tyrosine kinases (TKs): role downstream of particular types of cell surface receptor
- associated with PI3K-mTOR PW
- associated with MAPK PW
- regulate cytoskeletal organization
- Regulate cell cycle
- function in DNA repair responses
- function in gene transcription

Figure 4 [52]: Biological relevance of kinases in core signalling pathways

Kinases play a role in many cellular pathways and processes including e.g. cell cycle regulation (control of proper division of cell and decision about cell survival), migration, DNA repair and cell growth. Due to the high biological relevance, defective regulation of kinases is related to a variety of disorders, and in particular to cancer.

chromosomal rearrangements can lead to overexpression and/or aberrant activities of kinases and thereby step by step to the generation of abnormal cells with rapid, unregulated cell growth, i.e. to cancer [50, 53].

Cancer is the second leading cause of death globally (one in six deaths is caused by cancer) [54]. Cancer drivers are either up-regulated activities of proto-oncogenes (transforming them to oncogenes and leading to abnormal cell proliferation) or inhibition of tumor suppressors (i.e. inhibition of cell growth control). For instance the activity of the first identified cellular proto-oncogene kinase, namely SRC, is up-regulated in approximately 50% of tumors in colon, lung, breast, liver and pancreas [55]. Another example is the tumor suppressor PETN, a lipid phosphatase which is mutated in several common cancers. By dephosphorylating phosphatidylinositol 3,4,5-bisphosphate PETN counters the activity of the proto-oncogene kinases PI 3-kinase and downstream Akt, which in turn can promote survival [56]. Cancer is in the end caused by a combination of dysregulations of multiple oncogenes and tumor suppressors [56].

Kinase inhibitors are a fast growing class of cancer therapeutic agents and typically inhibit multiple targets [57]. Presently, all inhibitors in Phase III and FDA approved drugs together bind to less than 20% of the human kinome [58], whereby the majority of the main targets of FDA approved drugs are tyrosine kinases (Figure 5) [57].

Kinases can be categorized into groups according to their sequence homology in the catalytic domain

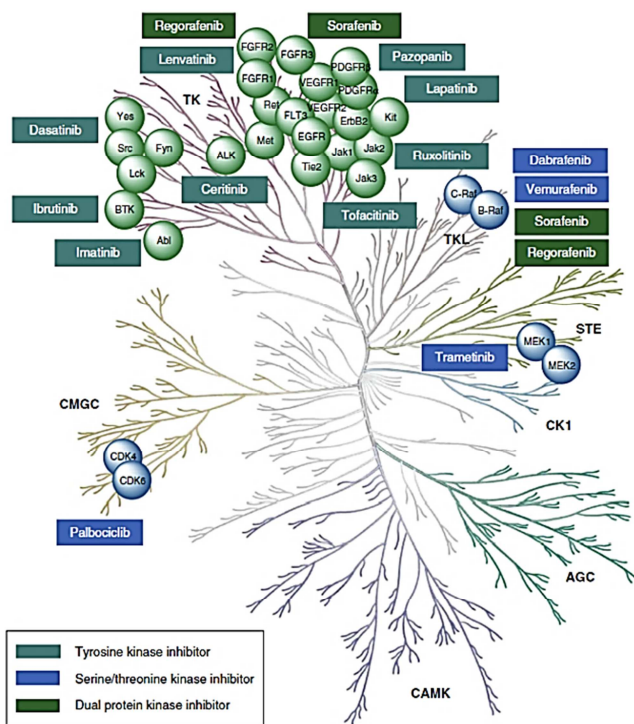


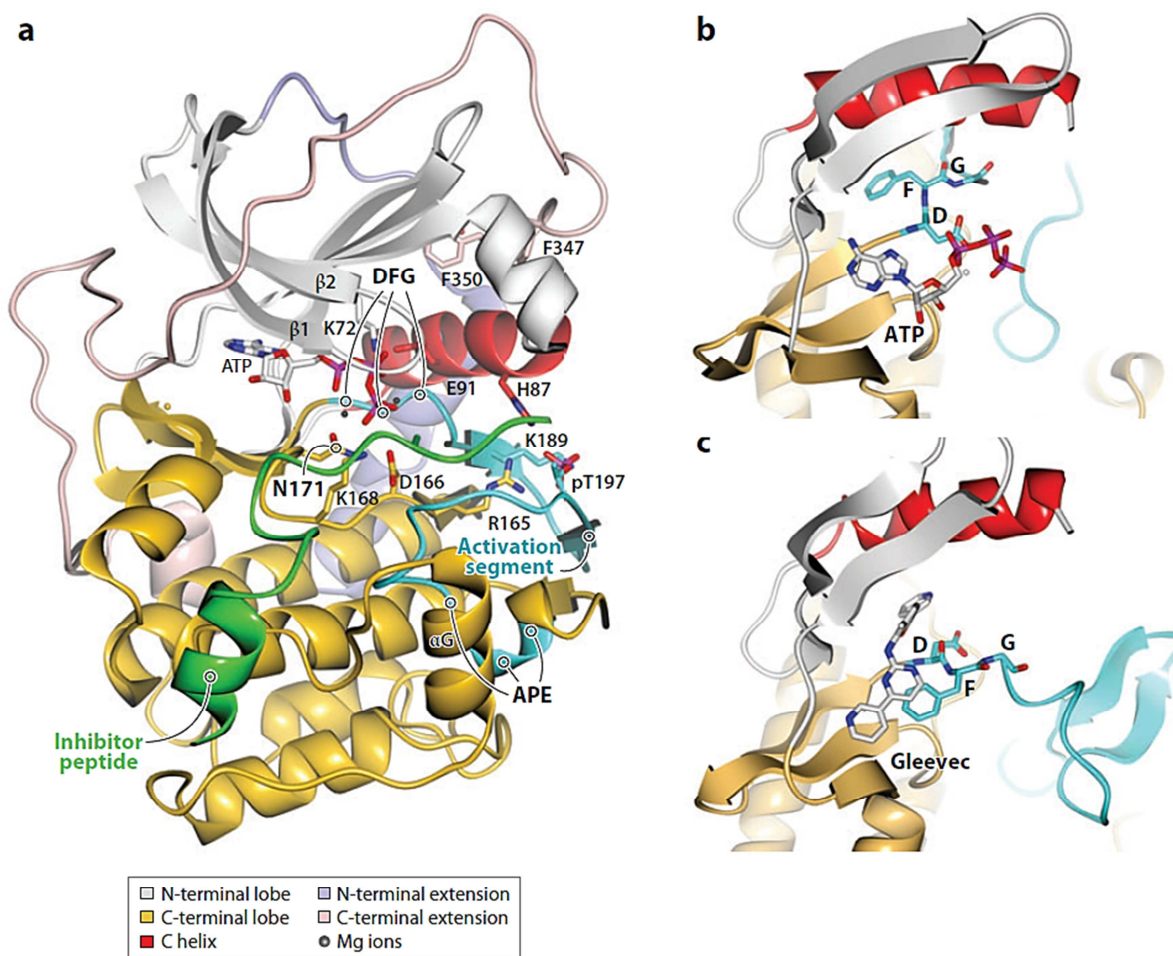
Figure 5 [57]: Phylogenetic trees of the human kinome with main targets of FDA approved small-molecule kinase inhibitors

(degree of relationship) with additional input from other sequence domains and the distinct functions of the kinases. For example tyrosine kinases are a kinase sub-family which exclusively phosphorylates tyrosine residues, while tyrosine kinase-like kinases are very similar to tyrosine kinases, but phosphorylate serine/threonine substrates. However, the kinase ATP site is highly structurally conserved [49], and very similar for active protein kinases and the phosphatidylinositol kinases (PI3Ks are lipid kinases) [50]. Therefore, targeting the highly conserved ATP binding site often results in promiscuous kinase inhibition (in particular for ATP mimics [50]). This may

lead to safety issues due to off-target-based toxicity (e.g. [59, 60]). Therefore, target selectivity is complementing efficacy as important optimization criterion in kinase inhibitor discovery [24, 61].

Although kinase dysregulation concerns a number of other non-life-threatening diseases, only very few kinase inhibitors are available for treating non-oncological indications, whereby one main obstacle are the lack of selective compounds and concerns that getting selective compounds is very difficult and would lead to failure due to side effects and safety issues [50, 62]. On the other hand, since pathologies usually involve many defective or deregulated proteins, reasonable unselectivity is argued to help rebalancing between the affected proteins [50, 61, 63]. Large-scale kinase inhibitor selectivity profiling studies (based on equilibrium metrics) revealed that drug discovery programs have generated fairly selective kinase inhibitors (albeit the molecular background explaining the selectivity have often been found in late stages of the development rather than being the result of design strategies) [62]. Knowledge about protein structures and the interaction of the kinase inhibitors with the kinase has an essential impact on the development of potent and selective kinase inhibitors.

In the catalytic domain of kinases, the ATP-binding site is located between two lobes, a C-terminal lobe and a smaller N-terminal lobe connected by the hinge region. The N-terminal lobe consists of the α C-helix and a β -sheet with several strands. The so called “gatekeeper” is a single amino acid in the hinge region that separates the binding site from an adjacent hydrophobic pocket [64]. The C-terminal lobe is mainly α -helical and includes the variable substrate binding region, the flexible activation loop with the conserved DFG motif (DFG aspartate binds Mg^{2+} and thereby contributes to correct orientation of ATP) and the catalytic loop with the conserved HRD motif (HRD aspartate is essential for activity; DFG and HRD are amino acid triads named according to the single letter amino acid code) [53, 62, 65]. Kinases in the active and inactive state possess different conformations (Figure 6): In the active state, the α C-helix is rotated towards the active site (α C-helix-in conformation) and the DFG aspartate points into the binding site (and chelates Mg^{2+}) accompanied by an open conformation of the activation loop (DFG-in conformation) [53], and the so-called hydrophobic spines are in place (hydrophobic interactions between residues in the C-lobe and N-lobe) [66]. Due to the need for distinct amino acids in the correct position for catalytic activity, the active conformation is rigid and highly conserved – a feature which hampers the development of selective compounds [62]. Inhibitors targeting the ATP-binding site in the active state are called Type I inhibitors. In the inactive conformation, the DFG phenylalanine points into the binding site (disrupting Mg^{2+} binding and the hydrophobic spines [66]), forming a catalytically inactive conformation (DFG-out conformation) and opening an additional pocket adjacent to the ATP binding site [67]. As the inactive state is structurally diverse and dynamic, it might be easier to achieve



DFG and APE: conserved amino acid sequences at start and end of activation segment

Figure 6 [53]: Schematic representation of structural features of active and inactive kinases

a, b) Protein kinase A (PKA) in active conformation with bound ATP and substrate (PDB ID: 1atp; panel **b**: zoom in for details of ATP binding site). The DFG aspartate (D) points into the binding site and the α C-helix is rotated towards the active site. **c)** ATP binding site of ABL in inactive conformation with bound inhibitor Gleevec (PDB ID: 1iep). DFG phenylalanine (F) points into the binding site.

selective compounds when targeting this newly formed pocket (type II inhibitors) [62]. For Type II inhibitor binding the DFG-out conformation is often accompanied by an outward-orientation of the α C-helix [67]. But there are also conformations somewhere in between the extremes, which are called DFG-out-like and α C-helix-out-like. In addition to type I and type II inhibitors, there are type III (allosteric) compounds binding outside the ATP binding site to the “back pocket” (introducing conformational changes forcing the α C-helix to the outward-orientation) and displacing ATP noncompetitively [67], and type IV inhibitors which bind distant from the ATP binding site and typically interfere with kinase regulators [62]. Apart from some exceptions (such as trametinib), most kinase inhibitors in Phase III and FDA approved drugs bind to the highly conserved ATP binding site [50]. Large-scale kinase inhibitor selectivity profiling studies revealed that also type I inhibitors can be highly selective and that there are some examples for type II inhibitors with promiscuous kinase

activity [68]. The precise molecular mechanisms contributing to selectivity are still discussed and not yet fully understood.

While there are several comprehensive studies assessing selectivity-based on equilibrium metrics (IC_{50} , K_D) [14, 15, 25], there are few studies investigating the effect of kinetic selectivity [69]. These studies are based on only a few target-compound pairs and usually do not evaluate binding kinetics in the context of pharmacokinetics. The kinetic-based studies propose relevance of slow off-rates for selectivity: For example the FDA approved slow-dissociating type I EGFR inhibitor lapatinib (EGFR: epidermal growth factor receptor) leads to prolonged down-regulation of EGFR activity in cells [70], and the FDA approved covalent type I BTK inhibitor ibrutinib [71] possess a quasi-infinite residence time and the target occupancy is only limited by target turnover.

Although there is no design strategy available allowing optimization for desired binding kinetics behavior rationally, the relevance of several structure-kinetic relationships is discussed: Major conformational changes as observed in type II inhibitors (DFG motif is displaced in the DFG-out conformation) [32, 33, 72, 73] or induced by some type I inhibitors (e.g. the above mentioned lapatinib causes a α C-helix displacement [70]) as well as minor conformational adaption of the DFG-loop [74] are thought to contribute to long residence times. But not all DFG-out binders possess long residence times implying that the DFG-out conformation *per se* is insufficient to explain how slow off-rates occur. The additional relevance of further factors such as hydrophobic interactions with the hinge region and especially the front pocket are proposed to block kinase motion (stabilize the destructed hydrophobic spine in the kinase) and increase residence time [75]. Recently, the interaction of halogens in drugs with aromatic residues in the target was suggested to lead to slow off-rates [76]. Furthermore, the replacement of water molecules unfavorably placed in hydrophobic regions of the binding pocket by the ligand is thought to be a rate determining step for association and dissociation [77]. In addition, target residence time is prolonged for reversible covalent inhibitors binding transiently covalent to cysteine residues of the target [78]. Finally, there are hints that physicochemical properties, in particular molecular weight and to a lesser extent lipophilicity and flexibility of compounds, influence dissociation rates [79]. A major challenge is to discriminate between structure-activity and structure-kinetic relationships.

To sum up, kinase inhibitors are a rapidly growing drug class [57] and selectivity is an important selection criteria during their development [80]. Binding kinetic rate constants are proposed to contribute to efficacy and a favorable selectivity profile [31, 69], but comprehensive studies are missing.

3 Aim of the thesis

To date, efforts to understand the role of binding kinetics in drug discovery have mainly been focused on a few targets and a few compounds and/or publication-biased drug-target interaction datasets (high affinity interactions and slow off-rates are more frequently published as compared to low affinities and fast off-rates). Several of these studies propose that the duration and extent of drug action are determined by binding kinetics, and that kinetic selectivity can mitigate off-target-based toxicity leading to improved safety [36, 39, 81]. On the other hand, critics of the drug-target residence-time concept point out that its usefulness is limited due to e.g. the high impact of low drug clearance (the drug's slow elimination from the body) on the duration of effect *in vivo* [29]. Despite the increasing awareness of the potential impact of binding kinetics, it is yet unclear how this information could be used to prioritize and optimize drug candidates during lead optimization, or whether and when binding kinetics could be integrated into the drug discovery process. So far, there is too little known about what structural features influence binding kinetics at the molecular level to enable prospective design of binding kinetic rate constants.

A good way for the discovery of new drugs is to analyze approved drugs and to understand their efficacy and safety profiles [82]. In that respect, the systematic analysis of the on-rates and off-rates of drugs and drug candidates from preclinical and clinical phases might provide new insights into the subject of binding kinetics. **The aim of this thesis** was to assess the role of binding kinetics for drug discovery in an unprecedented comprehensive fashion by analyzing an exemplary protein family and the drugs targeting it: Protein kinases and their inhibitors.

Objective 1:

Assessment of precision and accuracy of binding kinetic parameters determined with 'kinetic probe competition assays' and the 'kinetics of competitive binding equation'

The 'kinetics of competitive binding equation' [83] is frequently used for model fitting to data from 'kinetic probe competition assays' and accordingly for the calculation of binding kinetic rate constants. Due to the increasing interest in binding kinetics, this equation was particularly applied in recent years, albeit it was already introduced in 1984. The first objective of this thesis was to assess the precision and accuracy of the determined binding parameters within the parameter space by Monte Carlo analyses. The question is whether and to what extent particular model equation parameters influence the reproducibility and reliability of the results, and if the determined on-rates are accurate in cases where determination of affinity and off-rates was not possible (as presumed by Schiele, Ayaz and Fernández-Montalván [84]). The gained understanding of the limitations of the method should be applied to extract guidelines for 'kinetic probe competition' experiments.

Objective 2:

Establishment of assays for large-scale analysis of kinase inhibitors' target binding kinetics

Due to the central role of kinases in cellular signaling, kinase inhibitors belong to the most important and fastest growing classes of therapeutic agents [2, 49], but surprisingly little is known about the binding kinetics of these drugs. A TR-FRET-based kinetic probe competition assay (kPCA) was recently invented by Schiele, Ayaz and Fernández-Montalván to enable high-throughput determination of binding kinetic parameters [84]. The second objective of this thesis was to develop a kPCA-based profiling panel for a set of protein kinases, and to analyze the binding kinetics of 270 small molecules including most FDA approved and clinically relevant kinase inhibitors. Thereby, the applicability of kPCA for large-scale profiling should be validated, and the newly generated data were supposed to be used for addressing objectives 3-4 and to answer to following question: How is the distribution of on- and off-rates and is a long residence time a typical feature of clinically successful kinase inhibitors?

Objective 3:

Investigation of the influence of structural features on kinase inhibitors' target binding kinetics

Knowledge about structure-kinetic relationships is a prerequisite for the prospective design of binding kinetic rate constants. The third objective of this thesis was to investigate the effect of molecular features on binding kinetic parameters, by using the results from the large-scale profiling approach (objective 2). The large dataset should hypothetically foster the discrimination of effects on affinities and binding kinetic parameters. Consideration of known chemical properties and functionalities of both the compounds and the targets might provide new insights into structure-kinetic relationships. Also the analysis of available crystal structures can provide further information on the structural elements and binding modes leading to certain kinetic behaviors.

Objective 4:

Evaluation of the impact of kinase inhibitors' target binding kinetics on target occupancy profiles

Typically, kinase inhibitors bind to the highly conserved kinase ATP site, a motif present in all members of the human kinome [49]. This feature can result in promiscuous kinase inhibition, which may lead to safety issues due to off-target-based toxicity. Thus, assessment of target selectivity has become an important optimization criterion in the development of kinase inhibitors [61], but the impact and occurrence of kinetic selectivity has not yet been explored in detail. Target occupancy is essential for the (adverse) pharmacological effect on primary targets and off-targets [5]. A fourth objective of this thesis was to evaluate whether target occupancy and selectivity can be differently assessed from the affinity and binding kinetics perspectives, by using the results from the large-scale profiling approach (objective 2). It was planned to evaluate the impact of kinase inhibitors' target binding kinetics on target occupancy in cells and to address the question whether binding kinetics can alter the pharmacological effect in relation to the concentration-affinity effect *per se*.

4 Material and methods

4.1 Material

The material used in this work is listed in this chapter.

4.1.1 Equipment, accessories and consumables

equipment, accessories, consumable.....	manufacturer
HERAstar (FS) plate reader	BMG LABTECH
Hummingbird XL 384 Cartesian Dispensing Systems.....	Cartesian Technologies/DIGILAB
Precision Microplate Pipetting System.....	BioTek
Multidrop Combi Reagent Dispenser	Thermo Fischer Scientific
Biacore 4000 system.....	GE Healthcare
Series S Sensor Chip SA (streptavidin-coated, storage at 4°C).....	GE Healthcare
Milli-Q Integral Water Purification System.....	Millipore
Quick Combi-Sealer.....	HJ-Bioanalytik
Pipettes (single-channel; different sizes).....	Eppendorf
Pipettes Matrix Impact Equalizer (multi-channel; different sizes)...	Thermo Fischer Scientific
Pipetboy Acu.....	Integra Biosciences
Safe-Lock Tubes (different sizes).....	Eppendorf
Conical Tubes (different sizes).....	Corning
black 384 Well Small Volume™ HiBase Microplates	Greiner Bio-One
REMP Storage 384 Microplates.....	Brooks Automation
Microplate, 96 well, PP, U-bottom, natural.....	Greiner Bio-One
384-Well x 252 uL Assay Collection And Storage Microplate.....	NUNC
Reagent Plate and Foil.....	GE Healthcare
Plastic Vials and Caps (different sizes).....	GE Healthcare
White, nonbinding surface 96-well plates.....	Corning
Storage Bottles (different sizes).....	Corning and Schott
Reservoir, polystyrene: 10 mL and Transtar 96 Disposable 12-channel	Corning
Aluminum foil (adhesive) #538619.....	Beckman Coulter
Polypropylene foil (adhesive), # BR-1005-78.....	GE Healthcare
Polypropylene foil (adhesive).....	HJ-Bioanalytik
Microplate Foil, 96-well and 384-well.....	GE Healthcare
Costar disposable serological pipettes (different sizes).....	Corning
epT.I.P.S. reloads (different sizes).....	Eppendorf
Thermo Scientific Matrix Pipette Tips (different sizes).....	Thermo Fischer Scientific
Millipore Stericup filtration system, 0.22 µm.....	Sigma Aldrich
GloMax® Discover Instrument.....	Promega
pH meter 765 Calimatic & pH sensor SE101N.....	KNICK
Analytical balance - Analytic AC 120S.....	Sartorius
Vortex-Genie 2.....	Scientific Industries
Balance PM3000.....	METTLER TOLEDO
Centrifuge VWR Galaxy mini.....	Merck
Centrifuge 5810R.....	Eppendorf
Fridges (-4°C, -20°C, -80°C), ice machines and -20°C room.....	Different manufacturers

4.1.2 Chemicals, buffers, compounds, recombinant proteins and cells

chemicals, buffers, compounds, proteins, cells	manufacturer.....	storage temperature
Dimethyl sulfoxide (DMSO), # D2650.....	Sigma Aldrich.....	room temperature
1M Tris-HCl, pH 7.5, # T2319-1L.....	Sigma Aldrich.....	room temperature
1M Tris-HCl, pH 8, # T3038-1L.....	Sigma Aldrich.....	room temperature
5M sodium chloride (NaCl) solution, # S6546-1L	Sigma Aldrich.....	4°C
Tween 20, # P7949.....	Sigma Aldrich.....	room temperature
Bovines Serum Albumin (BSA), # A-7906.....	Sigma Aldrich.....	Powder: 4°C; solution: -20°C & 4°C ⁽¹⁾
Dithiothreitol (DTT), # D9779-50G.....	Sigma Aldrich.....	solid: 4°C; solution: -20°C ⁽²⁾
Nonident P-40 solution 10%, # A2239,0100.....	AppliChem.....	4°C
Magnesium chloride (MgCl ₂) solution, # M-1028....	Sigma Aldrich.....	room temperature
Sodium orthovanadate (Na ₃ VO ₄), # 22.059-0.....	Sigma Aldrich.....	solution: -20°C
Streptavidin - Tb (Terbium; St-Tb), #610SATLB.....	Cisbio Bioassays.....	lyophilisate: 4°C; solution: -20°C ⁽²⁾
Kinase Tracers 178, 199, 222, 236, 314 and 1710....	Thermo Fisher Scientific	stock and aliquots at -20°C
1M NaOH solution, # S2567.....	Sigma Aldrich.....	4°C & short term room temperature
NanoBRET Target Engagement Assay, # N2080.....	Promega.....	-20°C
DMEM (Dulbecco's Modified Eagle Medium), # 11995-065	Thermo Fisher Scientific	4°C
Fetal bovine serum, # SH30070.03.....	HyClone.....	-20°C
Kinase Tracer-05.....	Promega.....	-20
Opti-MEM I Reduced Serum Medium, no phenol red, # 11058-021.....	Life Technologies....	4°C
Cells expressing kinase fused to NanoLuc [®] luciferase..	Promega.....	cultured at 37°C
Trypsin/EDTA, # 25300.....	Thermo Fisher Scientific	-20°C
HBS-P+ buffer 10x, # 28-9950-84.....	GE Healthcare.....	room temperature
Normalizing Solution (Amine Coupling Kit), # BR-1000-50	GE Healthcare.....	4°C
Desorb Solution I + II (Desorp Kit), # BR-1008-23....	GE Healthcare.....	room temperature
50 M NaOH, # BR-1003-58.....	GE Healthcare.....	4°C
Biotin, # B4501.....	Sigma Aldrich.....	4°C
ATP disodium hydrate, # 34369-07-8.....	Sigma Aldrich.....	-20°C
Hepes, pH 7.4, # L1613.....	BIOCHROM AG.....	room temperature
Surfactant P20, # BR-1000-54.....	GE Healthcare.....	4°C
Biotinylated kinases ⁽³⁾⁽⁴⁾	Carna Biosciences ⁽⁵⁾ ...	stock and aliquots at -80°C ⁽⁶⁾
Kinase Inhibitors ⁽³⁾	Selleck Chemicals....	solution: -20°C

⁽¹⁾ initially -20°C, but upon thawing at 4°C

⁽²⁾ storage of aliquots (solution) at -20°C → use aliquots only once

⁽³⁾ detailed information about the kinases and inhibitors is provided in Table 4 and Table 5 (appendix A)

⁽⁴⁾ do not vortex proteins with >3000 rpm

⁽⁵⁾ exceptions: His-tagged, biotinylated CDK2 and CDK9 were synthesized inhouse

⁽⁶⁾ avoid repeated thawing and freezing

His-tagged, biotinylated CDK2 and CDK9 were synthesized inhouse according to previously described protocols [74, 84] and kindly provided by Pelin Ayaz, Uwe Eberspächer and Elisa Chemik. In brief, human full-length CDK9 (N-terminal AviTagTM fusion protein) and cyclin T1 (N-terminal His₆ fusion protein) were coexpressed in Hi5 insect cells along with BirA for *in vivo* biotinylation as indicated by the manufacturer (Avidity). Human full-length CDK2 (N-terminal His₆ and AviTagTM Fusion protein)

was coexpressed in BL21(DE3) competent *E. coli* cells along with BirA. Both CDK9/cyclin T1 complexes and CDK2 were purified by immobilized metal ion affinity chromatography (HisTrap HP, GE-Healthcare).

4.1.3 Software and databases

The following databases were used in this study:

- 1st OncologyTM database: for information about clinical phases of kinase inhibitors;
- IntegritySM database: for kinase inhibitors plasma half-lives and maximum plasma concentrations in healthy human adults;
- KLIFS – a structural kinase-ligand interaction database [85, 86]: for compound's binding mode information (including DFG- and α C-helix conformations) and kinase-ligand interaction fingerprints;
- Protein Data Bank (PDB): for protein crystal structures complexed to inhibitors

The following software was used in this study:

- Kinome Render [87] and KinMap [88]: for depicting kinases used in this thesis and their binding parameters within a phylogenetic tree of the human kinome, which was reproduced courtesy of Cell Signaling Technology, Inc. (www.cellsignal.com). The distance between two kinases in the phylogenetic tree is a measure for their degree of relationship based on sequence homology of the catalytic domain.
- The PyMOL Molecular Graphics System (Version 1.3): for superimposition of kinase-inhibitor cocrystal structures
- Discovery Studio Visualizer (v17.1.0.16143): for generation of ligand interaction diagrams
- Reader Control Software and MARS Data Analysis Software: for protocol and script writing to run the plate reader and for calculation of TR-FRET ratios
- Genedata Screener: for analyzing equilibrium probe competition assays and calculating IC₅₀ values
- Biacore 4000 Evaluation Software: for evaluation of surface plasmon resonance experiments
- GraphPad Prism 6.00, 6.07 and 7.00 for Windows (GraphPad Software, La Jolla California USA, www.graphpad.com): for linear and nonlinear regression, Monte Carlo analyses, statistical tests and visualization (e.g. scatterplots, histograms)
- TIBCO Spotfire (V.6.5.2): for data mining and visualization of results (e.g. scatterplots, bar charts)
- Microsoft Excel 2010: for raw data handling (using macros for repeating tasks in excel), analysis (e.g. Gini score calculation) and visualization (e.g. line charts, bar charts)
- Python 3 (available at <http://www.python.org>) [89]: for creating clustered distance matrices and their correlation
- Clustal Omega [90]: for multiple sequence alignment of kinase constructs
- Pipeline Pilot (Version 16.5.0.143): for generating compound structure similarity matrix and for multivariable linear regression based on a genetic function approximation algorithm
- Copasi 4.1.9.: for simulation of the dynamics of biochemical reactions and events [91]
- Phoenix version 6.4: for estimation of two-compartment model parameters on the basis of concentration-time profiles

4.2 Experimental Techniques

The assay formats and readout technologies utilized for the determination of binding kinetic parameters are presented in this chapter.

4.2.1 Probe competition assays (PCA) for large scale profiling

Overview and readout principle of large-scale binding kinetics profiling with kinetic Probe Competition Assays based on TR-FRET (time resolved-fluorescence resonance energy transfer) technology

Recently, the kinetic Probe Competition Assay (kPCA) has been reported as possible solution for high-throughput binding kinetics profiling [84]. Large-scale profiling of binding kinetic parameters based on this assay can be performed according to a standard workflow (Figure 7). Both assay development and compound screening (comprising test plate generation and readout) can be performed with the standard instrumentation of a screening laboratory, enabling measurement of 100s of compounds per day. Detailed information about the single steps is provided in the chapters below. Assay development comprises optimization of assay components and kinetic characterization of the probe (compound labeled with a fluorophore). kPCA allows determination of binding kinetic rate constants

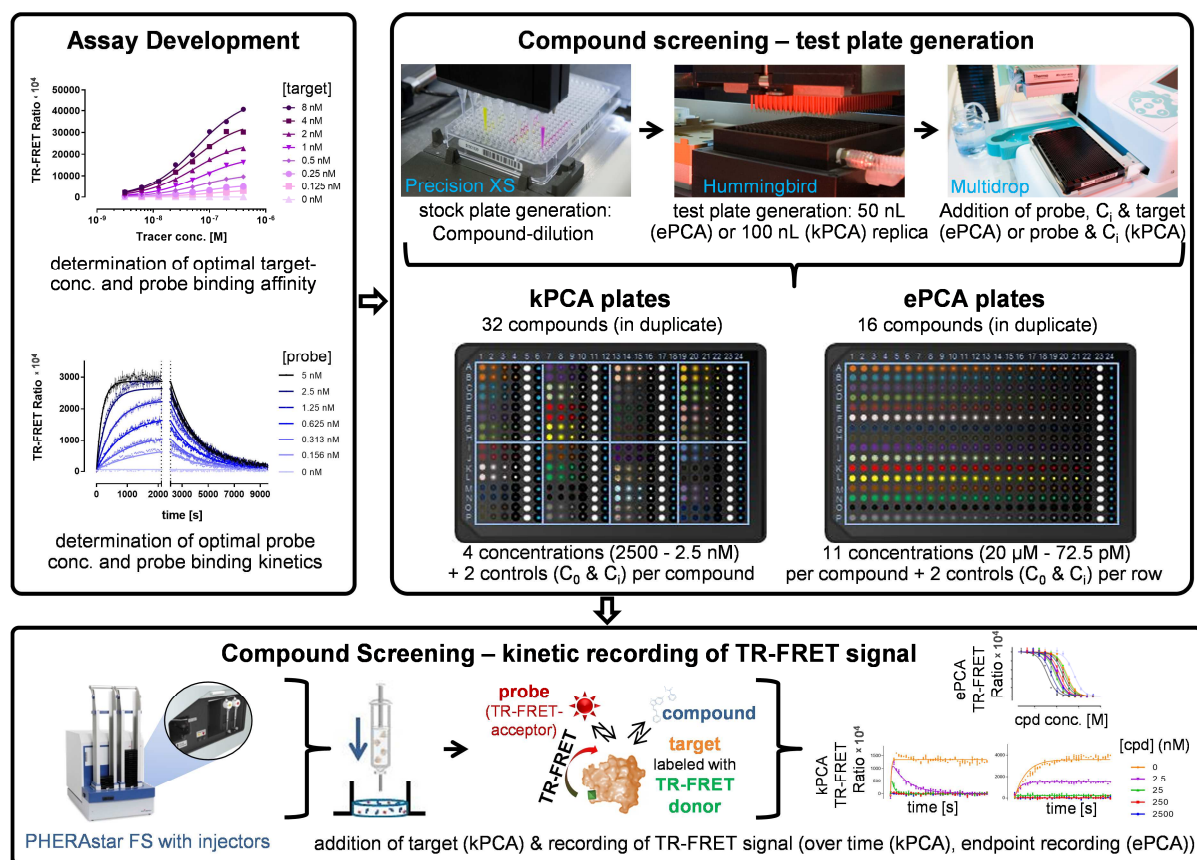


Figure 7: Workflow of binding kinetic profiling based on kinetic Probe Competition Assay (kPCA)

Assay development and compound screening (comprising test plate generation and readout) can be performed with the standard instrumentation of a screening laboratory. Binding kinetic rate constants and affinities are determined by kPCA, affinities are additionally determined by using equilibrium Probe Competition Assays (ePCA).

and affinities of compounds. Parallel performance of an equilibrium Probe Competition Assay (ePCA) for determination of affinities in equilibrium is used for cross validation.

The assay development assays, kPCA and ePCA rely on the TR-FRET (time resolved-fluorescence resonance energy transfer) readout technology. FRET is the non-radiative energy transfer from an excited donor fluorophore (that has absorbed light) to an acceptor fluorophore. This process will only occur if the acceptor molecule is in close proximity to the donor molecule (9 nm or less), i.e. if a probe labeled with a FRET acceptor molecule and the protein is labeled with a FRET donor molecule, the energy transfer will only occur if the probe is bound to the protein. Characteristic fluorescence emission from donors and acceptors are measured with a fluorescence reader, allowing direct discrimination between bound and unbound probe (without the need for separation by filtration). This feature makes kPCA a mix-and-read assay, where the binding signals can be directly measured after mixing of all assay components (homogenous assay), enabling miniaturization and immediate monitoring of the signal with high kinetic resolution. TR-FRET is the combination of FRET with time-resolved fluorometry: e.g. Lanthanide (such as Europium or Terbium) complexes are long-lived emitting fluorophores (milliseconds instead of nanoseconds) and can be used as FRET donors enabling a time delay (typically 50-150 μ s) between excitation of the donor and reading of the donor and acceptor fluorescence emission. The advantage of measuring with a time delay is that short-lived non-binding-specific background fluorescence (caused by other assay components) is reduced or even eliminated, which increases sensitivity. [92] Labeling of the kinases with lanthanide was performed by using biotinylated kinases and streptavidin-terbium conjugates. The interaction between streptavidin and biotin is the strongest non-covalent binding known (with a dissociation constant of 10^{-15} M) [93].

Procedure

In general, TR-FRET assays were conducted at room temperature in black 384 Well Small Volume™ HiBase Microplates using a buffer (50 mM Tris HCl, pH 7.5) containing 150 mM NaCl, 0.01% Tween20, 0.01% BSA and 2 mM DTT (exception: CDK9 buffer (50 mM Tris HCl, pH 8) with 10 mM $MgCl_2$, 0.1 mM Na_3VO_4 , 0.01% Nonident P-40, 1 mM DTT). Biotinylated kinases were incubated with 0.5 nM St-Tb (Streptavidin-Terbium) for labeling with the long-life fluorescent cryptate TR-FRET donor. Kinase Tracers (multikinase inhibitor - Alexa Fluor® conjugates) [94] served as fluorescent probe (TR-FRET acceptors). For all experiments, a nonspecific binding control (C_i) was performed in the presence of tracer and 0.5 nM St-Tb, but in the absence of protein (= background signal). Fluorescence signals were detected in a PHERAstar (FS) plate reader by excitation of the donor with 5 laser flashes at 337 nm, followed by a time delay of 100 μ s and readout of acceptor and donor emission for 400 μ s at 665 and 620 nm respectively. HTRF signal (homogenous time-resolved fluorescence signal; in the following often referred to as “probe binding signal”) was calculated from TR-FRET Ratio values as defined in the MARS data analysis software (Equation 1).

$$\text{HTRF signal} = \text{TR-FRET Ratio} \times 10\,000 = [\text{acceptor counts} / \text{donor counts}] \times 10\,000$$

Equation 1

4.2.1.1 *Development of Probe Competition Assays*

Principle

The endpoint and kinetic experiments performed for assay development are based on direct binding assays: The binding of the TR-FRET-acceptor-labeled tracer to the terbium-labeled kinase can be directly monitored. Tracer-target binding signal increases until it plateaus at equilibrium. For reasons of throughput, assay development for the respective kinase assay comprised only choosing a Kinase Tracer and optimization of the Kinase Tracer and kinase concentrations, but not optimization of the assay buffer (usage of a universal buffer for all kinases). Thereby, also the affinity and the binding kinetics of the Kinase Tracer were determined. The kinase concentration should be as low as possible (at the same time sufficiently high to reach a reasonable high signal-to-background ratio), since the lowest IC_{50} value determinable in the screening assay equals half the applied kinase concentration. Lower IC_{50} cannot be determined accurately, the determined value would always equal half the applied kinase concentration. This limitation is called assay wall [95]. The negative phenomenon of ligand depletion is reduced by lower kinase concentrations (ligands: tracer, compound): The analysis techniques applied for evaluation of both ePCA and kPCA (chapters 4.3.1.2 and 4.3.1.3) assume that the free concentration of ligand is more or less unchanged. If more than 10% of the ligands bind to the receptor it is possible to get problems due to ligand depletion (rule of thumb) [96]. In the kinetic assay setup ligand depletion can result in mass transfer limitations (due to diffusion: binding of the compound to the protein is faster than the transfer of the compound to the proximity of the protein) and inaccurately determined on-rates. When applying a compound with a certain affinity in a certain concentration the fraction of bound ligands is lower for lower kinase concentrations. Moreover lower kinase concentrations are also less expensive. Choosing tracers concentrations is a balance act between performance and costs: The concentration should be high enough to 1) avoid ligand depletion (e.g. $>10\times$ kinase concentration) and 2) reach equilibrium for kinase-tracer binding in absence of compound within the time course of the kPCA experiment (typically 400 sec), preferably within seconds. It should be mentioned that in the equilibrium assay (ePCA) with defined compound concentrations, higher tracer concentrations lead to an offset of the determinable dissociation constants to lower values (refer to Cheng-Prusoff relationship in chapter 4.3.1.2). Due to cost considerations, the tracer concentrations should not be too high. If more than one tracer is available, the tracer which is faster reaching equilibrium (fast on-rate and off-rate) at equal concentrations was preferred, whereby also the affinity should also be reasonable high to allow acceptable maximum signal (TR-FRET Ratio > 1000) and lower kinase concentrations.

Procedure

Experiment I: For assessment of the affinity of the fluorescent probe and for determination of the optimal amount of protein for the following TR-FRET experiments, an 8-point 2-fold serial dilution of the respective Kinase Tracer (volume: 2.5 μ L; final concentrations in assay: 3.125-400 nM) was

incubated for at least 30 min with increasing kinase concentrations (volume: 2.5 μ L; 7-point 2-fold serial dilution; final concentrations in assay: 0.125-8 nM). The minimal amount of protein for which the signal to background ratio is around 2.5-3.5 was selected for the following TR-FRET experiments, in order to obtain a sufficiently high signal at lowest possible target protein concentration (refer to assay wall / ligand depletion explained above). If there was no known tracer for a kinase, this experiment I was performed for Kinase Tracers 178, 199, 222, 236, 314 and 1710, respectively. Affinities were determined as described in chapter 4.3.1.1.

Experiment II: For measurement of the kinetic rate constants of probe binding and for determination of the optimal assay parameters with regard to probe concentration, kinetic time intervals and duration of observation, 5 μ L of target kinase (kinases concentrations as specified in Table 6 in appendix B) were added to an 8-point 2-fold serial dilution of tracer (volume: 5 μ L; concentrations depended on determined affinity; two or more replicates) with the reagent injectors of the plate reader followed by immediate time-resolved TR-FRET signal increase recording (refer to Table 8 in appendix E for information about applied tracer concentrations, time intervals and duration of observation). Prior to and after usage, the injectors were washed with 1 M NaOH and ddH₂O. Kinetic rate constants were determined as described in chapter 4.3.1.1.

4.2.1.2 Equilibrium Probe Competition Assay (ePCA)

Principle

ePCA is an indirect binding assay: The equilibrium dissociation constants of the compounds (the kinase inhibitors) are determined indirectly by measuring the competition binding of unlabeled compounds and labeled probes in a saturation binding experiment. The advantage of the indirect assay format is that many compounds can be analyzed with the same assay protocol, and compounds do not have to be labeled (steric hindrance caused by a bulky fluorescence label most probably influences binding properties) and targets do not have to be immobilized, allowing a higher throughput as direct binding assays [92]. The standard ePCA plate layout (as depicted in Figure 7) allows analysis of 16 compounds in duplicate per 384-well plate.

Procedure

For analysis of steady-state affinities of the kinase inhibitors, two independent experiments were performed with two duplicates each: The BioTek™ Precision™ Microplate Pipetting System and REMP Storage 384 Microplates were used for 11-point 3.5-fold serial dilutions of 100x concentrated compounds in DMSO (final concentration in assay: 72.5 pM - 20 μ M) and for application of DMSO into control wells (0% (C_i) and 100% (C₀) probe binding). 50 nL of these stock solutions (in stock plates) were transferred into the assay plates (black 384 Well Small Volume HiBase Microplates) with Digilab's Hummingbird Benchtop System. The stock plates were sealed with adhesive aluminum foil

by using the Quick Combi-Sealer and stored at -20°C . The assay plates were either sealed with adhesive polypropylene foil and stored at -20°C or immediately used to run the ePCA: $3\ \mu\text{L}$ of fluorescent probe and $2\ \mu\text{L}$ of target kinase (refer to Table 6 in appendix B for kinase specific assay parameters such as probe and target concentration) were added using a Multidrop™ Combi Reagent Dispenser (Thermo Fisher Scientific) to start the competitive target kinase binding process of compound and tracer. The system was incubated for more than 1 h. Subsequently the TR-FRET signals were measured. The signal for 100% probe binding was detected in the absence of inhibitor, while the signal for 0% probe binding was detected in the nonspecific binding control. TR-FRET traces were normalized and affinities were determined as described in chapter 4.3.1.2. Assay plates with many compounds with a low affinity were retested with a 1:10 dilution of the stock plates (final concentration in assay: $7.25\ \text{pM} - 2\ \mu\text{M}$).

4.2.1.3 Kinetic Probe Competition Assay (kPCA)

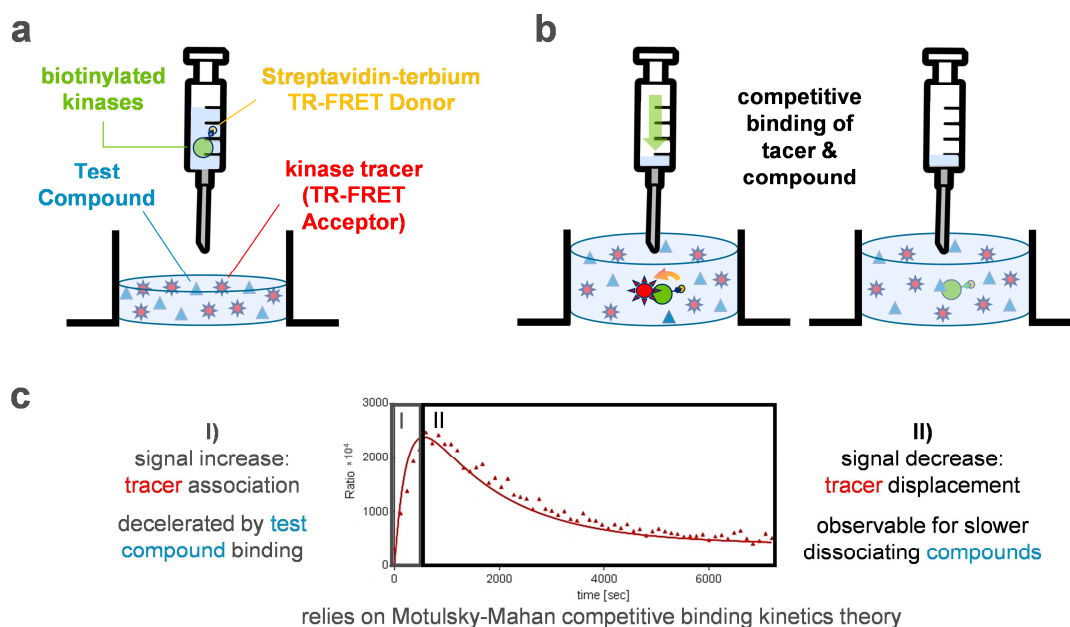


Figure 8: Principle of the kinetic Probe Competition Assay (kPCA)

a) The homogenous assay is based on the TR-FRET technology (time resolved-fluorescence resonance energy transfer). Biotinylated kinases are labeled with Streptavidin-Terbium, a long-life fluorescent cryptate TR-FRET donor. The assay 1) can discriminate between bound and unbound tracer molecules as FRET only occurs when the FRET-acceptor labeled tracer is in close proximity to the FRET-donor labeled protein, and 2) reduces background fluorescence by measuring with a time the delay ($50\text{-}150\ \mu\text{s}$) between excitation and reading.

b) The target protein is added with the injection device of the plate reader starting the competitive binding of compound and tracer to the target protein and allowing immediate signal recording after sample mixing.

c) Upon mixing of all assay components, the signal increases with tracer binding to the protein which is decelerated by simultaneous competitive binding of the test compound. If the test compound dissociates more slowly from the protein as the tracer, the signal will overshoot (compared to steady-state) and then decrease until equilibrium is reached. The signal traces are dependent on the compound and tracer binding kinetics and concentrations. The kinetic rate constants of the compound can be calculated by fitting of the Motulsky-Mahan equation [83] to the signal traces and fixing the tracer binding kinetics to previously determined values (refer to chapter 4.3.1.3).

Principle

kPCA is an indirect binding assay (providing the same advantages as described for ePCA): This homogenous assay measures by TR-FRET the simultaneous binding of unlabeled compounds and fluorescence labeled tracer (of known binding kinetics) to fluorescence-labeled targets over time [84]. The TR-FRET readout allows immediate monitoring of the signal with a high kinetic resolution. A major advantage of the kPCA is that there is virtually no delay (only a few seconds) between mixing of all assay components and reading, since the injection system of the plate reader is used to add target as final assay component (Figure 8). The standard kPCA plate layout (as depicted in Figure 7) allows analysis of 32 compounds in duplicate per 384-well plate.

Procedure

For analysis of kinetic rate constants of inhibitor binding to the respective kinase, two independent experiments were performed in duplicate using the same high throughput compatible automated machines as described for ePCA: 4-point 10-fold serial dilutions of 100x concentrated compounds were prepared in DMSO (final concentrations in assay: 2.5-2500 nM), and DMSO was applied into control wells (0% and 100% probe binding = C_i and C_0). 100 nL of these stock solutions and 5 μ L of fluorescent probe were pre-dispensed into the assay plates. To start the competitive target kinase binding process of tracer and compound, 5 μ L of target kinase were added with the reagent injectors of the plate reader followed by immediate time-resolved TR-FRET signal increase recording (refer to Table 6 in appendix B for kinase specific assay parameters such as probe and target concentration, measurement interval and observation time). The script mode of the plate reader was used to load (with St-Tb labeled kinase) and measure octants of the plate subsequently (as described in [84]), enabling a higher frequency of measurement (required since the reader loads and reads each well separately). Prior to and after usage, the injectors were washed with 1 M NaOH and ddH₂O. Binding kinetic and affinity parameters were determined as described in chapter 4.3.1.3.

4.2.2 Surface plasmon resonance (SPR) biosensor-based assay

Principle

SPR biosensors were used to detect the binding of compounds to proteins immobilized on a sensitive surface (glass coated with a thin metal film, typically gold) by surface plasmon resonance: During total internal reflection in glass, the electromagnetic field component of the light extends into and along the metal film at the opposite side of the sensor surface (where the protein is immobilized), and can excite delocalized electrons on the metal film by resonance energy transfer, creating surface plasmons (evanescent wave decreasing exponentially). The intensity of the reflected light is reduced at the specific angle of incidence if this resonance energy transfer on the metal film occurs. The local reflective index is changed by compound binding to the immobilized protein on the sensor surface.

The change in the refractive index, changes the surface plasmon resonance angle. SPR can be used to measure the mass concentration on the surface, as the change in the resonance angle is proportional to the bound mass on the surface. [92, 97] Since the binding event causes a physico-optical change, labeling is not required for detection but protein immobilization and special instrumentation. This method is highly sensitive and allows signal detection with a high frequency (10 Hz). The microfluidic sample delivery system is used in the immobilization step to provide reagents required for protein immobilization/capturing, in the association step to inject the compounds in a continuous flow, and in the dissociation step to separate bound from free compounds, limiting rebinding. Disadvantages are that immobilization can affect protein activity, that the changes in the refractive index of the surrounding medium (e.g. caused by differences in the concentration of DMSO, a standard solvent, in the running and the sample buffer) lead to background signal changes, and that mass transfer can contribute to determined binding kinetic data (especially at high levels of immobilized proteins). If the binding of the compound to the sensor surface (depending on association rate, concentration of immobilized target and concentration of compound) is faster than the transfer of the compound to the proximity of the sensor surface (= mass transfer due to convection and diffusion, influenced by the flow rate in the microfluidic delivery system), the calculated association rate is underestimated. Immobilizing less protein minimizes the mass transfer contribution issue. [92, 98]

Procedure

SPR assays were conducted at 25°C on a Biacore 4000 system. Before used in the Biacore system, the buffers were vacuum filtered to remove particles.

To prepare the S Sensor Chip SA for protein capture and analysis, the steps Normalize (system automatically adjusts responding behavior of the detection unit to chip specific optical properties) and Hydrodynamic addressing (automatic calibration of the flow system for precise addressing of sensor spots) were conducted according to the manufacturer's instructions. Reagents for protein capture were provided in a sealed 96-well microplate and in capped plastic vials located at 12°C in the plate hotel of the Biacore system. Protein capture on the streptavidin-coated chips was accomplished at 25°C by injecting biotinylated kinases (2-10 µg/mL in HBS-P+ buffer) for 6 min with a flow rate of 10 µL/min. Afterwards, the sensor surface was washed with a solution containing 1 M NaCl and 0.05 M NaOH, and remaining streptavidin was blocked with 0.5 mM biotin.

Compounds were serially diluted (5-point 10-fold) in DMSO and transferred to assay buffer (50 mM Hepes (pH 7.4) containing 100 mM NaCl, 0.001% Surfactant P20) in a 1:100 dilution step to achieve the final test concentration (0.5 nM - 5 µM) at 1% DMSO. Reagents for compound analysis were provided in sealed 384-Well x 252 µL Microplates (NUNC) and reagent plates located at 25°C in the plate hotel of the Biacore system. Compound binding measurements were performed at 25°C with a

flow rate of 30 $\mu\text{L}/\text{min}$ in the assay buffer containing 1% DMSO. All compound concentrations were injected for 30 s, followed by a dissociation time of 190 s. Zero compound concentration samples were used as blanks and to check for sample carry over, and 1 mM ATP with 10 mM Mg^{2+} served as positive control. Solvent correction cycles were done according to the manufacturer's instructions. Experiments were conducted for FGFR1, FLT3, FMS, FYN, IGF1R, LCK, LYNa, MAP2K1, Met, PI3KCA, Ret and SRC. Binding kinetics and affinity parameters were determined as described in chapter 4.3.1.4.

4.2.3 Cellular assay based on bioluminescence resonance energy transfer (BRET)

Principle

The NanoBRET™ Target Engagement Assay [99] was used to investigate compound-kinase binding characteristics within intact cells. A variety of factors can influence target engagement in cells: In addition to binding kinetics and/or affinity, also e.g. protein degradation upon compound binding, cellular compartmentalization, cellular redox potential or interaction with membranes can influence the readout signal. On the one hand, they are closer to the *in vivo* situation (compared to biochemical binding assays), but on the other hand the complexity hampers the interpretability and binding kinetic rate constants cannot be extracted in a straightforward manner [92]. The NanoBRET™ Target Engagement Assay relies on BRET technology. BRET works like FRET but uses a bioluminescence donor. An unfavorable feature is that a bioluminescence-inducing protein has to be fused to the target protein (which could alter binding properties) [92]. The setup of the washout experiment was as follows: In the first step, cells expressing the bright NanoLuc luciferase®-protein target fusion protein are preincubated with the test compounds. The next step is the washout, i.e. removal of “unbound” compounds by changing the medium, so that compounds outside cells are removed while compounds inside cells are not. Due to the low volume of cells compared to the assay buffer, the amount of compounds inside cells is comparatively small and when compounds are released from cells, they are rapidly diluted to virtually nothing. However, as long the compounds are inside the cell, they can rebind to the target after dissociation. After the washout, BRET-acceptor-labeled cell-permeable target-specific tracers and the substrate for the bright luciferase are added. Additionally, extracellular inhibitor for NanoLuc luciferase is used to inhibit signals which would otherwise arise from disrupted cells (while not affecting intact cells). The dissociation of the compound is monitored over time and indirectly by measuring tracer binding.

Procedure

The cellular NanoBRET™ Target Engagement Assays were kindly conducted at Promega according to the manufacturer's instructions [100] and the costumers' specifications. In brief, cells expressing the target kinase that is fused to the bright NanoLuc® luciferase (cultured in 90%DMEM + 10% fetal

bovine serum) were trypsinized to dissociate cells from flask, trypsin was neutralized with cell culture medium, cells were centrifuged at 200 g for 5 minutes and cell pellets were resuspended in assay medium (Opti-MEM® I Reduced Serum Medium, no phenol red). The cell density was adjusted to 2×10^5 cells/mL. Then, 1 μ L/mL of 1000x concentrated test compound was added (final concentrations: [staurosporine]: 0.5 μ M; [imatinib]: 2 μ M; [ibrutinib], [dasatinib], [ponatinib]: 0.2 μ M) and incubated at 37°C for 3 h. After removing unbound test compound (washout with prewarmed assay medium), cells were dispensed into white, nonbinding surface 96-well plates (18000 cells/well) and cell-permeable fluorescent Kinase Tracer-05 [99, 101], and the Complete NanoBRET™ NanoGlo® Substrate with Extracellular NanoLuc® Inhibitor Solution were added. Subsequently, bioluminescence resonance energy transfer was measured over 5 h in 3-minutes intervals with a GloMax® Discover Instrument. A positive control with saturating dose of kinase inhibitor (0% probe binding) served for background correction, and a probe signal control (100% probe binding) was conducted by adding only DMSO instead of compound solubilized in DMSO. The experiments were conducted for ABL, BTK, FYN, KIT, LCK, Ret, SRC and Tie2.

For better comparability with simulated target occupancy traces (refer to chapters 4.3.8 and 5.4.1.2), NanoBRET traces were normalized to get binding signals as percentage of control, according to Equation 2.

$$\text{Signal}_{\text{normalized}}(t) = (1 - (\text{Signal}(t) - \text{Signal}_{0\%}(t)) / (\text{Signal}_{100\%}(t) - \text{Signal}_{0\%}(t))) \times 100\%$$

Equation 2

t: time; $\text{Signal}_{0\%}(t)$: 0% probe binding signal; $\text{Signal}_{100\%}(t)$: 100% probe binding signal

Changes in cellular target occupancy were calculated as described in Equation 3.

$$\Delta\text{TO}_{0-t \text{ min}} [\%] = 100 - (\text{Signal}_{\text{normalized}}(t) / \text{Signal}_{\text{normalized}}(t=0)) * 100$$

Equation 3

ΔTO : target occupancy; t: time; $\text{Signal}_{\text{normalized}}(t)$: normalized signal at time = t; $\text{Signal}_{\text{normalized}}(t=0)$: normalized signal at time = 0

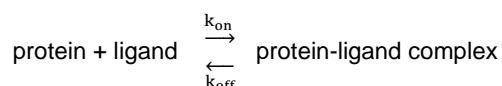
Constrains for experimental traces: $\text{Signal}_{\text{normalized}}(t=0)$ was estimated based on fitting of a “One phase decay” curve to the normalized trace using GraphPad Prism. $\Delta\text{TO}_{0-t \text{ min}}$ were set to 100% for all values >100% and to 0% for all values <0%.

Changes in simulated cellular target occupancy (see chapter 4.3.8 and appendix I) were calculated in the same way, but without consideration of the above mentioned constrains.

4.3 Computational Techniques and data analysis

4.3.1 Model fitting

The following chapters present the models used for nonlinear regression, i.e. the fitting of the respective model to the experimentally obtained binding curves and traces, in order to obtain best-fit values for binding kinetic and dissociation constants. All nonlinear regressions were performed without weighting, i.e. fitting was done ordinarily by minimizing the sum-of-squares of the vertical distances between data and fit curve (method of least squares) [102, 103]. All models assume that the free concentration of ligand (probe, compound) is approximately equal to the added concentration, i.e. no ligand depletion in FRET-based assays (assumed by models in chapters 4.3.1.1-4.3.1.3) and no mass transfer during association phase or rebinding during dissociation phase in SPR-based assay (assumed by model in chapter 4.3.1.4). The analyses further assume that binding is a one-step reversible 1:1 binding process and follows the law of mass action, i.e. that the rate of protein-ligand complex formation is proportional to the concentrations of free ligand and free protein, and that the rate of protein-ligand complex disengagement is proportional to the concentration of the protein-ligand complex, and that at equilibrium the ratio between 1) the product of the concentrations of protein and ligand and 2) the concentration of the protein-ligand complex is a characteristic constant value (the dissociation constant). According to the law of mass action, the reversible reaction



is at equilibrium when the concentrations do not change:

$$\frac{d[\text{protein ligand complex}]}{dt} = [\text{protein}] \times [\text{ligand}] \times k_{\text{on}} - [\text{protein ligand complex}] \times k_{\text{off}} = 0$$

In other words, equilibrium is reached when: $[\text{protein}] \times [\text{ligand}] \times k_{\text{on}} = [\text{protein ligand complex}] \times k_{\text{off}}$

The equilibrium dissociation constant can be calculated as: $K_D = \frac{[\text{protein}] \times [\text{ligand}]}{[\text{protein ligand complex}]} = \frac{k_{\text{off}}}{k_{\text{on}}}$

4.3.1.1 Determination of kinase-probe binding affinities and kinetic rate constants

The signal traces and curves obtained as described in chapter 4.2.1.1 were analyzed as follows: The baseline was removed (subtraction of nonspecific binding control signals) for all probe-target binding signals obtained in experiment I and II. The steady-state affinities of probe binding to the kinases were calculated by fitting of the “One site -- specific binding” model (GraphPad Prism, refer to next box) to the obtained probe-target binding signals from experiment I. This model assumes that the ligand-protein binding is at equilibrium.

“One site -- specific binding” model

$$Y = B_{\max} * X / (K_D + X)$$

X: concentration of probe (constrained as used in experiment); Y: specific binding signal; B_{\max} : maximum binding signal at very high probe concentrations in units of Y; K_D : equilibrium dissociation constant in units of X

The kinetic experiment was an association experiment, i.e. the rate of signal increase is influenced by the association rate constant k_{on} , the dissociation rate constant k_{off} , and the probe concentration. The measurement with several concentrations allows determination of the kinetic rate constants of the probe binding to the kinases by global fitting of the “Association kinetics -- two or more concentration of hot” model (GraphPad Prism, see box below) (under standard parameter constrains) to the probe concentration series traces from experiment II.

“Association kinetics -- two or more concentration of hot”

$$K_D = k_{\text{off}} / k_{\text{on}}$$

$$k_{\text{obs}} = k_{\text{on}} * L + k_{\text{off}}$$

$$\text{Occupancy} = L / (L + K_D)$$

$$Y_{\max} = \text{Occupancy} * B_{\max}$$

$$Y = Y_{\max} * (1 - \exp(-1 * k_{\text{obs}} * X))$$

K_D : calculated equilibrium dissociation constant in M, k_{obs} : observed rate of probe-target complex formation, k_{off} : dissociation rate constant of probe in inverse time, k_{on} : association rate constant of probe in inverse Molar times inverse time, L: probe concentration in M; Y is the specific binding signal; Y_{\max} is the maximum observable signal at equilibrium; B_{\max} : maximum binding signal at very high probe concentrations in units of Y

Parameter constrains:

L constrained to constant values as used in experiment

Shared parameters (between concentration traces) for global fit: k_{off} , k_{on} , B_{\max}

4.3.1.2 ePCA-based determination of kinase-inhibitor binding affinities

TR-FRET ratio values obtained as described in chapter 4.2.1.2 were normalized between 100% probe binding (= 0% inhibitor binding) and 0% probe binding (= 100% inhibition). 100% probe binding and 0% probe binding signals were calculated beforehand as mean of all signals in the respective control wells on a single microtiter plate (for 100% probe binding: wells with tracer but without compound; 0% probe binding: wells with St-Tb and tracer but without biotinylated kinase). A four-parameter sigmoidal dose-response curve (refer to next box) was then fitted to the normalized data under automated data- and model driven outlier masking (with Genedata Screener). The obtained IC_{50} value is the concentration of compound required to evoke a response (normalized probe binding signal) half way between minimum response and maximum response. The model assumes that competition of ligands reversibly binding to one site of the protein is in equilibrium, and the model is limited by the assay wall (refer to chapter 4.2.1.1). The IC_{50} value was converted into the equilibrium dissociation constant ($K_{D \text{ eq}}$) by using the Cheng-Prusoff equation [104] (Equation 4).

“Four-parameter sigmoidal dose-response curve” model

$$Y = \text{Bottom} + (\text{Top} - \text{Bottom}) / (1 + 10^{((\text{Log}(\text{IC}_{50}) - X) * \text{Hill slope}))}$$

Y: normalized probe binding signal (response); Bottom: bottom plateau (minimal response); Top: maximum response; X: logarithms of compound concentrations; IC₅₀: concentration of compound required to provoke a response half way between Bottom and Top (in units of compound concentration); Hill slope: slope factor describing steepness of dose-response curve

Parameter constrains:

X constrained to constant values as used in experiment

Genedata Screener software was allowed to automatically choose if to fix or not to fix the Hill slope to 1, Bottom to 0 and Top to 100, but was not allowed to extrapolate IC₅₀s. Thereby fixing of the parameters was enforced if the data range is <30% or R² < 0.1.

If not fixed, the parameters were constrained: Hill slope must be between 0.5 and 5; Bottom must be <30%; Top must be between 70 and 150%

Cheng-Prusoff equation:

Equation 4

$$K_D = \text{IC}_{50} / (1 + L / K_{D_L})$$

K_D: equilibrium dissociation constant of compound; IC₅₀: concentration of compound required to provoke a response half way between minimum and maximum response; L, K_{D_L}: concentration and equilibrium dissociation constant of probe

4.3.1.3 kPCA-based determination of kinase-inhibitor binding affinities and kinetic rate constants

Kinetic traces from kinetic Probe Competition Assays obtained as described in chapter 4.2.1.3 are dependent on the association rate constant k_{on} , the dissociation rate constant k_{off} , and the concentration of probe and compound, and were analyzed as follows: For baseline subtraction, the baseline signal (0% probe binding control) was assumed to be linear with time. Kinetic rate constants of inhibitor binding to kinases were then calculated by global curve fitting of Motulsky-Mahans' [83] “Kinetics of competitive binding” equation (see box below) to the inhibitor concentration series traces (GraphPad Prism) using the respective tracer binding kinetics (refer to Table 7 in appendix B). The zero compound concentration trace (100% probe binding control) was included in the analysis.

Motulsky-Mahans' “kinetics of competitive binding” model

$$Y(t) = \frac{B_{\max} \times K_1 \times L}{\text{Diff}} \left(\frac{K_4 \text{ Diff}}{K_F K_S} + \frac{K_4 - K_F}{K_F} e^{-K_F t} - \frac{K_4 - K_S}{K_S} e^{-K_S t} \right)$$

with

$$K_A = K_1 \times L + K_2$$

$$K_B = K_3 \times I + K_4$$

$$K_F = 0.5 \left(K_A + K_B + \sqrt{(K_A - K_B)^2 + 4 \times K_1 \times K_3 \times L \times I} \right)$$

$$K_S = 0.5 \left(K_A + K_B - \sqrt{(K_A - K_B)^2 + 4 \times K_1 \times K_3 \times L \times I} \right)$$

$$\text{Diff} = K_F - K_S$$

Parameters constrains:

K₁, L, K₂, I constrained to constant values as used in experiment or determined during assay development, respectively.

Shared parameters (between concentration traces) for global fit: K₃, K₄, B_{max} must be greater than 0

Y: specific probe binding signal (TR-FRET Ratio); t: time; K₁: association rate of probe in inverse Molar times inverse time; K₂: dissociation rate of probe in inverse time; L: concentration of probe in M; K₃: association rate of unlabeled compound (inverse Molar times inverse time); I: concentration of unlabeled compound in M; K₄: dissociation rate of unlabeled compound (inverse time); B_{max}: maximum binding signal at very high concentration of probe (and often exceeds what is measured in experiment)

Affinities from kinetic analysis were calculated as the ratio of the on- and off-rate (Equation 5). The results from Monte Carlo analyses performed in this thesis (chapter 5.1) were considered for evaluation of the data: If accurate determination of off-rates was not possible by nonlinear regression (if $CV(k_{on} \times K_{D\ eq}) < 50\%$ and either case I) $CV(k_{off}) > 50\%$ or case II) k_{off} is not determinable by regression), off-rates were calculated using Equation 6 as suggested by Schiele, Ayaz and Fernández-Montalván [84] and proved to be appropriate within this thesis (chapters 5.1.2.1 and 5.1.2.4). Off-rates were set to > 0.35 (2 times faster than the fastest determined off-rate with a relative model error $< 40\%$), if $CV(K_{D\ kin}) < 50\%$, the difference between $K_{D\ kin}$ and $K_{D\ eq}$ is less than five-fold and kinetic rate constants (k_{on} , k_{off}) are not determinable by regression (values far beyond assay quantitation limit and/or beyond diffusion limit: $k_{on} > 10^9\ M^{-1}s^{-1}$; $k_{off} > 10^4\ s^{-1}$ (case III); and/or $CV > 90\%$). Moreover, kinetic rate constants were considered as not evaluable, in all cases (which do not belong to case I-II but) with a more than five-fold difference between $K_{D\ kin}$ and $K_{D\ eq}$ (which could result from more complex interactions than simple 1:1 binding).

Residence times (RT) were calculated using Equation 7. The percentage of equilibrium reached in the probe binding control (without compound) at a given time can be approximated with Equation 8.

$$K_{D\ kin} = k_{off} / k_{on}$$

Equation 5

$K_{D\ kin}$: calculated equilibrium dissociation constant in M, k_{off} : dissociation rate constant in inverse time, k_{on} : association rate constant in inverse Molar times inverse time

$$k_{off} = K_{D\ eq} \times k_{on}$$

Equation 6

$K_{D\ eq}$: equilibrium dissociation constant in M as determined in endpoint experiment ePCA, k_{off} : calculated dissociation rate constant in inverse time, k_{on} : association rate constant in inverse Molar times inverse time as determined by using Motulsky-Mahans' equation

$$RT = 1/k_{off}$$

Equation 7

RT: residence time in units of time, k_{off} : dissociation rate constant in inverse time

$$\%eq\ reached = (1 - e^{-(t \times (k_{on} \times L + k_{off}))}) \times 100$$

Equation 8

$\%eq$: percentage of equilibrium reached at time t = response at time t divided by response at equilibrium multiplied by 100%; t : observation time; k_{on} : association rate constant of ligand in inverse Molar times inverse time; L : concentration of ligand in M; k_{off} : dissociation rate constant of ligand in inverse time

Finally, the affinities determined with kPCA were corrected by considering the affinities determined with ePCA to derive a K_D (PCA): K_D (PCA) = $K_{D\ kin}$, except for the following cases: (I) K_D (PCA) = $K_{D\ eq}$, if $CV(K_{D\ eq}) < 70\%$ and 1) $CV(K_{D\ kin}) > 70\%$ or 2) $K_{D\ kin}$ is n.e. or 3) reached assay quantitation limit or 4) there is at least a 5-fold discrepancy between $K_{D\ kin}$ and $K_{D\ eq}$; (II) else if $CV(K_{D\ kin})$ and $CV(K_{D\ eq}) > 70\%$, but there is a less than 5-fold discrepancy between $K_{D\ kin}$ and $K_{D\ eq}$, then K_D (PCA) = $\text{mean}(K_{D\ kin}, K_{D\ eq})$. These final PCA affinity values were used for all calculations (if not otherwise specified).

4.3.1.4 SPR-based determination of kinase-inhibitor binding affinities and kinetic rate constants

Data obtained as described in chapter 4.2.2 were analyzed with Biacore 4000 Evaluation Software using the kinetic model “1:1 Binding” (see box below) to determine on- and off-rates (BIAevaluation Software Handbook). Biacores “1:1 Binding” model relies on Langmuir’s isotherm [105, 106] for adsorption of substances to solid surfaces, and is composed of a Langmuir association and a Langmuir dissociation model used for global fitting to all signal traces of the association and dissociation phase. Kinase-inhibitor pairs with the following properties were not evaluable due to poor kinetic information in traces or unreliable values (model fit unreliable or parameter outside limits given by applied concentration, or diffusion): affinities $>5 \times 10^{-7}$ M or $k_{\text{off}} > 100 \text{ s}^{-1}$ or $k_{\text{on}} > 10^9 \text{ M}^{-1}\text{s}^{-1}$ or $R_{\text{max}} < 2 \text{ RU}$ or $R_{\text{max}} > 200 \text{ RU}$ or $\text{Chi}^2 > 1$ (parameters defined in box below; Chi^2 : information about goodness of fit; Equation 9).

Biacores “1:1 Binding” model

composed of Langmuir association model (for $t_0 - t_{\text{start disso}}$)

$$R(t) = R_{\text{eq}} * (1 - \exp(-(k_{\text{on}} * L + k_{\text{off}}) * (t - t_0))) + R_{\text{I}} \quad \text{with } R_{\text{eq}} = (k_{\text{on}} * C * R_{\text{max}}) / (k_{\text{on}} * C + k_{\text{off}})$$

and Langmuir dissociation model (for $t_{\text{start disso}} - t_{\text{end}}$)

$$R(t) = Y_0 * \exp(-k_{\text{off}} * (t - t_0))$$

t: time; t_0 : start association experiment; $t_{\text{start disso}}$: start dissociation experiment; t_{end} : end of observation time; k_{on} : association rate constant in $\text{M}^{-1}\text{s}^{-1}$; k_{off} : dissociation rate constant in s^{-1} ; R: binding signal in response units (RU); R_{eq} : binding signal at equilibrium; R_{max} : maximum analyte binding capacity in RU; R_0 : response at the beginning of dissociation experiment; R_{I} : bulk refractive index contribution (signal due to unbound molecules suspended in the medium and close ($< 300 \text{ nm}$) to the sensor surface)

additionally, an offset is allowed; i.e. curve is not forced to go through the original of the plot

Parameters constrains: L constrained to constant values as used in experiment; Shared parameters (between concentration traces) for global fit: k_{on} , k_{off} , R_{max}

$$\text{Chi}^2 = \sum (y_f - y_x)^2 / (n - p)$$

Equation 9

Chi^2 : value with information about goodness of fit; y_f : fitted value at a given time; y_x : data point at the same time; n: number of data points; p: number of parameters to be fitted

4.3.2 General statistics

Standard deviations were estimated from the output parameters of the individual experiments assuming that these arguments are a sample of the population (by applying Bessel's correction [107]).

For assessment of the direction and strength of relationship between k_{on} , k_{off} , K_{D} values determined in different assays or replicates (using GraphPad Prism), Spearman correlation calculations were utilized to compute correlation coefficients and two-tailed P values (binding parameters are approximately log normally distributed [108, 109], but skewed due to assay quantitation limits). Agreement between methods and replicates was evaluated by Bland-Altman analysis [110, 111] using mean log differences. Spearman correlation calculations were also done for comparison of 1) kinetic rate constants with affinity, 2) biochemical binding parameters (k_{on} , k_{off} , K_{D}) with cellular target occupancy changes, and 3) simulated and experimentally obtained cellular target occupancy changes.

Statistical analyses were performed with log values of binding parameters, including generation of histograms (bin: 0.5) and distance matrices calculations, Gini score calculation, percent difference calculations and multivariable regression analyses (more details are provided in the next chapters).

1) Calculation of frequencies (for bin n = no. of values (bin n)), relative frequencies (for bin n = no. of values (bin n) / no. of values (all bins) * 100) and cumulative frequencies (for bin n = no. of values (bin 1 to bin n) / no. of values (all bins) * 100), **2)** fitting of histograms to a “Gaussian” curve or “Cumulative Gaussian -- Percents” curve, respectively, and **3)** descriptive statistics was performed using GraphPad Prism.

Percent differences were calculated as defined in Equation 10.

$$\text{Percent difference} = (\text{value1} - \text{value2}) / (\text{value1} + \text{value2}) * 100$$

Equation 10

4.3.3 Monte Carlo simulations for assessment of precision and accuracy

Principle

Monte Carlo analyses can be performed to assess precision and accuracy of nonlinear multi-parametric models within the parameter space [112]. A set of data points determined in a series of the same experiment is precise if the data points are close to their average value, and accurate if the difference between the true parameter value and the determined values is small. It is possible that the determined data points are precise but inaccurate (low standard deviation between determined points, but not equal to the real value), or imprecise but accurate (high standard deviation, but the mean is close to the real value), or precise and accurate (all data points close to the real value). Monte Carlo analyses simulate pseudo-experiments with known input data, and the pseudo-measured signal traces can then be analyzed by fitting a model to the data. The advantage in comparison to real expensive biological experiments is that hundreds and thousands of pseudo experiments can be performed providing a larger draw from a probability distribution (statistically meaningful results), and that all input parameters are known so that accuracy can be evaluated without the need of an independent reference experiment.

Procedure

Monte Carlo analyses were performed (with GraphPad Prism) to assess precision and accuracy of the nonlinear multi-parametric Motulsky-Mahan model describing the kinetics of competitive target binding (model provided in chapter 4.3.1.3) within the parameter space: 1) Using the model equation, the biochemical experiment was emulated for a compound with a defined on- and off-rate and with the same input parameters (for tracer: on-rate, off-rate and concentration; for time: kinetic intervals and duration of observation; for compounds: concentrations) and a B_{\max} (= 5954.62 arbitrary HTRF units) and scatter in TR-FRET ratio signals as used and observed in a real experiment by the example of the BTK assay (refer to chapter 4.2.1.3 and appendix B) – except for the parameter for which the effect on precision and accuracy shall be analyzed. The scatter was estimated on the basis of the

standard deviations of the signal for the time when traces reached equilibrium and beyond (double Gaussian: 50% with SD = 72.9 arbitrary HTRF units, 50% with SD = 145.8 arbitrary HTRF units). The background signal (0% tracer binding) was emulated by assumption of 1000 M compound. 2) Afterwards, these synthetic experimental data were analyzed with the same model equation (and in the same way as real experimental data) to calculate optimal parameter (best fit) values (compound k_{on} , k_{off} , K_D). With perfect precision and accuracy of the model, these calculated outcome parameters equal the input parameters. 3) Step 1 and 2 were repeated 100 times by Monte Carlo Simulation. Step 1-3 were conducted for various meaningful changes in the model parameters (e.g. different combinations of on- and off-rates of the compound). Monte Carlo analyses were performed in the same way for assessment of models describing the association (and dissociation) of probe.

4.3.4 Distance matrices and clustering technique

Principle

Distance matrices are two-dimensional $m \times m$ arrays of the pairwise distances between m objects, e.g. compounds (the diagonal elements of the distance matrix are zero since there is the distance from the object to itself). These distances can be calculated based on the set of measured features, e.g. the compound binding characteristics (on-rates, off-rates or affinities) on a set of kinases. An often applied distance measure is the Euclidean distance [113].

Euclidean distance

$$d(x, y) = \sqrt{\sum_{i=1}^n (x_i - y_i)^2}$$

x_i is a feature of the object x , y_i is the corresponding feature of the object y and n is the total number of features

Distances between kinases can be determined in the same way based on the binding parameters of compounds targeting the respective kinase. (Side note: Pearson correlation would have been an alternative distance measure, where the distance is zero if the data of the objects correlate perfectly, but was not chosen for the analysis as it is very sensitive to outliers. Additionally, it was preferred that objects with high values (e.g. high affinities) cluster together and objects with low values cluster together, which is the case when using Euclidean distance.) Similarly, the calculation of distance between compounds based on chemical similarity and between kinases based on sequence alignment, respectively, can be performed automatically with various bioinformatics tool (for examples see below). Though, in these cases the features are often binary (e.g. fingerprints for compounds), i.e. each bit indicates the presence or absence of a certain feature. The distance between the objects (e.g. compound fingerprints) can be calculated by using the Tanimoto coefficient [113].

Tanimoto coefficient for binary variables

$$d(x, y) = \sum_{i=1}^n (x_i \times y_i) / (\sum_{i=1}^n (x_i^2) + \sum_{i=1}^n (y_i^2) - \sum_{i=1}^n (x_i \times y_i))$$

x_i is a feature of the object x , y_i is the corresponding feature of the object y and n is the total number of features

A clustering method can be used to sort the distance matrices (classify the objects into groups with small distances, i.e. similar features): e.g. average-linkage arranges objects on the basis of the average distances between all objects of both clusters (contrarily, complete linkage would use the maximum distance). In an agglomerative approach (typically used) each object is initially in its own cluster and the objects are joined by the clustering algorithm, while in a divisive approach all objects are initially in one cluster and the cluster are divided by the clustering algorithm.

Procedure

Distance matrices and hierarchical clustering: Distance matrices were calculated as '100 minus percent similarity'. Compound structure similarity matrix was generated with Pipeline Pilot (Version 16.5.0.143) using the component 'Fingerprint Similarity NxN' (distance measure: Tanimoto). Multiple sequence alignment of kinase constructs was performed using Clustal Omega [90]. Compound and kinase similarities were calculated with Python 3 (available at <http://www.python.org>) and the module SciPY (`scipy.spatial.distance` using the distance measure 'Euclidean') based on vectors of log values of binding parameters (pK_D , $-pk_{on}$, pk_{off}). No scaling or normalization was applied, on-rates and off-rates for kinase-inhibitor pairs with affinities below assay quantitation limit were set to $350 \text{ M}^{-1}\text{s}^{-1}$ and 3.5 s^{-1} , 'not evaluable' values were masked. Clustering/Visualization of distance matrices was performed with Python 3 using the modules Pandas, Seaborn and SciPY (`scipy.spatial`, `scipy.cluster.hierarchy` (routine linkage for agglomerative clustering based on clustering method 'average')). Pearson correlation coefficients were used as measure for correlation between distance matrices.

4.3.5 Definition and calculation of physicochemical properties of compounds

The molecular properties and chemical functionalities of the compounds used for the analyses in chapter 5.3 were calculated or are defined as described in the following: The molecular weight (MolWt) of the compounds was calculated based on the molecular formula and assuming standard isotope distribution. Flexibility is the number of rotatable bonds divided by number of bonds (between heavy atoms). Rotatable bonds are the single bonds between heavy atoms that are both not in a ring and not terminal (connected to a heavy atom which is attached to only hydrogens) as well as no amide C-N bonds. F, Cl, Br, and I atoms in a compound account for the number of halogens. The $sp^3 \text{ C} / \text{C}$ ratio is the number of sp^3 carbon atoms divided by the total number of carbon atoms. Hydrogen bond donors (HBD) are the heteroatoms (O,N,P,S) with one or more attached hydrogen atom(s), while hydrogen bond acceptors (HBA) are heteroatoms (O,N,P,S) with one or more lone pair(s), excluding atoms with positive formal charges, amide and pyrrole-type nitrogens, and aromatic oxygen and sulfur atoms in heterocyclic rings. The polar surface area was calculated from the molecular topology, considering all N and O atoms including attached H atoms

according to Ertl [114], but excluding sulfur and phosphorus polar fragments. The prediction of predominant charge state (predominantly positive, negative or neutral molecule, based on pKa prediction) relied on Simulations Plus' ADMET predictor (v.1, 2013.0620) software. The property was applied as a qualitative variable in the analyses below and set to 1 (positive), 0 (neutral) or -1 (negative). Likewise: The compound's binding mode information (involved subpockets and conformations, including DFG- and α C-helix conformations) and kinase-ligand interaction fingerprints (obtained from KLIFS database) are qualitative descriptors: 1 or 0 representing whether or not the kinase ligand interaction shows the respective binding feature.

4.3.6 Multivariable linear regression based on a genetic function approximation algorithm

Principle

Standard regression systematically varies the coefficients (independent variables) in the model equation with the goal to minimize the residues (distance between data points and fit line), which is often performed using the method of least squares. With too many independent variables (also called predictors or input variable), the problem of overfitting can occur: While the fit follows the data, extrapolation beyond the fitted data would not make good predictions, i.e. new unseen data could not be predicted with the generated model. An alternative approach to standard regression, the genetic function approximation (GFA) algorithm, is often used for structure-activity relationship analyses [115]: GFA generates models using the process of evolution (survival of the fittest) and thereby selects important predictors automatically and can estimate the most appropriate number of predictors to resist overfitting. At first, many models are created with random initial coefficients and their quality is estimated by analyzing how well they can describe the data (the dependent variable) based on e.g. the following criterion: The model r squared which is the percentage of variance in the dependent variable that can be explained by the model (not recommended, since no penalty for overfitting), or the adjusted model r squared which additionally considers the number of predictors in relation to the number of data points (penalizes equations with too many variables). The best models are then combined in several ways to create a new generation of models. This process is continued many times. When using Pareto improvement, i.e. during model optimization it is assessed if a change makes the optimization criterion better, at some point the quality of the new generation of models cannot be improved anymore. The Pareto optimum is reached and the models contain the best combination of coefficients to describe the data. [116] The variable usage count in the final model population, which is the number of models in the final generation using the respective variable, is a measure for the significance of the variable. If all variables are scaled equally, the coefficient of the variables can also be applied to compare their significance. That way, GFA is a technique for analyzing the influence of variables and generating hypotheses about their significance for prediction of the dependent response variable.

Procedure

Multivariable linear regression models for log values of binding parameters (as dependent variable) were built with a genetic function approximation algorithm using molecular descriptors (e.g. number of HBD and HBA, $sp^3 C / C$) and/or structural features (kinase-compound interactions or binding mode information) as predictors. This was computed with Pipeline Pilot (Version 16.5.0.143) using the component 'Learn Molecular GFA Model' with the following parameters: population size = 100, maximum generations: 1000; initial equation length: 4, maximum equation length = 15, Scoring method: Pareto (non-dominated sorting genetic algorithm II) with Score Function: Adjusted R-squared (estimates most appropriate number of variables and penalizes overfitting). Additionally, correlation matrices were generated with Pipeline Pilot (Version 16.5.0.143) using the component 'Correlation Matrix' calculating Pearson correlation coefficients.

4.3.7 Gini scores as metric for selectivity

Principle

Selectivity scores are used to rank compounds according to their target binding selectivity. One way to calculate a selectivity score is to divide the number of kinases targeted with at least an arbitrarily defined dissociation constant (e.g. $<10 \mu M$) by the total number of kinases tested [15, 25]. Using the ratio avoids the dependency of the selectivity score on the size of the tested kinase panel (neglecting the fact that in a larger panel there might indeed be a higher or lower percentage of kinase targets of the compound of interest than in the smaller panel). However, the selectivity score is still dependent on the arbitrary threshold. To cope with this problem, the Gini coefficient, which is a statistical measure for inequality, can be applied as selectivity score [14, 117]. It indicates how the compound inhibitory activities (or binding properties) vary among all kinases. A Gini selectivity score of 0 displays perfect equality: The compounds hits each target equally. A score of 1 indicates maximum inequality: Highly selective compound will possess a Gini coefficient very close to one. The mathematical background for the calculation of the Gini selectivity score is a Lorenz curve which plots the proportion of the cumulative binding activity (or binding strength) against the corresponding percentage of the cumulative number of kinases (sorted e.g. in order of their increasing inhibition by the compound). The ratio of the area under the curves of the straight line of perfect equality and the Lorenz curve is the Gini coefficient.

Procedure

Gini scores were determined based on normalized log values of binding parameters as described by Graczyk *et al.* [117]. Since Gini score calculation requires values normalized between 0 and 100, log values were normalized based on minimum and maximum values.

4.3.8 Quantitative systems biology and pharmacokinetics simulations with Copasi

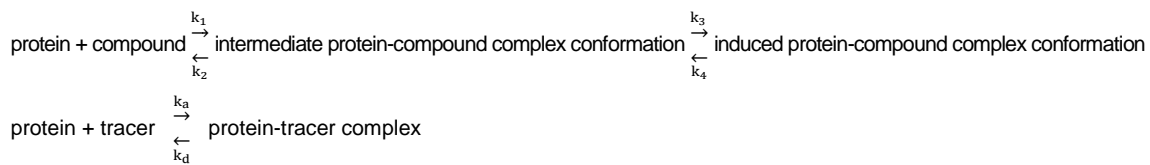
Simulation of biochemical reactions and events was performed with Copasi (version 4.1.9.) [91]. The underlying equations are provided in this chapter. The time course of a biochemical reaction is the function of the concentration of the substrates and products and the kinetic rate constants.

The one-step reversible 1:1 binding reaction following the law of mass action was introduced in chapter 4.3.1. The differential equations describing this binding reaction is given in the box below (left side). The reactions and equations on the right side of the box describe an alternative binding mechanism, namely covalent binding, where the formation of the protein-compound complex is irreversible, and additionally the competitive but one-step reversible 1:1 binding of tracer to the same target protein.

One-step reversible 1:1 drug-target binding model	One-step irreversible 1:1 drug-target binding and one-step reversible 1:1 tracer-target binding model
$\text{protein} + \text{compound} \xrightleftharpoons[k_{\text{off}}]{k_{\text{on}}} \text{protein-compound complex}$	$\text{protein} + \text{compound} \xrightarrow{k_{\text{on}}} \text{protein-compound complex}$ $\text{protein} + \text{tracer} \xrightleftharpoons[k_{\text{d}}]{k_{\text{a}}} \text{protein-tracer complex}$
1) $\frac{d([C](t))}{dt} = k_{\text{off}} \times [TC](t) - k_{\text{on}} \times [C](t) \times [T](t)$	1) $\frac{d([C](t))}{dt} = -k_{\text{on}} \times [C](t) \times [T](t)$
2) $\frac{d([TC](t))}{dt} = k_{\text{on}} \times [C](t) \times [T](t) - k_{\text{off}} \times [TC](t)$	2) $\frac{d([TC](t))}{dt} = k_{\text{on}} \times [C](t) \times [T](t)$
3) $\frac{d([T](t))}{dt} = k_{\text{off}} \times [TC](t) - k_{\text{on}} \times [C](t) \times [T](t)$	3) $\frac{d([T](t))}{dt} = k_{\text{d}} \times [TL](t) - k_{\text{a}} \times [L](t) \times [T](t) - k_{\text{on}} \times [C](t) \times [T](t)$
	4) $\frac{d([L](t))}{dt} = k_{\text{d}} \times [TL](t) - k_{\text{a}} \times [L](t) \times [T](t)$
	5) $\frac{d([TL](t))}{dt} = k_{\text{a}} \times [L](t) \times [T](t) - k_{\text{d}} \times [TL](t)$
<p>t: time; [C]: compound concentration; [T]: concentration of free target protein; [TC]: concentration of compound-complexed protein; k_{on} and k_{off}: rate constants for association and dissociation of the compound-target complex; [L]: concentration of free tracer; [TL]: concentration of tracer-complexed protein; k_{a} and k_{d}: rate constants for association and dissociation of the tracer-target complex</p>	

A more complex binding mechanism model is the induced fit model, which assumes that the binding of the compound to the target is followed by a conformational change in the target which strengthens binding. The reaction and differential equations for induced fit drug target binding along with additional one-step reversible 1:1 tracer-target binding are provided in the box below. In detail, simulations of more complex interaction mechanisms assumed a reaction volume of 5 μL , a target concentration of 0.1 nM and tracer parameters as in the BTK assay (refer to appendix B) as well as a 4-point 10-fold serial dilution of compound (starting at 2500 nM) and 0nM compound control.

Induced fit drug-target binding and one-step reversible 1:1 tracer-target binding model



- 1) $\frac{d[C](t)}{dt} = k_2 \times [TC](t) - k_1 \times [C](t) \times [T](t)$
- 2) $\frac{d[TC](t)}{dt} = k_1 \times [C](t) \times [T](t) - k_2 \times [TC](t) - k_3 \times [TC](t) + k_4 \times [T^*C](t)$
- 3) $\frac{d[T^*C](t)}{dt} = k_3 \times [TC](t) - k_4 \times [T^*C](t)$
- 4) $\frac{d[T](t)}{dt} = k_2 \times [TC](t) - k_1 \times [C](t) \times [T](t) + k_d \times [TL](t) - k_a \times [L](t) \times [T](t)$
- 5) $\frac{d[L](t)}{dt} = k_d \times [TL](t) - k_a \times [L](t) \times [T](t)$
- 6) $\frac{d[TL](t)}{dt} = k_a \times [L](t) \times [T](t) - k_d \times [TL](t)$

t: time; [C]: compound concentration; [T]: concentration of free target protein; [TC]: concentration of transitional intermediate of inhibitor-complexed protein; [T^{*}C]: concentration of conformationally changed inhibitor-complexed protein; k₁ and k₂: rate constants for association and dissociation of the compound from the target; k₃ and k₄: rate constants for TC-T^{*}C interconversion; [L]: concentration of free tracer; [TL]: concentration of tracer-complexed protein; k_a and k_d: rate constants for association and dissociation of the tracer-target complex

Permeation of a compound through the cellular membrane can be approximated by using Fick's First Law and the membrane permeability coefficient (see box below).

Fick's First Law – Permeation equation

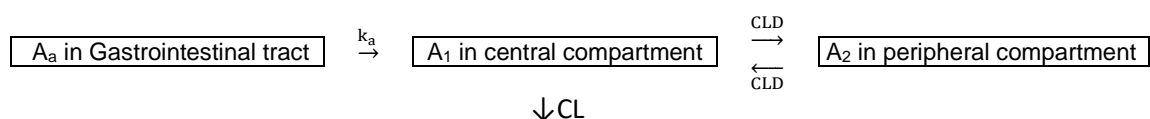
$$\frac{da_1}{dt} = -\frac{D}{\delta} \times A_o \times (C_1 - C_2)$$

t: time; a₁: amount of permeate (e.g. compound) on one side of the membrane; C₁ and C₂: permeate concentrations on the respective site of the membrane; D/δ: diffusion coefficient divided by thickness of the membrane is equal to the membrane permeability coefficient (P); A_o: membrane surface area

Pharmacokinetic modeling of the drug concentration-time profile in the body was performed with a simple two-compartment model which divides the body in a central and peripheral compartment:

Pharmacokinetic two-compartment model

(with the assumption of equal rate constants for distribution and redistribution between central and peripheral compartment)



$$\frac{d([C_1](t))}{dt} = \frac{k_a \times A_a(t)}{V_1} - CL \times [C_1](t) - CLD \times ([C_1](t) - [C_2](t))$$

$$\frac{d([C_2](t))}{dt} = CLD \times ([C_1](t) - [C_2](t))$$

$$\frac{d(A_a(t))}{dt} = -k_a \times A_a(t)$$

$[C_1]$ ($= A_1/V_1$) and $[C_2]$ ($= A_2/V_2$) are the total compound concentrations (= amount/distribution volume) in the central compartment (consisting of plasma and tissues where distribution is instantaneous) and peripheral compartment (consisting of the other tissues), respectively. A_a is the amount of drug in the gastrointestinal tract. k_a , CL , CLD represent the rate constants for absorption, elimination and distribution.

The models describing cellular and *in vivo* target occupancy were developed by combining the relevant equations and are given in appendix I and J.

5 Results

5.1 Assessment of precision and accuracy of binding kinetic parameters determined with kPCA and the ‘kinetics of competitive binding equation’

As described in chapter 4.2.1 probe competition assays can be applied for high-throughput assessment of binding kinetics data. The Motulsky-Mahan competitive binding kinetics theory [83] is frequently applied for the evaluation of this kind of assays. Also the calculation of binding kinetic rate constants from kPCA traces relies on this model. One main objective of this thesis was to assess the precision and accuracy of the non-linear multi-parametric Motulsky-Mahan model within the parameter space.

5.1.1 Precision and accuracy within the parameter space for exemplary kPCA setup

Monte Carlo analyses enable estimation of the impact of different parameters on precision and accuracy (and were performed as described in 4.3.3). As a first step, it was assessed how the Motulsky-Mahan model performs under the conditions (such as compound and tracer concentrations, kinetic intervals and durations of observation) applied in the standard kPCA setup (chapter 4.2.1.3; [84]). kPCA traces were simulated with tracer binding kinetics and a fluctuation of the TR-FRET signal as observed in a real experiment (BTK assay, appendix B, chapter 4.3.3). Figure 9 shows an example of real experimental traces compared to simulated traces for a compound with the same binding kinetic rate constants, illustrating that simulations are close-to-reality. To study the precision and accuracy across different on- and off-rates, 100 kPCA trace simulations were conducted for 35 hypothetical compounds, respectively. Thereby, each hypothetical compound possessed a defined on- and off-rates (for kinase binding) to span a wide range of binding properties: k_{on} : 10^3 - 10^9 $M^{-1}s^{-1}$, k_{off} : 10^{-5} - 1 s^{-1} and K_D : 10^{-5} - 10^{-12} M (see Figure 10a). The 100 simulated traces (per compound) were then analyzed by

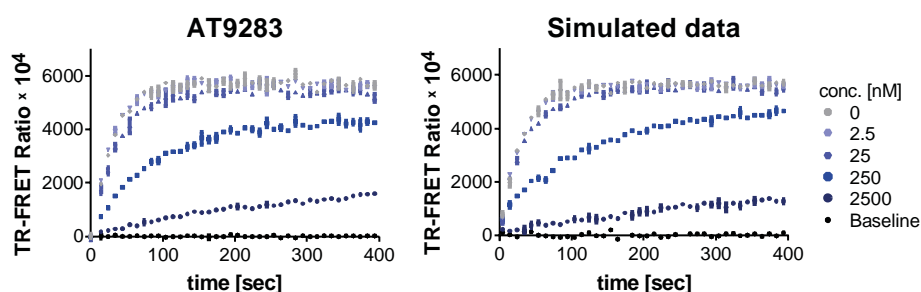


Figure 9: Comparison of experimental kPCA traces versus simulated kPCA traces

kPCA traces were simulated with a B_{max} and fluctuation in the TR-FRET signal as observed for the BTK assay (refer to chapter 4.3.3) and by using the same conditions as applied in the BTK assay: same kinetic interval, observation time, compound and tracer concentration and tracer binding kinetics (see appendix B). Therefore, the simulation of kPCA traces (right plot) for a compound with distinct binding kinetics is close-to-reality (left plot: experimental kPCA traces for AT9283).

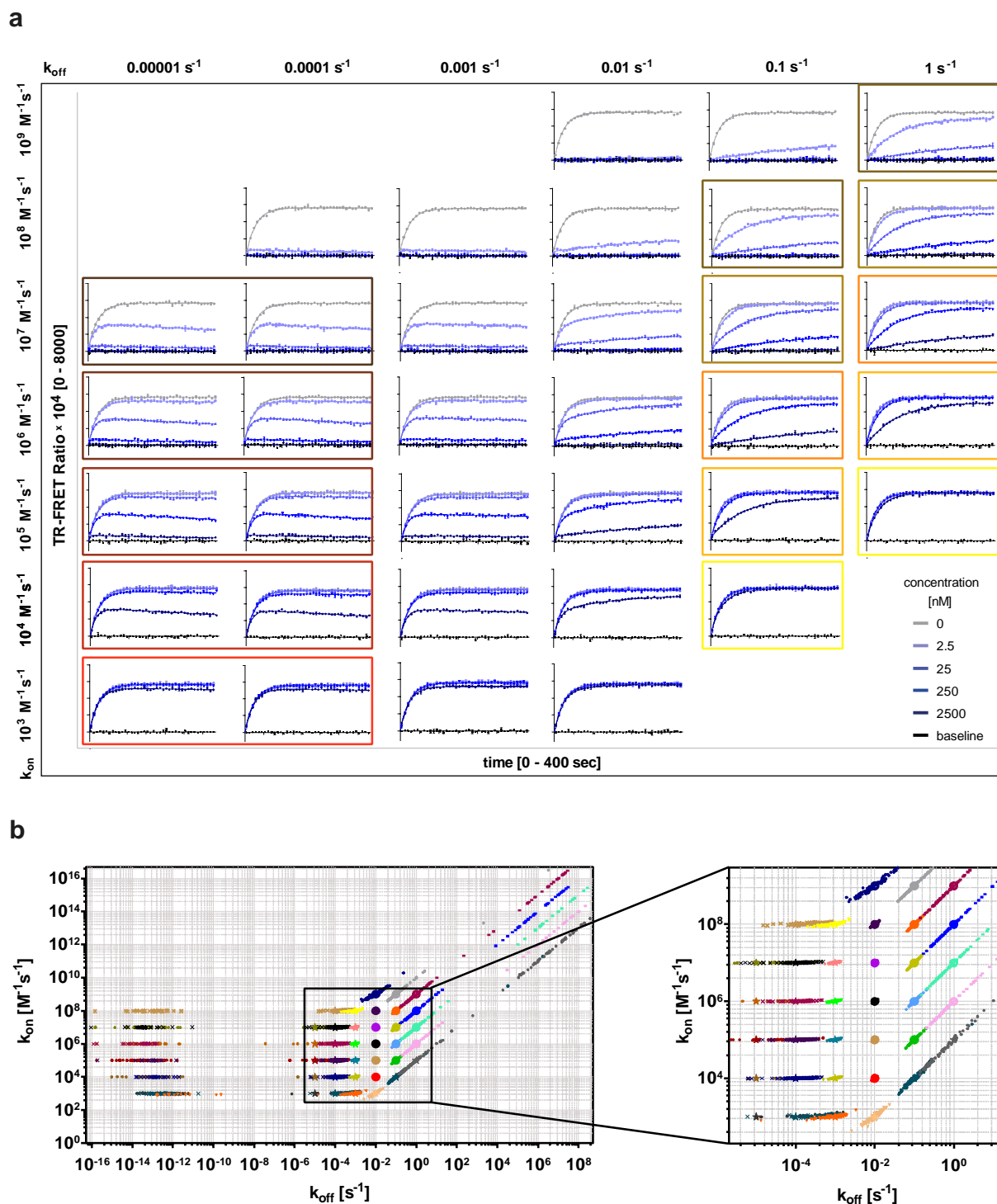


Figure 10: Precision and accuracy of the Motulsky-Mahan model under the conditions in a standard kPCA setup Monte Carlo analyses were performed for assessment of precision and accuracy of the Motulsky-Mahan model. These analyses comprised simulation of 100 kPCA traces with a B_{\max} and random fluctuation in the TR-FRET signal as observed in a real experiment (refer to chapter 4.3.3) and evaluation of the simulated data with the Motulsky-Mahan model.

a) Representative simulated kPCA traces and fit curves for 35 hypothetical compounds with different on- and off-rates.
b) Input (large symbols) and output binding kinetic parameters (small symbols) from Monte Carlo analyses. The same colors are applied for corresponding input and output data.

Ideally, the output data are consistent with the input data (same on-rate, off-rate and affinity), which is observed for compound-kinase dissociation rates between 0.1 and 0.001 s^{-1} . For compound-kinase pairs with slower off-rates solely the output on-rate was consistent with the input data and for compound-kinase pairs with faster off-rates solely output affinities are consistent with the input data.

using the Motulsky-Mahan model and thereby treated in the same way as experimentally obtained traces (e.g. subtraction of background signal, same parameter constrains for regression). Figure 10b depicts the input binding kinetics data along with the output binding kinetics data. This Monte Carlo analysis identified k_{off} as the main determinant for precision and accuracy: If the off-rate of the compound-kinase pair is between 0.1 and 0.001 s^{-1} , all output binding parameters are consistent with the input binding parameters (Figure 10b). Only very fast and very slowly associating pairs have a little higher scatter. Yet, this scatter can be eliminated by adaptation of the compound concentration in a way that the compound traces have a significantly larger or smaller area under the curve than compared to the control traces (background or tracer without compound, respectively). If the off-rate of the compound-kinase pair is 1 s^{-1} or faster, the kPCA traces are very similar for the pairs with the same affinity (Figure 10a) and accordingly only the affinity can be calculated with high precision and accuracy, while the fit-results for on- and off-rates are not consistent with the input data and often drift to extremely fast “non-sense” kinetic rate constants (Figure 10b). If the off-rate of the compound-kinase pair is 0.0001 s^{-1} or slower, the kPCA traces are very similar for the pairs with the same on-rate (Figure 10a) and accordingly solely the on-rate can be calculated with high precision and accuracy, while the fit-results for off-rates and affinities are not consistent with the input data and often drift to extremely low “non-sense” values (Figure 10b).

For cross-validation, dissociation rate constants determined by kPCA (using Equation 5 and kinetic rate constants determined with the Motulsky-Mahan model) are usually compared to dissociation rate constants determined in an endpoint assay [118]. Moreover, Schiele, Ayaz and Fernández-Montalván [84] also suggested calculation of off-rates that are not determinable by kPCA using equilibrium dissociation constants and the on-rate from kPCA (Equation 6). However, the question arose whether the on-rate is reliable. Moreover the dissociation constant can be underestimated in endpoint assays, if the target concentration is larger than twice the IC_{50} of the kinase-compound pair (assay wall) [95, 119], or if the incubation time is too short to reach equilibrium [120, 121]. In those cases also the off-rate will be underestimated. Yet, the Monte Carlo analyses in this study showed that the on-rate is reliable. A next step was to analyze exactly how long an endpoint assay would have to be incubated to reach equilibrium under the conditions applied for a standard ePCA experiment. For that reason, the TR-FRET signal arising from tracer-kinase binding in the presence of different concentrations of the compound was simulated over time (using compound concentrations as applied in the standard ePCA setting: 13-point 3.5-fold dilution series starting from $2 \times 10^{-5} \text{ M}$; and assuming 10 M for simulation of 0% tracer binding). This was performed for hypothetical compounds with different on- and off-rates and assuming the same tracer and B_{max} parameters as described for kPCA MC simulations (BTK assay). For each compound the TR-FRET signals of all concentrations after different “incubation” times were then fitted to a four-parameter sigmoidal dose-response curve (refer to chapter 4.3.1.2) to obtain the apparent IC_{50} values (and via Cheng-Prusoff [104] (Equation 4) the dissociation constants) that would

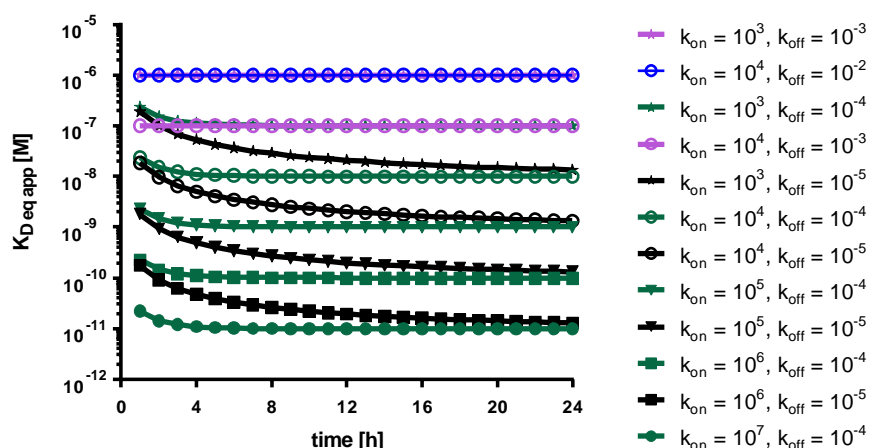


Figure 11: Effect of incubation times in equilibrium binding assays on apparent dissociation constants

The apparent dissociation constants obtained in an equilibrium binding experiment after different incubation times were simulated for compounds with different on- and off-rates (by using the conditions described for ePCA – chapter 4.2.1.2, BTK assay – appendix B). In detail, the TR-FRET signal arising from tracer-kinase binding in the presence of different concentrations of compounds with distinct on- and off-rates were simulated over time. The TR-FRET signals of all concentrations of a compound at a certain point in time were then fitted to a four-parameter sigmoidal dose-response curve to calculate the dissociation constants (using Cheng-Prusoff equation [104]). The plot depicts the obtained dissociation constants over time. Even for very slow off-rates (residence time of 27.78 h), the determined apparent K_D differs less than 3-fold from the true value after 12 h of incubation (overnight incubation).

be calculated at the respective time. As expected, Figure 11 illustrates that the underestimation of K_D due to incubation time is dependent on the off-rate. The slower the off-rate, the higher the underestimation or the longer the time required to reach equilibrium. However, usually incubation times of 12 h (e.g. overnight) are sufficient to reach K_D values with less than 3-fold deviation from the real values. Residence times of more than 27.78 h would lead to longer required incubations times.

Summary of the results: Monte Carlo analyses revealed boundaries for accurate and precise binding kinetic determinations when using the Motulsky-Mahan model. These boundaries are imposed by the drug-target k_{off} : Under standard kPCA conditions, all binding parameters (on-rate, off-rate, affinity) can be determined with high precision and accuracy for drug target pairs with dissociation rates in the range $0.1-0.001\text{ s}^{-1}$. For drug-target pairs with too slow k_{off} , only the k_{on} is reliable determinable (from now on called the “slow off-rate problem”) and for pairs with too fast k_{off} , solely the K_D is reliable (from now on called the “fast off-rate problem”). Simulations of the K_D determinable with standard ePCA settings after different incubation times revealed that for very long residence times (up to 27.78 h) 12 h are required to calculate an apparent K_D less than 3-fold off compared to the true value.

5.1.2 Effect of assay parameters and properties on precision and accuracy

In this chapter, the impact of further assay parameters, such as observation time, measurement intervals or binding kinetics of the tracer, on precision and accuracy of the Motulsky-Mahan model were analyzed, also in order to identify solutions for the k_{off} imposed boundaries.

5.1.2.1 Effect of total observation time

When comparing simulated kPCA traces with 394 s observation time for compound-kinase pairs with the same on-rates but different off-rates (Figure 12a), it becomes obvious that the traces are very similar for slower off-rates (10^{-4} s^{-1} or slower) – the areas under the curves are similar. With longer incubation times the traces become distinguishable – with smaller areas under the curve for slower off-rates (Figure 12b). It was assessed how the incubation time influences the precision and accuracy of the Motulsky-Mahan model equation. For that reason, kPCA traces were simulated with different incubation times for 1) a kinase-compound pair with a fast off-rate (0.1 s^{-1}) showing first signs of the fast off-rate problem and 2) a kinase-compound pair with a slow off-rate (0.0001 s^{-1}) as representative for the slow off-rate problem and with different on-rates. The kPCA traces were

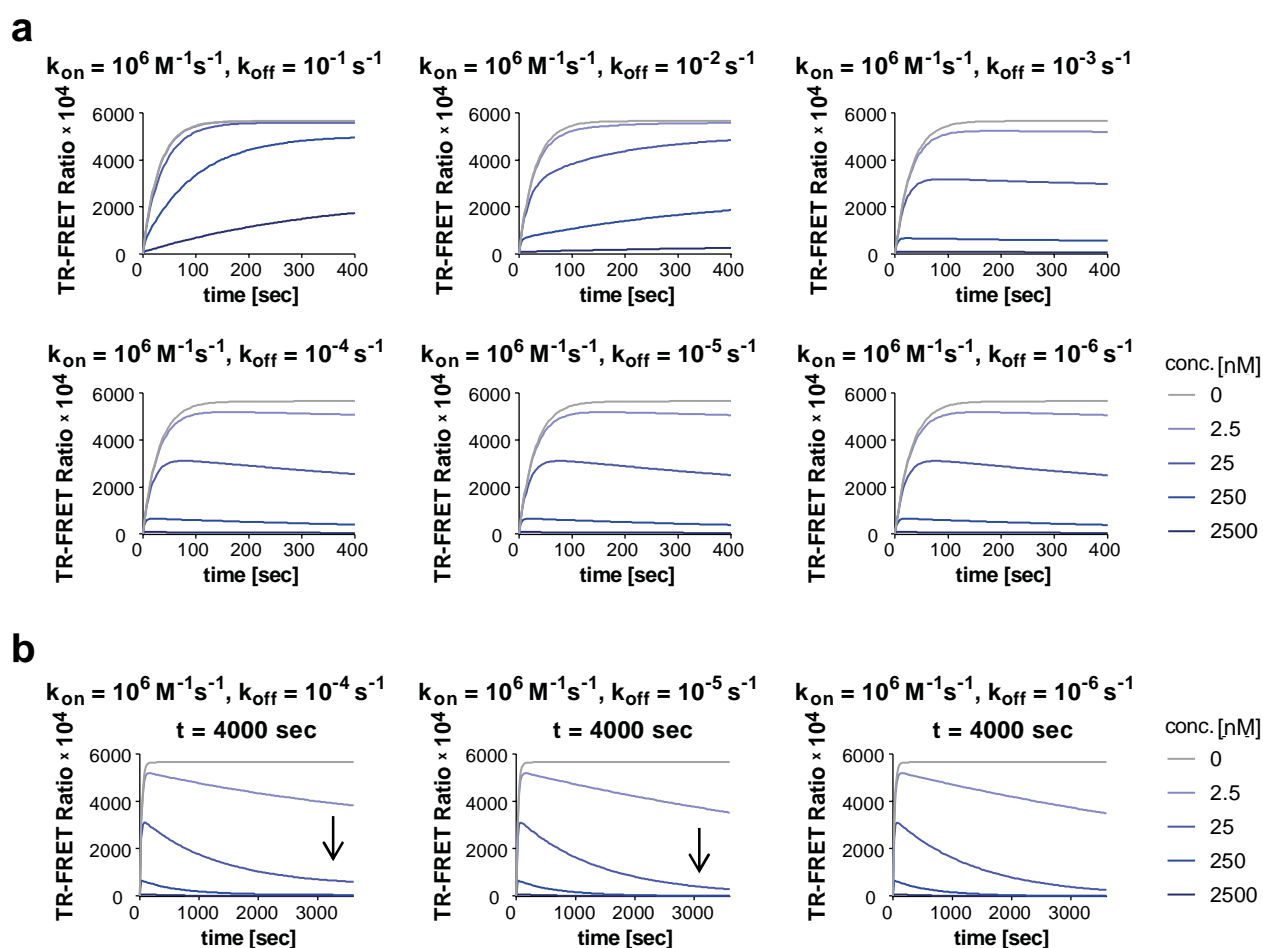


Figure 12: Effect of longer incubation times on traces of slow dissociating kinase-compound pairs

a) Simulation of kPCA traces illustrating the slow off-rate problem. The traces of fast dissociating kinase-compound pairs with the same on-rates are distinguishable, while the areas under the curves for traces of slow dissociating kinase-compound pairs are very similar.

b) Simulation of kPCA traces for the same slow off-rates and the same on-rates (where the slow off-rate problem occurs in a) but with longer observation times. The simulation illustrates, that longer incubation times lead to differences in the traces, especially in the last third of the observation time (indicated by arrows): the area under the curve is smaller for slower off-rates.

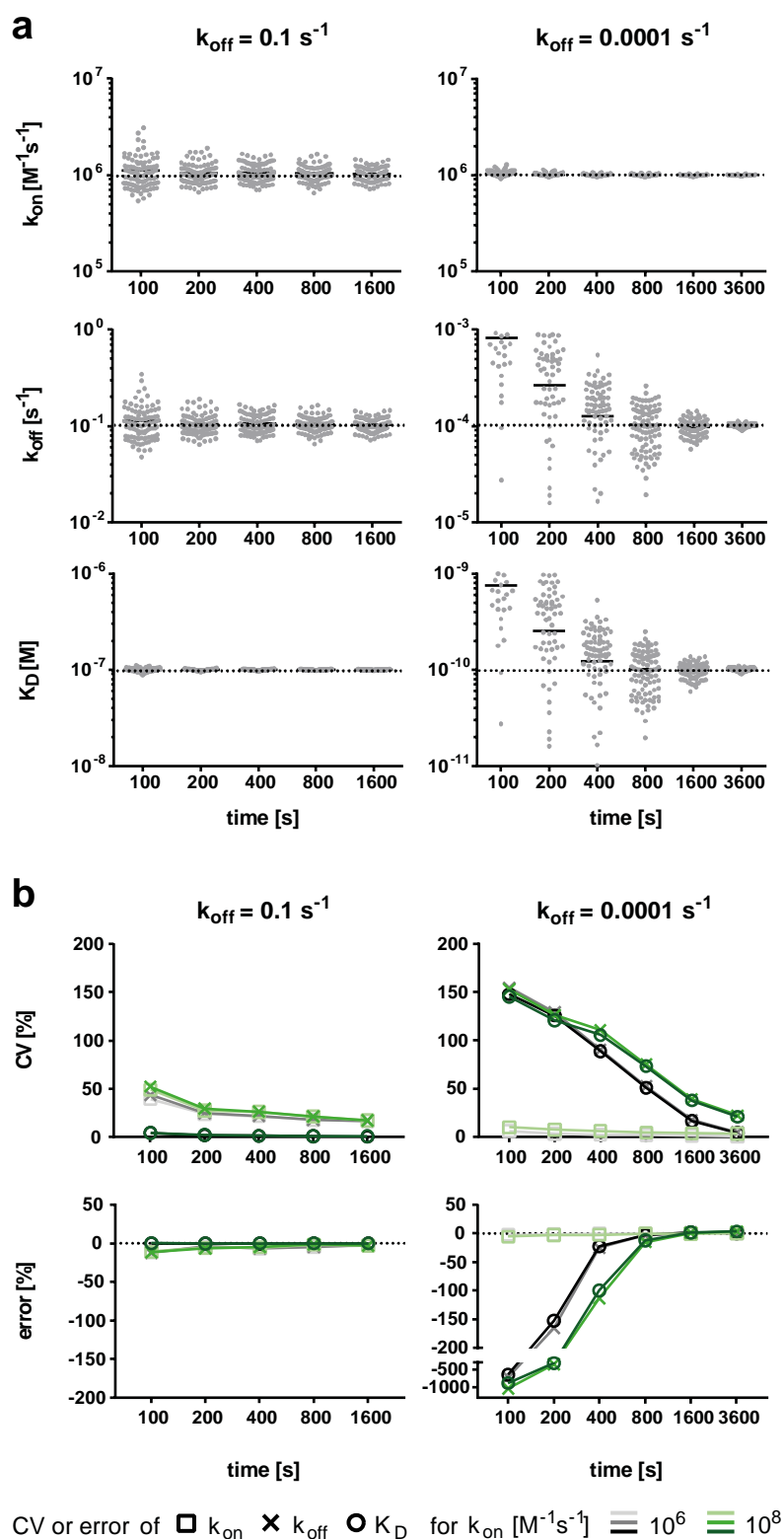


Figure 13: Effect of longer incubation times on precision and accuracy of the Motulsky-Mahan model

Results from Monte Carlo analyses for a fast and a slow dissociating kinase-compound pair (both with a k_{on} of $10^6 \text{ M}^{-1}\text{s}^{-1}$ (panel a, b) or alternatively $10^8 \text{ M}^{-1}\text{s}^{-1}$ (panel b)):

a) Output values (grey dots) and input values (dotted line) for on-rates, off-rates and affinities over incubation times. The mean of all output values is indicated as a black line. Not all output values are inside the range of the y-axis.

b) Coefficient of variation of the output values (as measure for precision) and the relative error between input and output value (as measure for accuracy) over incubation times.

The precision and accuracy of the determination of binding parameters is increasing with increasing observation times, especially for off-rates and affinities of the slow dissociating kinase-compound pairs.

simulated 100 times, respectively, and with the binding kinetics and a random fluctuation in the TR-FRET signal as observed in a real experiment (BTK assay, refer to chapter 4.3.3), and then analyzed with the Motulsky-Mahan model equation. These Monte Carlo analyses revealed that the longer the observation time, the higher the precision (lower coefficient of variation) and accuracy (smaller difference between results and true values) for the determination of off-rate and affinity for the slow off-rate kinase-compound pairs (Figure 13). In other words, with longer observation times, the slow-off-boundary for precise and accurate determination of binding parameters is shifted to slower off-rates (diminishing the slow off-rate problem). On the other hand, there is no appreciable improvement or deterioration of precision and accuracy with regard to the fast off-rate problem (Figure 13). With the exception of very short observation time of 100 seconds, where also determination of the binding parameters for the fast dissociating kinase-compound pairs is slightly less precise and accurate as compared to longer observation times. Nonetheless, also with long incubation times the precision is still too low, so that the fast off-rate problem cannot be solved by increased incubation times, but is also not negatively affected.

5.1.2.2 Effect of time interval of measurement

When comparing simulated kPCA traces with measurement intervals of 10 seconds for compound-kinase pairs with the same affinities but different off-rates (Figure 14a), it becomes obvious that the traces are very similar for fast off-rates (10^{-1} s^{-1} or faster) – the areas under the curves are similar. The only slight difference is observable in the first 10 seconds (Figure 14b). With higher frequency of measurement, the traces become better distinguishable (within the first 10 seconds) – with smaller areas under the curve for faster off-rates (Figure 14c). The influence of the time interval of measurement on precision and accuracy of the Motulsky-Mahan model equation was assessed. For that reason, Monte Carlo analyses were performed as described in 5.1.2.1 for 1) a kinase-compound pair with a fast off-rate (0.1 s^{-1}) and 2) a kinase-compound pair with a slow off-rate (0.0001 s^{-1}) and different on-rates, respectively. Thereby, kPCA traces were simulated with different measurement intervals (and 394 s observation times, respectively). The higher the frequency of measurement, the higher the precision (lower coefficient of variation) and accuracy (smaller difference between results and true values) for the determination of the on- and off-rate for the fast off-rate kinase-compound pairs (Figure 15). In other words, with shorter measurement intervals, the fast-off-boundary for precise and accurate determination of binding kinetics parameters is shifted to faster off-rates (diminishing the fast off-rate problem). Interestingly, there is also an improvement of precision and accuracy for the determination of off-rate and affinity for the slow off-rate kinase-compound pairs (Figure 15). However, the precision is still too low, implying that the slow off-rate problem cannot be solved by shorter measurement intervals.

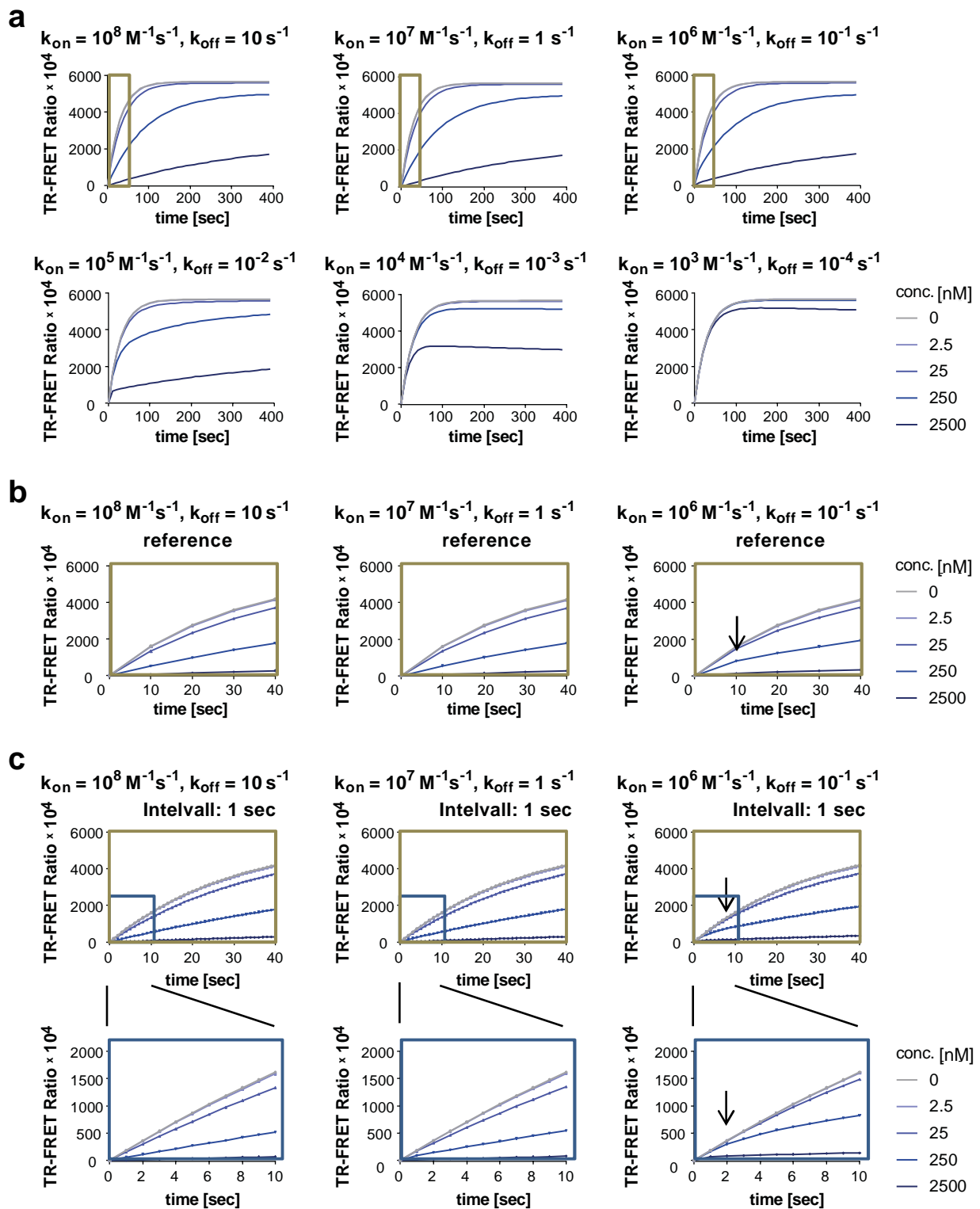
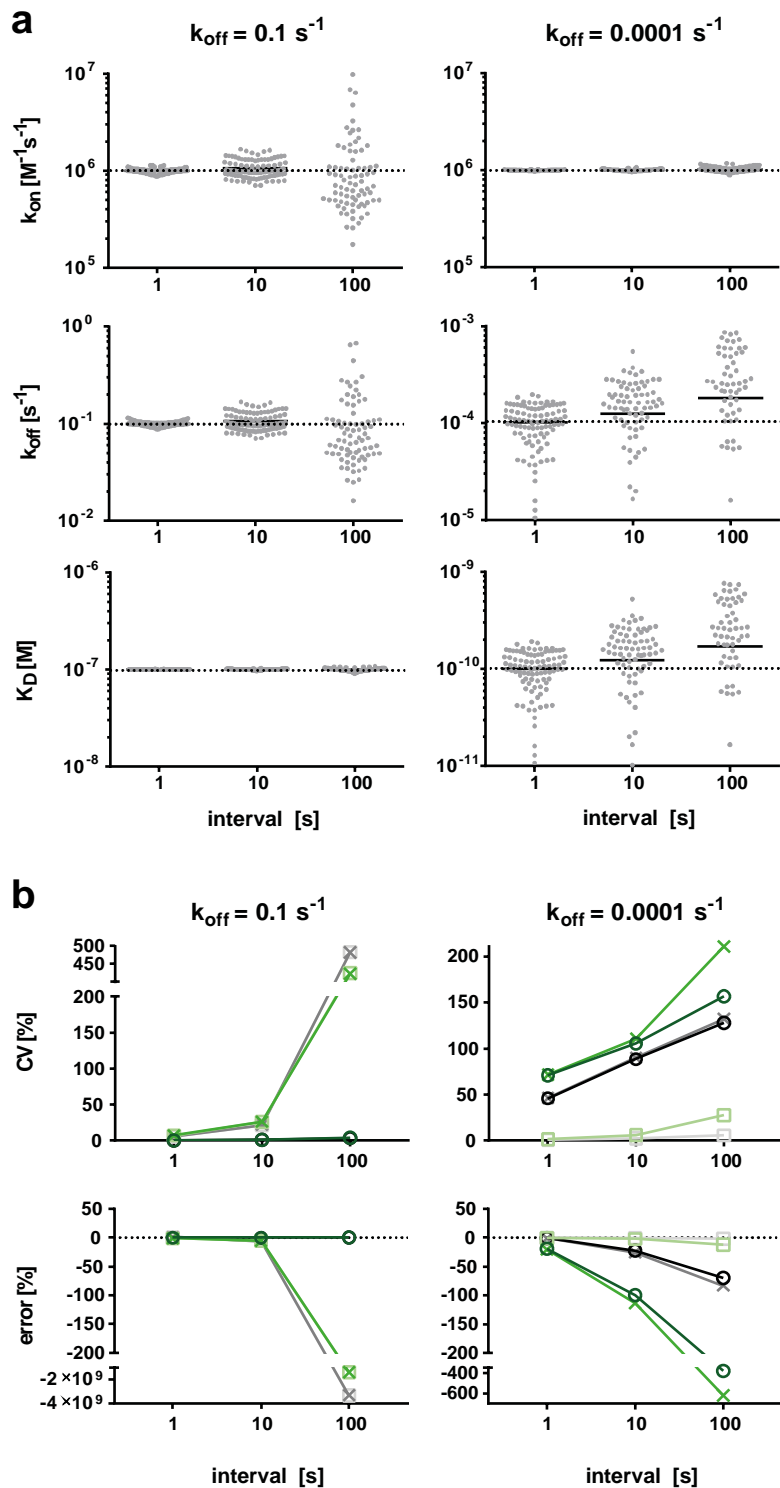


Figure 14: Effect of measurement intervals on traces of fast dissociating kinase-compound pairs

a) Simulation of kPCA traces illustrating the fast off-rate problem. The traces of slower dissociating kinase-compound pairs with the same affinities are distinguishable, while the areas under the curves for traces of fast dissociating kinase-compound pairs with the same affinity are very similar.

b) The zoom into the first 40 seconds indicates that there is a very slight difference in the first 10 seconds.

c) Simulation of kPCA traces for the same fast off-rates and the same on-rates (where the fast off-rate problem occurs in a and b) but higher frequency of measurement (observation time was 394 s). The simulation illustrates, that the shorter measurement intervals lead to higher differences in the traces within the first 10 seconds (illustrated by zoom, and indicated by arrows): the area under the curve is smaller for fast off-rates.



CV or error of \square k_{on} \times k_{off} \circ K_{D} for $k_{\text{on}} [\text{M}^{-1}\text{s}^{-1}]$ \equiv 10^6 \equiv 10^8

Figure 15: Effect of measurement intervals on precision and accuracy of the Motulsky-Mahan model

Results from Monte Carlo analyses for a fast and a slow dissociating kinase-compound pair (both with a k_{on} of $10^6 \text{ M}^{-1}\text{s}^{-1}$ (panel a, b) or alternatively $10^8 \text{ M}^{-1}\text{s}^{-1}$ (panel b)):

a) Output values (grey dots) and input values (dotted line) for on-rates, off-rates and affinities over measurement intervals. The mean of all output values is indicated as a black line. Output values with a more than 10-fold deviation from the input value are not shown, but considered for calculation of the mean, error and coefficient of variation.

b) Coefficient of variation of the output values (as measure for precision) and the relative error between input and output value (as measure for accuracy) over measurement intervals.

The precision and accuracy of the determination of binding parameters is increasing with increasing frequency of measurement, especially for the on- and off-rates of fast dissociating kinase-compound pairs.

5.1.2.3 Effect of concentration and binding kinetic rate constants of kPCA probe

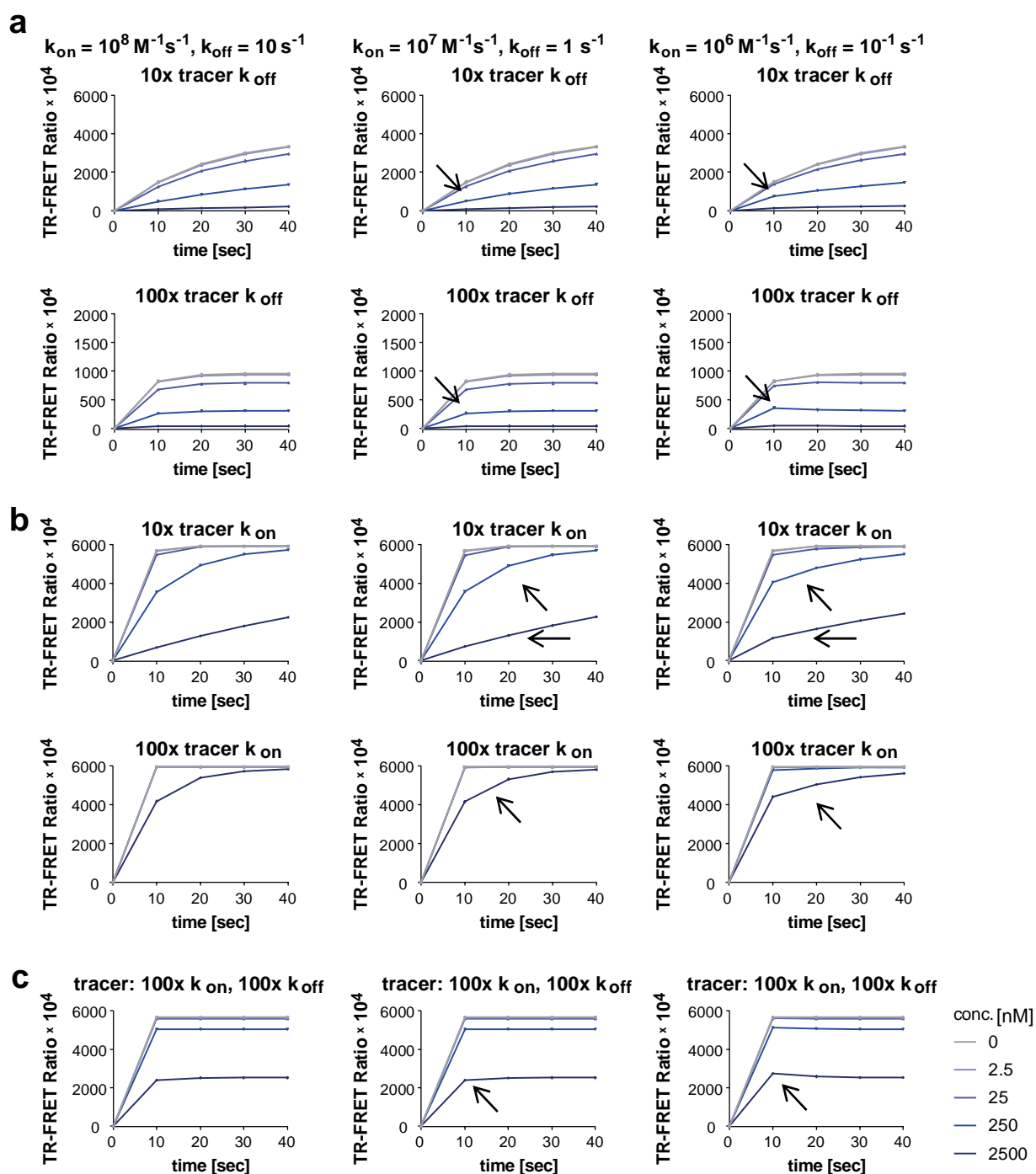


Figure 16: Effect of tracer binding kinetics on traces of fast dissociating kinase-compound pairs

Simulation of kPCA traces for the same fast off-rates and the same on-rates for the compound-kinase pair for which the fast off-rate problem occurs in Figure 14, but with a faster off-rate tracer **(a)** or a faster on-rate tracer **(b)** or a tracer with both a faster on- and off-rate **(c)**. 394 s are simulated, but only the first 40 seconds are depicted, so that the differences in this time period are more visible. The simulations illustrate, that a tracer with a faster on- and/or off-rate lead to higher differences in the traces within the first 10 seconds (illustrated by zoom, and indicated by arrows): the area under the curve is smaller for fast off-rates of the compound. Though, a tracer with a faster off-rate alone leads to lower TR-FRET signals. On the other hand, a tracer with a higher on-rate alone would require higher compound concentrations to get more than one compound trace distinguishable from the tracer trace (0 nM compound). A combination of both a higher on-rate and off-rate combines the effects on the trace (difference for fast off-rates visible) diminishing the negative effects (neither lower signal nor much higher compound concentration required).

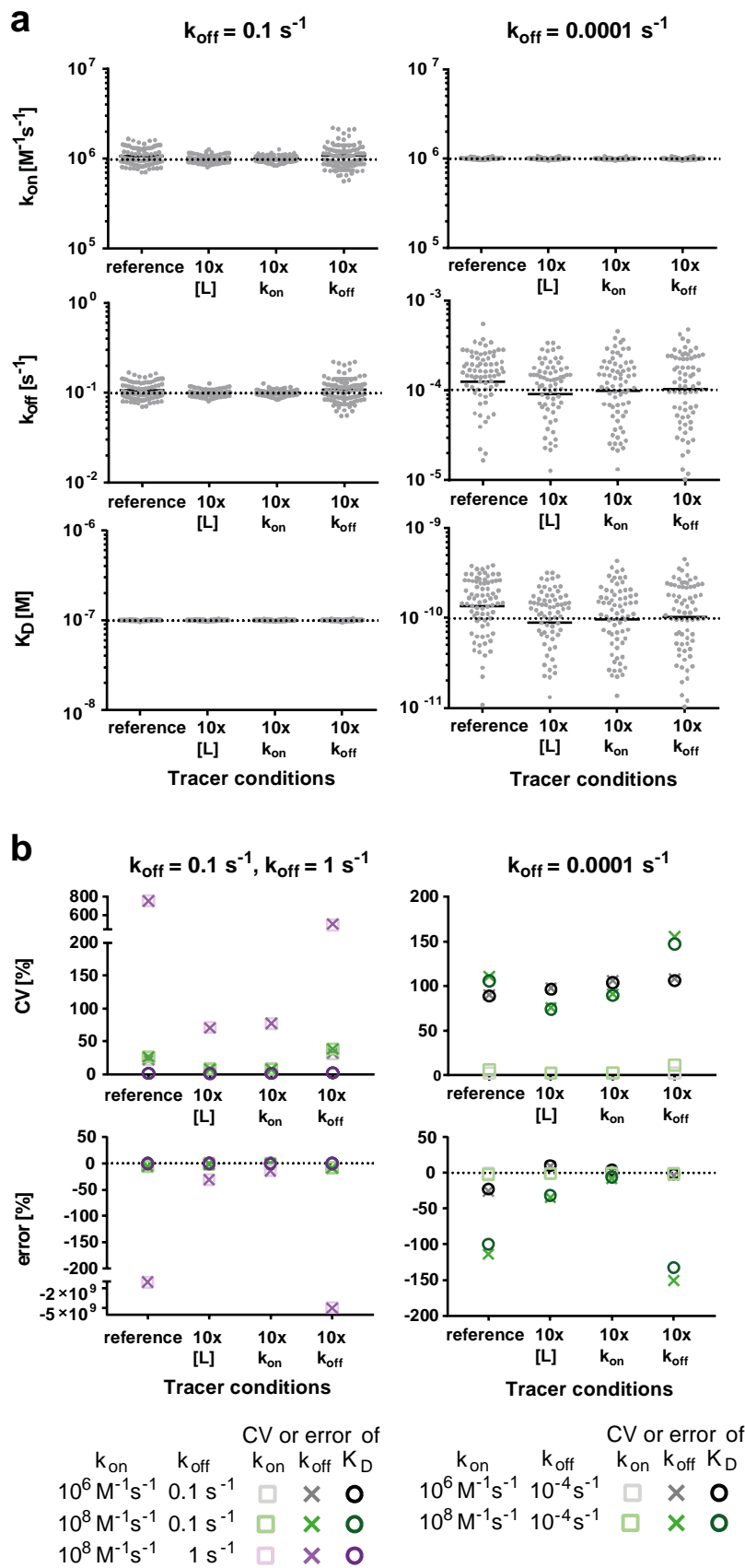


Figure 17: Effect of the concentration and the binding kinetics of the tracer on precision and accuracy of the Motulsky-Mahan model

Results from Monte Carlo analyses for a fast and a slow dissociating kinase-compound pair (both with a k_{on} of $10^6 \text{ M}^{-1}\text{s}^{-1}$ (panel a, b) or alternatively $10^8 \text{ M}^{-1}\text{s}^{-1}$ (panel b)):

a) Output values (grey dots) and input values (dotted line) for on-rates, off-rates and affinities for a higher concentration / on-rate / off-rate of the tracer. The mean of all output values is indicated as a black line. Output values with a more than 10-fold deviation from the input value are not shown, but considered for calculation of the mean, error and coefficient of variation.

b) Coefficient of variation of the output values (as measure for precision) and the relative error between input and output value (as measure for accuracy) over measurement intervals.

The precision and accuracy of the determination of binding parameters is increasing with increasing concentration or on-rate of the tracer, especially for the determination of on- and off-rates of fast dissociating kinase-compound pairs. The 10x higher off-rate was not sufficient to reach an improvement for precision and accuracy.

Another possibility to cope with the slow and/or fast off-rate problem could be the use of another tracer concentration or another tracer with other binding kinetic properties (tracer and kPCA probe are used synonymously). When comparing simulated kPCA traces (with measurement intervals of 10 seconds) for compound-kinase pairs with the same affinities but different off-rates (10^{-1} s^{-1} or faster), it becomes obvious that the traces become better distinguishable with higher tracer off-rates (Figure 16a+c) and higher tracer on-rates (Figure 16b+c) as compared to the reference traces (Figure 14b). A 10-fold higher tracer concentration rate leads to the same effect as a 10-fold faster tracer on-rate. A tracer with a slower off-rate alone has the disadvantage that the TR-FRET signal decreases (Figure 16a). To diminish this effect either the tracer has to be used in a higher concentration or should also have a higher on-rate (Figure 16c). It was assessed how the tracers' concentration and binding kinetics influence the precision and accuracy of the Motulsky-Mahan model equation. For that reason, Monte Carlo analyses were performed as described in 5.1.2.1 for 1) a kinase-compound pair with a fast off-rate (0.1 s^{-1}) and 2) a kinase-compound pair with a slow off-rate (0.0001 s^{-1}) and different on-rates, respectively. Thereby, kPCA traces were simulated with different tracer concentrations, on-rates and/or off-rates (and standard observation times of 394 s and measurement intervals of 10 s). A tracer with a higher on-rate or a higher tracer concentration, leads to a higher precision (lower coefficient of variation) and accuracy (smaller difference between results and true values) for the determination of on- and off-rates of the fast off-rate kinase-compound pair (Figure 17). In other words, the fast-off-rate-boundary for precise and accurate determination of binding kinetics parameters is shifted to faster off-rates (diminishing the fast off-rate problem). If the off-rate of the kinase-compound pair is 1 s^{-1} instead of 0.1 s^{-1} , precision and accuracy for the determination of binding kinetics parameters is also improved, but the precision is still too low (Figure 17b). On the other hand, a 10-fold faster off-rate cannot solve the fast off-rate problem. Interestingly, there is also an improvement of the accuracy for the determination of off-rates and affinities of the slow off-rate kinase-compound pair when using a faster-on tracer or a higher tracer concentration (Figure 17b). Yet, the precision is still too low so that the slow off-rate problem cannot be solved.

5.1.2.4 Combined effect of various parameters

In reality, it is not only one parameter that varies in different assays. Here it was simulated how the combined effect of tracer binding kinetics and concentration as well as incubation time and interval effect the precision and accuracy of the Motulsky-Mahan model within the parameter space. Thereby, real assays (as developed in chapter 5.2.1) served as basis for the simulations. To facilitate the comparison, the fluctuation observed in the BTK assay was also applied for simulation of the other kinase assays. The Monte Carlo analyses were performed as described in chapter 5.1.1 for hypothetical compounds with defined on- and off-rates (for kinase binding) to span a wide range of

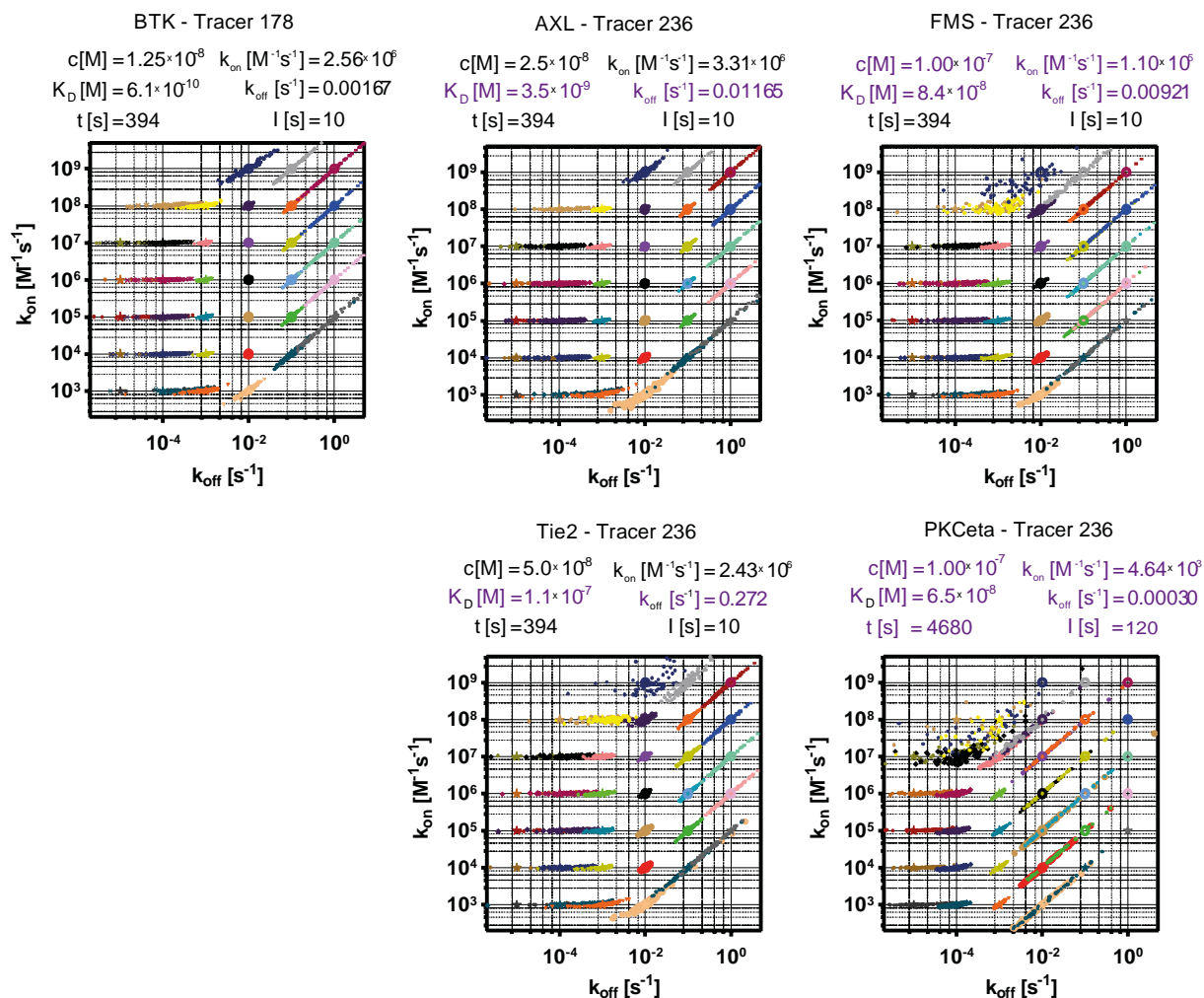


Figure 18: Combined effect of various parameters on the precision and accuracy of the Motulsky-Mahan model

The k_{on} - k_{off} plots represent the input (large symbols) and output binding kinetic parameters (small symbols) from Monte Carlo analyses. The same colors are applied for corresponding input and output data. Monte Carlo analyses comprised simulation of 100 kPCA traces for 35 hypothetical compounds with different on- and off-rates (= input data) and evaluation of the simulated data with the Motulsky-Mahan model to calculate the binding kinetics of the respective compound (= output data). For better comparability between the assays, the TR-FRET signal fluctuation observed in the BTK assay (in a real experiment; refer to chapter 4.3.3) was applied for all kinase assays. Otherwise the simulations were performed under the conditions used in the respective assay (tracer concentration c , tracer binding kinetics (k_{on} , k_{off} , and affinity K_D), observation time (t) and measurement interval (l); as indicated in the figure and listed in Table 6 and Table 7 in appendix B). Major deviations of the other kinase assays compared to the BTK assay are highlighted in purple.

The output data for the BTK assay and the AXL assay are very similar, despite the fact that the tracer in the AXL assay possesses approximately a 10-fold faster dissociation rate constant. The output data for FMS and Tie2 assay are similar to each other and similar to the BTK assay. Albeit there is an exception: The output data for fast on-rates of the compound are less scattered in the BTK assay as compared to the Tie2 and FMS assay. In comparison to the BTK assay, the tracer in the FMS assay possesses approx. a 10-fold faster off-rate and 10-fold slower on-rate, respectively, while the tracer in the Tie2 assay possesses approximately a 100-fold faster off-rate. This illustrates, that it is the affinity and concentration of the tracer (together with the applied compound concentration) which decide about the highest on-rates that can be determined with the assay. In general, the k_{off} imposed boundaries for precise and accurate determination of binding parameters are only very slightly affected by binding kinetics of the tracer: The precision is lower in the FMS assay with the approx. 10-fold slower on-tracer. The PKCeta assay illustrates, that these k_{off} imposed boundaries are mainly dependent on the observation time (for slow off-rate problem) and incubation interval (for fast off-rate problem): In comparison to BTK assay, the observation time and measurement interval is increased, shifting the boundaries to slower off-rates. Additionally, the effect of the slow on-rate and the low affinity of the tracer occurs (stronger than in FMS assay).

binding properties. Figure 18 depicts the input binding kinetics data along with the output binding kinetics data for the different kinase assays distinguishing themselves through the applied observation time, measurement intervals, tracer concentration and/or the tracer binding kinetics (and affinity). The examples show, that the binding kinetics of the tracer have a lower impact on the k_{off} imposed boundaries for precise and accurate determination of binding parameters as compared to the observation time and the measurement interval: The boundaries are only shifted to slower off-rates for the PKCeta assay where both the observation time and the measurement interval were longer as compared to the other assays. Moreover, also the slower on-rate of the tracer in the FMS and the PKCeta assay led to a lower precision in relation to the other assays. The tracer controls (without compound) of the BTK, AXL and Tie2 assays reached 100% equilibrium within the 394 seconds (observation time), while the FMS and PKCeta tracer reached $\approx 99.97\%$ and $\approx 97.25\%$ equilibrium within the observation time (Equation 8). This is also a result of the slow on-rate of the tracers. Monte Carlo analyses of PKCeta with a 10 seconds interval for 400 s observation time (tracer reached $\approx 26.33\%$ equilibrium) lead to imprecise and inaccurate results over the entire $k_{\text{on}}-k_{\text{off}}$ plot (not shown), illustrating that equilibrium of the tracer is also a prerequisite (whereby good results were also observed for $\approx 80\%$ equilibrium). However, also the analysis in chapter 5.1.2.3 showed that the on-rate of the tracer impacts the precision and in this analysis equilibrium was reached for both the tracer with the higher and the slower on-rate. The examples of simulations in Figure 18 further illustrate that especially the affinity and the concentration of the tracer determine the highest compound on-rate which is determinable for given compound concentrations. Possible explanations for the observed phenomenon are as follows: (Under given compound binding characteristics and concentrations) the concentration and affinity of the tracer, and to a lesser extent the on-rate of the tracer, determine whether the compound traces are distinguishable from the control traces (background or tracer without compound, respectively): e.g. for a lower tracer affinity and/or concentration with a relatively slow on-rate, a fast associating and high affinity compound immediately reduces the TR-FRET signal to the background signal so that there is no competition observable. Yet, higher compound on-rates can be determined if the compound concentration is reduced so that the compound trace is distinguishable from the background trace. The maximum TR-FRET signal is a result of the tracer concentration and affinity for the kinase (and the concentration of the kinase). The smaller the maximum TR-FRET signal, the higher the impact of the fluctuation in the TR-FRET signal and therefore, the higher the scatter in the signal trace. With a higher scatter, a low deviation between the compound trace and the background signal (or the tracer control) cannot be detected.

Summary of the results: The k_{off} imposed boundaries for precise and accurate determination of binding parameters when using the Motulsky-Mahan model can be stretched: Longer observation times reduce the slow off-rate problem and a higher frequency of measurement reduces the fast off-rate problem. Both a higher tracer concentration and a tracer with a higher on-rate, respectively, have the same effect and also contribute to the reduction of the fast off-rate problem, albeit to a

lesser extent than the measurement interval. However, the percentage of equilibrium reached in the tracer control within the observed time frame can have a high impact on precision and accuracy (around 80% equilibrium are sufficient). The tracer concentration and affinity (and to a lesser extent the on-rate of the tracer), together with the applied concentrations of the compound, have an impact on the lowest and highest determinable compound on-rate.

5.1.3 Effect of errors on accuracy

In this chapter, the robustness of the method (kPCA combined with the Motulsky-Mahan model) was investigated: It was assessed how errors influence the kPCA traces and the accuracy of the Motulsky-Mahan model equation. Monte Carlo simulations and analyses were performed as described in chapter 4.3.3 for 1) a kinase-compound pair with a fast off-rate (0.01 s^{-1}) and 2) a kinase-compound pair with a slow off-rate (0.0001 s^{-1}) and an on-rate of $10^{-6} \text{ M}^{-1}\text{s}^{-1}$, respectively. The kPCA traces were simulated by using the binding kinetics and a fluctuation in the TR-FRET signal as observed in a real experiment (BTK assay). The standard kPCA setting (394 s observation time, 10 s measurement interval) were applied for 1) the fast off-rate compound, while the observation time for the 2) slow off-rate compound was extended to 1594 s (using 10 s measurement intervals). That way, the reference kPCA simulation (without an error) has a good precision and accuracy for determination of binding parameters for both the fast and the slow dissociating compound. Otherwise, the kPCA traces were simulated with an error, but always analyzed in the same way with the Motulsky-Mahan model equation to evaluate the influence of this error.

A concentration error in a single well can result from transfer problems when using Digilab's Hummingbird Benchtop System (refer to methods chapter 4.2.1.3). This error can be detected in the kPCA plot: Discrepancy between best-fit curves and the corresponding data points for 2 or more whole concentration traces (Figure 19). Monte Carlo analysis revealed that such an error has almost no influence on accuracy of the determination of binding parameters for the slow dissociating compound and of off-rates for the fast dissociating compound (even for a relative concentration error of 80% for a single concentration: 50 nM instead of 250 nM compound). However, the on-rate and affinity of the fast dissociating compound is determined precisely but inaccurately (Figure 20). Even so, if the affected compound trace is removed from the analysis, also these parameters can be determined correctly again.

For an error in the stock concentration or a dilution error, the best-fit curves correspond with the data points, so that the error is not detectable in the kPCA traces (Figure 19). However, even a relative stock error of 40% (4-point 10-fold serial dilution starting with 3500 nM instead of 2500 nM) or a relative dilution error of 20% (12-fold instead of 10-fold dilution series, e.g. due to residuals on/in the pipette) is not severely hampering the accuracy of the determination of the binding parameters (Figure 20): the discrepancy between result and true value is less than 3-fold. In addition to human errors, solubility and stability of the compound could be reasons for errors in the stock concentration.

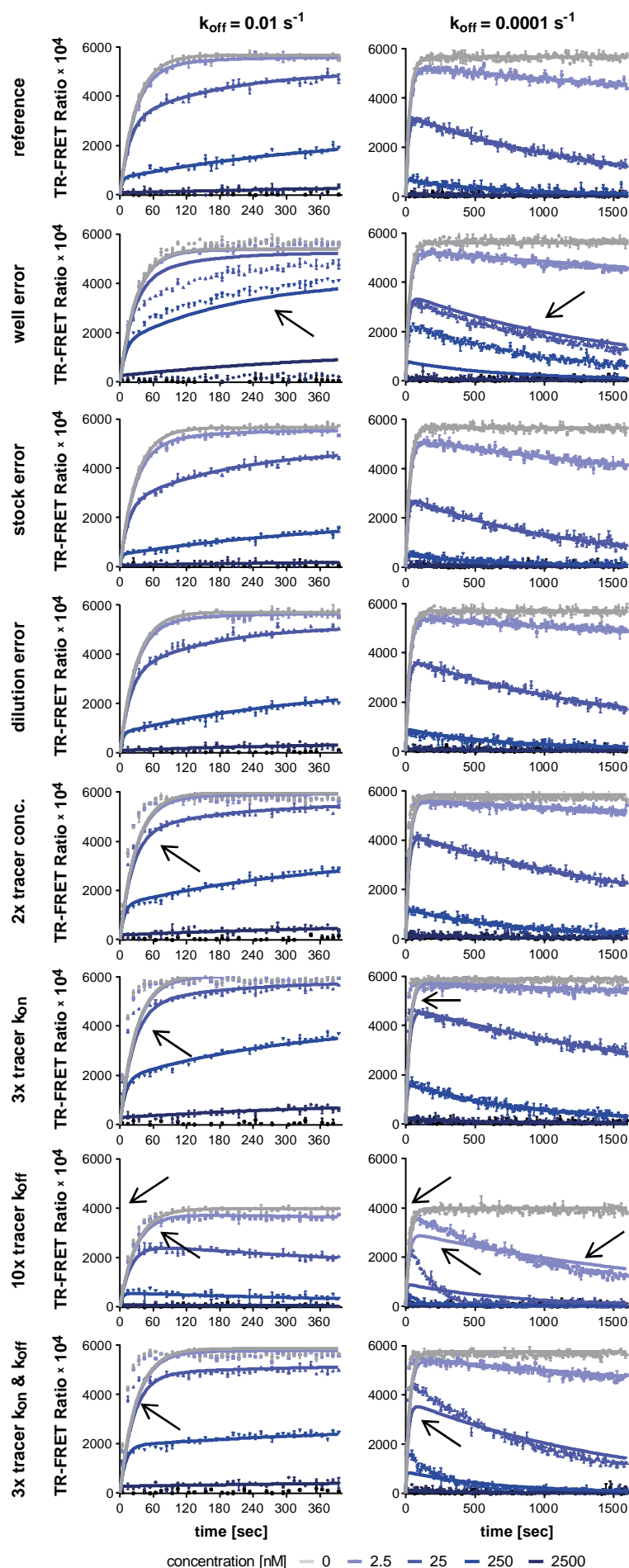


Figure 19: Effect of experiential errors on kPCA traces

Simulation of kPCA traces and fit curves for a fast off-rate and a slow off-rate compound-kinase pair (both with a k_{on} of $10^6 \text{ M}^{-1}\text{s}^{-1}$) in a way that neither the fast off-rate nor the slow off-rate problem occurs in the reference simulation.

The kPCA traces were simulated with errors:

- a single well error can result from transfer problems when using Digilab's Hummingbird Benchtop System (here: 50 nM instead of 250 nM compound),
- a stock concentration error can result from handling error, compound solubility or stability issues (here: 4-point 10-fold serial dilution starting with 3500 nM instead of 2500 nM),
- a dilution error can result from miscalibrated pipettes or handling errors (here: 12-fold instead of 10-fold dilution series),
- a wrong tracer concentration can result from tracer solubility or stability issues and handling errors,
- wrong tracer binding kinetics can be determined during assay development.

The plots show the influence of these errors on the kPCA trace. Visible discrepancies between best-fit curves and the corresponding data points are indicated with arrows.

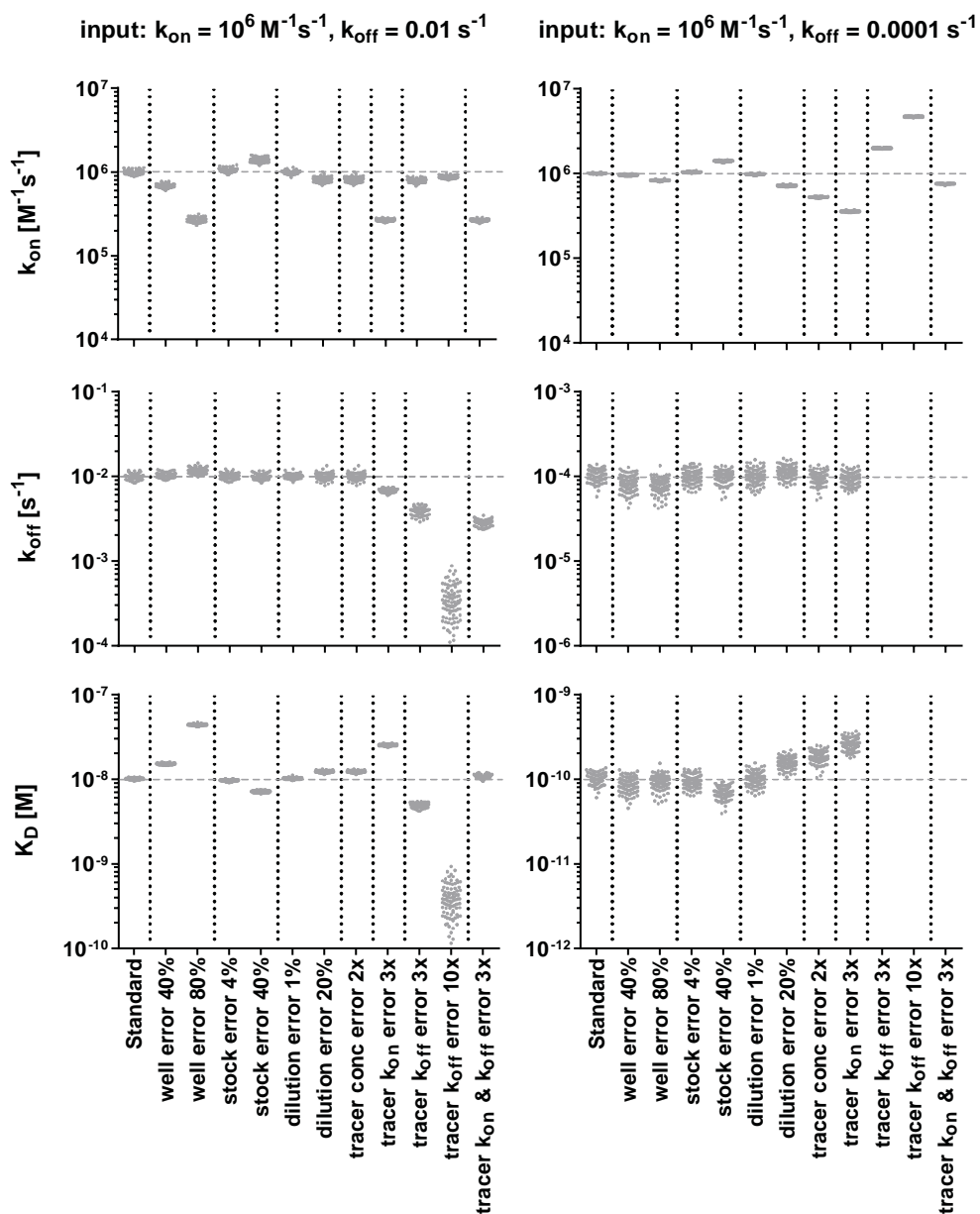


Figure 20: Effect of experiential errors on the accuracy of the Motulsky-Mahan model

Results from Monte Carlo analyses for a fast and a slow dissociating kinase-compound pair (both with a k_{on} of $10^6 \text{ M}^{-1} \text{ s}^{-1}$). Output values (grey dots) and input values (dashed line) for on-rates, off-rates and affinities over different experimental errors (related to Figure 19). In the cases, where the grey dots are not visible, the output values drifted to extremely low “non-sense” values (k_{off} : 10^{-13} - 10^{-14} s^{-1} , K_D : 10^{-19} - 10^{-20} s^{-1}).

Some errors have a negative impact on the accuracy of the determination of binding parameters. Thereby, the accuracy for slow and fast dissociating compounds is affected in a different manner. Highest accuracy issues are observed for the well error (concentration error for a single compound concentration) and for false on- and off-rate or concentration of the tracer. The well error can be easily eliminated during the analysis (mask the affected concentration for regression), while it is essential to avoid a tracer error.

Errors in the applied tracer concentration and assumed tracer binding kinetics were identified to have a great influence on the accuracy of the method. These errors can be detected in the kPCA plot: There is a discrepancy between the best-fit curves and the corresponding data points for all

concentration traces, whereby the best-fit curve approaches or crosses the data points (Figure 19). A 2-fold higher tracer concentration or on-rate (as assumed in the Motulsky-Mahan model) has almost no impact on the determination of binding parameters for fast dissociating compounds, but leads to an underestimation of the on-rate and affinity for slow dissociating compounds (Figure 20). A 3-fold higher tracer concentration or on-rate has the same effect for slow dissociating compounds, but with the 3-fold error also the accuracy of the determination of binding parameters for fast dissociating compounds is reduced: the calculated on-rates, off-rates and affinities are lower than the true values (Figure 20). Moreover, a faster off-rate of the tracer (as assumed in the Motulsky-Mahan model) also reduces the accuracy for slow and fast dissociating compounds in a different manner: For fast dissociating compounds, the on-rate is still determined accurately, while the calculated off-rate is lower and the calculated affinity is higher as compared to the true value. For slow dissociating compounds, the on-rate is overestimated, and the calculated off-rates and affinities drift to extremely low “non-sense” values (k_{off} : 10^{-13} - 10^{-14} s⁻¹, K_D : 10^{-19} - 10^{-20} s⁻¹). A 3-fold higher on-rate and off-rate of the tracer (as assumed in the Motulsky-Mahan model) also influences accuracy: For fast dissociating compounds, the calculated on-rate and off-rate of the compound are lower than the true values, while the affinity is still determined accurately. For slow dissociating compounds, the impact on the on-rate is low, while the calculated off-rates and affinities drift to extremely low “non-sense” values (k_{off} : 10^{-13} - 10^{-14} s⁻¹, K_D : 10^{-19} - 10^{-20} s⁻¹).

In addition to these experimental errors, there are also rather conceptual errors: The Motulsky-Mahan model assumes reversible one-step 1:1 binding. It was assessed, how the signal trace is affected if the binding mode is more complex, e.g. irreversible binding or induced fit, and how the calculated apparent on- and off-rates correspond with the real values. For that reason, the kPCA traces were simulated with COPASI as described in 4.3.8 by using an irreversible binding model or an induced fit model, respectively. Then, the simulated traces were analyzed by using the Motulsky-Mahan model (standard procedure in GraphPad Prism as applied for experimentally obtained traces). The best-fit curves match exactly to the data points from irreversible binding. The calculated on-rates are consistent with the true on-rates, while the calculated off-rate is very slow but obviously underestimated. On the other hand, there is a discrepancy between the best-fit curves and data points from induced fit binding, whereby the best-fit curve crosses the data points twice (Figure 21b). That way, induced fit binding could be detected in the kPCA traces. The calculated apparent on- and off-rates might be a kind of translation of the more complex interaction mode into simple one-step binding within the observed timeframe.

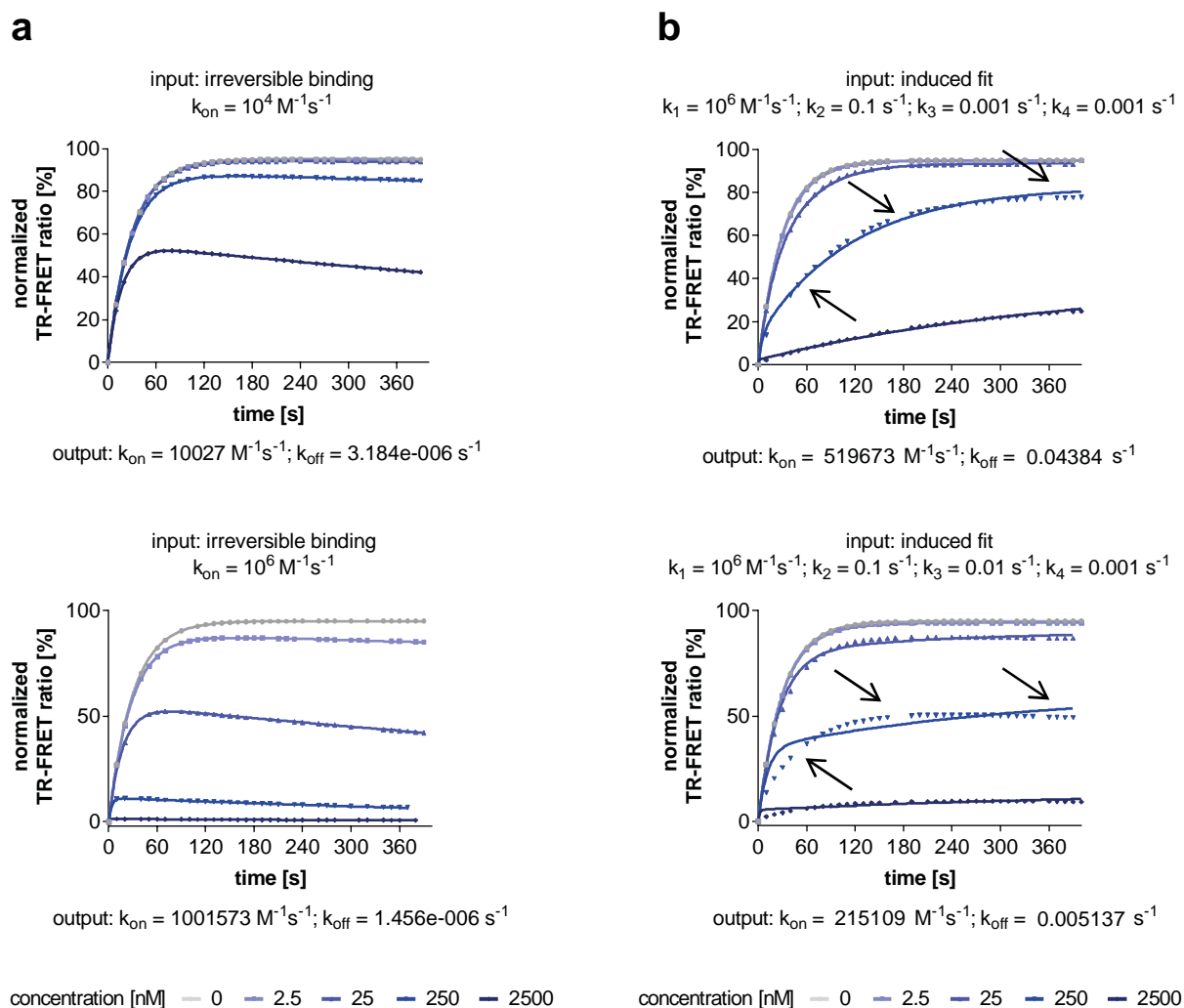


Figure 21: Effect of conceptual errors on kPCA traces and calculated on- and off-rates

kPCA traces were simulated with COPASI as described in 4.3.8 by using an irreversible binding model (a) or an induced fit model (b), respectively, and the traces were then analyzed by using the Motulsky-Mahan model (GraphPad Prism). The best-fit curves match exactly to the data points from irreversible binding (a), while the best-fit curve crosses the data points twice for induced fit binding (b). For irreversible binding, the on-rate was calculated accurately, while the determined off-rate was very slow but obviously underestimated (a). For induced fit binding, the apparent on- and off-rates could be seen as a 1:1 binding translation of the more complex interaction mode within the observed timeframe (b).

Summary of the results: The method is robust with regard to smaller concentration errors of the compound (e.g. stock concentration, dilution error). Other experimental errors usually reduce the accuracy for slow and fast dissociating compounds in a different manner. Highest accuracy issues arise from false on- and off-rates or concentration of the tracer. Most errors that have an impact on the accuracy of the determination of binding parameters are visible in the kPCA traces, whereby each error leads to certain discrepancies between the best-fit curves and the data points that are distinguishable from the effects of other errors. For instance, induced fit binding that is evaluated with the Motulsky-Mahan model assuming reversible one-step binding leads to best-fit curves which

cross the data points twice. On the other hand, the on-rate of an irreversible binder (assuming one-step binding) is determined accurately with the Motulsky-Mahan model and the best-fit curve matches exactly with the data points.

5.1.4 Limitations of approaches for analysis of kinetics of tracer-target binding

The “Association kinetics -- two or more concentration of hot” model (GraphPad Prism) is routinely used for the determination of tracer binding kinetics. Here, this model was assessed for precision and accuracy to get a better understanding of the method and to learn how to avoid an error in determination of the tracer binding kinetics. Moreover, an alternative experimental procedure for the determination of the binding kinetics was implemented: An association step was directly followed by a dissociation step for a concentration series of the tracer (refer to appendix C). For the analysis of this alternative experiment, the “Association then dissociation” model (GraphPad Prism) was extended to an “Association then dissociation - two or more concentration of hot” model (refer to appendix C), enabling global curve fitting of the model equation to the tracer concentration series “association then dissociation” traces. Monte Carlo analyses were performed as described in chapter 4.3.3 for both the standard “Association kinetics -- two or more concentration of hot” model (400 s association time, 10 s incubation interval) and the new “Association then dissociation - two or more concentration of hot” model (400 s association time, 1500 s dissociation time, 10 s incubation interval) enabling benchmarking of the two models. These analyses were performed for hypothetical tracers with different on- and off-rates (for kinase binding) to span a wide range of binding properties. Figure 22a shows typical examples of simulated signal traces for both models and for a fast, medium and slow dissociating tracer, respectively. Figure 22b depicts the input binding kinetics data along with the output binding kinetics data. For the majority of on- and off-rate combinations both models worked equally well and determined the parameters with high precision and accuracy. Yet, the precision for determination of the off-rates and affinities of the slowly dissociating tracers (10^{-5} s^{-1}) was low for the “Association kinetics -- two or more concentration of hot” model. But by increasing the observation time, also slow off-rates can be determined with high precision. Another problem is, that if the affinity of the tracer was 10^{-6} or 10^{-7} M, the binding kinetic parameters precisely determined with the “Association kinetics -- two or more concentration of hot” model are not consistent with the true values (input data), while the affinities are still determined accurately. In these cases, the “Association then dissociation - two or more concentration of hot” model performs a little better: Only, if the off-rate of the tracer was 1 or 10 s^{-1} , the binding kinetic parameters are not determined accurately and precisely by using this alternative model. However, when increasing the frequency of measurement the boundaries of both models can be shifted towards lower affinities or faster off-rates, respectively. Moreover, the accuracy issue is visible in the plots, where the

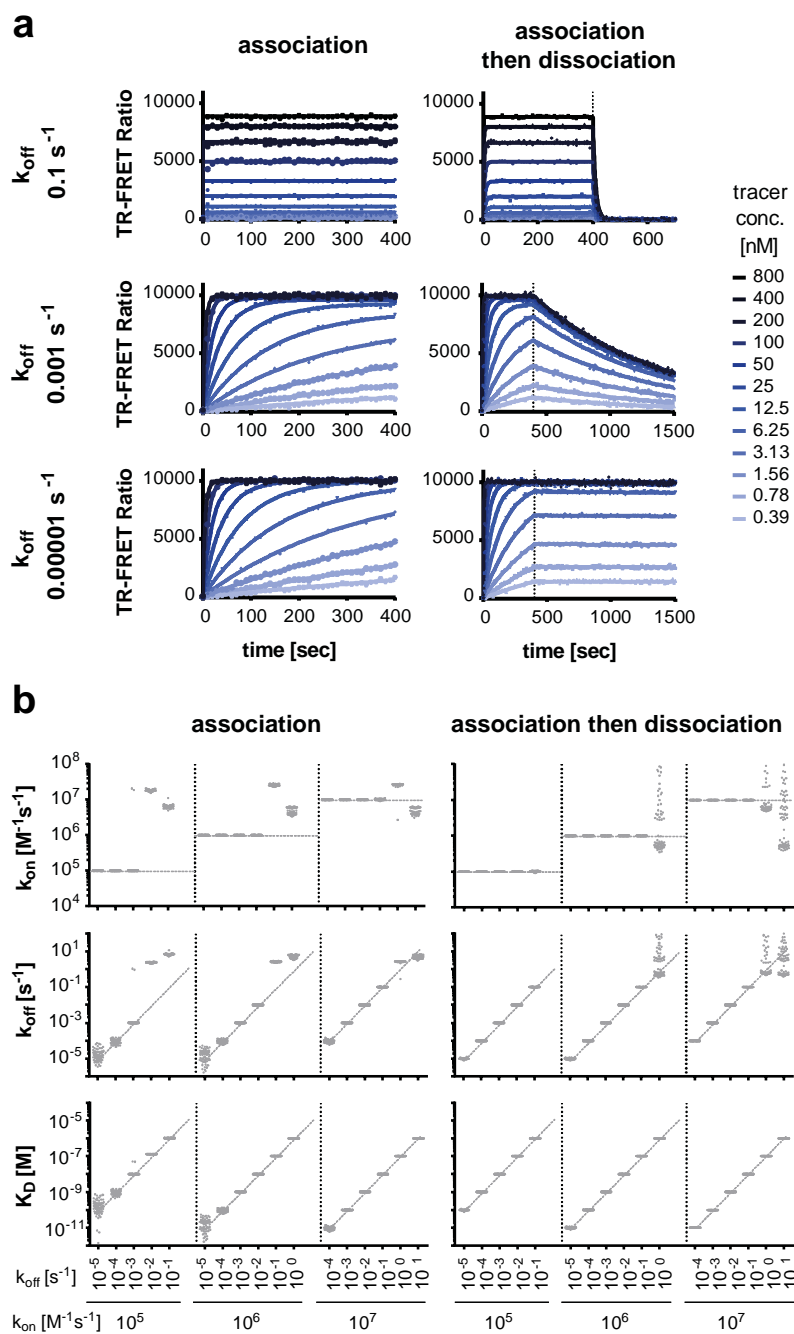


Figure 22: Comparison of two approaches for determination of kinetic rate constants of tracer-target binding

Determination of tracer binding kinetics can be performed with an “Association kinetics -- two or more concentration of hot” experiment and model or alternatively with a newly implemented “Association then Dissociation - two or more concentration of hot” experiment and model (refer to appendix C). Monte Carlo analyses were performed to assess precision and accuracy for determination of tracer binding kinetics and to benchmark the two models. A measurement interval of 10 s was used for the analysis.

a) Representative simulated tracer binding traces and fit curves for both models and for a fast-, medium- and slow-dissociating tracer (with a k_{on} of $10^6 \text{ M}^{-1}\text{s}^{-1}$, respectively).

b) Input (dashed line) and output binding kinetic parameters (grey dots) from Monte Carlo analyses. The output data are consistent with the input data (same on-rate, off-rate and affinity) for most on- and off-rate combinations (for both models). With the “association” model, there is a low precision for the analysis of tracers with slow off-rates of 10^{-5} s^{-1} ; which can be eliminated by increasing the observation time (not shown). Moreover, there is a low accuracy for the analysis of tracers with affinities of 10^{-6} or 10^{-7} M . The “association then dissociation” model performs a bit better, but there is a similar problem: There is a low precision and accuracy for the analysis of tracers with off-rates of 1 or 10 s^{-1} . For both models, a higher frequency of measurement diminishes these problems for the analysis of fast dissociating tracers (not shown).

measured signal goes up (and down) very fast und the best-fit curve even faster (mismatch). In real experiments, the dissociation in the “Association then Dissociation” experiment is initiated by addition of an excess of unlabeled competitor. Therefore this experiment can be hampered by rebinding effects, especially if the concentration of the unlabeled compound is too low.

Summary of the results: When using the “Association kinetics -- two or more concentration of hot” experiment and model for determination of the binding kinetics of the tracer, problems can arise for the analysis of fast and slow dissociating tracers. In case of uncertainty, Monte Carlo simulation can help to assess the situation. If the coefficient of variations for a slow off-rate and the corresponding affinity are high (depending on signal fluctuation; in this example $CV > 30\%$), the observation time should be increased to obtain reliable results. If the affinity is low (depending on measurement frequency and signal fluctuation; here: $> 10^{-7}$ M), fast off-rates and the corresponding on-rates might be determined inaccurately and the measurement frequency should be increased as far as possible. An alternative is the use of the “Association then Dissociation - two or more concentration of hot” experiment and model that performs a bit better for the fast dissociating tracers but still has a limit (depending on measurement frequency and signal fluctuation; here: $k_{off} > 1 \text{ s}^{-1}$). Moreover, fast and slow dissociating ligands can be spotted more intuitively in the signal trace plot. For the dissociation step, the unlabeled competitor should be provided in excess and should associate fast to avoid rebinding of the tracer and related problems.

5.1.5 The ‘kinetics of competitive binding equation’ and systematic signal decay

kPCA measurements can be influenced by fluorescence losses e.g. due to photobleaching or cell sedimentation. To cope with systematic signal decay Schiele, Ayaz and Fernández-Montalván [84] extended the Motulsky-Mahan model by multiplication with a signal drift term ($Y(\text{Drift}) = Y \times \exp(-K_{\text{drift}} \times \text{time})$) assuming mono-exponential decay (Figure 45a in appendix D). An alternative approach to overcome the problem is a Motulsky-Mahan model derived for normalized kinetic traces, where normalization eliminates the background fluorescence and signal drift (Figure 45b in appendix D). The normalization of the signal trace (and the model) is performed according to Equation 2. The model equation is provided in appendix D. In collaboration with Bosma *et al.* [122] it was demonstrated that the binding kinetic parameters determined with a radioligand competition assay are in good agreement with those determined with kPCA and the Motulsky-Mahan model with the drift term (to cope with systematic signal decay). There is a strong correlation (Spearman r for K_D : 0.97, k_{on} : 0.92, k_{off} : 0.97) and small mean log difference (K_D : 0.15; k_{on} : 0.09; k_{off} : 0.12) for binding kinetic rate constants and affinity (see Figure 23). Here, the kPCA data were normalized and reanalyzed with the derived Motulsky-Mahan model for normalized traces (see Figure 23a). With this alternative approach the correlation between radioligand data and kPCA data is even slightly stronger (Spearman r for K_D : 0.98, k_{on} : 0.93, k_{off} : 0.98) and the mean log differences are similar

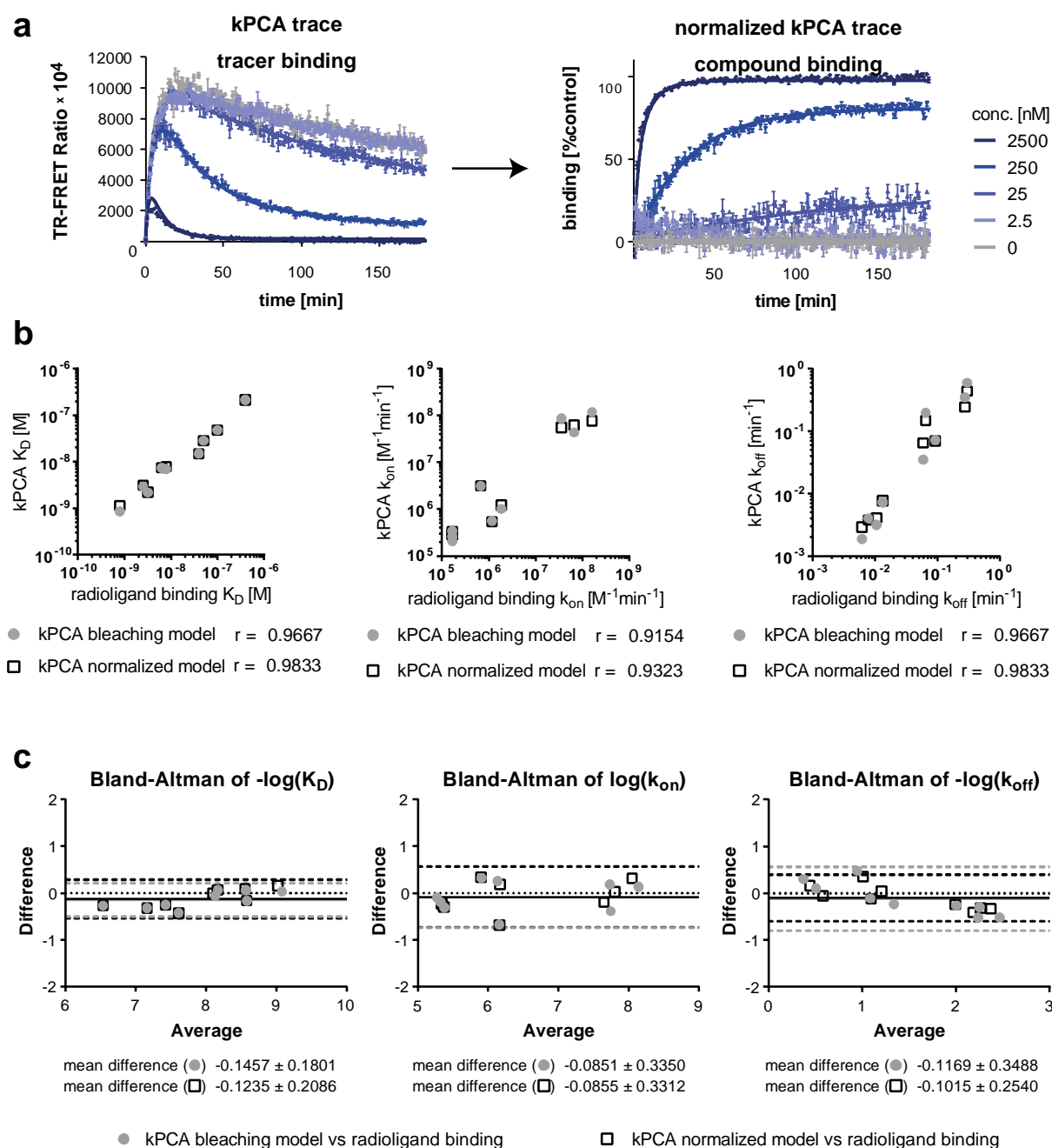


Figure 23: Comparison of two approaches coping with kPCA traces with systematic signal decay

Schiele, Ayaz and Fernández-Montalván used a Motulsky-Mahan model extended by a signal drift term (drift model) to analyze kPCA traces with systematic signal decay [84]. An alternative is the newly implemented analysis comprising normalization of the kPCA traces and a derived Motulsky-Mahan model (normalized model) able to analyze these traces (refer to appendix D).

a) Representative plots of a kPCA tracer trace analyzed with the drift model and a normalized kPCA trace (representing compound binding) analyzed with the normalized model (more examples in Figure 45 appendix D).

b) There are strong correlations between binding parameters determined by kPCA and those determined by a radioligand competition assay (correlation coefficients are indicated in the figure). The correlations are stronger when using the normalized model as compared to the drift model.

c) There are small log differences (solid horizontal line) between binding parameters determined by kPCA and those determined by a radioligand competition assay (means \pm standard deviations are indicated below the graphs). Analysis of the kPCA traces with signal decay by the normalized model (instead of the drift model) leads to a better agreement between the off-rates determined by kPCA and the radioligand assay (dashed lines represent the upper and lower 95% limits of agreement).

for on-rates and a little smaller for affinities and off-rates (K_D : 0.12, k_{on} : 0.09, k_{off} : 0.10) (see Figure 23b+c). Especially the off-rates determined with the normalized traces and model are more similar to the off-rates determined with the radioligand competition assay: The mean log difference of the off-rates and particularly the standard deviation of the mean are smaller (0.10 ± 0.25) as for the comparison between the drift model with the radioligand competition assay (0.12 ± 0.35). Moreover, the normalized kinetic traces can be more easily interpreted visually (normalization eliminates signal decay) and compared with traces from other experiments (normalized traces are independent from TR-FRET signal scaling).

Summary of the results: The Motulsky-Mahan model extended by a drift term and the normalized Motulsky-Mahan model were applied for the determination of binding parameters by global curve fitting to kPCA traces with systematic signal decay or the corresponding normalized traces, respectively. The results were compared to binding parameters determined with a radioligand competition assay. The binding data determined with the newly implemented normalized Motulsky-Mahan model correlated more strongly with the data determined by radioligand binding. Compared to the drift model, especially the off-rates obtained with the normalized model are in better agreement with the off-rates obtained by using the radioligand assay.

5.2 Large-scale analysis of kinase inhibitors' target binding kinetics

5.2.1 Binding kinetics and affinity profiling of kinase inhibitors

One main objective of this thesis was to determine the binding kinetics and affinity parameters of 270 small-molecule compounds' (listed in Table 5 in appendix A) interactions with clinically relevant kinases. In order to achieve this goal, the first necessary step is the development of a kinase assay panel allowing high-throughput profiling of these parameters. The TR-FRET-based kinetic probe competition assay (kPCA) [84] is a promising tool for this task. Additionally, the corresponding equilibrium probe competition assay (ePCA) allows cross-validation and provides affinity values required for calculation of slow off-rates (refer to reference [84], chapter 4.3.1.3 and chapter 5.1.1). The second step is the screening itself.

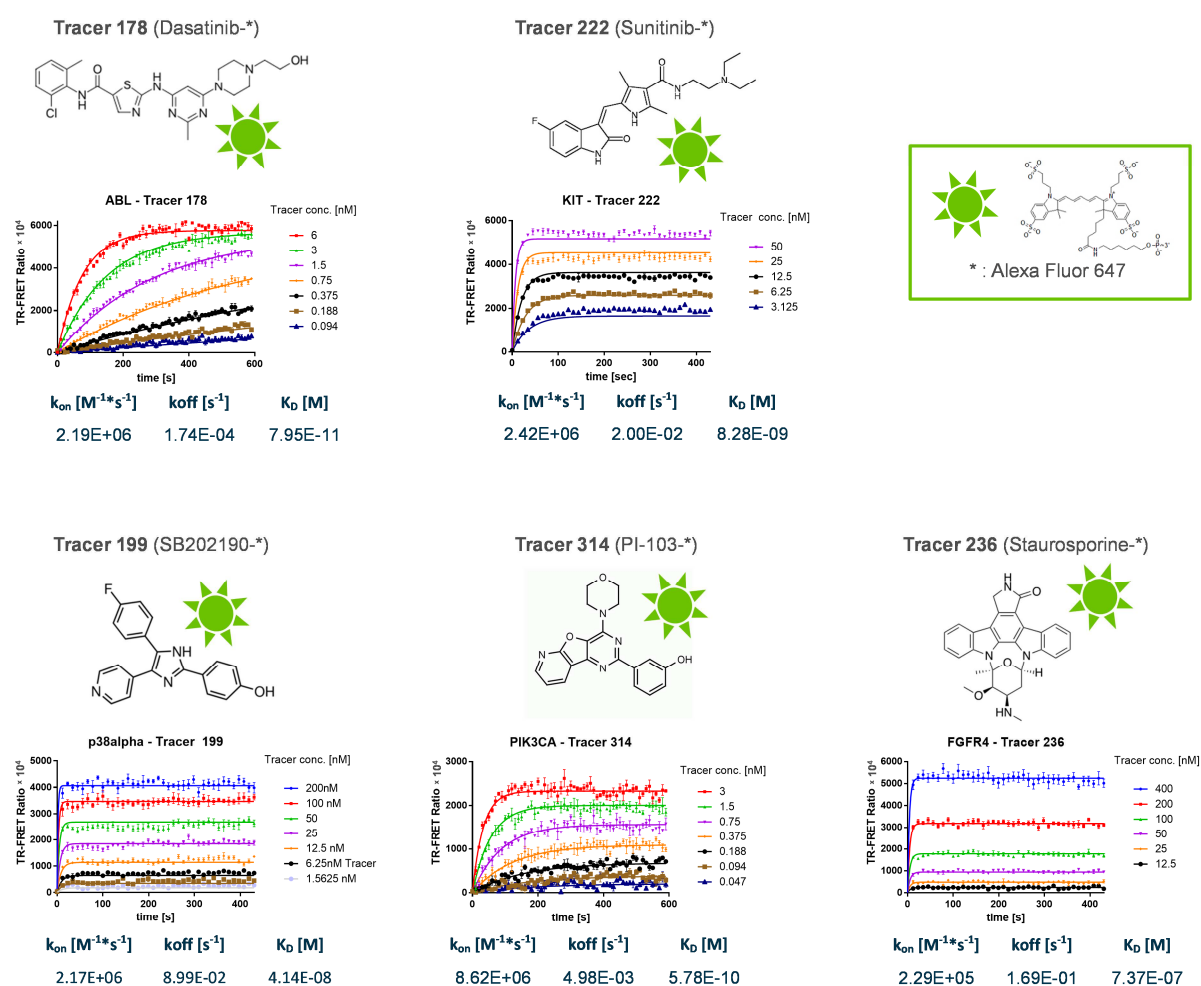


Figure 24: Kinetic characterization of probes – exemplary kinase binding traces

The 5 Kinase Tracers are multikinase inhibitor - Alexa Fluor® conjugates [94] and were used as probes for the competition assays. Their molecular background is undisclosed but the presumed inhibitor is indicated in the figure. The figure further shows exemplary kinase binding traces for increasing concentrations of these tracers (means and SD of 2 (ABL, PIK3CA) or 4 (KIT, p38 α , FGFR4) replicates) as well as the corresponding fitting curves and binding parameters determined by global nonlinear regression (refer to chapters 4.2.1.1 and 4.3.1.1). Binding traces and determined binding parameters for tracer binding to other kinases are given in Table 8 (appendix E) and Table 7 (appendix B).

Assay development

To set up the binding kinetics profiling panel, kinase assays were developed according to a standardized workflow as described in chapter 4.2.1.1, comprising tracer versus kinase titration experiments (endpoint assay) and kinetic tracer association assays (kinases are listed in Table 4 in appendix A). 32 of the kinase assays (80%) were established with the Kinase Tracer 236 as probe. Kinase Tracers 178, 199, 314 and 222 were used in 4, 2, 1 and 1 assay/s, respectively. For the 40 kinase assays, representative kinetic traces applied for determination of kinase specific assay parameters and kinetic characterization of the probes are given in Figure 24 and appendix E (Table 8). A summary about the results (such as determined assay composition, applied Kinase Tracers and their binding kinetics on kinases) is provided in appendix B (Table 6 and Table 7) and E (Figure 46a). In most assays, the ascertained tracer concentrations are in the range of the K_D of the respective tracer-kinase pair. Higher tracer concentrations were applied for tracers with the highest affinities, though (see Figure 46b in appendix E). Binding kinetic rate constants were determined by global curve fitting of the “Association kinetics -- two or more concentration of hot” equation (refer to chapter 4.3.1.1) to the tracer concentration series traces. Overall, the signal to noise ratios were (very) good, and the best-fit curves correspond with the data points (except for EGFR; refer to Table 8 in appendix E). The standard errors of the best fit parameters are low (even for the IKK β assay with the lowest signal to noise ratio). Remarkably, slightly higher errors are observed for very slow and fast off-rates of the tracers (see Figure 46a in appendix E). Accuracy of the tracer binding characteristics was validated by comparing the tracer affinities determined by endpoint analysis to affinities determined in the kinetic assay setup (calculated as described in chapter 4.3.1.1), which were in good agreement (see Figure 46c in appendix E). Additionally, the tracers’ kinetic rate constants were consistent with the values determined for the (presumed) corresponding unlabeled compound (see Figure 50 in appendix F). Almost all tracer-kinase association and dissociation rates are reasonably fast so that the kPCAs can be performed with the standard time settings (40 readings in intervals of 10 seconds). An exception is the slow Kinase Tracer 236 binding to PKC η . It was decided to choose 40 readings and time intervals of 120 seconds to achieve tracer binding equilibrium within the observed timeframe and simultaneously keep the number of readings low in order to protect the laser from wear. This also allowed using the PKC η assay to confirm the influence of kinetic intervals experimentally. Finally, it should be mentioned, that assay development was discontinued for 4 kinases: Under the applied test conditions, none of the six tested Kinase Tracers were binding to Tb-labeled HER2, JAK1 and SPHK. Although Kinase Tracer 236 was binding to Tb-labeled CHK1, the affinity is too low with the results that the required amount of tracer is too high for the high-throughput approach.

Screening

By using this newly developed binding kinetics profiling panel, the 270 known kinase inhibitors were screened against 40 kinases, including 25 targets of FDA approved inhibitors and further driver kinases to core cellular pathways and processes (a complete list of these kinases is given in Table 4 in

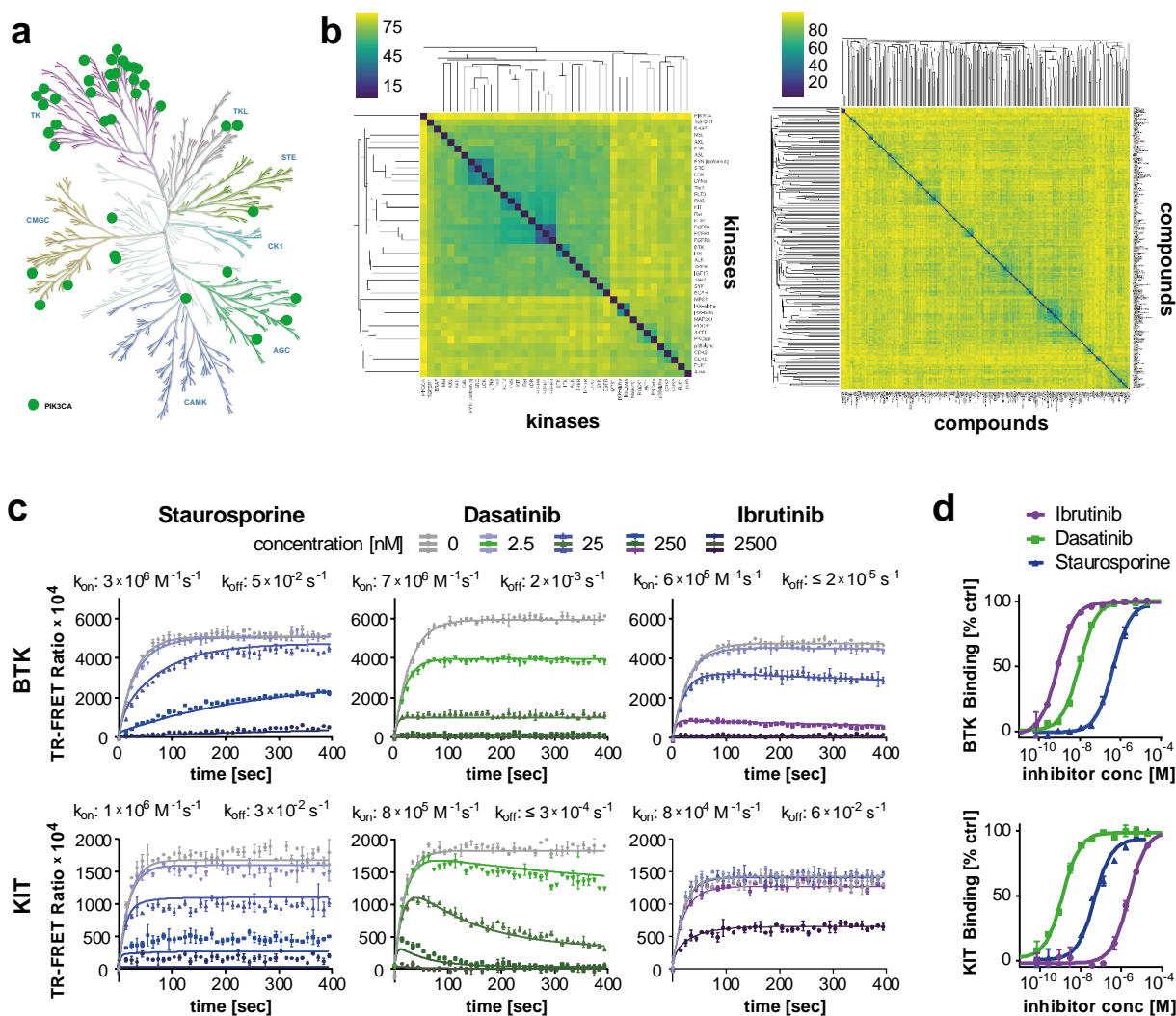


Figure 25: Overview of the large-scale binding kinetics profiling performed in this thesis

a) Visualization of the evolutionary distances of the kinases screened in this thesis within the framework of a phylogenetic tree of the human kinome (produced as described in 4.1.3). The majority of the kinases are tyrosine kinases, but there are also members of other protein kinase subfamilies and a PI3K member (PIK3CA).

b) Clustered distance matrices for kinase constructs and compound structures used in the screening panel were generated as described in 4.3.4. The right panel illustrates structural diversity of compounds (Tanimoto index was used for ECFP4 fingerprint-based similarity calculations). The left panel shows Euclidean distance matrix for kinases based on kinase sequence similarities (which were calculated with Clustal Omega). As expected, highest similarities (lowest dissimilarities) are among tyrosine kinase family members.

c) Representative traces from kinetic Probe Competition Assays (kPCAs) used for determination of compound-kinase binding kinetics. The plots show the tracer-kinase binding traces in the presence of increasing concentrations of the respective compound (means and SD from 2 replicates) as well as the corresponding fitting curves and binding kinetic parameters determined by global nonlinear regression (refer to chapters 4.2.1.3 and 4.3.1.3).

d) Representative curves from equilibrium Probe Competition Assays (ePCA) used for determination of compound-kinase equilibrium dissociation constants. The plots visualize the percentage of kinase binding for a series of compound concentrations in the presence of tracer (means and SD of 2 replicates) as well as corresponding fitting curves determined by nonlinear regression and applied to derive $K_{D,eq}$ values (for details refer to chapters 4.2.1.2 and 4.3.1.2).

Binding kinetic and affinity parameters for the 10800 kinase-inhibitor pairs screened were determined based on 108,000 kPCA traces and 21,600 ePCA curves and are given as mean from two independent experiments in the Supplementary Spreadsheet (appendix page 165ff).

appendix A). The majority of the kinases are tyrosine kinases, but there are also members of other protein kinase subfamilies and a PI3K member (see Figure 25a). PIK3CA was included in the panel in addition to the protein kinases, since the highly conserved ATP binding site is very similar for active protein kinases and PI3Ks [50], and thus PIK3CA is interesting for selectivity considerations. Moreover, the 270 small-molecule kinase inhibitors represent a diverse set of compounds: 1) comprising clinical and preclinical candidates, including 32 (91.4%) * FDA approved drugs, 2) comprising Type I, Type II, Type III and covalent inhibitors [62], and 3) covering a range of kinase targets (according to Selleck Chemicals datasheets > 58 known targets) and chemotypes. Distance matrices for kinase and compound structures illustrate structural diversity of compounds, and structural similarity of kinase sequences (Figure 25b). As expected, highest similarities (lowest dissimilarities) are observed for tyrosine kinase family members. These distance matrices were generated as described in chapter 4.3.4 and are required for the following analyses (see chapter 5.2.3).

In total, 10800 kinase-inhibitor pairs were profiled for their affinity and binding kinetic parameters in independent equilibrium (ePCA) and kinetic (kPCA) experiments as described in the methods section (chapters 4.2.1.2, 4.2.1.3, 4.3.1.2, 4.3.1.3). Typical kPCA traces (for k_{on} , k_{off} , $K_{D\ kin}$ determination) and ePCA curves (for $K_{D\ eq}$ determination) are depicted in Figure 25c-d. All experiments were conducted in quadruplicate (2 independent experiments with two replicates respectively). As expected from Monte Carlo analyses (chapter 5.1.1), the following three cases were frequently observed during evaluation of the large dataset: kinase-inhibitor pairs with **I**) model fit k_{on} similar to calculated k_{on} ($= k_{off} / K_{D\ eq}$), but model fit k_{off} and $K_{D\ kin}$ differ from calculated k_{off} ($= k_{on} \times K_{D\ eq}$) and equilibrium $K_{D\ eq}$,

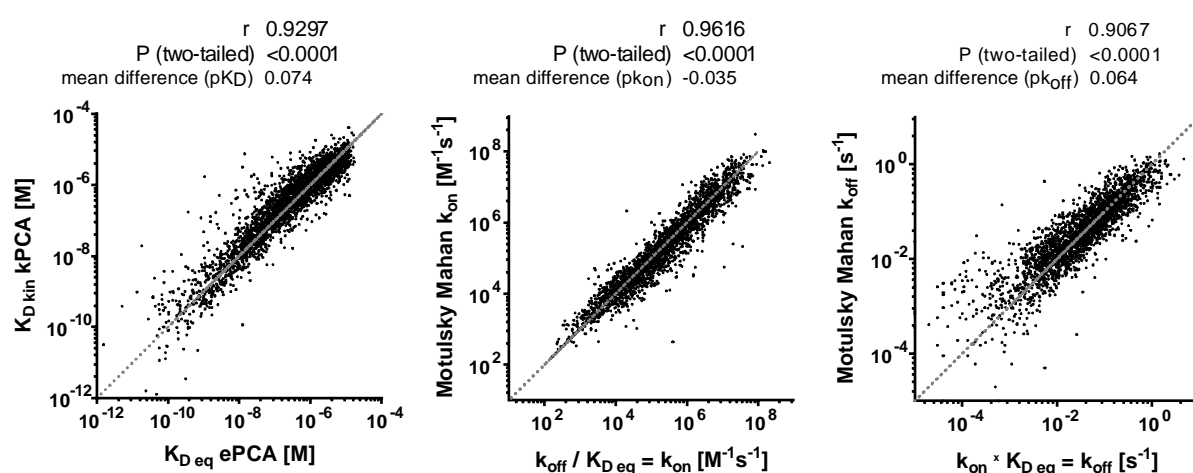


Figure 26: Comparison of binding parameters calculated from steady state (ePCA) versus kPCA model fit results
Correlation coefficients and Bland-Altman statistics are indicated above the plots. On- and off-rates were obtained from kPCA using the Motulsky-Mahan model (model fit parameters: $K_{D\ kin}$, Motulsky-Mahan k_{on} and k_{off}). The rate constants were additionally calculated by using the steady state affinities ($K_{D\ eq}$) and the relationship $K_D = k_{off} / k_{on}$ (calculated parameters). There is a good agreement between dissociation constants, on-rates and fast off-rates determined by using these two methods, but inconsistencies are observable for slow off-rates. As learned from Monte Carlo analyses (chapter 5.1.1), the calculated off-rates are more accurate and smaller than or equal to the true off-rates (smaller if equilibrium affinity was underestimated due to assay wall or unreached equilibrium).

* Current status (Jan. 2018)

respectively (refer to Figure 26), **II**) precisely determined k_{on} and $K_{D_{eq}}$, but imprecise and nonsensically low $K_{D_{kin}}$ and k_{off} (far beyond assay quantitation limit: $K_{D_{kin}} < 10^{-13}$ M; $k_{off} < 10^{-10}$ s⁻¹) and **III**) precisely determined $K_{D_{eq}}$ and $K_{D_{kin}}$, but imprecise and nonsensically high k_{on} and k_{off} (far beyond assay quantitation limit and/or beyond diffusion limit: $k_{on} > 10^9$ M⁻¹s⁻¹; $k_{off} > 10^4$ s⁻¹). The results from Monte Carlo analyses were considered for evaluation of these cases as described in chapter 4.3.1.3. The 3230 quantitative and 784 semi-quantitative binding kinetic and 4177 affinity parameters determined by this profiling approach are given as means from two independent experiments in the Supplementary Spreadsheet (appendix page 165ff). As expected from Monte Carlo analyses (Figure 18), the PKCeta kPCA enabled quantification of the lowest on-rates (refer to Figure 48 in appendix F).

Summary of the results: kPCAs and ePCAs were set up for 40 clinically relevant kinases including 25 targets of FDA approved drugs. Thereby, 5 Kinase Tracers were applied as kPCA probes and the binding kinetics of the 40 kinase-tracer pairs were precisely and accurately calculated. 10800 kinase-inhibitor pairs were profiled for their binding kinetics and affinity parameters by using this newly established panel. Insights from Monte Carlo analyses were applied for evaluation of the 32400 experimentally determined values.

5.2.2 Validation of determined binding kinetics and affinity data

The assays and results of the binding kinetics profiling panel were validated to demonstrate reliability of the method.

Typically, relative errors of the best fit parameters were below 30% and the TR-FRET traces of the two replicates were similar (Figure 25c-d), indicating good intra-assay precision. The mean log differences of the binding parameters determined in two independent experiments are below 0.015 (Figure 27) and the median coefficients of variation are low: $CV(K_{D_{eq}}) = 20\%$, $CV(k_{on}) = 26\%$, $CV(k_{off}) = 26\%$, $CV(K_{D_{kin}}) = 13\%$. Altogether, the intra- and inter-assay precision is as good as in other biochemical assays [84].

To validate the accuracy, the binding kinetics and affinity data acquired in this thesis were compared with reference values from orthogonal technologies and/or from previous studies analyzing kinase-inhibitor interactions. **I**) The affinities determined with the kinetic assay setup (kPCA) were cross-validated with the orthogonal assay technology ePCA (this study). There is a good agreement with the steady state affinities (Figure 28a): The mean log difference is 0.05. **II**) Previously, multiple high-throughput screening studies analyzed kinase-inhibitor interactions under equilibrium conditions. For example, Anastassiadis *et al.* [14] (study 1) determined binding affinities and Davis *et al.* [15] (study 2) detected remaining kinase activities. 677 (study 1) and 602 (study 2) kinase-inhibitor pairs overlapped with this study and their equilibrium binding metrics and kinase inhibition activities are

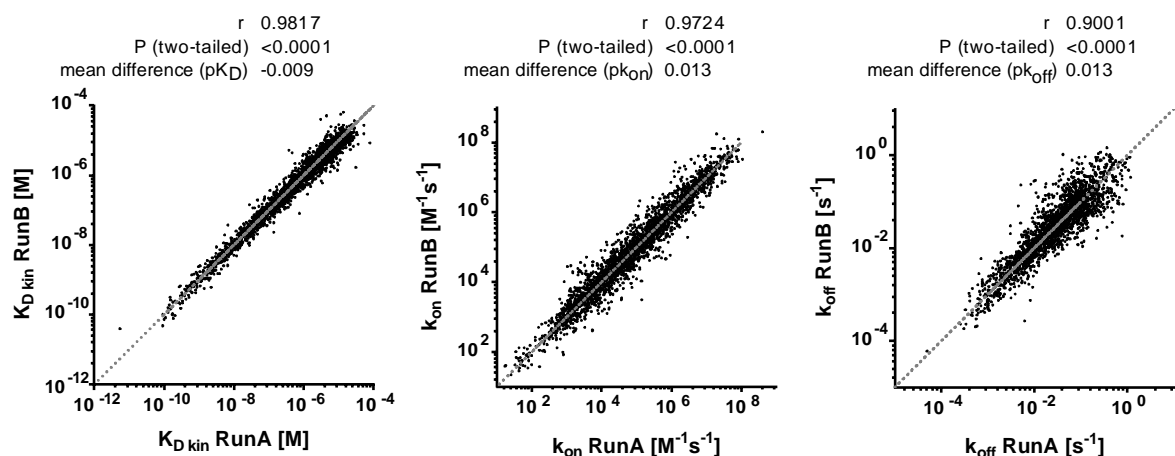


Figure 27: Comparison of binding parameters obtained in Run A versus Run B (two independent experiments)

Correlation coefficients and Bland-Altman statistics are indicated above the plots. The between-run precision is high: There is a good agreement between binding parameters determined in two independent experiments with mean log differences below 0.015.

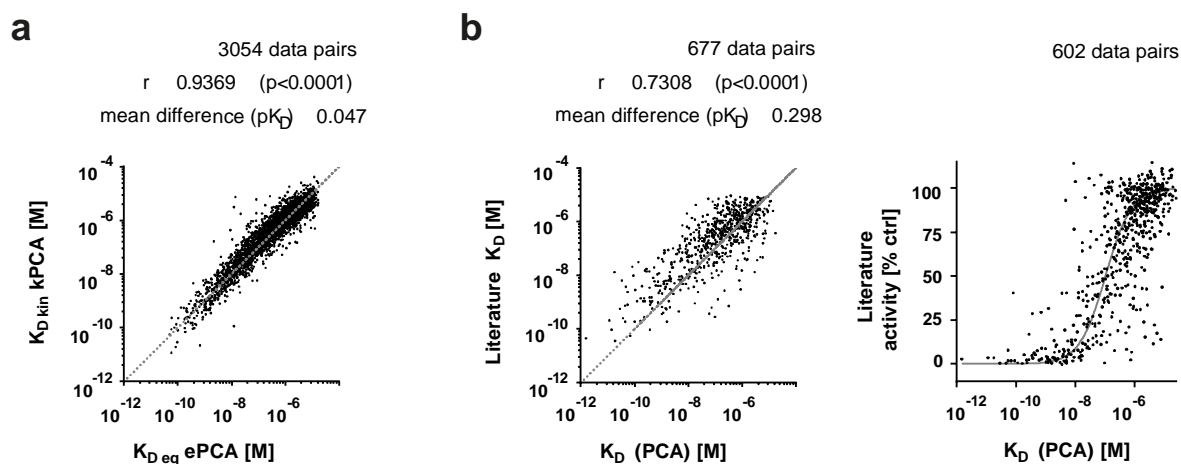


Figure 28: Comparison of affinity metrics obtained in this thesis versus literature reference values

Data pair numbers, correlation coefficients and Bland-Altman statistics are indicated above the plots. The binding kinetics profiling panel determines affinities accurately: **a)** affinities determined in the kinetic assay setup (kPCA) are in good agreement (mean log difference < 0.05) with the affinities determined in the endpoint assay (ePCA). **b)** Moreover, the affinities determined with the profiling panel (PCA, final affinity value derived from ePCA and kPCA experiments as described in chapter 4.3.1.3, last paragraph) are in good agreement with affinities determined in previous kinase-inhibitor interaction profiling studies (left: [15], mean log difference < 0.3 ; right: [14]). As anticipated, the plots illustrate linear relationships between affinities and a sigmoidal relationship between affinity and remaining kinase activity.

consistent with the affinities determined in this study (Figure 28b). **III)** So far, there was no truly comprehensive study analyzing binding kinetic rate constants of kinase inhibitors, yet some reference data can be found in the literature: e.g. Willemsen-Seegers *et al.* [69] (2017) and Kitagawa *et al.* [123] (2014). In order to validate the kinetic data with more data points, the orthogonal assay technology SPR was conducted in this study (as described in 4.2.2 and 4.3.1.4). As illustrated in Figure 29, there was a good agreement of these 97 reference values (including 41 literature values) with the off-rates obtained in this study (mean log difference ≈ 0.18). The kPCA on-rates correlate

moderately with the SPR data obtained in this study and strongly with the literature data, but the determined SPR on-rates are slower than on-rates determined by kPCA (mean log difference ≈ 1 ; potential reasons are discussed in chapter 6.2). Summarizing the findings from these comparisons, affinities, on- and off-rates determined in this study strongly correlate with literature values. Moreover, affinities and off-rates are in a similar range as compared to literature values, suggesting accuracy of determined affinities, off-rates and on-rates (since $K_D = k_{off} / k_{on}$).

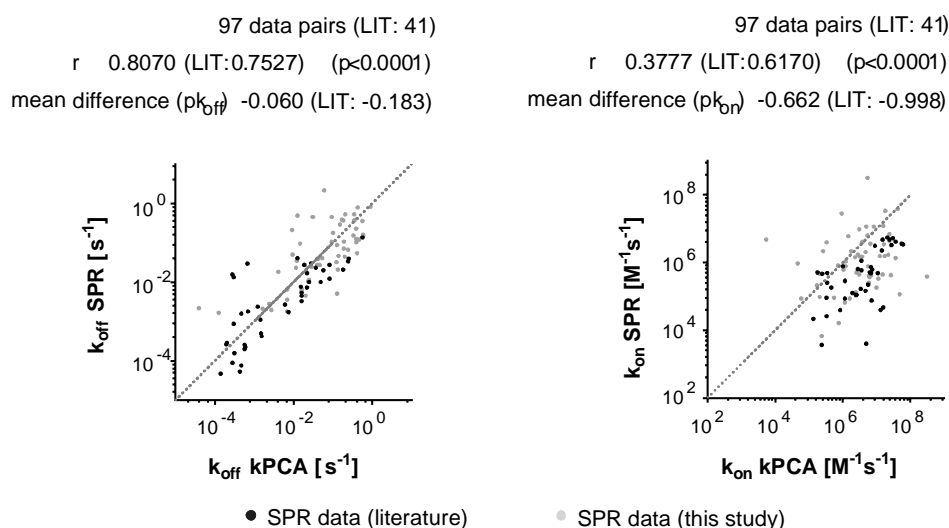


Figure 29: Comparison of binding kinetic parameters obtained with kPCA in this study versus own and literature values measured with SPR

Data pair numbers, correlation coefficients and Bland-Altman statistics are indicated above the plots. The binding kinetic parameters determined with the profiling panel are in good agreement with those obtained with the orthogonal assay technology SPR. There is a good correlation with literature data [69, 123] and the off-rates are in a similar range, but SPR on-rates are shifted towards lower values (mean log difference ≈ 1).

Six compounds were present in two different salt forms in the screening panel. Comparison of determined binding kinetic and affinity parameters (Figure 49 in appendix F) revealed good agreement between salt forms with one exception: slower on-rates and accordingly lower affinities were determined for R788 disodium in comparison to R788. Differences in calculated on-rates and affinities are expected for solubility issues: DMSO solubility of R788 (199.84 mM) is better than DMSO solubility of R788 disodium (9.6 mM) (according to Selleck Chemicals datasheets). As every assay technology, kPCA is susceptible to sparingly soluble compounds. However, the other five compounds can also be regarded as controls demonstrating repeatability.

Summary of the results: The kPCA-based screening platform provides accurate and precise binding kinetics and affinity data. Intra- and inter-assay precision is as good as in other biochemical assays. Accuracy was validated with reference values from orthogonal assay technologies and literature. There is a strong correlation between kPCA and literature binding data. Although on-rates determined with SPR are slower than on-rates determined with kPCA, affinities and off-rates were in

a similar range as compared to literature values, suggesting accuracy of determined affinities, off-rates and on-rates (since $k_{on} = k_{off} / K_D$).

5.2.3 Binding kinetics perspective on kinase-inhibitor interactions

The mean binding kinetic and affinity parameters quantified in this study are presented as k_{on} - k_{off} plot in Figure 30a. The diagonals illustrate iso-affinity lines. There are many compounds targeting various kinases with similar affinities, but different binding kinetic properties (e.g. cabozantinib, ponatinib). Interestingly, affinities correlate better with on-rates ($r = 0.8$) than with off-rates ($r = 0.1$) (Figure 30b). However, with increasing affinities, the correlation between k_{off} and K_D becomes better (to $r = 0.5$ for $K_D < 10^{-9}$ M), while the correlation between k_{on} and K_D is decreasing (to $r = 0.1$ for $K_D < 10^{-9}$ M). Together, this shows that consideration of on-rates and target residence times ($= 1/k_{off}$) might provide a different view on selectivity than affinities *per se*.

On-rates ranged from $10^2 - 10^8 \text{ M}^{-1}\text{s}^{-1}$ and off-rates from $10^0 - 10^6 \text{ s}^{-1}$ (residence times from 1 s to >10 days). The majority of the investigated kinase-inhibitor pairs possess fast off rates, while fewer pairs have slow off-rates: 78 % with $k_{off} \geq 0.01 \text{ s}^{-1}$ ($RT \leq 1.67$ min), 17 % with $k_{off}: 0.01-0.001 \text{ s}^{-1}$ ($RT: 1.67-16.67$ min), only 5 % with $k_{off} < 0.001 \text{ s}^{-1}$ ($RT > 16.67$ min). Interestingly, among the latter are many interactions of FDA approved drugs with their main targets (Figure 30a; refer to Table 4 in appendix A for main targets according to [124, 125]): 21 out of 37 (57%) with $RT > 16.67$ min, 5 (14%) with $RT: 1.67-16.67$ min.

To further characterize these trends, **1)** the distribution of on- and off-rates quantified in this study and **2)** its dependence on affinity was analyzed (Figure 30c):

1) Association and dissociation rates followed a log normal distribution (Gaussian curve fit $r^2 = 0.98$). The mean values of the kinetic rate constants for kinase binding are similar for both, all kinase inhibitors and those approved by the FDA: $-pk_{on}: 4.9 \pm 1.3$ versus 5.0 ± 1.3 and $pk_{off}: 1.6 \pm 0.8$ versus 1.7 ± 1.0 . On the other hand, the mean values for the subset of FDA-approved drugs interacting with their main target were different: $-pk_{on} = 6.2$ and $pk_{off} = 3.0$.

2) The frequency distributions of on- and off-rates across affinities (three affinity groups: $K_D < 10^{-9}$ M, $K_D: 10^{-7} - 10^{-9}$ M, $K_D \geq 10^{-7}$ M) from all kinase-inhibitor pairs are similar to those from kinase-FDA approved drug pairs: On-rates increase with increasing affinities ($-pk_{on}$ (all): 4.4, 6.1 and 6.7; $-pk_{on}$ (FDA): 4.5, 6.0 and 6.6), while the majority of off-rates remain fast in the first two affinity groups (pk_{off} (all): 1.5, 1.7; pk_{off} (FDA): 1.4, 1.7). But the exceptions are off-rates of high-affinity interactions ($< 10^{-9}$ M: pk_{off} (all) 3.0; pk_{off} (FDA): 3.2), for which off-rates are wide-spread from fast to slow and the slowest off-rates are exclusively observed for main targets of FDA approved drugs (refer to Table 4 in appendix A for main targets according to [124, 125]), not for their other targets (Figure 30c).

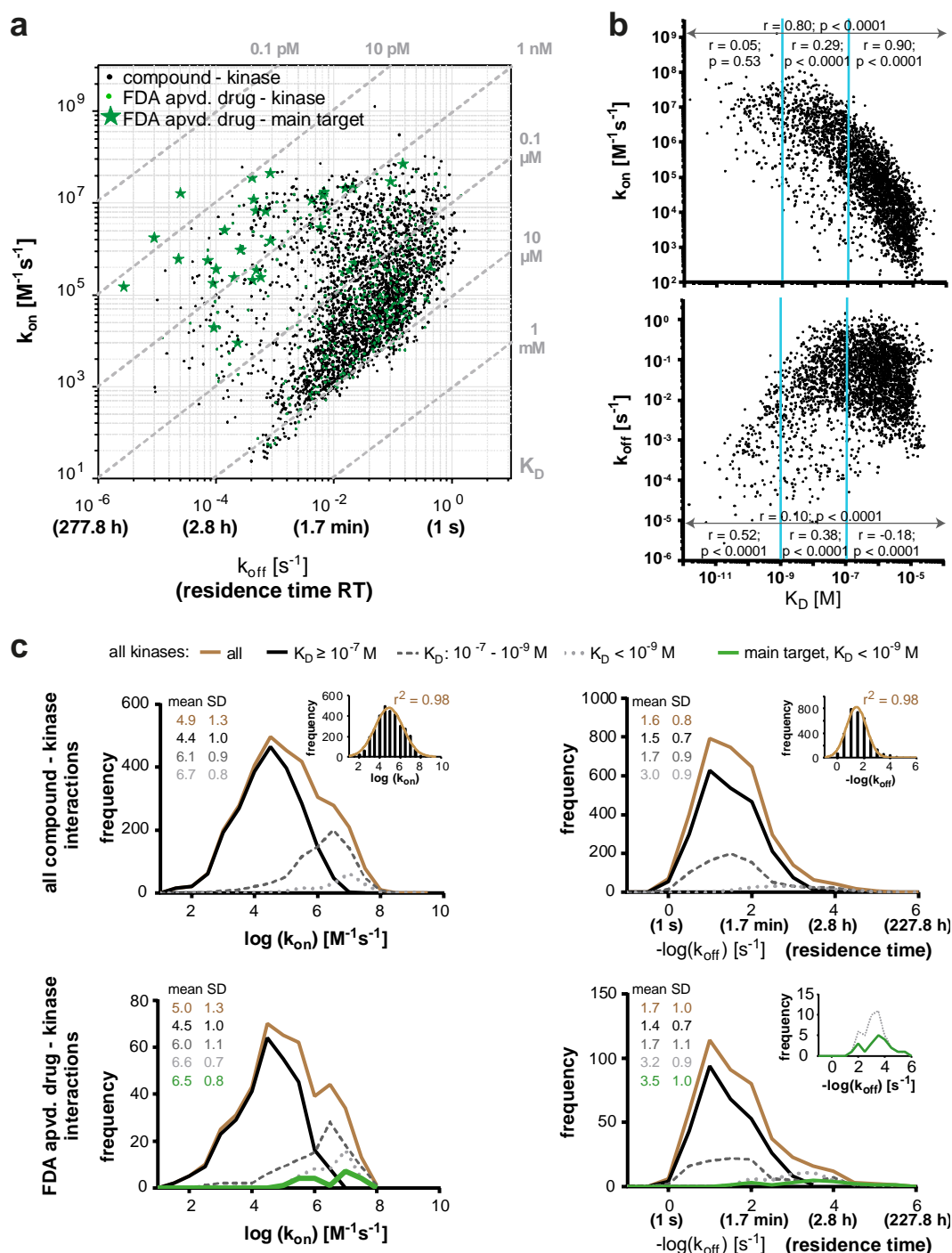


Figure 30: Distribution of on- and off-rates of 3230 kinase-inhibitor interactions quantified in this study

k_{on} - k_{off} plot (a) and the distributions of on- and off-rates of kinase-inhibitor pairs depending on their affinities (b-c). Binding with lower affinities or faster off-rates is not quantifiable with the applied assay setup and not represented in the plots. Binding with high affinities and/or slow off-rates might be underestimated due to the assay wall or unreached equilibrium but is included in these plots. **a**) The majority of the kinase-inhibitor dissociation rates is fast, but many FDA approved drugs dissociate slowly from their main targets (refer to Table 4 in appendix A for main targets [124, 125]). **b**) Affinity correlates better with on-rates than with off-rates, but this pattern is inverted with increasing affinities (correlation coefficients for complete dataset and three affinity groups (separated by cyan lines) are represented in the plots). **c**) Frequency distribution of on-rates (left) and off-rates (right) of kinase-inhibitor complexes across the corresponding affinities, considering all (top) or FDA-approved (bottom) kinase inhibitors. For better clarity, frequency values of adjacent bins are connected by lines and bars are omitted. Except for insets in the upper panels showing histograms (bars for bins) for all kinase-inhibitor pairs, the Gaussian curve fit and corresponding r^2 . On-rates increase with increasing affinities, while off-rates remain in a similar range. Exceptions are compound-kinase interactions with high affinities: here, the off rates are widespread from fast to slow. Considering only FDA approved drug interactions, the slowest off-rates are solely observed for their main targets (green), fulfilling a prerequisite for kinetic selectivity.

A prerequisite for kinetic selectivity is fulfilled: the residence time ($= 1/k_{\text{off}}$) on the main target is longer than on other targets. This assumption is strengthened by the observation, that the gap between slow and fast dissociating kinase-compound pairs becomes larger when comparing compounds in early and late stages of clinical development (see Figure 51 in appendix F). (How kinetics rate constants of clinically relevant kinase binding interactions (high affinities) differ for preclinical and FDA-approved compounds was analyzed in chapter 5.4.3.1 Figure 43a.)

Figure 31 displays kinase-compound interaction maps in the form of heatmaps of the kinases' and compounds' (Euclidean) distance matrices based on their K_D , k_{on} and k_{off} profiles, respectively. The compound-centric heatmaps represent the pairwise distances between compounds respective their on-rate, off-rate or affinity profiles on the kinases, and the kinase-centric heatmaps show the pairwise distance between kinases respective their on-rate, off-rate or affinity profiles. The correlations between distance matrices were analyzed in order to assess the overall similarity between K_D and k_{on} or k_{off} profiles: The Pearson correlation coefficient between k_{off} - and K_D -based matrices is 0.54 for the kinase-centric matrix and 0.78 for the compound-centric matrix. This is slightly lower than the correlations between k_{on} - and K_D -based matrices (in line with the analysis in Figure 30b), where the Pearson correlation coefficient amounts to 0.79 for the kinase-centric matrix and to 0.87 for the compound-centric matrix. These correlation coefficients suggest that the overall selectivity and drugability profiles are similar in terms of K_D and binding kinetic parameters when considering each parameter separately. However, it should be noted that even if some kinases, e.g. LCK, LYNa, FYN and SRC, possess comparable similar binding profiles and group together in the clustered k_{on} -, k_{off} - and K_D -based distance matrices (Figure 31), their similarity is highest in the K_D -based matrix (dark blue in the heatmap), less in the k_{on} -based matrix (lighter blue in the heatmap) and lowest in the k_{off} -based matrix (lightest blue in the heatmap). This illustrates that even if these kinases are targeted by some of the compounds with similar affinities, the corresponding on- and off-rates can be comparatively diverse. The distances in the k_{off} -based distance matrix is on average higher compared to the k_{on} and K_D -based distance matrices.

To start addressing the question whether binding parameters can be rationalized from structural features, the overall similarities between binding profiles (based on on-rate, off-rate or affinity; Figure 31) and structure profiles of kinases and compounds (Figure 25b) were analyzed: Correlations of the compound and kinase distance matrices based on affinity and binding kinetic parameters with the distance matrix based on compound or kinase structures, respectively, reveal that the overall binding profiles of the compounds differ from the compound structure profile (Pearson correlation coefficients < 0.05 for comparison between structure and k_{on} , k_{off} or K_D profiles, respectively, as indicated in Figure 31), while the binding profiles of the kinases correlate with the kinase structure profile (Pearson correlation coefficients: 0.57 for k_{on} , 0.22 for k_{off} , 0.42 for K_D versus structure profile,

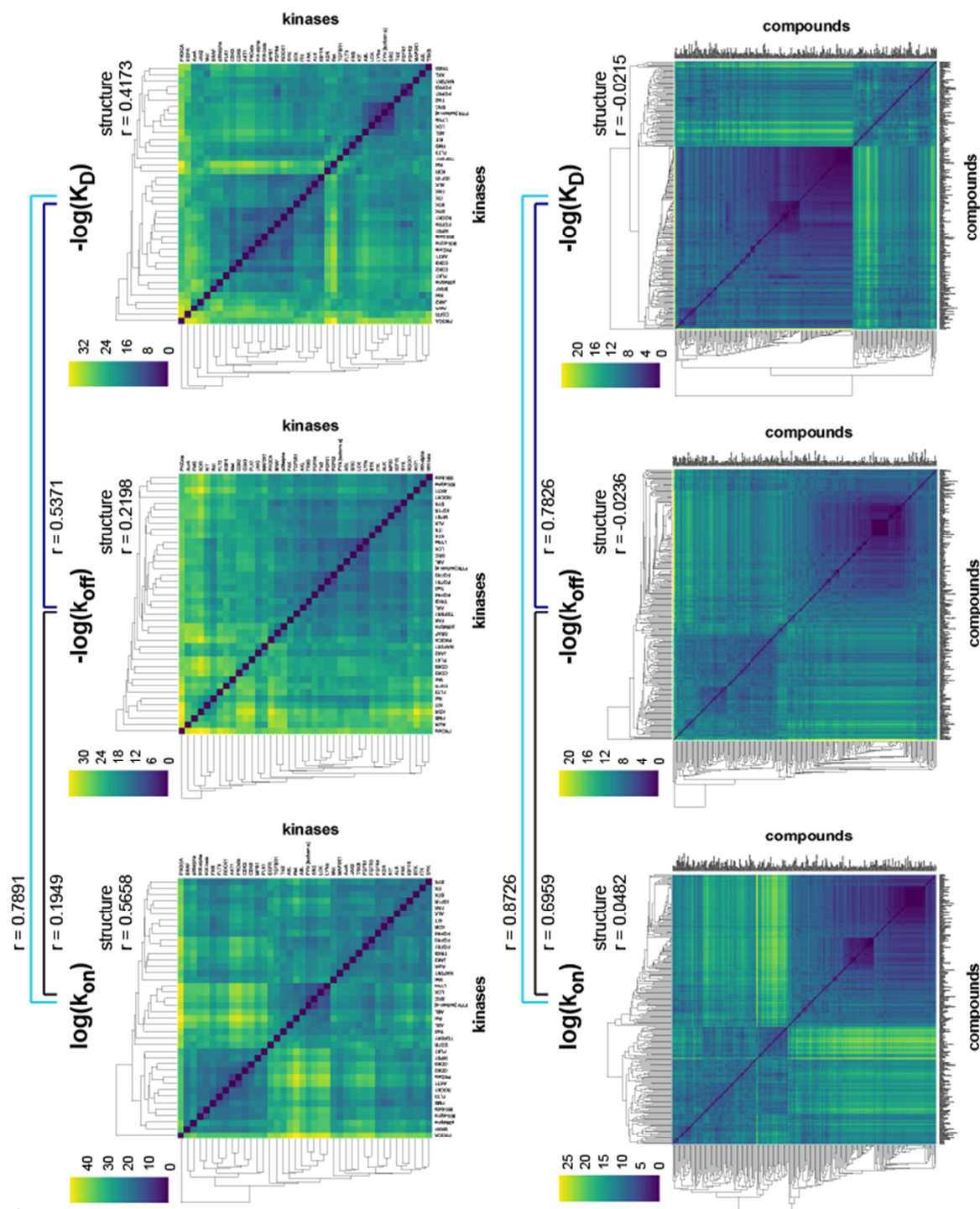


Figure 31: Kinase-inhibitor interaction maps from steady state and binding kinetics perspective

Clustered distance matrices for affinity and binding kinetic parameters per kinase (left side) and per compound (right side) were generated as described in chapter 4.3.4. The colors represent the Euclidean distances. Coefficients for correlation (r) between compound-centric distance matrices and between kinase-centric distance matrices and their correlation with compound- or kinase-structure-based distance matrices (as shown in Figure 25b) are indicated in the figure. The correlations between k_{on} - and K_D -based matrices are stronger than the correlations between k_{off} - and K_D -based matrices. Moreover, the sequence-based kinase distance matrix is less similar to the off-rate-based distance matrix than to the affinity-based distance matrix, and the similarity to the on-rate-based distance matrix is highest. Together, this indicates that selective targeting of structurally similar kinases could be reached best via off-rates. There is either no or a very weak correlation between structure-based compounds distance matrix and the binding-based compound distance matrices. Nevertheless, close derivatives among the compounds possess similar binding properties (refer to Figure 52) and group together in the binding-based matrices.

respectively). The structurally diverse set of compounds possesses comparatively similar binding profiles on kinases. One possible explanation is that similar binding profiles are determined by similar interactions of single compound moieties with distinct amino acids in the proteins' binding pockets, rather than due to overall structural similarity of the compounds (refer to chapter 5.3.2). Another factor is that there are many kinase-compound pairs with no detectable interaction. In other words, not all compounds bind to all kinases and there are even 11 compounds with no observed kinase binding activity at all. This leads to structural diverse compounds with similar "binding profiles", which is in fact due to no binding. Nevertheless, close derivatives present among the compounds possess only small differences in binding properties (refer to Table 9 and Figure 52 in appendix G) and appear as pairs in the clustered distance matrices. Likewise, kinases related by sequence identity are targeted by similar sets of compounds (for k_{off} weak correlation, k_{on} stronger correlation, K_D medium correlation with kinase structure distance matrix). For instance, the above mentioned kinases LCK, LYNa, FYN and SRC with comparable similar activity profiles are related by sequence identity. Yet, there are also exceptions for this finding: I) Similar kinases are targeted by different sets of compounds (e.g. the binding profile-based distances between FGFR1 and FGFR3 are shorter as compared to the distances between FGFR1 and FGFR4 as well as between FGFR3 and FGFR4 (color code in Figure 31). Especially the observed FGFR4 K_D profile is more different from FGFR1 and FGFR3 as compared to other kinases with the same similarity degree, which was similarly observed by Anastassiadis *et al.* [14]). II) Structurally different kinases are targeted by similar sets of compounds (e.g. PIK3CA off-rate profiles are generally more similar to protein kinases than assumed from sequence identity). This confirms that kinases related by sequence identity can be differentially targeted by compounds, but also that compounds can target not only closely related and but also less related kinases (less similar by sequence identity). Overall, the highest dissimilarities of the structurally related kinases were observed from the off-rate perspective.

Summary of the results: A prerequisite for kinetic selectivity is fulfilled: Among the relatively few observed slow off-rate interactions are many interactions of FDA approved drugs with their main targets. Kinase-inhibitor interaction maps from the affinity perspective are more similar in terms of on-rate profiles as compared to the off-rate profiles. Moreover, kinases' distances by sequence identity correspond better to their on-rate profiles than to their affinity profiles, and are least similar to their off-rate profiles. Hence, kinetic selectivity for structurally similar kinases might be reached better by different off-rates than by different on-rates. The observations from these general approaches suggest pertinence of more detailed analyses of both structure-kinetic relationships (refer to chapter 5.3) and kinetic selectivity (refer to chapter 5.4), i.e. to zoom in specific examples analyzing whether target occupancy dynamics and hence selectivity is dependent on binding kinetics.

5.3 Investigation of the influence of structural features on kinase inhibitors' binding kinetics (KI BK)

The next objective of this thesis was to investigate the effect of molecular features on binding kinetic parameters, by using the results from the large-scale profiling approach (chapter 5.2). Identification of structural aspects influencing the binding kinetic behavior might be a step forward towards rational optimization of binding kinetic rate constants.

5.3.1 Effect of molecular properties of kinase inhibitors & conformations of proteins on KI BK

As a first step the relationship between binding kinetics and chemical properties and functionalities of both the compounds and the targets was studied.

5.3.1.1 Dependence of binding parameters' relative distributions on compound properties and kinase conformations

Distribution of binding parameters across structural features revealed trends indicating influence of molecular properties of compounds (calculated as described in chapter 4.3.5) and conformations of proteins (source: KLIFS database) on binding kinetics (Figure 32, Figure 33). These trends are stronger for kinase-compound pairs with higher affinities in at least the double-digit nanomolar range (tighter interactions with $K_D < 10^{-8}$ M) than for lower affinity interactions. This could be explained by the fact that specific interactions between compound moieties and amino acid residues in the kinase's binding site are more important to describe binding than the overall molecular features, albeit these molecular features can influence the binding rate constants. Interestingly, property and functionality changes with trends toward slow off-rates also tend to slow on-rates diminishing the effect on affinities. The same applies for trends towards fast on- and off-rates (Figure 32).

The percentage of slow on-rates and slow off-rates was increasing with increasing molecular weight (MolWt), number of halogen atoms, total polar surface area and with decreasing ratio of number of sp^3 -hybridized carbon atoms to total number of carbon atoms (sp^3 C/C) (Figure 32). Possible explanations for the observed trends are as follows: Binding of large compounds (high MolWt) might be slowed down due to steric hindrance. In Addition, a larger (high MolWt) molecule can have more chemical moieties interacting with the protein, similarly a higher polar surface area might allow more hydrophobic contacts. The number of halogens might be important if specific interaction mechanisms of the halogen with the protein contribute to slow off-rates, as recently suggested [76]. Despite the flat ATP binding pocket, binding of flat compounds (low sp^3 C/C) seem to be slowed down compared to compounds with higher sp^3 C/C ratios. Most probably, all these influences of the molecular properties will have a maximum value above which further changes will have no further effect or even an opposite effect (visually spoken: if the molecule becomes too large, it might not fit in the binding pocket any more). There was no monotonic trend observed for binding parameters and the number of hydrogen bond acceptors or donors (HBA, HBD), flexibility or the number of rotatable bonds. Yet, an optimum of 5-7 HBA and 2 HBD for slow binding might be noticeable (Figure 32).

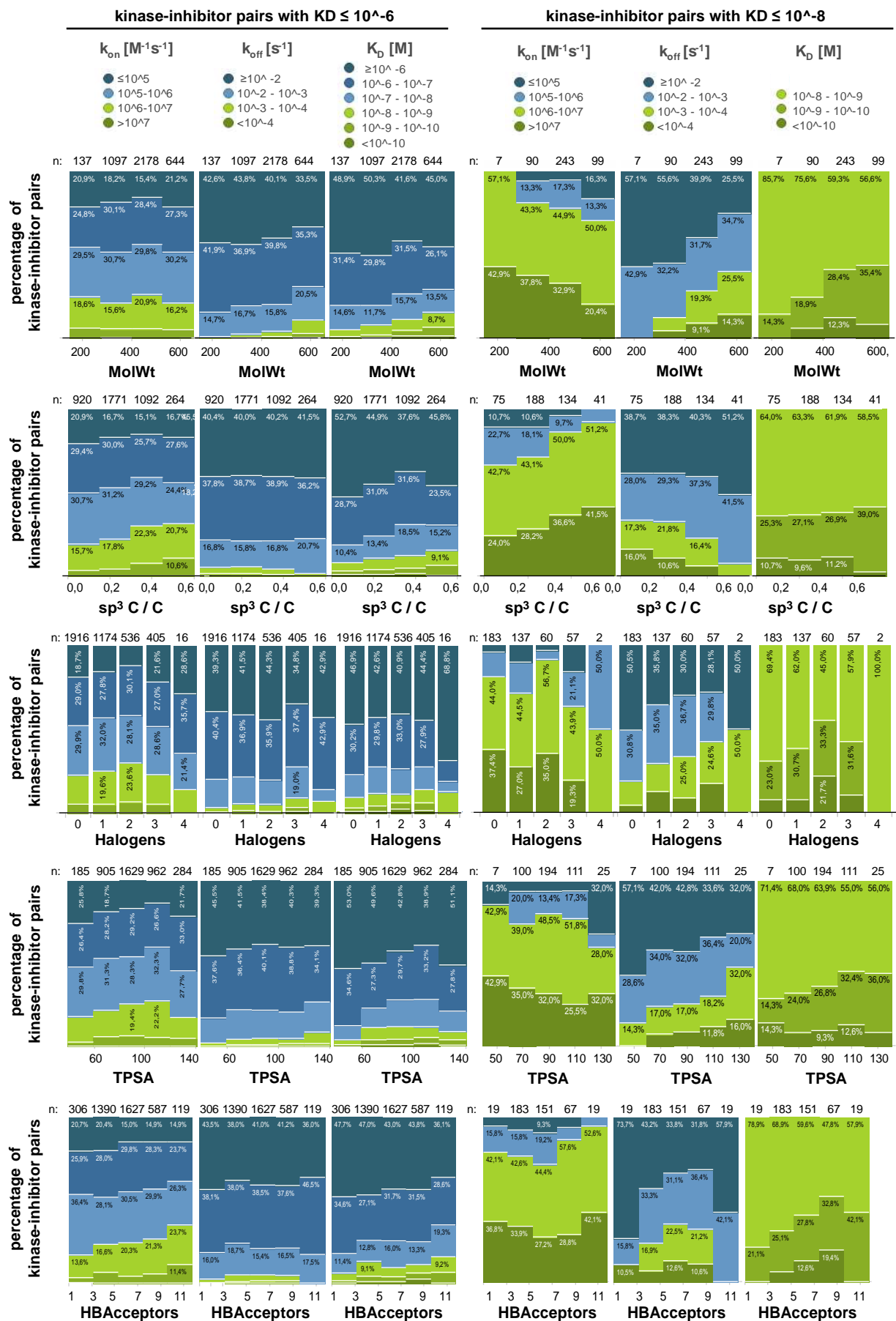


Figure 32 (part 1 of 2)

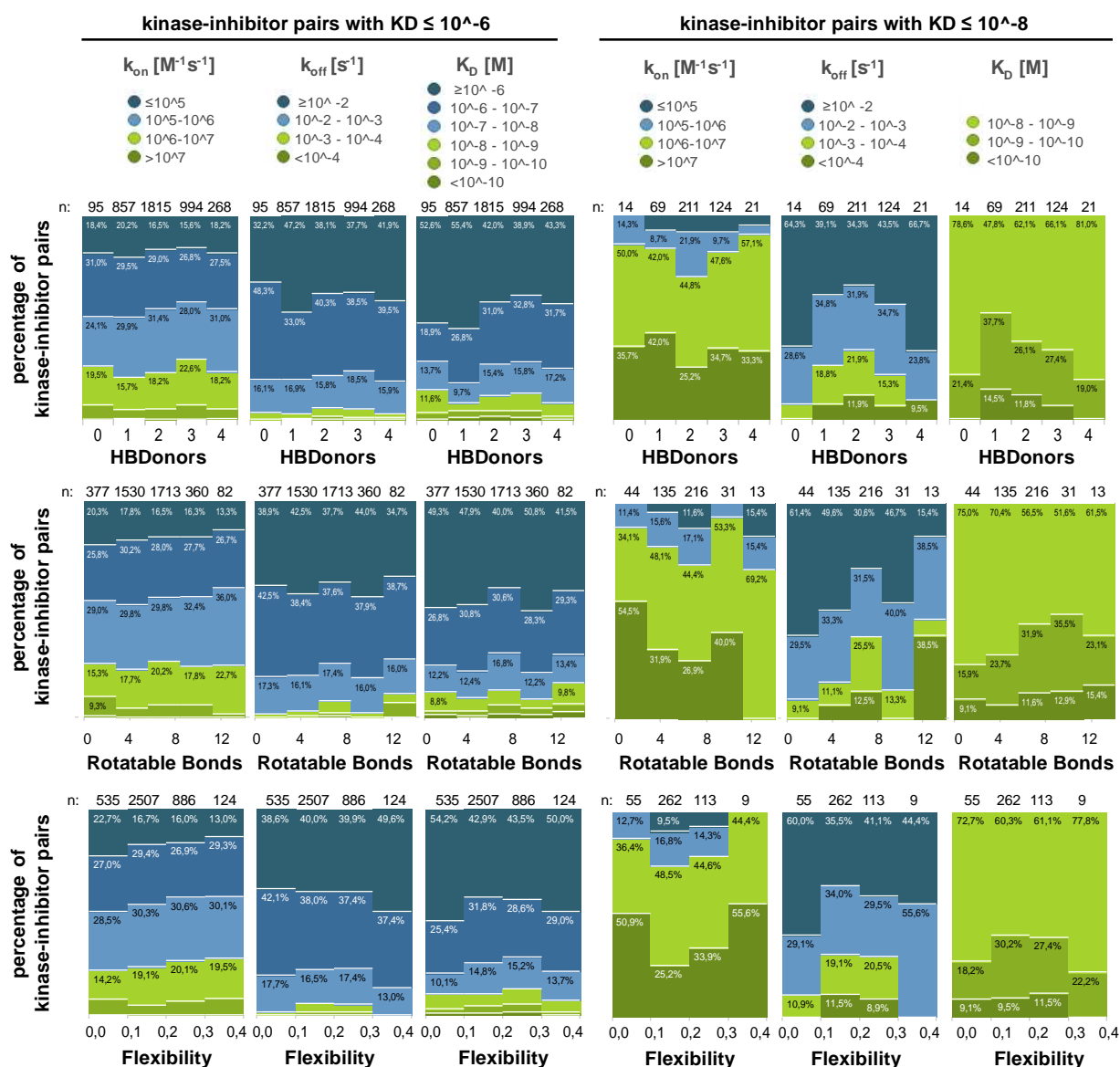


Figure 32 (part 2 of 2): Distributions of binding parameters across compound molecular properties

The bar charts depict the relative (percentage) on-rate, off-rate and affinity distribution for compound-kinase pairs with $K_D < 10^{-6}$ M (left) or $K_D < 10^{-8}$ M (right) depending on binned molecular properties of compounds (one property per row). The amount (n) of compound-kinase pairs in the molecular property bin is indicated on top of the bars.

All observable trends are stronger for tighter interactions ($K_D < 10^{-8}$ M) as for lower affinity interactions. Probably because molecular properties affect binding kinetics, while specific kinase-compound interactions are the key contributors.

There is a trend towards slow binding with increasing molecular weight (MolWt), decreasing number of sp^3 Carbone atoms over total number of Carbone atoms (sp^3 C / C), increasing number of halogen atoms and increasing total polar surface area (TPSA) of the compound. There might be an optimum for hydrogen bond (HB) donors and acceptors. There is no obvious trend for the number of rotatable bonds or flexibility of the compound. These observations indicate impact of steric hindrance and rebinding (within the kinase binding site) on binding kinetic rate constants.

Property changes with positive effects on on-rates (trend towards fast on-rates) have negative effects on off-rates (trend towards fast off-rate) and vice versa. These opposing effects diminish (neutralize) the effect on affinities (e.g. MolWt, sp^3 C/C).

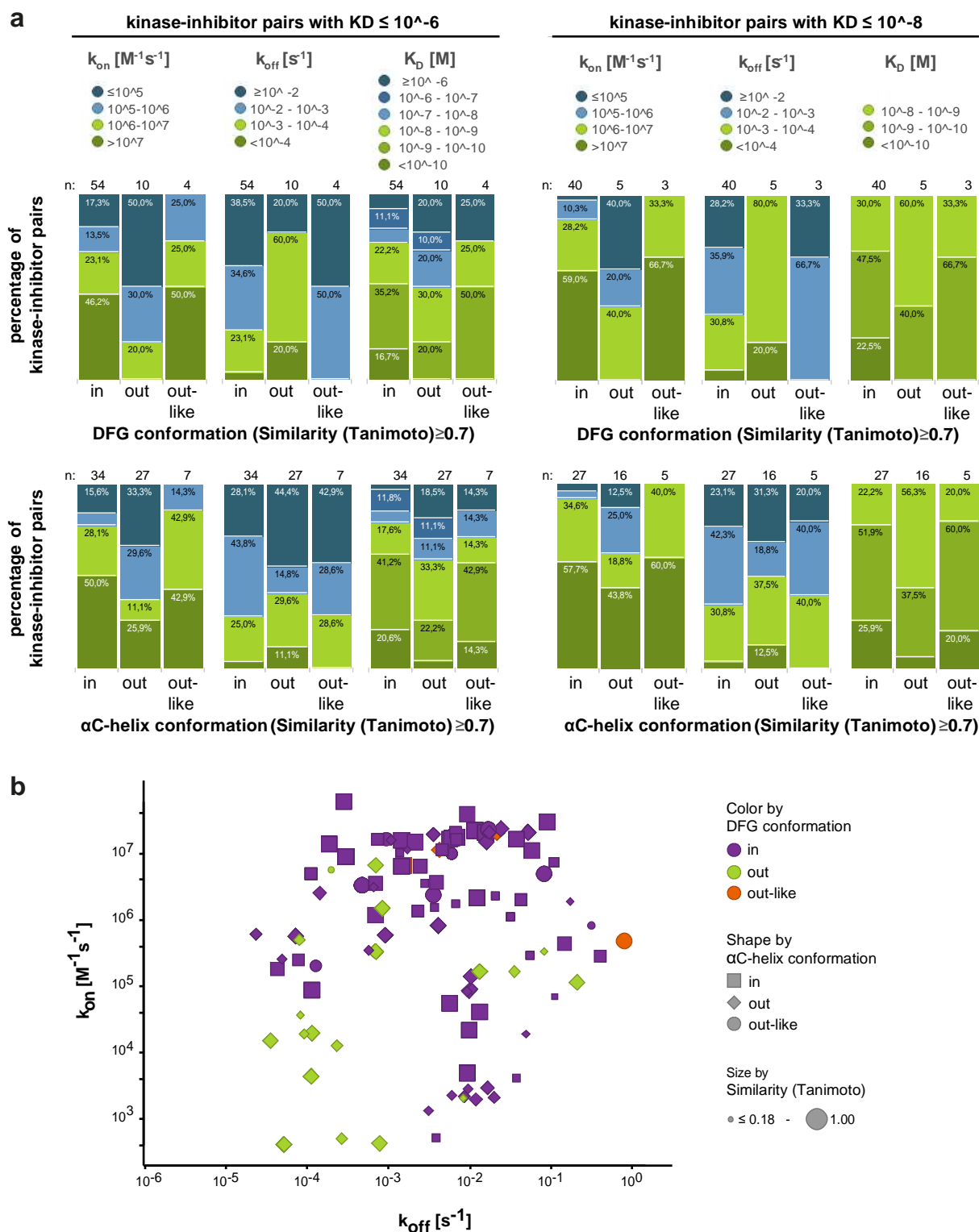


Figure 33: Distribution of binding parameters across kinase conformations

a) Bar charts representing relative frequencies (percentage) of on-rates, off-rates and affinities of kinase-inhibitor pairs (with $K_D < 10^{-6}$ M (left) or $K_D < 10^{-8}$ M (right)) across DFG and α C-helix conformations (as specified in KLIFS database: either derived from structure of kinase-inhibitor pair (PDB) or predicted based on Tanimoto similarity to compounds with a PDB entry for the respective kinase). The amount (n) of compound-kinase pairs with the specific conformation is indicated on top of the bars.

b) k_{on} - k_{off} plot of kinase-inhibitor pairs with known or predicted DFG and α C-helix conformation (KLIFS).

There is a trend towards fast binding for DFG-in/-out-like and α C-helix-in/-out-like conformations and towards slow binding for DFG-out binding (a). Combination of slow on-rates and off-rates (lower left part of k_{on} - k_{off} plot) is exclusively observed for combined DFG-out and α C-helix-out conformation (b). In contrast to the observations in Figure 32, all trends are similarly observable for all interactions ($K_D < 10^{-6}$ M) and the subgroup of tighter interactions ($K_D < 10^{-8}$ M).

In addition to the compounds' molecular properties, also DFG and α C-helix conformations of kinases displayed trends towards slow or fast binding kinetic rate constants. In general, the observations for the DFG-out-like and α C-helix-out-like conformation were very similar to those for the DFG-in and α C-helix-in conformation, while the DFG-out and α C-helix-out conformation revealed contrary trends: The majority of compound-kinase pairs in DFG-in, DFG-out-like, α C-helix-in or α C-helix-out-like conformation display fast on-rates and fast off-rates, while the majority of compound-kinase pairs in DFG-out conformation have slow off-rates and slow on-rates (Figure 33a), which was previously observed [72] and is thought to be caused by the required conformational change in the DFG-loop. However, there are also exceptions to these trends. But all kinase-compound pairs analyzed in this study with both slow on- and off-rates are in DFG-out and α C-helix-out conformation (Figure 33b, lower left quarter of k_{on} - k_{off} plot). Yet, there are also examples of fast associating or dissociating DFG-out and α C-helix-out binders.

All these observed trends illustrate that molecular properties of compounds and the conformation of the kinase might affect binding kinetics, although they are not the main contributors. However, this analysis does not allow estimation of the significance of the effect or identification of interdependencies of the properties or identification of confounders (properties that influence both the binding kinetic rate constants and other molecular properties causing untrue correlations).

Nonetheless and interestingly, also the comparison between binding parameters of the tracers and the presumed corresponding inhibitors suggests relevance of steric hindrance: In general there is a good agreement for the binding parameters, but the on-rates and affinities determined for the tracer are lower as compared to those of the corresponding inhibitors (see Figure 50 in appendix F). Most probably, the attached fluorescence label decelerated the on-rate of the tracer due to steric hindrance. In this case, the off-rate is not affected. Other reasons could be solubility or stability issues of the Kinase Tracer 236, but both should not lead to the observed steady shift.

5.3.1.2 Significance of the effect of compound properties and kinase conformations on KI BK

Correlation analysis and multivariable linear regression with a genetic function approximation (GFA) algorithm (refer to methods chapter 4.3.6) served to estimate the significance of the structural features for binding kinetic rate constants. Moreover, GFA uses the process of evolution to select the most important features automatically diminishing the problem of confounders. As expected from the previous analysis (chapter 5.3.1.1), there are no significant or very weak relationships between binding kinetics and molecular properties of compounds when considering all compound-kinase pairs. Whereas - on the other hand -, for compound-kinase pairs with tight interactions ($pKD > 8$), the strengths of the relationships and the percentage of the variability that can be explained by the model are higher but still weak/low (Figure 34a, Table 1). A reason might be that a compound with distinct molecular properties targets a variety of kinases with different on- and off-rates. Therefore, the effects of molecular properties on binding parameters were also investigated for single kinases, which allowed description of a higher percentage of the variability of the data (example in Figure 34b, Table 2).

Table 1: Percentage of variability of binding data explained by linear models with molecular properties as descriptors

The models with molecular properties as descriptors (built by GFA) can explain less than 7% of the variability of the binding data of all kinase-inhibitor pairs, but approximately 16% of the variability of on- and off-rates of kinase-inhibitor pairs in at least the double-digit nanomolar range (the trend was also expected from Figure 32). The models cannot (and where never meant to) be used for predictions, but they can be applied to estimate if a molecular feature has a significant positive or negative influence on binding kinetics (Figure 34).

r^2 of GFA model for	$\log(k_{on})$	$-\log(k_{off})$	$-\log(K_D)$
all kinase-inhibitor pairs	0.06	0.07	0.06
all kinase-inhibitor pairs with $pK_D > 8$	0.16	0.16	0.06

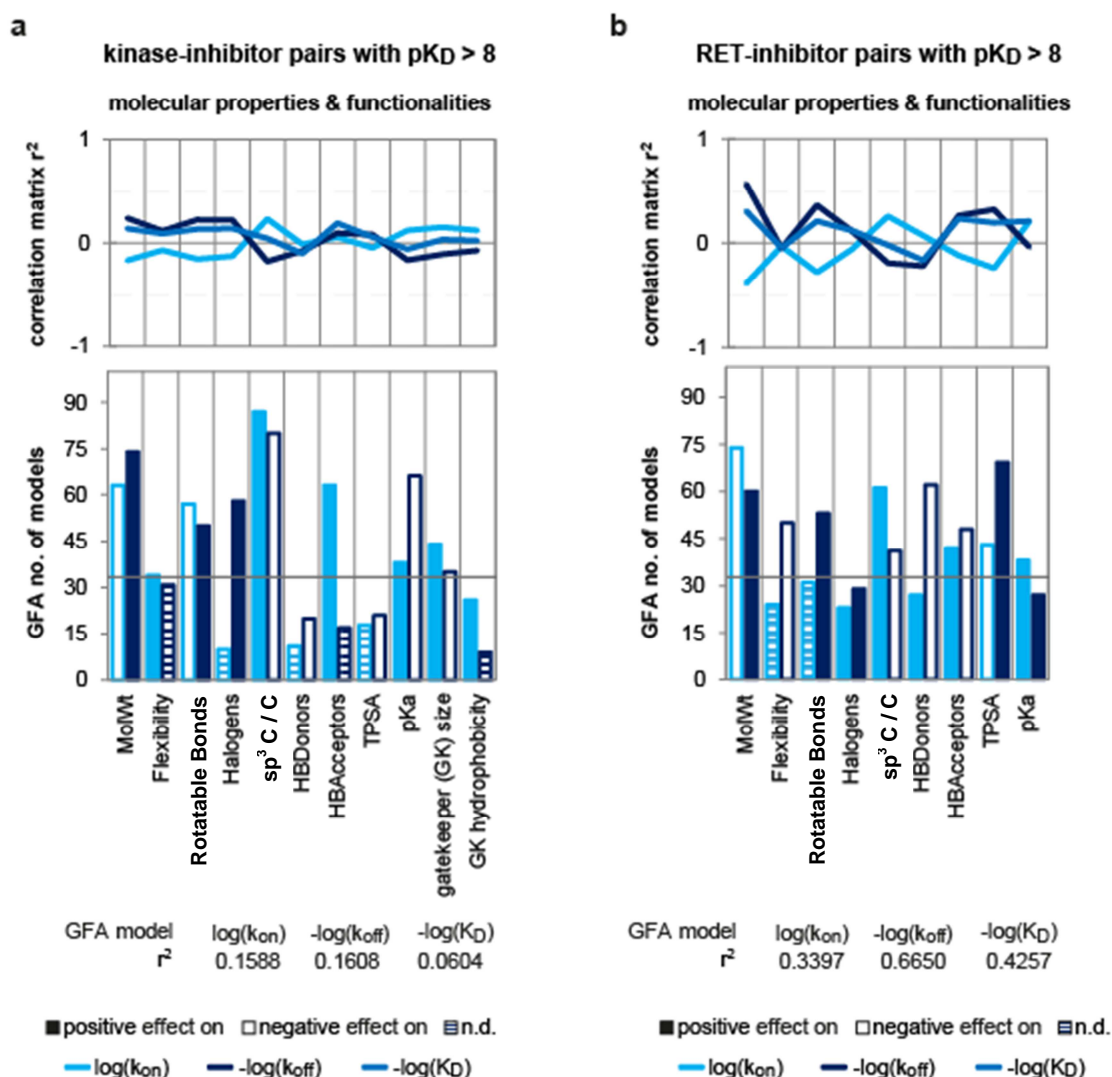


Figure 34: Relationships between binding parameters and molecular properties – correlation and linear regression

The charts depict r^2 from correlation analyses and the number of variable usage for multivariable linear regression models built by genetic function approximation (refer to methods chapter 4.3.6) using molecular features as descriptors for binding parameters (k_{on} , k_{off} or K_D , respectively) of kinase-inhibitor pairs (a) or RET-inhibitor pairs (b), both with $pK_D > 8$. Correlation r^2 and the number of variable usage were considered as measure for the significance and the direction of the relationship. The sign of the coefficient in the GFA built model indicates positive and negative effects (the direction of effect was labeled as not defined, if the respective feature was not selected in the top 10 GFA models).

Molecular weight (MolWt), rotatable bonds, hydrogen bond acceptors (HBA) and sp^3 C/C were frequently selected as important features for description of binding kinetic rate constants (with same direction of effect in a and b). These features either accelerate both on-rates (positive effect) and off-rates (negative effect) or decelerate both on rates (negative effect) and off-rates (positive effect).

Table 2: Percentage of variability of binding data on individual kinases explained by linear models with molecular properties as descriptors

The models with molecular properties as descriptors (built by GFA) can explain approximately 36% and 45% of the variability of the association and dissociation rate constants on individual kinases. This illustrates once more, that these molecular properties are not the key contributors but seem to have an impact on binding kinetic rate constants. The GFA built models were used to estimate if a molecular feature has a significant positive or negative influence on binding kinetics (Figure 34).

r^2 of GFA model for	$\log(k_{on})$	$-\log(k_{off})$
RET- inhibitor pairs	0.34	0.67
PIK3CA- inhibitor pairs	0.86	0.51
KDR- inhibitor pairs	0.30	0.45
AurA- inhibitor pairs	0.25	0.41
EGFR- inhibitor pairs	0.19	0.34
JAK2- inhibitor pairs	0.23	0.31

All in all, molecular properties seem to affect binding kinetics but as expected are not the key contributors explaining the full variability of the binding data. GFA frequently selected molecular weight, rotatable bonds, hydrogen bond acceptors (HBA) and sp^3 C/C as important features for description of the observed on- and off-rates. It should be noted that HBA have the problem that the percentage of slow off rates initially increases and then decreases with increasing number of HBA (as revealed by the descriptive analysis in chapter 5.3.1.1), which makes it inappropriate for linear regression (performed for the analysis in this chapter). Moreover, rotatable bonds have the problem to correlate with both molecular weight and flexibility, which could lead to spurious associations (confounding variables). Overall the findings and trends above (chapter 5.3.1.1) were confirmed: I) Increasing molecular weights (indirectly due to increasing number of interacting functional groups) and TPSA seem to be beneficial for slow dissociation, which might be due to improved interaction with the kinase binding site. II) Also steric hindrance could play a role: Large, flat molecules (high molecular weight, sp^3 C/C low) with low flexibility (rotatable bonds/total number of bonds) tend to display slower binding kinetics. III) Molecular properties with a positive effect on off-rates (deceleration) tend to have a negative effect on on-rates (deceleration) and vice versa.

Summary of the results: Trends towards slow binding (slow on- and off-rates, diminishing the effect on affinities) were observed for increasing molecular weight, TPSA, number of halogen atoms and decreasing sp^3 C/C. The significance of these effects was confirmed for molecular weight and sp^3 C/C by correlation analysis and by using a global function approximation algorithm (GFA). GFA further revealed potential importance of HBA and rotatable bonds for binding kinetic rate constants. Furthermore, slow off-rates are frequently observed for the DFG-out conformation (especially in combination with α C-helix-out conformation). Taken together, steric hindrance (e.g. due to large, flat, inflexible compounds), rebinding effects (e.g. due to number of functional groups, TPSA, HBA) and conformational changes (e.g. DFG-out) could explain how molecular properties of compounds and conformations of proteins might affect binding kinetics. Steric hindrance could also explain why

the on-rates and affinities of tracers are slower as compared to those of the corresponding unlabeled compounds.

5.3.2 Effect of kinase-inhibitor interaction fingerprints on KI BK

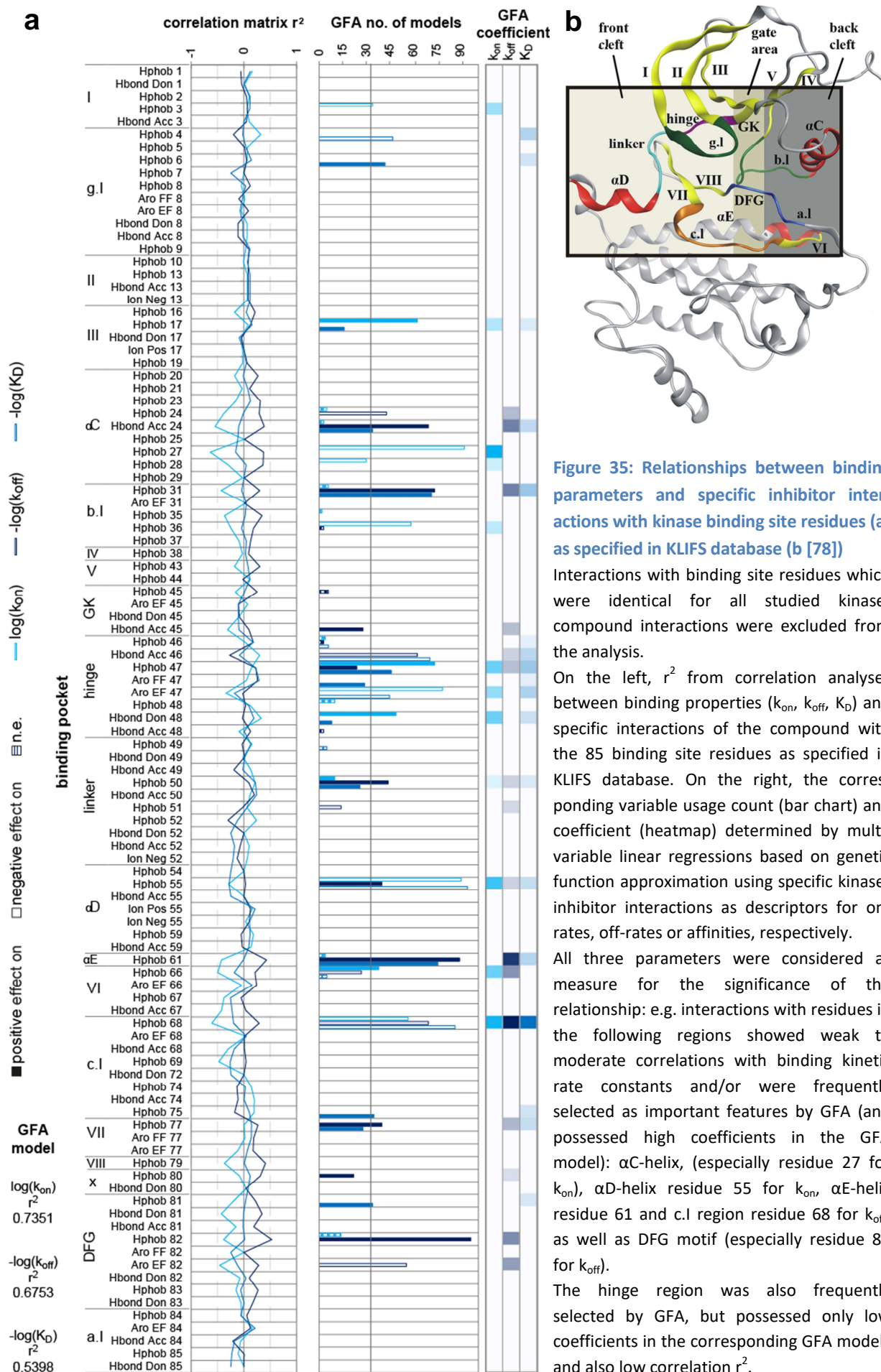
Chapter 5.3.1 deals with the influence of structural features of compounds and kinases on binding kinetics. The DFG and α C-helix conformations were the only studied features which are connected to the interaction of the compound with the kinase. In this chapter the focus is on the analysis of available cocrystal structures which could provide further information on the structural elements, binding modes and/or specific compound-kinase interactions leading to certain kinetic behaviors. Hence, the following analyses were performed for the compound-kinase pairs with PDB and KLIFS entry. The KLIFS database uses known kinase-compound cocrystal structures (available in the PDB), aligns predefined 85 kinase binding site residues and describes the kinase-compound interaction using molecular interaction fingerprints (IFPs; describing whether a compound undergoes a specific interaction with a particular kinase binding site residue) and extracts the involved subpockets and conformations (the compound's binding mode) [85, 86]. Thereby, KLIFS data enabled studying of the influence of specific kinase-compound interactions on binding properties. In the following, the binding site residue numbering and nomenclature was used as specified in KLIFS.

Multivariable linear regression with a genetic function approximation algorithm and using either molecular properties (same as studied in Figure 34) or kinase-compound binding mode information (KLIFS information about subpockets/conformations: DFG conformation, α C-helix conformation, Front pocket, Gate area, Back pocket, FP-I, FP-II, BP-I-A, BP-I-B, BP-II-in, BP-II-A-in, BP-II-B-in, BP-II-out, BP-II-B, BP-III, BP-IV, BP-V (refer to [86] and Figure 35b)) for description of binding properties led to models explaining less than 42% of the variability of the data (Table 3). On the other hand, usage of interaction fingerprints as descriptors explained 74% and 68% of the variability of the observed on-rates and off-rates. The percentage of variance that can be explained by the model can be

Table 3: Percentage of variability of binding data of kinase-compound interactions with known cocrystal structures explained by linear models with molecular properties or KLIFS binding mode information and/or KLIFS interaction fingerprints (IFPs) as descriptors

Models using molecular properties or KLIFS binding mode information as descriptors (built by GFA) can explain less than 42% of the variability of the binding kinetics data, while models using IFPs as descriptors can explain approximately 70% of the variability (which can be increased by additionally using molecular properties as descriptors). The models describing the variance of the observed binding kinetic rate constants were always better than those describing the observed affinities. The models based on IFP were applied to estimate if specific kinase-compound interactions have a significant positive or negative influence on binding kinetics (Figure 35 & Figure 53 in appendix H).

GFA model for	$\log(k_{\text{on}})$	$-\log(k_{\text{off}})$	$-\log(K_D)$
Molecular properties	0.41	0.38	0.27
KLIFS binding mode	0.43	0.33	0.15
KLIFS interaction fingerprints	0.74	0.68	0.54
KLIFS interaction fingerprints & molecular properties	0.79	0.69	0.58



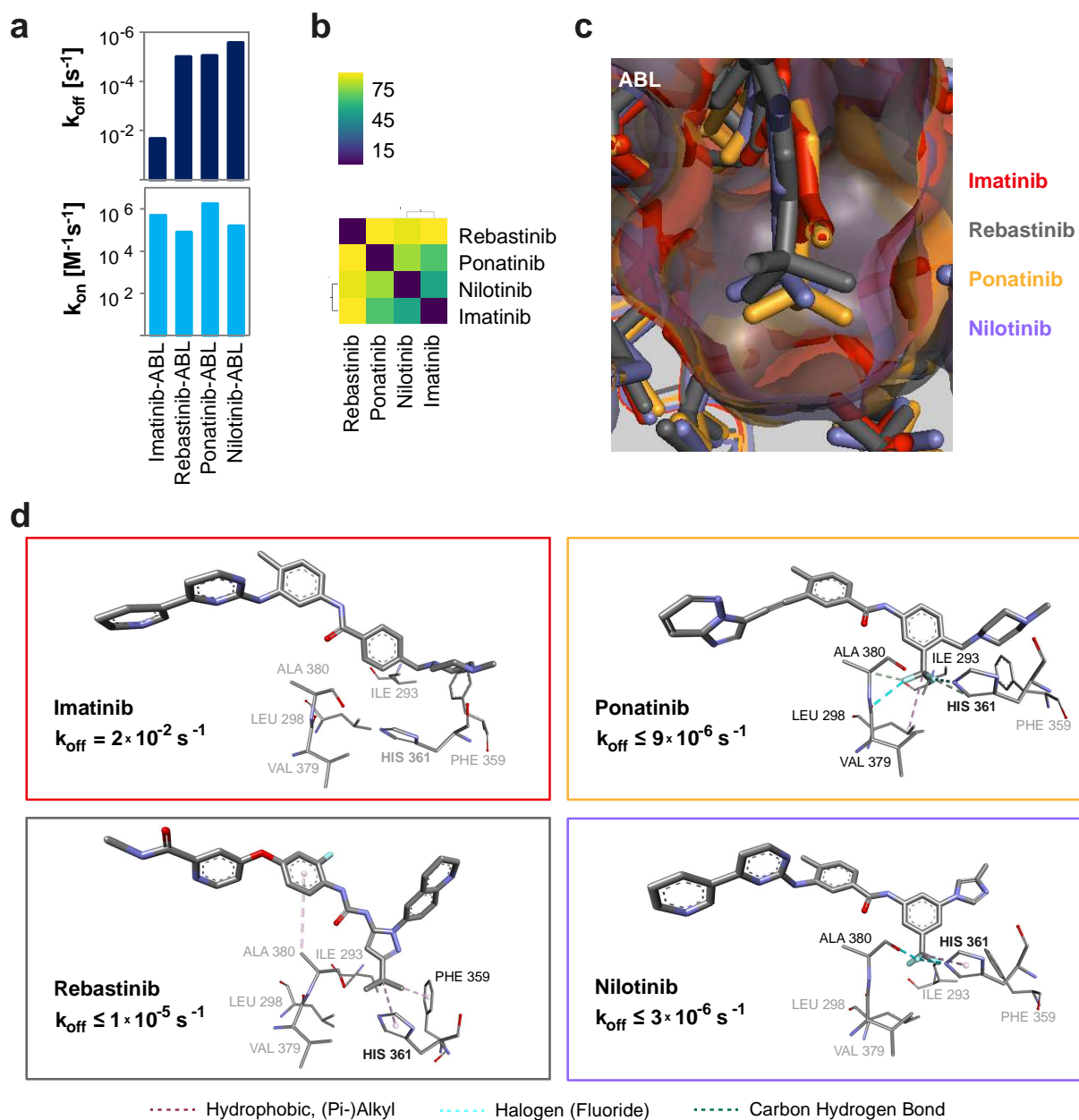


Figure 36: Comparison of imatinib, rebastinib, ponatinib and nilotinib binding to ABL

Imatinib, rebastinib, ponatinib and nilotinib bind to ABL in DFG- and αC -helix-out conformation.

a) The bar charts illustrate that the inhibitors have similar on-rates for ABL binding (see Supplementary Spreadsheet in appendix page 165ff), but imatinib has a 100-fold faster off-rates compared to the other compounds.

b) The structural distance matrix (generated as described in chapter 4.3.4) for of the inhibitors displays smallest differences between imatinib and nilotinib, followed by ponatinib. rebastinib structure is least similar to the other compounds.

c) ABL cocrystal structures with these four compounds (PDB IDs: 2hyy, 3qri, 3oxz, 3cs9): Superimposition depicts hydrophobic pocket around HIS 361 (KLIFS residue 68). The compounds with the slow off-rates, but not imatinib (with faster off-rate), occupy this pocket.

d) Compound-kinase interactions in this pocket are represented in the 3D diagrams. If the respective compound undergoes an interaction with a binding pocket residue, the residue is labeled in black. The compounds with the slow off-rates, but not imatinib (with faster off-rate), interact with HIS 361 (belonging to the HRD motif; printed in bold type in the figure).

increased when including molecular properties as descriptors in addition to KLIFS interaction fingerprints (Table 3). The corresponding models reveal significance of the same compound-amino acid interactions except for the hinge region interactions that seem to be less important, but instead the size of the gatekeeper is often used as descriptor variable in the GFA models (Figure 35 and Figure 53 in appendix H). Correlation analysis and multivariable linear regression based on GFA using IFPs indicate relevance of interactions with particular binding residues (named as defined in KLIFS): e.g. hydrophobic interactions with amino acid 27 in α C-helix and amino acid 55 in α D-helix for k_{on} ; or amino acid 61 in α E-helix, amino acid 68 in c.I region and amino acid 82 in DFG motive for k_{off} (Figure 35). Considering correlation matrix r^2 as a measure for the direction of the effect indicates again that interactions with a positive effect on on-rates mainly have negative effects on off-rates and vice versa (Figure 35). Thus, there is often no or a low impact on affinity. That could explain, why the percentage of variance that can be explained by the models (no matter whether using molecular properties, kinase-compound binding mode information or/and interaction fingerprints) is lower for description of K_D than for description of k_{on} and k_{off} (Table 3).

Analysis of kPCA data revealed four compounds binding to ABL in DFG-out and α C-helix-out mode with similar on-rates but different off-rates (Figure 36a). As mentioned in chapter 5.3.1.1, the majority of kinase-compound pairs in DFG- and α C-helix-out conformation has slow off-rates (Figure 33b), and so do three of the compounds, while one compound (imatinib) possesses a fast off-rate. Imatinib is dissimilar from the off-rate perspective, although it is structural relatively similar to nilotinib and also ponatinib (Figure 36b). On the other hand, rebastinib is similar to nilotinib and ponatinib from the binding kinetics perspective, although it is comparatively dissimilar from the structural perspective (Figure 36b). Examination of the compound-ABL interactions, considered as important by GFA, enabled identification of KLIFS binding site residue 68 as a potential key player for the observed phenomenon. The four compounds show differences in the binding to this residue (part of HRD-motif; HIS 361 in ABL) which lies in a hydrophobic pocket and is only accessible in the DFG-out conformation. Imatinib, the fast dissociating compound, is not interacting with this residue, while the slow dissociating compounds show hydrophobic interactions employing a trifluoromethyl (nilotinib and ponatinib) or a tert-butyl (rebastinib) substituent. Derivatives of the compounds modified at these functional groups should lead to altered off-rates. Indeed, the IC_{50} values on ABL of nilotinib derivatives with a hydrogen, fluorine or methyl instead of the trifluoromethyl decrease in that order [126], presumably due to decreasing off-rates (increasing residence times). Since imatinib, nilotinib, ponatinib and rebastinib possess similar on-rates but different off-rates, these affinity changes presumably result from different off-rates. (Further more detailed studies should follow as discussed in chapter 6.3.)

Summary of the results: Multivariable linear regression models built by GFA and using kinase-compound interaction fingerprints as descriptors explained about 73.5%, 67.5% and 54.0% of the variability of the on-rates, off-rates and affinities. Additional consideration of molecular properties improved the models by 5.3%, 2.0% and 4.3%, respectively. These regression models, together with results from correlation analysis, helped to generate hypotheses about which binding site residues or regions might be relevant for the binding kinetic behavior. For instance, interaction with the HIS in the HRD motif might play a role for binding kinetics and could explain, in part, why imatinib dissociates faster from ABL compared to the other DFG-out and α C-helix-out binders nilotinib, ponatinib and rebastinib (relevance of further factors is likely, e.g. also the additional interaction with the Ala380 preceding the DFG motif might have an impact). Finally, it is worth noting the percentage of the variance that can be explained by the models (no matter whether using molecular properties, kinase-compound binding mode information or/and interaction fingerprints) is lower for description of K_D than for description of k_{on} and k_{off} .

5.4 Evaluation of the effect of kinase inhibitors' binding kinetics on target occupancy profiles

The last objective of this thesis was to evaluate whether target occupancy and selectivity can be differently assessed from the affinity and binding kinetics perspectives, by using the results from the large-scale profiling approach (chapter 5.2). An important step towards increasing acceptance of binding kinetics in drug discovery would be to show that – in some cases – only binding kinetics, but not high affinities *per se*, can explain target occupancy onset and decline.

5.4.1 Target occupancy in intact cells

As a first step, the effect of kinase inhibitors' target binding kinetics on target occupancy in cells was studied. A subpanel of 40 kinase-compound pairs was selected for assessing the kinetic behavior in the cellular context with a recently published tracer displacement assay based on NanoBRET™ technology [101]. In detail, the five preferably unselective and clinically relevant compounds together with the eight kinases were selected to span a wide spectrum of different on-rates, off-rates and affinities (refer to Figure 37). The washout experiments were performed as described in chapter 4.2.3 and allowed

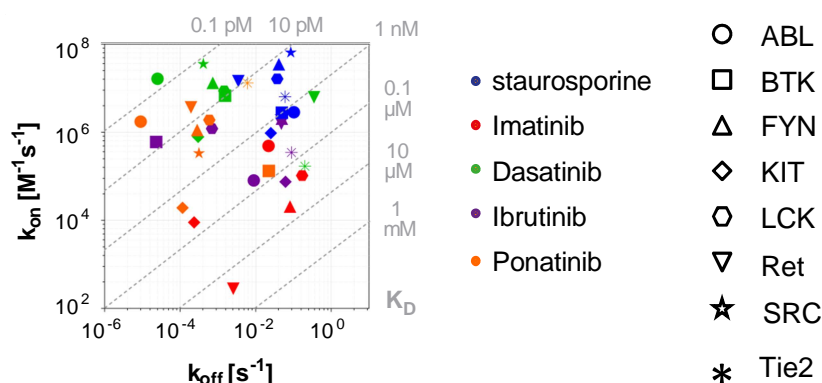


Figure 37: k_{on} - k_{off} plot representing the wide-spread distribution of on- and off-rates for 5 compounds binding to 8 kinases that were selected for cellular experiments.

qualitative and time-resolved evaluation of target engagement in cells. The cells were preincubated with the respective compound at a concentration around the maximum plasma concentrations (measured in healthy human adults, source: IntegritySM database) and were then washed to remove unbound compounds, followed by observation of signal increase arising from tracer binding to the target. The resulting plots are given in Figure 38 and were applied for evaluation of target engagement in cells. The signal losses during the experiment hampered the evaluation. Nevertheless, tracer binding curves (as measure for cellular target engagement) were significantly different: e.g. 100% target occupancy (0% tracer binding) could be observed for the covalent inhibitor ibrutinib binding to BTK till the end of the observation time, while tracer binding to BTK was faster than in the tracer binding control for cells pre-incubated with dasatinib and as fast as in the tracer binding control for all other compounds. Surprisingly, the tracers were binding significantly faster to ABL, KIT and LCK in cells pre-incubated with staurosporine as compared to the tracer binding controls without compound pre-incubation.

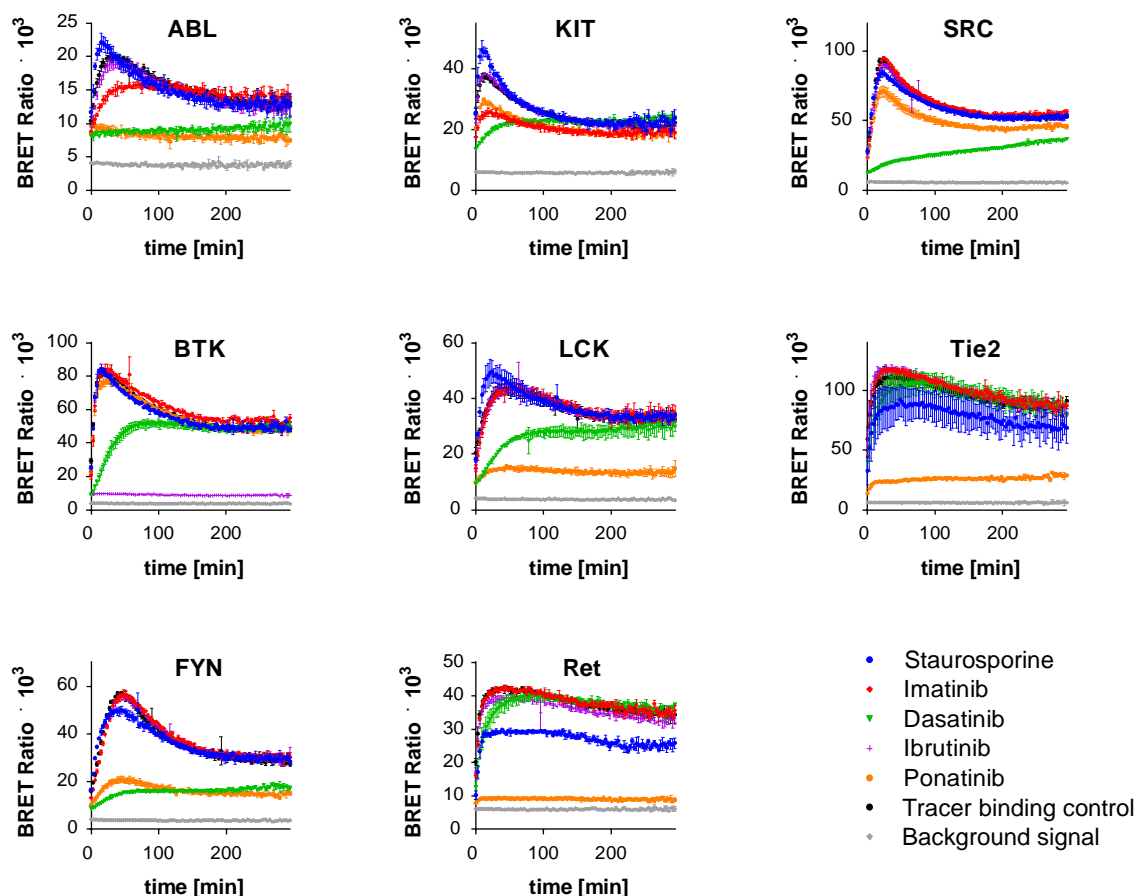


Figure 38: NanoBRET™ traces for analysis of the time course of target engagement in intact cells.

The plots show the time-resolved tracer binding to eight kinases in intact cells after compound washout (NanoBRET™ assays). A 0% (saturating inhibition) and 100% tracer binding control (vehicle DMSO instead of inhibitor) are labeled as “Background signal” and “Tracer binding control”. (Refer to chapter 4.2.3 for experimental procedure.)

5.4.1.1 Comparison between cellular target engagement and individual biochemical kinase-inhibitor binding properties (on-rate, off-rate and affinity viewed individually)

For quantitative analysis of cellular target occupancy dynamics, percent changes in target engagement during 30 min after compound washout were calculated from normalized cellular traces (as described in

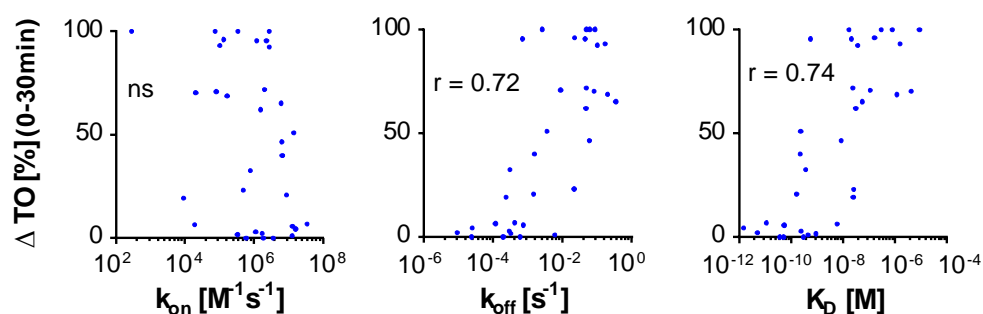


Figure 39: Comparison of biochemical binding parameters and duration of target binding in the cellular context

The percent changes in target occupancy ΔTO (in the normalized NanoBRET signal) during 30 min following compound washout were used as quantitative measure for intracellular target engagement. Off-rates and affinities correlate with ΔTO (correlation coefficient is indicated in the plots), while the correlation analysis for on-rates was not significant (n.s.).

chapter 4.2.3, Equation 2 and Equation 3) and compared to binding kinetic and affinity parameters (Figure 39). There is a good correlation of target occupancy changes with off-rates ($r = 0.7$) and with affinities ($r = 0.7$), while the different on-rates are not in agreement with target occupancy changes.

5.4.1.2 Simulation of the time-course of cellular target occupancy using biochemical kinase-inhibitor binding properties

Motivated by this observation, it was evaluated whether binding kinetics can be used to predict the time course of target occupancy in cells. In order to facilitate an easier comparison between simulated and experimental data, the observed NanoBRET tracer-target binding traces (Figure 38) were normalized (as described in chapter 4.2.3, Equation 2) to get the time course of compound-target binding signals as percentage of control (see Figure 41c). A Binding Kinetics (BK) - Permeation model was developed for simulation of cellular target occupancy profiles

(percentage of bound target fraction over time). The model equations are provided in appendix I. Several reactions and events had to be combined to improve the simulations of target occupancy decline in cells upon washout (illustrated in Figure 40). In brief, the following factors were included in the model: I) Association- and dissociation-kinetics of kinase-compound binding, II) available concentration of the compound over time calculated based on the permeation through the cellular membrane, III) competition with ATP for kinase binding (considering ATP binding kinetics and ATP concentration), and IV) the percentage of target occupancy at the beginning of the dissociation experiment (directly after the removal of the compound), which can be estimated by simulation of the pre-incubation step with the compound. Although, the kinase concentration could also have an impact, it was assumed to be constant. Only through the combinations of all these factors (I-IV), the simulations of target occupancy with ibrutinib and dasatinib in intact cells were in good agreement with the cellular experiments (Figure 41). The traces were best described, when assuming a lower ATP concentration to account for cytotoxic effects of the compounds (dead cells lose ATP [127]) – an example is BTK and SRC occupancy with dasatinib. The analysis further indicates that the residence times ($1/k_{off}$) of dasatinib-LCK, dasatinib-FYN and ibrutinib-BTK might be underestimated in the kPCA experiment (more details in chapters 5.1.1 and 5.4.3.2). Taken together, the simulation based on binding kinetics and the experimental traces indicated that there might be further mechanisms decelerating target occupancy increase and decline in cells for ponatinib and imatinib (such as e.g. active transport). Considering additional reduction of compound intake and release (as described in appendix I), improved the

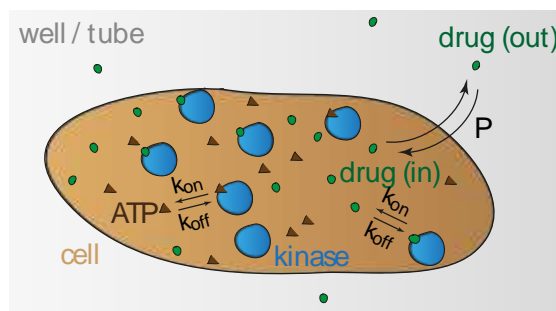


Figure 40: Reactions and events relevant for simulation of target occupancy.

The kinetics of competitive target kinase binding of ATP and drug was considered for the simulation of target occupancy profiles. Additionally, the availability of free drug in the cell was estimated based on permeation through the cell membrane.

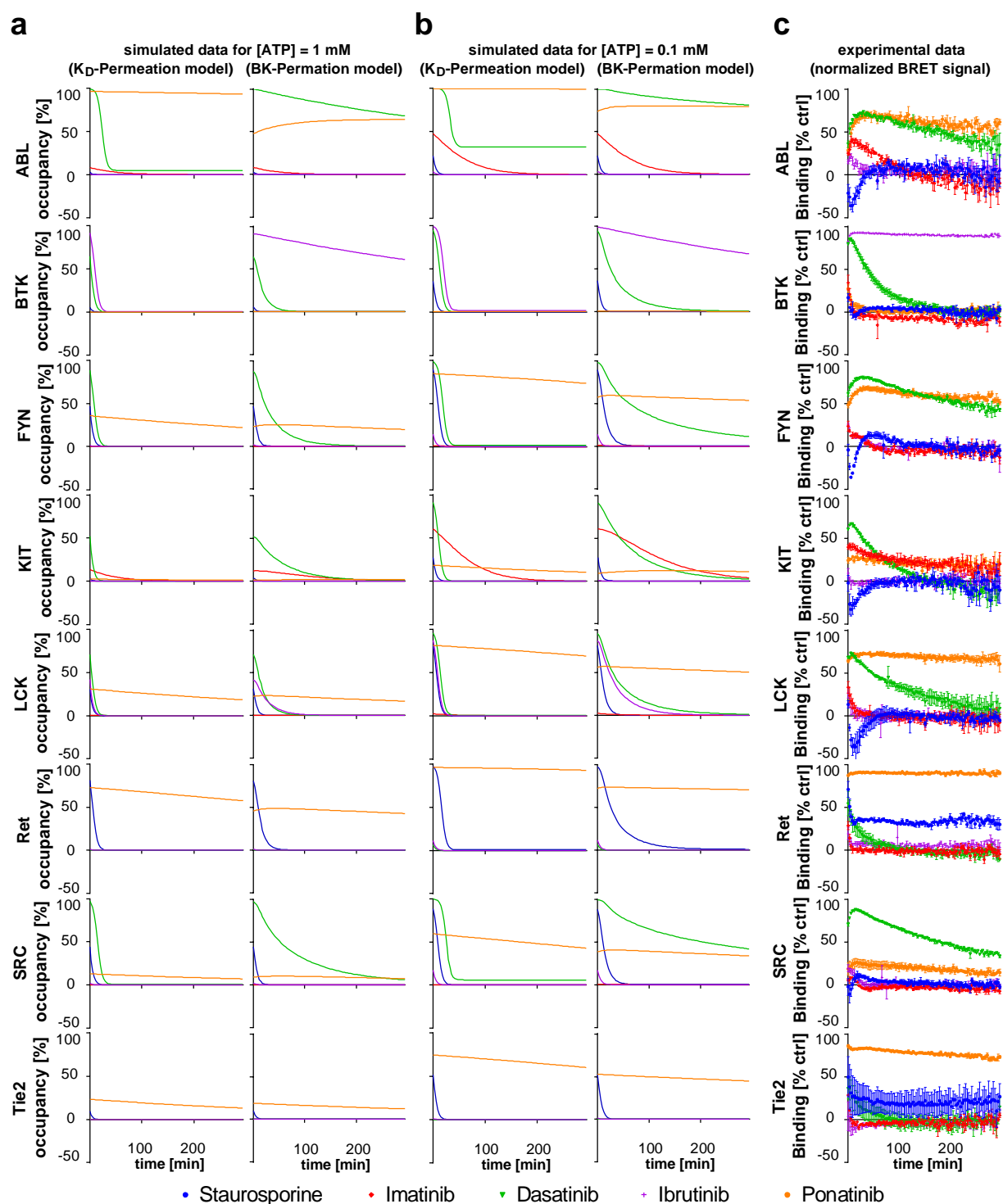


Figure 41: Simulated time course of target occupancy decline in cells compared to experimental traces

Simulated time courses of target occupancy decline upon compound washout assuming ATP concentrations for healthy (a) or dead (b) cells and using either affinities or binding kinetics (left and right panels in a and b, respectively) versus time course of kinase binding (as percentage of control = normalized from traces shown in Figure 38) as observed in NanoBRET™ washout experiments (c). The model equations used for the simulations are provided in appendix I. The traces from Figure 38 were normalized as described in chapter 4.2.3 (Equation 2). The cellular target engagement profiles can be better simulated under consideration of binding kinetics as by using the concentration-affinity effect *per se*. The time courses are best described by the BK-permeation model assuming the lower ATP (0.1 mM) concentration to account for cytotoxic effects of the compound (as observable in this figure and quantified in appendix K, Figure 54).

simulations for these drugs. The staurosporine traces from NanoBRET experiments are difficult to interpret, since tracer binding in cells preincubated with staurosporine exceeds tracer binding in the controls (without compound pre-incubation) in the beginning of the washout experiments (as mentioned in chapter 5.4.1; refer to Figure 38). However, target occupancy seems to be short in all cases, except for RET occupancy. This behavior corresponds with the fast off-rates determined by kPCA, where the slowest off-rate was also observed for RET.

Furthermore, it was assessed if target occupancy profiles predicted by binding kinetics parameters differ in relation to profiles predicted by the concentration-affinity effect *per se*. A K_D - Permeation model was developed. The equations for this model are provided in appendix I. In brief, the time course of the cellular compound concentrations was simulated with a permeation model (by using the same conditions as for the BK-Permeation simulations (including consideration of the pre-incubation step), but obviously without consideration of binding kinetics). The concentration profiles were then used together with the affinities (of compound- and ATP-kinase binding) to calculate the target occupancy profile. These simulations indeed differed from those obtained with the BK-Permeation model (Figure 41a-b). The comparison to the kinase-compound binding traces derived from the cellular experiments enabled to decide which prediction is closer-to-reality. In many cases, the time course of target occupancy was better predicted by using binding kinetics than by using affinities *per se* (Figure 41 – e.g. ABL-dasatinib). Quantitative comparison of target occupancy changes in the experimentally obtained and simulated traces reinforced this observation and confirmed the BK-Permeation model considering 0.1 mM ATP as best prediction (appendix K, Figure 54).

Summary of the results: Off-rates and affinities, but not on-rates correlate with target engagement in intact cells. Yet, simulation of the cellular target engagement profiles for 16 kinase-compound pairs reflected experimental traces under consideration of the following reactions and events: The kinetics of competitive ATP and compound binding to kinases, permeation through the cell membrane and the percentage of target occupancy at the beginning of the washout experiment (obtainable by simulation of the pre-incubation step). It was necessary to include binding kinetics (on- and off-rates) in the model. The concentration-affinity effect was not explaining the time course of target occupancy. Other simulated target engagement profiles differed from the experimental traces, revealing that there are further main factors which can determine the decline of kinase-compound occupancy in addition to binding kinetics. All in all, biochemical on- and off-rates contribute to a better understanding of the time course of cellular target occupancy and are better predictors than equilibrium affinity *per se*.

5.4.2 Binding kinetics perspective on selectivity

The cellular target engagement assay (chapter 5.4.1) illustrated how kinase occupancy and hence selectivity can change over time. For example, dasatinib initially occupies six kinases to more than

70%. After 200 min only 3 of the kinases remain occupied to about 50%, while the other 3 are no longer occupied with dasatinib. In this chapter, it will be assessed and discussed when and how selectivity can be differently weighted from the binding kinetics and affinity perspective. (In the next chapter, selectivity is assessed in *in vivo* simulations additionally considering the pharmacokinetic aspect.)

The Gini coefficients [128] was calculated (chapter 4.3.7) as known measure of compound selectivity (Figure 42a). This score expresses the degree to which the sum of the inhibitors affinities on all kinases under investigation hits a single kinase (Gini coefficient = 1) or all kinases with equal affinities (Gini coefficient = 0). Thus, it is independent on arbitrary thresholds. As expected, the known unselective compound staurosporine has one of the lowest Gini scores. Nevertheless, the number of kinases screened in this panel is not sufficient for reliable assessment of total selectivity; but it can serve for comparison of affinity and binding kinetic effects. Although, the Gini score is traditionally determined on the basis of affinities, it was additionally calculated (as described in chapter 4.3.7) on the basis of on-rates and off-rates, respectively (Figure 42a). The rank order is always similar. A possible explanation is that an unselective compound hits many kinases and a selective compound one or only a few kinases, so that the perspective on the overall selectivity of kinase inhibitors based on the Gini score is not significantly different, whether considering on-rates, off-rates or affinities (separately). Thus, this procedure turned out as not suitable to visualize kinetic selectivity.

Even so, the cellular experiment illustrated that there can be a difference between equilibrium and kinetic selectivity: A compound could be less unselective, at least over time, than assumed from the equilibrium perspective (e.g. based on affinities on kinases). The cellular experiment further indicated that it is insufficient to consider solely one of the binding parameters (on-rate, off-rate or affinity) separately for the estimation of target engagement level and time course. For a different perspective on selectivity, it would therefore be necessary to consider on-rates, off-rates, and affinities together, since the kinase-compound interaction is best described by all three parameters together. Figure 42b depicts how that could be accomplished qualitatively, and why consideration of only one parameter is not sufficient. The illustration reveals that e.g. staurosporine targets many kinases with fast on-rates and affinities, presumably leading to high target occupancies, but dissociates fast from many of them (especially from closely related non-receptor tyrosine kinases), which could increase selectivity for those with long residence times (slow off-rates) over time. On the other hand, imatinib, ibrutinib and ponatinib have slow off-rates on targets where they presumably never reach high target occupancy due to low on-rates and affinities. Moreover, all compounds in Figure 42b have fast on-rates on many targets, where they also possess low affinities and fast off-rates and thus will probably never reach long-term high target occupancies.

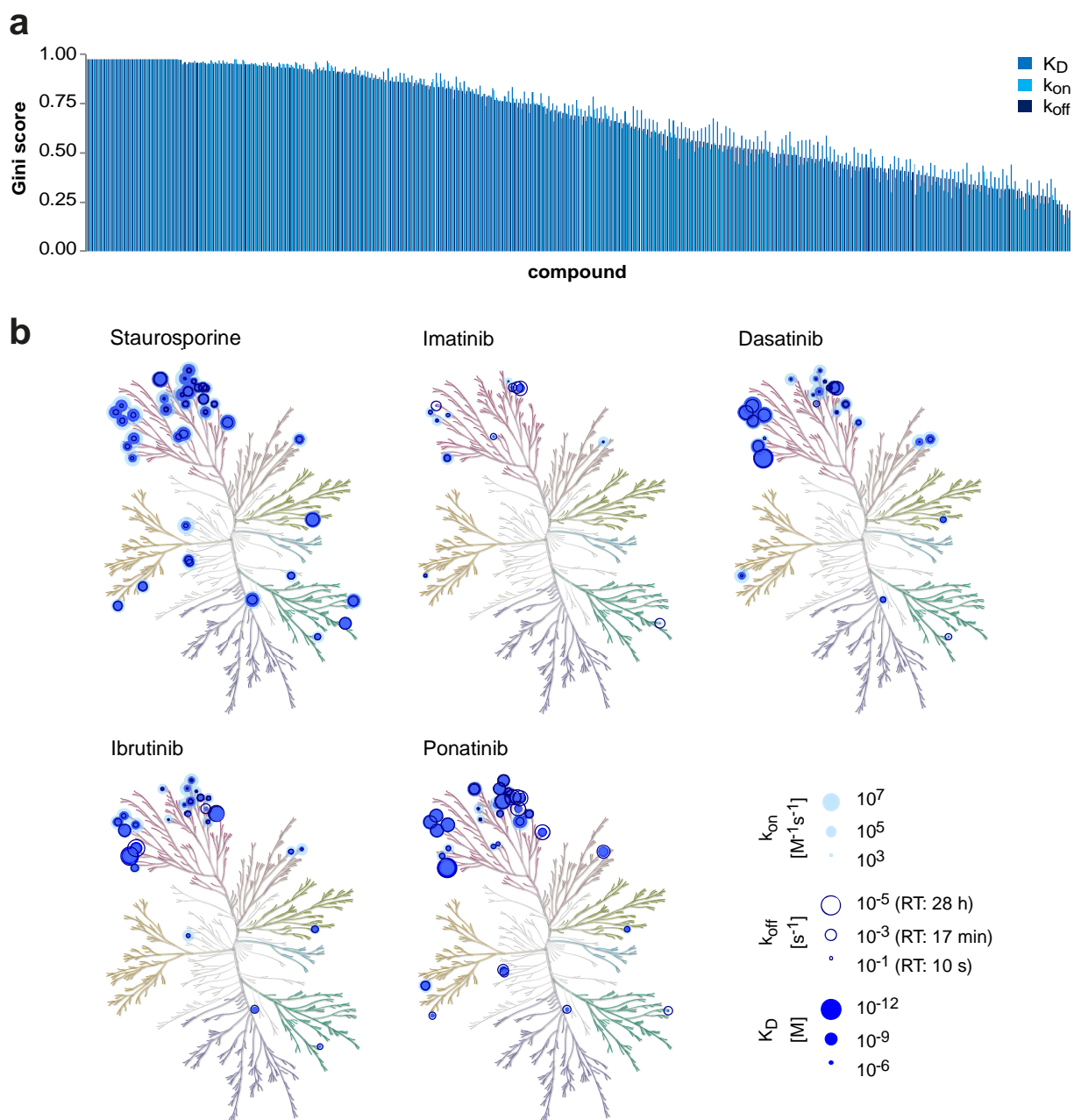


Figure 42: Influence of binding kinetics on target selectivity.

a) Bar chart of selectivity scores of kinase inhibitors calculated (with a procedure which is typically used to analyze equilibrium binding metrics; see methods chapter 4.3.7) based on their affinities, on-rates or off-rates on all kinases under investigation, respectively. Consideration of these parameters separately does not significantly change the rank order, since a highly selective compound still targets only one/a few kinases, while an unselective compound targets many kinases. Kinetic selectivity cannot be visualized with this approach.

b) Phylogenetic trees of the human kinome with kinases targeted by the respective compound (out of the targets screened in this study). The spot size quantifies the magnitude of the corresponding on-rate, off-rate and affinity. The cellular experiment (chapter 5.4.1) showed, that together these binding parameters determine the level of target occupancy that can be reached within a given timeframe and at a given drug concentration, as well as the rate of target occupancy decline upon removal of drug. E.g. a sufficiently fast on-rate and high affinity is required to reach the desired level of target occupancy and a slow off-rate, together with a preferably fast on-rate (facilitating rebinding), decelerates target occupancy decline. With respect to target selectivity, e.g. staurosporine could reach high occupancy for many targets (due to high affinity and on-rate), but cannot keep the level for all upon compound removal (due to fast off-rate).

It should be noted that in the *in vivo* context, all these considerations are also dependent on e.g. the drug dose (concentration), pharmacokinetic parameters (such as absorption, plasma elimination, bioavailability) as well as other micro-pharmacokinetic parameters (such as target concentration and turnover, active transport of the drug in cells) [29, 40, 129]. The example of ponatinib (Figure 41) shows that other micro-pharmacokinetic parameters can diminish e.g. the effect of binding kinetics on target occupancy decline. Here only the onset of target occupancy in cells is also determined by binding kinetics and affinity. Then, the level of target occupancy stays constant, presumably because the intracellular drug repository stays high.

However, binding kinetics and affinity are in addition to target concentration and target turnover the only parameters that are target specific, and as such one of the few parameters that can lead to a different perspective of selectivity in the *in vivo* context as compared to the test tube.

Summary of the results: Consideration of on-rates, off-rates or affinities separately cannot change the perspective on selectivity. However, the cellular experiment showed that the combined effect of these binding parameters can have an influence on the level of target occupancy that can be reached in a given timeframe and on the rate of target occupancy decline. Therefore, it was illustrated how they could be considered together to assess selectivity. Nonetheless, the knowledge about (other micro-)pharmacokinetic parameters is essential to estimate to what extent binding kinetics can change the selectivity of unselective compounds compared to the affinity perspective.

5.4.3 Combined effect of pharmacokinetics and binding kinetics on target occupancy

The question addressed in this chapter was whether binding kinetics can alter the *in vivo* target occupancy (a prerequisite for the pharmacological effect) in relation to the concentration-affinity effect *per se*.

5.4.3.1 Identification of trends for the effect of residence time on target occupancy and the pharmacological effect

Among the clinical relevant kinase-interactions ($K_D < 10^{-7}$ M) of FDA-approved drugs are more with slow off-rates as compared to those of compounds in earlier phases (Figure 43a; appendix K Figure 55), indicating that slow off-rates prevail. In detail: while means, medians and 75% percentiles of on-rates were similar for preclinical and FDA-approved compounds (0.3%, 1.0%, 0.5%), off-rates showed 12.6, 11.4 and 21.5 percent difference, respectively. Moreover, among the high affinity interactions the slowest off-rates were observed for the main targets, not for the other targets, of the FDA approved drugs (Figure 30c). Furthermore, the gap between slow and fast dissociating kinase-compound pairs becomes larger when comparing compounds in early and late stages of clinical development (see Figure 51 in appendix F). A possible explanation would be that the duration of

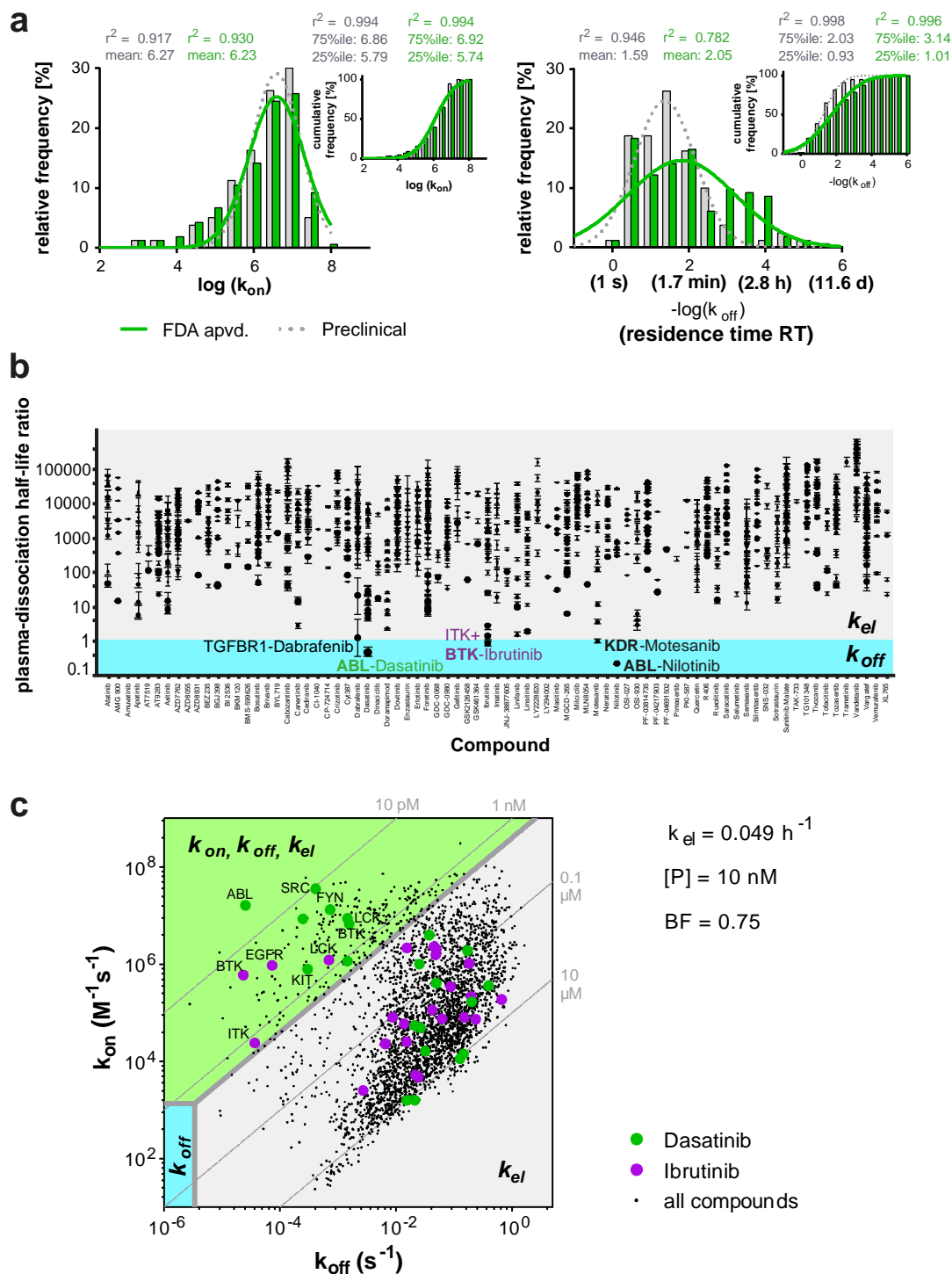


Figure 43: Trends for the effect of residence time on target occupancy and the pharmacological effect

a) Considered are kinase-compound pairs with affinities $<10^{-7}$ M (to account for potential clinical relevance): Relative and cumulative frequency distributions of target-compound binding kinetic parameters for preclinical and FDA-approved kinase inhibitors are shown as histograms (bars for bins) with Gaussian curve fit (and corresponding r^2). The frequency distribution of on-rates is similar for kinase inhibitors in different clinical phases, while the percentage of slow off-rates is increasing from preclinical drug candidates to FDA approved drugs. (more details in appendix K, Figure 55). **b)** Ratio of plasma half-life and dissociation half-life considering all compounds analyzed in this study with IntegritySM database entries about plasma half-life. The majority of kinase-compound dissociation half-lives is faster than the corresponding plasma elimination half-life. **c)** k_{on} - k_{off} plot of kinase-inhibitor pairs (with binding parameters within assay quantitation limits) divided in sections where either 1) plasma elimination rate (k_{el}) (grey), 2) k_{off} (cyan) or 3) k_{on} , k_{off} and k_{el} (green) determine the rate of target occupancy decline (sections were defined according to Witte *et al.* [39] based on an average k_{el} of 0.049 h^{-1} (of all k_{el} IntegritySM database entries for tested compounds), a protein concentration $[P]$ of 10 nM and a bound target fraction BF of 75%). The interactions of dasatinib and ibrutinib are highlighted, as *in vivo* target occupancy simulations were performed for these compounds (see Figure 44).

target occupancy on the main targets, and hence the pharmacological effect, is indeed prolonged by slow off-rates increasing kinetic selectivity.

Therefore, different published approaches were pursued to assess the potential impact of binding kinetics (BK) on target occupancy (TO) decline in the *in vivo* situation. According to Dahl and Akerud (2013) [29] drug–target dissociation will prolong target occupancy if the dissociation half-life is greater than the (systemic) plasma half-life. Figure 43b shows the plasma-dissociation half-life ratio for all inhibitors profiled in this study with entries in the IntegritySM database. The Plasma half-lives of the kinase inhibitors were calculated as median (with 25% and 75% quantil) of all entries in Integrity database for healthy human adults. The dissociation half-lives were calculated as $\ln 2 / k_{\text{off}}$. The minority of inhibitors has a longer dissociation half-life than plasma half-life (Figure 43b): Among them are dasatinib, nilotinib, ibrutinib, dabrafenib and mosatinib. On the other hand, the recently published approach by Witte *et al.* (2016) [39], adds further complexity: According to them, binding to the target can modify local pharmacokinetics, may lead to a decrease in free drug concentration and only unbound drugs can be eliminated by pharmacokinetic effects. They derived equations allowing partition of the $k_{\text{on}}-k_{\text{off}}$ plot in sections where especially 1) the elimination rate, or 2) the off-rate or 3) the elimination rate, the on-rate and the off-rate determine target occupancy decline [39]. Figure 43c depicts such a sectioned $k_{\text{on}}-k_{\text{off}}$ plot for all kinase-compound pairs screened in this study. The median of all known plasma half-lives (of all inhibitors profiled in this study with entries in the IntegritySM database) was used to calculate an average elimination rate k_{el} ($= \ln 2 / \text{plasma-half-life}$). Plasma elimination (k_{el}) is the rate-limiting step for TO decline for the majority of compound-kinase pairs (3927 pairs; thereof: 14.3% FDA-approved drug interactions, 0.2% FDA-approved drug interactions with their main target), but there are also many cases where the TO decline rate is determined by k_{el} , k_{on} and k_{off} (250; thereof: 24.0% FDA-approved drug interactions, 11.6% FDA-approved drug interactions with their main target) - Figure 43c. Among the latter are many interactions of the FDA approved drugs with their main targets (Figure 43c and Figure 30a). It should be noted, that assuming another target concentration would lead to an offset of the margins of the $k_{\text{on}}/k_{\text{off}}/k_{\text{el}}$ section and assuming another k_{el} would affect the margins of the k_{off} section.

5.4.3.2 Simulation of the time-course of target occupancy using pharmacokinetics and kinase-inhibitor binding parameters

Motivated by the previous analysis, the goal was not only to explore the potential of binding kinetics to influence target occupancy decline (as with the previous approaches), but also its potential to influence the whole target engagement profile in the *in vivo* situation. For that reasons, the combined influence of pharmacokinetics and binding kinetics on *in vivo* target occupancy profiles was simulated (PK-BK model) for selected examples and compared to the traditional pharmacokinetic model considering the concentration-affinity effect (PK- K_D model) - Figure 44. The

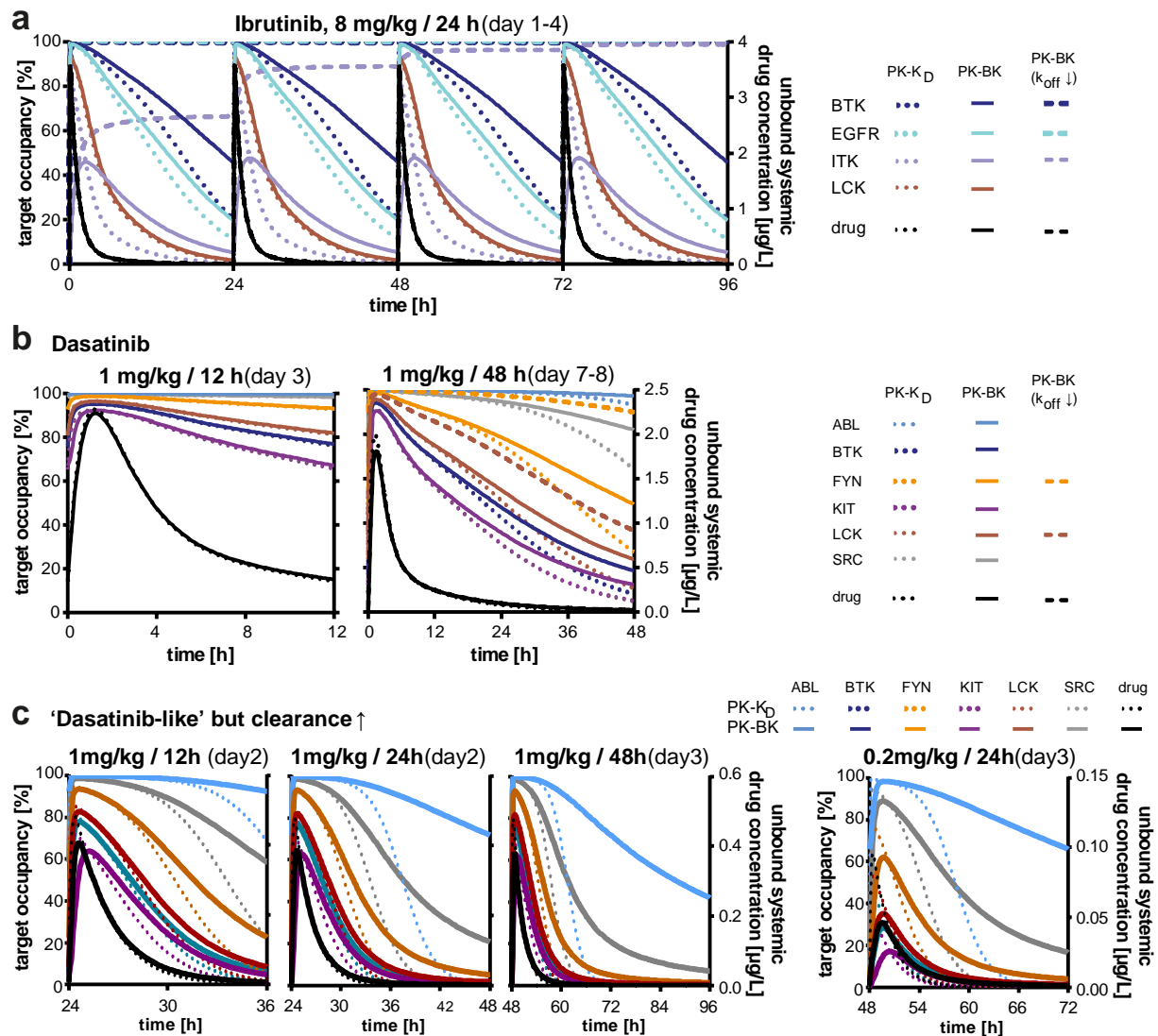


Figure 44: Comparison of simulations of the time course of *in vivo* target occupancy with drug from the binding kinetics (PK-BK) versus the affinity perspective (PK-K_D)

a) for ibrutinib (day 1-4, current clinical administration schedule) and **b)** for dasatinib (left: current clinical administration schedule; right: alternative dosing schedule with 4x longer intervals) and **c)** for a hypothetical 'dasatinib-like' compound with a faster clearance (4x intercompartmental clearance; 10x plasma clearance) but otherwise identical BK and PK parameters (b, c with different dosing schedules: day where target occupancy traces reached equilibrium, respectively). The model equations used for the simulations are provided in appendix J.

Target occupancy simulations on the basis of pharmacokinetics and binding kinetics (PK-BK) can be significantly different to those derived from pharmacokinetics models and the concentration-affinity effect (PK-K_D): Target occupancies can be prolonged (e.g. ibrutinib-BTK) and/or the target occupancy level expected from PK-K_D models is not reached in PK-BK models (e.g. ibrutinib-ITK). The simulations further illustrate that thereby, the extent of the influence of binding kinetics on the target occupancy profiles is dependent on various factors: (I) the on- and off-rate: e.g. no deviation between the models for fast binding (e.g. ibrutinib LCK), and underestimation of slow off rates (frequent problem (see chapter 5.1.1)) leads to underestimation of duration of target occupancy (e.g. covalent binding of ibrutinib, but also 2x or 10x slower dasatinib binding to LCK or FYN). (II) The administration interval: frequent dosing diminishes the effect of binding kinetics (see the different dosing intervals for dasatinib and the "dasatinib-like" compound). (III) Administered dose and clearance (e.g. 'dasatinib-like' drug): lower doses and faster clearance enhance the effect of binding kinetics, that target occupancy levels expected from PK-K_D models are not reached (dosing effect) and/or sustained longer (= hysteresis due to slow dissociation rates).

model equations are provided in appendix J. For comparison between different target occupancy profiles, the area under the curves (AUC) and maximum target occupancies (TO_{max}) were calculated (appendix K, Table 10). If not otherwise specified, the binding parameters determined in the profiling (supplementary spreadsheet in appendix page 165ff) were applied for the simulations, even though affinities and off-rates might be underestimated (as for the covalent inhibitor ibrutinib [71]). Nonetheless, the simulated target occupancy profile for ibrutinib is significantly different in traditional PK models based on affinities (PK- K_D) and in PK-BK models (20% and 14% difference for average AUC and TO_{max}), with the exception of LCK occupancy (4% and 0% difference for AUC and TO_{max}) – see Figure 44a. Ibrutinib has both a fast on-rate and fast-off-rate for LCK, with the result that binding kinetics do not influence target occupancy. On the other hand, the slow binding kinetic rate constants for the other targets lead to a modified time course of target occupancy compared to the concentration-affinity effect. The affinities for BTK and EGFR are similar, but the off-rate from BTK is slower, accordingly the target occupancy decline is decelerated for BTK (to a greater extent compared to EGFR: 16% versus 11% difference between AUC in PK-BK and PK- K_D models). The ibrutinib concentration together with its on-rates and affinities on LCK, BTK and EGFR are sufficient to reach 100% target occupancy (and 0% difference between TO_{max} in PK-BK and PK- K_D models), whereas the ibrutinib-ITK association-rate is too slow, so that the target occupancy presumed by PK- K_D simulation is not reached in PK-BK simulation (55% difference in TO_{max}). In contrast, PK- K_D and PK-BK simulated target occupancies are not significantly different for dasatinib administered as in the clinic (0% difference for average AUC and TO_{max}). Yet, when decreasing the frequency of drug administration, a decreased target occupancy decline is observed in PK-BK models (7% and 0% difference for average AUC and TO_{max}) – see Figure 44b.

Due to the long time frame required to reach equilibrium, off-rates and affinities are likely to be underestimated, regardless of the applied assay technology. As mentioned above (chapter 5.1.1 and 5.2.3), this also applies for kinetic Probe Competition Assays: For example, determined ibrutinib-BTK, -EGFR and -ITK off-rates are smaller or equal to the value used for these simulations (as indicated in the supplementary spreadsheet (appendix page 165ff)). The same applies for slow dasatinib off-rates. As ibrutinib is a well-known covalent inhibitor [71] and cellular experiments indicate a longer residence time on BTK (Figure 41), the PK-BK simulations were repeated with the assumption of covalent binding to BTK, EGFR and ITK. As expected, ibrutinib now sustains 100% BTK and EGFR occupancy and repeated administration of ibrutinib leads to higher and higher ITK occupancy levels before reaching equilibrium at 100% target occupancy (Figure 44a). Target degradation and resynthesis are not considered in the simulations, but with repeated drug dosing the level of target occupancy will be regained fast for BTK and EGFR and more slowly for ITK. Cellular experiments also indicate a longer residence time of dasatinib on FYN and LCK (Figure 41). Simulations considering the slower off-rates (10x slower for FYN, 2x slower for LCK) lead to higher FYN and LCK occupancies (Figure 44b).

Traditionally clearance, as a metric for drug removal from the body (or body compartment) per unit time, has to be slow enough for sufficient drug exposure to maintain target occupancy between doses [18]. In contrast, the clearance should be fast to make use of kinetic selectivity. Therefore, target occupancy traces were simulated for a hypothetical 'dasatinib-like' inhibitor optimized for fast clearance (intercompartmental clearance CLD: 4x; plasma clearance CL: 10x) administered with different dosing schedules (1mg/kg/12h, 1mg/kg/24h, 1mg/kg/48h or 0.2mg/kg/24h), but otherwise using the same BK and PK parameters as for dasatinib (Figure 44c). As observed for dasatinib before, longer dosing intervals enhance the effect of BK on the target occupancy traces: Higher discrepancies between the PK-BK and PK-K_D models are observed and indicate hysteresis (prolonged duration of effect as assumed from the concentration-affinity effect). On the other hand, longer dosing intervals also lead to lower target occupancies at the end of the dosing interval (also for the PK-BK model). To allow a high ABL occupancy at all times between dosing, once-daily dosing was chosen for the dasatinib-like compound. Moreover, by using a lower dose (0.2mg/kg/24h), lower target occupancies are reached for most of the targets (especially those with slower on-rates) as a result of the lower drug concentration (30% difference in average TO_{max} between PK-BK and BK-K_D), but the main targets ABL and SRC with fast on-rates are less affected (1% and 6% difference in TO_{max}). On the other hand, the fast clearance, once-daily dosing and long residence times on the primary targets lead to greater AUC in the PK-BK compared to the PK-K_D model (35% difference in average AUC), especially for the main targets ABL and SRC (65% and 56% difference in AUC). Therefore, a high target occupancy level (>66 % in PK-BK model) throughout the 24 h between dosing is only reached for ABL. This theoretic example illustrates the applicability of the concept of kinetic selectivity.

Summary of the results: For the majority of kinase-compound pairs, plasma half-life is longer than the dissociation half-life, and the plasma elimination rate is the rate limiting step for target occupancy decline. On the other hand, there are much more kinase-compound pairs, where in addition to the elimination rate, also the on-rate and off-rate could play a role for target occupancy decline as compared to kinase-compound pairs with longer dissociation half-lives than plasma half-lives. Simulations of the combined effect of pharmacokinetics and binding kinetics in the *in vivo* situation showed that slow off-rates have the potential to prolong target occupancy beyond the concentration-affinity effect and that slow on-rates can lead to lower target occupancy than expected from the concentration-affinity effect. The simulations further illustrated how knowledge about binding kinetics could be used to influence *in vivo* selectivity: In addition to drug administration dose and interval, also optimization towards fast plasma clearance during lead optimization can be deployed to make use of the concept of kinetic selectivity (if required). Finally, it was observed that throughout clinical development phases, the frequency distribution of on-rates was similar, while the percentage of slow off-rates was increasing towards the group of FDA-approved drugs. This observation might indicate that slow off-rates are indeed beneficial – either for the pharmacological effect or for selectivity or for both.

6 Discussion

In the past decade, the potential impact of drug-target binding kinetics on the duration of target occupancy and thereby on the pharmacological properties efficacy and safety has become a topic of intense debate. Major questions are whether and when binding kinetics can influence drug action in the complex context of pharmacokinetics and pharmacodynamics, and how the kinetic rate constants can be optimized rationally. One major obstacle for a better understanding was the lack of cost-effective assay technologies with sufficient throughput for the systematic assessment of compound's on- and off-rates and the generation of comprehensive datasets. To meet this challenge, the universal kinetic Probe Competition Assay (kPCA), which relies on the Motulsky-Mahan competitive binding kinetics theory, was recently developed.

In this study, 1) the scope and limitations of this method were assessed to generate guidelines for 'kinetic probe competition' experiments, 2) the applicability of kPCA for large-scale profiling was demonstrated by analyzing the binding kinetics of a large kinase inhibitor set against a panel of clinically relevant kinases, and 3) it was illustrated how the data generated with this kPCA panel can provide new insights into structural features influencing kinase inhibitors' target binding kinetics and into the impact of binding kinetics on target occupancy profiles. These outcomes are discussed in detail in the following chapters.

6.1 Recommendations for the analysis and design of 'kinetics of competitive binding' experiments

The Monte Carlo analyses and simulations (chapter 5.1) enhanced the theoretical knowledge and understanding of the Motulsky-Mahan model of competitive binding. The observations from this study allow derivation of recommendations about how to setup assays and how to evaluate experimental data, which will be discussed in this chapter.

The analyses were based on the example of a standard kPCA setting (as proposed in reference [84]) and in the timescale of seconds, but the mathematical background is identical for a time scale of minutes, and the results can be transferred to other competition assays applied for the analysis of binding kinetics. It should also be noted that the analyses assumed a fluctuation in the experimental signal as it was observed in an experiment. The fluctuation was assumed equal for all concentration traces (all wells), albeit there could be differences. For higher and lower fluctuations (in all or in single concentration traces), the quantitative results of the Monte Carlo analyses will differ, but the qualitative conclusions should be the same.

One case that frequently occurred in the experiments (in this study and beyond) was that the on-rate can be determined precisely (low coefficients of variation), but the off-rate cannot be calculated or only with high uncertainty (high coefficient of variation), and at the same time the affinity determined in the kinetic experiment differs from the equilibrium experiment. Schiele, Ayaz and Fernández-Montalván [84] suggested calculation of the off-rate for slow dissociating compounds, that cannot be determined by kPCA, by using the Motusky-Mahan on-rate and the equilibrium dissociation constant determined in an endpoint assay ($k_{\text{off}} = K_D \times k_{\text{on}}$). The Monte Carlo analyses in this dissertation (Figure 10) illustrate that for too slow-dissociating interactions the determined on-rate is reliable (accurate), while the slow off-rate could be either not determined (drift to non-sense low values), underestimated or overestimated. The conclusion is that the proposal of Schiele, Ayaz and Fernández-Montalván is useful not only in those cases where the off-rate cannot be determined but also in the cases where the on-rate, but not the off-rate, possesses a low coefficient of variation.

However, when calculating the off-rate using equilibrium affinities it is important to pay attention to the assay wall [95, 119] and incubation time in the endpoint assay [120]. Accordingly, if the dissociation constant is likely to be underestimated in the endpoint assays, also the off-rate is smaller or equal to the calculated value. This is much better than not to know if it is underestimated or overestimated (as for too slow Motulsky-Mahan k_{off} values). The affinity underestimation due to incubation time in the endpoint assay is highly dependent on the off-rate, and was used for the identification of slow dissociating compounds before [121]. The simulations of the equilibrium

experiment in this dissertation (Figure 11) reflect the same phenomenon and visualize that the smaller the off-rate, the slower the rate with which the determined apparent dissociation constant decreases over time. Also Motulsky and Mahan themselves pointed out that reaching equilibrium for all concentrations of an endpoint assay takes about 3.5-fold of the residence time [83]. Nonetheless, the simulations in this dissertation demonstrate that for the typical ePCA setup an incubation time of half the residence time will lead to reliable results (less than 3-fold difference), i.e. if applicable overnight incubation of the endpoint assay for very slow dissociating compounds.

The incubation time in the equilibrium assays used for the screening was shorter, but the following example of the irreversible (covalent) binder ibrutinib illustrates that calculation of slow off-rates using the equilibrium affinity and the Motulsky-Mahan on-rate should be preferred over the Motulsky-Mahan off-rate: While the residence time on BTK calculated from the Motulsky-Mahan off-rate was 40 min, the residence time obtained with the “calculated off-rate” for BTK was >12 h which is much closer to reality (and the possible underestimation is known).

Motulsky and Mahan further highlighted that an advantage of the kinetic assay setup is that affinities can be determined in a shorter period of time as compared to the equilibrium setup, which is advantageous since effects such as protein target degradation, cell death or changes in the composition of the assay buffer often hamper long incubation times [83]. However, the Monte Carlo analyses in Figure 10 demonstrated that the dissociation constant cannot always be determined accurately with the Motulsky-Mahan method. This finding reinforces the observations by Schiele, Ayaz and Fernández-Montalván [84], that the off-rate (and affinity) cannot be determined when none of the compound concentrations reaches at least 50% equilibrium. On the other hand, this dissertation showed that not the equilibrium but rather the off-rate (independent from the on-rate) of the compounds determines the lowest calculable off-rate. Neglecting influence of tracer binding characteristics, Monte Carlo experiments (Figure 12, Figure 13, Figure 18) allow derivation of the following rule of thumb: The highest residence time (and corresponding off-rate and affinity) that can be determined accurately in a kinetic probe competition assays is maximal five times the observation time (i.e. $RT \approx 1970$ s or $k_{off} \approx 5 \times 10^{-4} \text{ s}^{-1}$ for 394 s observation time and $RT \approx 23400$ s or $k_{off} \approx 4 \times 10^{-5} \text{ s}^{-1}$ for 4680 s incubation time). Coming back to Motulsky and Mahans’ claim, an incubation time of 0.2-fold the residence time (required for affinity determination in kinetic assay setup) is less than half the incubation time (required for affinity determination in equilibrium assay setup), and if it takes hours to reach equilibrium that might make a difference. However, this only applies for low-throughput applications, since for higher-throughput applications the readout for the equilibrium assay is much faster (less than one minute per 384 well plate) than the readout for the kinetic assay (currently at least 1x the observation time per 384 well plate). Therefore, for higher throughput

applications a short observation time in the kinetic assay combined with a parallel equilibrium assay as proposed by Schiele, Ayaz and Fernández-Montalván [84] is preferable.

Another case that frequently occurred in real experiments (in this study and beyond) is that neither the on-rate nor the off-rate can be determined (drift to non-sense high values) or determined precisely (high coefficients of variation), but the ratio of the on- and off-rate (the dissociation constant determined with the Motulsky-Mahan model) is consistent with the dissociation constant determined in the endpoint assay. The Monte Carlo method (Figure 10) illustrates that this case occurs for compound-target pairs with fast off-rates which can result in both overestimation and underestimation of the compounds off-rate and corresponding on-rate, while the dissociation constant is determined precisely and accurately. Further analyses (Figure 14, Figure 15, Figure 18) allow derivation of the following rule of thumb (neglecting influence of tracer binding characteristics): The fastest off-rate (and corresponding on-rate) that can be determined accurately in a kinetic probe competition assays is defined by the frequency of measurement (i.e. $k_{\text{off}} \approx 1 \times 10^{-1} \text{ s}^{-1}$ for a measurement frequency of 0.1 Hz (a measurement interval of 10 seconds), and $k_{\text{off}} \approx 8 \times 10^{-3} \text{ s}^{-1}$ for a measurement interval of 120 seconds). Similarly, but less quantitative, the GraphPad Curve Fitting Guide states that the “kinetics of competitive binding” equation “will only give reliable results if you have plenty of data points at early time points”, and at the same time points out: „The ratio K_4/K_3 is the equilibrium dissociation constant of the cold ligand in Molar. You should compare this value (determined via kinetics) with the same value determined by equilibrium competition” [118]. The first advice was reinforced by Monte Carlo simulations, but it should be noted that many data points covering the signal increase phase of the concentration traces is not necessarily sufficient (Figure 10), since the fastest reliably determinable off-rate depends especially on the length of the first measuring interval (Figure 14). The second advice helps to identify problems caused by slow off-rates, while it will not reveal errors arising from too fast off-rates (Figure 10).

In addition to measurement interval and the observation time, also the tracer binding characteristics have an influence on the reliably obtainable compound on- and off-rates: **1)** The maximum observable signal in the kPCA plot is dependent on the tracer affinity and concentration as well as the kinase concentration. The latter has to be low to avoid compound or tracer depletion. Therefore, the tracer concentration and affinity have to be high enough for a good signal to noise ratio. The interplay between compound and tracer concentration and affinity (and to a lesser extent also the tracer on-rate) determines the range of quantifiable affinities and on-rates of the compound (Figure 18). For lower throughput applications, it is therefore recommended to adapt the applied compound concentrations to the affinity and concentration of the tracer in the respective assay – and if known the expected affinity of the compound (e.g. not generally use a 4-point 10fold serial dilution starting

from 2500 nM compound, but higher or lower concentrations). **2)** Monte Carlo analyses (Figure 16, Figure 17, Figure 18) further visualize that if the fast off-rate limit is reached and the highest possible measurement interval is utilized, a last possibility that can have an impact for reliable determination of the kinetic rate constants is to increase the tracer concentration (or when available to use a tracer with a higher on-rate). **3)** It was also observed that the percentage of equilibrium reached in the tracer control has a high impact on precision and accuracy.

The third and last tip in the GraphPad Curve Fitting Guide is that the “kinetics of competitive binding” equation “does not account for ligand depletion. It assumes that only a small fraction of radioligand binds to receptors, so that the free concentration of radioligand is very close to the added concentration.” [118]. The analyses for robustness (Figure 20) showed that compound concentration errors in a single well can give inaccurate results. As long as tracer depletion is solely observed for the lowest compound concentration, this concentration should be removed from the analysis and the results are reliable again. The analysis is not robust for errors in the tracer binding characteristics (Figure 20), and special care is required for the determination of these parameters (Figure 22).

Finally, binding kinetic traces obtained by fluorescence-based readout can be influenced by fluorescence losses, leading to significant deviation from the standard Motulsky-Mahan competitive binding model. Schiele, Ayaz and Fernández-Montalván [84] provide a solution for this problem by multiplying with a signal drift term assuming mono-exponential decay. This dissertation validated the approach and additionally showed that an alternative method performs even better (Figure 23): A model for normalized curves (appendix D) was introduced in which normalization eliminates the signal drift completely without the need to add a further variable. Possible explanations for the better performance are proposed: On the one hand, photobleaching is typically more complex than a single-exponential process [130, 131], on the other hand also cell sedimentation or protein target degradation can lead to a decay in TR-FRET signals.

Conclusion and Outlook

kPCA is a robust method allowing for reliable determination of compound binding kinetics: kPCA gives accurate results in comparison with a radioligand assay. As all kinetic probe competition assays, kPCA is typically evaluated with the Motulsky-Mahan model. Monte Carlo analyses performed in this thesis confirmed and disclosed limitations of the Motulsky-Mahan model and allowed to derive recommendations for design of the assays and assessment of the data. Compared to multiple-compound-concentration traces, evaluation of single-compound-concentration traces is less robust and should be handled with care. The percentage of equilibrium reached in the tracer control was found to be important for precision and accuracy. A next step could be to analyze the minimum

required percentage in detail. The major drawback of the Motulsky-Mahan competitive binding kinetics theory is the assumption of one-step reversible 1:1 binding. It was demonstrated by simulation that the method can equally cope with irreversible one-step binding. However, it should be mentioned that an induced fit model would be better, as covalent inhibitors usually as first step form the drug-target complex followed by a second phase of covalent binding [132]. It would be interesting to implement and test alternative models (to the Motulsky-Mahan model) assuming more complex interaction mechanisms, such as induced fit or conformational selection. The choice of the model can be supported by the goodness of fit but should in the end be based on the knowledge about the molecular binding mechanism. Likewise the effect of the binding mechanism of the tracer should be implemented and tested. With regard to all biochemical studies comparing affinities (including drug discovery projects), it should be mentioned again (as it has been discussed several times [92] but is still often neglected) that for high IC_{50} values (e.g. in early stages of drug discovery projects typically >100 nM), where the off-rates are accordingly relatively fast, an incubation time of one hour will most often be sufficient for reliable determination of affinities, but on the other hand for interactions with low IC_{50} values (e.g. in lead evaluation and optimization phase typically < 100 nM) accompanied by slow off-rates the affinity can be underestimated if incubation times are too short.

6.2 Suitability of the ‘kinetic probe competition assay’ for large-scale binding kinetics profiling

This study confirmed the suitability of the kinetic Probe Competition Assay (kPCA) for the large scale analysis of binding kinetic data. 270 kinase inhibitors were screened against a panel of 40 kinases and 32400 binding parameters were evaluated. The details are discussed in this chapter.

The data experimentally obtained with the binding kinetic profiling panel were in accordance with the simulated data, not only for the signal traces (Figure 9) but also for the expected limits for precise determination of data (Figure 18 versus Figure 26 and Figure 48). Accordingly, it was possible to apply the learnings from the last chapter for the evaluation of the data set and to cope with initially hard to interpret but repeating artifacts. Thus, the method enabled collection of binding data with high intra- and inter-assay precision (chapter 5.2.2).

However, some limitations regarding accuracy could not be avoided: The Motulsky-Mahan equation assumes one-step reversible competitive 1:1 binding [83], which is not true for all compounds. Although the tracers (according to Thermo Fisher Scientific datasheet) as well as most inhibitors in Phase III and FDA approved drugs [50] bind to the ATP site, and typically via 1:1 binding, especially the assumption of the one-step process will lead to problems for some compounds. This error was reduced by considering kinase-compound pairs binding kinetics as not evaluable if the variation between precisely determined $K_{D\text{ eq}}$ and $K_{D\text{ kin}}$ is more than 5-fold. Another problem is that the assay wall was reached for some high affinity interactions, and the incubation time in the equilibrium assay was too short to reach equilibrium for slow dissociating compounds. Therefore the affinity [95, 119-121] and residence time (determined by calculated off-rate) is underestimated in those cases. Moreover, in some assays (especially for CDK2, IGF1R, IKK α , ITK, PLK1, ROCK1) and at low concentrations for the potent compounds depletion could occur, but is not considered in the analysis [83] (but tracer depletion was prevented completely). Moreover, stability and solubility issues (Figure 49), transfer problems with e.g. the Hummingbird Benchtop System and dust can cause concentration and/or readout errors. Finally, also temperature, buffer composition (pH, ionic strength) and the phosphorylation state of the protein affect the binding characteristics and not necessarily to the same extent or in the same direction [133].

Despite all these sources of error, the results correlated strongly with literature values [14, 69, 123] (Figure 28, Figure 29). The mean log differences were small for affinity and off-rates, only the on-rates determined by SPR were lower as compared to those determined by kPCA (which was similarly observed before [84]). It was described before, that different assay technologies with

different readout and assay setups have their individual advantages and disadvantages, which can impact the obtained kinetic parameters [92]. SPR and kPCA differ in many aspects: **1)** Target immobilization on surface (SPR) versus measurement in solution with labeled target (kPCA), both could alter binding characteristics of the proteins. Importantly, Kitagawa *et al.* [123] (so far the largest available study of kinase inhibitor binding kinetics and accordingly a major source for comparison) immobilized 4000-7000 RU protein on the sensor surface which could result in mass transfer effects [98] and accordingly underestimation of on-rates. **2)** Direct detection mode (SPR) versus indirect detection based on binding competition with labeled ligand (tracer): kPCA results depended on tracer concentration, and therefore its solubility and shelf-life, while SPR results depend on stability of immobilized protein. **3)** Kinetic resolution: 10Hz (SPR), but injection peak has to be removed in the beginning of the association phase versus 0.1Hz (kPCA): Higher kinetic resolution is better for fast kinetics, but as demonstrated by Monte Carlo analyses this especially affects the off-rates (at least for kPCA). **4)** Batch (kPCA) versus continuous flow (SPR): Compound residuals remaining after dissociation time on the sensor surface will hamper the accurate analysis of the following compounds (SPR). Despite all these differences, there was a good correlation of binding kinetic data obtained with the high-throughput method kPCA and the lower throughput method SPR. The difference in on-rates are most probably, at least in part, due to mass transfer effects [98] in the SPR system, a factor influencing on-rates to a larger extent than off-rates. Since kPCA results were in good agreement with literature affinities [14, 15] and off-rates [69, 123], it can be concluded that the kPCA results are reliable ($k_{on} = k_{off} / K_D$).

41 data points overlapped between this study and the so far largest available study of kinase inhibitor binding kinetics. This dissertation provides in total on-rates and off-rates for 4177 different kinase-inhibitor pairs, which were all measured with the same assay technology allowing an unprecedented comprehensive analysis (as presented in the following chapters).

Conclusion and Outlook

The profiling approach presented in this study can be performed using standard high-throughput compatible automated machines and meets the need for cost-effective determination of BK parameters at sufficient throughput to enable leveraging kinetic information - also in early drug discovery stages. In addition to high throughput capability, further compelling benefits compared to other assay setups comprise 1) high kinetic resolution (sec instead of min) [92] since there is no bound-unbound separation required (homogenous assay) and no delay between sample mixing and reading, 2) high sensitivity and miniaturized format allow low protein and tracer concentrations (nM instead of μ M – compared to [78]).

This dissertation validated that kPCA combined with ePCA is indeed a high-throughput compatible assay format and (when considering the recommendations mentioned in the chapter above) can provide accurate and precise results that are comparable to other methods for quantification of kinase-inhibitor binding kinetics and affinities. However, as is true for other biochemical assay technologies, high affinities and long residence times could be underestimated, and the binding parameters are *inter alia* dependent on temperature and buffer composition. For exact quantification of the slow off-rates and the corresponding affinities, it would be interesting to retest the respective kinase-compound pairs using longer incubation times for the endpoint assay and/or to enhance the observation time in the kinetic assay (and, if applicable, to reduce the kinase concentration by assay optimization). The PKCeta assay was used to prove the influence of the kinetic measurement interval experimentally. To allow a larger range of off-rates that can be determined precisely and accurately, the PKeta assay could be retested with the same long observation time, but a higher frequency of measurement in the early time points, which can be implemented by using the script mode of the plate reader (or alternatively with a faster equilibrating tracer and the standard kPCA setup). Compounds with mechanisms of action other than one-step binding could be re-analyzed by more complex models to get a deeper insight into the kinetics of the multiple steps. Future studies could also include the analysis of the impact of the pH value and the temperature. Preliminary studies (not shown) indicate that kPCA could even enable thermodynamics analyses. kPCA is an universally applicable technology: This was demonstrated by Schiele, Ayaz and Fernández-Montalván [84] presenting assays for a kinase, a G protein-coupled receptor and a protein-protein interaction. Moreover, it is supported by the broad study of 40 kinases presented in this dissertation, showing that 5 Kinase Tracers (236, 178, 199, 222, 314) are compatible with the TR-FRET-based probe competition assay and will be valuable tools for further studies in this field: 50% of human kinome is targeted by these tracers (Figure 47, according to Thermo Fisher Scientific). In addition, G protein-coupled receptor kPCAs were implemented and applied in parallel efforts to the kinase study [46, 122, 134]. In the future, a large-scale analysis of G protein-coupled receptor agonists and antagonists binding kinetics might provide novel insights into the role of binding kinetics for this drug class.

6.3 Structural features influencing binding kinetic parameters

The newly generated comprehensive dataset allowed for new insights into the relationships between molecular features and binding kinetic parameters and to identify potentially relevant interactions with the kinase binding site residues, which will be discussed in this chapter.

Derivation of structure-activity or structure-kinetic relationships was not possible by analyzing the few close derivatives of inhibitors in the panel (appendix G), but the chemical diversity and variety of the compounds allowed a study of both the influence of molecular properties and of specific interactions of compounds with particular amino acids in the kinase binding site (interaction fingerprints). As expected, the latter plays a greater role for binding affinities and kinetic rate constants as the molecular properties (GFA models can explain a higher percentage of the variability of the data; refer to Table 1 and Table 3).

The impact of physicochemical properties on residence times was assessed before by Miller *et al.*: They analyzed a diverse set of literature data, including different target classes (G protein coupled receptors, kinases, other enzymes), different biochemical and biophysical assays and temperatures, and found hints that in particular molecular weight and to a lesser extent lipophilicity and flexibility of compounds influence dissociation rates [79]. The effect of lipophilicity was investigated based on the octanol-water partition coefficient LogP and was especially observed for receptors, suggesting longer duration of target binding due to membrane interactions. The strength of the analysis in this dissertation is on the one hand the large set of compounds that was tested with the same temperature and assay technology, and on the other hand the comprehensive dataset providing the possibility to directly compare the structural effects on dissociation rates with those on association rates and affinities. Without the literature bias (high affinity interactions and slow off-rates are more frequently published as compared to low affinities and fast off-rates), it was observable that the impact of molecular properties on binding parameters is restricted to higher affinity interactions (in at least the double-digit nanomolar range (Figure 32, Table 1)), and as mentioned above is not as important as the interaction fingerprints. Moreover, for the data analyzed, changes in molecular properties and functionalities of compounds often either decelerated or accelerated both the on-rates and off-rates, diminishing the effect on affinities (Figure 32, Figure 34). However, an exception is e.g. the (presumed) steric hindrance due to the fluorescence label linked by a spacer to the compound [92], which decelerates the on-rates but not the off-rates (Figure 50). Taken together, rebinding of the compound moieties within the binding site before the compound has completely dissociated (indicated by relevance of MW, HBA, TPSA) and steric hindrance (indicated by relevance of MW, sp^3 C/C, flexibility, fluorescence label) might explain how molecular properties of compounds affect binding rates. It should be mentioned that a low sp^3 C/C ratio points to a flat

molecule, while a higher ratio does not necessarily mean more three dimensionality, since also the number of all carbon atoms could be low due to e.g. more N atoms in the compound. Therefore the relevance of the sp^3 C/C ratio could also have other reasons than steric hindrance. Especially since the ATP binding site is rather flat. In addition, halogens seemed to have an impact on slow binding rate constants (Figure 32), which supports another study reporting that interactions between halogens and aromatic side chains might contribute to increased residence times [76].

Furthermore, the trend towards longer residence times for DFG-out binders was confirmed [32, 33, 72] (Figure 33a). The conformational change is thought to stabilize the compound-target complex and thereby to increase target residence time. This dissertation further revealed a trend towards fast binding for DFG-in, DFG-out-like, α C-helix-in and α C-helix-out-like conformation, suggesting that binding towards DFG-out-like conformation is more similar to DFG-in binding than to DFG-out binding (Figure 33). The slowest on- and off-rates were observed for combined DFG-out and α C-helix-out conformations (Figure 33b), but as pointed out before for the relationship between long residence times and DFG-out binding [75], there are exceptions to all these trends, indicating that the DFG and α C-helix conformations (and conformational changes) might not be the key contributors (one of these exceptions is discussed below in “conclusions and outlook”).

The next step was to assess the influence of the detailed kinase-compound binding mode (including DFG and α C-helix conformations which turned out to be less important, Table 3) and of specific interactions of the compound with particular amino acids in the kinase binding site on binding parameters. Interestingly, the percentage of variability in the binding data that were explained by the GFA models was always higher for the description of kinetic rate constants than for the description of affinities (Table 3), suggesting that a thorough knowledge about structure-kinetic relationships might improve the understanding of how to modulate affinities. The GFA models further allowed deriving hypotheses: The particular interactions of the compound with the kinase binding site which were frequently selected (by the process of evolution generating the models) are potentially important for the description of the binding (and inhibition) process (Figure 35, Figure 53). Note that, especially hydrophobic interactions were identified, and among those are interactions with the DFG Phenylalanin and HRD Histidine. In the active conformation (DFG-in, α C-helix-in) these residues interact with each other as part of the hydrophobic regulatory spine, while in the inactive conformation the spine is disrupted [66, 135]. Furthermore, also other hydrophobic interactions identified by GFA as potential key players for kinetic rate constants (Figure 35, Figure 53) are close to regulatory or catalytic spine residues. This suggests that the spine theory might be more relevant than the DFG or α C-helix conformation *per se*. Schneider *et al.* also presume a connection between the spine theory and their finding that hydrophobic interactions in the CDK8 front pocket seem to be

main contributors to their observed long residence times [75]. Future in-depth analysis and follow-up studies based on the large data set provided in this dissertation might help to get a better understanding of the interplay between spine disordering by compound binding (or stabilization of the destructed state) and binding kinetic rate constants.

A limitation to all the structure-related observations is that on the one hand, the observed trends could arise from another not considered factor, which influence both the dependent (binding parameters) and the independent variables (investigated structural features), on the other hand the observed variables themselves can be interdependent. For instance, Miller *et al.* [79] pointed out that relatively large, stretched compounds are required to occupy the hinge region and the DFG-out pocket, which could also be a reason for the impact of molecular weight on binding properties. Likewise, large stretched molecules might be required to stabilize the destructed spine by the synergistic effect on several residues in the spine. Nonetheless, the observed influences of molecular properties, kinase conformations and specific kinase-compound interactions in the kinase binding site on binding rate constants could be a good starting point to get a better understanding of how to modulate binding rate constants. Naturally, the observed trends are often also relevant from the affinity perspective, but an increased understanding how these structural features influence on- and off-rates adds a new layer of information.

Conclusion and Outlook

The observed influence of molecular properties on binding kinetics and the hypothesized relevance of particular compound interactions with the kinase binding site for kinetic rate constants provide a rational basis for further detailed SKR studies and thereby contribute to make a step forward towards prospective design of kinetic rate constants. Remarkably, the GFA models describing binding kinetic rate constants were better than those describing affinities, presumably because the impact on affinity can be considered as the combined effect on on-rates and off-rates (but the effect on on-rates and off-rates can go in opposite directions). The GFA model *inter alia* proposes impact of interaction with the HRD Histidine. In a simplified use case demonstrating a possible way to start testing the hypotheses, it was observed that out of four ABL DFG-out and α C-helix-out binders, namely imatinib, nilotinib, ponatinib and rebastinib, only three interact with the HRD Histidine and possess longer residence times, while imatinib, which is not occupying the pocket burying the HRD Histidine, possesses a shorter residence time. Indeed, Duveau *et al.* describe changes in the IC₅₀ values of nilotinib derivatives modified at the functional group interacting with the HRD Histidine [126]. The next important step would be to measure the binding kinetics of these derivatives to demonstrate that the increasing affinities correlate to increasing residence times. A point mutation of the Histidine might be helpful to further prove this hypothesis. Also the local hydrophobic area

and the combined interaction with other residues could be investigated: E.g. all the three slow binders (but not imatinib) also interact with the Ala380 preceding the DFG motif. Thus, the combined interaction with both residues might contribute to stabilize the inactive conformation and to cause long residence times (which could also be tested by point mutation of the residue). The interaction pattern and residence time of the slow-dissociating ABL binders on other kinases might provide additional information and ideas, but will make the analysis increasingly complex. It should be emphasized that imatinib and other compounds can also possess long residence times on kinases due to other interactions (maybe also contributing to disordering of the spines). Likewise, the generated kinase-inhibitor binding kinetics data set contains other interesting cases, and considering the hypothesized relevant compound interactions with kinase binding site residues might provide starting points to analyze why DFG-in binding can result in slow on-rates and off-rates, or what leads to slow or fast on-rates for DFG-out binders. Furthermore, a more detailed analysis of the impact of the spines in new GFA models might reveal further insights into compound interactions required to disassemble the regulatory and/or catalytic spine. It would also be interesting to apply the data set for assessment of the effect of “unhappy” waters displacement (replacement of water molecules unfavorably placed in hydrophobic regions of the binding pocket by compound) on kinetic rate constants, or to include kinase descriptors not only qualitatively (as in this dissertation) but quantitatively by using proximity or angle of interacting compound moieties and kinase residues. Moreover, similar analyses of another set of compounds or with more kinases could provide new possibilities: With respect to equilibrium metrics, there are many studies with a larger number of kinases as a valuable source to identify which kinase family members might be targeted differentially by small molecules [14, 15, 136]. Additional kinases in the binding kinetics panel will provide a larger data set and might provide further insights into SKR and could help to identify kinases that can be targeted differentially from the kinetics perspective. Regarding the compound set, there are compounds with diverse chemotypes in the panel leading to large compounds’ distances by structural similarity. More compounds with more close derivatives and matched molecular pairs among the compounds in the screening panel would make up an interesting alternative and straightforward type of analysis. New starting points for such studies can *inter alia* be derived based on the binding kinetic data and hypotheses generated in this dissertation (as described above, refer to nilotinib derivatives).

6.4 Binding kinetics impact on target occupancy profiles and pharmacological effects

This dissertation demonstrated that binding kinetics of kinase inhibitors can have an impact on the time course of target occupancy in cells and has the potential to alter the target occupancy profile *in vivo*. Although other micro-pharmacokinetic parameters will also have an impact and there is not yet a proof that the altered target occupancy time course affects the time course of the pharmacological effect, it was interesting to observe that slow off-rates seem to be a favorable feature of compounds which prevails through clinical development. The details are discussed in this chapter.

So far there was no comprehensive study of kinase inhibitors binding kinetics. The large-scale profiling approach performed in this dissertation enabled analysis of kinetic and affinity parameters for 10800 kinase-inhibitors pairs, including inhibitors from different phases of clinical development. One of the first questions which was addressed is how on-rates and off-rate of kinase-inhibitor complexes are distributed in general, how they behave compared to affinities and if long residence times are a typical feature of FDA-approved kinase inhibitors:

- 1) The on-rates and off-rates of all tested kinase-inhibitor pairs are approximately log-normal distributed especially around the mean. The tails are skewed due to the limits of fast off-rate quantitation (caused by measurement interval, refer to chapters 6.1-6.2) and on-rate quantitation (caused by applied concentrations and affinities of compound and tracer, and the diffusion limit, refer to chapters 6.1-6.2). A tail with slow decay was observed for the slow off-rates (Figure 30c). These observations are in accordance with the work by Zheng and Wang who also describe a log-normal distribution near the mean, but a slower decaying power law distribution for the tails for binding to the cyclooxygenase-2 [108, 109].

- 2) While Copeland claims that affinity is often driven by off-rates [36], this dissertation observes an increase in on-rates, but not in off-rates, with increasing affinities (Figure 30b-c). Similarly, David Swinney and Steven Charlton described that affinities for G protein-coupled receptors are driven rather by on-rates than by off-rates (personal communication during K4DD Scientific Meeting "Binding kinetics: Time is of the essence", 16.-18. October 2017). Consistently, the overall distances between kinases based on binding affinities correlate better with the distances based on on-rates than with those based on off-rates, and interestingly, the kinases' distances by sequence identity are more similar to on-rate profiles than to affinity profiles than to off-rate profiles (Figure 31, left side). Together this suggests that if there is kinetic selectivity, it might be reached rather by differences in off-rates than by differences in on-rates (for structurally related kinases). On the other hand, it is also in line with the idea that the association rate reflects the energy of the transition state and is thus an important optimization parameter [137].

3) Although only 5% of all kinase-inhibitor pairs possess off-rates $<0.001\text{ s}^{-1}$, 57% of the FDA approved kinase inhibitors dissociate with off-rates $<0.001\text{ s}^{-1}$ from their main targets (chapter 5.2.3; main targets are given in Table 4). Moreover, off-rates $<0.0001\text{ s}^{-1}$ are exclusively observed for the main targets of FDA approved drugs, but not for their other targets (Figure 30a/c, Figure 51), fulfilling a prerequisite for kinetic selectivity as described by Copeland [31]. For higher affinity interactions with potential clinical relevance (dissociation constants $< 10^{-7}\text{ M}$) and when comparing compounds in early and late stages of clinical development, the frequency distribution of on-rates is not changing, while the percentage of slow off-rates is increasing (Figure 43a, Figure 55). Together, these findings indicate that slow off-rates on the primary target are indeed a frequently observed feature of FDA approved drugs, although the optimized affinities are rather connected with higher on-rates. However, it should be noted that not all FDA approved kinase inhibitors possess a fast residence time on their primary target.

Referencing Swinneys analysis [37] of biochemical mechanisms of FDA approved (2001-2004) new molecular entities, where he pointed out that about one third act via non-equilibrium kinetics, the observed slow off-rates for the kinase inhibitors found in this dissertation could be one factor contributing to non-equilibrium kinetics and e.g. hysteresis (prolonged duration of effect), which was analyzed in more detail:

With regard to traditional pharmacokinetics simulations, Dahl and Akerud [29] proposed that long residence times can only lead to a longer duration of target occupancy compared to the drugs' plasma concentration-affinity effect *per se*, if the dissociation half-lives are longer than the plasma half-lives. In this dissertation, only a few kinase inhibitors showed this feature (6% of the compounds analyzed according to this method). Recently, Witte *et al.* [39] provided an alternative perspective by suggesting a more detailed approach, additionally considering induced changes in the free drug concentration and rebinding effects in target vicinity, i.e. considering both on-rates and off-rates. Although only a few kinase inhibitors possessed a longer dissociation half-life than plasma half-life (Figure 43b), the target occupancy decline of many kinase-compound pairs (250, including 76% of the analyzed FDA approved drug interactions with their main targets) is potentially influenced by on-rates, off-rates and elimination rates (Figure 43c, Figure 30a). While this rate-limiting step approximation suggested by Witte *et al.* [39] is a step forward to assess whether a compound has the potential to show hysteresis, e.g. 1) the impact of binding kinetics on the onset of the drug-target interaction is not described, 2) non-specific binding is not considered but decreases the free drug concentration, and 3) it only allows to judge the impact on target occupancy decline at a distinct point in time, but not over the whole time course.

Previously, binding kinetics was incorporated into PK(PD) models to illustrate whether and how the time courses of target occupancy by the drug depend on binding kinetics or if binding kinetics can explain the time course of the pharmacological effect (e.g. [29, 31, 38, 42, 138]). Unfortunately, the profiles are most often not compared to the concentration-affinity effect *per se*, which might sometimes lead to exactly the same target occupancy profile (e.g. [138]). In some simulation studies decreasing off-rates are accompanied by likewise decreasing affinities [138], hampering the judgment whether the observed target occupancy time course is a result of the slow off-rates or the low affinities. Other simulation studies therefore fix the affinities and analyze the target occupancy profiles for different binding rate constants [29]. Other articles hypothesize that slow off-rates can only prove to be beneficial over affinities if also the on-rates are slow, because otherwise slow off-rates would mean high affinities [30]. However, the insufficiency of this thought is illustrated based on the PK-BK simulations performed in this dissertation with experimentally determined and thus various combinations of on- and off-rates and the direct comparison to traditional PK simulations considering the concentration-affinity effect (Figure 44). The simulations illustrate that there are rather ranges of affinities, on-rates and off-rates and their interaction with concentration-time profile which influence target occupancy profiles similarly and thresholds which have to be reached to enable the onset and perpetuation of the desired percentage of target occupancy:

- 1) The affinity and drug concentration describe the percentage of the target fraction bound in equilibrium and together have to be sufficiently high to potentially enable the target engagement required for the therapeutic effect, but
- 2) on-rate, drug concentration and off-rate together determine the required time to reach equilibrium and therefore the percentage of equilibrium reached within the available time frame (similarly to Equation 8), while
- 3) slow off-rates (which can be additionally combined with fast on-rates to enable rebinding) can prolong target occupancy beyond the concentration-affinity effect, and
- 4) thereby the drug concentration time profile is determined by PK properties. Sometimes multiple doses or higher drug concentrations are required to reach equilibrium of target occupancy traces.

Therefore, especially the on-rate and concentration have to be sufficiently high to reach the required target engagement level and the slower the off-rate the longer the biochemical residence time on the target preventing elimination (and the higher the on-rate the higher the probability for rebinding). One could argue that this is exactly what Folmer [30] meant: fast on-rate, slow off-rate, and ergo high affinity - so why care about binding kinetics? At the same time he suggests that a residence-time concept can only exist if the on- and off-rates of advanced compounds are slower

than that of initially discovered compounds [30], but this view is still restricted by the idea of equilibrium binding: Since also on-rates and affinities are relevant, it is, admittedly, insufficient to exclusively optimize for slow off-rates. On the other hand, that does not mean that optimization of off-rates can generally not prolong the duration of effect beyond the concentration-affinity effect or does not have the potential to lead to kinetic selectivity, as exemplified in Figure 44. It is the whole point of view that has to be changed: The PK-BK simulations showed that consideration of binding kinetics can lead to a slower onset, lower maximum target engagement and hysteresis when comparing the traces with the concentration-affinity effect *per se* (Figure 44a, c). Thus, drugs with poor pharmacokinetics in terms of fast clearance may be rescued if they are having long residence times. For the extreme cases, namely covalent inhibitors, this is frequently pursued (e.g. omeprazole with plasma half-life of less than 1h [139]) and might be interesting to consider for slow off-rate compounds too.

The above mentioned points 1-4 are required for the intended target. Regarding selectivity and safety, the opposite is the goal for the off-targets: As known from the equilibrium perspective, one goal is a sufficiently low affinity on off-targets so that target engagement is low. However, if affinity on off-targets is high, the concept of kinetic selectivity should be considered: If k_{on} and/or K_D on the off-target is lower than for the main target, an aim could be to use the minimum required dose (which can be better predicted by considering all effecting parameters, including binding kinetics rate constants) to decrease the available time with the right concentration and to prevent that equilibrium is reached on the off-target, while it is faster reached on the main target. If k_{off} is faster from the off-target than from the main-target, a consideration could be if dosing frequency can be reduced leading to faster target occupancy decline on the main-target than on the off-target and thereby to a better selectivity profile over time (as e.g. suggested by Copeland *et al.* [31]). Moreover, knowledge about long residence times (at high affinities) can be considered during lead identification and optimization, since the safety profile might be better if the plasma clearance is fast. How taking advantage of all these effects can be utilized to turn an unselective drug into a compound with a better selectivity profile as expected from the equilibrium perspective was exemplified in the simulations in Figure 44c: Target binding kinetics were different for main targets than for other targets, so that adaption of the dosing schedule could lead to a better selectivity profile.

Moreover, the slower the off-rate, the higher the probability that the affinity is underestimated (refer to chapter 6.1). Therefore knowledge about binding kinetics is useful from the experimentally point of view, but false estimation also impacts the target occupancy profiles (such as in Figure 44). Taking binding kinetics into account might also change the perspective on the percentage of target occupancy required over time to reach the desired effect and might help to identify minimum drug

exposure for a safe and effective pharmacological drug action (consideration of binding kinetics might reveal that a lower and less frequently administered dose still leads to 100% target occupancy between dosing).

However, also the PK-BK simulations in this dissertation are a simplification of the human body, which is more complex than a two compartment model and further factors influence the duration of drug action. While the simulations shall illustrate the potential and combine the fundamental ideas of binding kinetics effects, it is neither anticipated that they perfectly reflect the reality nor that they are valid in all cases. Additionally other micro-pharmacokinetic and pharmacodynamics factors can play a role [29, 31, 40, 41, 129] and could be integrated in the PK-BK simulation approach in the future to study their impact and interplay with binding kinetics: Particularly worth mentioning are

- 1) the influence of target protein concentration and turnover (of on- and off-targets; e.g. Is main target up-regulated?) on target occupancy (higher target concentrations (e.g. due to overexpression in cancer cells) are expected to enhance the effect of binding kinetics, while fast target turnover is expected to reduce the effect),
- 2) additional compartmentalization by e.g. the cellular membrane, interaction with membranes and active transport of drug as resistance mechanisms,
- 3) competition with endogenous ligands (ATP), and
- 4) the impact of target occupancy levels and profiles on downstream signaling and the drug effect.

Moreover, it should be recalled that in some cases a reasonable unselectively, meaning interaction with more than one target, might be beneficial and desired [50, 61, 63].

Within this dissertation, it was demonstrated that binding kinetics is a better predictor for target occupancy profiles in cells than steady-state affinity *per se* (Figure 41, Figure 54), if the system is not in equilibrium: The washout experiment revealed prolonged kinase occupancy in comparison to the concentration-affinity effect which was simulated well when considering binding kinetics. Thereby also the compartmentalization by the cellular membrane, i.e. diffusion through the membrane, and competition with ATP were included in the model: Competition with ATP changes the available target concentration and leads to a lower level of target occupancy in the beginning of the washout experiment, and permeation through the cell membrane (affects available compound concentration) as well as competition with ATP can influence the time course of target occupancy decline. The knowledge about binding kinetics, together with the Permeation-BK model and the cellular experiment, helped to identify in which cases target occupancy is alternatively affected by other micro-pharmacokinetic effects, which could be, inter alia, active transport or interactions with

cellular membranes (impacts available cellular compound concentration). Taken together, biochemical on- and off-rates contribute to a better understanding of the time course of cellular target occupancy.

Although other mechanisms can contribute to protracted target occupancy decline, only binding kinetics and affinity parameters are tunable and target specific and can contribute to selectivity (also other factors are “target specific” and should be considered but are not tunable: target concentration and turnover and the surrounding environment of the target (e.g. pH value might change membrane permeability, binding kinetic behavior and affinity of the compound)).

Finally, it was recently observed in a proliferation assay that cellular IC_{50} values correlate better with off-rates than with affinities of TTK inhibitors [140], illustrating that a long RT could also positively contribute to the desired therapeutic effect itself.

Conclusion and Outlook

This dissertation demonstrated that in some cases target occupancy profiles in cells can be better simulated by using binding kinetic parameters as descriptors than by the concentration-affinity effect *per se*. In other cases other micro-pharmacokinetic aspects influenced the time courses. It was further shown that simulation of *in vivo* profiles using standard PK and a modified PK model considering binding kinetics (PK-BK) can lead to different kinase occupancy time profiles. It was illustrated by simulations how the concept of kinetic selectivity could be applied to turn an unselective compound in equilibrium conditions into a more selective compound in the open system (*in vivo* situation). Furthermore, it was revealed that slow off-rates seem to be a favorable feature of kinase inhibitors that prevails through clinical development. However, other micro-pharmacokinetic and pharmacodynamics aspects will have to be considered in future models, and compared to the real time courses of drug actions, to judge whether in some cases BK alter the time course of the pharmacological effect and in the end is contributing to safety and/or efficacy.

With respect to the cellular experiments in this study, multiple future efforts are conceivable:

- 1) So far, the concentration and binding kinetic rate constants of the tracer were not considered in the simulations, but in some cases it might influence the BRET traces: E.g. the tracer was binding faster to the cells pre-incubated with staurosporine than to the tracer binding controls without pre-incubation with the compound (Figure 38). A possible explanation might be that in the tracer binding control, the kinases are occupied with ATP which is displaced by the tracer, but probably not completely (there might be an equilibrium with bound tracer and ATP in the end). In the staurosporine pre-incubated cells, the kinases are initially occupied with ATP or staurosporine.

If staurosporine dissociates, competition for the binding site starts: it could be possible that the tracer can now bind faster to the target than ATP, leading to a signal overshoot, but is then displaced by ATP until the same equilibrium is reached as in the tracer binding control. On the other hand, it would also be conceivable that staurosporin treatment led to a higher permeability of the cells, allowing the tracer to bind faster. However, these speculations will have to be verified experimentally.

2) Further cellular target occupancy decline experiments and simulations with the new BK-permeation model can now help to judge to what extent rebinding plays a role if the target binding site is in the cell: What conditions are required to allow rebinding to the target prior to diffusion through the cell membrane? Are there additional effects which cannot be explained by the model and which might have a background in high local drug concentrations upon dissociation and accordingly more rebinding?

3) Likewise, it could be interesting to track the pre-incubation step to check the influence of binding kinetics and affinity on the onset of target occupancy, and also to assess to what extent the on-rate might lead to depletion of ligand in target vicinity upon binding and thereby changes the time course of target occupancy formation. As pointed out last year by Witte *et al.* [39] effects caused by on-rates might especially apply for high target concentrations. Therefore, also the impact of target concentration should be considered. (This was not studied in detail in this dissertation, since the same concentration of target was assumed for all targets. For more accuracy, the target concentration could be determined experimentally and included in the model. However, NanoBret™ assay development at Promega involves ensuring low and constant expression levels of each target, enabling comparability with endogenous expression levels and thus also between targets.)

4) It would be interesting to perform such cellular experiments in a flow system (e.g. using impedance readout) allowing gradual changes of the drug concentration as expected in the human body (instead of the washout). In such a system it will be essential again to compare the BK-permeation model with the concentration affinity effect *per se*.

5) Fick's law of diffusion does not apply for charged molecules. Consideration of the electrical potential difference across the membrane and net charges of the compounds within and outside the cell could be interesting.

6) Finally, the permeation-BK model was obviously not the right model for ponatinib. It would be interesting to find an explanation for the time courses. Remarkably, occupancy by ponatinib was better described for the tyrosine kinase receptors than for the other kinases (albeit also the

receptors possess an intracellular binding site). Vauquelin reviewed in 2016 the role of cell membranes in PK-PD modeling [141]: membranes can serve as a reservoir increasing local drug concentrations around the membrane, and a lateral approach of drug binding through the membrane to the target is discussed. Moreover, it is described that accumulation of drug in the membrane is better described by the ratio between membrane and aqueous phase (accounts for hydrophobicity and interaction with polar head groups of membrane lipids) than by the octanol-water (or buffer) ratio [141-143], which could be a starting point for the analyses. On the other hand, post-translational modifications, such as phosphorylation, of the protein can affect the binding characteristics and could be a reason for the discrepancies between simulated data (based on binding parameters determined in the biochemical probe competition assay) and data from the cellular experiment (not the same protein as in biochemical probe competition assays).

With respect to the PK-BK simulations in this study, next steps could focus on

- 1) Consideration of different target concentrations and turnover, and
- 2) combination of the PK-BK model with the Permeation-BK model: Besides the additional compartmentalization by the cell membranes, especially the competition with ATP will be highly relevant. For intracellular target sites this might provide a new perspective compared to the rate-limiting step approximation [144] (might better describe onset and provide an alternative view on the TO decline).
- 3) The ultimate goal would be to demonstrate or invalidate that BK can affect TO and thereby the therapeutic effect. It could be tested whether the incorporation of binding kinetics into PK-PD models can improve the predictability of efficacy and safety for kinase inhibitors in examples where predictions based on steady-state data are not accurate enough and where other micro-pharmacokinetic aspects are not expected as main contributors. In that respect, the kinetic information gathered within this thesis could lay a foundation for a broad analysis of non-equilibrium PK-PD models.

With respect to the FDA approved kinase inhibitors with fast on-rates on their main target, it would be interesting to check how many of them also act via non-equilibrium mechanisms and lead to slower onset of target occupancy on off-targets or hysteresis for main targets, but caused by other effects such as contribution of on-rates, target or substrate inactivation, non-reversibly inducing a pathway or probably due to membrane interactions or tissue accumulation. Finally, it should be mentioned that kinetic selectivity is of course not required if the drug is selective by affinity.

With regard to selectivity screening the first step should always be the standard screen with equilibrium metrics, but if the drug is unselective a second step could be to check the potential for kinetic selectivity: The visualization in a kinome tree gives a qualitative impression of selectivity (Figure 42), but does not allow ranking between candidates. It would be interesting to develop an approach to assess the potential for kinetic selectivity quantitatively. One measure could be the calculated time required to reach equilibrium (Equation 8), but it would be required to combine both the affinity values and the time to reach equilibrium. This, however, will only describe the onset of target occupancy and also not yet considers the effect of different target concentrations. Another measure will have to be implemented to judge the potential for hysteresis, but there is not yet a convincing approach. Knowledge about other micro-pharmacokinetic effects (which can be partly already detected in cellular experiments as demonstrated by nanoBRET experiments) and later on PK properties of compounds should be considered to decide whether kinetic selectivity is achievable or not.

6.5 Concluding remarks

This study derived general guidelines for the setup and assessment of competitive binding kinetics experiments, demonstrated that binding kinetic data can be easily measured in large scales and contributed evidence for the importance of binding kinetics in drug discovery.

In principle the drug-target residence time concept is an interesting and promising approach [31], but agreeing with Dahl, Akerud [29] and Folmer [30] the consideration of off-rates *per se* is not sufficient for a better prediction of the therapeutic effect: The combined effect of on-rates, off-rates and affinities can be relevant if other micro-pharmacokinetic processes are not more relevant. Based on the results of the thesis and in the context of other research activities, the suggestion is to broaden and rename the drug-target residence time concept into the “kinetics of target engagement concept”. In some cases, it might be sufficient to simply use the concentration-affinity effect to describe target engagement. In other cases, however, the inclusion of binding kinetics as link between pharmacokinetics and pharmacodynamics might be a better predictor. Besides target affinity and binding kinetics, which are both target specific and modulatable, other micro-pharmacokinetic parameters could additionally influence the time course of target occupancy (and thereby diminish or enhance the effect of binding kinetics). A better understanding of this complex topic and the interplay between the various effects is thought to improve the prediction of the therapeutic effect.

Binding kinetics can be understood as a tool which can be applied during the drug discovery process, and as every tool it is sometimes useful and sometimes not. Binding kinetic rate constants provide more information than steady state affinity *per se*, and this knowledge can help to decide about the right incubation times with compounds or/and e.g. contribute to better comprehend the time courses of compound action in cellular experiments. It is further hypothesized that a deeper understanding of structure-kinetic relationships could help medicinal chemist during lead optimization. Of course, so far pursued structure-activity relationships are valid as they summarize the effects of on- and off-rates. However, knowledge about the binding kinetics of the compound and about how to modulate association and dissociation rates might be beneficial, not only when trying to achieve a desired on-rate or off-rate (e.g. if the on-rates are already at the diffusion limit, it is better to focus on optimization of the off-rate to optimize affinity). Moreover, it would help to know what structural changes modulate both on- and off-rates and diminish the effect on affinity. With regard to (clinical) pharmacokinetics, knowledge about binding kinetics (and other micro-pharmacokinetic aspects), can help to determine the optimal dosing regimen. In some cases slow dissociation and fast rebinding could help to minimize drug exposure for maximal target occupancy on

primary targets and minimal target occupancy on off-targets (but this requires fast drug clearance, which then would have to be considered during lead optimization). This is what was illustrated by simulation in this thesis, but beyond that other studies show further potential of the tool binding kinetics: E.g. with regard to pharmacodynamics, binding kinetics could help to cope with on-target side effects or in some cases lead to improved therapeutic effects.

Binding kinetics should not be neglected during drug discovery, and more efforts have to be spent to understand structure-kinetic relationships and the translation of *in vitro* experiment into *in vivo* effect. The large-scale profiling of kinase inhibitors' binding kinetics in this dissertation represents a valuable resource for future studies in this field.

7 References

7.1 Literature references

- [1] K. Lybecker, "The Biologics Revolution in the Production of Drugs," *Fraser institute*. <http://fraserinstitute.org>, 2016.
- [2] R. Santos, O. Ursu, A. Gaulton, A. P. Bento, R. S. Donadi, C. G. Bologa, *et al.*, "A comprehensive map of molecular drug targets," *Nature Reviews Drug Discovery*, vol. 16, pp. 19-34, 2016.
- [3] T. T. Ashburn and K. B. Thor, "Drug repositioning: identifying and developing new uses for existing drugs," *Nature Reviews Drug Discovery*, vol. 3, pp. 673-683, 2004.
- [4] U. Egner, J. Krätzschar, B. Kreft, H.-D. Pohlenz, and M. Schneider, "The Target Discovery Process," *ChemBioChem*, vol. 6, pp. 468-479, 2005.
- [5] S. H. Kaufmann, "Paul Ehrlich: founder of chemotherapy," *Nat Rev Drug Discov*, vol. 7, p. 373, May 2008.
- [6] P. Ehrlich, "Chemotherapeutics: scientific principles, methods and results," *Lancet*, vol. 2, pp. 353-359, 1913.
- [7] J. Hüser, *High-Throughput Screening in Drug Discovery*. Weinheim: WILEY-VCH Verlag GmbH & Co. KGaA, 2006.
- [8] S. Fox, S. Farr-Jones, L. Sopchak, A. Boggs, H. W. Nicely, R. Khoury, *et al.*, "High-throughput screening: update on practices and success," *J Biomol Screen*, vol. 11, pp. 864-9, Oct 2006.
- [9] K. H. Bleicher, H. J. Bohm, K. Muller, and A. I. Alanine, "Hit and lead generation: beyond high-throughput screening," *Nat Rev Drug Discov*, vol. 2, pp. 369-78, May 2003.
- [10] M. Glick, J. L. Jenkins, J. H. Nettles, H. Hitchings, and J. W. Davies, "Enrichment of high-throughput screening data with increasing levels of noise using support vector machines, recursive partitioning, and laplacian-modified naive bayesian classifiers," *J Chem Inf Model*, vol. 46, pp. 193-200, Jan-Feb 2006.
- [11] A. Steinmeyer, "The hit-to-lead process at Schering AG: strategic aspects," *ChemMedChem*, vol. 1, pp. 31-6, Jan 2006.
- [12] M. W. Parker, "Protein structure from x-ray diffraction," *J Biol Phys*, vol. 29, pp. 341-62, Dec 2003.
- [13] J. Bajorath, "Integration of virtual and high-throughput screening," *Nat Rev Drug Discov*, vol. 1, pp. 882-94, Nov 2002.
- [14] T. Anastasiadis, S. W. Deacon, K. Devarajan, H. Ma, and J. R. Peterson, "Comprehensive assay of kinase catalytic activity reveals features of kinase inhibitor selectivity," *Nature biotechnology*, vol. 29, pp. 1039-1045, 2011.
- [15] M. I. Davis, J. P. Hunt, S. Herrgard, P. Ciceri, L. M. Wodicka, G. Pallares, *et al.*, "Comprehensive analysis of kinase inhibitor selectivity," *Nature biotechnology*, vol. 29, pp. 1046-1051, 2011.
- [16] C. A. Lipinski, F. Lombardo, B. W. Dominy, and P. J. Feeney, "Experimental and computational approaches to estimate solubility and permeability in drug discovery and development settings," *Adv Drug Deliv Rev*, vol. 46, pp. 3-26, Mar 01 2001.
- [17] M. A. Hedaya, *Basic Pharmacokinetics, Second Edition*: Taylor & Francies Group, 2012.
- [18] D. Zhang, G. Luo, X. Ding, and C. Lu, "Preclinical experimental models of drug metabolism and disposition in drug discovery and development," *Acta Pharmaceutica Sinica B*, vol. 2, pp. 549-561, 2012.
- [19] D. G. Rudmann, "On-target and off-target-based toxicologic effects," *Toxicol Pathol*, vol. 41, pp. 310-4, Feb 2013.
- [20] B. A. Rasool Hassan, "Overview on Pharmaceutical Formulation and Drug Design," *Pharmaceutica Analytica Acta*, vol. 03, 2012.
- [21] G. Chilkoti, C. S. Sharma, A. Kochhar, D. Agrawal, and A. K. Sethi, "An overview of clinical research for anesthesiologists," *J Anaesthesiol Clin Pharmacol*, vol. 26, pp. 446-50, Oct 2010.
- [22] J. M. Reichert, "Trends in development and approval times for new therapeutics in the United States," *Nat Rev Drug Discov*, vol. 2, pp. 695-702, Sep 2003.
- [23] J. Gilbert, H. P., and A. Singh, "Rebuilding Big Pharma's Business Model," *IN VIVO*, vol. 21, 2003.
- [24] J. C. Uitdehaag, F. Verkaar, H. Alwan, J. de Man, R. C. Buijsman, and G. J. Zaman, "A guide to picking the most selective kinase inhibitor tool compounds for pharmacological validation of drug targets," *Br J Pharmacol*, vol. 166, pp. 858-76, Jun 2012.
- [25] M. W. Karaman, S. Herrgard, D. K. Treiber, P. Gallant, C. E. Atteridge, B. T. Campbell, *et al.*, "A quantitative analysis of kinase inhibitor selectivity," *Nature biotechnology*, vol. 26, pp. 127-132, 2008.
- [26] J. M. Berg, J. L. Tymoczko, and L. Stryer, *Biochemie* vol. 6. Heidelberg: Spektrum Akademischer Verlag, 2007.

- [27] R. Parker and D. Waud, "Pharmacological estimation of drug-receptor dissociation constants. Statistical evaluation. I. Agonists," *Journal of Pharmacology and Experimental Therapeutics*, vol. 177, pp. 1-12, 1971.
- [28] J. Drews, "Paul Ehrlich: magister mundi," *Nat Rev Drug Discov*, vol. 3, pp. 797-801, Sep 2004.
- [29] G. Dahl and T. Akerud, "Pharmacokinetics and the drug–target residence time concept," *Drug discovery today*, vol. 18, pp. 697-707, 2013.
- [30] R. H. A. Folmer, "Drug target residence time: a misleading concept," *Drug Discov Today*, Aug 03 2017.
- [31] R. A. Copeland, D. L. Pompliano, and T. D. Meek, "Drug–target residence time and its implications for lead optimization," *Nature reviews Drug discovery*, vol. 5, pp. 730-739, 2006.
- [32] K. Okamoto, M. Ikemori-Kawada, A. Jestel, K. von König, Y. Funahashi, T. Matsushima, *et al.*, "Distinct Binding Mode of Multikinase Inhibitor Lenvatinib Revealed by Biochemical Characterization," *ACS Medicinal Chemistry Letters*, vol. 6, pp. 89-94, 2015.
- [33] L. T. Alexander, H. Möbitz, P. Drueckes, P. Savitsky, O. Fedorov, J. M. Elkins, *et al.*, "Type II Inhibitors Targeting CDK2," *ACS Chemical Biology*, vol. 10, pp. 2116-2125, 2015.
- [34] R. A. Copeland, "Conformational adaptation in drug-target interactions and residence time," *Future medicinal chemistry*, vol. 3, pp. 1491-1501, 2011.
- [35] G. Vauquelin, I. Van Liefde, and D. C. Swinney, "On the different experimental manifestations of two-state 'induced-fit' binding of drugs to their cellular targets," *Br J Pharmacol*, vol. 173, pp. 1268-85, Apr 2016.
- [36] R. A. Copeland, "The drug-target residence time model: a 10-year retrospective," *Nat Rev Drug Discov*, vol. 15, pp. 87-95, Feb 2016.
- [37] D. C. Swinney, "Biochemical mechanisms of new molecular entities (NMEs) approved by United States FDA during 2001-2004: mechanisms leading to optimal efficacy and safety," *Current topics in medicinal chemistry*, vol. 6, pp. 461-478, 2006.
- [38] R. A. Copeland, "The dynamics of drug-target interactions: drug-target residence time and its impact on efficacy and safety," *Expert opinion on drug discovery*, vol. 5, pp. 305-310, 2010.
- [39] W. E. A. de Witte, M. Danhof, P. H. van der Graaf, and E. C. M. de Lange, "In vivo Target Residence Time and Kinetic Selectivity: The Association Rate Constant as Determinant," *Trends in Pharmacological Sciences*, vol. 37, pp. 831-842, 2016.
- [40] G. Vauquelin, "Effects of target binding kinetics on in vivo drug efficacy: koff, kon and rebinding," *Br J Pharmacol*, vol. 173, pp. 2319-34, Aug 2016.
- [41] K. E. Hightower, R. Wang, F. Deanda, B. A. Johns, K. Weaver, Y. Shen, *et al.*, "Dolutegravir (S/GSK1349572) exhibits significantly slower dissociation than raltegravir and elvitegravir from wild-type and integrase inhibitor-resistant HIV-1 integrase-DNA complexes," *Antimicrob Agents Chemother*, vol. 55, pp. 4552-9, Oct 2011.
- [42] F. Daryaei, A. Chang, J. Schiebel, Y. Lu, Z. Zhang, K. Kapilashrami, *et al.*, "Correlating Drug-Target Kinetics and In vivo Pharmacodynamics: Long Residence Time Inhibitors of the FabI Enoyl-ACP Reductase," *Chem Sci*, vol. 7, pp. 5945-5954, Sep 01 2016.
- [43] D. C. Swinney, "Biochemical mechanisms of drug action: what does it take for success?," *Nature reviews Drug discovery*, vol. 3, pp. 801-808, 2004.
- [44] D. A. Sykes, H. Moore, L. Stott, N. Holliday, J. A. Javitch, J. R. Lane, *et al.*, "Extrapyramidal side effects of antipsychotics are linked to their association kinetics at dopamine D2 receptors," *Nat Commun*, vol. 8, p. 763, Oct 02 2017.
- [45] S. Kapur and P. Seeman, "Antipsychotic agents differ in how fast they come off the dopamine D2 receptors. Implications for atypical antipsychotic action," *J Psychiatry Neurosci*, vol. 25, pp. 161-6, Mar 2000.
- [46] W. E. A. de Witte, J. W. Versfelt, M. Kuzikov, S. Rolland, V. Georgi, P. Gribbon, *et al.*, "In vitro and in silico analysis of the influence of D2 antagonist target binding kinetics on the cellular response to fluctuating dopamine concentrations," *British Journal of Pharmacology*, *accepted article*, 2018.
- [47] B. Maschera, G. Darby, G. Palu, L. L. Wright, M. Tisdale, R. Myers, *et al.*, "Human immunodeficiency virus. Mutations in the viral protease that confer resistance to saquinavir increase the dissociation rate constant of the protease-saquinavir complex," *J Biol Chem*, vol. 271, pp. 33231-5, Dec 27 1996.
- [48] E. Eden, N. Geva-Zatorsky, I. Issaeva, A. Cohen, E. Dekel, T. Danon, *et al.*, "Proteome half-life dynamics in living human cells," *Science*, vol. 331, pp. 764-8, Feb 11 2011.
- [49] G. Manning, D. B. Whyte, R. Martinez, T. Hunter, and S. Sudarsanam, "The protein kinase complement of the human genome," *Science*, vol. 298, pp. 1912-1934, 2002.
- [50] D. Fabbro, S. W. Cowan-Jacob, and H. Moebitz, "Ten things you should know about protein kinases: IUPHAR Review 14," *British Journal of Pharmacology*, vol. 172, pp. 2675-2700, 2015.
- [51] V. V. H. Ghukasyan, A. A., *Natural Biomarkers for Cellular Metabolism. Biology, Techniques, and Applications*. Boca Raton: Taylor & Francis Group, LLC, 2015.

- [52] E. D. Fleuren, L. Zhang, J. Wu, and R. J. Daly, "The kinome 'at large' in cancer," *Nat Rev Cancer*, vol. 16, pp. 83-98, Feb 2016.
- [53] J. A. Endicott, M. E. Noble, and L. N. Johnson, "The structural basis for control of eukaryotic protein kinases," *Annu Rev Biochem*, vol. 81, pp. 587-613, 2012.
- [54] World Health Organization, "Cancer fact sheet," *WHO Media center*, 02.2017.
- [55] S. M. Dehm and K. Bonham, "SRC gene expression in human cancer: the role of transcriptional activation," *Biochem Cell Biol*, vol. 82, pp. 263-74, Apr 2004.
- [56] G. M. Cooper, *The Cell: A Molecular Approach. 2nd edition*. Sunderland (MA): Sinauer Associates, 2000.
- [57] P. Wu, T. E. Nielsen, and M. H. Clausen, "Small-molecule kinase inhibitors: an analysis of FDA-approved drugs," *Drug Discov Today*, vol. 21, pp. 5-10, Jan 2016.
- [58] O. Fedorov, S. Muller, and S. Knapp, "The (un)targeted cancer kinome," *Nat Chem Biol*, vol. 6, pp. 166-169, Mar 2010.
- [59] H. Cheng and T. Force, "Why do kinase inhibitors cause cardiotoxicity and what can be done about it?," *Prog Cardiovasc Dis*, vol. 53, pp. 114-20, Sep-Oct 2010.
- [60] H. Cheng and T. Force, "Molecular mechanisms of cardiovascular toxicity of targeted cancer therapeutics," *Circ Res*, vol. 106, pp. 21-34, Jan 08 2010.
- [61] P. M. LoRusso and J. P. Eder, "Therapeutic potential of novel selective-spectrum kinase inhibitors in oncology," *Expert Opin Investig Drugs*, vol. 17, pp. 1013-28, Jul 2008.
- [62] S. Muller, A. Chaikuad, N. S. Gray, and S. Knapp, "The ins and outs of selective kinase inhibitor development," *Nat Chem Biol*, vol. 11, pp. 818-21, Nov 2015.
- [63] S. K. Mencher and L. G. Wang, "Promiscuous drugs compared to selective drugs (promiscuity can be a virtue)," *BMC Clin Pharmacol*, vol. 5, p. 3, Apr 26 2005.
- [64] R. Roskoski, Jr., "RAF protein-serine/threonine kinases: structure and regulation," *Biochem Biophys Res Commun*, vol. 399, pp. 313-7, Aug 27 2010.
- [65] C. S. Gibbs and M. J. Zoller, "Rational scanning mutagenesis of a protein kinase identifies functional regions involved in catalysis and substrate interactions," *J Biol Chem*, vol. 266, pp. 8923-31, May 15 1991.
- [66] J. Hu, L. G. Ahuja, H. S. Meharena, N. Kannan, A. P. Kornev, S. S. Taylor, *et al.*, "Kinase regulation by hydrophobic spine assembly in cancer," *Mol Cell Biol*, vol. 35, pp. 264-76, Jan 2015.
- [67] R. S. Vijayan, P. He, V. Modi, K. C. Duong-Ly, H. Ma, J. R. Peterson, *et al.*, "Conformational analysis of the DFG-out kinase motif and biochemical profiling of structurally validated type II inhibitors," *J Med Chem*, vol. 58, pp. 466-79, Jan 08 2015.
- [68] Z. Zhao, H. Wu, L. Wang, Y. Liu, S. Knapp, Q. Liu, *et al.*, "Exploration of type II binding mode: A privileged approach for kinase inhibitor focused drug discovery?," *ACS Chem Biol*, vol. 9, pp. 1230-41, Jun 20 2014.
- [69] N. Willemsen-Seegers, J. C. Uitdehaag, M. B. Prinsen, J. R. de Vetter, J. de Man, M. Sawa, *et al.*, "Compound Selectivity and Target Residence Time of Kinase Inhibitors Studied with Surface Plasmon Resonance," *J Mol Biol*, vol. 429, pp. 574-586, Feb 17 2017.
- [70] E. R. Wood, A. T. Truesdale, O. B. McDonald, D. Yuan, A. Hassell, S. H. Dickerson, *et al.*, "A unique structure for epidermal growth factor receptor bound to GW572016 (Lapatinib): relationships among protein conformation, inhibitor off-rate, and receptor activity in tumor cells," *Cancer Res*, vol. 64, pp. 6652-9, Sep 15 2004.
- [71] S. Ponader, S. S. Chen, J. J. Buggy, K. Balakrishnan, V. Gandhi, W. G. Wierda, *et al.*, "The Bruton tyrosine kinase inhibitor PCI-32765 thwarts chronic lymphocytic leukemia cell survival and tissue homing in vitro and in vivo," *Blood*, vol. 119, pp. 1182-9, Feb 02 2012.
- [72] Y. Liu and N. S. Gray, "Rational design of inhibitors that bind to inactive kinase conformations," *Nat Chem Biol*, vol. 2, pp. 358-64, Jul 2006.
- [73] C. Pargellis, L. Tong, L. Churchill, P. F. Cirillo, T. Gilmore, A. G. Graham, *et al.*, "Inhibition of p38 MAP kinase by utilizing a novel allosteric binding site," *Nat Struct Biol*, vol. 9, pp. 268-72, Apr 2002.
- [74] P. Ayaz, D. Andres, D. A. Kwiatkowski, C. C. Kolbe, P. Lienau, G. Siemeister, *et al.*, "Conformational Adaption May Explain the Slow Dissociation Kinetics of Roniciclib (BAY 1000394), a Type I CDK Inhibitor with Kinetic Selectivity for CDK2 and CDK9," *ACS Chem Biol*, vol. 11, pp. 1710-9, Jun 17 2016.
- [75] E. V. Schneider, J. Bottcher, R. Huber, K. Maskos, and L. Neumann, "Structure-kinetic relationship study of CDK8/CycC specific compounds," *Proc Natl Acad Sci U S A*, vol. 110, pp. 8081-6, May 14 2013.
- [76] C. Heroven, V. Georgi, G. K. Ganotra, P. Brennan, F. Wolfreys, R. C. Wade, *et al.*, "Halogen-Aromatic π Interactions Modulate Inhibitor Residence Times," *Angewandte Chemie*, vol. 57, pp. 7220-7224, 2018.
- [77] R. A. Pearlstein, W. Sherman, and R. Abel, "Contributions of water transfer energy to protein-ligand association and dissociation barriers: Watermap analysis of a series of p38alpha MAP kinase inhibitors," *Proteins*, vol. 81, pp. 1509-26, Sep 2013.

- [78] J. M. Bradshaw, J. M. McFarland, V. O. Paavilainen, A. Bisconte, D. Tam, V. T. Phan, *et al.*, "Prolonged and tunable residence time using reversible covalent kinase inhibitors," *Nat Chem Biol*, vol. 11, pp. 525-31, Jul 2015.
- [79] D. C. Miller, G. Lunn, P. Jones, Y. Sabnis, N. L. Davies, and P. Driscoll, "Investigation of the effect of molecular properties on the binding kinetics of a ligand to its biological target," *MedChemComm*, vol. 3, p. 449, 2012.
- [80] M. C. Munson, "Introduction to Kinase Antitargets," in *Antitargets and Drug Safety*, ed: Wiley-VCH Verlag GmbH & Co. KGaA, 2015, pp. 329-364.
- [81] G. K. Walkup, Z. You, P. L. Ross, E. K. Allen, F. Daryaei, M. R. Hale, *et al.*, "Translating slow-binding inhibition kinetics into cellular and in vivo effects," *Nat Chem Biol*, vol. 11, pp. 416-23, Jun 2015.
- [82] T. N. Raju, "The Nobel chronicles. 1988: James Whyte Black, (b 1924), Gertrude Elion (1918-99), and George H Hitchings (1905-98)," *Lancet*, vol. 355, p. 1022, Mar 18 2000.
- [83] H. J. Motulsky and L. Mahan, "The kinetics of competitive radioligand binding predicted by the law of mass action," *Molecular pharmacology*, vol. 25, pp. 1-9, 1984.
- [84] F. Schiele, P. Ayaz, and A. Fernández-Montalván, "A universal homogeneous assay for high-throughput determination of binding kinetics," *Anal Biochem*, vol. 468, pp. 42-9, Jan 01 2015.
- [85] A. J. Kooistra, G. K. Kanev, O. P. J. van Linden, R. Leurs, I. J. P. de Esch, and C. de Graaf, "KLIFS: a structural kinase-ligand interaction database," *Nucleic Acids Research*, vol. 44, pp. D365-D371, 2016.
- [86] O. P. J. van Linden, A. J. Kooistra, R. Leurs, I. J. P. de Esch, and C. de Graaf, "KLIFS: A Knowledge-Based Structural Database To Navigate Kinase–Ligand Interaction Space," *Journal of Medicinal Chemistry*, vol. 57, pp. 249-277, 2014.
- [87] M. Chartier, T. Chénard, J. Barker, and R. Najmanovich, "Kinome Render: a stand-alone and web-accessible tool to annotate the human protein kinome tree," *PeerJ*, vol. 1, p. e126, 2013.
- [88] S. Eid, S. Turk, A. Volkamer, F. Rippmann, and S. Fulle, "KinMap: a web-based tool for interactive navigation through human kinome data," *BMC Bioinformatics*, vol. 18, 2017.
- [89] G. van Rossum, "Python tutorial, Technical Report CS-R9526. ," presented at the Centrum voor Wiskunde en Informatica (CWI), Available at <http://www.python.org>, Amsterdam, 1995.
- [90] F. Sievers, A. Wilm, D. Dineen, T. J. Gibson, K. Karplus, W. Li, *et al.*, "Fast, scalable generation of high-quality protein multiple sequence alignments using Clustal Omega," *Mol Syst Biol*, vol. 7, p. 539, Oct 11 2011.
- [91] S. Hoops, S. Sahle, R. Gauges, C. Lee, J. Pahle, N. Simus, *et al.*, "COPASI—a COmplex PATHway Simulator," *Bioinformatics*, vol. 22, pp. 3067-74, Dec 15 2006.
- [92] V. Georgi, D. Andres, A. E. Fernández-Montalván, C. M. Stegmann, A. Becker, and A. Mueller-Fahrnow, "Binding kinetics in drug discovery - A current perspective," *Front Biosci (Landmark Ed)*, vol. 22, pp. 21-47, Jan 01 2017.
- [93] N. M. Green, "Avidin," *Adv Protein Chem*, vol. 29, pp. 85-133, 1975.
- [94] C. S. Lebakken, S. M. Riddle, U. Singh, W. J. Frazee, H. C. Eliason, Y. Gao, *et al.*, "Development and applications of a broad-coverage, TR-FRET-based kinase binding assay platform," *Journal of biomolecular screening*, vol. 14, pp. 924-935, 2009.
- [95] B. Klebl, G. Müller, and M. Hamacher, *Protein Kinases as Drug Targets* vol. 49. Weinheim: WILEY-VCH Verlag GmbH & Co. KGaA, 2011.
- [96] GraphPad Software Inc. (11.2017). *Ligand depletion*. Available: <https://www.graphpad.com/guides/prism/7/curve-fitting/index.htm?liganddepletion.htm>
- [97] T. M. Davis and W. D. Wilson, "Determination of the refractive index increments of small molecules for correction of surface plasmon resonance data," *Anal Biochem*, vol. 284, pp. 348-53, Sep 10 2000.
- [98] R. W. Glaser, "Antigen-antibody binding and mass transport by convection and diffusion to a surface: a two-dimensional computer model of binding and dissociation kinetics," *Anal Biochem*, vol. 213, pp. 152-61, Aug 15 1993.
- [99] M. B. Robers, M. L. Dart, C. C. Woodroffe, C. A. Zimprich, T. A. Kirkland, T. Machleidt, *et al.*, "Target engagement and drug residence time can be observed in living cells with BRET," *Nat Commun*, vol. 6, p. 10091, Dec 3 2015.
- [100] Promega, "Technical manual: NanoBRET™ Target Engagement Intracellular HDAC Assay," *Instructions for Use of Products*, pp. 16-20.
- [101] J. D. Vasta, C. R. Corona, J. Wilkinson, C. A. Zimprich, J. R. Hartnett, M. R. Ingold, *et al.*, "Quantitative, Wide-Spectrum Kinase Profiling in Live Cells for Assessing the Effect of Cellular ATP on Target Engagement," *Cell Chem Biol*, Nov 13 2017.
- [102] K. Levenberg, "A Method for the Solution of Certain Non-Linear Problems in Least Squares," *The Quarterly of Applied Mathematics*, vol. 2, pp. 164-168, 1944.

- [103] D. W. Marquardt, "An algorithm for least-squares estimation of non-linear parameters," *Journal of the Society for Industrial and Applied Mathematics*, vol. 11, pp. 431-441, 1963.
- [104] Y.-C. Cheng and W. H. Prusoff, "Relationship between the inhibition constant (K₁) and the concentration of inhibitor which causes 50 per cent inhibition (I₅₀) of an enzymatic reaction," *Biochemical pharmacology*, vol. 22, pp. 3099-3108, 1973.
- [105] I. Langmuir, "The constitution and fundamental properties of solids and liquids. Part I. Solids.," *J. Am. Chem. Soc.*, vol. 38, pp. 2221-225, 1916.
- [106] I. Langmuir, "The adsorption of gases on plane surfaces of glass, mica and platinum.," *J. Am. Chem. Soc.*, vol. 40, pp. 1361-1404, 1918.
- [107] W. J. Reichmann, *Use and abuse of statistics*. London: Methuen & Co Ltd., 1963.
- [108] X. Zheng and J. Wang, "Universal statistical fluctuations in thermodynamics and kinetics of single molecular recognition," *Phys. Chem. Chem. Phys.*, vol. 18, pp. 8570-8578, 2016.
- [109] G. Wei, X. Zheng, and J. Wang, "The Universal Statistical Distributions of the Affinity, Equilibrium Constants, Kinetics and Specificity in Biomolecular Recognition," *PLOS Computational Biology*, vol. 11, p. e1004212, 2015.
- [110] J. M. Bland and D. G. Altman, "Statistical methods for assessing agreement between two methods of clinical measurement," *Lancet*, vol. 1, pp. 307-10, Feb 08 1986.
- [111] J. M. Bland and D. G. Altman, "Measuring agreement in method comparison studies," *Stat Methods Med Res*, vol. 8, pp. 135-60, Jun 1999.
- [112] N. Metropolis and S. Ulam, "The Monte Carlo method," *J Am Stat Assoc*, vol. 44, pp. 335-41, Sep 1949.
- [113] D. Bajusz, A. Racz, and K. Heberger, "Why is Tanimoto index an appropriate choice for fingerprint-based similarity calculations?," *J Cheminform*, vol. 7, p. 20, 2015.
- [114] P. Ertl, B. Rohde, and P. Selzer, "Fast calculation of molecular polar surface area as a sum of fragment-based contributions and its application to the prediction of drug transport properties," *J Med Chem*, vol. 43, pp. 3714-7, Oct 05 2000.
- [115] D. Rogers and A. J. Hopfinger, "Application of Genetic Function Approximation to Quantitative Structure-Activity Relationships and Quantitative Structure-Property Relationships," *Journal of Chemical Information and Modeling*, vol. 34, pp. 854-866, 1994.
- [116] K. Deb, *Multi-Objective Optimization using Evolutionary Algorithms*. Chichester: Wiley, 2001.
- [117] P. P. Graczyk, "Gini coefficient: a new way to express selectivity of kinase inhibitors against a family of kinases," *Journal of medicinal chemistry*, vol. 50, pp. 5773-5779, 2007.
- [118] GraphPadSoftware Inc. (11/2017). *Equation: Kinetics of competitive binding*. Available: https://www.graphpad.com/guides/prism/7/curve-fitting/index.htm?reg_kinetics_of_competitive_bindin.htm
- [119] L. H. Easson and E. Stedman, "The Absolute Activity of Choline-Esterase," *Proceedings of the Royal Society B: Biological Sciences*, vol. 121, pp. 142-164, 1936.
- [120] P. Aranyi, "Kinetics of the hormone-receptor interaction. Competition experiments with slowly equilibrating ligands," *Biochim Biophys Acta*, vol. 628, pp. 220-7, Mar 03 1980.
- [121] C. E. Heise, S. K. Sullivan, and P. D. Crowe, "Scintillation proximity assay as a high-throughput method to identify slowly dissociating nonpeptide ligand binding to the GnRH receptor," *J Biomol Screen*, vol. 12, pp. 235-9, Mar 2007.
- [122] R. Bosma, L. A. Stoddart, V. Georgi, M. Bouzo-Lorenzo, N. Bushby, L. Inkoom, *et al.*, "Probe dependency in the determination of ligand binding kinetics at a G protein coupled receptor via competitive association kinetics," *manuscript in clearance for submission*, expected in 2018.
- [123] D. Kitagawa, M. Gouda, and Y. Kirii, "Quick evaluation of kinase inhibitors by surface plasmon resonance using single-site specifically biotinylated kinases," *J Biomol Screen*, vol. 19, pp. 453-61, Mar 2014.
- [124] P. Wu, T. E. Nielsen, and M. H. Clausen, "FDA-approved small-molecule kinase inhibitors," *Trends Pharmacol Sci*, vol. 36, pp. 422-39, Jul 2015.
- [125] K. L. Kim and W. Suh, "Apatinib, an Inhibitor of Vascular Endothelial Growth Factor Receptor 2, Suppresses Pathologic Ocular Neovascularization in Mice," *Invest Ophthalmol Vis Sci*, vol. 58, pp. 3592-3599, Jul 01 2017.
- [126] D. Y. Duveau, X. Hu, M. J. Walsh, S. Shukla, A. P. Skoumbourdis, M. B. Boxer, *et al.*, "Synthesis and biological evaluation of analogues of the kinase inhibitor nilotinib as Abl and Kit inhibitors," *Bioorganic & Medicinal Chemistry Letters*, vol. 23, pp. 682-686, 2013.
- [127] H. Imamura, K. P. Huynh Nhat, H. Togawa, K. Saito, R. Iino, Y. Kato-Yamada, *et al.*, "Visualization of ATP levels inside single living cells with fluorescence resonance energy transfer-based genetically encoded indicators," *Proceedings of the National Academy of Sciences*, vol. 106, pp. 15651-15656, 2009.

- [128] P. P. Graczyk, "Gini coefficient: a new way to express selectivity of kinase inhibitors against a family of kinases," *J Med Chem*, vol. 50, pp. 5773-9, Nov 15 2007.
- [129] S. Shugarts and L. Z. Benet, "The role of transporters in the pharmacokinetics of orally administered drugs," *Pharm Res*, vol. 26, pp. 2039-54, Sep 2009.
- [130] J. P. Rigaut and J. Vassy, "High-resolution three-dimensional images from confocal scanning laser microscopy. Quantitative study and mathematical correction of the effects from bleaching and fluorescence attenuation in depth," *Anal Quant Cytol Histol*, vol. 13, pp. 223-32, Aug 1991.
- [131] L. Song, E. J. Hennink, I. T. Young, and H. J. Tanke, "Photobleaching kinetics of fluorescein in quantitative fluorescence microscopy," *Biophys J*, vol. 68, pp. 2588-600, Jun 1995.
- [132] Q. Liu, Y. Sabnis, Z. Zhao, T. Zhang, S. J. Buhrlage, L. H. Jones, *et al.*, "Developing irreversible inhibitors of the protein kinase cysteinome," *Chem Biol*, vol. 20, pp. 146-59, Feb 21 2013.
- [133] E. C. Hulme and M. A. Trevethick, "Ligand binding assays at equilibrium: validation and interpretation," *British Journal of Pharmacology*, vol. 161, pp. 1219-1237, 2010.
- [134] I. Nederpelt, V. Georgi, F. Schiele, K. Nowak-Reppel, A. E. Fernández-Montalván, I. J. AP, *et al.*, "Characterization of 12 GnRH peptide agonists - a kinetic perspective," *Br J Pharmacol*, vol. 173, pp. 128-41, Jan 2016.
- [135] A. P. Kornev, N. M. Haste, S. S. Taylor, and L. F. Eyck, "Surface comparison of active and inactive protein kinases identifies a conserved activation mechanism," *Proc Natl Acad Sci U S A*, vol. 103, pp. 17783-8, Nov 21 2006.
- [136] J. M. Elkins, V. Fedele, M. Szklarz, K. R. Abdul Azeez, E. Salah, J. Mikolajczyk, *et al.*, "Comprehensive characterization of the Published Kinase Inhibitor Set," *Nat Biotechnol*, vol. 34, pp. 95-103, Jan 2016.
- [137] A. Schoop and F. Dey, "On-rate based optimization of structure-kinetic relationship--surfing the kinetic map," *Drug Discov Today Technol*, vol. 17, pp. 9-15, Oct 2015.
- [138] P. J. Tummino and R. A. Copeland, "Residence time of receptor- ligand complexes and its effect on biological function," *Biochemistry*, vol. 47, pp. 5481-5492, 2008.
- [139] C. Cederberg, T. Andersson, and I. Skanberg, "Omeprazole: pharmacokinetics and metabolism in man," *Scand J Gastroenterol Suppl*, vol. 166, pp. 33-40; discussion 41-2, 1989.
- [140] J. C. M. Uitdehaag, J. de Man, N. Willemsen-Seegers, M. B. W. Prinsen, M. A. A. Libouban, J. G. Sterrenburg, *et al.*, "Target Residence Time-Guided Optimization on TTK Kinase Results in Inhibitors with Potent Anti-Proliferative Activity," *J Mol Biol*, vol. 429, pp. 2211-2230, Jul 07 2017.
- [141] G. Vauquelin, "Cell membranes... and how long drugs may exert beneficial pharmacological activity in vivo," *Br J Clin Pharmacol*, vol. 82, pp. 673-82, Sep 2016.
- [142] R. P. Mason, D. G. Rhodes, and L. G. Herbet, "Reevaluating equilibrium and kinetic binding parameters for lipophilic drugs based on a structural model for drug interaction with biological membranes," *J Med Chem*, vol. 34, pp. 869-77, Mar 1991.
- [143] Y. N. Abdiche and D. G. Myszka, "Probing the mechanism of drug/lipid membrane interactions using Biacore," *Anal Biochem*, vol. 328, pp. 233-43, May 15 2004.
- [144] W. E. A. de Witte, G. Vauquelin, P. H. van der Graaf, and E. C. M. de Lange, "The influence of drug distribution and drug-target binding on target occupancy: The rate-limiting step approximation," *Eur J Pharm Sci*, May 12 2017.
- [145] A. K. Eaton and R. C. Stewart, "Kinetics of ATP and TNP-ATP Binding to the Active Site of CheA from *Thermotoga maritima*," *Biochemistry*, vol. 49, pp. 5799-5809, 2010.
- [146] N. J. Yang and M. J. Hinner, "Getting Across the Cell Membrane: An Overview for Small Molecules, Peptides, and Proteins," vol. 1266, pp. 29-53, 2015.
- [147] R. Milo, P. Jorgensen, U. Moran, G. Weber, and M. Springer, "BioNumbers--the database of key numbers in molecular and cell biology," *Nucleic Acids Res*, vol. 38, pp. D750-3, Jan 2010.

7.2 Collaboration partners and published parts of the thesis

If not otherwise stated by reference or acknowledgment, I generated the presented work on my own under supervision of my advisors during my doctoral studies. All contributions from colleagues are explicitly referenced within the thesis and/or in the following. The material listed below was obtained in the context of collaborative research:

- Biotinylated proteins CDK2, CDK9: Dr. Uwe Eberspächer, Elisa Chemik and Dr. Pelin Ayaz produced and provided CDK2 and CDK9
- Normalized Motulsky-Mahan equation: Alexey Dubrovskiy (Genedata AG at the time of his contribution to this work) and I developed the equation independently from each other and ended up with the same result.
- Fig. 24, Tables 6 - 8, Supplementary Spreadsheet:
For some kinases M.Sc. Benedict-Tilman Berger and Robert Karmauss (Bayer AG at the time of their contribution to this work) performed the development of probe competition assays and the respective screening for binding parameters of kinase inhibitors. I supervised RK and (re-)evaluated all kPCA traces generated by B-TB and RK according to an automated standard procedure which I developed by myself. I also performed assay development and the screening for the majority of the kinases.
- Fig. 29: For some kinases M.Sc. Benedict-Tilman Berger and B.Sc. Nicole Dittmar (Bayer AG at the time of their contribution to this work) performed the SPR experiments. I supervised ND and (re-)evaluated all of the sensograms generated by B-TB and ND and I also performed SPR experiments.
- Fig. 38, 41c: Dr. James. D. Vasta and Dr. Matthew B. Robers (Promega) performed the nanoBRET Target Engagement assays. I designed the experimental setup: Run of experiments for which kinase-compound pairs and at which compound concentration. I developed the normalization procedure for the nanoBRET data and the permeation models and performed the normalization and simulations accordingly.
- Fig. 25b, 31: Dr. Andreas Steffen (Bayer AG) and me: Together we discussed how best 1) to generate the distance matrices and 2) to perform the clustering for the binding parameters. AS helped with Python scripting.
- PK-BK model, Fig. 44: With my idea, Dr. Stephan Menz (Bayer AG) and I developed the model together. I designed and performed all simulations. Dr. Cornelia Preusse (Bayer AG) estimated PK parameters on the basis of concentration-time profiles using Phoenix 6.4 (I provided her the time profiles).

Whenever results figures, results tables, scientific content or text in this thesis are identical to a previous publication or submitted manuscript, it is stated explicitly here.

- The following parts of the thesis will be published in

[148] Georgi, V.; Dubrovskiy, A.; Steigele, S.; Fernández-Montalván, A. E.: "Precision and accuracy of the 'Motulsky-Mahan' model for the analysis of kinetic competition association assays", *manuscript submitted*, expected in 2018.:

- Methods Chapters (scientific content): 4.3.3, 4.3.8
- Results Chapters (scientific content): 5.1
- Discussion Chapters (scientific content): 6.1
- Figures: 10 - 23, 45
- Appendix (scientific content): C, D

- The following parts of the thesis are published in

[149] Georgi, V.; Schiele, F.; Berger, B.-T.; Steffen, A.; Zapata, P. M.; Briem, H.; Menz, S. ; Preusse, C.; Vasta, J. D.; Robers, M. B.; Brands, M.; Knapp, S.; Fernández-Montalván, A. E.: "Binding kinetics survey of the drugged kinome", *J Am Chem Soc*, vol. 140, pp. 15774-82, Oct 2018.:

- Methods Chapters (scientific content, text):
4.1.2, 4.2.1 & 4.2.3 (Procedures), 4.3.1.1 - 4.3.1.3, 4.3.2 & 4.3.4 - 4.3.7 (Procedures)
- Results Chapters (scientific content): 5.2 - 5.4
- Discussion Chapters (scientific content): 6.2 - 6.4
- Figures: 25, 27 - 39, 41 - 44, 46, 54 - 55
- Tables: 1 - 7, 9 - 10, Supplementary Spreadsheet
- Appendix (scientific content, text): A, B, E, G - K

Appendix

A Kinase constructs and compounds

Table 4: 40 kinases screened using equilibrium and kinetic Probe Competition Assay

Biotinylated Kinase	Gene ID	UniProt	Amino acids	Main target of FDA approved drug [124, 125] screened in this study
ABL	25	P00519	Full-length 2-1130	Bosutinib, Dasatinib, Imatinib, Nilotinib, Ponatinib
AKT1	207	P31749	catalytic domain 104-480	
ALK	238	Q9UM73	cytoplasmic domain 1058-1620	CH5424802 (Alectinib), Crizotinib
AurA	6790	O14965	Full-length 1-403	
AXL	558	P30530	cytoplasmic domain 464-885	
BRAF	673	P15056	catalytic domain 433-726	Dabrafenib, Vemurafenib
BTK*	695	Q06187	Full-length 2-659	Ibrutinib
CDK2	1017	P24941	Full-length 1-298	
CDK9	1025	P50750	Full-length	
CHK1	1111	O14757	Full-length 1-476	
EGFR	1956	P00533	cytoplasmic domain 669-1210	Afatinib, Vargatef (Nintedanib), Desmethyl Erlotinib, Gefitinib, Lapatinib, Vandetanib
FAK	5747	Q05397	Truncated 376-1052	
FGFR1*	2260	P11362	cytoplasmic domain 398-822	
FGFR3*	2261	P22607	cytoplasmic domain 436-806	
FGFR4	2264	P22455	cytoplasmic domain 460-802	
FLT3	2322	P36888	cytoplasmic domain 564-993	
FMS	1436	P07333	cytoplasmic domain 538-972	
FYN**	2534	P06241	Full-length 1-537	
IGF1R*	3480	P08069	cytoplasmic domain 959-1367	
IKK- α	1147	O15111	Full-length 1-745	
IKK- β	3551	O14920	Truncated 1-662	
ITK*	3702	Q08881	Full-length 2-620	
JAK2	3717	O60674	catalytic domain 826-1132	Ruxolitinib, Tofacitinib
KDR	3791	P35968	cytoplasmic domain 790-1356	Apatinib, Axitinib, Vargatef (Nintedanib), Lenvatinib, Pazopanib, Sunitinib, Vandetanib, Cabozantinib
KIT*	3815	P10721	cytoplasmic domain 544-976	Axitinib, Imatinib, Nilotinib, Pazopanib, Sunitinib
LCK	3932	P06239	Full-length human 1-509	
LYNa	4067	P07948	Full-length1-512	
MAP2K1	5604	Q02750	Full-length 1-393	Selumetinib, Trametinib
Met	4233	P08581	cytoplasmic domain 956-1390	Crizotinib, Cabozantinib
MPS1 (TTK)	7272	P33981	Full-length 1-857	
p38 α ***	1432	Q16539	Truncated 9-352	
PIK3CA****	5290	P42336	Full-length1-1068	
PKC η	5583	P24723	Full-length human 1-683	
PLK1	5347	P53350	Full-length1-603	
Ret	5979	P07949	cytoplasmic domain 658-1114	Sunitinib
ROCK1	6093	Q13464	catalytic domain 1-477	
SRC	6714	P12931	Full-length 1-536	Bosutinib, Dasatinib
SYK*	6850	P43405	Full-length 1-635	
TGFB β 1	7046	P36897	catalytic domain 200-503	
Tie2*	7010	Q02763	cytoplasmic domain 771-1124	
TRKB*	4915	Q16620	cytoplasmic domain 456-822	

* preactivated with ATP treatment; ** FYN [isoform a]; *** co-expression with NP_002749.2 and NP_002410.1; **** co-expression with NP_852664.1

Screening was not performed for

- CHK1 (Gene ID: 1111): assay developed, but high amount of tracer and kinase required
- HER2 (Gene ID: 2064), JAK1 (Gene ID: 3716), SPHK (Gene ID: 8877): no kPCA probe identified

Table 5: 270 compounds screened using equilibrium and kinetic Probe Competition Assay

Compound name	CAS Number	Compound name	CAS Number
3-Methyladenine	5142-23-4	BIX 02188	1094614-84-2
A66	1166227-08-2	BIX 02189	1094614-85-3
A-674563	552325-73-2	BKM120 (NVP-BKM120)	944396-07-0
A-769662	844499-71-4	BMS 777607	1025720-94-8
AEE788 (NVP-AEE788)	497839-62-0	BMS 794833	1174046-72-0
Afatinib (BIBW2992)	439081-18-2	BMS-265246	582315-72-8
AG-1024	65678-07-1	BMS-599626 (AC480)	714971-09-2
AG-1478 (Tyrphostin AG-1478)	153436-53-4	Bosutinib (SKI-606)	380843-75-4
AG-490	133550-30-8	Brivanib (BMS-540215)	649735-46-6
AMG 900	945595-80-2	Brivanib alaninate (BMS-582664)	649735-63-7
AMG-208	1002304-34-8	BS-181 HCl	1397219-81-6
AMG458	913376-83-7	BX-795	702675-74-9
Amuvatinib (MP-470)	850879-09-3	BX-912	702674-56-4
Apatinib (YN968D1)	811803-05-1	BYL719	1217486-61-7
ARQ 197 (Tivantinib)	905854-02-6	CAL-101 (GS-1101)	870281-82-6
ARRY334543	845272-21-1	CAY10505	1218777-13-9
Arry-380	937265-83-3	CCT128930	885499-61-6
AS-252424	900515-16-4	CCT129202	942947-93-5
AS-604850	648449-76-7	CCT137690	1095382-05-0
AS-605240	648450-29-7	Cediranib (AZD2171)	288383-20-0
AS703026 (pimasertib)	1236699-92-5	CEP33779	1257704-57-6
AST-1306	1050500-29-2	CH5424802	1256580-46-7
AT7519	844442-38-2	CHIR-124	405168-58-3
AT7867	857531-00-1	CHIR-98014	252935-94-7
AT9283	896466-04-9	CI-1033 (Canertinib)	267243-28-7
Aurora A Inhibitor I	1158838-45-9	CI-1040 (PD184352)	212631-79-3
Axitinib	319460-85-0	CP 673451	343787-29-1
AZ 960	905586-69-8	CP-724714	537705-08-1
AZ628	878739-06-1	Crenolanib (CP-868596)	670220-88-9
AZD2014	1009298-59-2	Crizotinib (PF-02341066)	877399-52-5
AZD4547	1035270-39-3	CX-4945 (Silmitasertib)	1009820-21-6
AZD5438	602306-29-6	CYC116	693228-63-6
AZD6244 (Selumetinib)	606143-52-6	Cyt387	1056634-68-4
AZD7762	860352-01-8	Dabrafenib (GSK2118436)	1195765-45-7
AZD8055	1009298-09-2	Dacomitinib (PF299804 - PF-00299804)	1110813-31-4
AZD8330	869357-68-6	Danuserib (PHA-739358)	827318-97-8
AZD8931	848942-61-0	Dasatinib (BMS-354825)	302962-49-8
Barasertib (AZD1152-HQPA)	722544-51-6	DCC-2036 (Rebastinib)	1020172-07-9
Baricitinib (LY3009104 - incb28050)	1187594-09-7	Deforolimus (Ridaforolimus)	572924-54-0
BEZ235 (NVP-BEZ235)	915019-65-7	Desmethyl Erlotinib (CP-473420)	183320-51-6
BGJ398 (NVP-BGJ398)	872511-34-7	Dinaciclib (SCH727965)	779353-01-4
BI 2536	755038-02-9	Dovitinib (TKI-258)	405169-16-6
BI6727 (Volasertib)	755038-65-4	Dovitinib Dilactic acid (TKI258 Dilactic acid)	852433-84-2
BIBF1120 (Vargatef)	656247-17-5	E7080 (Lenvatinib)	417716-92-8
BIRB 796 (Doramapimod)	285983-48-4		

Compound name	CAS Number
ENMD-2076	1291074-87-7
Enzastaurin (LY317615)	170364-57-5
Erlotinib HCl	183319-69-9
Everolimus (RAD001)	159351-69-6
Flavopiridol HCl	131740-09-5
Foretinib (GSK1363089 - XL880)	849217-64-7
GDC-0068	1001264-89-6
GDC-0879	905281-76-7
GDC-0941	957054-30-7
GDC-0980 (RG7422)	1032754-93-0
Gefitinib (Iressa)	184475-35-2
Golitinib (E7050)	928037-13-2
GSK1059615	958852-01-2
GSK1070916	942918-07-2
GSK1120212 (Trametinib)	871700-17-3
GSK1838705A	1116235-97-2
GSK1904529A	1089283-49-7
GSK2126458	1086062-66-9
GSK461364	929095-18-1
GSK690693	937174-76-0
Hesperadin	422513-13-1
HMN-214	173529-46-9
IC-87114	371242-69-2
Imatinib (Gleevec)	152459-95-5
Imatinib Mesylate	220127-57-1
IMD 0354	978-62-1
INCB28060	1029712-80-8
Indirubin	479-41-4
INK 128 (MLN0128)	1224844-38-5
JNJ-38877605	943540-75-8
JNJ-7706621	443797-96-4
Ki8751	228559-41-9
KRN 633	286370-15-8
Ku-0063794	938440-64-3
KU-55933	587871-26-9
KU-60019	925701-49-1
KW 2449	1000669-72-6
KX2-391	897016-82-9
Lapatinib Ditosylate (Tykerb)	388082-77-7
LDN193189	1062368-24-4
Linifanib (ABT-869)	796967-16-3
Linsitinib (OSI-906)	867160-71-2
LY2228820	862507-23-1
LY2603618 (IC-83)	911222-45-2
LY2784544	1229236-86-5
LY294002	154447-36-6
Masitinib (AB1010)	790299-79-5

Compound name	CAS Number
MGCD-265	875337-44-3
Milciclib (PHA-848125)	802539-81-7
MK-2206 2HCl	1032350-13-2
MK-2461	917879-39-1
MK-5108 (VX-689)	1010085-13-8
MLN8054	869363-13-3
MLN8237 (Alisertib)	1028486-01-2
Motesanib Diphosphate (AMG-706)	857876-30-3
Mubritinib (TAK 165)	366017-09-6
Neratinib (HKI-272)	698387-09-6
Nilotinib (AMN-107)	641571-10-0
NU7441 (KU-57788)	503468-95-9
NVP-ADW742	475488-23-4
NVP-BGT226	1245537-68-1
NVP-BHG712	940310-85-0
NVP-BSK805	1092499-93-8
NVP-BVU972	1185763-69-2
NVP-TAE226	761437-28-9
ON-01910	1225497-78-8
OSI-027	936890-98-1
OSI-420	183320-51-6
OSI-930	728033-96-3
OSU-03012	742112-33-0
Palomid 529	914913-88-5
Pazopanib HCl	635702-64-6
PCI-32765 (Ibrutinib)	936563-96-1
PD 0332991 (Palbociclib) HCl	827022-32-2
PD0325901	391210-10-9
PD153035 HCl	183322-45-4
PD173074	219580-11-7
PD318088	391210-00-7
PD98059	167869-21-8
Pelitinib (EKB-569)	257933-82-7
PF-00562271	939791-38-5
PF-03814735	942487-16-3
PF-04217903	956905-27-4
PF-04691502	1013101-36-4
PF-05212384 (PKI-587)	1197160-78-3
PH-797804	586379-66-0
PHA-665752	477575-56-7
PHA-680632	398493-79-3
PHA-767491	845714-00-3
PHA-793887	718630-59-2
Phenformin HCl	834-28-6
PHT-427	1191951-57-1
PI-103	371935-74-9

Compound name	CAS Number
Piceatannol	10083-24-6
PIK-293	900185-01-5
PIK-294	900185-02-6
PIK-75	372196-77-5
PIK-90	677338-12-4
PIK-93	593960-11-3
PKI-402	1173204-81-3
PLX-4720	918505-84-7
Ponatinib (AP24534)	943319-70-8
PP-121	1092788-83-4
PP242	1092351-67-1
Quercetin (Sophoretin)	117-39-5
Quizartinib (AC220)	950769-58-1
R406	841290-81-1
R406 (free base)	841290-80-0
R788 (Fostamatinib)	901119-35-5
R935788 (Fostamatinib disodium - R788 disodium)	1025687-58-4
Raf265 derivative	n.a.; Selleck Chemicals Cat.No. S2200
Rapamycin (Sirolimus)	53123-88-9
Roscovitine (Seliciclib - CYC202)	186692-46-6
Ruxolitinib (INCB018424)	941678-49-5
SAR131675	1433953-83-3
Saracatinib (AZD0530)	379231-04-6
SB 202190	152121-30-7
SB 203580	152121-47-6
SB 216763	280744-09-4
SB 415286	264218-23-7
SB 431542	301836-41-9
SB 525334	356559-20-1
SB590885	405554-55-4
Semaxanib (SU5416)	194413-58-6
SGX-523	1022150-57-7
SNS-032 (BMS-387032)	345627-80-7
SNS-314	1146618-41-8
Sotrastaurin (AEB071)	425637-18-9
SP600125	129-56-6
Staurosporine	62996-74-1
SU11274	658084-23-2
Sunitinib Malate (Sutent)	341031-54-7
TAE684 (NVP-TAE684)	761439-42-3
TAK-285	871026-44-7
TAK-733	1035555-63-5
TAK-901	934541-31-8
Tandutinib (MLN518)	387867-13-2
Temsirolimus (Torisel)	162635-04-3

Compound name	CAS Number
TG 100713	925705-73-3
TG100-115	677297-51-7
TG101209	936091-14-4
TG101348 (SAR302503)	936091-26-8
TGX-221	663619-89-4
Thiazovivin	1226056-71-8
Tideglusib	865854-05-3
Tie2 kinase inhibitor	948557-43-5
Tivozanib (AV-951)	475108-18-0
Tofacitinib (CP-690550 - Tasocitinib)	477600-75-2
Tofacitinib citrate (CP-690550 citrate)	540737-29-9
Torin 1	1222998-36-8
Torin 2	1223001-51-1
TPCA-1	507475-17-4
Triciribine (Triciribine phosphate)	35943-35-2
TSU-68 (SU6668)	252916-29-3
TWS119	601514-19-6
Tyrphostin AG 879 (AG 879)	148741-30-4
U0126-EtOH	1173097-76-1
Vandetanib (Zactima)	443913-73-3
Vatalanib 2HCl (PTK787)	212141-51-0
Vemurafenib (PLX4032)	918504-65-1
VX-680 (MK-0457 - Tozasertib)	639089-54-6
VX-702	745833-23-2
WAY-600	1062159-35-6
WHI-P154	211555-04-3
Wortmannin	19545-26-7
WP1066	857064-38-1
WP1130	856243-80-6
WYE-125132	1144068-46-1
WYE-354	1062169-56-5
WYE-687	1062161-90-3
WZ3146	1214265-56-1
WZ4002	1213269-23-8
WZ8040	1214265-57-2
XL147	956958-53-5
XL-184 (Cabozantinib)	849217-68-1
XL765	1349796-36-6
Y-27632 2HCl	129830-38-2
YM201636	371942-69-7
ZM 336372	208260-29-1
ZM-447439	331771-20-1
ZSTK474	475110-96-4

B Binding kinetic rate constants of tracers and kinase specific assay parameters

Table 6: Assay conditions for equilibrium and kinetic Probe Competition Assay

	Probe (Kinase Tracer)	Probe conc. [nM] ¹	Kinase conc. [nM] ¹	Kinetic intervals [s] ²
ABL	178	10	0.1	10
AKT1	236	50	0.5	10
ALK	236	10	0.5	10
AurA	236	12.5	0.3	10
AXL	236	25	0.2	10
BRAF	178	125 (kPCA), 50 (ePCA)	2	10
BTK	178	12.5	0.2	10
CDK2	236	200	2.0	10
CDK9	236	200 (kPCA), 50 (ePCA)	1	10
CHK1	236	400	2.0	10
EGFR	199	25	0.5	10
FAK	236	25	0.3	10
FGFR1	236	50	0.3	10
FGFR3	236	50	0.3	10
FGFR4	236	120	0.4	10
FLT3	236	50	0.3	10
FMS	236	100	0.5	10
FYN	236	50	0.2	10
IGF1R	236	100	1.0	10
IKK- α	236	70	2.0	10
IKK- β	236	100	0.5	10
ITK	236	50	1.0	10
JAK2	236	5	0.4	10
KDR	236	50	0.3	10
KIT	222	12.5	0.3	10
LCK	236	50	0.3	10
LYNa	236	25	0.3	10
MAP2K1	236	25	0.1	10
Met	236	50	0.2	10
MPS1 (TTK)	236	250 (kPCA), 50 (ePCA)	1	10
p38 α	199	50	0.124	10
PIK3CA	314	5	0.121	10
PKC η	236	100	0.4	120
PLK1	236	50	4.0	10
Ret	236	25	0.3	10
ROCK1	236	200	1.0	10
SRC	236	25	0.3	10
SYK	236	5	0.2	10
TGFBR1	178	25	0.3	10
Tie2	236	50	0.3	10
TRKB	236	25	0.2	10

1) were determined as described in chapter 4.2.1.1.; 2) first cycle 14 s instead of 10 s (due to parallel injection and reading); Further reader settings: excitation - 337 nm / emission - A: 665 nm, B: 620 nm / 40 cycles

Table 7: Binding kinetic and affinity parameters of Kinase Tracers (the kPCA probes)

were determined as described in chapter 4.2.1.1 & 4.3.1.1 and required for evaluation of kPCA (chapter 4.3.1.3)

Kinase	Probe (Kinase Tracer)	$k_{on} [M^{-1}s^{-1}]$		$k_{off} [s^{-1}]$		$K_D [nM]$	
		mean	error	mean	error	mean	error
ABL	178	$2.185 \cdot 10^6$	$1.952 \cdot 10^4$	0.00017	0.00004	0.08	0.02
AKT1	236	$8.089 \cdot 10^4$	$1.154 \cdot 10^3$	0.00399	0.00009	49.26	1.18
ALK	236	$3.746 \cdot 10^6$	$2.177 \cdot 10^5$	0.09023	0.00533	24.09	0.23
AurA	236	$1.338 \cdot 10^6$	$1.502 \cdot 10^4$	0.00155	0.00006	1.16	0.04
AXL	236	$3.305 \cdot 10^6$	$1.593 \cdot 10^5$	0.01165	0.00081	3.52	0.13
BRAF	178	$1.790 \cdot 10^6$	$3.038 \cdot 10^5$	0.21070	0.03576	117.7	1.93
BTK	178	$2.563 \cdot 10^6$	$5.200 \cdot 10^4$	0.00167	0.00016	0.61	0.08
CDK2	236	$7.935 \cdot 10^4$	$4.458 \cdot 10^3$	0.01346	0.00087	169.7	5.85
CDK9	236	$1.672 \cdot 10^5$	$4.297 \cdot 10^3$	0.01173	0.00023	70.14	1.85
CHK1	236	$2.752 \cdot 10^4$	$1.339 \cdot 10^3$	0.00453	0.00034	164.6	11.92
EGFR	199	$8.897 \cdot 10^5$	$5.115 \cdot 10^4$	0.02250	0.00140	25.29	0.58
FAK	236	$1.053 \cdot 10^6$	$5.319 \cdot 10^4$	0.04273	0.00266	40.57	1.45
FGFR1	236	$9.046 \cdot 10^5$	$9.875 \cdot 10^4$	0.07235	0.00881	79.98	3.78
FGFR3	236	$5.971 \cdot 10^5$	$3.950 \cdot 10^4$	0.05370	0.00415	89.93	3.56
FGFR4	236	$2.292 \cdot 10^5$	$2.287 \cdot 10^4$	0.1689	0.01670	736.7	22.03
FLT3	236	$6.886 \cdot 10^4$	$6.844 \cdot 10^2$	0.00423	0.00007	61.49	0.91
FMS	236	$1.099 \cdot 10^5$	$3.302 \cdot 10^3$	0.00921	0.00034	83.77	1.94
FYN	236	$3.004 \cdot 10^6$	$6.026 \cdot 10^5$	0.14270	0.02999	47.51	1.92
IGF1R	236	$4.760 \cdot 10^5$	$5.766 \cdot 10^4$	0.13220	0.01454	277.7	19.51
IKK- α	236	$1.646 \cdot 10^5$	$2.908 \cdot 10^3$	0.01483	0.00031	90.06	1.11
IKK- β	236	$3.164 \cdot 10^5$	$3.291 \cdot 10^4$	0.04886	0.00513	154.4	7.85
ITK	236	$1.012 \cdot 10^6$	$8.064 \cdot 10^4$	0.07774	0.00680	76.80	3.30
JAK2	236	$3.428 \cdot 10^6$	$7.051 \cdot 10^4$	0.01356	0.00032	3.96	0.06
KDR	236	$1.441 \cdot 10^5$	$1.681 \cdot 10^3$	0.00446	0.00009	30.93	0.44
KIT	222	$2.419 \cdot 10^6$	$1.191 \cdot 10^5$	0.02002	0.00112	8.28	0.23
LCK	236	$1.579 \cdot 10^6$	$2.269 \cdot 10^5$	0.12210	0.01860	77.34	3.58
LYNa	236	$2.270 \cdot 10^6$	$3.417 \cdot 10^5$	0.08538	0.01363	37.62	1.63
MAP2K1	236	$1.710 \cdot 10^5$	$1.386 \cdot 10^3$	0.00021	0.00004	1.23	0.23
Met	236	$2.569 \cdot 10^5$	$8.434 \cdot 10^3$	0.02865	0.00100	111.5	1.57
MPS1 (TTK)	236	$1.156 \cdot 10^6$	$1.244 \cdot 10^5$	0.1483	0.01582	128.2	2.79
p38 α	199	$2.170 \cdot 10^6$	$2.630 \cdot 10^5$	0.08989	0.01112	41.41	0.78
PIK3CA	314	$8.620 \cdot 10^6$	$1.743 \cdot 10^5$	0.00498	0.00016	0.58	0.01
PKC η	236	$4.640 \cdot 10^3$	$8.773 \cdot 10^1$	0.00030	0.00001	65.52	1.89
PLK1	236	$3.029 \cdot 10^6$	$2.747 \cdot 10^5$	0.01950	0.00194	6.44	0.23
Ret	236	$9.785 \cdot 10^5$	$2.879 \cdot 10^4$	0.00740	0.00029	7.57	0.17
ROCK1	236	$9.213 \cdot 10^4$	$3.421 \cdot 10^3$	0.03257	0.00121	353.6	8.44
SRC	236	$6.007 \cdot 10^6$	$2.255 \cdot 10^6$	0.16850	0.06482	28.05	1.42
SYK	236	$2.734 \cdot 10^6$	$5.134 \cdot 10^4$	0.00383	0.00013	1.40	0.04
TGFBR1	178	$2.104 \cdot 10^6$	$2.285 \cdot 10^5$	0.08545	0.00944	40.62	0.71
Tie2	236	$2.429 \cdot 10^6$	$1.012 \cdot 10^6$	0.27200	0.11490	112.0	6.21
TRKB	236	$7.683 \cdot 10^6$	$1.319 \cdot 10^4$	0.00117	0.00009	1.52	0.11

C „Association then dissociation – two or more concentration of hot” model for determination of tracer binding kinetics

An alternative experimental procedure (to an association experiment) for the determination of the binding kinetics was implemented, where an association step was directly followed by a dissociation step for a concentration series of the tracer: Serial dilutions of fluorescent tracer were pre-dispensed in a microtiter plate. The script mode and injection device of the plate reader was used to start 1) the association phase by injection of St-Tb labeled kinase and subsequently 2) the dissociation phase by injection of an excess of unlabeled inhibitor (inhibitor in a least 10x highest concentration and 100x K_D compared to tracer). (refer to chapter 4.2.1 for more information about the assay components)

The “Association then dissociation” model (GraphPad Prism) was extended to an “Association then dissociation - two or more concentration of hot” model to enable global fitting to the concentration series traces:

“Association then dissociation - two or more concentration of hot” model

$$K_D = k_{\text{off}} / k_{\text{on}}$$

$$k_{\text{obs}} = k_{\text{on}} * L + k_{\text{off}}$$

$$\text{Occupancy} = L / (L + K_D)$$

$$Y_{\text{max}} = \text{Occupancy} * B_{\text{max}}$$

$$\text{Association} = Y_{\text{max}} * (1 - \exp(-1 * k_{\text{obs}} * X))$$

$$Y_{\text{Time0}} = Y_{\text{max}} * (1 - \exp(-1 * k_{\text{obs}} * \text{Time0}))$$

$$\text{Dissociation} = Y_{\text{Time0}} * \exp(-1 * k_{\text{off}} * (X - \text{Time0}))$$

$$Y = \text{IF}(X < \text{Time0}, \text{Association}, \text{Dissociation}) + \text{NS}$$

Parameter constrains:

L, Time0 constrained to constant values as used in experiment

Shared parameters (between concentration traces) for global fit: k_{off} , k_{on} , B_{max}

K_D : calculated equilibrium dissociation constant in M, k_{obs} : observed rate of probe-target complex formation, k_{off} : dissociation rate constant of probe in inverse time, k_{on} : association rate constant of probe in inverse Molar times inverse time, L: probe concentration in M; Y is the binding signal; Y_{max} is the maximum observable signal at equilibrium; B_{max} : maximum binding signal at very high probe concentrations in units of Y; Time0: time at which dissociation is initiated; Y_{Time0} : binding signal at Time0; NS: non-specific binding signal (constrain to 0 if specific binding signal is used)

Optional: Accounting for signal drift:

$$Y(\text{drift}) = Y * \exp(-K_{\text{drift}} * t)$$

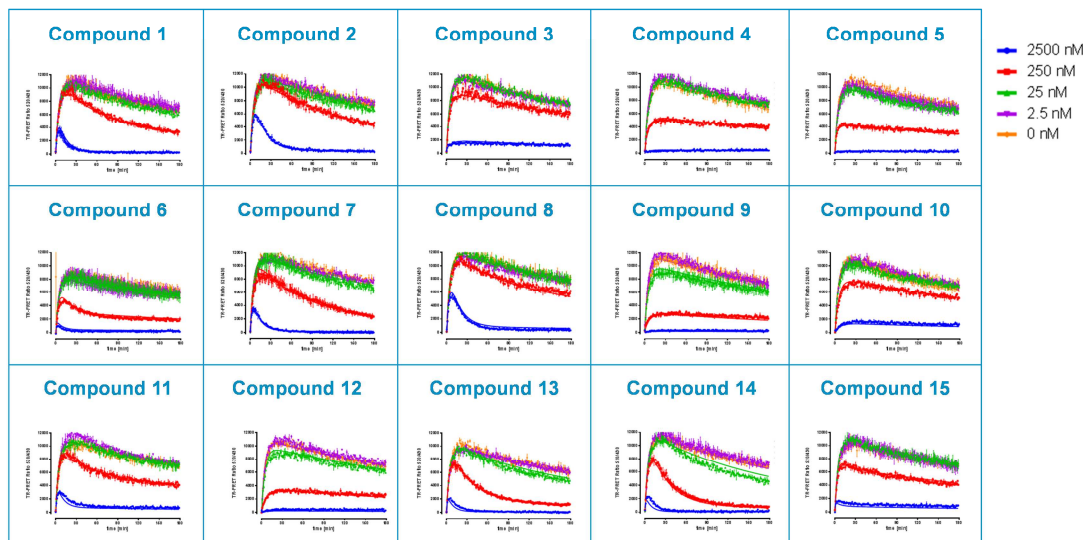
Y is the binding signal with observed signal drift

K_{drift} is the rate of signal drift and a shared parameter between all concentration traces for global fit

D kPCA traces with signal decrease and their evaluation based on normalization

kPCA measurements can be influenced by fluorescence losses, e.g. due to photobleaching or cell sedimentation (signal traces in Figure 45a). Fluorescence losses are identifiable by the decreasing signal in the tracer binding control (without compound), where normally tracer binding leads to an increase in the signal until equilibrium is reached. As demonstrated within this thesis (chapter 5.1.5), the problem can be solved best by normalization of kPCA traces (normalized signal traces in Figure 45b) and evaluation with an adapted Motulsky-Mahan model as provided below. However, kPCAs applied for the binding kinetics profiling panel (chapter 5.2) showed no significant systematic signal decay and were evaluated with standard Motulsky-Mahan model.

a kPCA traces with signal decrease → tracer binding



b normalized kPCA traces: compound binding [%control]

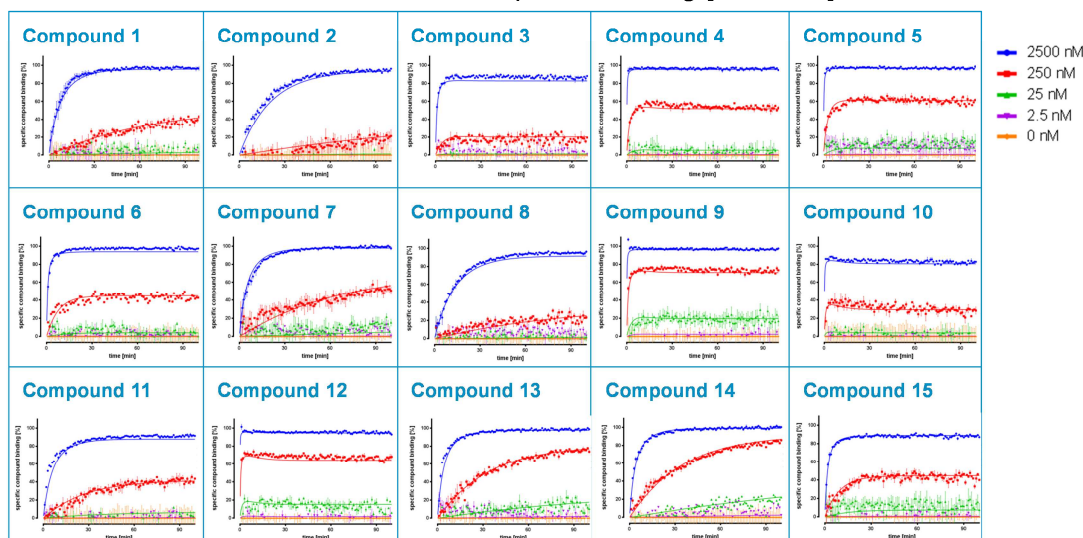


Figure 45: Exemplary kPCA traces influenced by systematic signal decay (a) and their corresponding normalized traces representing the percentage of compound binding (b)

Motulsky-Mahan Model for normalized Data

Note: due to normalization this model is independent of trace scaling & photo-bleaching

Normalization of TR-FRET traces:

percentage of probe binding (TR-FRET signal: 0% = max. inhibition control, 100% = probe signal control); and inverting signal to get compound traces:

$$\hat{y}(t) = \left(1 - \frac{y(t) - y_{0\%}(t)}{y_{100\%}(t) - y_{0\%}(t)}\right) \times 100\%$$

t: time; \hat{y} : normalized binding signal; y: tracer binding signal (TR-FRET ratio); $y_{100\%}$: median trace of TR-FRET Ratio traces from probe signal control wells (without compound); $y_{0\%}$: median trace of TR-FRET Ratio traces from background signal wells (max. inhibition control)

kPCA model for normalized TR-FRET traces:

$$\hat{y}(t > 0) = \left(1 - \frac{K_A}{\text{Diff}(1 - e^{-K_A t})} \left(\frac{K_4 \text{Diff}}{K_F K_S} + \frac{K_4 - K_F}{K_F} e^{-K_F t} - \frac{K_4 - K_S}{K_S} e^{-K_S t} \right)\right) \times 100\%$$

$$\hat{y}(t = 0) = 0$$

with

$$K_A = K_1 \times L + K_2$$

$$K_B = K_3 \times I + K_4$$

$$K_F = 0.5 \left(K_A + K_B + \sqrt{(K_A - K_B)^2 + 4 \times K_1 \times K_3 \times L \times I} \right)$$

$$K_S = 0.5 \left(K_A + K_B - \sqrt{(K_A - K_B)^2 + 4 \times K_1 \times K_3 \times L \times I} \right)$$

$$\text{Diff} = K_F - K_S$$

\hat{y} : normalized binding signal; t: time; K_1 : association rate of probe in inverse Molar times inverse time; K_2 : dissociation rate of probe in inverse time; L: concentration of probe in M, K_3 : association rate of unlabeled compound (inverse Molar times inverse time); I: concentration of unlabeled compound in M; K_4 : dissociation rate of unlabeled compound (inverse time)

Parameters constrains:

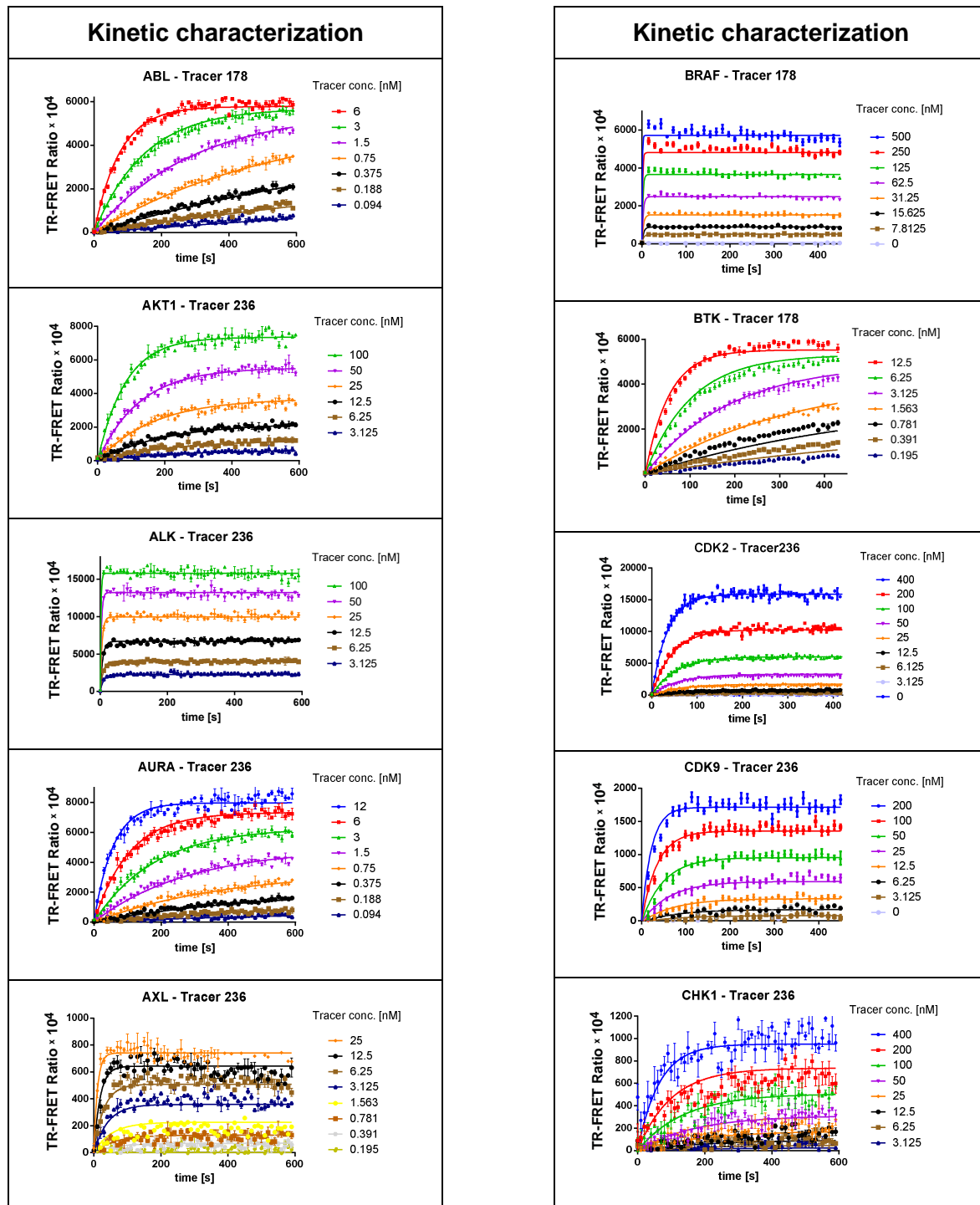
K_1 , L, K_2 , I constrained to constant values as used in experiment or determined during assay development, respectively.

Shared parameters (between concentration traces) for global fit: K_3 , K_4

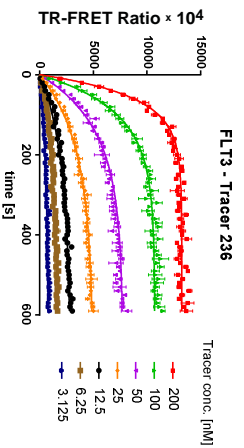
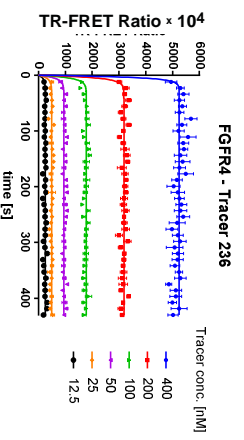
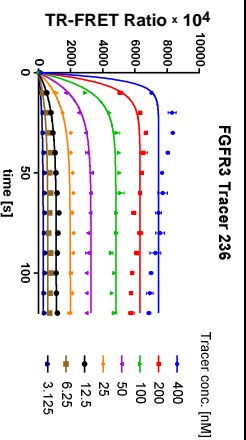
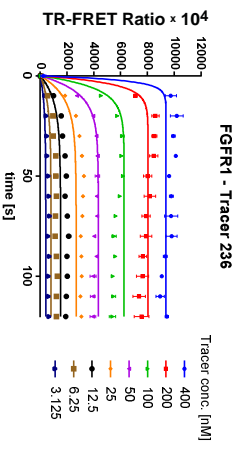
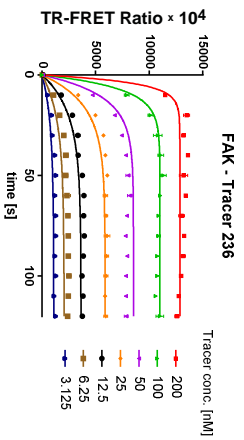
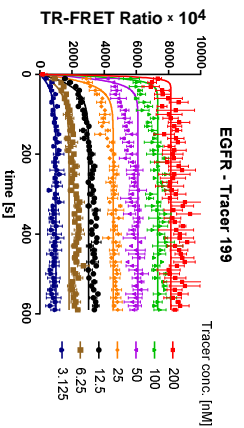
E Determination of kinase specific assay parameters and kinetic characterization of kPCA probe

Table 8: Determination of kinase specific assay parameters and kinetic characterization of kPCA probe

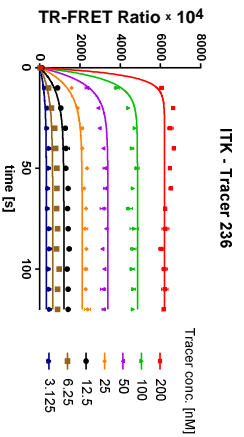
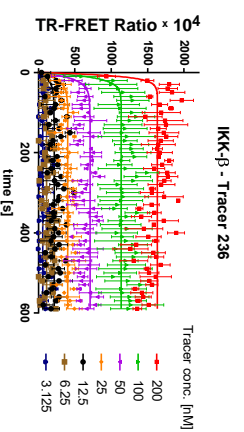
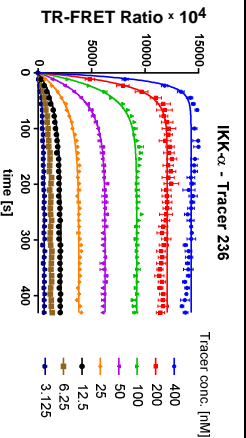
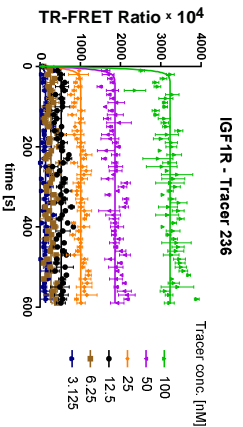
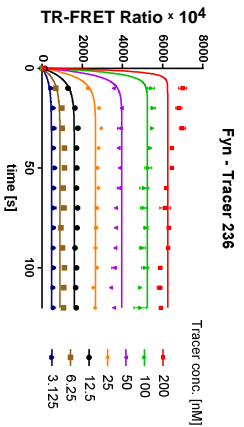
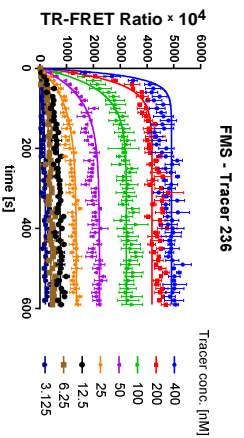
Kinase Tracers (multikinase inhibitor - Alexa Fluor® conjugates) were used as probes for the competition assays. The table lists the graphs representing kinase binding traces (tracer association) for increasing concentrations of these tracers as well as the corresponding fitting curves (for more details refer to chapters 4.2.1.1 and 4.3.1.1). The determined binding parameters for tracer binding to kinases are given in Table 7 (appendix B).



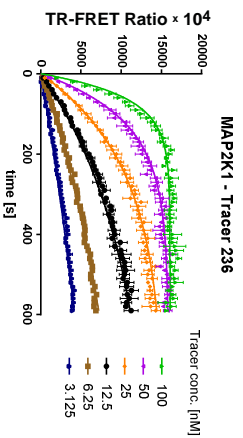
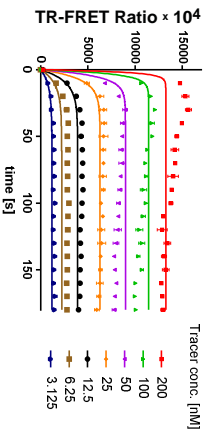
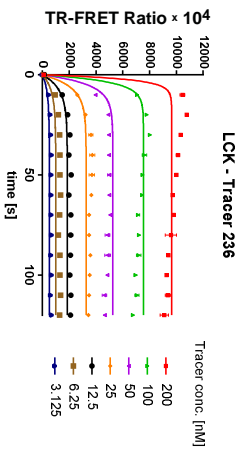
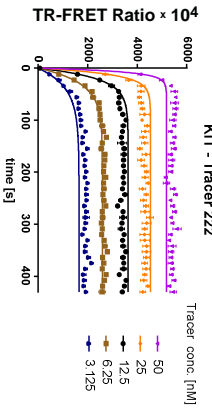
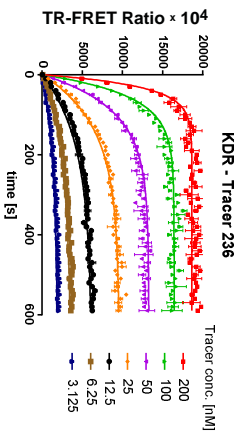
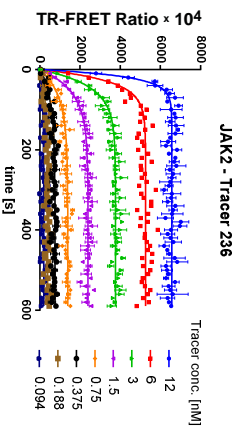
Kinetic characterization



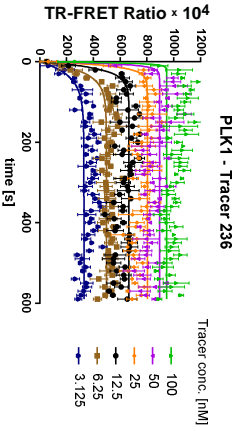
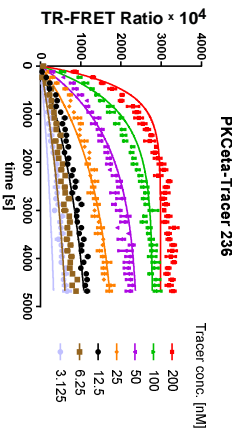
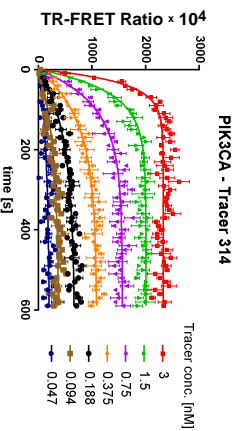
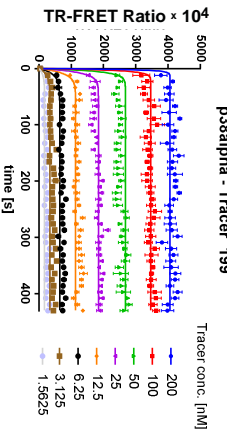
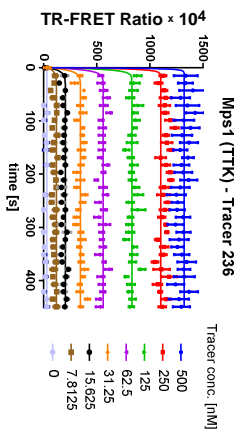
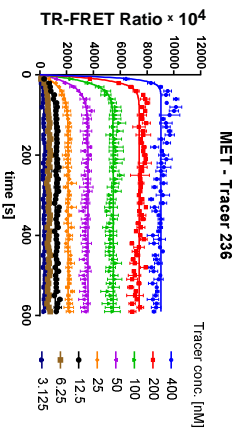
Kinetic characterization

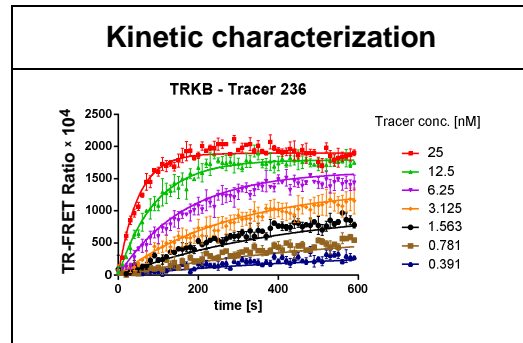
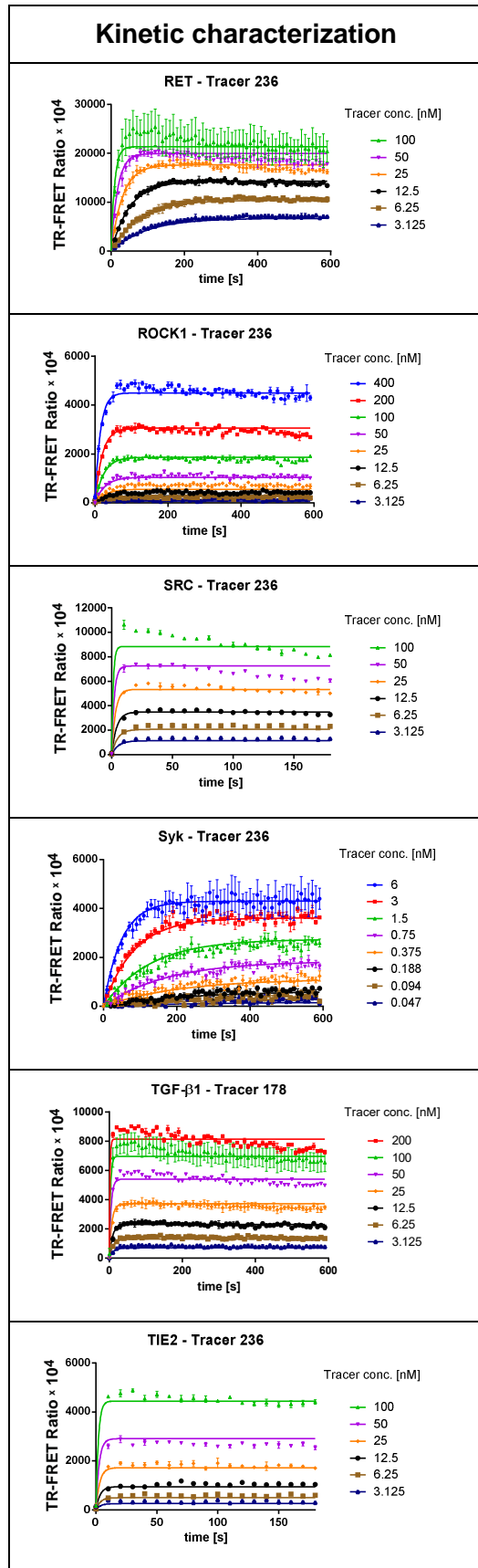


Kinetic characterization



Kinetic characterization





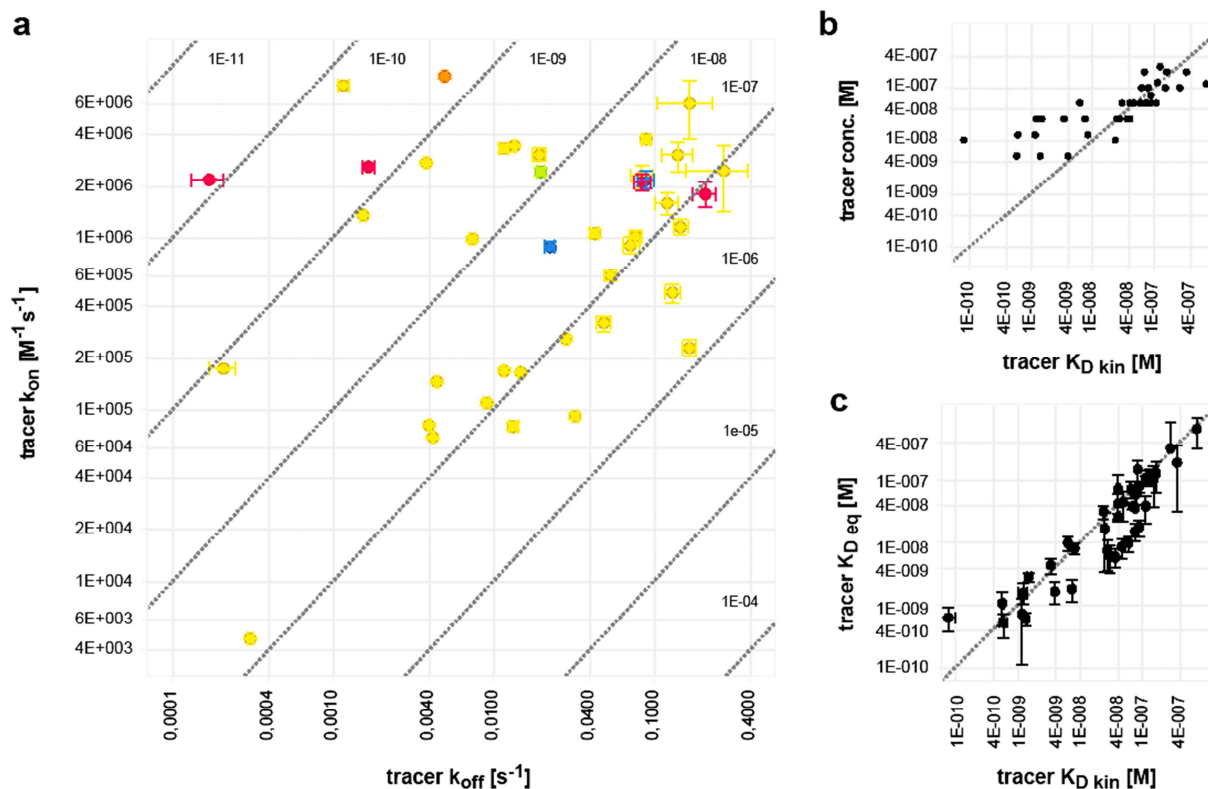


Figure 46: Binding kinetics, affinities and concentrations of Kinase Tracers investigated in this thesis

a) Binding kinetic parameters determined by kinetic association assays for binding of Kinase Tracers 236 (yellow), 178 (pink), 199 (blue), 222 (green) and 314 (orange) to kinases used in this study (procedure described in chapter 4.2.1.1 and 4.3.1.1, corresponding plots are depicted in Table 8). Standard errors of the best fit parameters are shown in the figure. Higher errors were observed for very low and high off-rates of the tracers, as compared to errors of off-rates in between.

b) In most assays, the tracers were applied at a concentration in the range of the K_D of the respective tracer-kinase pair. Higher tracer concentrations were applied for tracers with high affinities.

c) Accuracy of determined tracer binding characteristics: Good agreement of tracer affinities determined in equilibrium (K_{Deq} from endpoint tracer titration assays) and in the kinetic assay setup (K_{Dkin} from kinetic tracer association assays). (For more information about experimental setup and non-linear regression models refer to chapters 4.2.1.1 and 4.3.1.1)

F Large-scale binding kinetics profiling

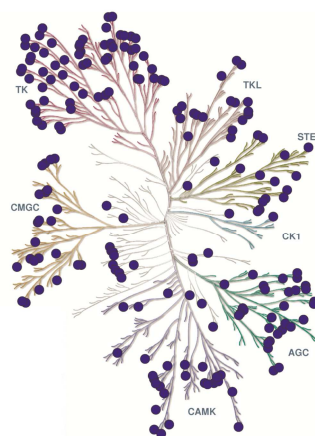


Figure 47: Phylogenetic tree of the human kinome with kinases targeted by kPCA compatible tracers

More than 286 kinases (>50% of human kinome) are targeted by kPCA compatible tracers (according to Thermo Fisher Scientific's datasheets).

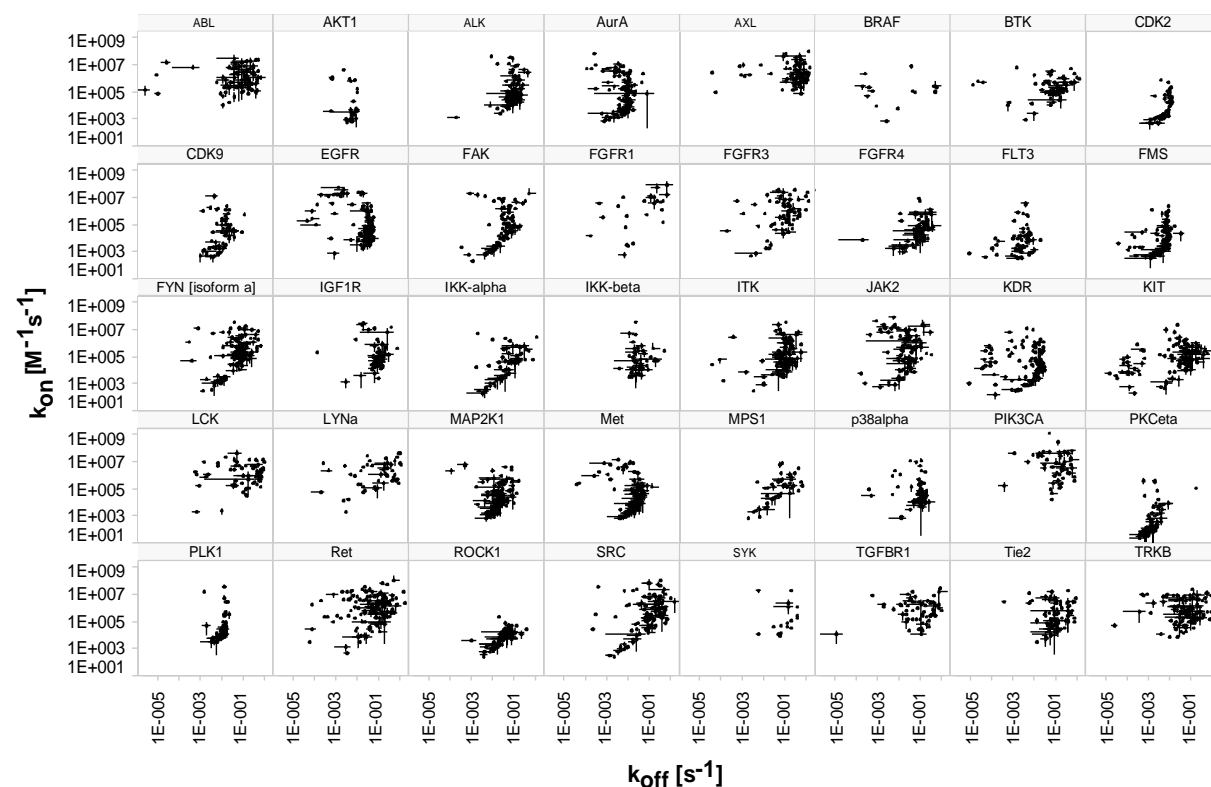


Figure 48: Binding parameters of 270 kinase inhibitors for individual kinases

Determined binding kinetic and affinity parameters for the kinase-inhibitor pairs screened by kPCA in this dissertation are given as mean from two independent experiments in the Supplementary Spreadsheet (appendix page 165ff) and are represented in this figure as k_{on} - k_{off} plots for individual kinases (for more information about experimental setup and data acquisition refer to chapters 4.2.1.3 and 4.3.1.3).

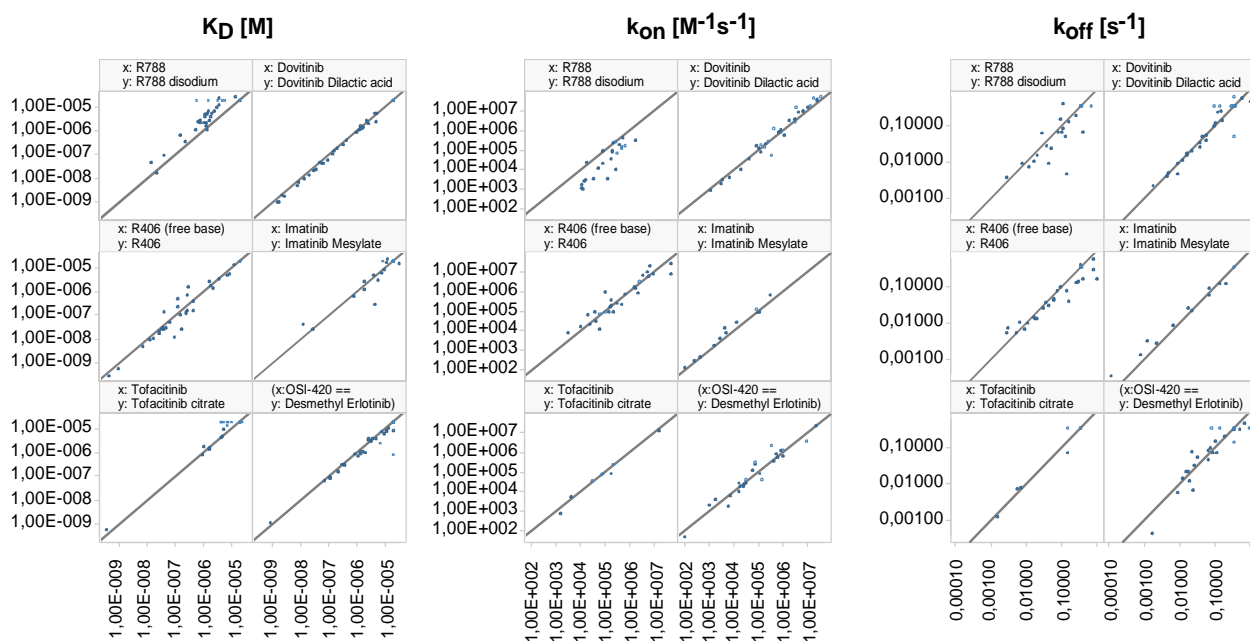


Figure 49: Comparison of binding kinetic and affinity parameters determined for different salt forms of kinase inhibitors

There is a good agreement between salt forms with one exception: slower on-rates and accordingly lower affinities were determined for R788 disodium in comparison to R788. Differences in calculated on-rates and affinities are expected for solubility issues: As all assay technologies, kPCA is susceptible to sparingly soluble compounds.

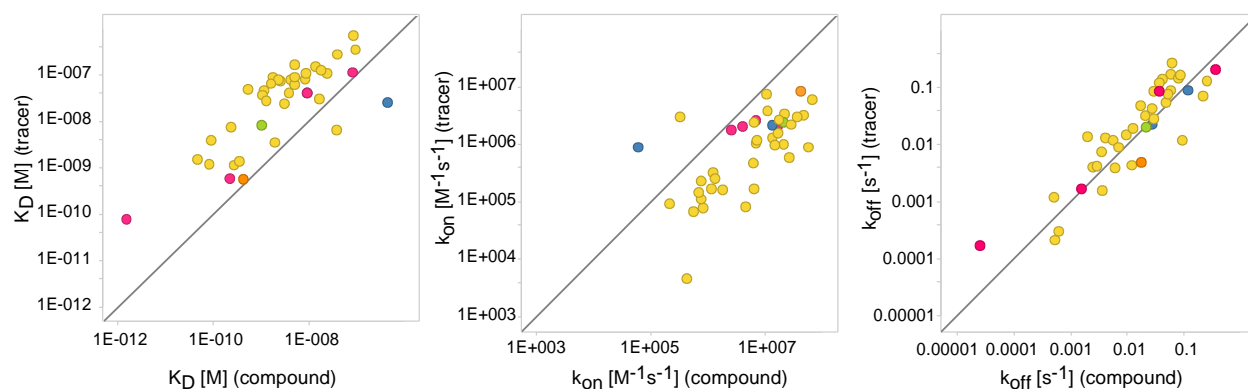


Figure 50: Comparison of binding kinetic and affinity parameters determined for labeled and unlabeled compounds

Kinase Tracers 236 (yellow), 178 (pink), 199 (blue), 222 (green) and 314 (orange) are multikinase inhibitors conjugated via a rather long linker with the fluorophore Alexa Fluor[®]. The represented plots compare the binding parameters of the tracers and the presumed corresponding inhibitors. In general there is a good agreement, but the on-rates and affinities determined for the tracer are lower as compared to those of the corresponding inhibitors. Most probably, the attached fluorescence label decelerated the on-rate of the tracer due to steric hindrance.

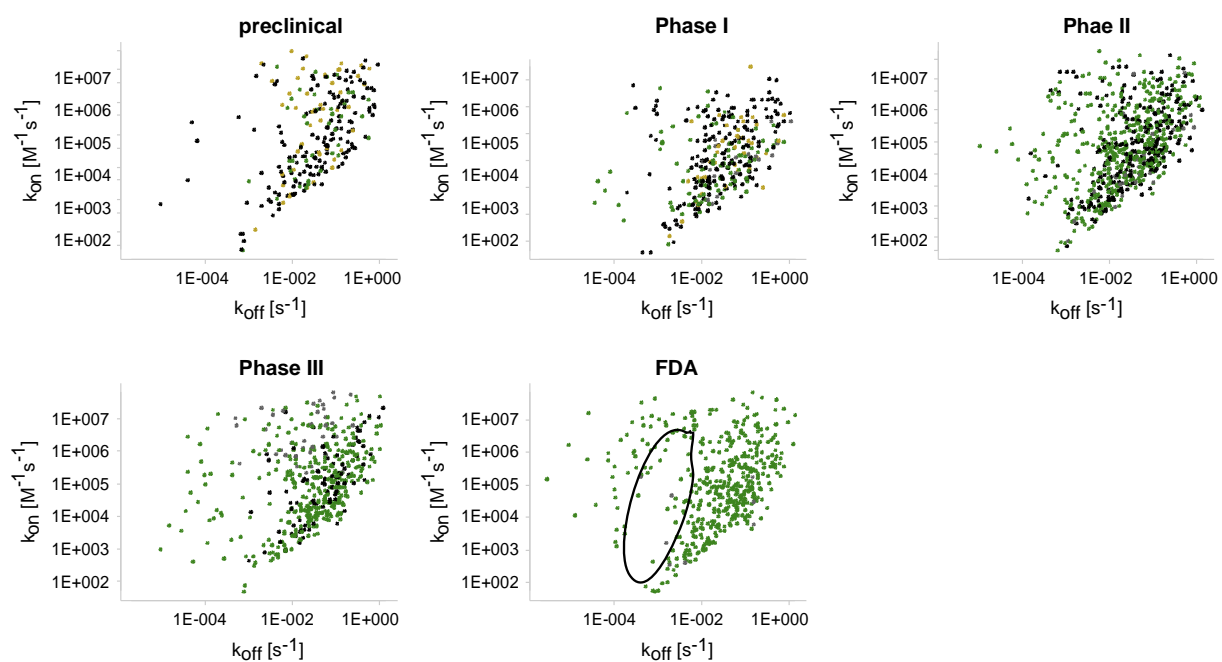


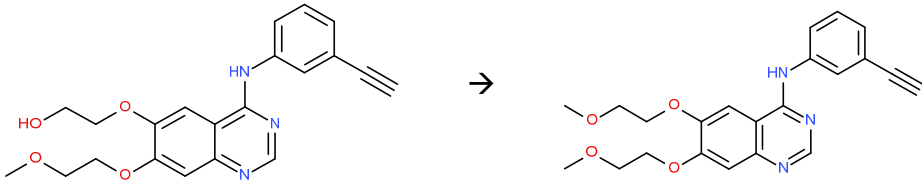
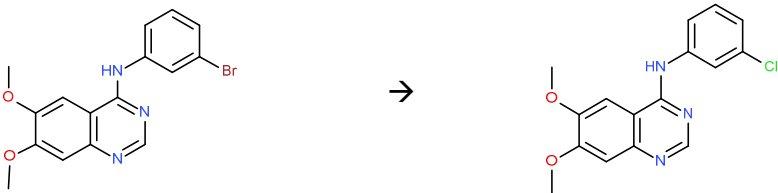

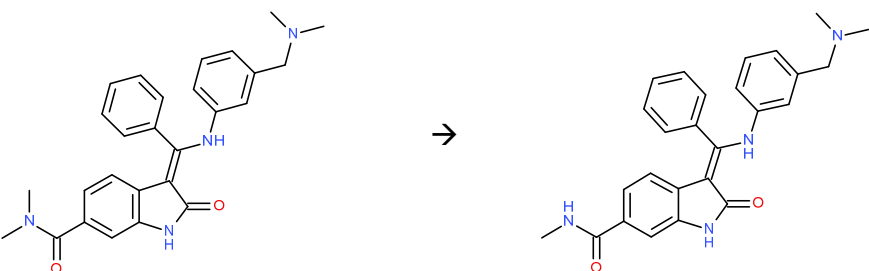
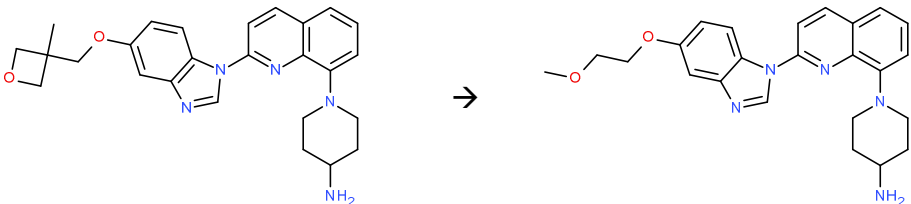
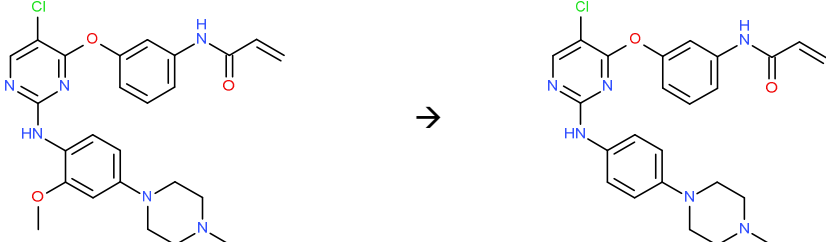
Figure 51: Binding parameters of kinase inhibitors in different clinical phases

The binding parameters of kinase inhibitor in different clinical phases are represented in individual k_{on} - k_{off} plots. The gap between slow and fast dissociating kinase-compound pairs becomes larger when comparing compounds in early and late stages of clinical development (the gap is encircled in the plot for FDA approved drugs). Since among the slow dissociating compounds are especially main targets of FDA approved drugs (refer to Figure 30), this observation strengthens the assumption that a prerequisite for kinetic selectivity is fulfilled: A significantly longer residence time on the primary targets as compared to the off-targets.

G Close derivatives among the inhibitors in the profiling panel

Table 9: Close derivatives among the 270 analyzed compounds screened

Close derivatives with differences in binding properties are printed in bold type and the direction of the change is indicated in brackets.

<p>Desmethyl Erlotinib → Erlotinib</p>	
<p>PD153035 → Tyrphostin AG-1478</p>	
<p>WHI-P154 → PD153035</p>	
<p>BIX 02189 → BIX 02188 ($k_{on} \uparrow$, $K_D \downarrow$)</p>	
<p>Crenolanib → CP 673451 ($k_{on} \uparrow$, $k_{off} \uparrow$)</p>	
<p>WZ4002 → WZ3146 ($k_{on} \uparrow$, $K_D \downarrow$)</p>	

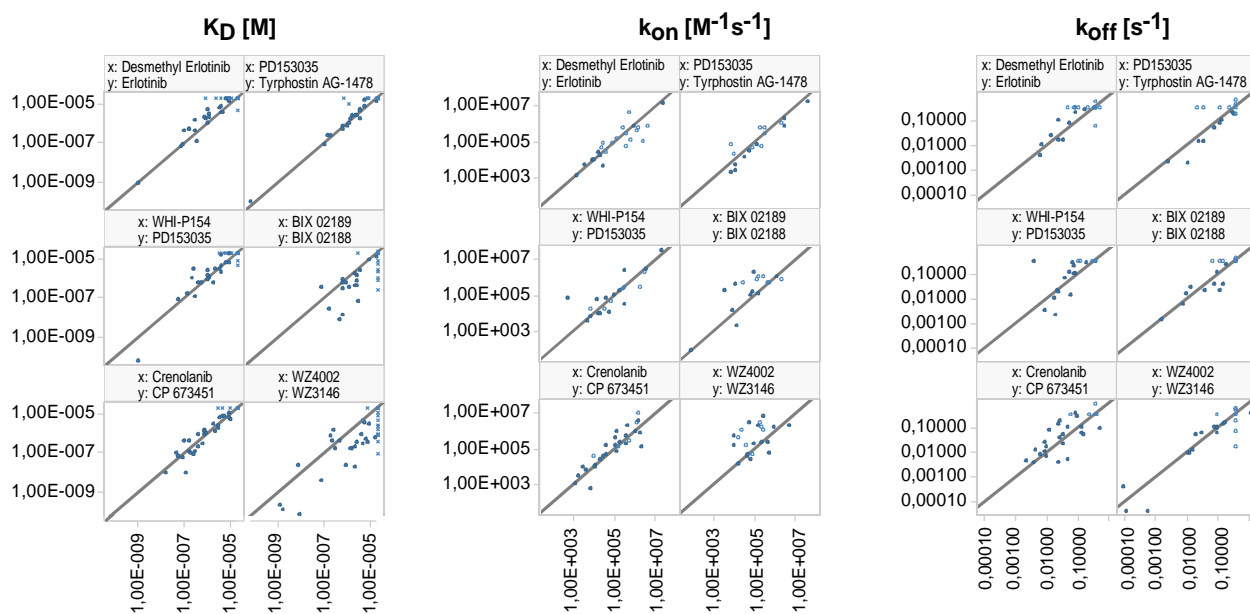


Figure 52: Comparison of binding kinetic and affinity parameters determined for close derivatives among the compounds in the screening panel

Observable trends: BIX 02189 => BIX 02188 ($k_{on} \uparrow$, $K_D \downarrow$); Crenolanib => CP 673451 ($k_{on} \uparrow$, $k_{off} \uparrow$); WZ4002 => WZ3146 ($k_{on} \uparrow$, $K_D \downarrow$); otherwise similar binding parameters

H Effect of specific inhibitor-kinase interactions on binding parameters

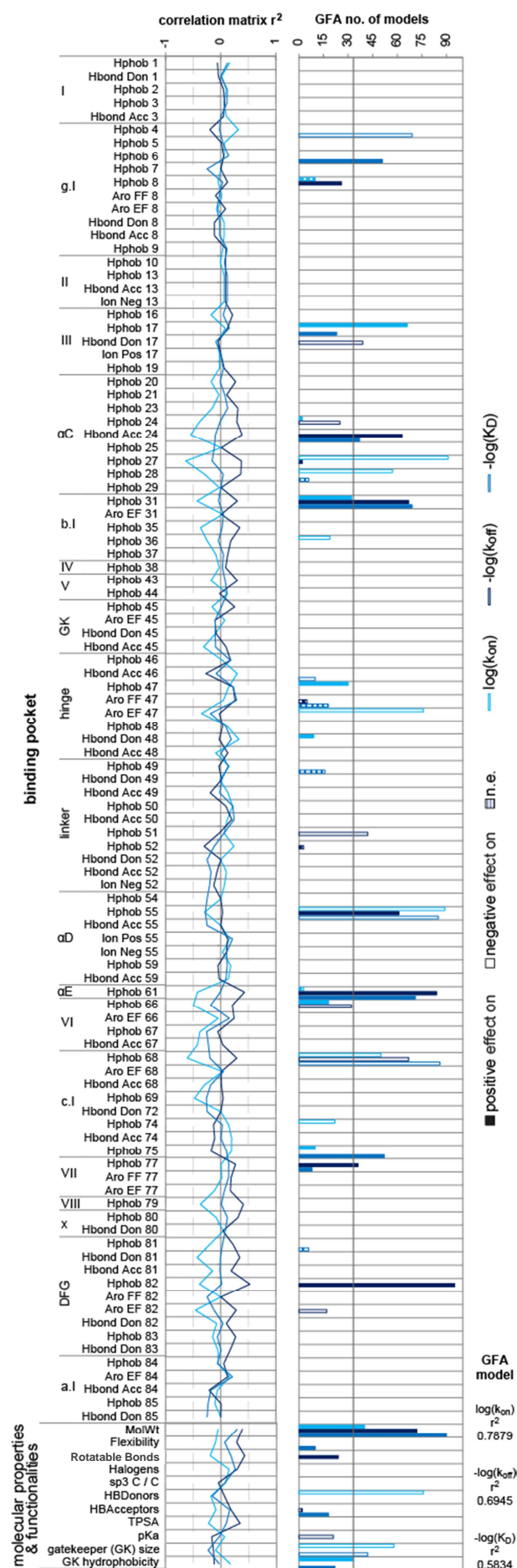


Figure 53: Relationships between binding parameters and molecular properties and/or specific inhibitor-kinase interactions as specified in KLIFS database

Interactions with binding site residues which were identical for all studied kinase-compound interactions were excluded from the analysis.

The chart depicts r^2 from correlation analyses (left) and the number of variable usage for multivariable linear regression models built by genetic function approximation (with molecular properties and specific inhibitor-kinase interactions as descriptors for on-rates, off-rates or affinities, respectively) (right). Both were considered as measure for the significance of the relationship.

The percentage of variance that can be explained by the models was increased compared to the models without molecular properties as descriptors (only KLIFS interaction fingerprints as predictors, see Table 3). The corresponding models reveal significance of the same compound-amino acid interactions. The exceptions are the hinge region interactions that seem to be less important (this figure compared to Figure 35), but instead the size of the gatekeeper might have an impact.

I Model equations for simulations of target occupancy in cells

Binding Kinetics - Permeation model

A Binding Kinetics (BK) - Permeation model was developed for simulation of cellular target occupancy profiles. To describe compound binding to protein targets, a simple 1:1 drug-target binding model with competition between compound and ATP was used (refer to chapter 4.3.8). The total protein target concentration was assumed to be constant. Permeation of the compound through the cellular membrane was added (refer to chapter 4.3.8). The BK-Permeation model is given by the following equations and was simulated in Copasi 4.1.9.:

BK-Permeation model

- 1) $\frac{d([C_1](t))}{dt} = k_{\text{off}} \times [\text{TC}](t) - k_{\text{on}} \times [C_1](t) \times [T](t) - P \times A_{\text{O,cell}} \times ([C_1](t) - [C_2](t)) / V_1$
- 2) $\frac{d([\text{TC}](t))}{dt} = k_{\text{on}} \times [C_1](t) \times [T](t) - k_{\text{off}} \times [\text{TC}](t)$
- 3) $\frac{d([T](t))}{dt} = k_{\text{off}} \times [\text{TC}](t) - k_{\text{on}} \times [C_1](t) \times [T](t) + k_{\text{off,ATP}} \times [\text{T.ATP}](t) - k_{\text{on,ATP}} \times [\text{ATP}](t) \times [T](t)$
- 4) $\frac{d([\text{ATP}](t))}{dt} = k_{\text{off,ATP}} \times [\text{T.ATP}](t) - k_{\text{on,ATP}} \times [\text{ATP}](t) \times [T](t)$
- 5) $\frac{d([\text{T.ATP}](t))}{dt} = k_{\text{on,ATP}} \times [\text{ATP}](t) \times [T](t) - k_{\text{off,ATP}} \times [\text{T.ATP}](t)$
- 6) $\frac{d([A_2](t))}{dt} = P \times A_{\text{O,cell}} \times ([C_1](t) - [C_2](t))$

Target occupancy can be calculated using $\text{TO}(t) = [\text{TC}](t) / [\text{T}_{\text{total}}] \times 100\%$

The total concentration of target protein $[\text{T}_{\text{total}}]$ is equal to the sum of free protein $[T]$ and inhibitor-complexed protein $[\text{TC}]$ and ATP-complexed protein $[\text{T.ATP}]$ concentrations. k_{on} and k_{off} represent the rate constants for association and dissociation of the compound-target complex. $[\text{ATP}]$ and $[\text{T.ATP}]$ are the concentrations of ATP and ATP-complexed protein. $k_{\text{on,ATP}}$ and $k_{\text{off,ATP}}$ represent the rate constants for association and dissociation of the ATP-target complex. $[C_1]$ ($= A_1/V_1$) and $[C_2]$ ($= A_2/V_2$) are the compound concentrations ($=$ amount/volume) within cells and outside cells, respectively. P is the permeability coefficient of compound through membrane. $A_{\text{O,cell}}$ is the total surface area of the cells.

The following assumptions and initial values were used for the simulations:

- I) For simulation of the pre-incubation step: $A_{\text{O,cell}} = 0.0154 \text{ dm}^2$ and $V_1 = 4 \times 10^{-7} \text{ L}$ (cumulated sphere surface area & volume of 2×10^5 cells); $V_2 = 0.001 \text{ L}$ (2×10^5 cells / mL were applied in the nanoBRET pre-incubation step); $[\text{TC}](t=0) = 0$; $[\text{T.ATP}](t=0) = [\text{ATP}] / ([\text{ATP}] + K_{\text{D,ATP}}) \times [\text{T}_{\text{total}}]$ (equilibrated ATP-target complex); $[T](t=0) = [\text{T}_{\text{total}}] - [\text{T.ATP}]$; $A_1(t=0) = 0$; $A_2(t=0)$ is the compound concentration applied in the nanoBRET pre-incubation step.
- II) For simulation of target occupancy decline after washout: $[T]$, $[\text{TC}]$, $[\text{T.ATP}]$, $[C_1]$ and $[\text{ATP}]$ at $t=0$ were set to the output parameters of pre-incubation simulations; $A_2(t=0) = 0$ (washout); $A_{\text{O,cell}} = 0.0014 \text{ dm}^2$ and $V_1 = 3.6 \times 10^{-8} \text{ L}$ (cumulated sphere surface area and volume of 18000 cells (90 μL of 2×10^5 cells / mL were applied in the nanoBRET washout experiment)); $V_2 = 0.0002 \text{ L}$ (applied assay volume).

III) In both parts of the simulation, the total concentration of the expressed target protein $[T_{\text{total}}]$ was fixed to 100 nM. ATP concentration was fixed to 0.0001 M (lower than typical cellular ATP concentrations as dead cells lose ATP [127] to account for cytotoxic effects of compounds) or 0.001 M. ATP k_{on} and k_{off} were assumed to be similar for the studied kinases and were fixed to $9.2 \times 10^5 \text{ M}^{-1}\text{s}^{-1}$ and 1.9 s^{-1} [145]. Permeability coefficients (P) were set to 10^{-6} cm/s [146] initially, but were reduced for imatinib (10^{-7}) and ponatinib (10^{-8}) to simulate additional effects reducing compound intake and release. A cell size of $2000 \mu\text{m}^3$ in volume (typical size according to Milo *et al.* BioNumbers database [147]) was assumed for calculation of the cumulated surface area and volume of the cells.

K_D- Permeation model

To check if binding kinetics lead to target occupancy profiles different from concentration-K_D effect profiles, the BK-Permeation model simulations were compared to K_D-Permeation simulations.

K_D- Permeation model

The compound-concentration-time profile was simulated by:

$$\frac{d([C_1](t))}{dt} = -P \times A_{O,\text{cell}} \times ([C_1](t) - [C_2](t))/V_1 \text{ and } \frac{d([C_2](t))}{dt} = P \times A_{O,\text{cell}} \times ([C_1](t) - [C_2](t))/V_2$$

and target occupancy traces were calculated using

$$\text{TO}(t) = \frac{[C_1](t)}{K_D \left(1 + \frac{[\text{ATP}](t)}{K_{D,\text{ATP}}}\right) + [C_1](t)} \times 100\%$$

K_D represents the equilibrium dissociation constant of the compound-target complex. $[\text{ATP}]$ and is the concentration of ATP. $K_{D,\text{ATP}}$ represents the equilibrium dissociation constant of the ATP-target complex. $[C_1]$ ($= A_1/V_1$) and $[C_2]$ ($= A_2/V_2$) are the compound concentrations (= amount/volume) within cells and outside cells, respectively. P is the permeability coefficient of compound through membrane. $A_{O,\text{cell}}$ is the total surface area of the cells.

Otherwise, the simulations (of pre-incubation step and target occupancy decline after washout) were conducted by using the same assumptions and initial values as described above (for the BK-Permeation model).

It should be noted, that the BK-Permeation model indeed led to better simulations of cellular target-occupancy (closer-to-realty → refer to Figure 41, and Figure 54 in appendix K).

J Model equations for simulations of target occupancy in the *in vivo* situation

Pharmacokinetics-binding kinetics (PK-BK) model

A two-compartment model was used to simulate the compound-concentration-time profile after oral administration of a kinase inhibitor (refer to chapter 4.3.8). To describe compound binding to protein targets, a simple 1:1 drug-target binding model was added (refer to chapter 4.3.8), assuming the free drug hypotheses and constant total protein target concentrations. This PK-BK model for compound binding to n proteins is given by the following equations and was simulated in Copasi 4.1.9.

PK-BK model

- 1)
$$\frac{d([C_1](t))}{dt} = \frac{k_a \times A_a(t)}{V_1} - CL \times [C_1](t) - CLD \times ([C_1](t) - [C_2](t)) + \sum_{i=1}^n (k_{off_i} \times [TC]_i(t) - k_{on_i} \times (fu \times [C_1](t)) \times [T]_i(t))$$
- 2)
$$\frac{d([TC]_i(t))}{dt} = k_{on_i} \times (fu \times [C_1](t)) \times [T]_i(t) - k_{off_i} \times [TC]_i(t) \quad \text{for } i = 1, 2, \dots, n$$
- 3)
$$\frac{d([C_2](t))}{dt} = CLD \times ([C_1](t) - [C_2](t))$$
- 4)
$$\frac{d(A_a(t))}{dt} = -k_a \times A_a(t)$$

Target occupancies can be calculated using $TO_i(t) = [TC]_i(t) / [T_{total}]_i \times 100\%$ for $i = 1, 2, \dots, n$

n is the number of target kinases. The total target concentrations $[T_{total}]$ are equal to the sum of the respective free protein $[T]$ and inhibitor-complexed protein $[TC]$ concentrations. k_{on} and k_{off} represent the rate constants for association and dissociation of the compound-target complex. $[C_1]$ ($= A_1/V_1$) and $[C_2]$ ($= A_2/V_2$) are the total compound concentrations ($=$ amount/distribution volume) in the central and peripheral compartment, respectively. A_a is the amount of drug in the gastrointestinal tract (effective dose $=$ dose \times bioavailability F). fu is the unbound fraction of the compound in plasma. k_a , CL , CLD represent the rate constants for absorption, elimination and distribution.

The following assumptions and initial values were used for the simulations:

The total target concentrations $[T_{total}]$ were fixed to 10 nM (within the lower range of a typical concentration of signaling protein according to Milo *et al.* BioNumbers database [147] and as reported in literature and assumed in previous analyses [39]); $[TC](t=0) = 0$; $A_1(t=0) = A_2(t=0) = 0$; The model parameters k_a , V_1 , V_2 , CL and CLD were estimated on the basis of the concentration-time profiles (using Phoenix version 6.4, Pharsight), F was fixed to 1. Administered dose, dosing interval, fu and concentration-time profiles are given in Clinical Pharmacology and Biopharmaceutics Review documents for ibrutinib (NDA: 205552) and dasatinib (NDA: 21-986; 22-072). For simulation of covalent binding of ibrutinib, the off-rate was set to 10^{-7} s^{-1} (residence time of 116 days).

Pharmacokinetics and the concentration-affinity effect – PK- K_D model

To check if binding kinetics lead to target occupancy profiles differing from concentration- K_D effect profiles, the PK-BK model simulations were compared to PK- K_D simulations. The compound-concentration-time profiles were simulated with the two-compartment model as described above, but without consideration of the drug-target binding model terms and the target occupancy traces were calculated using

$$TO(t) = \frac{fu \times [C_1](t)}{K_D + fu \times [C_1](t)} \times 100\%.$$

K Effect of binding kinetics on target occupancy and the pharmacological effect

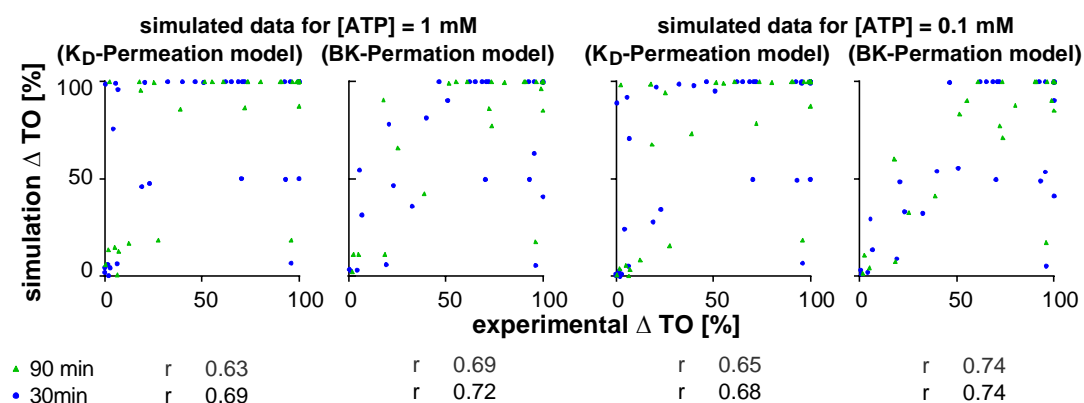


Figure 54: Comparison of percent changes in target occupancy Δ TO (30 and 90 min upon compound washout) derived from simulated and experimental traces (as shown in Figure 41)

As shown in Figure 41, the cellular target occupancy decline can be better simulated under consideration of binding kinetics (BK-Permeation model) as by using the concentration-affinity effect *per se* (K_D-Permeation model). For quantitative comparison, the percent target occupancy changes were calculated as described in Equation 3 in chapter 4.2.3. Correlation coefficients are indicated in the figure ($p < 0.001$, respectively). Experimentally obtained changes in target occupancy correlate best with the Δ TO derived from the BK-permeation model assuming the lower ATP (0.1 mM) concentration to account for cytotoxic effects of the compound.

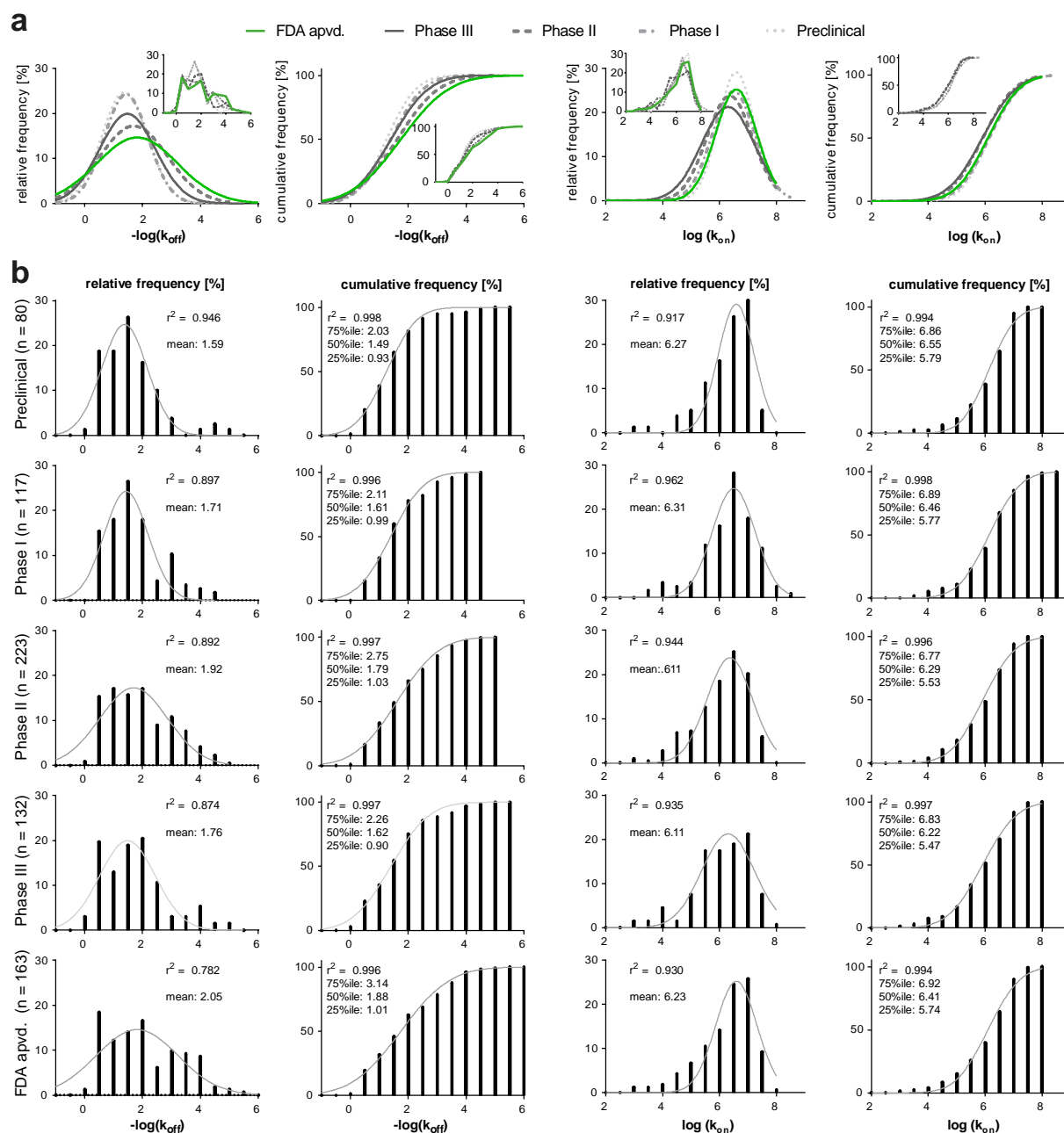


Figure 55: Distribution of kinase-compound binding kinetic rate constants depending on the clinical phase of the kinase inhibitor

Considered are kinase-compound pairs with affinities $<10^{-7}$ M (to account for potential clinical relevance). The frequency distribution of on-rates is similar for kinase inhibitors in different clinical phases. On the other hand, the percentage of slow off-rates is increasing from preclinical drug candidates to FDA approved drugs.

a) Gaussian curve fits to the relative and cumulative frequency distributions of target-compound binding kinetic parameters for kinase inhibitors in different phases of clinical development. The corresponding relative or cumulative frequency distribution histograms are shown as inset (for better comparability, frequency values of adjacent bins are connected by lines and bars are omitted).

b) Detailed view on the same data as shown in a: Relative and cumulative frequency distributions of target-compound binding kinetic parameters for kinase inhibitors in different phases of clinical development shown as histograms (bars for bins) with the corresponding Gaussian curve fit (and corresponding r^2). Descriptive statistics values of the raw data are indicated in the figure.

Table 10: Area under the curve (AUC) and maximal target occupancy (TO_{max}) for the simulated *in vivo* target occupancy profiles (TO) (as shown in Figure 44).

Drug	Administration schedule	Kinase	AUC of TO trace simulated with PK-KD model	AUC of TO trace simulated with PK-BK model	TO_{max} for simulation with PK-KD model	TO_{max} for simulation with PK-BK model
Dasatinib	1 mg/kg / 12h (day 3)	ABL	11.99	11.99	0.9997	0.9997
		FYN	11.55	11.56	0.9880	0.9878
		KIT	9.58	9.63	0.9237	0.9222
		LCK	10.76	10.78	0.9650	0.9641
		SRC	11.90	11.91	0.9970	0.9974
		BTK	10.39	10.41	0.9530	0.9517
Dasatinib	1 mg/kg / 48h (day 7-8)	ABL	47.19	47.52	0.9996	0.9996
		FYN	33.65	36.72	0.9862	0.9848
		KIT	17.65	19.56	0.9126	0.9042
		LCK	24.45	27.05	0.9590	0.9554
		SRC	43.04	44.75	0.9970	0.9968
		BTK	21.82	24.11	0.9450	0.9402
'Dasatinib-like' but clearance \uparrow (4x intercompartmental CL; 10x plasma CL)	0.2 mg/kg / 24h (day 3)	ABL	10.28	20.28	0.9920	0.9830
		FYN	3.44	4.98	0.7742	0.6206
		KIT	1.00	1.14	0.3343	0.1705
		LCK	1.82	2.25	0.5320	0.3524
		SRC	6.33	11.24	0.9430	0.8881
		BTK	1.47	1.75	0.4550	0.2853
Ibrutinib (assuming kPCA k_{off})	8 mg/kg / 24h (day 4)	BTK	15.58	18.22	0.9953	0.9939
		LCK	5.62	5.83	0.9343	0.9322
		EGFR	12.74	14.22	0.9906	0.9894
		ITK	3.34	5.54	0.8410	0.4785
Ibrutinib (assuming covalent binding)	8 mg/kg / 24h (day 4)	BTK	-	24.00	-	1.000
		LCK	-	5.81	-	0.9326
		EGFR	-	24.00	-	1.000
		ITK	-	23.66	-	0.9877

Supplementary Spreadsheet:

Profiling results – Kinase inhibitors' target binding kinetics and affinities

The interactions of 270 kinase inhibitors with 40 clinically relevant kinases were characterized. The library contained 6 compounds in different salt forms or in duplicate (R788/R788 disodium; Imatinib/Imatinib Mesylate; R406 (free base)/R406; Dovitinib/Dovitinib Dilactic acid; Tofacitinib/Tofacitinib citrate; OSI-420/Desmethyl Erlotinib). They served as internal standards demonstrating excellent reproducibility. Their binding parameters were averaged in this table.

* calculated according to Cheng-Prusoff

** $K_{D\text{ kin corrected}} = K_{D\text{ kin}}$, except for the following cases: (I) $K_{D\text{ kin corrected}} = K_{D\text{ eq}}$, if $CV(K_{D\text{ eq}}) < 70\%$ and 1) $CV(K_{D\text{ kin}}) > 70\%$ or 2) $K_{D\text{ kin}}$ is n.e. or 3) reached assay limit or 4) there is at least a 5fold discrepancy between $K_{D\text{ kin}}$ and $K_{D\text{ eq}}$; (II) else if $CV(K_{D\text{ kin}}) \& CV(K_{D\text{ eq}}) > 70\%$, then $K_{D\text{ kin corrected}} = \text{mean}(K_{D\text{ kin}}, K_{D\text{ eq}})$

1 ePCA: $S_{\text{inf}} - S_0 < 80\%$

2 kPCA: Discrepancy between best-fit curves and data points

3 k_{on} was determined by Motulsky k_{off} / K_i

4 k_{off} was determined by $K_i \times \text{Motulsky } k_{\text{on}}$

n.e. not evaluable

≈ if $CV > 100\%$ or $n=1$ (one run n.e.)

empty no binding observed; Kinase-Inhibitors pairs are not shown if not binding was observed in ePCA and kPCA

kinase	Compound	IC ₅₀ [M] ePCA	K _{D eq} [M] ePCA *	K _{D kin} [M] kPCA	K _D [M] PCA **	k _{on} [M ⁻¹ s ⁻¹] kPCA	k _{off} [s ⁻¹] kPCA	comment
ABL	AEE788 (NVP-AEE788)	1,8E-06	1,4E-08	1,0E-08	1,0E-08	1,7E+07	1,6E-01	
ABL	Afatinib (BIBW2992)	≥ 2,0E-05		1,0E-06	1,0E-06	3,8E+05	3,8E-01	2
ABL	AG-1024	≥ 2,0E-05		5,7E-07	5,7E-07	4,3E+05	2,2E-01	
ABL	AG-1478 (Typhostin AG-1478)	1,8E-05	1,4E-07	2,6E-07	2,6E-07	7,8E+05	1,9E-01	
ABL	AMG 900	≥ 2,0E-05		9,9E-07	9,9E-07	5,2E+04	4,1E-02	
ABL	AMG458	≥ 2,0E-05		2,1E-07	2,1E-07	8,3E+04	1,5E-02	2
ABL	Apatinib (YN968D1)	≥ 2,0E-05		≈ 5,6E-06	≈ 5,6E-06	8,6E+04	3,9E-01	
ABL	AS-252424	≥ 2,0E-05		3,0E-06	3,0E-06	≥ 1,2E+05	≥ 3,5E-01	
ABL	AT9283	≈ 2,4E-06	≈ 1,9E-08	1,3E-08	1,3E-08	≈ 2,3E+07	≈ 3,7E-01	
ABL	Aurora A Inhibitor I	1,7E-05	1,3E-07	1,8E-06	1,3E-07	≈ 1,7E+05	≈ 1,7E-01	2
ABL	Axitinib	1,7E-06	1,4E-08	9,6E-09	9,6E-09	6,2E+06	6,0E-02	2
ABL	AZ 960	≥ 2,0E-05		8,3E-07	8,3E-07	≥ 4,2E+05	≥ 3,5E-01	
ABL	AZ628	≥ 2,0E-05		1,3E-07	1,3E-07	2,0E+05	2,3E-02	
ABL	AZD4547	≥ 2,0E-05		1,9E-07	1,9E-07	≈ 8,5E+05	1,3E-01	2
ABL	AZD5438	≥ 2,0E-05		1,6E-06	1,6E-06	≥ 2,2E+05	≥ 3,5E-01	
ABL	AZD7762	1,1E-06	8,9E-09	1,3E-08	1,3E-08	≈ 1,8E+07	≈ 2,3E-01	
ABL	AZD8931	≥ 2,0E-05		5,1E-07	5,1E-07	≈ 3,1E+05	≈ 1,7E-01	
ABL	Barasertib (AZD1152-HQPA)	≥ 2,0E-05		4,7E-07	4,7E-07	≈ 2,5E+05	≈ 3,7E-02	
ABL	Baricitinib (LY3009104 - incb28050)	≥ 2,0E-05		3,3E-06	3,3E-06	≥ 1,1E+05	≥ 3,5E-01	
ABL	BGJ398 (NVP-BGJ398)	≥ 2,0E-05		9,5E-07	9,5E-07	≈ 3,6E+04	≈ 3,9E-02	
ABL	BI 2536	≥ 2,0E-05		2,4E-06	2,4E-06	≥ 1,5E+05	≥ 3,5E-01	
ABL	BI6727 (Volasertib)	≥ 2,0E-05		2,6E-06	2,6E-06	≥ 1,3E+05	≥ 3,5E-01	
ABL	BIBF1120 (Vargatef)	1,6E-06	1,3E-08	8,7E-09	8,7E-09	≈ 8,4E+06	6,4E-02	
ABL	BIRB 796 (Doramapimod)	≥ 2,0E-05		3,5E-06	3,5E-06	≥ 1,0E+05	≥ 3,5E-01	
ABL	BIX 02188	≥ 2,0E-05		1,6E-06	1,6E-06	≈ 1,5E+05	≈ 2,5E-01	2
ABL	BIX 02189	≥ 2,0E-05		2,5E-06	2,5E-06	≈ 7,2E+04	≈ 1,8E-01	
ABL	BMS 777607	1,7E-05	1,3E-07	1,0E-07	1,0E-07	2,2E+05	2,2E-02	
ABL	BMS 794833	1,8E-05	1,4E-07	2,5E-07	2,5E-07	4,7E+04	1,1E-02	2
ABL	Bosutinib (SKI-606)	≈ 8,8E-09	≈ 7,0E-11	n.e.	≈ 7,0E-11	6,8E+06	≤ 4,7E-04	4
ABL	Brivanib (BMS-540215)	≥ 2,0E-05		2,1E-07	2,1E-07	8,8E+05	1,7E-01	2
ABL	Brivanib alaninate (BMS-582664) - prodrug	1,7E-05	1,4E-07	1,5E-07	1,5E-07	≈ 1,9E+06	≈ 3,4E-01	
ABL	BX-795	≥ 2,0E-05		5,1E-07	5,1E-07	≥ 6,9E+05	≥ 3,5E-01	
ABL	BX-912	1,7E-05	1,3E-07	1,2E-07	1,2E-07	1,4E+06	1,6E-01	
ABL	BYL719	≥ 2,0E-05		1,4E-06	1,4E-06	≥ 2,4E+05	≥ 3,5E-01	
ABL	CCT137690	≥ 2,0E-05		4,3E-07	4,3E-07	≥ 8,1E+05	≥ 3,5E-01	
ABL	Cediranib (AZD2171)	≥ 2,0E-05		3,1E-08	3,1E-08	≈ 5,3E+06	≈ 2,0E-01	
ABL	CEP33779	≥ 2,0E-05		4,7E-07	4,7E-07	≥ 7,5E+05	≥ 3,5E-01	
ABL	CH5424802	≥ 2,0E-05		4,4E-07	4,4E-07	1,2E+06	5,0E-01	
ABL	CI-1033 (Canertinib)	≥ 2,0E-05		5,1E-08	5,1E-08	≈ 3,5E+06	1,6E-01	
ABL	CP 673451	9,1E-06	7,2E-08	2,3E-07	2,3E-07	≈ 2,1E+05	≈ 5,4E-02	
ABL	Crenolanib (CP-868596)	≥ 2,0E-05		4,0E-07	4,0E-07	3,5E+05	1,4E-01	
ABL	Crizotinib (PF-02341066)	2,4E-06	1,9E-08	≈ 1,4E-08	1,9E-08	≥ 2,4E+07	≥ 3,5E-01	
ABL	CX-4945 (Silmatasertib)	≥ 2,0E-05		2,9E-06	2,9E-06	≥ 1,2E+05	≥ 3,5E-01	
ABL	CYC116	≥ 2,0E-05		1,3E-07	1,3E-07	≥ 2,7E+06	≥ 3,5E-01	
ABL	Cyt387	≥ 2,0E-05		5,3E-07	5,3E-07	3,6E+05	1,9E-01	
ABL	Dabrafenib (GSK2118436)	≥ 2,0E-05		6,5E-08	6,5E-08	1,9E+06	1,2E-01	
ABL	Dacomitinib (PF299804 - PF-00299804)	≥ 2,0E-05		5,4E-07	5,4E-07	≥ 6,5E+05	≥ 3,5E-01	
ABL	Danuseritib (PHA-739358)	1,6E-06	1,2E-08	2,1E-08	2,1E-08	7,2E+05	1,4E-02	
ABL	Dasatinib (BMS-354825)	≤ 1,9E-10	≤ 1,5E-12	n.e.	≤ 1,5E-12	1,6E+07	≤ 2,5E-05	4
ABL	DCC-2036 (Rebastinib)	1,7E-08	1,3E-10	n.e.	1,3E-10	7,7E+04	≤ 1,0E-05	4
ABL	Desmethyl Erlotinib (CP-473420)	8,1E-06	6,4E-08	6,7E-08	6,7E-08	6,9E+05	4,4E-02	
ABL	Dovitinib (TKI-258)	6,8E-06	5,4E-08	2,9E-08	2,9E-08	6,6E+06	2,1E-01	
ABL	E7080 (Lenvatinib)	≥ 2,0E-05		1,6E-07	1,6E-07	≈ 3,5E+06	≈ 5,0E-01	
ABL	ENMD-2076	1,1E-05	8,5E-08	8,0E-08	8,0E-08	≥ 4,4E+06	≥ 3,5E-01	
ABL	Erlotinib HCl	1,8E-05	1,4E-07	7,7E-08	7,7E-08	≈ 7,9E+05	≈ 8,6E-02	
ABL	Foretinib (GSK1363089 - XL880)	3,9E-07	3,1E-09	1,1E-08	1,1E-08	1,1E+06	1,1E-02	

kinase	Compound	IC ₅₀ [M] ePCA	K _D eq [M] ePCA *	K _D kin [M] kPCA	K _D [M] PCA **	k _{on} [M ⁻¹ s ⁻¹] kPCA	k _{off} [s ⁻¹] kPCA	comment
ABL	GDC-0980 (RG7422)	≥ 2,0E-05		8,1E-07	8,1E-07	≈ 1,1E+05	≈ 1,0E-01	
ABL	Gefitinib (Iressa)	≈ 1,1E-05	≈ 9,0E-08	5,3E-07	5,3E-07	≈ 4,5E+05	≈ 2,7E-01	
ABL	Golitinib (E7050)	1,8E-05	1,4E-07	6,8E-08	6,8E-08	2,0E+05	1,3E-02	2
ABL	GSK1070916	≥ 2,0E-05		2,9E-07	2,9E-07	3,1E+05	8,9E-02	
ABL	Hesperadin	2,6E-06	2,1E-08	1,6E-08	1,6E-08	≈ 7,6E+06	≈ 1,2E-01	
ABL	Imatinib (Gleevec)	1,9E-06	1,5E-08	5,1E-08	2,7E-08	4,9E+05	2,2E-02	
ABL	INK 128 (MLN0128)	1,6E-05	1,3E-07	4,4E-07	4,4E-07	≈ 9,9E+05	≈ 4,7E-01	
ABL	JNJ-38877605	≥ 2,0E-05		2,9E-06	2,9E-06	≥ 1,2E+05	≥ 3,5E-01	
ABL	JNJ-7706621	1,9E-05	1,5E-07	1,3E-07	1,3E-07	≥ 2,8E+06	≥ 3,5E-01	
ABL	Ki8751	≥ 2,0E-05		5,3E-08	5,3E-08	5,1E+05	2,6E-02	2
ABL	KRN 633	≥ 2,0E-05		1,7E-06	1,7E-06	1,5E+05	2,5E-01	
ABL	KW 2449	3,8E-06	3,0E-08	1,9E-07	3,0E-08	1,8E+06	3,4E-01	
ABL	LDN193189	3,4E-06	2,7E-08	7,8E-08	7,8E-08	1,4E+06	1,1E-01	1
ABL	Linsitinib (OSI-906)	≥ 2,0E-05		3,4E-06	3,4E-06	≥ 1,0E+05	≥ 3,5E-01	
ABL	LY2784544	≥ 2,0E-05		1,4E-07	1,4E-07	7,7E+05	1,1E-01	
ABL	Masitinib (AB1010)	2,7E-06	2,2E-08	3,9E-08	3,9E-08	≈ 1,7E+06	5,7E-02	
ABL	MGCD-265	≈ 3,7E-07	≈ 2,9E-09	1,1E-08	1,1E-08	5,0E+05	5,7E-03	12
ABL	Milciclib (PHA-848125)	1,7E-05	1,3E-07	4,7E-08	4,7E-08	≈ 7,6E+06	3,1E-01	
ABL	MK-2206 2HCl	≥ 2,0E-05		2,7E-06	2,7E-06	≥ 1,3E+05	≥ 3,5E-01	
ABL	MK-2461	≥ 2,0E-05		5,6E-07	5,6E-07	≥ 6,3E+05	≥ 3,5E-01	
ABL	MK-5108 (VX-689)	2,1E-07	1,6E-09	1,6E-09	1,6E-09	≈ 2,6E+07	≈ 3,9E-02	
ABL	MLN8054	1,5E-05	1,2E-07	1,1E-07	1,1E-07	≥ 3,2E+06	≥ 3,5E-01	
ABL	MLN8237 (Alisertib)	1,6E-05	1,2E-07	9,9E-08	9,9E-08	≥ 3,5E+06	≥ 3,5E-01	
ABL	Motesanib Diphosphate (AMG-706)	≥ 2,0E-05		1,5E-06	1,5E-06	≈ 5,9E+05	≈ 4,5E-01	
ABL	Neratinib (HKI-272)	≥ 2,0E-05		2,3E-06	2,3E-06	≥ 1,5E+05	≥ 3,5E-01	
ABL	Nilotinib (AMN-107)	≤ 2,3E-09	≤ 1,8E-11	n.e.	≤ 1,8E-11	1,5E+05	≤ 2,7E-06	24
ABL	NVP-BGT226	≥ 2,0E-05		2,2E-06	2,2E-06	≥ 1,6E+05	≥ 3,5E-01	
ABL	NVP-BHG712	≥ 2,0E-05		1,1E-06	1,1E-06	1,1E+04	1,1E-02	
ABL	NVP-BSK805	1,4E-05	1,1E-07	1,7E-07	1,7E-07	≥ 2,1E+06	≥ 3,5E-01	
ABL	NVP-TAE226	≥ 2,0E-05		1,4E-06	1,4E-06	≥ 2,4E+05	≥ 3,5E-01	
ABL	OSI-930	≥ 2,0E-05		1,5E-06	1,5E-06	≥ 2,3E+05	≥ 3,5E-01	
ABL	Pazopanib HCl	≥ 2,0E-05		1,1E-07	1,1E-07	≥ 3,3E+06	≥ 3,5E-01	
ABL	PCI-32765 (Ibrutinib)	5,4E-06	4,3E-08	1,1E-07	1,1E-07	8,1E+04	8,9E-03	2
ABL	PD153035 HCl	1,8E-05	1,4E-07	1,3E-07	1,3E-07	≈ 2,7E+06	3,1E-01	
ABL	Pelitinib (EKB-569)	8,7E-06	6,9E-08	1,5E-07	1,5E-07	4,4E+05	6,8E-02	
ABL	PF-00562271	≥ 2,0E-05		1,2E-06	1,2E-06	≥ 3,0E+05	≥ 3,5E-01	
ABL	PF-03814735	5,6E-06	4,4E-08	5,7E-08	5,7E-08	≈ 6,5E+06	≈ 2,8E-01	
ABL	PHA-665752	≥ 2,0E-05		2,7E-07	2,7E-07	≥ 1,3E+06	≥ 3,5E-01	
ABL	PHA-680632	3,2E-06	2,5E-08	2,1E-08	2,1E-08	2,5E+06	5,1E-02	
ABL	PIK-75	≥ 2,0E-05		8,2E-07	8,2E-07	≈ 5,0E+05	≈ 4,5E-01	
ABL	PLX-4720	≥ 2,0E-05		3,6E-07	3,6E-07	≈ 4,9E+05	≈ 1,6E-01	
ABL	Ponatinib (AP24534)	≤ 6,5E-10	≤ 5,1E-12	n.e.	≤ 5,1E-12	1,8E+06	≤ 9,0E-06	4
ABL	PP-121	5,5E-07	4,4E-09	2,2E-08	2,2E-08	2,0E+06	4,0E-02	2
ABL	PP242	1,9E-05	1,5E-07	1,9E-07	1,9E-07	2,4E+05	4,7E-02	
ABL	Quercetin (Sophoretin)	≥ 2,0E-05		1,4E-06	1,4E-06	≥ 2,5E+05	≥ 3,5E-01	
ABL	R406	≥ 2,0E-05		3,6E-06	3,6E-06	≥ 9,7E+04	≥ 3,5E-01	
ABL	Saracatinib (AZD0530)	5,9E-07	4,7E-09	7,3E-09	7,3E-09	5,0E+06	3,7E-02	
ABL	SB 203580	≥ 2,0E-05		2,1E-06	2,1E-06	≥ 1,7E+05	≥ 3,5E-01	
ABL	SB590885	≥ 2,0E-05		7,5E-07	7,5E-07	2,2E+05	1,6E-01	
ABL	Semaxanib (SU5416)	≥ 2,0E-05		3,6E-06	3,6E-06	≈ 1,3E+05	≈ 4,5E-01	
ABL	SNS-314	≥ 2,0E-05		1,9E-06	1,9E-06	≥ 1,9E+05	≥ 3,5E-01	
ABL	Sotrastaurin (AEB071)	≥ 2,0E-05		1,6E-06	1,6E-06	≥ 2,2E+05	≥ 3,5E-01	
ABL	SP600125	≥ 2,0E-05		1,6E-06	1,6E-06	≈ 1,6E+04	≈ 2,3E-02	
ABL	Staurosporine	2,6E-06	2,0E-08	3,9E-08	3,9E-08	2,9E+06	1,0E-01	
ABL	SU11274	≥ 2,0E-05		4,8E-07	4,8E-07	≥ 7,2E+05	≥ 3,5E-01	
ABL	Sunitinib Malate (Sutent)	1,6E-05	1,3E-07	8,5E-08	8,5E-08	≥ 4,1E+06	≥ 3,5E-01	
ABL	TAE684 (NVP-TAE684)	≥ 2,0E-05		1,1E-07	1,1E-07	≈ 1,1E+06	≈ 1,4E-01	
ABL	TAK-901	3,8E-07	3,0E-09	6,6E-09	6,6E-09	6,3E+06	4,2E-02	
ABL	TG101209	3,0E-06	2,4E-08	5,9E-08	5,9E-08	≥ 6,0E+06	≥ 3,5E-01	
ABL	TG101348 (SAR302503)	1,3E-05	1,0E-07	1,4E-07	1,4E-07	≈ 2,6E+06	≈ 2,8E-01	
ABL	Tie2 kinase inhibitor	≥ 2,0E-05		3,9E-06	3,9E-06	1,1E+05	4,3E-01	
ABL	Tivozanib (AV-951)	5,3E-07	4,2E-09	3,5E-09	3,5E-09	6,4E+06	2,3E-02	
ABL	Torin 2	≥ 2,0E-05		1,5E-06	1,5E-06	≥ 2,4E+05	≥ 3,5E-01	
ABL	TPCA-1	≥ 2,0E-05		6,3E-07	6,3E-07	≥ 5,5E+05	≥ 3,5E-01	
ABL	TSU-68 (SU6668)	≥ 2,0E-05		2,1E-06	2,1E-06	≥ 1,7E+05	≥ 3,5E-01	
ABL	TWS119	4,5E-07	3,5E-09	3,9E-09	3,9E-09	1,1E+07	4,3E-02	
ABL	Vandetanib (Zactima)	9,6E-07	7,6E-09	1,8E-08	1,8E-08	≈ 2,1E+07	≈ 4,9E-01	
ABL	VX-680 (MK-0457 - Tozasertib)	7,9E-07	6,3E-09	7,5E-09	7,5E-09	≈ 1,5E+07	9,0E-02	
ABL	WHI-P154	1,9E-05	1,5E-07	2,7E-07	2,7E-07	≈ 2,8E+05	≈ 6,8E-02	
ABL	WZ3146	≥ 2,0E-05		3,5E-07	3,5E-07	≥ 9,9E+05	≥ 3,5E-01	
ABL	WZ8040	≥ 2,0E-05		6,9E-07	6,9E-07	≈ 1,0E+05	≈ 8,3E-02	
ABL	XL-184 (Cabozantinib)	≈ 3,3E-06	≈ 2,6E-08	3,6E-08	3,6E-08	≈ 1,2E+06	≈ 3,8E-02	12
ABL	ZM 336372	≥ 2,0E-05		3,3E-06	3,3E-06	≥ 1,0E+05	≥ 3,5E-01	
ABL	ZM-447439	≥ 2,0E-05		4,2E-07	4,2E-07	≈ 2,4E+05	≈ 9,2E-02	
AKT1	A-674563	2,3E-08	1,2E-08	9,1E-09	9,1E-09	5,9E+05	5,5E-03	
AKT1	AS703026 (pimasertib)	1,5E-05	7,3E-06	≥ 2,0E-05	≥ 7,3E-06			
AKT1	AT7867	3,1E-08	1,5E-08	1,2E-08	1,2E-08	7,1E+05	7,8E-03	
AKT1	AT9283	3,2E-07	1,6E-07	n.e.	1,6E-07	3,7E+03	≤ 5,8E-04	4
AKT1	AZD7762	1,1E-07	5,7E-08	1,1E-07	1,1E-07	9,5E+04	9,9E-03	

kinase	Compound	IC ₅₀ [M] ePCA	K _D eq [M] ePCA *	K _D kin [M] kPCA	K _D [M] PCA **	k _{on} [M ⁻¹ s ⁻¹] kPCA	k _{off} [s ⁻¹] kPCA	comment
AKT1	Baricitinib (LY3009104 - incb28050)	2,8E-06	1,4E-06	2,2E-06	2,2E-06	4,9E+03	1,1E-02	
AKT1	Bosutinib (SKI-606)	≥ 2,0E-05		4,6E-06	4,6E-06	9,6E+02	4,5E-03	
AKT1	BX-795	8,5E-06	4,2E-06	2,6E-06	2,6E-06	3,6E+03	9,6E-03	
AKT1	BX-912	9,3E-06	4,6E-06	1,7E-06	1,7E-06	5,5E+03	9,0E-03	
AKT1	CCT128930	2,0E-08	1,0E-08	4,8E-09	4,8E-09	9,5E+05	4,4E-03	
AKT1	CEP33779	≈ 1,1E-05	≈ 5,3E-06	2,4E-06	2,4E-06	2,9E+03	7,1E-03	
AKT1	CHIR-124	1,0E-06	5,1E-07	1,1E-06	1,1E-06	5,1E+03	5,4E-03	
AKT1	CP 673451	1,0E-05	5,2E-06	≥ 2,0E-05	≥ 2,0E-05			
AKT1	Crenolanib (CP-868596)	1,8E-05	8,7E-06	n.e.	8,7E-06	6,5E+02	≤ 5,7E-03	4
AKT1	CYC116	≥ 2,0E-05		≈ 5,5E-06	≈ 5,5E-06	5,3E+02	≈ 3,4E-03	
AKT1	Cyt387	≥ 1,5E-05		≥ 2,0E-05	≥ 2,0E-05			
AKT1	GDC-0068	1,2E-09	5,8E-10	n.e.	5,8E-10	1,2E+06	≤ 6,8E-04	4
AKT1	GSK690693	1,6E-09	7,9E-10	n.e.	7,9E-10	8,5E+05	≤ 6,7E-04	4
AKT1	LDN193189	1,3E-05	6,4E-06	≥ 2,0E-05	≥ 2,0E-05			
AKT1	PF-00562271	n.e.	n.e.	≥ 2,0E-05	≥ 2,0E-05			
AKT1	PF-03814735	8,3E-06	4,1E-06	≈ 5,4E-06	4,1E-06	≈ 1,0E+03	≈ 8,4E-03	
AKT1	PHA-767491	6,2E-06	3,1E-06	1,9E-06	1,9E-06	4,7E+03	8,9E-03	
AKT1	PIK-75	7,7E-08	3,8E-08	5,5E-08	5,5E-08	1,9E+05	1,0E-02	
AKT1	Ponatinib (AP24534)	1,5E-05	7,3E-06	n.e.	7,3E-06	7,6E+02	≤ 5,5E-03	4
AKT1	PP-121	5,7E-06	2,8E-06	2,6E-06	2,6E-06	2,2E+03	5,6E-03	
AKT1	PP242	≥ 2,0E-05		≈ 2,4E-06	≈ 2,4E-06	1,1E+03	≈ 3,1E-03	
AKT1	Sotrastaurin (AEB071)	≥ 2,0E-05		≈ 3,7E-06	≈ 3,7E-06	1,1E+03	≈ 5,7E-03	
AKT1	Staurosporine	3,3E-09	1,6E-09	5,4E-10	5,4E-10	4,5E+06	2,4E-03	
AKT1	Sunitinib Malate (Sutent)	≈ 5,9E-06	≈ 2,9E-06	2,3E-06	2,3E-06	4,6E+03	1,1E-02	
AKT1	TAK-901	≈ 9,3E-06	≈ 4,6E-06	3,8E-06	3,8E-06	2,1E+03	7,9E-03	
AKT1	TG101209	7,6E-06	3,8E-06	n.e.	3,8E-06	8,6E+02	≤ 3,3E-03	4
AKT1	TG101348 (SAR302503)	8,7E-06	4,3E-06	1,5E-06	1,5E-06	≈ 3,4E+03	≈ 4,9E-03	
AKT1	Thiazovivin	1,8E-06	9,1E-07	3,7E-07	3,7E-07	1,9E+04	7,1E-03	1
ALK	AEE788 (NVP-AEE788)	7,3E-07	5,1E-07	3,7E-07	3,7E-07	3,3E+05	1,3E-01	
ALK	Afatinib (BIBW2992)	1,3E-05	9,3E-06	3,4E-06	3,4E-06	2,7E+04	8,9E-02	2
ALK	AG-1478 (Typhostin AG-1478)	5,1E-06	3,6E-06	5,6E-06	5,6E-06	1,5E+04	8,1E-02	
ALK	AT9283	2,0E-06	1,4E-06	9,3E-07	9,3E-07	≈ 1,1E+05	≈ 1,0E-01	
ALK	AZ 960	1,1E-07	7,5E-08	2,8E-08	2,8E-08	3,2E+06	8,7E-02	1
ALK	AZD4547	1,1E-06	7,9E-07	2,6E-07	2,6E-07	6,9E+05	≈ 1,8E-01	
ALK	AZD7762	4,4E-07	3,1E-07	2,4E-07	2,4E-07	6,9E+05	1,5E-01	
ALK	AZD8931	3,2E-06	2,2E-06	1,1E-06	1,1E-06	1,7E+05	1,9E-01	
ALK	Baricitinib (LY3009104 - incb28050)	9,5E-06	6,7E-06	5,2E-06	5,2E-06	3,1E+04	1,6E-01	
ALK	BEZ235 (NVP-BEZ235)	≥ 2,0E-05		3,2E-06	3,2E-06	1,7E+04	4,8E-02	
ALK	BI 2536	4,1E-07	2,9E-07	3,8E-07	3,8E-07	≈ 3,3E+05	≈ 1,3E-01	
ALK	BI6727 (Volasertib)	≈ 1,0E-06	≈ 7,1E-07	7,7E-07	7,7E-07	1,3E+05	9,7E-02	
ALK	BIBF1120 (Vargatef)	3,3E-08	2,3E-08	1,0E-08	1,0E-08	≈ 3,9E+06	9,1E-02	3
ALK	BMS 777607	1,0E-05	7,1E-06	8,2E-06	8,2E-06	≈ 4,2E+03	≈ 3,0E-02	
ALK	BMS-265246	1,7E-06	1,2E-06	3,0E-06	3,0E-06	6,1E+03	1,8E-02	2
ALK	Bosutinib (SKI-606)	2,5E-06	1,8E-06	2,0E-06	2,0E-06	≈ 7,1E+04	≈ 1,3E-01	
ALK	BS-181 HCl	7,0E-06	4,9E-06	7,6E-06	7,6E-06	2,4E+04	1,9E-01	
ALK	BX-912	2,4E-06	1,7E-06	1,8E-06	1,8E-06	5,7E+04	1,0E-01	
ALK	CCT137690	5,5E-06	3,9E-06	≈ 1,1E-05	3,9E-06	n.e.	n.e.	
ALK	Cediranib (AZD2171)	≥ 2,0E-05		1,9E-06	1,9E-06	5,1E+04	9,4E-02	
ALK	CEP33779	8,0E-06	5,6E-06	3,4E-06	3,4E-06	≈ 3,7E+04	≈ 1,1E-01	
ALK	CH5424802	2,7E-08	1,9E-08	3,4E-09	1,9E-08	3,0E+07	9,1E-02	
ALK	CI-1033 (Canertinib)	≥ 2,0E-05		4,1E-06	4,1E-06	2,5E+04	1,0E-01	
ALK	Crizotinib (PF-02341066)	9,0E-09	6,4E-09	1,0E-08	1,0E-08	≥ 3,4E+07	≥ 3,5E-01	
ALK	CYC116	6,4E-06	4,5E-06	2,5E-06	2,5E-06	4,9E+04	1,2E-01	
ALK	Dabrafenib (GSK2118436)	≥ 2,0E-05		6,9E-06	6,9E-06	6,6E+03	4,5E-02	
ALK	Dacomitinib (PF299804 - PF-00299804)	2,7E-06	1,9E-06	2,3E-06	2,3E-06	2,0E+04	4,5E-02	
ALK	Danuseritib (PHA-739358)	3,1E-07	2,2E-07	3,4E-07	3,4E-07	4,3E+05	1,5E-01	
ALK	DCC-2036 (Rebastinib)	2,0E-07	1,4E-07	n.e.	1,4E-07	1,3E+03	≤ 1,9E-04	4
ALK	Desmethyl Erlotinib (CP-473420)	2,9E-06	2,0E-06	3,1E-06	3,1E-06	2,8E+04	8,8E-02	
ALK	Dovitinib (TKI-258)	3,4E-07	2,4E-07	2,9E-07	2,9E-07	≈ 4,3E+05	≈ 1,4E-01	
ALK	ENMD-2076	1,2E-05	8,4E-06	≈ 9,3E-06	8,4E-06	6,2E+03	5,7E-02	
ALK	Erlotinib HCl	8,6E-06	6,1E-06	3,7E-06	3,7E-06	≥ 9,5E+04	≥ 3,5E-01	
ALK	Flavopiridol HCl	7,9E-07	5,6E-07	1,3E-06	1,3E-06	1,8E+05	2,2E-01	
ALK	Foretinib (GSK1363089 - XL880)	1,4E-07	9,5E-08	1,1E-07	1,1E-07	1,1E+06	1,2E-01	
ALK	GDC-0879	≥ 2,0E-05		8,4E-06	8,4E-06	2,5E+03	2,1E-02	
ALK	GDC-0980 (RG7422)	≈ 1,8E-06	≈ 1,3E-06	1,3E-06	1,3E-06	7,9E+04	9,8E-02	
ALK	Gefitinib (Iressa)	≥ 2,0E-05		6,0E-06	6,0E-06	≈ 3,2E+04	≈ 1,9E-01	
ALK	Golvatinitib (E7050)	1,8E-07	1,3E-07	7,2E-08	7,2E-08	5,8E+05	4,2E-02	
ALK	GSK1059615	≥ 2,0E-05		5,6E-06	5,6E-06	≥ 6,3E+04	≥ 3,5E-01	
ALK	GSK1070916	3,7E-06	2,6E-06	1,4E-06	1,4E-06	3,5E+04	4,7E-02	
ALK	GSK1838705A	2,2E-09	1,5E-09	n.e.	1,5E-09	1,1E+07	1,7E-02	3
ALK	Hesperadin	4,3E-09	3,0E-09	1,9E-09	1,9E-09	3,3E+07	6,3E-02	
ALK	INK 128 (MLN0128)	4,4E-06	3,1E-06	5,2E-06	5,2E-06	1,7E+04	8,7E-02	
ALK	JNJ-7706621	1,7E-06	1,2E-06	1,1E-06	1,1E-06	1,1E+05	1,2E-01	
ALK	Ki8751	≥ 2,0E-05		5,4E-06	5,4E-06	9,1E+03	4,8E-02	2
ALK	KW 2449	2,3E-07	1,6E-07	3,9E-07	3,9E-07	≥ 8,9E+05	≥ 3,5E-01	
ALK	LDN193189	≈ 5,1E-06	≈ 3,6E-06	4,1E-06	4,1E-06	5,5E+04	≈ 2,4E-01	
ALK	Linifanib (ABT-869)	1,1E-06	7,5E-07	8,4E-07	8,4E-07	6,5E+04	5,4E-02	
ALK	LY2603618 (IC-83)	1,6E-05	1,2E-05	≈ 1,2E-05	1,2E-05	1,6E+04	1,9E-01	
ALK	LY2784544	8,6E-08	6,1E-08	1,6E-08	1,6E-08	9,6E+06	1,5E-01	

kinase	Compound	IC ₅₀ [M] ePCA	K _D eq [M] ePCA *	K _D kin [M] kPCA	K _D [M] PCA **	k _{on} [M ⁻¹ s ⁻¹] kPCA	k _{off} [s ⁻¹] kPCA	comment
ALK	MGCD-265	≥ 2,0E-05		6,8E-06	6,8E-06	7,2E+03	4,7E-02	
ALK	MK-2206 2HCl	1,1E-05	8,1E-06	6,7E-06	6,7E-06	≈ 2,3E+04	≈ 1,4E-01	
ALK	MK-5108 (VX-689)	5,8E-08	4,1E-08	7,7E-08	7,7E-08	4,0E+06	3,0E-01	
ALK	MLN8054	7,5E-06	5,3E-06	3,1E-06	3,1E-06	3,7E+04	≈ 1,2E-01	
ALK	MLN8237 (Alisertib)	4,5E-06	3,2E-06	3,4E-06	3,4E-06	≈ 3,0E+04	≈ 1,1E-01	
ALK	NVP-ADW742	9,7E-07	6,8E-07	1,1E-06	1,1E-06	≈ 7,4E+04	≈ 8,5E-02	
ALK	NVP-BSK805	8,4E-07	5,9E-07	1,7E-06	1,7E-06	3,7E+04	6,2E-02	
ALK	NVP-TAE226	3,3E-08	2,3E-08	1,1E-08	1,1E-08	7,3E+06	1,1E-01	
ALK	Pazopanib HCl	≥ 2,0E-05		1,0E-06	1,0E-06	1,2E+05	1,2E-01	
ALK	PCI-32765 (Ibrutinib)	1,3E-05	9,0E-06	8,1E-06	8,1E-06	≥ 4,3E+04	≥ 3,5E-01	
ALK	PD 0332991 (Palbociclib) HCl	1,3E-05	9,4E-06	7,8E-06	7,8E-06	≈ 1,1E+04	8,5E-02	
ALK	PD153035 HCl	≈ 8,8E-06	≈ 6,2E-06	3,2E-06	3,2E-06	3,5E+04	1,1E-01	
ALK	Pelitinib (EKB-569)	≈ 5,7E-06	≈ 4,0E-06	2,9E-06	2,9E-06	≈ 2,6E+04	≈ 7,5E-02	
ALK	PF-00562271	9,5E-08	6,7E-08	7,4E-08	7,4E-08	1,4E+06	≈ 1,1E-01	
ALK	PF-03814735	8,4E-08	5,9E-08	1,4E-07	1,4E-07	2,9E+06	4,2E-01	
ALK	PHA-665752	6,3E-06	4,5E-06	2,1E-06	2,1E-06	≈ 8,9E+04	≈ 2,0E-01	
ALK	PHA-680632	1,9E-06	1,3E-06	9,0E-07	9,0E-07	9,9E+07	8,9E-02	
ALK	PIK-75	2,4E-07	1,7E-07	4,5E-07	4,5E-07	7,3E+05	1,7E-01	
ALK	Ponatinib (AP24534)	≈ 1,2E-05	≈ 8,1E-06	4,5E-06	4,5E-06	3,5E+04	1,7E-01	1
ALK	PP-121	4,9E-07	3,4E-07	6,9E-07	6,9E-07	1,6E+05	1,1E-01	
ALK	PP242	6,9E-06	4,9E-06	3,5E-06	3,5E-06	1,9E+04	6,8E-02	
ALK	R406	≈ 3,2E-06	≈ 2,2E-06	6,8E-06	6,8E-06	1,3E+04	7,7E-02	
ALK	R788 (Fostamatinib) - prodrug	3,7E-06	2,6E-06	4,5E-06	4,5E-06	5,0E+04	1,4E-01	
ALK	Roscovitine (Seliciclib - CYC202)	4,4E-06	3,1E-06	3,4E-06	3,4E-06	3,3E+04	1,1E-01	
ALK	Ruxolitinib (INCB018424)	1,4E-06	9,5E-07	2,1E-06	2,1E-06	≈ 7,3E+04	≈ 1,4E-01	
ALK	Saracatinib (AZD0530)	4,9E-06	3,4E-06	2,9E-06	2,9E-06	4,2E+04	1,2E-01	
ALK	SB590885	1,4E-05	9,8E-06	6,2E-06	6,2E-06	1,4E+04	8,3E-02	
ALK	Semaxanib (SU5416)	6,7E-07	4,7E-07	4,5E-07	4,5E-07	1,1E+05	4,8E-02	
ALK	SNS-314	7,7E-06	5,4E-06	5,0E-06	5,0E-06	2,3E+04	1,2E-01	
ALK	SP600125	≈ 2,6E-06	≈ 1,8E-06	2,6E-06	2,6E-06	3,7E+04	9,8E-02	1
ALK	Staurosporine	7,5E-09	5,3E-09	3,1E-09	3,1E-09	1,1E+07	5,8E-02	3
ALK	SU11274	1,8E-06	1,3E-06	3,9E-06	3,9E-06	3,9E+04	1,5E-01	
ALK	Sunitinib Malate (Sutent)	≈ 1,4E-07	≈ 9,8E-08	1,5E-07	1,5E-07	≈ 1,3E+06	≈ 1,8E-01	
ALK	TAE684 (NVP-TAE684)	1,2E-09	8,6E-10	2,4E-10	2,4E-10	3,9E+07	9,3E-03	
ALK	TAK-901	1,1E-08	7,7E-09	2,4E-08	2,4E-08	2,8E+06	6,8E-02	
ALK	TG101209	4,4E-07	3,1E-07	6,0E-07	6,0E-07	≈ 1,6E+05	≈ 9,9E-02	
ALK	TG101348 (SAR302503)	9,1E-07	6,4E-07	1,0E-06	1,0E-06	≈ 6,0E+04	≈ 6,1E-02	
ALK	Tivozanib (AV-951)	9,7E-06	6,8E-06	2,6E-06	2,6E-06	2,7E+04	7,1E-02	
ALK	Torin 1	≥ 2,0E-05		7,9E-06	7,9E-06	1,8E+04	1,4E-01	
ALK	Torin 2	≥ 2,0E-05		6,4E-06	6,4E-06	1,4E+04	8,6E-02	
ALK	TPCA-1	2,7E-06	1,9E-06	2,2E-06	2,2E-06	6,1E+04	1,3E-01	
ALK	TSU-68 (SU6668)	1,3E-06	8,9E-07	2,6E-07	2,6E-07	2,6E+05	6,8E-02	
ALK	TWS119	1,4E-06	9,7E-07	≈ 3,5E-07	9,7E-07	≥ 1,0E+06	≥ 3,5E-01	
ALK	Tyrphostin AG 879 (AG 879)	≥ 2,0E-05		≈ 2,5E-06	≈ 2,5E-06	≈ 8,9E+03	7,5E-03	
ALK	Vandetanib (Zactima)	1,1E-06	7,6E-07	1,2E-06	1,2E-06	5,0E+04	6,1E-02	
ALK	Vatalanib 2HCl (PTK787)	4,8E-06	3,4E-06	7,0E-06	7,0E-06	n.e.	n.e.	
ALK	VX-680 (MK-0457 - Tozasertib)	8,6E-06	6,1E-06	3,8E-06	3,8E-06	4,4E+04	1,7E-01	
ALK	WHI-P154	6,0E-07	4,2E-07	2,6E-07	2,6E-07	3,1E+05	8,0E-02	
ALK	WZ3146	1,7E-06	1,2E-06	1,5E-06	1,5E-06	6,1E+04	9,2E-02	
ALK	WZ4002	8,1E-07	5,7E-07	2,4E-07	2,4E-07	≈ 5,4E+05	9,4E-02	
ALK	WZ8040	6,3E-07	4,5E-07	7,3E-07	7,3E-07	8,4E+04	6,2E-02	
ALK	XL-184 (Cabozantinib)	9,9E-07	7,0E-07	7,0E-07	7,0E-07	3,4E+05	≈ 2,7E-01	
ALK	ZM-447439	2,0E-06	1,4E-06	3,2E-06	3,2E-06	≈ 5,8E+04	≈ 2,0E-01	
AurA	A-674563	1,0E-05	8,9E-07	1,0E-06	1,0E-06	3,6E+03	3,5E-03	
AurA	AEE788 (NVP-AEE788)	3,8E-06	3,2E-07	3,1E-07	3,1E-07	3,2E+04	9,9E-03	
AurA	Afatinib (BIBW2992)	n.e.	n.e.	≥ 2,0E-05	≥ 2,0E-05			
AurA	AG-1478 (Tyrphostin AG-1478)	8,8E-06	7,4E-07	n.e.	7,4E-07	2,7E+03	≤ 2,0E-03	4
AurA	AMG 900	≤ 4,1E-10	≤ 3,5E-11	n.e.	≤ 3,5E-11	5,6E+06	≤ 2,0E-04	4
AurA	AMG458	≈ 2,8E-06	≈ 2,4E-07	4,7E-07	4,7E-07	2,0E+04	9,6E-03	
AurA	Apatinib (YN968D1)	≥ 2,0E-05		1,1E-06	1,1E-06	1,3E+03	1,5E-03	
AurA	AS-252424	≥ 2,0E-05		3,1E-06	3,1E-06	2,1E+03	6,5E-03	
AurA	AS-605240	7,0E-06	5,9E-07	n.e.	5,9E-07	1,6E+03	≤ 9,6E-04	4
AurA	AT7867	4,6E-06	3,9E-07	6,5E-07	6,5E-07	1,6E+04	1,0E-02	
AurA	AT9283	≈ 2,0E-08	≈ 1,7E-09	7,9E-10	7,9E-10	3,5E+06	2,8E-03	
AurA	Aurora A Inhibitor I	2,6E-09	2,2E-10	3,8E-10	3,8E-10	6,4E+06	2,4E-03	
AurA	Axitinib	5,6E-08	4,7E-09	6,0E-09	6,0E-09	≈ 2,6E+06	1,1E-02	
AurA	AZ 960	≈ 3,6E-08	≈ 3,0E-09	1,1E-09	1,1E-09	3,6E+06	4,0E-03	
AurA	AZD4547	≈ 5,7E-07	≈ 4,8E-08	3,1E-08	3,1E-08	2,9E+05	9,1E-03	
AurA	AZD5438	3,4E-07	2,9E-08	5,9E-08	5,9E-08	3,4E+05	2,0E-02	
AurA	AZD7762	4,1E-07	3,5E-08	5,4E-08	5,4E-08	1,4E+05	7,8E-03	
AurA	Barasertib (AZD1152-HQPA)	≈ 2,5E-07	≈ 2,1E-08	1,6E-08	1,6E-08	7,3E+05	1,2E-02	
AurA	Baricitinib (LY3009104 - incb28050)	3,8E-06	3,2E-07	3,5E-07	3,5E-07	2,5E+04	8,9E-03	
AurA	BIBF1120 (Vargatef)	1,5E-06	1,2E-07	n.e.	1,2E-07	1,1E+05	≤ 1,3E-02	4
AurA	BIX 02188	1,7E-05	1,5E-06	2,2E-06	2,2E-06	3,2E+03	7,2E-03	
AurA	BMS 777607	1,2E-06	1,0E-07	1,6E-07	1,6E-07	6,3E+04	9,8E-03	
AurA	BMS 794833	1,8E-05	1,5E-06	3,4E-06	3,4E-06	1,5E+03	2,2E-03	3
AurA	BMS-265246	6,9E-07	5,8E-08	n.e.	5,8E-08	1,4E+05	≤ 8,3E-03	24
AurA	BMS-599626 (AC480)	≥ 2,0E-05		2,9E-06	2,9E-06	3,3E+03	9,4E-03	
AurA	BX-795	1,2E-08	1,0E-09	1,0E-09	1,0E-09	2,7E+06	2,8E-03	

kinase	Compound	IC ₅₀ [M] ePCA	K _D eq [M] ePCA *	K _D kin [M] kPCA	K _D [M] PCA **	k _{on} [M ⁻¹ s ⁻¹] kPCA	k _{off} [s ⁻¹] kPCA	comment
AurA	BX-912	2,9E-08	2,4E-09	4,0E-09	4,0E-09	3,3E+06	1,3E-02	
AurA	CCT128930	≥ 2,0E-05		2,6E-06	2,6E-06	2,8E+03	7,3E-03	
AurA	CCT129202	2,2E-08	1,9E-09	3,9E-09	3,9E-09	1,8E+06	6,7E-03	
AurA	CCT137690	1,2E-08	1,1E-09	n.e.	1,1E-09	3,7E+06	≤ 3,9E-03	4
AurA	Cediranib (AZD2171)	≥ 2,0E-05		1,5E-06	1,5E-06	9,5E+03	1,4E-02	
AurA	CEP33779	≈ 1,7E-06	≈ 1,4E-07	2,2E-07	2,2E-07	4,0E+04	9,1E-03	
AurA	CHIR-124	2,6E-06	2,2E-07	5,6E-07	5,6E-07	2,7E+04	5,8E-03	3
AurA	CI-1033 (Canertinib)	4,5E-06	3,8E-07	1,2E-06	1,2E-06	≈ 6,8E+04	≈ 8,1E-02	
AurA	CP 673451	8,8E-06	7,5E-07	1,6E-06	1,6E-06	7,4E+03	1,2E-02	
AurA	CP-724714	≥ 2,0E-05		1,6E-06	1,6E-06	3,7E+03	5,9E-03	
AurA	Crenolanib (CP-868596)	≈ 7,8E-06	≈ 6,6E-07	≈ 7,9E-07	≈ 7,2E-07	4,5E+03	≈ 4,5E-03	
AurA	Crizotinib (PF-02341066)	2,2E-07	1,9E-08	2,5E-08	2,5E-08	2,2E+06	5,3E-02	
AurA	CX-4945 (Siltitasertib)	≥ 2,0E-05		1,1E-06	1,1E-06	6,2E+03	7,0E-03	
AurA	CYC116	2,5E-08	2,1E-09	2,1E-09	2,1E-09	2,7E+06	5,7E-03	
AurA	Cyt387	4,9E-07	4,2E-08	3,2E-08	3,2E-08	2,4E+05	7,6E-03	
AurA	Dabrafenib (GSK2118436)	≈ 6,6E-07	≈ 5,6E-08	2,8E-08	2,8E-08	2,1E+05	5,9E-03	
AurA	Danuserib (PHA-739358)	2,0E-08	1,7E-09	n.e.	1,7E-09	1,8E+05	≤ 3,0E-04	4
AurA	Dasatinib (BMS-354825)	5,5E-06	4,7E-07	3,9E-07	3,9E-07	5,4E+04	2,1E-02	
AurA	Desmethyl Erlotinib (CP-473420)	3,6E-06	3,1E-07	3,6E-07	3,6E-07	2,1E+04	7,5E-03	
AurA	Dovitinib (TKI-258)	1,6E-06	1,4E-07	1,9E-07	1,9E-07	1,1E+05	2,2E-02	
AurA	E7080 (Lenvatinib)	4,4E-06	3,8E-07	3,7E-07	3,7E-07	2,4E+04	9,0E-03	
AurA	ENMD-2076	1,6E-08	1,4E-09	2,3E-09	2,3E-09	1,5E+06	3,6E-03	
AurA	Erlotinib HCl	1,5E-06	1,3E-07	n.e.	1,3E-07	3,0E+04	≤ 3,9E-03	4
AurA	Flavopiridol HCl	≥ 2,0E-05		2,5E-06	2,5E-06	1,4E+03	3,4E-03	
AurA	Foretinib (GSK1363089 - XL880)	1,8E-07	1,5E-08	5,0E-08	5,0E-08	2,0E+05	1,0E-02	
AurA	GDC-0941	≥ 2,0E-05		1,9E-06	1,9E-06	5,7E+03	1,1E-02	
AurA	GSK1059615	≥ 2,0E-05		2,1E-06	2,1E-06	≈ 6,0E+03	9,9E-03	
AurA	GSK1070916	6,8E-08	5,8E-09	2,6E-09	2,6E-09	4,6E+05	1,2E-03	
AurA	GSK2126458	≥ 2,0E-05		2,6E-06	2,6E-06	≥ 1,4E+05	≥ 3,5E-01	
AurA	Hesperadin	1,3E-08	1,1E-09	8,3E-10	8,3E-10	7,1E+06	5,8E-03	
AurA	INK 128 (MLN0128)	≈ 1,1E-05	≈ 9,2E-07	2,1E-06	2,1E-06	3,9E+03	8,4E-03	
AurA	JNJ-38877605	≥ 2,0E-05		2,4E-06	2,4E-06	2,2E+03	5,3E-03	
AurA	JNJ-7706621	7,1E-08	6,1E-09	5,8E-09	5,8E-09	2,1E+06	1,2E-02	
AurA	Ki8751	1,0E-07	8,7E-09	n.e.	8,7E-09	1,5E+05	≤ 1,3E-03	124
AurA	KRN 633	≥ 2,0E-05		1,1E-06	1,1E-06	5,4E+03	6,0E-03	
AurA	KW 2449	1,1E-07	9,0E-09	n.e.	9,0E-09	2,5E+05	≤ 2,2E-03	4
AurA	Lapatinib Ditosylate (Tykerb)	≥ 2,0E-05		2,9E-06	2,9E-06	2,5E+03	7,4E-03	
AurA	LDN193189	1,4E-05	1,2E-06	9,8E-07	9,8E-07	8,8E+03	8,7E-03	
AurA	Linifanib (ABT-869)	≈ 3,1E-06	≈ 2,6E-07	≈ 2,5E-07	≈ 2,5E-07	2,3E+03	≈ 6,3E-04	
AurA	Linsitinib (OSI-906)	≥ 2,0E-05		1,5E-06	1,5E-06	1,9E+03	2,9E-03	
AurA	LY2784544	7,5E-09	6,4E-10	6,1E-10	6,1E-10	3,5E+06	2,1E-03	
AurA	MGCD-265	2,4E-06	2,1E-07	3,9E-07	3,9E-07	1,0E+04	3,9E-03	
AurA	Milciclib (PHA-848125)	≈ 1,9E-06	≈ 1,6E-07	1,2E-07	1,2E-07	9,5E+04	1,1E-02	
AurA	MK-2461	8,4E-07	7,1E-08	9,5E-08	9,5E-08	4,7E+05	4,4E-02	
AurA	MK-5108 (VX-689)	≤ 5,4E-11	≤ 4,6E-12	n.e.	≤ 4,6E-12	6,0E+07	≤ 2,8E-04	4
AurA	MLN8054	≤ 3,9E-10	≤ 3,3E-11	n.e.	≤ 3,3E-11	8,9E+06	≤ 3,0E-04	4
AurA	MLN8237 (Alisertib)	≤ 2,6E-10	≤ 2,2E-11	n.e.	≤ 2,2E-11	5,0E+06	≤ 1,1E-04	4
AurA	NVP-ADW742	1,4E-05	1,2E-06	1,4E-06	1,4E-06	6,7E+03	9,5E-03	
AurA	NVP-BSK805	6,2E-06	5,3E-07	8,9E-07	8,9E-07	1,0E+04	8,7E-03	
AurA	NVP-TAE226	≈ 7,5E-08	≈ 6,4E-09	7,5E-09	7,5E-09	1,3E+06	9,7E-03	
AurA	OSI-027	3,2E-06	2,8E-07	7,7E-07	7,7E-07	5,3E+03	4,1E-03	
AurA	Pazopanib HCl	4,4E-07	3,8E-08	5,5E-08	5,5E-08	2,7E+05	1,4E-02	
AurA	PCI-32765 (Ibrutinib)	1,6E-06	1,4E-07	2,9E-07	2,9E-07	2,3E+04	6,5E-03	
AurA	PD153035 HCl	9,3E-06	7,9E-07	9,3E-07	9,3E-07	1,2E+04	1,1E-02	
AurA	PF-00562271	1,6E-07	1,3E-08	1,5E-08	1,5E-08	5,2E+05	7,8E-03	
AurA	PF-03814735	2,4E-09	2,0E-10	2,3E-10	2,3E-10	5,0E+06	1,1E-03	
AurA	PHA-665752	1,7E-06	1,4E-07	1,4E-07	1,4E-07	1,0E+05	1,4E-02	
AurA	PHA-680632	2,0E-08	1,7E-09	n.e.	1,7E-09	1,4E+06	≤ 2,3E-03	4
AurA	PHT-427	1,6E-05	1,3E-06	≥ 2,0E-05	≥ 1,3E-06			
AurA	PIK-294	≥ 2,0E-05		9,7E-07	9,7E-07	4,0E+03	4,1E-03	
AurA	PIK-75	6,6E-07	5,6E-08	9,6E-08	9,6E-08	1,1E+05	1,0E-02	2
AurA	PLX-4720	≈ 4,0E-06	≈ 3,4E-07	4,0E-07	4,0E-07	2,4E+04	9,3E-03	
AurA	Ponatinib (AP24534)	7,8E-06	6,6E-07	1,0E-06	1,0E-06	6,4E+03	6,5E-03	
AurA	PP-121	7,1E-06	6,0E-07	1,0E-06	1,0E-06	6,1E+03	6,2E-03	
AurA	PP242	6,8E-06	5,8E-07	6,2E-07	6,2E-07	6,0E+03	3,7E-03	
AurA	Quercetin (Sophoretin)	≥ 2,0E-05		2,0E-06	2,0E-06	3,1E+03	6,3E-03	
AurA	R406	7,5E-08	6,4E-09	1,1E-08	1,1E-08	7,3E+05	7,8E-03	2
AurA	R788 (Fostamatinib) - prodrug	1,8E-07	1,5E-08	2,0E-08	2,0E-08	4,8E+05	9,8E-03	
AurA	Ruxolitinib (INCB018424)	2,9E-06	2,5E-07	4,6E-07	4,6E-07	1,8E+04	8,4E-03	
AurA	SAR131675	≥ 2,0E-05		1,1E-06	1,1E-06	8,1E+02	8,8E-04	
AurA	Semaxanib (SU5416)	≈ 5,2E-06	≈ 4,4E-07	4,5E-07	4,5E-07	2,7E+04	1,3E-02	
AurA	SNS-032 (BMS-387032)	1,5E-05	1,3E-06	1,3E-06	1,3E-06	8,1E+03	1,1E-02	
AurA	SNS-314	≈ 1,2E-08	≈ 1,0E-09	5,7E-10	5,7E-10	8,4E+06	4,8E-03	
AurA	SP600125	9,2E-07	7,8E-08	8,8E-08	8,8E-08	1,1E+05	9,3E-03	
AurA	Staurosporine	3,2E-09	2,7E-10	n.e.	2,7E-10	1,3E+07	≤ 3,6E-03	4
AurA	SU11274	7,3E-08	6,2E-09	1,3E-08	1,3E-08	9,3E+05	1,2E-02	
AurA	Sunitinib Malate (Sutent)	2,3E-06	1,9E-07	2,1E-07	2,1E-07	8,8E+04	1,9E-02	
AurA	TAE684 (NVP-TAE684)	2,4E-08	2,1E-09	7,6E-10	7,6E-10	4,5E+06	3,4E-03	
AurA	TAK-901	2,2E-09	1,9E-10	n.e.	1,9E-10	5,1E+06	≤ 9,5E-04	4

kinase	Compound	IC ₅₀ [M] ePCA	K _D eq [M] ePCA *	K _D kin [M] kPCA	K _D [M] PCA **	k _{on} [M ⁻¹ s ⁻¹] kPCA	k _{off} [s ⁻¹] kPCA	comment
AurA	Tandutinib (MLN518)	1,9E-05	1,6E-06	3,6E-06	3,6E-06	5,0E+03	1,8E-02	
AurA	TG101209	1,6E-07	1,3E-08	2,8E-08	2,8E-08	1,8E+05	5,0E-03	
AurA	TG101348 (SAR302503)	1,1E-06	9,3E-08	1,3E-07	1,3E-07	5,8E+04	7,3E-03	
AurA	Thiazovivin	≥ 2,0E-05		1,4E-06	1,4E-06	6,3E+03	9,2E-03	
AurA	Tivozanib (AV-951)	3,8E-07	3,2E-08	3,6E-08	3,6E-08	2,5E+05	8,9E-03	
AurA	Tofacitinib (CP-690550 - Tasocitinib)	1,2E-05	9,8E-07	1,7E-06	1,7E-06	4,6E+03	7,7E-03	
AurA	Torin 2	≥ 2,0E-05		9,3E-07	9,3E-07	1,2E+04	1,1E-02	
AurA	TPCA-1	1,4E-06	1,2E-07	1,7E-07	1,7E-07	4,6E+04	7,7E-03	
AurA	TSU-68 (SU6668)	1,4E-07	1,2E-08	1,7E-08	1,7E-08	5,4E+05	9,2E-03	
AurA	TWS119	1,0E-06	8,6E-08	9,9E-08	9,9E-08	1,0E+05	1,0E-02	
AurA	Vandetanib (Zactima)	≥ 2,0E-05		1,6E-06	1,6E-06	3,6E+03	6,1E-03	
AurA	Vatalanib 2HCl (PTK787)	1,8E-05	1,6E-06	n.e.	1,6E-06	8,1E+02	≤ 1,3E-03	4
AurA	VX-680 (MK-0457 - Tozasertib)	2,3E-09	1,9E-10	n.e.	1,9E-10	3,6E+06	≤ 6,9E-04	4
AurA	WHI-P154	6,9E-06	5,8E-07	1,0E-06	1,0E-06	1,7E+04	1,6E-02	
AurA	WZ3146	2,9E-08	2,4E-09	4,2E-09	4,2E-09	2,2E+06	9,3E-03	
AurA	WZ4002	8,6E-07	7,3E-08	n.e.	7,3E-08	≈ 1,6E+05	1,1E-02	3
AurA	WZ8040	3,6E-08	3,0E-09	8,9E-09	8,9E-09	7,4E+05	6,4E-03	
AurA	XL-184 (Cabozantinib)	1,6E-06	1,4E-07	≈ 3,7E-07	1,4E-07	5,7E+04	7,8E-03	3
AurA	ZM 336372	1,3E-05	1,1E-06	n.e.	1,1E-06	7,1E+02	≤ 7,6E-04	4
AurA	ZM-447439	1,7E-07	1,4E-08	2,5E-08	2,5E-08	4,0E+05	1,0E-02	
AXL	A-674563	≥ 2,0E-05		3,2E-06	3,2E-06	2,0E+05	6,2E-01	
AXL	AEE788 (NVP-AEE788)	1,5E-05	1,8E-06	1,2E-06	1,2E-06	≈ 3,6E+05	≈ 4,4E-01	
AXL	Afatinib (BIBW2992)	8,1E-06	9,9E-07	8,9E-07	8,9E-07	≥ 3,9E+05	≥ 3,5E-01	
AXL	AG-1478 (Typhostin AG-1478)	5,5E-06	6,8E-07	1,8E-06	1,8E-06	≈ 3,1E+05	≈ 5,0E-01	
AXL	AMG 900	≥ 2,0E-05		2,3E-06	2,3E-06	≥ 1,5E+05	≥ 3,5E-01	
AXL	AMG458	7,2E-09	8,8E-10	n.e.	8,8E-10	1,5E+06	≤ 1,3E-03	4
AXL	ARRY334543	≥ 2,0E-05		2,9E-06	2,9E-06	≥ 1,2E+05	≥ 3,5E-01	
AXL	AT9283	4,2E-07	5,2E-08	3,1E-08	3,1E-08	1,2E+07	3,7E-01	
AXL	Aurora A Inhibitor I	≥ 2,0E-05		1,2E-06	1,2E-06	≈ 8,4E+05	≈ 1,0E+00	2
AXL	Axitinib	1,8E-06	2,2E-07	2,9E-07	2,9E-07	≥ 1,2E+06	≥ 3,5E-01	
AXL	AZ 960	≥ 2,0E-05		2,1E-06	2,1E-06	≥ 1,7E+05	≥ 3,5E-01	
AXL	AZD4547	4,9E-06	6,0E-07	6,1E-07	6,1E-07	2,5E+06	≈ 1,2E+00	
AXL	AZD5438	1,9E-05	2,3E-06	1,2E-06	1,2E-06	≥ 2,8E+05	≥ 3,5E-01	
AXL	AZD7762	3,1E-07	3,8E-08	4,4E-08	4,4E-08	≈ 7,8E+06	≈ 3,0E-01	
AXL	Barasertib (AZD1152-HQPA)	6,6E-07	8,2E-08	7,4E-08	7,4E-08	4,5E+06	3,3E-01	
AXL	Baricitinib (LY3009104 - incb28050)	1,4E-05	1,8E-06	1,3E-06	1,3E-06	≥ 2,6E+05	≥ 3,5E-01	
AXL	BEZ235 (NVP-BEZ235)	≥ 2,0E-05		1,6E-06	1,6E-06	≈ 2,5E+05	≈ 2,8E-01	
AXL	BIBF1120 (Vargatef)	7,7E-07	9,5E-08	7,5E-08	7,5E-08	≈ 7,4E+06	≈ 5,3E-01	
AXL	BIX 02188	2,1E-06	2,6E-07	4,2E-07	4,2E-07	≈ 1,1E+06	≈ 4,8E-01	
AXL	BIX 02189	1,1E-05	1,4E-06	2,1E-06	2,1E-06	≥ 1,7E+05	≥ 3,5E-01	
AXL	BMS 777607	3,3E-09	4,0E-10	9,6E-11	9,6E-11	7,5E+06	7,2E-04	
AXL	BMS 794833	9,7E-09	1,2E-09	1,2E-09	1,2E-09	1,8E+06	2,1E-03	
AXL	Bosutinib (SKI-606)	6,1E-08	7,5E-09	1,3E-08	1,3E-08	≈ 4,2E+07	≈ 5,1E-01	
AXL	Brivanib alaninate (BMS-582664) - prodrug	≥ 2,0E-05		3,9E-06	3,9E-06	≥ 9,1E+04	≥ 3,5E-01	
AXL	BX-795	1,6E-06	2,0E-07	3,1E-07	3,1E-07	≥ 1,1E+06	≥ 3,5E-01	
AXL	BX-912	3,5E-06	4,3E-07	1,1E-06	1,1E-06	≥ 3,2E+05	≥ 3,5E-01	
AXL	CCT128930	1,9E-05	2,3E-06	1,7E-06	1,7E-06	≈ 5,0E+05	≈ 9,6E-01	
AXL	CCT129202	≥ 2,0E-05		1,0E-06	1,0E-06	≈ 5,3E+05	≈ 5,6E-01	2
AXL	CCT137690	5,6E-07	6,9E-08	3,0E-07	3,0E-07	n.e.	n.e.	2
AXL	Cediranib (AZD2171)	1,2E-05	1,5E-06	n.e.	1,5E-06	n.e.	n.e.	
AXL	CEP33779	8,2E-07	1,0E-07	1,8E-07	1,8E-07	≈ 1,5E+06	≈ 2,1E-01	
AXL	CH5424802	6,9E-07	8,6E-08	≈ 6,9E-08	8,6E-08	≈ 7,4E+06	≈ 5,1E-01	2
AXL	CHIR-124	≈ 2,1E-06	≈ 2,6E-07	5,8E-07	5,8E-07	≈ 1,1E+06	≈ 3,3E-01	
AXL	CI-1033 (Canertinib)	2,2E-06	2,7E-07	≈ 4,3E-07	2,7E-07	≈ 2,4E+06	≈ 1,0E+00	
AXL	CP 673451	3,8E-06	4,7E-07	1,2E-06	1,2E-06	≥ 2,9E+05	≥ 3,5E-01	
AXL	Crenolanib (CP-868596)	4,9E-06	6,1E-07	6,9E-07	6,9E-07	≥ 5,1E+05	≥ 3,5E-01	
AXL	Crizotinib (PF-02341066)	≈ 5,1E-08	≈ 6,3E-09	1,0E-08	1,0E-08	n.e.	n.e.	2
AXL	CX-4945 (Silmintasertib)	4,7E-07	5,7E-08	6,9E-08	6,9E-08	≈ 1,3E+07	7,7E-01	
AXL	CYC116	1,2E-06	1,4E-07	1,6E-07	1,6E-07	4,6E+06	7,2E-01	
AXL	Cyt387	≈ 1,2E-05	≈ 1,5E-06	1,1E-06	1,1E-06	≈ 5,8E+05	≈ 6,7E-01	
AXL	Dabrafenib (GSK2118436)	2,0E-06	2,5E-07	1,2E-06	2,5E-07	n.e.	n.e.	
AXL	Dacomitinib (PF299804 - PF-00299804)	≈ 1,2E-05	≈ 1,5E-06	9,1E-07	9,1E-07	≈ 3,2E+05	≈ 2,8E-01	
AXL	Danuseritib (PHA-739358)	8,8E-06	1,1E-06	1,3E-06	1,3E-06	≥ 2,8E+05	≥ 3,5E-01	
AXL	Dasatinib (BMS-354825)	≈ 2,0E-05	≈ 2,5E-06	≈ 1,9E-06	≈ 2,2E-06	≥ 1,9E+05	≥ 3,5E-01	
AXL	DCC-2036 (Rebastinib)	5,6E-09	6,9E-10	n.e.	6,9E-10	8,4E+04	≤ 5,8E-05	24
AXL	Desmethyl Erlotinib (CP-473420)	9,0E-06	1,1E-06	8,4E-07	8,4E-07	8,1E+05	6,0E-01	
AXL	Dovitinib (TKI-258)	1,2E-06	1,5E-07	1,2E-07	1,2E-07	≥ 2,9E+06	≥ 3,5E-01	
AXL	E7080 (Lenvatinib)	≥ 2,0E-05		1,0E-06	1,0E-06	4,3E+05	4,4E-01	
AXL	ENMD-2076	6,5E-07	8,1E-08	1,0E-07	1,0E-07	≈ 2,4E+06	≈ 2,4E-01	
AXL	Erlotinib HCl	≈ 1,3E-05	≈ 1,6E-06	≈ 2,3E-06	≈ 2,0E-06	≥ 1,5E+05	≥ 3,5E-01	
AXL	Flavopiridol HCl	1,9E-05	2,3E-06	2,3E-06	2,3E-06	≥ 1,5E+05	≥ 3,5E-01	
AXL	Foretinib (GSK1363089 - XL880)	≤ 1,1E-10	≤ 1,4E-11	n.e.	≤ 1,4E-11	2,8E+06	≤ 3,8E-05	4
AXL	GDC-0941	≥ 2,0E-05		2,6E-06	2,6E-06	≥ 1,3E+05	≥ 3,5E-01	
AXL	GDC-0980 (RG7422)	5,8E-06	7,1E-07	9,2E-07	9,2E-07	≥ 3,8E+05	≥ 3,5E-01	
AXL	Gefitinib (Iressa)	5,6E-06	6,9E-07	≈ 1,1E-06	6,9E-07	≥ 3,3E+05	≥ 3,5E-01	
AXL	Golvatinib (E7050)	≈ 6,0E-09	≈ 7,4E-10	7,3E-10	7,3E-10	1,0E+07	7,5E-03	
AXL	GSK1059615	≈ 7,7E-06	≈ 9,6E-07	4,1E-07	4,1E-07	≥ 8,6E+05	≥ 3,5E-01	1
AXL	GSK1070916	8,5E-08	1,0E-08	9,1E-09	9,1E-09	2,3E+06	2,1E-02	
AXL	GSK1838705A	≥ 2,0E-05		1,7E-06	1,7E-06	≈ 1,4E+05	≈ 2,4E-01	

kinase	Compound	IC ₅₀ [M] ePCA	K _D eq [M] ePCA *	K _D kin [M] kPCA	K _D [M] PCA **	k _{on} [M ⁻¹ s ⁻¹] kPCA	k _{off} [s ⁻¹] kPCA	comment
AXL	Hesperadin	1,9E-08	2,3E-09	1,6E-09	1,6E-09	6,8E+07	1,1E-01	
AXL	INCB28060	1,2E-05	1,4E-06	1,1E-06	1,1E-06	≈ 1,3E+06	≈ 1,2E+00	
AXL	JNJ-38877605	8,6E-06	1,1E-06	1,7E-06	1,7E-06	≥ 2,0E+05	≥ 3,5E-01	
AXL	JNJ-7706621	2,9E-06	3,5E-07	4,1E-07	4,1E-07	≈ 2,2E+06	≈ 9,0E-01	
AXL	K8751	5,6E-08	6,9E-09	2,1E-08	2,1E-08	5,6E+06	1,2E-01	2
AXL	KRN 633	≈ 1,1E-05	≈ 1,4E-06	8,3E-07	8,3E-07	≈ 8,5E+05	≈ 7,2E-01	
AXL	KW 2449	1,6E-06	2,0E-07	5,7E-07	5,7E-07	≥ 6,1E+05	≥ 3,5E-01	
AXL	Lapatinib Ditosylate (Tykerb)	≈ 2,0E-05	≈ 2,5E-06	≈ 2,7E-06	≈ 2,6E-06	≥ 1,3E+05	≥ 3,5E-01	
AXL	Linifanib (ABT-869)	6,6E-07	8,1E-08	9,6E-07	8,1E-08	≈ 1,3E+05	≈ 7,7E-02	1
AXL	Linsitinib (OSI-906)	≥ 2,0E-05		3,1E-06	3,1E-06	≥ 1,1E+05	≥ 3,5E-01	
AXL	LY2784544	2,1E-06	2,6E-07	5,9E-07	5,9E-07	≥ 5,9E+05	≥ 3,5E-01	
AXL	MGCD-265	1,4E-09	1,7E-10	5,4E-10	5,4E-10	1,8E+06	9,2E-04	2
AXL	Milciclib (PHA-848125)	7,7E-07	9,5E-08	6,9E-08	6,9E-08	4,5E+06	3,1E-01	
AXL	MK-2461	1,4E-06	1,7E-07	≈ 1,7E-07	1,7E-07	≥ 2,0E+06	≥ 3,5E-01	1
AXL	MK-5108 (VX-689)	8,7E-08	1,1E-08	n.e.	1,1E-08	n.e.	n.e.	
AXL	MLN8054	1,3E-06	1,6E-07	2,5E-07	2,5E-07	2,2E+06	5,7E-01	
AXL	MLN8237 (Alisertib)	2,4E-06	3,0E-07	7,5E-07	7,5E-07	≥ 4,6E+05	≥ 3,5E-01	
AXL	Neratinib (HKI-272)	3,9E-06	4,8E-07	2,0E-07	2,0E-07	5,8E+05	1,2E-01	2
AXL	NVP-ADW742	7,8E-06	9,6E-07	9,6E-07	9,6E-07	≥ 3,6E+05	≥ 3,5E-01	
AXL	NVP-BGT226	1,7E-05	2,1E-06	5,8E-07	5,8E-07	≈ 4,1E+05	≈ 2,8E-01	
AXL	NVP-BSK805	2,7E-07	3,3E-08	4,1E-08	4,1E-08	≈ 4,9E+06	≈ 1,7E-01	
AXL	NVP-TAE226	7,1E-07	8,8E-08	7,7E-08	7,7E-08	≥ 4,5E+06	≥ 3,5E-01	
AXL	Pazopanib HCl	≈ 2,0E-05	≈ 2,5E-06	≈ 6,7E-07	≈ 1,6E-06	≥ 5,2E+05	≥ 3,5E-01	
AXL	PCI-32765 (Ibrutinib)	8,5E-06	1,0E-06	8,8E-07	8,8E-07	≥ 4,0E+05	≥ 3,5E-01	
AXL	PD 0332991 (Palbociclib) HCl	1,5E-05	1,9E-06	1,6E-06	1,6E-06	≥ 2,2E+05	≥ 3,5E-01	
AXL	PD153035 HCl	6,8E-06	8,4E-07	1,2E-06	1,2E-06	≥ 2,9E+05	≥ 3,5E-01	
AXL	PD173074	≈ 2,0E-05	≈ 2,5E-06	4,9E-06	4,9E-06	≥ 7,2E+04	≥ 3,5E-01	
AXL	PD318088	≈ 2,0E-05	≈ 2,5E-06	2,9E-06	2,9E-06	≥ 1,2E+05	≥ 3,5E-01	
AXL	Pelitinib (EKB-569)	7,6E-07	9,4E-08	1,3E-07	1,3E-07	1,0E+06	1,4E-01	
AXL	PF-00562271	2,0E-06	2,5E-07	3,1E-07	3,1E-07	≈ 1,7E+06	5,2E-01	
AXL	PF-03814735	7,0E-08	8,6E-09	1,4E-08	1,4E-08	≈ 2,5E+07	≥ 3,5E-01	
AXL	PHA-665752	2,9E-07	3,6E-08	5,3E-08	5,3E-08	≈ 1,3E+07	≈ 7,4E-01	
AXL	PHA-680632	6,2E-06	7,6E-07	4,1E-07	4,1E-07	2,5E+06	≈ 1,0E+00	
AXL	PHT-427	1,1E-05	1,4E-06	6,7E-06	6,7E-06	8,2E+04	5,6E-01	
AXL	PIK-75	1,4E-07	1,7E-08	2,9E-08	2,9E-08	≈ 2,4E+07	5,8E-01	2
AXL	Ponatinib (AP24534)	1,1E-06	1,4E-07	1,5E-07	1,5E-07	2,9E+06	4,4E-01	
AXL	PP-121	1,4E-05	1,8E-06	1,6E-06	1,6E-06	≈ 1,4E+05	≈ 2,2E-01	
AXL	PP242	1,5E-05	1,9E-06	8,3E-07	8,3E-07	≈ 5,0E+05	≈ 3,3E-01	
AXL	R406	1,1E-05	1,3E-06	1,8E-06	1,8E-06	2,6E+05	3,9E-01	
AXL	R788 (Fostatinib) - prodrug	1,1E-05	1,4E-06	1,6E-06	1,6E-06	≈ 1,6E+05	≈ 3,5E-01	
AXL	Ruxolitinib (INCB018424)	≥ 2,0E-05		2,3E-06	2,3E-06	≥ 1,5E+05	≥ 3,5E-01	
AXL	Saracatinib (AZD0530)	4,5E-06	5,6E-07	4,7E-07	4,7E-07	1,5E+06	6,7E-01	
AXL	SB590885	≥ 2,0E-05		4,3E-06	4,3E-06	≥ 8,1E+04	≥ 3,5E-01	
AXL	Semaxanib (SU5416)	1,2E-06	1,5E-07	4,1E-07	4,1E-07	7,3E+05	3,0E-01	
AXL	SGX-523	1,9E-05	2,3E-06	4,1E-06	4,1E-06	≥ 8,6E+04	≥ 3,5E-01	
AXL	SNS-314	7,2E-08	8,9E-09	1,1E-08	1,1E-08	3,3E+07	3,5E-01	
AXL	SP600125	3,5E-06	4,4E-07	6,9E-07	6,9E-07	1,1E+06	7,6E-01	
AXL	Staurosporine	2,6E-08	3,2E-09	2,0E-09	2,0E-09	4,6E+07	9,2E-02	
AXL	SU11274	1,3E-07	1,6E-08	3,2E-08	3,2E-08	≈ 1,0E+07	≈ 3,3E-01	
AXL	Sunitinib Malate (Sutent)	4,8E-08	5,9E-09	1,1E-08	1,1E-08	≈ 4,3E+07	≈ 5,3E-01	
AXL	TAE684 (NVP-TAE684)	1,8E-07	2,2E-08	1,2E-08	1,2E-08	≈ 1,6E+07	≈ 1,4E-01	
AXL	TAK-901	7,0E-08	8,6E-09	1,7E-08	1,7E-08	1,8E+07	3,2E-01	
AXL	Tandutinib (MLN518)	1,5E-05	1,8E-06	2,4E-06	2,4E-06	≥ 1,5E+05	≥ 3,5E-01	
AXL	TG101209	3,2E-07	3,9E-08	6,1E-08	6,1E-08	≈ 1,5E+07	≈ 9,0E-01	
AXL	TG101348 (SAR302503)	6,4E-07	7,9E-08	6,4E-08	6,4E-08	≥ 5,5E+06	≥ 3,5E-01	
AXL	Thiazovivin	≥ 2,0E-05		3,4E-06	3,4E-06	≥ 1,0E+05	≥ 3,5E-01	
AXL	Tivozanib (AV-951)	1,2E-07	1,5E-08	2,2E-08	2,2E-08	≈ 1,4E+07	≈ 3,8E-01	
AXL	Torin 2	2,0E-05	2,4E-06	2,1E-06	2,1E-06	≥ 1,7E+05	≥ 3,5E-01	
AXL	TPCA-1	≈ 1,3E-05	≈ 1,6E-06	1,7E-06	1,7E-06	≈ 5,5E+05	≈ 1,0E+00	
AXL	TSU-68 (SU6668)	7,2E-07	8,9E-08	2,9E-07	2,9E-07	≈ 9,3E+05	2,4E-01	
AXL	TWS119	8,9E-06	1,1E-06	2,0E-06	2,0E-06	≥ 1,7E+05	≥ 3,5E-01	
AXL	Vandetanib (Zactima)	9,9E-07	1,2E-07	1,7E-07	1,7E-07	2,5E+06	4,0E-01	
AXL	VX-680 (MK-0457 - Tozasertib)	3,4E-06	4,2E-07	5,1E-07	5,1E-07	≈ 2,1E+06	≈ 9,6E-01	
AXL	WHI-P154	4,2E-06	5,1E-07	1,1E-06	1,1E-06	≈ 3,3E+05	≈ 3,5E-01	
AXL	WZ3146	1,6E-06	1,9E-07	2,3E-07	2,3E-07	≈ 1,7E+06	≈ 4,0E-01	
AXL	WZ4002	≈ 1,4E-05	≈ 1,7E-06	2,1E-06	2,1E-06	≈ 8,3E+05	≈ 1,1E+00	
AXL	WZ8040	3,0E-06	3,7E-07	9,4E-07	9,4E-07	≈ 4,4E+05	≈ 3,1E-01	
AXL	XL-184 (Cabozantinib)	8,4E-10	1,0E-10	n.e.	1,0E-10	1,0E+07	≤ 1,1E-03	4
AXL	ZM-447439	4,4E-07	5,4E-08	2,3E-07	2,3E-07	≥ 1,6E+06	≥ 3,5E-01	1
BRAF	AEE788 (NVP-AEE788)	≥ 2,0E-05		3,4E-06	3,4E-06	7,8E+02	2,7E-03	
BRAF	Apatinib (YN968D1)	5,9E-06	2,9E-06	≈ 5,6E-06	2,9E-06	≥ 6,3E+04	≥ 3,5E-01	
BRAF	ARRY334543	≥ 2,0E-05		3,1E-06	3,1E-06	≥ 1,1E+05	≥ 3,5E-01	
BRAF	Arry-380	1,7E-05	8,3E-06	≥ 2,0E-05	≥ 8,3E-06			
BRAF	AS-252424	1,0E-05	5,1E-06	≥ 2,0E-05	≥ 5,1E-06			
BRAF	AT9283	3,5E-06	1,7E-06	1,7E-06	1,7E-06	≥ 2,0E+05	≥ 3,5E-01	
BRAF	Aurora A Inhibitor I	≥ 2,0E-05		5,7E-06	5,7E-06	≥ 6,1E+04	≥ 3,5E-01	
BRAF	AZ628	6,0E-09	2,9E-09	4,5E-09	4,5E-09	1,3E+05	5,7E-04	
BRAF	Barasertib (AZD1152-HQPA)	≥ 2,0E-05		5,9E-06	5,9E-06	≥ 5,9E+04	≥ 3,5E-01	
BRAF	BIRB 796 (Doramapimod)	1,0E-06	5,0E-07	n.e.	5,0E-07	n.e.	n.e.	

kinase	Compound	IC ₅₀ [M] ePCA	K _D eq [M] ePCA *	K _D kin [M] kPCA	K _D [M] PCA **	k _{on} [M ⁻¹ s ⁻¹] kPCA	k _{off} [s ⁻¹] kPCA	comment
BRAF	BKM120 (NVP-BKM120)	n.e.	n.e.	≥ 2,0E-05	≥ 2,0E-05			
BRAF	BMS 777607	1,3E-05	6,3E-06	≥ 2,0E-05	≥ 6,3E-06			
BRAF	BMS 794833	1,1E-06	5,2E-07	n.e.	5,2E-07	n.e.	n.e.	1
BRAF	Bosutinib (SKI-606)	6,6E-06	3,2E-06	≈ 1,5E-06	3,2E-06	≥ 2,4E+05	≥ 3,5E-01	
BRAF	CCT137690	4,5E-06	2,2E-06	5,5E-06	5,5E-06	≥ 6,4E+04	≥ 3,5E-01	
BRAF	CEP33779	≈ 2,7E-05	≈ 1,3E-05	3,7E-06	3,7E-06	≥ 9,5E+04	≥ 3,5E-01	
BRAF	CHIR-98014	1,6E-05	7,7E-06	≥ 2,0E-05	≈ 7,7E-06			
BRAF	Crenolanib (CP-868596)	≈ 2,8E-05	≈ 1,4E-05	≈ 4,8E-06	≈ 9,3E-06	≥ 7,3E+04	≥ 3,5E-01	
BRAF	CX-4945 (Silmisaterib)	≈ 2,6E-05	≈ 1,2E-05	4,9E-07	4,9E-07	n.e.	n.e.	
BRAF	CYC116	3,5E-06	1,7E-06	1,9E-06	1,9E-06	≥ 1,9E+05	≥ 3,5E-01	
BRAF	Cyt387	1,1E-05	5,3E-06	≈ 4,6E-06	5,3E-06	≥ 7,5E+04	≥ 3,5E-01	
BRAF	Dabrafenib (GSK2118436)	1,7E-09	8,4E-10	n.e.	8,4E-10	2,4E+05	≤ 2,0E-04	4
BRAF	Dasatinib (BMS-354825)	1,7E-07	8,2E-08	≈ 1,4E-07	8,2E-08	≥ 2,6E+06	≥ 3,5E-01	
BRAF	DCC-2036 (Rebastinib)	1,3E-07	6,1E-08	1,1E-07	1,1E-07	9,0E+03	9,4E-04	
BRAF	E7080 (Lenvatinib)	≥ 2,0E-05		5,3E-06	5,3E-06	≥ 6,6E+04	≥ 3,5E-01	
BRAF	Foretinib (GSK1363089 - XL880)	2,4E-05	1,2E-05	≥ 2,0E-05	≥ 1,2E-05			
BRAF	GDC-0879	4,5E-09	2,2E-09	1,7E-07	2,2E-09	n.e.	n.e.	
BRAF	Golvatinib (E7050)	1,2E-06	5,7E-07	n.e.	5,7E-07	n.e.	n.e.	
BRAF	Imatinib (Gleevec)	9,4E-06	4,6E-06	3,5E-06	3,5E-06	≥ 1,1E+05	≥ 3,5E-01	
BRAF	INK 128 (MLN0128)	≥ 2,8E-05		≥ 2,0E-05	≥ 1,4E-05			
BRAF	JNJ-7706621	3,6E-06	1,8E-06	n.e.	1,8E-06	n.e.	n.e.	
BRAF	LDN193189	9,1E-06	4,4E-06	≥ 2,0E-05	≥ 4,4E-06			
BRAF	LY2228820	9,7E-06	4,7E-06	2,6E-06	2,6E-06	≥ 1,3E+05	≥ 3,5E-01	
BRAF	LY2603618 (IC-83)	≥ 1,4E-05		≥ 2,0E-05	≥ 6,7E-06			
BRAF	LY2784544	2,0E-05	9,7E-06	5,0E-06	5,0E-06	≥ 7,1E+04	≥ 3,5E-01	
BRAF	Milciclib (PHA-848125)	2,5E-05	1,2E-05	6,4E-06	6,4E-06	≥ 5,5E+04	≥ 3,5E-01	
BRAF	Motesanib Diphosphate (AMG-706)	7,3E-06	3,5E-06	n.e.	3,5E-06	n.e.	n.e.	
BRAF	Nilotinib (AMN-107)	≈ 1,3E-05	≈ 6,2E-06	≈ 2,4E-06	≈ 4,3E-06	≥ 1,5E+05	≥ 3,5E-01	1
BRAF	NVP-BHG712	1,7E-07	8,3E-08	6,0E-06	8,3E-08	n.e.	n.e.	
BRAF	NVP-BSK805	1,5E-05	7,4E-06	4,1E-06	4,1E-06	≥ 8,6E+04	≥ 3,5E-01	
BRAF	OSI-930	3,3E-07	1,6E-07	≥ 2,0E-05	≥ 1,6E-07			1
BRAF	Pazopanib HCl	≈ 2,1E-06	≈ 1,0E-06	≈ 6,2E-07	≈ 8,2E-07	≈ 9,1E+04	≈ 5,7E-02	1
BRAF	PCI-32765 (Ibrutinib)	1,4E-06	6,7E-07	3,2E-07	3,2E-07	≈ 1,1E+05	≈ 4,2E-02	
BRAF	PF-03814735	1,2E-05	5,9E-06	≈ 6,4E-06	5,9E-06	≥ 5,5E+04	≥ 3,5E-01	
BRAF	PHA-767491	≥ 2,7E-05		≥ 2,0E-05	≥ 1,3E-05			
BRAF	PIK-75	8,9E-07	4,3E-07	≈ 2,9E-06	4,3E-07	n.e.	n.e.	
BRAF	PLX-4720	2,5E-08	1,2E-08	≤ 1,2E-10	1,2E-08	2,1E+06	2,5E-04	
BRAF	Ponatinib (AP24534)	1,6E-08	7,6E-09	n.e.	7,6E-09	4,6E+04	≤ 3,5E-04	4
BRAF	PP-121	4,5E-08	2,2E-08	1,8E-06	2,2E-08	n.e.	n.e.	
BRAF	PP242	3,9E-06	1,9E-06	3,4E-06	3,4E-06	≥ 1,0E+05	≥ 3,5E-01	
BRAF	Quercetin (Sophoretin)	1,6E-05	7,7E-06	3,1E-06	3,1E-06	≥ 1,1E+05	≥ 3,5E-01	
BRAF	R406	2,7E-05	1,3E-05	≥ 2,0E-05	≥ 1,3E-05			
BRAF	R788 (Fostatinib) - prodrug	1,6E-05	7,8E-06	≥ 2,0E-05	≥ 7,8E-06			
BRAF	Raf265 derivative	2,4E-06	1,2E-06	≥ 2,0E-05	≥ 1,2E-06			
BRAF	Ruxolitinib (INCB018424)	1,8E-05	8,9E-06	≥ 2,0E-05	≈ 8,9E-06			
BRAF	Saracatinib (AZD0530)	1,1E-05	5,2E-06	5,4E-06	5,4E-06	≥ 6,5E+04	≥ 3,5E-01	
BRAF	SB 202190	4,6E-07	2,2E-07	7,2E-07	7,2E-07	≥ 4,8E+05	≥ 3,5E-01	
BRAF	SB 203580	4,6E-07	2,3E-07	6,9E-07	6,9E-07	≥ 5,1E+05	≥ 3,5E-01	
BRAF	SB590885	≤ 7,6E-10	≤ 3,7E-10	4,5E-09	≤ 3,7E-10	8,7E+06	3,8E-02	
BRAF	SNS-032 (BMS-387032)	1,0E-05	4,9E-06	≥ 2,0E-05	≥ 4,9E-06			
BRAF	SNS-314	4,7E-06	2,3E-06	2,3E-06	2,3E-06	≥ 1,5E+05	≥ 3,5E-01	1
BRAF	TAK-901	1,1E-05	5,4E-06	≥ 2,0E-05	≥ 5,4E-06			
BRAF	TG 100713	1,2E-05	5,7E-06	≥ 2,0E-05	≥ 5,7E-06			
BRAF	TG100-115	5,0E-06	2,4E-06	≈ 5,8E-06	2,4E-06	≥ 6,0E+04	≥ 3,5E-01	
BRAF	TG101209	2,1E-05	1,0E-05	≈ 5,7E-06	1,0E-05	≥ 6,1E+04	≥ 3,5E-01	
BRAF	Tie2 kinase inhibitor	9,5E-06	4,6E-06	2,1E-06	2,1E-06	≥ 1,7E+05	≥ 3,5E-01	
BRAF	Tivozanib (AV-951)	5,7E-07	2,7E-07	≈ 1,3E-06	2,7E-07	≈ 6,4E+03	≈ 8,2E-03	
BRAF	TPCA-1	1,3E-06	6,5E-07	2,5E-07	2,5E-07	≥ 1,4E+06	≥ 3,5E-01	
BRAF	TWS119	1,9E-06	9,1E-07	2,2E-06	2,2E-06	≥ 1,6E+05	≥ 3,5E-01	
BRAF	Vemurafenib (PLX4032)	4,2E-09	2,0E-09	n.e.	2,0E-09	2,1E+05	≤ 4,2E-04	4
BRAF	ZM 336372	2,6E-07	1,2E-07	≥ 2,0E-05	≥ 1,2E-07			
BTK	AEE788 (NVP-AEE788)	≥ 2,0E-05		1,1E-06	1,1E-06	3,1E+05	3,3E-01	
BTK	AMG 900	≥ 2,0E-05		≈ 9,5E-06	≈ 9,5E-06	≥ 3,7E+04	≥ 3,5E-01	
BTK	ARRY334543	≥ 2,0E-05		7,9E-06	7,9E-06	n.e.	n.e.	
BTK	AST-1306	≥ 1,1E-05		≥ 2,0E-05	≥ 4,9E-07			
BTK	AT9283	1,9E-06	8,9E-08	7,1E-08	7,1E-08	5,2E+05	3,7E-02	2
BTK	Aurora A Inhibitor I	≥ 2,0E-05		3,5E-06	3,5E-06	n.e.	n.e.	2
BTK	AZ 960	≥ 2,0E-05		8,7E-07	8,7E-07	5,6E+04	4,9E-02	2
BTK	AZD4547	≥ 2,0E-05		1,5E-06	1,5E-06	≈ 4,9E+05	≈ 7,5E-01	
BTK	AZD5438	≥ 2,0E-05		3,2E-06	3,2E-06	≥ 1,1E+05	≥ 3,5E-01	
BTK	AZD7762	8,8E-07	4,1E-08	6,6E-08	6,6E-08	3,8E+05	2,4E-02	2
BTK	AZD8931	≥ 2,0E-05		1,1E-06	1,1E-06	7,6E+04	8,5E-02	
BTK	Barasertib (AZD1152-HQPA)	≥ 2,0E-05		1,0E-06	1,0E-06	7,8E+04	8,2E-02	
BTK	BIBF1120 (Vargatef)	1,8E-06	8,5E-08	8,0E-08	8,0E-08	5,7E+05	4,4E-02	12
BTK	BIX 02188	≥ 2,0E-05		2,5E-06	2,5E-06	≈ 1,0E+05	≈ 2,1E-01	
BTK	BMS 777607	≥ 2,0E-05		3,8E-06	3,8E-06	≥ 9,1E+04	≥ 3,5E-01	
BTK	BMS-599626 (AC480)	≥ 2,0E-05		9,3E-06	9,3E-06	≥ 3,8E+04	≥ 3,5E-01	
BTK	Bosutinib (SKI-606)	6,7E-08	3,1E-09	6,1E-09	6,1E-09	1,8E+06	1,1E-02	
BTK	BX-795	≥ 2,0E-05		8,4E-06	8,4E-06	≥ 4,2E+04	≥ 3,5E-01	

kinase	Compound	IC ₅₀ [M] ePCA	K _D eq [M] ePCA *	K _D kin [M] kPCA	K _D [M] PCA **	k _{on} [M ⁻¹ s ⁻¹] kPCA	k _{off} [s ⁻¹] kPCA	comment
BTK	BX-912	≥ 2,0E-05		1,8E-06	1,8E-06	≈ 1,3E+05	≈ 2,2E-01	
BTK	Cediranib (AZD2171)	≥ 2,0E-05		1,2E-06	1,2E-06	1,8E+05	2,2E-01	
BTK	CEP33779	≥ 2,0E-05		4,5E-06	4,5E-06	≥ 7,8E+04	≥ 3,5E-01	
BTK	CHIR-124	≥ 2,0E-05		4,4E-06	4,4E-06	2,3E+03	9,4E-03	
BTK	CI-1033 (Canertinib)	7,5E-07	3,5E-08	n.e.	3,5E-08	1,8E+04	≤ 6,4E-04	124
BTK	CP-724714	≥ 2,0E-05		1,1E-05	1,1E-05	n.e.	n.e.	
BTK	Crizotinib (PF-02341066)	≥ 2,0E-05		3,9E-06	3,9E-06	≥ 9,0E+04	≥ 3,5E-01	
BTK	CX-4945 (Silmitasertib)	≥ 2,0E-05		5,9E-06	5,9E-06	≈ 2,7E+04	≈ 1,8E-01	
BTK	CYC116	≥ 2,0E-05		1,6E-06	1,6E-06	1,8E+05	2,9E-01	
BTK	Dabrafenib (GSK2118436)	2,7E-06	1,2E-07	1,2E-07	1,2E-07	4,2E+05	5,0E-02	
BTK	Danuseritib (PHA-739358)	≈ 1,8E-05	≈ 8,5E-07	6,7E-07	6,7E-07	3,8E+05	2,6E-01	
BTK	Dasatinib (BMS-354825)	8,8E-09	4,1E-10	2,3E-10	2,3E-10	6,8E+06	1,5E-03	
BTK	DCC-2036 (Rebastinib)	1,1E-05	5,3E-07	5,7E-07	5,7E-07	1,3E+04	7,5E-03	
BTK	Desmethyl Erlotinib (CP-473420)	≥ 2,0E-05		3,8E-06	3,8E-06	9,8E+04	3,5E-01	
BTK	Dovitinib (TKI-258)	2,0E-05	9,3E-07	9,1E-07	9,1E-07	8,6E+05	7,5E-01	
BTK	E7080 (Lenvatinib)	≥ 2,0E-05		5,0E-06	5,0E-06	1,1E+04	5,7E-02	
BTK	ENMD-2076	8,7E-06	4,0E-07	2,8E-07	2,8E-07	1,0E+06	2,7E-01	
BTK	Erlotinib HCl	≥ 2,0E-05		4,0E-06	4,0E-06	≥ 8,7E+04	≥ 3,5E-01	
BTK	Foretinib (GSK1363089 - XL880)	4,3E-07	2,0E-08	2,8E-08	2,8E-08	4,2E+05	1,2E-02	
BTK	GDC-0980 (RG7422)	≈ 1,2E-05	≈ 5,8E-07	3,7E-07	3,7E-07	9,0E+04	3,4E-02	2
BTK	Gefitinib (Iressa)	≥ 2,0E-05		2,7E-06	2,7E-06	≥ 1,3E+05	≥ 3,5E-01	
BTK	Golvatinib (E7050)	≥ 2,0E-05		4,3E-06	4,3E-06	≥ 8,2E+04	≥ 3,5E-01	
BTK	GSK1059615	≥ 2,0E-05		6,8E-06	6,8E-06	≥ 5,1E+04	≥ 3,5E-01	
BTK	GSK1070916	≥ 2,0E-05		7,0E-06	7,0E-06	n.e.	n.e.	
BTK	Hesperadin	6,4E-07	3,0E-08	2,1E-08	2,1E-08	3,2E+06	6,7E-02	
BTK	JNJ-7706621	≥ 2,0E-05		1,2E-06	1,2E-06	8,6E+04	1,0E-01	
BTK	Ki8751	≥ 2,0E-05		2,1E-06	2,1E-06	≈ 1,3E+05	≈ 1,9E-01	2
BTK	KW 2449	≈ 1,3E-05	≈ 6,0E-07	6,8E-06	6,8E-06	n.e.	n.e.	
BTK	LY2784544	≥ 2,0E-05		1,3E-06	1,3E-06	≈ 1,0E+06	≈ 1,3E+00	
BTK	MGCD-265	≥ 2,0E-05		4,1E-06	4,1E-06	1,8E+04	7,5E-02	2
BTK	Milciclib (PHA-848125)	≥ 2,0E-05		1,5E-06	1,5E-06	1,1E+05	1,7E-01	
BTK	MK-5108 (VX-689)	1,5E-06	7,0E-08	1,2E-07	1,2E-07	≈ 5,1E+06	≈ 5,3E-01	
BTK	MLN8054	≥ 2,0E-05		2,1E-06	2,1E-06	≈ 6,2E+04	≈ 1,2E-01	
BTK	MLN8237 (Alisertib)	≥ 2,0E-05		1,2E-06	1,2E-06	≥ 3,0E+05	≥ 3,5E-01	
BTK	Neratinib (HKI-272)	≥ 2,0E-05		6,1E-06	6,1E-06	≈ 2,6E+04	≈ 1,4E-01	
BTK	NVP-ADW742	≥ 2,0E-05		7,1E-07	7,1E-07	7,9E+04	5,6E-02	2
BTK	NVP-BSK805	1,4E-05	6,3E-07	5,6E-07	5,6E-07	4,7E+05	2,7E-01	
BTK	NVP-TAE226	≈ 1,5E-05	≈ 6,8E-07	1,8E-07	1,8E-07	4,5E+05	8,3E-02	
BTK	Pazopanib HCl	≥ 2,0E-05		1,6E-06	1,6E-06	8,5E+04	1,4E-01	2
BTK	PCI-32765 (Ibrutinib)	≤ 8,3E-10	≤ 3,9E-11	n.e.	≤ 3,9E-11	6,0E+05	≤ 2,3E-05	4
BTK	PD153035 HCl	≥ 2,0E-05		6,7E-06	6,7E-06	≥ 5,2E+04	≥ 3,5E-01	
BTK	PD173074	n.e.	n.e.	≥ 2,0E-05	≥ 2,0E-05			
BTK	Pelitinib (EKB-569)	1,2E-05	5,5E-07	2,0E-06	2,0E-06	3,1E+04	6,1E-02	
BTK	PF-00562271	≥ 2,0E-05		8,9E-07	8,9E-07	≈ 9,0E+04	7,6E-02	2
BTK	PF-03814735	4,8E-06	2,2E-07	1,9E-07	1,9E-07	1,2E+06	2,3E-01	
BTK	PHA-680632	1,7E-05	7,8E-07	7,4E-07	7,4E-07	1,0E+05	7,5E-02	
BTK	PIK-75	≥ 2,0E-05		1,8E-06	1,8E-06	≥ 1,9E+05	≥ 3,5E-01	
BTK	PLX-4720	≥ 2,0E-05		7,7E-06	7,7E-06	≥ 4,5E+04	≥ 3,5E-01	
BTK	Ponatinib (AP24534)	≈ 7,3E-06	≈ 3,4E-07	1,7E-07	1,7E-07	1,3E+05	2,2E-02	1
BTK	PP-121	9,4E-06	4,4E-07	5,1E-07	5,1E-07	9,0E+04	4,6E-02	
BTK	PP242	≥ 2,0E-05		1,2E-06	1,2E-06	5,9E+04	7,2E-02	
BTK	R406	≥ 2,0E-05		2,3E-06	2,3E-06	3,5E+05	5,5E-01	2
BTK	R788 (Fostamatinib) - prodrug	≥ 2,0E-05		2,8E-06	2,8E-06	≥ 1,4E+05	≥ 3,5E-01	
BTK	Saracatinib (AZD0530)	7,4E-06	3,4E-07	2,9E-07	2,9E-07	4,3E+05	1,2E-01	
BTK	Staurosporine	4,2E-07	1,9E-08	1,8E-08	1,8E-08	2,8E+06	4,9E-02	
BTK	Sunitinib Malate (Sutent)	≥ 2,0E-05		1,1E-06	1,1E-06	≥ 3,3E+05	≥ 3,5E-01	
BTK	TAE684 (NVP-TAE684)	2,8E-06	1,3E-07	5,7E-08	5,7E-08	5,8E+05	3,3E-02	
BTK	TAK-285	≥ 2,0E-05		4,7E-06	4,7E-06	≈ 4,3E+04	≈ 1,7E-01	
BTK	TAK-901	4,2E-07	2,0E-08	3,5E-08	3,5E-08	1,7E+06	5,7E-02	
BTK	TG101209	7,9E-06	3,7E-07	3,1E-07	3,1E-07	2,3E+06	7,2E-01	
BTK	TG101348 (SAR302503)	≥ 2,0E-05		1,1E-06	1,1E-06	1,9E+05	2,0E-01	
BTK	Tivozanib (AV-951)	≥ 2,0E-05		5,2E-07	5,2E-07	1,5E+05	7,8E-02	
BTK	Torin 1	≥ 2,0E-05		4,7E-06	4,7E-06	8,4E+02	4,0E-03	
BTK	TPCA-1	≈ 1,6E-05	≈ 7,4E-07	4,8E-07	4,8E-07	1,2E+05	5,8E-02	
BTK	TWS119	≈ 1,1E-05	≈ 4,9E-07	7,3E-07	7,3E-07	1,7E+05	1,3E-01	1
BTK	Vandetanib (Zactima)	1,6E-05	7,6E-07	5,1E-07	5,1E-07	2,8E+05	1,4E-01	
BTK	VX-680 (MK-0457 - Tozasertib)	≥ 2,0E-05		1,5E-06	1,5E-06	≈ 3,8E+05	≈ 5,9E-01	
BTK	WHI-P154	≥ 2,0E-05		5,7E-06	5,7E-06	≥ 6,2E+04	≥ 3,5E-01	
BTK	WZ3146	1,6E-09	7,6E-11	n.e.	7,6E-11	5,2E+05	≥ 4,0E-05	24
BTK	WZ4002	1,9E-07	8,9E-09	≈ 4,1E-08	8,9E-09	1,0E+04	≈ 5,8E-04	
BTK	WZ8040	≤ 9,0E-10	≤ 4,2E-11	n.e.	≤ 4,2E-11	3,3E+05	≤ 1,4E-05	24
BTK	XL-184 (Cabozantinib)	≥ 2,0E-05		6,2E-07	6,2E-07	1,9E+05	1,2E-01	2
BTK	ZM-447439	≥ 2,0E-05		9,9E-07	9,9E-07	≈ 5,2E+05	≈ 5,1E-01	
CDK2	A-674563	≈ 1,5E-05	≈ 6,9E-06	2,4E-06	2,4E-06	4,7E+02	1,1E-03	
CDK2	AS-252424	≥ 2,0E-05		2,3E-06	2,3E-06	1,3E+03	3,1E-03	
CDK2	AS-605240	≥ 2,0E-05		3,2E-06	3,2E-06	1,3E+03	4,2E-03	
CDK2	AT7519	3,6E-07	1,6E-07	1,2E-07	1,2E-07	8,2E+04	9,3E-03	12
CDK2	AT9283	≈ 8,6E-07	≈ 3,9E-07	3,8E-07	3,8E-07	2,9E+04	1,1E-02	
CDK2	AZ 960	7,9E-07	3,6E-07	6,2E-07	6,2E-07	1,6E+04	9,5E-03	

kinase	Compound	IC ₅₀ [M] ePCA	K _D eq [M] ePCA *	K _D kin [M] kPCA	K _D [M] PCA **	k _{on} [M ⁻¹ s ⁻¹] kPCA	k _{off} [s ⁻¹] kPCA	comment
CDK2	AZD4547	≈ 1,0E-05	≈ 4,7E-06	3,1E-06	3,1E-06	1,9E+03	5,6E-03	2
CDK2	AZD5438	≈ 5,2E-08	≈ 2,4E-08	1,2E-07	1,2E-07	9,0E+04	1,1E-02	2
CDK2	BMS 794833	≈ 7,6E-07	≈ 3,5E-07	5,4E-07	5,4E-07	1,6E+04	8,7E-03	
CDK2	BMS-265246	2,2E-08	1,0E-08	5,1E-08	5,1E-08	2,3E+05	1,2E-02	12
CDK2	Bosutinib (SKI-606)	≥ 2,0E-05		2,1E-06	2,1E-06	1,6E+03	3,5E-03	
CDK2	BX-795	7,9E-07	3,6E-07	2,5E-07	2,5E-07	4,0E+04	1,0E-02	
CDK2	BX-912	2,9E-06	1,3E-06	1,0E-06	1,0E-06	9,8E+03	9,8E-03	1
CDK2	CEP33779	≈ 5,8E-06	≈ 2,7E-06	2,7E-06	2,7E-06	1,8E+03	4,8E-03	
CDK2	CHIR-124	3,4E-07	1,6E-07	5,2E-07	5,2E-07	1,6E+04	8,4E-03	
CDK2	CP 673451	6,6E-08	3,0E-08	6,3E-08	6,3E-08	1,7E+05	1,0E-02	2
CDK2	Crenolanib (CP-868596)	5,3E-08	2,4E-08	8,0E-08	8,0E-08	1,0E+05	8,2E-03	2
CDK2	CX-4945 (Silmatasertib)	7,9E-08	3,6E-08	1,5E-07	1,5E-07	5,4E+04	8,2E-03	
CDK2	CYC116	4,1E-07	1,9E-07	4,5E-07	4,5E-07	2,2E+04	9,8E-03	
CDK2	Cyt387	2,2E-06	1,0E-06	8,0E-07	8,0E-07	1,4E+04	1,1E-02	
CDK2	Dabrafenib (GSK2118436)	≈ 2,3E-08	≈ 1,1E-08	2,0E-07	2,0E-07	3,0E+04	5,5E-03	
CDK2	DCC-2036 (Rebastinib)	3,1E-08	1,4E-08	3,6E-08	3,6E-08	5,1E+04	1,9E-03	2
CDK2	Dinaciclib (SCH727965)	9,4E-08	4,3E-08	7,5E-08	7,5E-08	1,4E+05	1,0E-02	2
CDK2	Dovitinib (TKI-258)	1,8E-05	8,3E-06	4,8E-06	4,8E-06	1,0E+03	4,9E-03	
CDK2	Flavopiridol HCl	9,4E-07	4,3E-07	8,2E-07	8,2E-07	1,4E+04	1,2E-02	1
CDK2	GDC-0879	2,0E-05	9,1E-06	2,5E-06	2,5E-06	n.e.	n.e.	
CDK2	Golvatinib (E7050)	6,2E-06	2,9E-06	2,6E-06	2,6E-06	1,8E+03	4,7E-03	2
CDK2	GSK1059615	≥ 2,0E-05		4,5E-06	4,5E-06	2,1E+03	8,5E-03	
CDK2	GSK690693	≥ 2,0E-05		4,1E-06	4,1E-06	5,8E+02	2,5E-03	
CDK2	Hesperadin	1,5E-05	7,0E-06	2,6E-06	2,6E-06	3,2E+03	8,3E-03	
CDK2	JNJ-7706621	5,6E-08	2,6E-08	1,6E-08	1,6E-08	5,3E+05	8,5E-03	2
CDK2	KW 2449	4,4E-06	2,0E-06	n.e.	2,0E-06	1,0E+03	≤ 2,0E-03	4
CDK2	Linifanib (ABT-869)	1,3E-05	6,0E-06	1,7E-06	1,7E-06	1,3E+03	2,2E-03	
CDK2	LY2784544	1,7E-06	7,7E-07	4,4E-07	4,4E-07	1,8E+04	7,7E-03	
CDK2	Miliciclib (PHA-848125)	≈ 5,8E-07	≈ 2,7E-07	3,3E-07	3,3E-07	4,1E+04	1,3E-02	2
CDK2	MK-2461	≥ 2,0E-05		3,6E-06	3,6E-06	1,8E+03	6,3E-03	
CDK2	MK-5108 (VX-689)	≈ 1,4E-06	≈ 6,3E-07	8,6E-07	8,6E-07	1,6E+04	1,4E-02	
CDK2	Neratinib (HKI-272)	≥ 2,0E-05		3,5E-06	3,5E-06	1,6E+03	5,7E-03	
CDK2	NVP-BGT226	≥ 2,0E-05		2,9E-06	2,9E-06	1,7E+03	5,0E-03	
CDK2	NVP-TAE226	≥ 2,0E-05		3,8E-06	3,8E-06	1,1E+03	4,4E-03	
CDK2	PD 0332991 (Palbociclib) HCl	5,9E-06	2,7E-06	2,4E-06	2,4E-06	2,7E+03	6,6E-03	
CDK2	PF-00562271	1,1E-07	5,2E-08	1,6E-07	1,6E-07	5,9E+04	9,6E-03	2
CDK2	PF-03814735	1,2E-07	5,7E-08	3,2E-07	5,7E-08	3,8E+04	1,2E-02	2
CDK2	PHA-767491	1,9E-05	8,7E-06	3,6E-06	3,6E-06	9,9E+02	3,5E-03	
CDK2	PHA-793887	1,7E-07	7,9E-08	1,1E-07	1,1E-07	5,5E+04	5,6E-03	2
CDK2	PIK-75	≈ 1,0E-06	≈ 4,8E-07	5,9E-07	5,9E-07	2,1E+04	1,3E-02	2
CDK2	PLX-4720	≥ 2,0E-05		2,6E-06	2,6E-06	3,1E+03	8,0E-03	
CDK2	Ponatinib (AP24534)	7,3E-06	3,3E-06	1,2E-06	1,2E-06	8,8E+03	1,0E-02	
CDK2	PP242	1,3E-05	6,1E-06	n.e.	6,1E-06	1,5E+03	≤ 9,1E-03	4
CDK2	Quercetin (Sphoretin)	≈ 6,5E-06	≈ 3,0E-06	2,5E-06	2,5E-06	1,4E+03	3,5E-03	
CDK2	Raf265 derivative	≥ 2,0E-05		3,5E-06	3,5E-06	1,0E+03	3,3E-03	
CDK2	Roscovitine (Seliciclib - CYC202)	≥ 2,0E-05		2,1E-06	2,1E-06	4,8E+03	9,3E-03	
CDK2	Saracatinib (AZD0530)	≥ 2,0E-05		3,1E-06	3,1E-06	1,3E+03	3,4E-03	
CDK2	SB 216763	≥ 2,0E-05		2,5E-06	2,5E-06	2,6E+03	6,3E-03	
CDK2	SB 415286	2,6E-06	1,2E-06	≥ 2,0E-05	≥ 1,2E-06			
CDK2	SNS-032 (BMS-387032)	≈ 2,5E-07	≈ 1,1E-07	1,2E-07	1,2E-07	8,6E+04	9,7E-03	2
CDK2	SNS-314	1,3E-05	6,1E-06	3,3E-06	3,3E-06	4,3E+02	1,4E-03	
CDK2	Sotrastaurin (AEB071)	≥ 2,0E-05		2,4E-06	2,4E-06	2,2E+03	5,4E-03	
CDK2	SP600125	≥ 2,0E-05		2,7E-06	2,7E-06	2,4E+03	6,3E-03	
CDK2	Staurosporine	1,0E-08	4,8E-09	5,2E-09	5,2E-09	8,2E+05	4,1E-03	2
CDK2	TAE684 (NVP-TAE684)	9,2E-06	4,2E-06	1,3E-06	1,3E-06	8,7E+03	1,1E-02	
CDK2	TAK-901	2,4E-06	1,1E-06	1,8E-06	1,8E-06	3,9E+03	6,9E-03	
CDK2	TG101209	1,1E-05	4,9E-06	2,4E-06	2,4E-06	1,7E+03	4,0E-03	
CDK2	Thiazovivin	9,5E-06	4,4E-06	3,0E-06	3,0E-06	1,2E+03	3,5E-03	
CDK2	TPCA-1	≈ 1,2E-05	≈ 5,6E-06	2,3E-06	2,3E-06	3,4E+03	7,7E-03	
CDK2	Tyrphostin AG 879 (AG 879)	≈ 1,0E-05	≈ 4,8E-06	≈ 6,2E-06	≈ 5,5E-06	4,2E+02	≈ 3,1E-03	
CDK2	VX-680 (MK-0457 - Tozasertib)	9,9E-06	4,5E-06	≈ 2,1E-06	4,5E-06	5,3E+02	≈ 1,1E-03	
CDK2	WZ3146	1,1E-05	5,1E-06	2,9E-06	2,9E-06	1,3E+03	3,8E-03	
CDK2	XL765	≥ 2,0E-05		1,7E-06	1,7E-06	7,8E+02	1,4E-03	
CDK9	A-674563	9,1E-08	2,4E-08	3,9E-08	3,9E-08	3,8E+05	1,4E-02	
CDK9	A-769662	3,9E-05	1,0E-05	≥ 2,0E-05	≥ 1,0E-05			
CDK9	AEE788 (NVP-AEE788)	9,0E-06	2,3E-06	1,3E-06	1,3E-06	≈ 3,4E+04	4,0E-02	
CDK9	Arry-380	1,9E-05	4,9E-06	≥ 2,0E-05	≥ 4,9E-06			
CDK9	AS-252424	3,6E-05	9,2E-06	≈ 5,8E-06	9,2E-06	≈ 2,2E+03	≈ 1,3E-02	
CDK9	AS-605240	5,2E-06	1,4E-06	7,5E-07	7,5E-07	3,3E+04	≈ 3,1E-02	
CDK9	AST-1306	4,2E-05	1,1E-05	≈ 1,9E-06	1,1E-05	9,8E+02	≈ 1,3E-03	
CDK9	AT7519	8,7E-09	2,3E-09	1,2E-09	1,2E-09	1,4E+06	3,1E-03	
CDK9	AT9283	8,6E-07	2,2E-07	1,1E-07	1,1E-07	8,9E+04	2,0E-02	
CDK9	Aurora A Inhibitor I	1,2E-05	3,1E-06	n.e.	3,1E-06	2,3E+03	≤ 7,0E-03	4
CDK9	AZ 960	1,9E-06	4,8E-07	6,6E-07	6,6E-07	3,2E+04	2,1E-02	
CDK9	AZD4547	≥ 2,0E-05		2,4E-06	2,4E-06	≈ 5,7E+02	≈ 1,9E-03	
CDK9	AZD5438	7,2E-08	1,9E-08	3,3E-08	3,3E-08	5,9E+05	2,0E-02	
CDK9	BI 2536	4,2E-05	1,1E-05	n.e.	1,1E-05	3,6E+02	≤ 3,9E-03	4
CDK9	BI6727 (Volasertib)	1,2E-05	3,1E-06	n.e.	3,1E-06	1,7E+03	≤ 5,1E-03	4
CDK9	BIRB 796 (Doramapimod)	8,6E-06	2,2E-06	n.e.	2,2E-06	n.e.	n.e.	

kinase	Compound	IC ₅₀ [M] ePCA	K _D eq [M] ePCA *	K _D kin [M] kPCA	K _D [M] PCA **	k _{on} [M ⁻¹ s ⁻¹] kPCA	k _{off} [s ⁻¹] kPCA	comment
CDK9	BMS-265246	7,6E-08	2,0E-08	2,2E-08	2,2E-08	1,1E+06	2,2E-02	
CDK9	BS-181 HCl	3,3E-06	8,6E-07	6,6E-07	6,6E-07	3,7E+04	2,4E-02	
CDK9	BX-795	5,7E-07	1,6E-07	1,6E-07	1,6E-07	9,8E+04	1,6E-02	
CDK9	BX-912	2,7E-06	7,1E-07	8,3E-07	8,3E-07	4,0E+04	3,2E-02	
CDK9	CCT129202	1,7E-06	4,4E-07	1,8E-06	1,8E-06	4,8E+03	5,4E-03	1
CDK9	CCT137690	3,3E-06	8,5E-07	1,7E-06	1,7E-06	3,0E+04	4,1E-02	
CDK9	CEP33779	1,7E-05	4,4E-06	1,9E-06	1,9E-06	1,8E+03	8,0E-03	3
CDK9	CHIR-124	1,4E-07	3,8E-08	2,9E-08	2,9E-08	2,6E+05	9,8E-03	
CDK9	CHIR-98014	2,1E-07	5,5E-08	1,1E-07	1,1E-07	9,0E+04	9,7E-03	
CDK9	CP 673451	3,1E-07	8,0E-08	7,0E-08	7,0E-08	2,5E+05	1,8E-02	
CDK9	Crenolanib (CP-868596)	3,1E-07	8,1E-08	5,4E-08	5,4E-08	1,8E+05	9,8E-03	
CDK9	Crizotinib (PF-02341066)	4,4E-05	1,1E-05	≈ 1,0E-05	1,1E-05	≈ 4,6E+02	≈ 4,8E-03	
CDK9	CX-4945 (Siltitasertib)	4,1E-07	1,1E-07	3,7E-07	3,7E-07	4,6E+04	1,7E-02	1
CDK9	CYC116	8,8E-07	2,3E-07	1,8E-07	1,8E-07	9,0E+04	1,6E-02	
CDK9	Cyt387	2,6E-07	6,8E-08	8,4E-08	8,4E-08	1,8E+05	1,5E-02	
CDK9	DCC-2036 (Rebastinib)	8,8E-06	2,3E-06	n.e.	2,3E-06	8,9E+02	≤ 2,0E-03	4
CDK9	Dinaciclib (SCH727965)	5,0E-09	1,3E-09	1,2E-09	1,2E-09	1,0E+06	1,2E-03	
CDK9	Enzastaurin (LY317615)	≥ 2,0E-05		1,9E-06	1,9E-06	1,4E+04	2,3E-02	
CDK9	Flavopiridol HCl	2,6E-09	6,8E-10	1,8E-09	1,8E-09	1,7E+06	2,8E-03	
CDK9	GDC-0941	≥ 2,0E-05		4,1E-06	4,1E-06	≈ 1,1E+04	≈ 3,7E-02	
CDK9	GDC-0980 (RG7422)	2,6E-05	6,9E-06	≥ 2,0E-05	≥ 6,9E-06			
CDK9	Golvtatinib (E7050)	2,9E-05	7,5E-06	≥ 2,0E-05	≥ 7,5E-06			
CDK9	GSK1059615	1,1E-06	2,8E-07	2,2E-07	2,2E-07	5,4E+05	1,1E-01	1
CDK9	Hesperadin	6,8E-06	1,8E-06	7,1E-07	7,1E-07	2,1E+04	1,5E-02	
CDK9	JNJ-7706621	5,8E-08	1,5E-08	≈ 1,2E-08	1,5E-08	1,1E+06	1,6E-02	
CDK9	KW 2449	1,9E-05	4,9E-06	≈ 1,1E-05	4,9E-06	≈ 6,5E+02	≈ 6,8E-03	
CDK9	LDN193189	6,4E-06	1,7E-06	n.e.	1,7E-06	1,6E+03	≤ 2,6E-03	14
CDK9	LY2784544	4,0E-06	1,0E-06	3,6E-07	3,6E-07	2,8E+04	1,0E-02	
CDK9	Milciclib (PHA-848125)	6,1E-06	1,6E-06	1,0E-06	1,0E-06	1,5E+04	1,4E-02	
CDK9	NVP-BGT226	3,4E-05	8,8E-06	≥ 2,0E-05	≥ 8,8E-06			
CDK9	Pazopanib HCl	7,0E-06	1,8E-06	9,1E-07	9,1E-07	≈ 3,5E+04	≈ 4,6E-02	
CDK9	PD 0332991 (Palbociclib) HCl	2,1E-06	5,4E-07	3,8E-07	3,8E-07	5,7E+04	2,2E-02	
CDK9	Pelitinib (EKB-569)	1,4E-05	3,6E-06	1,7E-06	1,7E-06	2,2E+03	3,9E-03	
CDK9	PF-00562271	1,5E-07	3,9E-08	5,4E-08	5,4E-08	2,3E+05	1,2E-02	
CDK9	PF-03814735	1,7E-06	4,3E-07	5,3E-07	5,3E-07	3,9E+04	2,0E-02	
CDK9	PHA-665752	4,4E-06	1,2E-06	1,0E-06	1,0E-06	3,9E+04	3,5E-02	
CDK9	PHA-767491	3,0E-08	7,8E-09	8,1E-09	8,1E-09	2,1E+06	1,7E-02	
CDK9	PHA-793887	5,0E-07	1,3E-07	4,9E-08	4,9E-08	1,2E+05	6,0E-03	
CDK9	Piceatannol	9,2E-06	2,4E-06	1,6E-07	2,4E-06	2,6E+04	4,1E-03	2
CDK9	PIK-75	1,4E-09	3,8E-10	n.e.	3,8E-10	1,1E+07	≤ 4,3E-03	4
CDK9	PP-121	≥ 2,0E-05		3,8E-06	3,8E-06	2,3E+03	7,9E-03	
CDK9	PP242	2,6E-05	6,9E-06	n.e.	6,9E-06	1,7E+03	≤ 1,1E-02	4
CDK9	Quercetin (Sophoretin)	2,2E-06	5,7E-07	8,1E-07	8,1E-07	6,3E+03	3,6E-03	
CDK9	Roscovitine (Seliciclib - CYC202)	1,7E-06	4,5E-07	3,0E-07	3,0E-07	8,8E+04	2,5E-02	
CDK9	SAR131675	≥ 3,8E-05		≥ 2,0E-05	≥ 9,9E-06			
CDK9	SB 415286	1,3E-05	3,4E-06	1,2E-06	1,2E-06	1,3E+03	1,6E-03	
CDK9	SB590885	≈ 4,1E-05	≈ 1,1E-05	≈ 1,3E-05	≈ 1,2E-05	≈ 5,4E+02	≈ 7,1E-03	
CDK9	SNS-032 (BMS-387032)	4,9E-08	1,3E-08	4,7E-09	4,7E-09	1,3E+06	6,3E-03	
CDK9	Sotrastaurin (AEB071)	3,1E-05	8,1E-06	≈ 3,2E-06	8,1E-06	≈ 3,5E+03	≈ 1,1E-02	
CDK9	Stauroporine	5,1E-08	1,3E-08	4,9E-09	4,9E-09	1,1E+06	5,5E-03	
CDK9	Sunitinib Malate (Sutent)	1,4E-05	3,5E-06	2,0E-06	2,0E-06	2,6E+04	9,2E-02	
CDK9	TAK-901	4,3E-07	1,1E-07	2,3E-07	2,3E-07	5,2E+04	1,2E-02	
CDK9	TG101348 (SAR302503)	3,6E-05	9,4E-06	n.e.	9,4E-06	4,5E+02	≤ 1,0E-03	4
CDK9	Thiazovivin	1,9E-06	5,0E-07	5,6E-07	5,6E-07	3,1E+04	1,7E-02	
CDK9	TPCA-1	≈ 4,4E-05	≈ 1,1E-05	≈ 5,5E-06	≈ 8,4E-06	4,4E+02	≈ 3,2E-03	
CDK9	TWS119	3,7E-06	9,7E-07	4,0E-07	4,0E-07	5,4E+04	2,0E-02	
CDK9	WZ3146	1,5E-05	4,0E-06	2,4E-06	2,4E-06	9,8E+03	2,4E-02	
CDK9	WZ8040	1,8E-05	4,7E-06	2,4E-06	2,4E-06	3,2E+03	1,5E-02	
CDK9	Y-27632 2HCl	4,2E-05	1,1E-05	n.e.	1,1E-05	8,2E+02	≤ 8,8E-03	4
EGFR	A-769662	9,3E-07	4,7E-07	2,1E-06	2,1E-06	≈ 6,2E+03	≈ 9,7E-03	
EGFR	AEE788 (NVP-AEE788)	4,2E-10	2,1E-10	5,1E-10	5,1E-10	2,3E+07	1,2E-02	
EGFR	Afatinib (BIBW2992)	≤ 7,3E-11	≤ 3,7E-11	n.e.	≤ 3,7E-11	1,2E+07	≤ 4,3E-04	4
EGFR	AG-1478 (Tyrphostin AG-1478)	≤ 2,3E-10	≤ 1,1E-10	n.e.	≤ 1,1E-10	2,0E+07	≤ 2,3E-03	4
EGFR	AG-490	≈ 1,0E-05	≈ 5,2E-06	≈ 4,7E-06	≈ 4,9E-06	2,7E+03	2,1E-02	
EGFR	Apatinib (YN968D1)	≈ 7,1E-07	≈ 3,6E-07	6,2E-07	6,2E-07	2,2E+04	1,3E-02	2
EGFR	ARQ 197 (Tivantinib)	n.e.	n.e.	≥ 2,0E-05	≥ 2,0E-05			
EGFR	ARRY334543	≈ 7,2E-10	≈ 3,6E-10	≤ 9,0E-11	≤ 9,0E-11	2,3E+07	2,1E-03	
EGFR	Arry-380	≈ 9,2E-08	≈ 4,6E-08	6,8E-08	6,8E-08	4,7E+05	3,2E-02	
EGFR	AS-252424	≥ 2,0E-05		1,0E-06	1,0E-06	3,2E+04	3,3E-02	
EGFR	AST-1306	4,3E-10	2,1E-10	n.e.	2,1E-10	3,1E+06	≤ 6,6E-04	4
EGFR	AT9283	≈ 7,2E-07	≈ 3,6E-07	4,2E-07	4,2E-07	1,1E+05	4,8E-02	
EGFR	Aurora A Inhibitor I	6,1E-06	3,1E-06	5,5E-06	5,5E-06	1,1E+04	3,3E-02	3
EGFR	AZ628	≈ 6,8E-07	≈ 3,4E-07	9,8E-07	9,8E-07	2,4E+04	2,2E-02	
EGFR	AZD2014	n.e.	n.e.	≥ 2,0E-05	≥ 2,0E-05			
EGFR	AZD7762	≈ 5,2E-08	≈ 2,6E-08	5,3E-08	5,3E-08	7,0E+05	3,5E-02	
EGFR	AZD8931	≈ 5,5E-11	≈ 2,8E-11	n.e.	≈ 2,8E-11	4,8E+07	≤ 1,3E-03	4
EGFR	Barasertib (AZD1152-HQPA)	≈ 3,4E-07	≈ 1,7E-07	1,9E-07	1,9E-07	3,0E+05	5,5E-02	
EGFR	BGJ398 (NVP-BGJ398)	≥ 2,0E-05		4,9E-06	4,9E-06	2,8E+03	1,5E-02	
EGFR	BI 2536	1,1E-06	5,6E-07	7,6E-07	7,6E-07	5,1E+04	3,9E-02	

kinase	Compound	IC ₅₀ [M] ePCA	K _D eq [M] ePCA *	K _D kin [M] kPCA	K _D [M] PCA **	k _{on} [M ⁻¹ s ⁻¹] kPCA	k _{off} [s ⁻¹] kPCA	comment
EGFR	BI6727 (Volasertib)	8,9E-07	4,5E-07	1,0E-06	1,0E-06	2,7E+04	2,6E-02	
EGFR	BIBF1120 (Vargatef)	≥ 2,0E-05		5,2E-06	5,2E-06	≈ 8,9E+03	≈ 4,9E-02	
EGFR	BIRB 796 (Doramapimod)	1,7E-06	8,5E-07	1,5E-06	1,5E-06	7,5E+03	1,1E-02	
EGFR	BMS 777607	≥ 2,0E-05		4,5E-06	4,5E-06	1,1E+04	4,7E-02	
EGFR	BMS-599626 (AC480)	5,9E-10	3,0E-10	1,5E-10	1,5E-10	1,1E+07	1,7E-03	
EGFR	Bosutinib (SKI-606)	≈ 2,3E-08	≈ 1,1E-08	9,2E-09	9,2E-09	3,2E+06	2,9E-02	
EGFR	Brivanib (BMS-540215)	≈ 3,6E-06	≈ 1,8E-06	1,4E-06	1,4E-06	2,5E+04	3,6E-02	
EGFR	Brivanib alaninate (BMS-582664) - prodrug	≈ 2,8E-06	≈ 1,4E-06	1,1E-06	1,1E-06	2,7E+04	2,9E-02	
EGFR	BX-795	≥ 2,0E-05		5,7E-06	5,7E-06	7,2E+03	4,1E-02	
EGFR	BX-912	1,8E-06	8,9E-07	1,1E-06	1,1E-06	3,0E+04	3,4E-02	
EGFR	CCT137690	≈ 1,2E-05	≈ 6,2E-06	≈ 6,1E-06	≈ 6,1E-06	7,5E+03	5,9E-02	
EGFR	Cediranib (AZD2171)	3,0E-07	1,5E-07	2,9E-08	1,5E-07	1,1E+06	3,2E-02	
EGFR	CEP33779	≈ 1,1E-05	≈ 5,7E-06	4,6E-06	4,6E-06	1,2E+04	5,5E-02	
EGFR	CH5424802	≥ 2,0E-05		9,7E-07	9,7E-07	4,7E+04	4,1E-02	2
EGFR	CI-1033 (Canertinib)	≤ 8,9E-11	≤ 4,5E-11	n.e.	≤ 4,5E-11	1,6E+07	≤ 7,2E-04	4
EGFR	CP 673451	≈ 4,2E-06	≈ 2,1E-06	1,9E-06	1,9E-06	1,2E+04	2,3E-02	
EGFR	CP-724714	≈ 1,3E-08	≈ 6,6E-09	8,9E-09	8,9E-09	2,3E+06	2,1E-02	
EGFR	Crenolanib (CP-868596)	4,5E-06	2,3E-06	2,9E-06	2,9E-06	1,1E+04	3,2E-02	
EGFR	CX-4945 (Silmisertib)	2,2E-06	1,1E-06	1,2E-06	1,2E-06	3,4E+04	4,1E-02	1
EGFR	CYC116	2,0E-06	1,0E-06	8,8E-07	8,8E-07	6,6E+04	5,8E-02	
EGFR	Cyt387	1,4E-05	7,1E-06	3,7E-06	3,7E-06	1,3E+04	4,7E-02	
EGFR	Dabrafenib (GSK2118436)	1,8E-05	9,2E-06	5,3E-07	9,2E-06	≈ 5,1E+04	2,4E-02	2
EGFR	Dacomitinib (PF299804 - PF-00299804)	≤ 2,7E-11	≤ 1,3E-11	n.e.	≤ 1,3E-11	1,4E+07	≤ 1,9E-04	4
EGFR	Dasatinib (BMS-354825)	≈ 6,3E-08	≈ 3,2E-08	2,5E-08	2,5E-08	≈ 1,0E+06	≈ 2,5E-02	
EGFR	DCC-2036 (Rebastinib)	1,4E-07	6,9E-08	n.e.	6,9E-08	8,2E+03	≤ 5,6E-04	4
EGFR	Desmethyl Erlotinib (CP-473420)	2,0E-09	9,9E-10	9,6E-10	9,6E-10	2,1E+07	2,0E-02	
EGFR	Dovitinib (TKI-258)	5,9E-06	3,0E-06	2,5E-06	2,5E-06	1,4E+04	3,3E-02	
EGFR	E7080 (Lenvatinib)	5,8E-07	2,9E-07	6,5E-07	6,5E-07	1,5E+05	4,4E-02	3
EGFR	ENMD-2076	2,2E-06	1,1E-06	1,2E-06	1,2E-06	3,4E+04	4,3E-02	
EGFR	Enzastaurin (LY317615)	≈ 1,7E-05	≈ 8,7E-06	≈ 9,0E-06	≈ 8,9E-06	2,9E+03	3,8E-02	
EGFR	Erlotinib HCl	≈ 4,7E-09	≈ 2,4E-09	1,1E-09	1,1E-09	1,5E+07	1,6E-02	
EGFR	Flavopiridol HCl	2,8E-06	1,4E-06	2,6E-06	2,6E-06	1,4E+04	3,5E-02	
EGFR	Foretinib (GSK1363089 - XL880)	1,9E-07	9,4E-08	2,2E-07	2,2E-07	1,6E+05	3,5E-02	
EGFR	GDC-0879	≥ 2,0E-05		8,7E-06	8,7E-06	3,4E+03	3,0E-02	
EGFR	GDC-0980 (RG7422)	5,9E-07	3,0E-07	4,4E-07	4,4E-07	1,0E+05	4,5E-02	
EGFR	Gefitinib (Iressa)	8,8E-10	4,4E-10	7,4E-10	7,4E-10	2,1E+07	1,6E-02	
EGFR	GSK1070916	8,7E-07	4,4E-07	4,4E-07	4,4E-07	6,1E+04	2,7E-02	
EGFR	GSK1838705A	9,5E-07	4,8E-07	1,6E-06	1,6E-06	2,6E+04	4,1E-02	
EGFR	GSK1904529A	≥ 2,0E-05		4,7E-06	4,7E-06	8,7E+03	4,1E-02	
EGFR	Hesperadin	≈ 4,2E-06	≈ 2,1E-06	1,2E-06	1,2E-06	4,5E+04	5,3E-02	
EGFR	INCB28060	≥ 2,0E-05		7,1E-06	7,1E-06	5,7E+03	3,9E-02	
EGFR	INK 128 (MLN0128)	≈ 1,4E-05	≈ 7,0E-06	4,1E-06	4,1E-06	8,3E+03	3,1E-02	
EGFR	JNJ-7706621	7,1E-06	3,6E-06	1,9E-06	1,9E-06	2,9E+04	5,5E-02	
EGFR	Ki8751	6,3E-06	3,1E-06	≈ 9,8E-06	3,1E-06	3,0E+03	3,2E-02	
EGFR	KRN 633	≥ 2,0E-05		2,5E-06	2,5E-06	1,0E+04	2,5E-02	
EGFR	KW 2449	5,7E-06	2,9E-06	6,8E-06	6,8E-06	5,0E+03	3,4E-02	
EGFR	Lapatinib Ditosylate (Tykerb)	≤ 1,1E-10	≤ 5,5E-11	n.e.	≤ 5,5E-11	2,5E+06	≤ 1,4E-04	4
EGFR	LDN193189	≥ 2,0E-05		6,7E-06	6,7E-06	4,6E+03	3,1E-02	
EGFR	Linifanib (ABT-869)	4,6E-06	2,3E-06	≈ 6,6E-06	2,3E-06	5,4E+03	≈ 3,6E-02	
EGFR	Linsitinib (OSI-906)	3,2E-06	1,6E-06	1,7E-06	1,7E-06	3,4E+04	5,6E-02	
EGFR	LY2228820	≈ 4,8E-07	≈ 2,4E-07	3,5E-07	3,5E-07	6,8E+04	2,4E-02	
EGFR	LY2603618 (IC-83)	≥ 1,1E-05		≥ 2,0E-05	≥ 5,7E-06			
EGFR	LY2784544	≥ 2,0E-05		7,8E-06	7,8E-06	3,3E+03	2,6E-02	
EGFR	Masitinib (AB1010)	8,6E-06	4,3E-06	5,8E-06	5,8E-06	5,0E+03	3,0E-02	
EGFR	MGCD-265	≈ 1,1E-06	≈ 5,7E-07	1,6E-06	1,6E-06	1,7E+04	2,7E-02	
EGFR	Milciclib (PHA-848125)	≥ 2,0E-05		1,5E-06	1,5E-06	≈ 2,9E+04	3,9E-02	
EGFR	MK-5108 (VX-689)	7,1E-07	3,6E-07	4,9E-07	4,9E-07	6,2E+04	3,0E-02	
EGFR	MLN8054	≈ 4,9E-06	≈ 2,5E-06	7,4E-07	7,4E-07	5,4E+04	4,0E-02	
EGFR	MLN8237 (Alisertib)	≈ 6,4E-07	≈ 3,2E-07	2,8E-07	2,8E-07	1,6E+05	4,5E-02	12
EGFR	Motesanib Diphosphate (AMG-706)	3,8E-07	1,9E-07	8,2E-07	8,2E-07	2,0E+04	1,6E-02	
EGFR	Neratinib (HKI-272)	3,5E-10	1,8E-10	2,1E-10	2,1E-10	1,9E+07	3,6E-03	
EGFR	NVP-ADW742	2,6E-06	1,3E-06	1,7E-06	1,7E-06	1,9E+04	3,3E-02	
EGFR	NVP-BGT226	≥ 2,0E-05		4,5E-06	4,5E-06	7,9E+03	3,6E-02	
EGFR	NVP-TAE226	≈ 1,1E-07	≈ 5,4E-08	1,8E-08	1,8E-08	1,8E+06	3,2E-02	
EGFR	OSI-027	≥ 2,0E-05		4,8E-06	4,8E-06	7,2E+03	3,5E-02	
EGFR	Pazopanib HCl	≥ 2,0E-05		2,1E-06	2,1E-06	1,8E+04	3,8E-02	
EGFR	PCI-32765 (Ibrutinib)	≤ 1,5E-10	≤ 7,7E-11	n.e.	≤ 7,7E-11	9,4E+05	≤ 7,3E-05	4
EGFR	PD153035 HCl	≤ 1,4E-10	≤ 6,9E-11	n.e.	≤ 6,9E-11	3,4E+07	≤ 2,3E-03	4
EGFR	PD173074	≥ 1,2E-05		≥ 2,0E-05	≥ 6,0E-06			
EGFR	Pelitinib (EKB-569)	≤ 1,3E-10	≤ 6,7E-11	n.e.	≤ 6,7E-11	1,6E+07	≤ 1,1E-03	4
EGFR	PF-00562271	6,8E-06	3,4E-06	4,7E-06	4,7E-06	5,8E+03	2,7E-02	
EGFR	PF-03814735	1,4E-06	7,1E-07	1,9E-06	1,9E-06	2,0E+04	3,9E-02	
EGFR	PHA-665752	≈ 2,8E-06	≈ 1,4E-06	2,3E-06	2,3E-06	1,2E+04	2,9E-02	
EGFR	PHA-680632	≥ 2,0E-05		7,2E-06	7,2E-06	5,1E+03	3,7E-02	
EGFR	PHA-767491	2,8E-07	1,4E-07	≥ 2,0E-05	≥ 1,4E-07			
EGFR	Phenformin HCl	≥ 2,0E-05		4,2E-06	4,2E-06	≈ 5,9E+03	2,0E-02	
EGFR	PHT-427	≥ 3,8E-06		≥ 2,0E-05	≥ 1,9E-06			
EGFR	PIK-75	≈ 4,7E-06	≈ 2,4E-06	1,4E-06	1,4E-06	3,8E+04	5,3E-02	
EGFR	PLX-4720	≥ 2,0E-05		6,5E-06	6,5E-06	6,6E+03	4,3E-02	

kinase	Compound	IC ₅₀ [M] ePCA	K _D eq [M] ePCA *	K _D kin [M] kPCA	K _D [M] PCA **	k _{on} [M ⁻¹ s ⁻¹] kPCA	k _{off} [s ⁻¹] kPCA	comment
EGFR	Ponatinib (AP24534)	1,5E-07	7,7E-08	7,4E-08	7,4E-08	9,6E+04	7,2E-03	2
EGFR	PP-121	1,7E-07	8,7E-08	9,7E-08	9,7E-08	3,5E+05	3,5E-02	
EGFR	PP242	≈ 1,3E-06	≈ 6,6E-07	6,4E-07	6,4E-07	5,6E+04	3,5E-02	
EGFR	Quercetin (Sophoretin)	3,9E-06	1,9E-06	2,0E-06	2,0E-06	2,6E+04	5,0E-02	
EGFR	R406	3,4E-07	1,7E-07	1,6E-07	2,2E-07	1,8E+05	3,8E-02	2
EGFR	R788 (Fostamatinib) - prodrug	7,8E-06	3,9E-06	2,2E-06	2,2E-06	2,1E+04	4,5E-02	
EGFR	Raf265 derivative	2,9E-06	1,5E-06	n.e.	1,5E-06	6,4E+02	≤ 9,4E-04	4
EGFR	Saracatinib (AZD0530)	≈ 5,9E-08	≈ 3,0E-08	1,7E-08	1,7E-08	1,2E+06	2,0E-02	
EGFR	SB 202190	1,2E-06	6,1E-07	4,5E-07	4,5E-07	6,0E+04	2,7E-02	
EGFR	SB 203580	3,4E-07	1,7E-07	7,5E-07	7,5E-07	4,5E+04	3,4E-02	
EGFR	SB590885	≥ 2,0E-05		3,2E-06	3,2E-06	≈ 1,1E+04	3,5E-02	
EGFR	SNS-314	≈ 6,5E-06	≈ 3,3E-06	1,1E-06	1,1E-06	1,5E+04	1,5E-02	
EGFR	Sotrastaurin (AEB071)	≈ 1,1E-05	≈ 5,4E-06	3,2E-06	3,2E-06	8,3E+03	2,5E-02	
EGFR	Staurosporine	1,3E-07	6,4E-08	8,1E-08	8,1E-08	3,4E+05	2,8E-02	
EGFR	SU11274	≥ 2,0E-05		3,3E-06	3,3E-06	7,5E+03	2,5E-02	
EGFR	Sunitinib Malate (Sutent)	1,4E-06	7,1E-07	n.e.	7,1E-07	7,1E+03	≤ 5,0E-03	4
EGFR	TAE684 (NVP-TAE684)	4,5E-07	2,3E-07	5,3E-08	5,3E-08	8,5E+05	4,5E-02	
EGFR	TAK-285	≈ 3,7E-09	≈ 1,8E-09	1,5E-09	1,5E-09	5,9E+05	9,1E-04	
EGFR	TAK-901	8,1E-09	4,1E-09	4,3E-08	4,1E-09	1,0E+06	4,4E-02	
EGFR	TG 100713	≈ 7,7E-06	≈ 3,9E-06	2,3E-06	2,3E-06	1,2E+04	2,9E-02	
EGFR	TG100-115	8,8E-07	4,4E-07	1,6E-06	1,6E-06	2,8E+04	4,5E-02	
EGFR	TG101209	≈ 1,2E-06	≈ 6,0E-07	4,6E-07	4,6E-07	8,0E+04	3,7E-02	
EGFR	TG101348 (SAR302503)	2,6E-06	1,3E-06	1,3E-06	1,3E-06	1,8E+04	2,5E-02	
EGFR	Tideglusib	n.e.	n.e.	≥ 2,0E-05	≥ 2,0E-05			
EGFR	Tie2 kinase inhibitor	4,9E-06	2,5E-06	7,3E-07	7,3E-07	4,2E+04	3,1E-02	
EGFR	Tivozanib (AV-951)	3,9E-07	1,9E-07	2,2E-07	2,2E-07	1,5E+05	3,2E-02	
EGFR	Torin 1	≥ 2,0E-05		9,3E-06	9,3E-06	4,1E+03	3,8E-02	
EGFR	Torin 2	≈ 1,0E-05	≈ 5,0E-06	≈ 8,8E-06	≈ 6,9E-06	3,3E+03	3,7E-02	
EGFR	TPCA-1	9,3E-07	4,7E-07	1,1E-06	1,1E-06	4,2E+04	4,6E-02	
EGFR	TWS119	≈ 4,1E-08	≈ 2,1E-08	1,2E-08	1,2E-08	1,5E+06	1,8E-02	
EGFR	Vandetanib (Zactima)	4,0E-09	2,0E-09	n.e.	2,0E-09	2,9E+06	≤ 5,9E-03	4
EGFR	Vemurafenib (PLX4032)	4,7E-06	2,4E-06	≈ 8,1E-06	2,4E-06	1,8E+03	1,8E-02	
EGFR	VX-680 (MK-0457 - Tozasertib)	3,7E-06	1,9E-06	7,6E-06	7,6E-06	5,0E+03	3,9E-02	
EGFR	WAY-600	≥ 2,0E-05		6,7E-06	6,7E-06	6,1E+03	4,1E-02	
EGFR	WHI-P154	3,7E-09	1,9E-09	1,0E-09	1,0E-09	1,9E+07	1,9E-02	
EGFR	WP1130	≥ 2,0E-05		9,5E-06	9,5E-06	n.e.	n.e.	
EGFR	WZ3146	4,6E-10	2,3E-10	n.e.	2,3E-10	1,8E+05	≤ 4,3E-05	4
EGFR	WZ4002	≈ 2,6E-09	≈ 1,3E-09	n.e.	≈ 1,3E-09	8,7E+04	≤ 1,1E-04	4
EGFR	WZ8040	≈ 6,3E-10	≈ 3,2E-10	n.e.	≈ 3,2E-10	2,5E+05	≤ 7,9E-05	4
EGFR	XL-184 (Cabozantinib)	2,0E-06	1,0E-06	1,3E-06	1,3E-06	2,9E+04	3,9E-02	
EGFR	ZM-447439	4,0E-08	2,0E-08	2,4E-08	2,4E-08	2,0E+06	4,3E-02	
FAK	A-674563	3,7E-06	2,3E-06	2,3E-06	2,3E-06	1,4E+04	3,2E-02	
FAK	AEE788 (NVP-AEE788)	4,0E-06	2,5E-06	2,6E-06	2,6E-06	7,5E+04	1,9E-01	
FAK	AMG458	2,5E-06	1,6E-06	1,3E-06	1,3E-06	1,4E+04	1,9E-02	
FAK	AT9283	4,3E-07	2,7E-07	1,8E-07	1,8E-07	3,0E+05	5,2E-02	
FAK	Aurora A Inhibitor I	3,9E-07	2,4E-07	5,4E-07	5,4E-07	1,0E+05	5,4E-02	2
FAK	Axitinib	7,4E-06	4,6E-06	2,5E-06	2,5E-06	2,6E+04	6,6E-02	
FAK	AZ 960	1,0E-08	6,5E-09	2,2E-09	2,2E-09	5,5E+06	1,2E-02	
FAK	AZD4547	5,6E-07	3,5E-07	2,8E-07	2,8E-07	3,1E+05	8,5E-02	
FAK	AZD5438	8,1E-07	5,0E-07	4,9E-07	4,9E-07	1,2E+05	6,0E-02	
FAK	AZD7762	1,9E-08	1,2E-08	1,6E-08	1,6E-08	6,8E+06	1,1E-01	
FAK	Barasertib (AZD1152-HQPA)	4,5E-06	2,8E-06	4,6E-06	4,6E-06	2,6E+03	1,2E-02	
FAK	Baricitinib (LY3009104 - incb28050)	1,2E-05	7,4E-06	6,0E-06	6,0E-06	8,6E+03	5,2E-02	
FAK	BEZ235 (NVP-BEZ235)	≥ 2,0E-05		3,1E-06	3,1E-06	1,0E+04	3,2E-02	
FAK	BGJ398 (NVP-BGJ398)	7,7E-06	4,7E-06	2,5E-06	2,5E-06	2,2E+04	5,2E-02	
FAK	BI 2536	7,3E-08	4,5E-08	5,0E-08	5,0E-08	1,2E+06	6,1E-02	
FAK	BI6727 (Volasertib)	7,9E-08	4,9E-08	7,7E-08	7,7E-08	6,6E+05	3,3E-02	
FAK	BIBF1120 (Vargatef)	1,9E-06	1,2E-06	6,9E-07	6,9E-07	7,6E+04	5,2E-02	
FAK	BIRB 796 (Doramapimod)	2,1E-06	1,3E-06	n.e.	1,3E-06	5,7E+02	≤ 7,2E-04	4
FAK	BMS 794833	2,5E-06	1,6E-06	1,3E-06	1,3E-06	2,1E+04	2,6E-02	
FAK	BMS-265246	4,7E-07	2,9E-07	1,4E-06	1,4E-06	6,1E+04	8,8E-02	12
FAK	Bosutinib (SKI-606)	2,8E-07	1,7E-07	2,7E-07	2,7E-07	1,2E+05	3,3E-02	
FAK	BS-181 HCl	3,5E-06	2,2E-06	2,2E-06	2,2E-06	2,4E+04	5,4E-02	
FAK	BX-795	1,1E-07	6,7E-08	8,9E-08	8,9E-08	1,3E+06	1,2E-01	
FAK	BX-912	2,8E-08	1,7E-08	3,3E-08	3,3E-08	2,1E+06	7,1E-02	
FAK	CCT137690	4,4E-06	2,7E-06	≥ 2,0E-05	≥ 2,7E-06			
FAK	CEP33779	1,5E-06	9,5E-07	1,0E-06	1,0E-06	9,6E+04	1,0E-01	
FAK	CH5424802	4,3E-07	2,7E-07	7,3E-08	7,3E-08	≈ 5,7E+06	≈ 3,2E-01	
FAK	CHIR-124	2,6E-06	1,6E-06	2,2E-06	2,2E-06	2,7E+04	5,3E-02	
FAK	CP 673451	1,4E-05	8,8E-06	6,3E-06	6,3E-06	1,2E+03	7,5E-03	
FAK	Crenolanib (CP-868596)	≥ 2,0E-05		8,4E-06	8,4E-06	1,2E+03	9,5E-03	
FAK	Crizotinib (PF-02341066)	2,6E-08	1,6E-08	4,3E-08	4,3E-08	n.e.	n.e.	2
FAK	CYC116	1,4E-07	8,8E-08	7,2E-08	7,2E-08	8,3E+05	6,2E-02	
FAK	Cyt387	2,3E-06	1,4E-06	9,3E-07	9,3E-07	7,8E+04	7,2E-02	
FAK	Dabrafenib (GSK2118436)	1,5E-05	9,5E-06	3,5E-06	3,5E-06	4,7E+03	1,6E-02	
FAK	Danuserib (PHA-739358)	7,7E-08	4,8E-08	7,9E-08	7,9E-08	8,9E+04	7,0E-03	
FAK	DCC-2036 (Rebastinib)	2,9E-07	1,8E-07	n.e.	1,8E-07	1,9E+03	≤ 3,5E-04	4
FAK	Dinaciclib (SCH727965)	1,0E-05	6,2E-06	≈ 8,1E-06	6,2E-06	≈ 1,7E+03	≈ 1,4E-02	
FAK	Dovitinib (TKI-258)	2,8E-06	1,7E-06	1,6E-06	1,6E-06	1,2E+05	1,8E-01	

kinase	Compound	IC ₅₀ [M] ePCA	K _D eq [M] ePCA *	K _D kin [M] kPCA	K _D [M] PCA **	k _{on} [M ⁻¹ s ⁻¹] kPCA	k _{off} [s ⁻¹] kPCA	comment
FAK	E7080 (Lenvatinib)	≥ 2,0E-05		8,9E-06	8,9E-06	1,3E+03	1,1E-02	
FAK	ENMD-2076	3,9E-06	2,4E-06	1,2E-06	1,2E-06	3,3E+04	4,0E-02	
FAK	Enzastaurin (LY317615)	≥ 2,0E-05		8,2E-06	8,2E-06	8,7E+02	7,0E-03	
FAK	Flavopiridol HCl	3,2E-06	2,0E-06	2,9E-06	2,9E-06	2,7E+04	7,8E-02	
FAK	Foretinib (GSK1363089 - XL880)	1,3E-07	7,9E-08	1,2E-07	1,2E-07	2,4E+05	2,8E-02	
FAK	GDC-0941	≥ 2,0E-05		4,7E-06	4,7E-06	2,4E+03	1,1E-02	
FAK	GDC-0980 (RG7422)	7,3E-06	4,5E-06	5,4E-06	5,4E-06	3,3E+03	1,8E-02	
FAK	Golitinib (E7050)	2,4E-06	1,5E-06	1,3E-06	1,3E-06	5,0E+04	6,6E-02	
FAK	GSK1070916	≥ 2,0E-05		8,3E-06	8,3E-06	1,1E+03	9,1E-03	
FAK	GSK1838705A	1,1E-07	6,6E-08	5,7E-08	5,7E-08	5,2E+05	2,9E-02	
FAK	Hesperadin	1,4E-08	8,5E-09	3,9E-09	3,9E-09	8,5E+06	3,4E-02	
FAK	Imatinib (Gleevec)	1,2E-05	7,5E-06	7,1E-06	7,1E-06	3,3E+03	2,2E-02	
FAK	INK 128 (MLN0128)	1,2E-05	7,3E-06	6,4E-06	6,4E-06	7,7E+02	4,9E-03	
FAK	JNJ-38877605	7,4E-06	4,5E-06	≥ 2,0E-05	≥ 4,5E-06			
FAK	JNJ-7706621	1,5E-06	9,3E-07	9,2E-07	9,2E-07	8,0E+04	7,4E-02	
FAK	Ki8751	≥ 2,0E-05		5,7E-06	5,7E-06	1,3E+03	7,6E-03	2
FAK	KW 2449	6,5E-07	4,0E-07	1,8E-06	1,8E-06	5,8E+04	1,0E-01	
FAK	Linifanib (ABT-869)	8,7E-06	5,4E-06	7,0E-07	5,4E-06	4,5E+04	3,1E-02	
FAK	Linsitinib (OSI-906)	≥ 2,0E-05		7,3E-06	7,3E-06	2,0E+03	1,5E-02	
FAK	LY2784544	6,6E-08	4,1E-08	1,7E-08	1,7E-08	1,6E+06	2,8E-02	
FAK	MGCD-265	≥ 2,0E-05		6,6E-06	6,6E-06	1,2E+03	8,0E-03	
FAK	Milciclib (PHA-848125)	8,8E-07	5,4E-07	4,0E-07	4,0E-07	1,2E+05	4,7E-02	
FAK	MK-5108 (VX-689)	4,9E-08	3,0E-08	3,1E-08	3,1E-08	≈ 1,9E+07	≈ 5,2E-01	
FAK	MLN8054	8,3E-07	5,1E-07	5,5E-07	5,5E-07	9,6E+04	4,9E-02	
FAK	MLN8237 (Alisertib)	9,3E-08	5,8E-08	5,6E-08	5,6E-08	4,5E+05	2,5E-02	
FAK	Neratinib (HKI-272)	7,8E-06	4,8E-06	3,1E-06	3,1E-06	9,6E+03	3,0E-02	
FAK	NVP-ADW742	1,1E-05	6,9E-06	7,0E-06	7,0E-06	≈ 2,8E+03	≈ 1,9E-02	
FAK	NVP-BGT226	≥ 2,0E-05		8,7E-06	8,7E-06	8,4E+02	7,3E-03	
FAK	NVP-BSK805	≥ 2,0E-05		7,3E-06	7,3E-06	≈ 1,6E+03	1,1E-02	
FAK	NVP-BVU972	≥ 2,0E-05		≈ 4,3E-06	≈ 4,3E-06	≥ 8,1E+04	≥ 3,5E-01	
FAK	NVP-TAE226	5,4E-10	3,3E-10	n.e.	3,3E-10	1,3E+07	≤ 4,3E-03	4
FAK	Pazopanib HCl	6,4E-07	4,0E-07	5,2E-07	5,2E-07	1,8E+05	9,3E-02	
FAK	PD 0332991 (Palbociclib) HCl	1,7E-05	1,1E-05	1,0E-05	1,0E-05	n.e.	n.e.	
FAK	Pelitinib (EKB-569)	2,8E-06	1,7E-06	2,8E-06	2,8E-06	8,4E+03	2,3E-02	
FAK	PF-00562271	≤ 8,0E-11	≤ 4,9E-11	≤ 5,6E-11	≤ 5,6E-11	1,7E+07	9,4E-04	
FAK	PF-03814735	3,0E-09	1,8E-09	2,4E-09	2,4E-09	8,4E+06	2,0E-02	
FAK	PHA-665752	5,8E-07	3,6E-07	2,7E-07	2,7E-07	2,4E+05	6,5E-02	
FAK	PHA-680632	1,4E-07	8,7E-08	6,2E-08	6,2E-08	4,7E+05	2,9E-02	
FAK	Phenformin HCl	9,3E-06	5,8E-06	≥ 2,0E-05	≥ 5,8E-06			
FAK	PIK-75	6,3E-08	3,9E-08	3,5E-08	3,5E-08	3,8E+06	1,4E-01	
FAK	PLX-4720	1,4E-05	8,8E-06	1,1E-05	1,1E-05	n.e.	n.e.	
FAK	Ponatinib (AP24534)	3,6E-06	2,2E-06	2,0E-06	2,0E-06	2,2E+04	4,3E-02	
FAK	PP-121	3,3E-07	2,0E-07	4,1E-07	4,1E-07	1,2E+05	4,8E-02	
FAK	R406	6,0E-08	3,7E-08	3,4E-08	3,4E-08	1,6E+06	5,2E-02	2
FAK	R788 (Fostatinib) - prodrug	3,9E-07	2,4E-07	2,9E-07	2,9E-07	2,9E+05	7,6E-02	
FAK	Roscovitine (Seliciclib - CYC202)	5,2E-06	3,2E-06	2,7E-06	2,7E-06	5,6E+04	1,5E-01	
FAK	Ruxolitinib (INCB018424)	1,4E-06	8,8E-07	1,6E-06	1,6E-06	6,7E+04	1,1E-01	
FAK	SAR131675	≥ 2,0E-05		7,1E-06	7,1E-06	7,3E+02	4,9E-03	
FAK	SB590885	9,3E-06	5,7E-06	n.e.	5,7E-06	2,0E+02	≤ 1,2E-03	4
FAK	Semaxanib (SU5416)	2,2E-07	1,4E-07	1,7E-07	1,7E-07	2,3E+05	4,0E-02	
FAK	SNS-314	3,0E-07	1,8E-07	1,6E-07	1,6E-07	2,3E+05	3,6E-02	1
FAK	Sotrastaurin (AEB071)	1,1E-05	6,6E-06	5,1E-06	5,1E-06	6,6E+03	3,3E-02	
FAK	SP600125	1,1E-06	7,1E-07	4,9E-07	4,9E-07	1,9E+05	9,3E-02	
FAK	Staurosporine	1,2E-08	7,6E-09	3,9E-09	3,9E-09	7,0E+06	2,7E-02	
FAK	SU11274	2,7E-06	1,7E-06	2,6E-06	2,6E-06	2,8E+04	7,2E-02	
FAK	Sunitinib Malate (Sutent)	7,9E-08	4,9E-08	7,2E-08	7,2E-08	3,4E+06	2,4E-01	
FAK	TAE684 (NVP-TAE684)	5,8E-10	3,6E-10	1,2E-10	1,2E-10	1,6E+07	1,9E-03	
FAK	TAK-901	1,2E-08	7,5E-09	1,6E-08	1,6E-08	2,0E+06	3,2E-02	
FAK	TG101209	4,7E-09	2,9E-09	5,8E-09	5,8E-09	5,3E+06	3,1E-02	
FAK	TG101348 (SAR302503)	7,9E-09	4,9E-09	5,5E-09	5,5E-09	5,6E+06	3,0E-02	
FAK	Tivozanib (AV-951)	1,7E-06	1,1E-06	1,4E-06	1,4E-06	3,0E+04	4,1E-02	
FAK	Torin 2	≥ 2,0E-05		4,8E-06	4,8E-06	4,0E+03	2,0E-02	
FAK	TPCA-1	1,5E-06	9,2E-07	1,2E-06	1,2E-06	8,1E+04	1,0E-01	
FAK	TSU-68 (SU6668)	1,6E-06	9,7E-07	7,1E-07	7,1E-07	6,0E+04	4,2E-02	
FAK	TWS119	5,9E-06	3,6E-06	3,7E-06	3,7E-06	1,1E+04	4,1E-02	
FAK	Vandetanib (Zactima)	1,4E-05	8,9E-06	7,7E-06	7,7E-06	5,5E+02	4,3E-03	
FAK	Vatalanib 2HCl (PTK787)	1,5E-05	9,2E-06	≈ 1,0E-05	9,2E-06	n.e.	n.e.	
FAK	VX-680 (MK-0457 - Tozasertib)	3,2E-06	2,0E-06	3,0E-06	3,0E-06	3,1E+04	9,2E-02	
FAK	WHI-P154	1,3E-05	n.e.	9,5E-06	9,5E-06	n.e.	n.e.	
FAK	WZ3146	4,5E-08	2,8E-08	2,6E-08	2,6E-08	2,4E+06	6,2E-02	
FAK	WZ4002	2,1E-08	1,3E-08	7,4E-09	7,4E-09	4,7E+06	3,1E-02	
FAK	WZ8040	3,5E-08	2,2E-08	2,4E-08	2,4E-08	1,4E+06	3,4E-02	
FAK	XL147	≥ 2,1E-06		≥ 2,0E-05	≥ 1,3E-06			
FAK	XL-184 (Cabozantinib)	1,2E-06	7,7E-07	6,4E-07	6,4E-07	7,9E+04	5,0E-02	
FAK	ZM-447439	2,9E-06	1,8E-06	3,2E-06	3,2E-06	2,4E+04	7,5E-02	
FGFR1	A-674563	≥ 2,0E-05		1,5E-05	1,5E-05	≥ 2,3E+04	≥ 3,5E-01	
FGFR1	AEE788 (NVP-AEE788)	1,2E-06	7,4E-07	≈ 7,7E-07	7,4E-07	≥ 4,6E+05	≥ 3,5E-01	
FGFR1	Apatinib (YN968D1)	≥ 2,0E-05		5,7E-06	5,7E-06	≥ 6,2E+04	≥ 3,5E-01	
FGFR1	AT9283	3,3E-08	2,0E-08	1,1E-08	1,1E-08	5,4E+06	6,1E-02	

kinase	Compound	IC ₅₀ [M] ePCA	K _D eq [M] ePCA *	K _D kin [M] kPCA	K _D [M] PCA **	k _{on} [M ⁻¹ s ⁻¹] kPCA	k _{off} [s ⁻¹] kPCA	comment
FGFR1	Aurora A Inhibitor I	1,5E-06	9,0E-07	1,6E-06	1,6E-06	n.e.	n.e.	2
FGFR1	Axitinib	7,7E-08	4,7E-08	2,4E-08	2,4E-08	≥ 1,4E+07	≥ 3,5E-01	
FGFR1	AZ 960	1,4E-07	8,7E-08	≈ 6,4E-08	8,7E-08	≥ 5,5E+06	≥ 3,5E-01	
FGFR1	AZ628	8,8E-06	5,4E-06	3,6E-06	3,6E-06	≈ 2,7E+03	≈ 9,8E-03	
FGFR1	AZD4547	1,8E-09	1,1E-09	6,1E-10	6,1E-10	1,0E+07	6,1E-03	
FGFR1	AZD5438	1,4E-05	8,4E-06	1,4E-05	1,4E-05	≥ 2,5E+04	≥ 3,5E-01	
FGFR1	AZD7762	3,9E-07	2,4E-07	≈ 3,5E-07	2,4E-07	≥ 1,0E+06	≥ 3,5E-01	
FGFR1	AZD8931	≥ 2,0E-05		≈ 1,8E-05	≈ 1,8E-05	≥ 1,9E+04	≥ 3,5E-01	
FGFR1	Barasertib (AZD1152-HQPA)	≥ 2,0E-05		1,8E-05	1,8E-05	≥ 2,0E+04	≥ 3,5E-01	
FGFR1	Baricitinib (LY3009104 - incb28050)	3,6E-06	2,2E-06	2,1E-06	2,1E-06	≥ 1,7E+05	≥ 3,5E-01	
FGFR1	BGJ398 (NVP-BGJ398)	5,6E-10	3,5E-10	1,5E-10	1,5E-10	3,4E+06	4,8E-04	
FGFR1	BIBF1120 (Vargatef)	9,8E-08	6,0E-08	3,2E-08	3,2E-08	≥ 1,1E+07	≥ 3,5E-01	
FGFR1	BIRB 796 (Doramapimod)	7,6E-06	4,7E-06	4,2E-06	4,2E-06	4,1E+03	1,7E-02	
FGFR1	BIX 02188	1,5E-06	9,0E-07	6,2E-07	6,2E-07	≥ 5,7E+05	≥ 3,5E-01	
FGFR1	BIX 02189	1,2E-06	7,2E-07	6,5E-07	6,5E-07	≥ 5,4E+05	≥ 3,5E-01	
FGFR1	BMS 794833	6,8E-06	4,2E-06	3,3E-06	3,3E-06	≥ 1,1E+05	≥ 3,5E-01	
FGFR1	Bosutinib (SKI-606)	4,9E-06	3,0E-06	1,2E-06	1,2E-06	≥ 2,8E+05	≥ 3,5E-01	
FGFR1	Brivanib (BMS-540215)	1,1E-07	6,6E-08	6,7E-08	6,7E-08	≥ 5,2E+06	≥ 3,5E-01	
FGFR1	Brivanib alaninate (BMS-582664) - prodrug	2,5E-07	1,6E-07	7,7E-08	7,7E-08	≈ 4,3E+06	≈ 3,6E-01	
FGFR1	BX-795	4,3E-07	2,6E-07	≈ 3,4E-07	2,6E-07	≥ 1,0E+06	≥ 3,5E-01	
FGFR1	BX-912	7,5E-08	4,6E-08	7,7E-08	7,7E-08	≈ 5,0E+06	≈ 4,5E-01	
FGFR1	CCT128930	1,8E-05	1,1E-05	1,0E-05	1,0E-05	≥ 3,4E+04	≥ 3,5E-01	
FGFR1	CCT129202	4,7E-08	2,9E-08	5,5E-08	5,5E-08	3,2E+06	1,6E-01	2
FGFR1	CCT137690	6,0E-08	3,7E-08	6,2E-07	3,7E-08	n.e.	n.e.	2
FGFR1	Cediranib (AZD2171)	3,0E-07	1,9E-07	1,7E-08	1,9E-07	n.e.	n.e.	
FGFR1	CEP33779	6,7E-07	4,2E-07	3,9E-07	3,9E-07	≥ 9,0E+05	≥ 3,5E-01	
FGFR1	CHIR-124	2,3E-06	1,4E-06	2,3E-06	2,3E-06	≥ 1,5E+05	≥ 3,5E-01	
FGFR1	CI-1033 (Canertinib)	1,9E-05	1,2E-05	1,1E-05	1,1E-05	≥ 3,1E+04	≥ 3,5E-01	
FGFR1	CP 673451	6,0E-06	3,7E-06	2,7E-06	2,7E-06	≥ 1,3E+05	≥ 3,5E-01	
FGFR1	Crenolanib (CP-868596)	9,0E-06	5,5E-06	2,8E-06	2,8E-06	≈ 1,5E+05	≈ 4,2E-01	
FGFR1	Crizotinib (PF-02341066)	5,4E-06	3,3E-06	6,3E-06	6,3E-06	≥ 5,5E+04	≥ 3,5E-01	
FGFR1	CX-4945 (Silmisertib)	≥ 2,0E-05		≈ 2,0E-05	≈ 2,0E-05	≥ 1,7E+04	≥ 3,5E-01	
FGFR1	CYC116	2,6E-07	1,6E-07	2,2E-07	2,2E-07	≥ 1,6E+06	≥ 3,5E-01	
FGFR1	Cyt387	8,1E-07	5,0E-07	5,8E-07	5,8E-07	≥ 6,1E+05	≥ 3,5E-01	
FGFR1	Dabrafenib (GSK2118436)	≥ 2,0E-05		3,9E-06	3,9E-06	≥ 8,9E+04	≥ 3,5E-01	
FGFR1	Danuserib (PHA-739358)	1,0E-07	6,4E-08	1,4E-07	1,4E-07	5,5E+04	7,6E-03	
FGFR1	Dasatinib (BMS-354825)	1,4E-06	8,7E-07	7,9E-07	7,9E-07	≥ 4,4E+05	≥ 3,5E-01	
FGFR1	DCC-2036 (Rebastinib)	2,2E-08	1,4E-08	n.e.	1,4E-08	1,2E+04	≤ 1,7E-04	4
FGFR1	Desmethyl Erlotinib (CP-473420)	≥ 2,0E-05		1,0E-05	1,0E-05	≥ 3,6E+04	≥ 3,5E-01	
FGFR1	Dinaciclib (SCH727965)	1,9E-05	1,2E-05	≈ 1,1E-05	1,2E-05	≥ 3,1E+04	≥ 3,5E-01	
FGFR1	Dovitinib (TKI-258)	3,4E-08	2,1E-08	1,2E-08	1,2E-08	≥ 3,1E+07	≥ 3,5E-01	
FGFR1	E7080 (Lenvatinib)	5,4E-08	3,3E-08	4,0E-08	4,0E-08	≈ 5,2E+06	≈ 2,3E-01	
FGFR1	ENMD-2076	7,5E-08	4,6E-08	4,5E-08	4,5E-08	1,4E+07	6,6E-01	
FGFR1	Enzastaurin (LY317615)	≥ 2,0E-05		1,0E-05	1,0E-05	≥ 3,5E+04	≥ 3,5E-01	
FGFR1	Erlotinib HCl	≥ 2,0E-05		1,3E-05	1,3E-05	≥ 2,7E+04	≥ 3,5E-01	
FGFR1	Foretinib (GSK1363089 - XL880)	2,5E-07	1,6E-07	2,3E-07	2,3E-07	≥ 1,5E+06	≥ 3,5E-01	
FGFR1	Golitinib (E7050)	7,3E-06	4,5E-06	3,9E-06	3,9E-06	≥ 8,9E+04	≥ 3,5E-01	
FGFR1	GSK1070916	2,1E-07	1,3E-07	1,5E-07	1,5E-07	4,9E+05	7,2E-02	
FGFR1	GSK461364	6,2E-06	3,8E-06	3,3E-06	3,3E-06	≥ 1,1E+05	≥ 3,5E-01	
FGFR1	Hesperadin	2,7E-08	1,7E-08	7,8E-09	7,8E-09	≈ 8,2E+07	≈ 6,6E-01	
FGFR1	INK 128 (MLN0128)	7,2E-07	4,4E-07	6,3E-07	6,3E-07	≥ 5,6E+05	≥ 3,5E-01	
FGFR1	JNJ-7706621	2,7E-07	1,7E-07	1,3E-07	1,3E-07	≥ 2,8E+06	≥ 3,5E-01	
FGFR1	Ki8751	≥ 2,0E-05		4,6E-06	4,6E-06	≈ 2,7E+03	≈ 1,1E-02	2
FGFR1	KRN 633	≥ 2,0E-05		3,2E-06	3,2E-06	≥ 1,1E+05	≥ 3,5E-01	
FGFR1	KW 2449	3,0E-07	1,9E-07	1,4E-06	1,9E-07	n.e.	n.e.	
FGFR1	LDN193189	1,6E-06	9,7E-07	1,8E-06	1,8E-06	≥ 2,0E+05	≥ 3,5E-01	
FGFR1	Linifanib (ABT-869)	1,4E-05	8,6E-06	1,0E-06	8,6E-06	n.e.	n.e.	
FGFR1	Linsitinib (OSI-906)	≥ 2,0E-05		1,5E-05	1,5E-05	≥ 2,4E+04	≥ 3,5E-01	
FGFR1	LY2784544	8,3E-08	5,1E-08	7,5E-07	5,1E-08	n.e.	n.e.	2
FGFR1	MGCD-265	2,1E-06	1,3E-06	1,7E-06	1,7E-06	≥ 2,0E+05	≥ 3,5E-01	
FGFR1	Milciclib (PHA-848125)	6,0E-07	3,7E-07	2,8E-07	2,8E-07	≥ 1,2E+06	≥ 3,5E-01	
FGFR1	MK-2206 2HCl	≥ 2,0E-05		1,6E-05	1,6E-05	≥ 2,2E+04	≥ 3,5E-01	
FGFR1	MK-2461	1,0E-07	6,4E-08	1,7E-07	1,7E-07	n.e.	n.e.	2
FGFR1	MK-5108 (VX-689)	2,2E-07	1,3E-07	≈ 2,2E-07	1,3E-07	≥ 1,6E+06	≥ 3,5E-01	
FGFR1	MLN8054	1,4E-06	8,4E-07	6,6E-07	6,6E-07	≥ 5,3E+05	≥ 3,5E-01	
FGFR1	MLN8237 (Alisertib)	5,4E-07	3,3E-07	3,2E-07	3,2E-07	≥ 1,1E+06	≥ 3,5E-01	
FGFR1	Motesanib Diphosphate (AMG-706)	≥ 2,0E-05		4,6E-06	4,6E-06	≥ 7,5E+04	≥ 3,5E-01	
FGFR1	NVP-ADW742	3,6E-06	2,2E-06	2,5E-06	2,5E-06	≥ 1,4E+05	≥ 3,5E-01	
FGFR1	NVP-BSK805	9,7E-07	6,0E-07	5,9E-07	5,9E-07	≥ 5,9E+05	≥ 3,5E-01	
FGFR1	NVP-TAE226	8,6E-07	5,3E-07	5,7E-07	5,7E-07	≥ 6,2E+05	≥ 3,5E-01	
FGFR1	OSI-930	≥ 2,0E-05		1,0E-05	1,0E-05	≥ 3,4E+04	≥ 3,5E-01	
FGFR1	Pazopanib HCl	9,1E-08	5,6E-08	9,8E-08	9,8E-08	≥ 3,6E+06	≥ 3,5E-01	
FGFR1	PCI-32765 (Ibrutinib)	3,2E-07	2,0E-07	2,3E-07	2,3E-07	≥ 1,5E+06	≥ 3,5E-01	
FGFR1	PD 0332991 (Palbociclib) HCl	1,6E-05	9,9E-06	7,7E-06	7,7E-06	≥ 4,5E+04	≥ 3,5E-01	
FGFR1	PD173074	2,8E-09	1,8E-09	1,5E-09	1,5E-09	2,4E+06	3,5E-03	
FGFR1	PD98059	8,4E-06	5,2E-06	≥ 2,0E-05	≥ 5,2E-06			
FGFR1	Pelitinib (EKB-569)	1,8E-05	1,1E-05	n.e.	1,1E-05	5,6E+02	≤ 6,4E-03	4
FGFR1	PF-00562271	3,0E-07	1,9E-07	2,6E-07	2,6E-07	≥ 1,4E+06	≥ 3,5E-01	
FGFR1	PF-03814735	1,2E-08	7,1E-09	1,1E-08	1,1E-08	1,1E+07	1,2E-01	

kinase	Compound	IC ₅₀ [M] ePCA	K _D eq [M] ePCA *	K _D kin [M] kPCA	K _D [M] PCA **	k _{on} [M ⁻¹ s ⁻¹] kPCA	k _{off} [s ⁻¹] kPCA	comment
FGFR1	PHA-665752	3,1E-06	1,9E-06	1,5E-06	1,5E-06	≥ 2,3E+05	≥ 3,5E-01	
FGFR1	PHA-680632	4,3E-08	2,6E-08	2,3E-08	2,3E-08	3,9E+05	9,0E-03	
FGFR1	PHT-427	1,3E-05	8,2E-06	≥ 2,0E-05	≥ 8,2E-06			
FGFR1	PIK-75	6,2E-07	3,8E-07	9,9E-07	9,9E-07	n.e.	n.e.	2
FGFR1	PLX-4720	5,3E-06	3,3E-06	2,6E-06	2,6E-06	≥ 1,3E+05	≥ 3,5E-01	
FGFR1	Ponatinib (AP24534)	3,3E-09	2,1E-09	n.e.	2,1E-09	3,3E+05	≤ 6,9E-04	4
FGFR1	PP-121	3,2E-08	2,0E-08	4,4E-08	4,4E-08	≥ 7,9E+06	≥ 3,5E-01	
FGFR1	PP242	9,3E-07	5,7E-07	3,6E-07	3,6E-07	≥ 9,8E+05	≥ 3,5E-01	
FGFR1	Quercetin (Sophoretin)	6,8E-06	4,2E-06	5,7E-06	5,7E-06	≥ 6,1E+04	≥ 3,5E-01	
FGFR1	R406	4,0E-08	2,5E-08	3,1E-08	3,1E-08	1,4E+07	3,8E-01	2
FGFR1	R788 (Fostamatinib) - prodrug	2,9E-06	1,8E-06	1,6E-06	1,6E-06	≥ 3,0E+05	≥ 3,5E-01	
FGFR1	Ruxolitinib (INCB018424)	2,1E-06	1,3E-06	2,0E-06	2,0E-06	≥ 1,7E+05	≥ 3,5E-01	
FGFR1	SAR131675	2,1E-06	1,3E-06	1,5E-06	1,5E-06	≥ 2,3E+05	≥ 3,5E-01	
FGFR1	SB 202190	≥ 2,0E-05		1,4E-05	1,4E-05	≥ 2,5E+04	≥ 3,5E-01	
FGFR1	SB590885	1,4E-05	8,6E-06	≥ 2,0E-05	≥ 8,6E-06			
FGFR1	Semaxanib (SU5416)	3,0E-06	1,8E-06	1,9E-06	1,9E-06	≥ 1,9E+05	≥ 3,5E-01	
FGFR1	SNS-314	1,8E-05	1,1E-05	7,0E-06	7,0E-06	≥ 5,0E+04	≥ 3,5E-01	
FGFR1	Sotrastaurin (AEB071)	≥ 2,0E-05		7,8E-06	7,8E-06	≥ 4,5E+04	≥ 3,5E-01	
FGFR1	SP600125	1,0E-06	6,4E-07	5,8E-07	5,8E-07	≥ 6,1E+05	≥ 3,5E-01	
FGFR1	Staurosporine	1,5E-08	9,1E-09	4,3E-09	4,3E-09	5,5E+07	2,2E-01	
FGFR1	SU11274	9,8E-07	6,0E-07	1,2E-06	1,2E-06	≥ 2,9E+05	≥ 3,5E-01	
FGFR1	Sunitinib Malate (Sutent)	2,4E-07	1,5E-07	2,0E-07	2,0E-07	≥ 1,7E+06	≥ 3,5E-01	
FGFR1	TAE684 (NVP-TAE684)	5,8E-08	3,6E-08	1,0E-08	1,0E-08	1,1E+07	1,1E-01	
FGFR1	TAK-901	1,2E-08	7,1E-09	1,9E-08	1,9E-08	9,3E+06	1,6E-01	
FGFR1	TG101209	3,6E-08	2,2E-08	2,5E-08	2,5E-08	≥ 1,4E+07	≥ 3,5E-01	
FGFR1	TG101348 (SAR302503)	1,7E-07	1,0E-07	1,3E-07	1,3E-07	≥ 2,6E+06	≥ 3,5E-01	
FGFR1	Tie2 kinase inhibitor	1,7E-05	1,0E-05	5,3E-06	5,3E-06	≥ 6,6E+04	≥ 3,5E-01	
FGFR1	Tivozanib (AV-951)	2,7E-07	1,7E-07	1,6E-07	1,6E-07	≥ 2,2E+06	≥ 3,5E-01	
FGFR1	Tofacitinib (CP-690550 - Tasocitinib)	1,0E-05	6,3E-06	5,0E-06	5,0E-06	≥ 7,1E+04	≥ 3,5E-01	
FGFR1	Torin 2	8,2E-06	5,1E-06	5,1E-06	5,1E-06	≥ 6,9E+04	≥ 3,5E-01	
FGFR1	TPCA-1	5,4E-07	3,3E-07	5,6E-07	5,6E-07	≥ 6,3E+05	≥ 3,5E-01	
FGFR1	TSU-68 (SU6668)	1,9E-06	1,2E-06	9,3E-07	9,3E-07	≥ 3,8E+05	≥ 3,5E-01	
FGFR1	TWS119	6,3E-07	3,9E-07	3,3E-07	3,3E-07	≈ 1,1E+06	≈ 3,8E-01	
FGFR1	U0126-EtOH	2,3E-06	1,4E-06	≥ 2,0E-05	≥ 1,4E-06			
FGFR1	Vandetanib (Zactima)	6,4E-07	3,9E-07	1,0E-06	1,0E-06	≥ 3,4E+05	≥ 3,5E-01	
FGFR1	Vemurafenib (PLX4032)	≥ 2,0E-05		9,4E-06	9,4E-06	≥ 3,7E+04	≥ 3,5E-01	
FGFR1	VX-680 (MK-0457 - Tozasertib)	3,3E-07	2,0E-07	3,1E-07	3,1E-07	≥ 1,1E+06	≥ 3,5E-01	
FGFR1	WHI-P154	4,8E-06	2,9E-06	3,2E-06	3,2E-06	2,9E+03	9,2E-03	
FGFR1	WZ3146	1,1E-07	6,5E-08	1,8E-07	1,8E-07	≥ 1,9E+06	≥ 3,5E-01	
FGFR1	WZ4002	≈ 9,5E-07	≈ 5,8E-07	1,5E-06	1,5E-06	≥ 2,3E+05	≥ 3,5E-01	
FGFR1	WZ8040	2,7E-07	1,7E-07	3,6E-07	3,6E-07	≥ 9,7E+05	≥ 3,5E-01	
FGFR1	XL-184 (Cabozantinib)	≥ 2,0E-05		2,1E-06	2,1E-06	≥ 1,7E+05	≥ 3,5E-01	
FGFR1	ZM-447439	1,7E-05	1,1E-05	≈ 9,0E-06	1,1E-05	≥ 3,9E+04	≥ 3,5E-01	
FGFR3	AEE788 (NVP-AEE788)	9,2E-07	5,9E-07	≈ 6,1E-07	5,9E-07	≈ 2,3E+05	≈ 1,4E-01	
FGFR3	AG-1024	≥ 2,0E-05		6,6E-06	6,6E-06	≥ 5,3E+04	≥ 3,5E-01	
FGFR3	AG-1478 (Tyrosinase AG-1478)	2,8E-06	1,8E-06	≈ 6,8E-06	1,8E-06	≥ 5,2E+04	≥ 3,5E-01	
FGFR3	AT9283	1,9E-08	1,2E-08	4,0E-09	4,0E-09	4,9E+06	2,0E-02	
FGFR3	Aurora A Inhibitor I	4,4E-07	2,9E-07	≈ 2,6E-07	2,9E-07	≥ 1,4E+06	≥ 3,5E-01	
FGFR3	Axitinib	8,8E-08	5,6E-08	1,3E-08	1,3E-08	≈ 1,4E+07	≈ 1,7E-01	
FGFR3	AZ 960	3,2E-07	2,0E-07	7,1E-08	7,1E-08	≥ 4,9E+06	≥ 3,5E-01	
FGFR3	AZ628	5,7E-06	3,7E-06	5,3E-06	5,3E-06	≥ 6,6E+04	≥ 3,5E-01	
FGFR3	AZD4547	2,1E-09	1,3E-09	1,2E-09	1,2E-09	1,4E+07	1,6E-02	
FGFR3	AZD5438	6,0E-06	3,8E-06	≈ 5,8E-06	3,8E-06	≥ 6,0E+04	≥ 3,5E-01	
FGFR3	AZD7762	1,7E-07	1,1E-07	2,1E-07	2,1E-07	≥ 1,7E+06	≥ 3,5E-01	
FGFR3	AZD8931	≈ 5,3E-06	≈ 3,4E-06	5,3E-06	5,3E-06	≥ 6,6E+04	≥ 3,5E-01	
FGFR3	Barasertib (AZD1152-HQPA)	6,4E-06	4,1E-06	5,1E-06	5,1E-06	≥ 6,8E+04	≥ 3,5E-01	
FGFR3	Baricitinib (LY3009104 - incb28050)	3,2E-06	2,0E-06	2,0E-06	2,0E-06	≈ 8,7E+04	≈ 1,8E-01	
FGFR3	BGJ398 (NVP-BGJ398)	≈ 7,6E-10	≈ 4,9E-10	1,3E-10	1,3E-10	4,7E+06	5,6E-04	
FGFR3	BIBF1120 (Vargatef)	7,1E-08	4,6E-08	9,0E-09	4,6E-08	≈ 3,9E+06	≈ 4,2E-02	
FGFR3	BIRB 796 (Doramapimod)	1,4E-05	8,8E-06	7,4E-06	7,4E-06	3,3E+03	2,2E-02	
FGFR3	BIX 02188	1,7E-07	1,1E-07	3,0E-07	3,0E-07	≥ 1,2E+06	≥ 3,5E-01	
FGFR3	BIX 02189	1,3E-06	8,3E-07	6,0E-07	6,0E-07	≈ 2,4E+05	≈ 1,5E-01	
FGFR3	BMS 794833	≥ 2,0E-05		3,2E-06	3,2E-06	≈ 4,0E+04	≈ 1,2E-01	
FGFR3	Bosutinib (SKI-606)	1,2E-06	7,6E-07	2,8E-07	2,8E-07	9,1E+04	2,5E-02	
FGFR3	Brivanib (BMS-540215)	≈ 1,4E-07	≈ 8,7E-08	5,2E-08	5,2E-08	≥ 6,7E+06	≥ 3,5E-01	
FGFR3	Brivanib alaninate (BMS-582664) - prodrug	3,0E-07	1,9E-07	8,5E-08	8,5E-08	≥ 4,1E+06	≥ 3,5E-01	
FGFR3	BX-795	≈ 5,2E-07	≈ 3,3E-07	3,0E-07	3,0E-07	≥ 1,2E+06	≥ 3,5E-01	
FGFR3	BX-912	6,1E-08	3,9E-08	4,2E-08	4,2E-08	≈ 3,4E+06	≈ 1,6E-01	
FGFR3	CCT128930	≥ 2,0E-05		6,2E-06	6,2E-06	≥ 5,6E+04	≥ 3,5E-01	
FGFR3	CCT129202	2,3E-08	1,5E-08	3,3E-08	3,3E-08	3,1E+06	9,3E-02	2
FGFR3	CCT137690	6,9E-08	4,4E-08	6,0E-07	4,4E-08	n.e.	n.e.	2
FGFR3	Cediranib (AZD2171)	1,4E-07	8,9E-08	5,7E-09	8,9E-08	1,1E+07	6,6E-02	
FGFR3	CEP33779	2,9E-07	1,9E-07	2,3E-07	2,3E-07	n.e.	n.e.	2
FGFR3	CH5424802	≥ 2,0E-05		5,0E-06	5,0E-06	≥ 7,0E+04	≥ 3,5E-01	
FGFR3	CHIR-124	7,3E-07	4,7E-07	7,9E-07	7,9E-07	n.e.	n.e.	2
FGFR3	CI-1033 (Canertinib)	1,2E-06	7,8E-07	1,4E-06	1,4E-06	≈ 1,9E+05	≈ 2,5E-01	2
FGFR3	CP 673451	1,3E-06	8,5E-07	1,0E-06	1,0E-06	4,1E+05	4,2E-01	
FGFR3	Crenolanib (CP-868596)	1,3E-06	8,4E-07	8,1E-07	8,1E-07	≈ 1,1E+05	≈ 7,9E-02	
FGFR3	Crizotinib (PF-02341066)	1,1E-06	7,4E-07	1,7E-06	1,7E-06	n.e.	n.e.	2

kinase	Compound	IC ₅₀ [M] ePCA	K _D eq [M] ePCA *	K _D kin [M] kPCA	K _D [M] PCA **	k _{on} [M ⁻¹ s ⁻¹] kPCA	k _{off} [s ⁻¹] kPCA	comment
FGFR3	CX-4945 (Silmnitasertib)	≥ 2,0E-05		6,7E-06	6,7E-06	≥ 5,2E+04	≥ 3,5E-01	
FGFR3	CYC116	1,2E-07	8,0E-08	7,7E-08	7,7E-08	≈ 2,1E+06	≈ 1,8E-01	
FGFR3	Cyt387	6,6E-07	4,2E-07	3,2E-07	3,2E-07	≈ 7,6E+05	≈ 2,8E-01	
FGFR3	Dabrafenib (GSK2118436)	1,0E-05	6,6E-06	1,6E-06	1,6E-06	≥ 2,1E+05	≥ 3,5E-01	
FGFR3	Danuserib (PHA-739358)	4,6E-08	2,9E-08	8,1E-08	8,1E-08	6,9E+04	5,5E-03	
FGFR3	Dasatinib (BMS-354825)	1,9E-06	1,2E-06	8,5E-07	8,5E-07	≥ 4,1E+05	≥ 3,5E-01	
FGFR3	DCC-2036 (Rebastinib)	8,8E-09	5,6E-09	n.e.	5,6E-09	3,4E+04	≤ 1,9E-04	4
FGFR3	Desmethyl Erlotinib (CP-473420)	1,6E-06	1,0E-06	1,1E-06	1,1E-06	4,1E+05	4,2E-01	
FGFR3	Dovitinib (TKI-258)	1,8E-08	1,1E-08	7,7E-09	7,7E-09	3,6E+07	3,1E-01	
FGFR3	E7080 (Lenvatinib)	6,9E-08	4,4E-08	2,6E-08	2,6E-08	6,9E+06	1,8E-01	
FGFR3	ENMD-2076	7,2E-08	4,6E-08	4,4E-08	4,4E-08	2,2E+06	9,6E-02	
FGFR3	Enzastaurin (LY317615)	≥ 2,0E-05		6,2E-06	6,2E-06	≈ 2,3E+04	≈ 1,5E-01	
FGFR3	Erlotinib HCl	≈ 1,4E-06	≈ 9,1E-07	1,2E-06	1,2E-06	≥ 3,0E+05	≥ 3,5E-01	1
FGFR3	Foretinib (GSK1363089 - XL880)	2,1E-07	1,4E-07	1,9E-07	1,9E-07	3,1E+05	5,9E-02	
FGFR3	GDC-0980 (RG7422)	≥ 2,0E-05		7,4E-06	7,4E-06	≥ 4,7E+04	≥ 3,5E-01	
FGFR3	Gefitinib (Iressa)	≥ 2,0E-05		≈ 8,4E-06	≈ 8,4E-06	≥ 4,2E+04	≥ 3,5E-01	
FGFR3	Golvatinib (E7050)	9,3E-06	6,0E-06	1,8E-06	1,8E-06	≈ 2,4E+05	≈ 4,1E-01	
FGFR3	GSK1070916	9,3E-08	6,0E-08	7,5E-08	7,5E-08	≥ 4,7E+06	≥ 3,5E-01	
FGFR3	GSK461364	1,2E-05	8,0E-06	≈ 4,1E-06	8,0E-06	≥ 8,6E+04	≥ 3,5E-01	
FGFR3	Hesperadin	1,1E-08	6,9E-09	4,5E-09	4,5E-09	≈ 2,1E+07	≈ 8,6E-02	
FGFR3	INK 128 (MLN0128)	1,0E-06	6,5E-07	7,6E-07	7,6E-07	≥ 4,6E+05	≥ 3,5E-01	
FGFR3	JNJ-7706621	2,0E-07	1,3E-07	6,5E-08	6,5E-08	≥ 5,4E+06	≥ 3,5E-01	
FGFR3	Ki8751	≥ 2,0E-05		4,2E-06	4,2E-06	≈ 2,8E+04	≈ 1,5E-01	2
FGFR3	KRN 633	≥ 2,0E-05		2,5E-06	2,5E-06	≈ 6,2E+03	≈ 1,5E-02	
FGFR3	KW 2449	2,6E-07	1,7E-07	7,0E-07	7,0E-07	≈ 6,3E+05	≈ 5,4E-01	
FGFR3	LDN193189	4,9E-07	3,1E-07	9,9E-07	9,9E-07	3,8E+04	3,7E-02	
FGFR3	Linifanib (ABT-869)	≥ 2,0E-05		1,4E-06	1,4E-06	≈ 1,5E+05	≈ 1,2E-01	
FGFR3	Linsitinib (OSI-906)	≥ 2,0E-05		6,0E-06	6,0E-06	6,8E+02	≈ 4,6E-03	
FGFR3	LY2784544	8,2E-08	5,3E-08	6,5E-08	6,5E-08	≈ 2,1E+06	≈ 1,4E-01	
FGFR3	MGCD-265	2,0E-06	1,3E-06	1,1E-06	1,1E-06	≈ 1,3E+05	≈ 1,5E-01	
FGFR3	Milciclib (PHA-848125)	7,7E-07	5,0E-07	2,8E-07	2,8E-07	≈ 8,2E+04	≈ 2,3E-02	
FGFR3	MK-2461	2,0E-08	1,3E-08	≈ 2,0E-08	1,3E-08	n.e.	n.e.	2
FGFR3	MK-5108 (VX-689)	1,4E-07	8,8E-08	1,0E-07	1,0E-07	≥ 3,5E+06	≥ 3,5E-01	
FGFR3	MLN8054	4,4E-07	2,8E-07	3,9E-07	3,9E-07	≈ 1,1E+06	≈ 4,8E-01	
FGFR3	MLN8237 (Alisertib)	4,3E-07	2,8E-07	1,8E-07	1,8E-07	9,3E+05	1,6E-01	
FGFR3	Neratinib (HKI-272)	≥ 2,0E-05		≈ 3,6E-06	≈ 3,6E-06	≈ 1,3E+05	≈ 1,6E-01	
FGFR3	NVP-ADW742	6,1E-06	3,9E-06	2,3E-06	2,3E-06	≥ 1,5E+05	≥ 3,5E-01	
FGFR3	NVP-BSK805	3,0E-07	1,9E-07	1,7E-07	1,7E-07	≈ 1,5E+06	≈ 2,5E-01	
FGFR3	NVP-TAE226	3,1E-07	2,0E-07	1,5E-07	1,5E-07	≈ 9,0E+05	≈ 1,6E-01	
FGFR3	Pazopanib HCl	3,7E-08	2,4E-08	≈ 7,7E-08	2,4E-08	≥ 4,6E+06	≥ 3,5E-01	
FGFR3	PCI-32765 (Ibrutinib)	2,5E-07	1,6E-07	2,1E-07	2,1E-07	≥ 1,0E+06	1,8E-01	
FGFR3	PD 0332991 (Palbociclib) HCl	1,1E-05	7,0E-06	≈ 9,8E-06	7,0E-06	≈ 1,6E+03	≈ 1,7E-02	
FGFR3	PD153035 HCl	≈ 1,2E-05	≈ 7,8E-06	3,2E-06	3,2E-06	≈ 8,3E+04	≈ 2,4E-01	
FGFR3	PD173074	3,0E-09	1,9E-09	1,4E-09	1,4E-09	2,8E+06	3,9E-03	
FGFR3	Pellitinib (EKB-569)	≥ 2,0E-05		4,4E-06	4,4E-06	1,9E+04	8,4E-02	
FGFR3	PF-00562271	3,7E-07	2,4E-07	2,5E-07	2,5E-07	≈ 1,1E+05	≈ 3,3E-02	
FGFR3	PF-03814735	2,4E-09	1,5E-09	3,1E-09	3,1E-09	3,1E+07	4,8E-02	3
FGFR3	PHA-665752	7,4E-07	4,7E-07	5,0E-07	5,0E-07	≈ 9,3E+05	≈ 4,4E-01	
FGFR3	PHA-680632	4,6E-08	2,9E-08	1,8E-08	1,8E-08	6,6E+05	1,2E-02	
FGFR3	PIK-75	3,2E-07	2,1E-07	3,8E-07	3,8E-07	n.e.	n.e.	2
FGFR3	PLX-4720	3,8E-06	2,5E-06	≈ 3,2E-06	2,5E-06	≥ 1,1E+05	≥ 3,5E-01	
FGFR3	Ponatinib (AP24534)	4,4E-09	2,8E-09	1,9E-09	1,9E-09	5,8E+05	1,1E-03	
FGFR3	PP-121	2,6E-08	1,7E-08	6,3E-08	6,3E-08	≈ 6,0E+06	≈ 4,2E-01	
FGFR3	PP242	7,4E-07	4,8E-07	2,6E-07	2,6E-07	≈ 5,0E+05	≈ 1,3E-01	
FGFR3	Quercetin (Sophoretin)	3,0E-06	2,0E-06	1,2E-06	1,2E-06	≥ 2,9E+05	≥ 3,5E-01	
FGFR3	R406	2,6E-08	1,7E-08	1,4E-08	1,4E-08	5,9E+06	9,7E-02	
FGFR3	R788 (Fostamatinib) - prodrug	1,7E-06	1,1E-06	8,4E-07	8,4E-07	2,4E+05	2,5E-01	
FGFR3	Ruxolitinib (INCB018424)	2,9E-06	1,8E-06	2,8E-06	2,8E-06	≥ 1,3E+05	≥ 3,5E-01	
FGFR3	SAR131675	9,2E-07	5,9E-07	3,2E-07	3,2E-07	≈ 1,1E+06	≈ 3,5E-01	
FGFR3	Saracatinib (AZD0530)	1,4E-05	8,9E-06	4,7E-06	4,7E-06	≈ 4,9E+04	≈ 2,4E-01	
FGFR3	Semaxanib (SU5416)	5,2E-07	3,3E-07	3,7E-07	3,7E-07	≈ 3,9E+05	≈ 1,4E-01	1
FGFR3	SNS-314	≥ 2,0E-05		5,7E-06	5,7E-06	≥ 6,1E+04	≥ 3,5E-01	
FGFR3	Sotrastaurin (AEB071)	≥ 2,0E-05		4,1E-06	4,1E-06	≥ 8,5E+04	≥ 3,5E-01	
FGFR3	SP600125	7,4E-07	4,8E-07	3,1E-07	3,1E-07	≥ 1,1E+06	≥ 3,5E-01	
FGFR3	Staurosporine	6,6E-09	4,2E-09	1,8E-09	1,8E-09	2,6E+07	4,8E-02	
FGFR3	SU11274	1,3E-07	8,4E-08	2,5E-07	2,5E-07	≥ 1,4E+06	≥ 3,5E-01	
FGFR3	Sunitinib Malate (Sutent)	6,7E-08	4,3E-08	5,9E-08	5,9E-08	≥ 5,9E+06	≥ 3,5E-01	
FGFR3	TAE684 (NVP-TAE684)	4,9E-08	3,1E-08	7,9E-09	7,9E-09	7,4E+06	5,6E-02	
FGFR3	TAK-901	4,9E-09	3,1E-09	1,2E-08	1,2E-08	3,9E+06	4,6E-02	
FGFR3	TG101209	3,5E-08	2,2E-08	2,7E-08	2,7E-08	≥ 1,3E+07	≥ 3,5E-01	
FGFR3	TG101348 (SAR302503)	2,5E-07	1,6E-07	1,6E-07	1,6E-07	≈ 4,1E+05	≈ 8,6E-02	
FGFR3	Tie2 kinase inhibitor	5,0E-06	3,2E-06	5,2E-06	5,2E-06	≈ 2,1E+04	≈ 9,2E-02	
FGFR3	Tivozanib (AV-951)	2,2E-07	1,4E-07	1,9E-07	1,9E-07	≈ 9,8E+05	≈ 2,1E-01	
FGFR3	Tofacitinib (CP-690550 - Tasocitinib)	1,3E-05	8,3E-06	4,4E-06	4,4E-06	8,0E+04	3,5E-01	
FGFR3	Torin 2	3,5E-06	2,3E-06	3,3E-06	3,3E-06	≥ 1,1E+05	≥ 3,5E-01	
FGFR3	TPCA-1	5,2E-07	3,3E-07	4,5E-07	4,5E-07	≥ 7,8E+05	≥ 3,5E-01	
FGFR3	TSU-68 (SU6668)	8,1E-07	5,2E-07	≈ 2,0E-07	5,2E-07	≈ 7,1E+05	≈ 1,4E-01	
FGFR3	TWS119	3,8E-07	2,4E-07	1,5E-07	1,5E-07	≈ 2,3E+06	≈ 3,5E-01	
FGFR3	U0126-EtOH	1,2E-06	7,6E-07	≈ 5,5E-06	7,6E-07	≈ 4,5E+02	≈ 2,5E-03	

kinase	Compound	IC ₅₀ [M] ePCA	K _D eq [M] ePCA *	K _D kin [M] kPCA	K _D [M] PCA **	k _{on} [M ⁻¹ s ⁻¹] kPCA	k _{off} [s ⁻¹] kPCA	comment
FGFR3	Vandetanib (Zactima)	≈ 1,7E-07	≈ 1,1E-07	2,2E-07	2,2E-07	≥ 1,6E+06	≥ 3,5E-01	
FGFR3	Vemurafenib (PLX4032)	≥ 2,0E-05		7,4E-06	7,4E-06	1,8E+03	1,3E-02	
FGFR3	VX-680 (MK-0457 - Tozasertib)	2,4E-07	1,5E-07	≈ 2,6E-07	1,5E-07	≥ 1,3E+06	≥ 3,5E-01	
FGFR3	WHI-P154	2,9E-06	1,9E-06	1,9E-06	1,9E-06	3,8E+04	7,5E-02	
FGFR3	WZ3146	7,8E-08	5,0E-08	1,7E-07	1,7E-07	≈ 1,1E+06	≈ 2,0E-01	
FGFR3	WZ4002	≈ 9,8E-07	≈ 6,3E-07	1,4E-06	1,4E-06	≥ 2,5E+05	≥ 3,5E-01	
FGFR3	WZ8040	3,1E-07	2,0E-07	≈ 4,1E-07	2,0E-07	≈ 2,6E+05	≈ 1,1E-01	
FGFR3	XL-184 (Cabozantinib)	≥ 2,0E-05		1,8E-06	1,8E-06	≥ 2,0E+05	≥ 3,5E-01	
FGFR3	ZM-447439	1,7E-06	1,1E-06	4,6E-06	4,6E-06	≥ 7,7E+04	≥ 3,5E-01	
FGFR4	AEE788 (NVP-AEE788)	≈ 4,0E-06	≈ 3,5E-06	5,3E-06	5,3E-06	≈ 2,3E+04	≈ 9,4E-02	1
FGFR4	Afatinib (BIBW2992)	≥ 2,0E-05		1,9E-05	1,9E-05	≥ 1,8E+04	≥ 3,5E-01	
FGFR4	AG-1024	≥ 1,9E-05		≥ 2,0E-05	≥ 1,7E-05			
FGFR4	AG-1478 (Typhostin AG-1478)	≥ 1,7E-05		≥ 2,0E-05	≥ 1,5E-05			
FGFR4	Amuvatinib (MP-470)	≥ 2,0E-05		≈ 1,5E-05	≈ 1,5E-05	≈ 2,2E+03	≈ 5,4E-02	
FGFR4	Apatinib (YN968D1)	9,9E-06	8,5E-06	4,8E-06	4,8E-06	≈ 1,6E+04	≈ 7,0E-02	
FGFR4	AT9283	6,5E-07	5,6E-07	7,2E-07	7,2E-07	≈ 9,0E+04	≈ 8,5E-02	
FGFR4	Axitinib	6,6E-07	5,7E-07	1,4E-06	1,4E-06	≈ 1,9E+05	≈ 2,0E-01	1
FGFR4	AZ 960	5,9E-07	5,1E-07	1,2E-06	1,2E-06	≈ 1,8E+05	≈ 2,4E-01	1
FGFR4	AZ628	≈ 1,8E-05	≈ 1,6E-05	3,7E-06	3,7E-06	≈ 1,7E+03	5,9E-03	
FGFR4	AZD2014	≈ 1,8E-05	≈ 1,6E-05	≈ 1,1E-05	≈ 1,4E-05	≈ 5,1E+03	1,0E-01	
FGFR4	AZD4547	1,9E-08	1,6E-08	1,7E-08	1,7E-08	5,5E+06	9,4E-02	
FGFR4	AZD7762	3,4E-06	2,9E-06	5,6E-06	5,6E-06	≈ 5,2E+04	≈ 3,4E-01	
FGFR4	AZD8931	≥ 2,0E-05		9,7E-06	9,7E-06	≥ 3,6E+04	≥ 3,5E-01	
FGFR4	Baricitinib (LY3009104 - incb28050)	1,5E-05	1,3E-05	4,2E-06	4,2E-06	≈ 1,2E+04	≈ 5,5E-02	
FGFR4	BGJ398 (NVP-BGJ398)	2,0E-08	1,7E-08	1,2E-08	1,2E-08	7,3E+06	8,3E-02	
FGFR4	BIBF1120 (Vargatef)	5,5E-07	4,7E-07	5,7E-07	5,7E-07	≈ 7,2E+05	≈ 3,4E-01	1
FGFR4	BIRB 796 (Doramapimod)	≈ 1,4E-05	≈ 1,2E-05	4,5E-06	4,5E-06	≈ 2,7E+03	1,1E-02	
FGFR4	BIX 02188	≥ 2,0E-05		1,0E-05	1,0E-05	≈ 2,4E+03	≈ 2,2E-02	
FGFR4	BIX 02189	≥ 2,0E-05		7,8E-06	7,8E-06	≈ 1,5E+04	≈ 1,2E-01	
FGFR4	BMS-599626 (AC480)	≥ 1,9E-05		≥ 2,0E-05	≥ 1,7E-05			
FGFR4	Bosutinib (SKI-606)	≈ 1,9E-05	≈ 1,6E-05	5,7E-06	5,7E-06	≈ 7,2E+04	≈ 4,0E-01	
FGFR4	Brivanib (BMS-540215)	5,4E-07	4,7E-07	9,9E-07	9,9E-07	8,1E+04	8,3E-02	
FGFR4	Brivanib alaninate (BMS-582664) - prodrug	1,3E-06	1,1E-06	1,5E-06	1,5E-06	≥ 2,4E+05	≥ 3,5E-01	
FGFR4	BX-795	1,9E-06	1,6E-06	1,7E-06	1,7E-06	4,7E+04	7,9E-02	
FGFR4	BX-912	6,2E-07	5,3E-07	≈ 8,7E-07	5,3E-07	≈ 1,5E+05	≈ 1,3E-01	
FGFR4	CCT129202	1,6E-07	1,4E-07	≈ 1,9E-07	1,4E-07	≥ 1,9E+06	≥ 3,5E-01	1
FGFR4	CCT137690	1,2E-06	1,1E-06	3,3E-06	3,3E-06	n.e.	n.e.	12
FGFR4	Cediranib (AZD2171)	≈ 3,0E-06	≈ 2,6E-06	6,3E-07	6,3E-07	≈ 5,4E+05	≈ 3,3E-01	1
FGFR4	CEP33779	4,3E-06	3,7E-06	7,2E-06	7,2E-06	≈ 3,9E+04	≈ 2,6E-01	
FGFR4	CH5424802	5,0E-06	4,3E-06	3,9E-06	3,9E-06	≥ 9,0E+04	≥ 3,5E-01	
FGFR4	CI-1033 (Canertinib)	1,6E-06	1,4E-06	1,8E-05	1,4E-06	n.e.	n.e.	
FGFR4	CYC116	≈ 2,9E-06	≈ 2,5E-06	1,4E-06	1,4E-06	1,3E+05	1,8E-01	
FGFR4	Cyt387	1,1E-06	9,5E-07	1,9E-06	1,9E-06	≈ 1,2E+05	≈ 2,3E-01	1
FGFR4	Dabrafenib (GSK2118436)	1,7E-05	1,5E-05	≈ 2,9E-05	1,5E-05	≥ 1,2E+04	≥ 3,5E-01	
FGFR4	Danuserib (PHA-739358)	2,3E-06	2,0E-06	2,3E-06	2,3E-06	≈ 4,9E+04	≈ 1,2E-01	
FGFR4	Dasatinib (BMS-354825)	6,6E-06	5,7E-06	1,0E-05	1,0E-05	1,4E+04	1,4E-01	1
FGFR4	DCC-2036 (Rebastinib)	≈ 3,4E-08	≈ 3,0E-08	n.e.	≈ 3,0E-08	6,7E+03	≤ 2,0E-04	4
FGFR4	Desmethyl Erlotinib (CP-473420)	≥ 2,0E-05		1,0E-05	1,0E-05	9,0E+03	7,8E-02	
FGFR4	Dovitinib (TKI-258)	2,1E-07	1,8E-07	4,3E-07	4,3E-07	≈ 8,3E+05	≈ 3,1E-01	
FGFR4	E7080 (Lenvatinib)	9,1E-08	7,8E-08	1,2E-07	1,2E-07	5,0E+05	5,9E-02	
FGFR4	ENMD-2076	2,3E-06	2,0E-06	2,1E-06	2,1E-06	≥ 1,6E+05	≥ 3,5E-01	1
FGFR4	Erlotinib HCl	≥ 2,0E-05		1,8E-05	1,8E-05	≈ 9,7E+03	≈ 2,3E-01	
FGFR4	Foretinib (GSK1363089 - XL880)	7,0E-06	6,0E-06	8,3E-06	8,3E-06	≥ 4,2E+04	≥ 3,5E-01	
FGFR4	Golvatinib (E7050)	≥ 2,0E-05		2,1E-05	2,1E-05	≈ 8,3E+03	≈ 1,4E-01	
FGFR4	GSK1059615	≥ 2,0E-05		7,1E-06	7,1E-06	≥ 4,9E+04	≥ 3,5E-01	
FGFR4	GSK1070916	9,2E-06	7,9E-06	6,1E-06	6,1E-06	≈ 1,7E+04	≈ 1,1E-01	1
FGFR4	GSK1838705A	≈ 2,0E-05	≈ 1,7E-05	≈ 4,4E-06	≈ 1,1E-05	n.e.	n.e.	
FGFR4	GSK2126458	≥ 2,0E-05		1,3E-05	1,3E-05	≈ 6,6E+03	≈ 1,0E-01	
FGFR4	Hesperadin	4,6E-07	4,0E-07	3,5E-07	3,5E-07	≥ 9,9E+05	≥ 3,5E-01	1
FGFR4	IC-87114	≥ 2,0E-05		1,3E-05	1,3E-05	≈ 1,2E+04	≈ 1,4E-01	
FGFR4	Imatinib (Gleevec)	≥ 2,0E-05		1,5E-05	1,5E-05	1,9E+04	3,5E-01	
FGFR4	INK 128 (MLN0128)	2,1E-06	1,8E-06	3,0E-06	3,0E-06	7,1E+04	2,1E-01	
FGFR4	JNJ-7706621	4,1E-06	3,6E-06	1,3E-06	1,3E-06	≥ 2,6E+05	≥ 3,5E-01	1
FGFR4	KRN 633	≈ 1,3E-05	≈ 1,1E-05	1,4E-05	1,4E-05	2,9E+03	≈ 4,7E-02	
FGFR4	KW 2449	2,6E-06	2,2E-06	9,2E-06	9,2E-06	≥ 3,8E+04	≥ 3,5E-01	1
FGFR4	Lapatinib Ditosylate (Tykerb)	≥ 2,0E-05		1,6E-05	1,6E-05	≥ 2,1E+04	≥ 3,5E-01	
FGFR4	LDN193189	≈ 5,3E-06	≈ 4,6E-06	2,0E-05	2,0E-05	≥ 1,8E+04	≥ 3,5E-01	
FGFR4	Linifanib (ABT-869)	5,8E-06	5,0E-06	1,4E-05	1,4E-05	≈ 7,8E+03	≈ 6,9E-02	
FGFR4	Linsitinib (OSI-906)	≥ 2,0E-05		8,6E-06	8,6E-06	2,5E+03	2,3E-02	
FGFR4	LY2228820	≥ 2,0E-05		1,7E-05	1,7E-05	9,4E+02	1,7E-02	
FGFR4	LY2784544	6,4E-06	5,5E-06	3,1E-06	3,1E-06	≈ 5,0E+04	1,5E-01	
FGFR4	Milcicib (PHA-848125)	3,5E-06	3,0E-06	3,5E-06	3,5E-06	≈ 2,5E+04	≈ 1,1E-01	1
FGFR4	MK-2461	3,2E-07	2,8E-07	1,3E-06	1,3E-06	≥ 2,6E+05	≥ 3,5E-01	
FGFR4	MK-5108 (VX-689)	5,1E-07	4,4E-07	9,7E-07	9,7E-07	1,3E+05	1,3E-01	
FGFR4	MLN8054	5,3E-06	4,6E-06	3,9E-06	3,9E-06	≈ 1,7E+04	≈ 5,6E-02	
FGFR4	MLN8237 (Alisertib)	6,6E-06	5,7E-06	4,1E-06	4,1E-06	2,6E+04	1,0E-01	
FGFR4	Motesanib Diphosphate (AMG-706)	≈ 1,5E-06	≈ 1,3E-06	1,4E-06	1,4E-06	3,9E+04	5,5E-02	1
FGFR4	NVP-ADW742	≈ 4,2E-06	≈ 3,6E-06	4,2E-06	4,2E-06	6,4E+03	2,6E-02	1
FGFR4	NVP-BSK805	≈ 5,6E-06	≈ 4,8E-06	4,7E-06	4,7E-06	≥ 7,4E+04	≥ 3,5E-01	

kinase	Compound	IC ₅₀ [M] ePCA	K _D eq [M] ePCA *	K _D kin [M] kPCA	K _D [M] PCA **	k _{on} [M ⁻¹ s ⁻¹] kPCA	k _{off} [s ⁻¹] kPCA	comment
FGFR4	NVP-TAE226	4,0E-08	3,4E-08	1,2E-07	1,2E-07	6,4E+05	7,8E-02	
FGFR4	OSI-027	1,5E-05	1,3E-05	≥ 2,0E-05	≥ 1,3E-05			
FGFR4	Pazopanib HCl	2,7E-07	2,3E-07	4,1E-07	4,1E-07	2,3E+05	9,3E-02	1
FGFR4	PCI-32765 (Ibrutinib)	9,3E-07	8,0E-07	3,0E-06	3,0E-06	≈ 7,4E+04	≈ 2,4E-01	
FGFR4	PD153035 HCl	≥ 2,0E-05		1,8E-05	1,8E-05	≥ 1,9E+04	≥ 3,5E-01	
FGFR4	PD173074	3,5E-07	3,0E-07	2,6E-07	2,6E-07	≈ 6,5E+05	≈ 1,7E-01	
FGFR4	PF-00562271	2,4E-06	2,1E-06	2,4E-06	2,4E-06	≈ 3,0E+04	≈ 7,4E-02	
FGFR4	PF-03814735	2,7E-08	2,3E-08	1,5E-07	2,3E-08	n.e.	n.e.	
FGFR4	PHA-680632	4,0E-07	3,5E-07	6,9E-07	6,9E-07	3,0E+05	2,0E-01	
FGFR4	PIK-75	≈ 5,2E-06	≈ 4,5E-06	5,1E-06	5,1E-06	≈ 3,6E+04	≈ 2,4E-01	
FGFR4	Ponatinib (AP24534)	5,0E-08	4,3E-08	8,2E-08	8,2E-08	1,7E+05	1,3E-02	
FGFR4	PP-121	6,9E-08	5,9E-08	2,8E-07	2,8E-07	1,1E+06	3,0E-01	
FGFR4	PP242	9,4E-07	8,1E-07	9,5E-07	9,5E-07	7,0E+04	6,6E-02	
FGFR4	Quercetin (Sophoretin)	4,6E-06	4,0E-06	4,5E-06	4,5E-06	≈ 1,9E+04	≈ 8,2E-02	
FGFR4	R406	1,0E-05	8,6E-06	6,2E-06	6,2E-06	6,9E+04	3,5E-01	1
FGFR4	R788 (Fostamatinib) - prodrug	6,0E-06	5,1E-06	2,0E-05	2,0E-05	≈ 6,6E+03	8,9E-02	
FGFR4	Ruxolitinib (INCB018424)	≈ 1,2E-05	≈ 1,1E-05	1,4E-05	1,4E-05	n.e.	n.e.	
FGFR4	SAR131675	1,1E-05	9,5E-06	3,8E-06	3,8E-06	≥ 9,3E+04	≥ 3,5E-01	
FGFR4	Semaxanib (SU5416)	≥ 2,0E-05		8,7E-06	8,7E-06	1,6E+03	≈ 1,5E-02	
FGFR4	SP600125	7,2E-06	6,2E-06	2,9E-06	2,9E-06	≈ 1,9E+04	≈ 6,4E-02	
FGFR4	Staurosporine	1,4E-07	1,2E-07	8,9E-08	8,9E-08	≈ 7,4E+05	≈ 5,7E-02	1
FGFR4	Sunitinib Malate (Sutent)	1,7E-06	1,5E-06	2,5E-06	2,5E-06	≈ 5,5E+04	≈ 1,5E-01	
FGFR4	TAE684 (NVP-TAE684)	2,5E-08	2,2E-08	1,8E-08	1,8E-08	6,8E+05	1,2E-02	
FGFR4	TAK-901	1,8E-07	1,6E-07	6,3E-07	6,3E-07	≥ 5,5E+05	≥ 3,5E-01	
FGFR4	TG101209	5,6E-07	4,8E-07	3,8E-07	3,8E-07	≈ 3,7E+05	≈ 1,2E-01	
FGFR4	TG101348 (SAR302503)	1,3E-06	1,1E-06	1,6E-06	1,6E-06	1,1E+05	1,6E-01	1
FGFR4	Tivozanib (AV-951)	6,1E-07	5,3E-07	1,0E-06	1,0E-06	≈ 2,0E+05	≈ 2,4E-01	1
FGFR4	Tofacitinib (CP-690550 - Tasocitinib)	1,9E-05	1,6E-05	2,5E-05	2,5E-05	6,2E+03	1,6E-01	
FGFR4	TPCA-1	1,2E-05	1,0E-05	3,0E-06	3,0E-06	≈ 2,2E+04	≈ 7,7E-02	
FGFR4	TSU-68 (SU6668)	3,4E-06	2,9E-06	2,1E-06	2,1E-06	2,9E+04	5,9E-02	
FGFR4	TWS119	6,4E-07	5,5E-07	6,1E-07	6,1E-07	≥ 5,7E+05	≥ 3,5E-01	
FGFR4	Vandetanib (Zactima)	3,3E-06	2,9E-06	6,0E-06	6,0E-06	≈ 1,1E+04	≈ 5,7E-02	
FGFR4	VX-680 (MK-0457 - Tozasertib)	≈ 3,3E-06	≈ 2,9E-06	≈ 7,8E-06	≈ 5,3E-06	≥ 4,5E+04	≥ 3,5E-01	1
FGFR4	WHI-P154	9,7E-06	8,3E-06	≈ 1,4E-05	8,3E-06	≈ 7,5E+03	≈ 1,0E-01	
FGFR4	WYE-687	≥ 2,0E-05		9,2E-06	9,2E-06	1,9E+03	1,9E-02	
FGFR4	WZ3146	6,1E-07	5,2E-07	3,2E-06	3,2E-06	≈ 4,3E+04	≈ 1,5E-01	
FGFR4	WZ4002	≈ 3,5E-06	≈ 3,0E-06	5,9E-06	5,9E-06	≈ 4,7E+04	≈ 1,4E-01	
FGFR4	WZ8040	≈ 3,5E-06	≈ 3,0E-06	6,1E-06	6,1E-06	n.e.	n.e.	1
FLT3	AEE788 (NVP-AEE788)	6,3E-06	3,5E-06	1,7E-06	1,7E-06	1,4E+03	2,2E-03	
FLT3	AMG458	≈ 2,7E-06	≈ 1,5E-06	≈ 6,6E-07	≈ 1,1E-06	n.e.	n.e.	
FLT3	AT9283	≈ 3,6E-06	≈ 2,0E-06	8,8E-07	8,8E-07	5,1E+03	4,5E-03	
FLT3	Aurora A Inhibitor I	≥ 2,0E-05		1,0E-06	1,0E-06	≥ 3,4E+05	≥ 3,5E-01	2
FLT3	Axitinib	3,8E-06	2,1E-06	1,3E-06	1,3E-06	2,5E+03	3,1E-03	
FLT3	AZ 960	5,3E-06	2,9E-06	1,6E-06	1,6E-06	2,0E+03	3,2E-03	
FLT3	AZD2014	≥ 1,1E-05		≥ 2,0E-05	≥ 6,2E-06			
FLT3	AZD4547	2,0E-05	1,1E-05	n.e.	1,1E-05	5,7E+02	≤ 6,2E-03	24
FLT3	AZD7762	7,9E-08	4,4E-08	2,1E-07	2,1E-07	8,6E+03	1,8E-03	
FLT3	Barasertib (AZD1152-HQPA)	≈ 4,1E-07	≈ 2,3E-07	8,0E-08	8,0E-08	1,4E+04	1,1E-03	
FLT3	BIBF1120 (Vargatef)	1,2E-08	6,8E-09	1,5E-09	1,5E-09	3,0E+06	4,1E-03	
FLT3	BIX 02188	4,6E-07	2,6E-07	4,8E-08	2,6E-07	9,6E+04	4,6E-03	
FLT3	BMS 777607	2,2E-06	1,2E-06	n.e.	1,2E-06	1,1E+03	≤ 1,3E-03	4
FLT3	BMS 794833	5,0E-07	2,8E-07	n.e.	2,8E-07	5,9E+02	≤ 1,6E-04	4
FLT3	BX-795	2,0E-06	1,1E-06	9,1E-07	9,1E-07	4,7E+03	4,2E-03	
FLT3	BX-912	3,7E-07	2,0E-07	2,5E-07	2,5E-07	2,5E+04	6,1E-03	
FLT3	CCT137690	1,0E-06	5,6E-07	2,7E-06	2,7E-06	7,1E+03	1,9E-02	
FLT3	CEP33779	≈ 2,0E-06	≈ 1,1E-06	1,7E-06	1,7E-06	2,6E+03	4,5E-03	
FLT3	CHIR-124	2,7E-07	1,5E-07	≈ 2,4E-07	1,5E-07	1,3E+04	2,3E-03	
FLT3	CP 673451	7,4E-07	4,1E-07	4,7E-07	4,7E-07	9,6E+03	4,5E-03	
FLT3	Crenolanib (CP-868596)	3,7E-07	2,1E-07	1,6E-07	1,6E-07	1,2E+04	2,0E-03	
FLT3	CYC116	8,2E-07	4,5E-07	2,8E-07	2,8E-07	1,7E+04	4,8E-03	
FLT3	Dabrafenib (GSK2118436)	1,7E-05	9,5E-06	n.e.	9,5E-06	8,8E+02	≤ 8,4E-03	4
FLT3	DCC-2036 (Rebastinib)	4,9E-06	2,7E-06	n.e.	2,7E-06	4,2E+02	≤ 1,1E-03	4
FLT3	Dovitinib (TKI-258)	3,7E-09	2,1E-09	n.e.	2,1E-09	9,8E+05	≤ 2,0E-03	4
FLT3	ENMD-2076	1,1E-08	5,8E-09	n.e.	5,8E-09	1,9E+05	≤ 1,1E-03	4
FLT3	Foretinib (GSK1363089 - XL880)	3,1E-08	1,7E-08	n.e.	1,7E-08	8,9E+03	≤ 1,5E-04	4
FLT3	GDC-0980 (RG7422)	1,9E-05	1,0E-05	n.e.	1,0E-05	8,0E+02	≤ 8,2E-03	4
FLT3	Golvatinib (E7050)	9,7E-07	5,3E-07	n.e.	5,3E-07	3,3E+03	≤ 1,7E-03	24
FLT3	GSK1070916	1,3E-06	7,2E-07	n.e.	7,2E-07	2,6E+03	≤ 1,9E-03	4
FLT3	Hesperadin	5,0E-07	2,8E-07	2,4E-07	2,4E-07	1,8E+04	4,3E-03	
FLT3	INK 128 (MLN0128)	≈ 2,6E-06	≈ 1,5E-06	5,2E-07	5,2E-07	1,0E+04	5,4E-03	
FLT3	Ki8751	2,2E-08	1,2E-08	n.e.	1,2E-08	7,7E+02	≤ 9,4E-06	4
FLT3	KW 2449	1,1E-07	5,9E-08	1,1E-07	1,1E-07	4,6E+04	5,1E-03	
FLT3	Linifanib (ABT-869)	1,3E-07	7,4E-08	n.e.	7,4E-08	1,5E+03	≤ 1,1E-04	4
FLT3	LY2603618 (IC-83)	1,1E-05	6,2E-06	n.e.	6,2E-06	2,7E+02	≤ 1,7E-03	4
FLT3	LY2784544	8,8E-08	4,9E-08	5,5E-07	4,9E-08	n.e.	n.e.	
FLT3	MGCD-265	8,6E-08	4,7E-08	1,3E-07	1,3E-07	8,2E+03	1,1E-03	
FLT3	Milciclib (PHA-848125)	≈ 5,1E-06	≈ 2,8E-06	1,0E-06	1,0E-06	1,8E+03	1,9E-03	
FLT3	MK-5108 (VX-689)	1,2E-05	6,6E-06	n.e.	6,6E-06	4,0E+02	≤ 2,6E-03	4
FLT3	NVP-ADW742	6,1E-07	3,4E-07	4,8E-07	4,8E-07	1,0E+04	4,9E-03	

kinase	Compound	IC ₅₀ [M] ePCA	K _D eq [M] ePCA *	K _D kin [M] kPCA	K _D [M] PCA **	k _{on} [M ⁻¹ s ⁻¹] kPCA	k _{off} [s ⁻¹] kPCA	comment
FLT3	NVP-BSK805	1,3E-05	7,4E-06	n.e.	7,4E-06	1,4E+03	≤ 1,1E-02	4
FLT3	PCI-32765 (Ibrutinib)	3,6E-06	2,0E-06	1,0E-06	1,0E-06	2,5E+03	2,7E-03	
FLT3	PF-00562271	2,9E-06	1,6E-06	n.e.	1,6E-06	1,7E+03	≤ 2,8E-03	4
FLT3	PF-03814735	2,9E-08	1,6E-08	1,3E-08	1,3E-08	4,3E+05	5,4E-03	
FLT3	PHA-665752	2,4E-06	1,3E-06	3,6E-07	3,6E-07	7,4E+03	2,7E-03	
FLT3	PIK-75	3,2E-07	1,7E-07	4,6E-07	4,6E-07	1,6E+04	6,8E-03	2
FLT3	Ponatinib (AP24534)	1,0E-07	5,5E-08	n.e.	5,5E-08	3,1E+03	≤ 1,7E-04	4
FLT3	Quercetin (Sophoretin)	9,7E-06	5,3E-06	1,3E-06	1,3E-06	1,3E+03	1,7E-03	2
FLT3	Quizartinib (AC220)	2,3E-07	1,3E-07	n.e.	1,3E-07	4,1E+02	≤ 5,1E-05	4
FLT3	R406	1,8E-07	1,0E-07	3,2E-07	3,2E-07	2,2E+04	5,3E-03	2
FLT3	R788 (Fostamatinib) - prodrug	2,6E-06	1,5E-06	n.e.	1,5E-06	5,8E+02	≤ 8,4E-04	4
FLT3	Raf265 derivative	8,2E-06	4,5E-06	n.e.	4,5E-06	3,4E+02	≤ 1,5E-03	4
FLT3	Semaxanib (SU5416)	3,0E-08	1,7E-08	5,7E-08	5,7E-08	5,3E+04	3,1E-03	
FLT3	SNS-314	≈ 5,7E-08	≈ 3,2E-08	n.e.	≈ 3,2E-08	6,1E+03	≤ 1,9E-04	4
FLT3	Sotrastaurin (AEB071)	≈ 1,0E-05	≈ 5,6E-06	n.e.	≈ 5,6E-06	4,0E+02	≤ 2,2E-03	4
FLT3	SP600125	3,3E-06	1,8E-06	8,7E-07	8,7E-07	5,7E+03	4,9E-03	
FLT3	Staurosporine	1,4E-08	7,4E-09	5,1E-09	5,1E-09	5,6E+05	2,9E-03	
FLT3	Sunitinib Malate (Sutent)	2,6E-09	1,4E-09	1,2E-09	1,2E-09	3,4E+06	4,0E-03	
FLT3	TAE684 (NVP-TAE684)	5,8E-06	3,2E-06	9,8E-07	9,8E-07	6,1E+03	5,8E-03	
FLT3	TAK-901	2,7E-07	1,5E-07	3,5E-07	3,5E-07	1,9E+04	6,8E-03	
FLT3	Tandutinib (MLN518)	1,6E-06	8,9E-07	n.e.	8,9E-07	1,5E+03	≤ 1,3E-03	4
FLT3	TG101209	1,8E-06	1,0E-06	1,1E-06	1,1E-06	2,5E+03	2,8E-03	
FLT3	TG101348 (SAR302503)	5,3E-06	2,9E-06	n.e.	2,9E-06	7,9E+02	≤ 2,3E-03	4
FLT3	Tivozanib (AV-951)	5,6E-07	3,1E-07	1,2E-07	1,2E-07	9,2E+03	1,0E-03	
FLT3	Torin 2	≥ 2,0E-05		1,1E-06	1,1E-06	2,6E+03	3,0E-03	
FLT3	TPCA-1	1,4E-05	7,8E-06	n.e.	7,8E-06	7,1E+02	≤ 5,5E-03	4
FLT3	TSU-68 (SU6668)	3,6E-08	2,0E-08	9,5E-09	9,5E-09	4,9E+05	4,8E-03	
FLT3	TWS119	2,8E-06	1,5E-06	1,2E-06	1,2E-06	7,8E+03	8,9E-03	
FLT3	Vandetanib (Zactima)	1,5E-05	8,5E-06	n.e.	8,5E-06	3,2E+02	≤ 2,7E-03	4
FLT3	VX-680 (MK-0457 - Tozasertib)	1,1E-06	6,2E-07	8,1E-07	8,1E-07	7,8E+03	6,3E-03	
FLT3	WZ3146	2,2E-06	1,2E-06	7,4E-07	7,4E-07	6,5E+03	4,8E-03	
FLT3	WZ8040	6,2E-07	3,4E-07	2,7E-07	2,7E-07	1,2E+04	3,3E-03	
FLT3	XL-184 (Cabozantinib)	1,1E-07	5,8E-08	n.e.	5,8E-08	1,8E+03	≤ 1,0E-04	24
FMS	AEE788 (NVP-AEE788)	2,8E-07	1,3E-07	1,1E-07	1,1E-07	7,0E+04	7,8E-03	
FMS	AMG458	5,0E-06	2,3E-06	≥ 2,0E-05	≥ 2,3E-06			
FMS	Apatinib (YN968D1)	2,8E-07	1,3E-07	n.e.	1,3E-07	1,8E+03	≤ 2,4E-04	4
FMS	AT9283	4,1E-07	1,9E-07	2,4E-07	2,4E-07	3,8E+04	8,4E-03	
FMS	Aurora A Inhibitor I	≥ 2,0E-05		2,3E-06	2,3E-06	2,8E+03	6,7E-03	
FMS	Axitinib	1,8E-07	8,1E-08	9,7E-08	9,7E-08	6,4E+04	5,7E-03	
FMS	AZ 960	2,8E-06	1,3E-06	1,0E-06	1,0E-06	9,7E+03	9,7E-03	
FMS	AZ628	5,2E-07	2,4E-07	n.e.	2,4E-07	2,2E+03	≤ 5,2E-04	4
FMS	AZD4547	2,0E-07	8,9E-08	3,3E-08	3,3E-08	1,9E+05	6,5E-03	2
FMS	AZD5438	4,9E-07	2,2E-07	8,2E-07	8,2E-07	1,2E+04	1,0E-02	
FMS	AZD7762	3,7E-06	1,7E-06	n.e.	1,7E-06	2,3E+03	≤ 3,9E-03	4
FMS	Barasertib (AZD1152-HQPA)	9,4E-06	4,3E-06	3,4E-06	3,4E-06	2,9E+03	9,6E-03	
FMS	BEZ235 (NVP-BEZ235)	4,9E-06	2,2E-06	7,7E-07	7,7E-07	1,4E+04	1,0E-02	
FMS	BGJ398 (NVP-BGJ398)	≈ 4,4E-08	≈ 2,0E-08	n.e.	≈ 2,0E-08	2,4E+04	≤ 4,8E-04	4
FMS	BIBF1120 (Vargatef)	5,4E-08	2,5E-08	1,0E-08	1,0E-08	1,0E+06	9,3E-03	
FMS	BIX 02188	7,9E-08	3,6E-08	1,4E-08	1,4E-08	4,5E+05	6,6E-03	2
FMS	BIX 02189	1,8E-06	8,3E-07	6,3E-07	6,3E-07	1,2E+04	7,6E-03	
FMS	BKM120 (NVP-BKM120)	9,5E-07	4,3E-07	6,1E-07	6,1E-07	1,3E+04	8,2E-03	
FMS	BMS-265246	≥ 2,0E-05		3,3E-06	3,3E-06	7,4E+02	2,5E-03	
FMS	Bosutinib (SKI-606)	8,2E-06	3,7E-06	1,8E-06	1,8E-06	4,2E+03	7,7E-03	
FMS	BX-795	≥ 2,0E-05		1,9E-06	1,9E-06	1,2E+03	≈ 2,4E-03	
FMS	BX-912	1,8E-06	8,4E-07	1,2E-06	1,2E-06	6,0E+03	6,9E-03	
FMS	CCT137690	8,4E-07	3,8E-07	1,8E-06	1,8E-06	2,0E+04	3,2E-02	
FMS	Cediranib (AZD2171)	8,2E-06	3,7E-06	5,2E-07	3,7E-06	1,9E+04	9,7E-03	
FMS	CEP33779	2,6E-06	1,2E-06	1,2E-06	1,2E-06	6,6E+03	8,0E-03	
FMS	CH5424802	≥ 2,0E-05		4,8E-06	4,8E-06	≈ 9,8E+02	≈ 5,3E-03	
FMS	CHIR-124	7,5E-09	3,4E-09	8,4E-09	8,4E-09	5,9E+05	4,4E-03	
FMS	CP 673451	1,9E-07	8,7E-08	1,0E-07	1,0E-07	7,5E+04	7,9E-03	
FMS	Crenolanib (CP-868596)	7,3E-08	3,3E-08	4,4E-08	4,4E-08	1,4E+05	6,1E-03	
FMS	Crizotinib (PF-02341066)	3,9E-07	1,8E-07	2,1E-07	2,1E-07	8,2E+04	1,7E-02	
FMS	CX-4945 (Silmatasertib)	4,4E-06	2,0E-06	1,2E-06	1,2E-06	5,5E+03	6,7E-03	
FMS	CYC116	5,9E-07	2,7E-07	3,4E-07	3,4E-07	2,3E+04	7,8E-03	
FMS	Dabrafenib (GSK2118436)	8,5E-07	3,9E-07	1,3E-07	1,3E-07	3,3E+04	4,4E-03	
FMS	Danuserib (PHA-739358)	5,0E-06	2,3E-06	2,1E-06	2,1E-06	2,2E+03	4,7E-03	
FMS	Dasatinib (BMS-354825)	2,7E-09	1,2E-09	n.e.	1,2E-09	1,2E+06	≤ 1,4E-03	4
FMS	Dovitinib (TKI-258)	1,7E-07	7,9E-08	4,7E-08	4,7E-08	1,9E+05	9,1E-03	
FMS	E7080 (Lenvatinib)	2,9E-07	1,3E-07	1,1E-07	1,1E-07	2,2E+04	2,4E-03	
FMS	ENMD-2076	2,8E-07	1,3E-07	1,2E-07	1,2E-07	5,0E+04	6,3E-03	
FMS	Enzastaurin (LY317615)	≥ 2,0E-05		3,9E-06	3,9E-06	7,4E+02	3,0E-03	
FMS	Erlotinib HCl	≥ 2,0E-05		4,8E-06	4,8E-06	5,4E+02	2,6E-03	
FMS	Foretinib (GSK1363089 - XL880)	4,9E-08	2,2E-08	n.e.	2,2E-08	1,1E+04	≤ 2,4E-04	4
FMS	GDC-0941	≥ 2,0E-05		4,4E-06	4,4E-06	4,1E+02	1,8E-03	
FMS	GDC-0980 (RG7422)	2,7E-06	1,2E-06	1,4E-06	1,4E-06	5,2E+03	7,2E-03	
FMS	Golitinib (E7050)	6,7E-07	3,1E-07	5,3E-08	3,1E-07	8,1E+04	4,2E-03	2
FMS	GSK1059615	1,1E-05	5,1E-06	2,9E-06	2,9E-06	2,8E+03	7,5E-03	
FMS	GSK1070916	2,8E-06	1,3E-06	8,5E-07	8,5E-07	6,0E+03	5,2E-03	

kinase	Compound	IC ₅₀ [M] ePCA	K _D eq [M] ePCA *	K _D kin [M] kPCA	K _D [M] PCA **	k _{on} [M ⁻¹ s ⁻¹] kPCA	k _{off} [s ⁻¹] kPCA	comment
FMS	GSK1904529A	≥ 2,0E-05		4,0E-06	4,0E-06	8,9E+02	3,4E-03	
FMS	GSK690693	≥ 2,0E-05		3,0E-06	3,0E-06	2,3E+03	6,4E-03	
FMS	Hesperadin	5,9E-06	2,7E-06	1,4E-06	1,4E-06	4,0E+03	5,5E-03	
FMS	Imatinib (Gleevec)	5,1E-06	2,3E-06	n.e.	2,3E-06	4,5E+02	≤ 1,0E-03	4
FMS	INCB28060	≥ 2,0E-05		3,2E-06	3,2E-06	1,1E+03	3,5E-03	
FMS	INK 128 (MLN0128)	2,0E-06	8,9E-07	6,5E-07	6,5E-07	1,5E+04	9,6E-03	
FMS	JNJ-38877605	3,9E-06	1,8E-06	2,4E-06	2,4E-06	3,1E+03	7,3E-03	
FMS	JNJ-7706621	7,8E-07	3,6E-07	1,9E-07	1,9E-07	2,9E+04	5,4E-03	
FMS	Ki8751	2,1E-08	9,5E-09	n.e.	9,5E-09	4,2E+03	≤ 4,0E-05	24
FMS	KRN 633	2,9E-06	1,3E-06	7,7E-07	7,7E-07	7,1E+03	5,4E-03	
FMS	KW 2449	2,6E-07	1,2E-07	3,6E-07	3,6E-07	2,3E+04	8,0E-03	
FMS	Linifanib (ABT-869)	2,7E-08	1,2E-08	n.e.	1,2E-08	1,5E+04	≤ 1,9E-04	4
FMS	LY2784544	1,4E-07	6,2E-08	n.e.	6,2E-08	1,2E+05	≤ 7,1E-03	4
FMS	Masitinib (AB1010)	1,2E-06	5,3E-07	n.e.	5,3E-07	5,0E+02	≤ 2,7E-04	4
FMS	MGCD-265	8,9E-08	4,1E-08	1,6E-07	1,6E-07	1,7E+04	2,7E-03	
FMS	MK-5108 (VX-689)	6,6E-07	3,0E-07	5,7E-07	5,7E-07	1,7E+04	9,8E-03	
FMS	Motesanib Diphosphate (AMG-706)	4,6E-07	2,1E-07	n.e.	2,1E-07	1,9E+03	≤ 4,0E-04	4
FMS	Nilotinib (AMN-107)	≥ 2,0E-05		5,7E-06	5,7E-06	6,9E+02	3,9E-03	
FMS	NVP-ADW742	1,0E-05	4,6E-06	2,8E-06	2,8E-06	1,0E+03	2,9E-03	
FMS	NVP-BGT226	≥ 2,0E-05		1,1E-06	1,1E-06	5,1E+03	5,7E-03	
FMS	NVP-BSK805	2,2E-07	9,9E-08	9,6E-08	9,6E-08	5,9E+04	5,9E-03	
FMS	NVP-TAE226	7,8E-07	3,6E-07	5,4E-07	5,4E-07	1,6E+04	8,7E-03	
FMS	OSI-930	1,3E-07	6,0E-08	n.e.	6,0E-08	2,1E+03	≤ 1,3E-04	24
FMS	Pazopanib HCl	3,7E-08	1,7E-08	7,4E-08	7,4E-08	3,7E+04	2,6E-03	
FMS	PD173074	≥ 2,0E-05		3,7E-06	3,7E-06	8,4E+02	3,1E-03	
FMS	PD318088	≥ 2,0E-05		3,1E-06	3,1E-06	1,2E+03	4,0E-03	
FMS	PF-00562271	1,2E-05	5,6E-06	n.e.	5,6E-06	1,5E+03	≤ 8,6E-03	4
FMS	PF-03814735	1,5E-07	6,7E-08	1,9E-07	1,9E-07	3,5E+04	6,5E-03	
FMS	PHA-665752	4,2E-06	1,9E-06	1,1E-06	1,1E-06	7,6E+03	8,7E-03	
FMS	PHA-680632	≥ 2,0E-05		3,0E-06	3,0E-06	1,2E+03	3,6E-03	
FMS	PLX-4720	1,4E-05	6,2E-06	n.e.	6,2E-06	1,5E+03	≤ 9,3E-03	4
FMS	Ponatinib (AP24534)	1,9E-07	8,6E-08	n.e.	8,6E-08	1,3E+03	≤ 1,1E-04	4
FMS	PP-121	2,1E-07	9,7E-08	2,2E-07	2,2E-07	2,7E+04	5,9E-03	
FMS	PP242	≥ 2,0E-05		1,1E-06	1,1E-06	≥ 3,1E+05	≥ 3,5E-01	
FMS	R406	≥ 1,1E-06		1,8E-06	1,8E-06	5,7E+03	8,6E-03	2
FMS	R788 (Fostamatinib) - prodrug	1,2E-05	5,6E-06	4,1E-06	5,6E-06	≈ 4,4E+02	≈ 3,3E-03	
FMS	Raf265 derivative	1,0E-05	4,6E-06	≈ 2,6E-06	4,6E-06	≈ 3,2E+02	≈ 1,4E-03	
FMS	Ruxolitinib (INCB018424)	≥ 2,0E-05		2,9E-06	2,9E-06	5,5E+02	≈ 1,7E-03	
FMS	Saracatinib (AZD0530)	2,3E-06	1,1E-06	3,1E-07	3,1E-07	1,4E+04	4,5E-03	
FMS	SB 203580	≥ 2,0E-05		5,1E-06	5,1E-06	7,8E+02	3,9E-03	
FMS	Semaxanib (SU5416)	2,0E-07	8,9E-08	3,5E-07	3,5E-07	2,7E+04	9,2E-03	
FMS	SGX-523	≥ 2,0E-05		3,3E-06	3,3E-06	4,1E+02	1,3E-03	
FMS	SNS-032 (BMS-387032)	≥ 2,0E-05		3,3E-06	3,3E-06	1,1E+03	3,7E-03	
FMS	SNS-314	1,7E-06	7,9E-07	7,8E-07	7,8E-07	9,4E+03	7,3E-03	
FMS	SP600125	3,4E-06	1,5E-06	1,2E-06	1,2E-06	7,3E+03	8,9E-03	
FMS	Staurosporine	2,0E-08	9,2E-09	8,4E-09	8,4E-09	7,6E+05	7,0E-03	3
FMS	SU11274	8,4E-07	3,8E-07	7,4E-07	7,4E-07	9,2E+03	6,7E-03	
FMS	Sunitinib Malate (Sutent)	5,9E-09	2,7E-09	4,3E-09	4,3E-09	2,2E+06	9,3E-03	
FMS	TAE684 (NVP-TAE684)	1,9E-05	8,8E-06	2,2E-06	2,2E-06	2,8E+03	6,3E-03	
FMS	TAK-901	3,0E-07	1,4E-07	4,9E-07	4,9E-07	1,6E+04	7,6E-03	
FMS	Tandutinib (MLN518)	2,0E-06	9,3E-07	9,3E-07	9,3E-07	6,0E+03	5,6E-03	
FMS	TG101209	2,4E-06	1,1E-06	1,8E-06	1,8E-06	3,5E+03	6,5E-03	
FMS	TG101348 (SAR302503)	7,9E-06	3,6E-06	n.e.	3,6E-06	1,7E+03	≤ 5,3E-03	4
FMS	Tivozanib (AV-951)	1,5E-07	6,7E-08	1,9E-08	1,9E-08	3,8E+04	7,2E-04	
FMS	Torin 1	2,4E-06	1,1E-06	5,3E-07	5,3E-07	1,5E+04	7,9E-03	
FMS	Torin 2	5,7E-08	2,6E-08	5,9E-08	5,9E-08	1,3E+05	7,9E-03	
FMS	TPCA-1	1,0E-06	4,6E-07	5,3E-07	5,3E-07	1,7E+04	9,1E-03	
FMS	TSU-68 (SU6668)	7,4E-08	3,4E-08	5,0E-08	5,0E-08	1,4E+05	7,0E-03	
FMS	TWS119	3,5E-08	1,6E-08	1,0E-08	1,0E-08	9,3E+05	9,3E-03	
FMS	Tyrphostin AG 879 (AG 879)	≥ 2,0E-05		4,1E-06	4,1E-06	6,3E+02	2,6E-03	
FMS	Vatalanib 2HCl (PTK787)	6,0E-06	2,7E-06	n.e.	2,7E-06	8,9E+02	≤ 2,4E-03	4
FMS	VX-680 (MK-0457 - Tozasertib)	9,0E-06	4,1E-06	3,7E-06	3,7E-06	1,5E+03	5,4E-03	
FMS	WP1130	≥ 2,0E-05		2,8E-06	2,8E-06	1,3E+03	3,8E-03	
FMS	WZ3146	4,1E-07	1,9E-07	1,9E-07	1,9E-07	5,1E+04	9,7E-03	
FMS	WZ4002	1,2E-06	5,7E-07	2,8E-07	2,8E-07	4,7E+04	1,1E-02	
FMS	WZ8040	2,7E-08	1,2E-08	2,0E-08	2,0E-08	4,3E+05	7,9E-03	
FMS	XL-184 (Cabozantinib)	1,9E-06	8,7E-07	3,7E-07	3,7E-07	7,0E+03	2,5E-03	2
FMS	XL765	≥ 2,0E-05		3,4E-06	3,4E-06	1,1E+03	3,7E-03	
FMS	ZM-447439	≈ 7,8E-06	≈ 3,6E-06	4,1E-06	4,1E-06	1,7E+03	7,1E-03	
FYN	A-674563	≥ 2,0E-05		5,7E-06	5,7E-06	2,2E+03	1,3E-02	
FYN	AEE788 (NVP-AEE788)	7,3E-08	3,6E-08	5,9E-08	5,9E-08	≈ 7,6E+06	≈ 4,9E-01	
FYN	Afatinib (BIBW2992)	2,6E-06	1,3E-06	1,9E-06	1,9E-06	≈ 5,0E+04	≈ 8,9E-02	
FYN	AG-1024	3,7E-06	1,8E-06	1,2E-06	1,2E-06	≈ 6,2E+04	≈ 9,1E-02	
FYN	AG-1478 (Tyrphostin AG-1478)	7,5E-07	3,7E-07	7,5E-07	7,5E-07	≈ 7,2E+04	≈ 5,7E-02	
FYN	AMG458	2,4E-06	1,2E-06	1,1E-06	1,1E-06	2,3E+04	2,6E-02	
FYN	Apatinib (YN968D1)	4,4E-06	2,1E-06	1,7E-06	1,7E-06	≈ 3,5E+04	≈ 4,9E-02	
FYN	ARRY334543	5,3E-06	2,6E-06	1,8E-06	1,8E-06	1,2E+05	2,1E-01	
FYN	AT9283	7,6E-08	3,7E-08	3,3E-08	3,3E-08	3,8E+06	1,3E-01	
FYN	Aurora A Inhibitor I	≥ 2,0E-05		2,1E-06	2,1E-06	≈ 5,4E+04	8,5E-02	

kinase	Compound	IC ₅₀ [M] ePCA	K _D eq [M] ePCA *	K _D kin [M] kPCA	K _D [M] PCA **	k _{on} [M ⁻¹ s ⁻¹] kPCA	k _{off} [s ⁻¹] kPCA	comment
FYN	Axitinib	7,6E-06	3,7E-06	1,1E-06	1,1E-06	≥ 3,3E+05	≥ 3,5E-01	
FYN	AZ 960	6,3E-08	3,1E-08	2,6E-08	2,6E-08	1,8E+06	4,7E-02	
FYN	AZ628	9,9E-07	4,8E-07	3,9E-07	3,9E-07	9,9E+04	3,7E-02	
FYN	AZD4547	9,7E-07	4,7E-07	2,8E-07	2,8E-07	2,8E+05	7,7E-02	
FYN	AZD5438	3,5E-06	1,7E-06	1,9E-06	1,9E-06	≈ 3,4E+04	≈ 5,9E-02	
FYN	AZD7762	1,7E-08	8,2E-09	7,4E-09	7,4E-09	1,8E+07	1,3E-01	
FYN	AZD8931	4,0E-07	1,9E-07	2,0E-07	2,0E-07	≈ 9,9E+05	≈ 2,0E-01	
FYN	Barasertib (AZD1152-HQPA)	5,1E-06	2,5E-06	2,8E-06	2,8E-06	1,9E+04	5,0E-02	
FYN	Baricitinib (LY3009104 - incb28050)	4,2E-06	2,1E-06	1,6E-06	1,6E-06	≈ 2,7E+04	≈ 5,1E-02	
FYN	BEZ235 (NVP-BEZ235)	≥ 2,0E-05		2,4E-06	2,4E-06	≈ 2,4E+04	≈ 6,2E-02	
FYN	BGJ398 (NVP-BGJ398)	3,2E-06	1,6E-06	1,0E-06	1,0E-06	8,1E+04	8,6E-02	
FYN	BIBF1120 (Vargatef)	6,9E-08	3,4E-08	9,2E-09	9,2E-09	1,2E+07	1,1E-01	
FYN	BIX 02188	1,2E-06	6,1E-07	3,6E-07	3,6E-07	≈ 1,2E+05	≈ 3,9E-02	
FYN	BIX 02189	2,4E-06	1,1E-06	1,1E-06	1,1E-06	6,6E+04	7,4E-02	1
FYN	BMS 77607	8,7E-07	4,2E-07	3,3E-07	3,3E-07	2,9E+05	9,1E-02	
FYN	BMS 794833	1,6E-06	7,6E-07	6,0E-07	6,0E-07	8,2E+04	4,9E-02	
FYN	BMS-599626 (AC480)	≥ 2,0E-05		6,4E-06	6,4E-06	1,5E+03	9,5E-03	
FYN	Bosutinib (SKI-606)	8,6E-10	4,2E-10	7,0E-10	7,0E-10	5,6E+06	3,9E-03	
FYN	Brivanib (BMS-540215)	3,0E-06	1,5E-06	1,1E-06	1,1E-06	1,1E+05	1,1E-01	
FYN	Brivanib alaninate (BMS-582664) - prodrug	≥ 2,0E-05		6,2E-07	6,2E-07	≈ 1,6E+05	≈ 1,0E-01	
FYN	BX-795	1,2E-06	5,7E-07	7,0E-07	7,0E-07	≈ 1,4E+05	≈ 9,7E-02	
FYN	BX-912	4,8E-07	2,3E-07	2,9E-07	2,9E-07	5,3E+05	1,5E-01	
FYN	CCT129202	≥ 2,0E-05		7,1E-06	7,1E-06	n.e.	n.e.	
FYN	CCT137690	6,6E-07	3,2E-07	3,0E-06	3,2E-07	n.e.	n.e.	2
FYN	Cediranib (AZD2171)	2,9E-06	1,4E-06	1,4E-07	1,4E-06	1,0E+06	1,4E-01	
FYN	CEP33779	1,3E-06	6,1E-07	5,6E-07	5,6E-07	1,5E+05	8,4E-02	
FYN	CH5424802	≥ 2,0E-05		1,1E-06	1,1E-06	6,5E+05	6,5E-01	2
FYN	CHIR-124	9,0E-08	4,4E-08	1,2E-07	1,2E-07	6,6E+05	7,0E-02	
FYN	CI-1033 (Canertinib)	≈ 4,1E-07	≈ 2,0E-07	2,9E-07	2,9E-07	≥ 1,2E+06	≥ 3,5E-01	
FYN	CP 673451	2,5E-07	1,2E-07	1,2E-07	1,2E-07	8,1E+05	9,5E-02	
FYN	Crenolanib (CP-868596)	5,0E-07	2,4E-07	2,8E-07	2,8E-07	≈ 1,7E+06	≈ 4,9E-01	
FYN	Crizotinib (PF-02341066)	7,3E-07	3,5E-07	9,7E-07	9,7E-07	n.e.	n.e.	2
FYN	CX-4945 (Silmisertib)	3,4E-06	1,7E-06	1,2E-06	1,2E-06	≈ 1,3E+05	≈ 1,6E-01	
FYN	CYC116	2,7E-07	1,3E-07	1,3E-07	1,3E-07	≈ 7,0E+05	≈ 8,3E-02	
FYN	Cyt387	2,0E-06	9,9E-07	6,8E-07	6,8E-07	1,2E+05	8,0E-02	
FYN	Dabrafenib (GSK2118436)	3,2E-07	1,5E-07	1,9E-07	1,9E-07	2,7E+05	5,1E-02	
FYN	Dacomitinib (PF299804 - PF-00299804)	9,7E-07	4,7E-07	1,2E-06	1,2E-06	≈ 8,0E+04	≈ 1,1E-01	
FYN	Danuserib (PHA-739358)	3,5E-08	1,7E-08	3,0E-08	3,0E-08	9,6E+04	2,9E-03	
FYN	Dasatinib (BMS-354825)	≤ 1,1E-10	≤ 5,5E-11	n.e.	≤ 5,5E-11	1,3E+07	≤ 7,3E-04	4
FYN	DCC-2036 (Rebastinib)	1,8E-08	8,8E-09	n.e.	8,8E-09	4,6E+04	≤ 4,0E-04	4
FYN	Desmethyl Erlotinib (CP-473420)	4,3E-07	2,1E-07	1,9E-07	1,9E-07	≈ 3,3E+05	≈ 7,9E-02	
FYN	Dovitinib (TKI-258)	8,8E-08	4,3E-08	2,5E-08	2,5E-08	3,3E+06	9,3E-02	
FYN	E7080 (Lenvatinib)	4,6E-06	2,3E-06	1,6E-06	1,6E-06	6,1E+04	9,8E-02	
FYN	ENMD-2076	9,4E-08	4,6E-08	3,2E-08	3,2E-08	1,5E+06	4,9E-02	
FYN	Erlotinib HCl	1,1E-06	5,5E-07	5,6E-07	5,6E-07	1,1E+05	6,0E-02	
FYN	Flavopiridol HCl	8,8E-06	4,3E-06	3,3E-06	3,3E-06	≥ 1,0E+05	≥ 3,5E-01	
FYN	Foretinib (GSK1363089 - XL880)	2,6E-08	1,2E-08	2,3E-08	2,3E-08	5,5E+05	1,2E-02	
FYN	GDC-0941	≥ 2,0E-05		7,1E-06	7,1E-06	6,7E+02	4,7E-03	
FYN	GDC-0980 (RG7422)	3,1E-07	1,5E-07	5,3E-07	5,3E-07	≈ 1,2E+05	≈ 5,3E-02	
FYN	Gefitinib (Iressa)	1,0E-06	4,9E-07	1,0E-06	1,0E-06	≈ 4,8E+05	≈ 4,3E-01	
FYN	Golvatinib (E7050)	1,2E-06	6,0E-07	4,4E-07	4,4E-07	1,2E+05	5,2E-02	
FYN	GSK1070916	2,4E-06	1,2E-06	1,0E-06	1,0E-06	≈ 3,7E+05	≈ 4,2E-01	
FYN	Hesperadin	5,3E-09	2,6E-09	2,2E-09	2,2E-09	1,3E+07	2,7E-02	
FYN	Imatinib (Gleevec)	6,8E-06	3,3E-06	4,4E-06	4,4E-06	2,1E+04	8,1E-02	
FYN	INK 128 (MLN0128)	1,7E-06	8,2E-07	5,8E-07	5,8E-07	1,9E+05	1,1E-01	
FYN	JNJ-7706621	1,6E-06	7,6E-07	4,8E-07	4,8E-07	1,3E+05	6,2E-02	
FYN	Ki8751	≈ 4,0E-07	≈ 1,9E-07	6,8E-07	6,8E-07	≈ 1,1E+05	≈ 8,1E-02	2
FYN	KRN 633	≥ 2,0E-05		4,9E-06	4,9E-06	3,2E+03	1,5E-02	
FYN	KW 2449	2,3E-06	1,1E-06	3,0E-06	3,0E-06	≥ 1,2E+05	≥ 3,5E-01	
FYN	LDN193189	7,1E-07	3,5E-07	2,5E-07	2,5E-07	1,1E+06	2,8E-01	
FYN	Linifanib (ABT-869)	≥ 2,0E-05		3,4E-06	3,4E-06	9,8E+03	3,4E-02	
FYN	Linsitinib (OSI-906)	≥ 2,0E-05		5,1E-06	5,1E-06	1,3E+03	6,5E-03	
FYN	LY2784544	5,8E-08	2,8E-08	1,1E-08	1,1E-08	2,6E+06	3,0E-02	
FYN	Masitinib (AB1010)	3,3E-07	1,6E-07	1,0E-07	1,0E-07	1,1E+05	1,1E-02	
FYN	MGCD-265	2,4E-08	1,2E-08	1,8E-08	1,8E-08	9,7E+05	1,7E-02	
FYN	Milcicli (PHA-848125)	1,0E-07	5,1E-08	3,0E-08	3,0E-08	2,2E+06	6,6E-02	
FYN	MK-2461	≈ 5,1E-06	≈ 2,5E-06	3,3E-06	3,3E-06	≥ 1,0E+05	≥ 3,5E-01	
FYN	MK-5108 (VX-689)	1,2E-07	6,0E-08	9,7E-08	9,7E-08	4,0E+06	3,7E-01	
FYN	MLN8054	2,9E-07	1,4E-07	1,2E-07	1,2E-07	5,1E+05	5,8E-02	
FYN	MLN8237 (Alisertib)	7,5E-08	3,6E-08	2,4E-08	2,4E-08	1,2E+06	2,7E-02	
FYN	Motesanib Diphosphate (AMG-706)	1,1E-05	5,3E-06	4,2E-06	4,2E-06	2,6E+03	1,1E-02	
FYN	Neratinib (HKI-272)	3,1E-06	1,5E-06	5,7E-07	5,7E-07	2,3E+05	1,2E-01	
FYN	Nilotinib (AMN-107)	≥ 2,0E-05		1,9E-06	1,9E-06	4,1E+03	7,0E-03	
FYN	NVP-ADW742	1,9E-06	9,5E-07	1,1E-06	1,1E-06	6,9E+04	7,7E-02	
FYN	NVP-BGT226	≥ 2,0E-05		1,6E-06	1,6E-06	≈ 2,9E+05	≈ 4,4E-01	
FYN	NVP-BHG712	≈ 5,1E-06	≈ 2,5E-06	9,3E-07	9,3E-07	2,2E+03	2,1E-03	
FYN	NVP-BSK805	1,2E-06	5,9E-07	3,9E-07	3,9E-07	1,7E+05	6,5E-02	
FYN	NVP-TAE226	9,6E-07	4,7E-07	3,4E-07	3,4E-07	3,9E+05	1,3E-01	
FYN	OSI-930	1,3E-06	6,2E-07	7,6E-07	7,6E-07	≈ 5,8E+04	≈ 3,9E-02	

kinase	Compound	IC ₅₀ [M] ePCA	K _D eq [M] ePCA *	K _D kin [M] kPCA	K _D [M] PCA **	k _{on} [M ⁻¹ s ⁻¹] kPCA	k _{off} [s ⁻¹] kPCA	comment
FYN	Pazopanib HCl	≈ 2,6E-07	≈ 1,3E-07	3,1E-07	3,1E-07	3,5E+05	1,1E-01	
FYN	PCI-32765 (Ibrutinib)	2,4E-08	1,2E-08	2,4E-08	2,4E-08	2,0E+06	4,9E-02	
FYN	PD153035 HCl	7,8E-07	3,8E-07	6,0E-07	6,0E-07	1,2E+05	7,1E-02	
FYN	PD173074	≥ 2,0E-05		7,4E-06	7,4E-06	1,1E+03	8,3E-03	
FYN	Pellitinib (EKB-569)	1,4E-07	6,8E-08	1,0E-07	1,0E-07	≈ 4,6E+05	≈ 4,9E-02	
FYN	PF-00562271	3,3E-07	1,6E-07	1,4E-07	1,4E-07	≈ 6,7E+05	8,8E-02	
FYN	PF-03814735	7,1E-08	3,4E-08	3,1E-08	3,1E-08	≈ 2,7E+06	≈ 9,2E-02	2
FYN	PHA-665752	≈ 8,8E-06	≈ 4,3E-06	2,1E-06	2,1E-06	≥ 1,7E+05	≥ 3,5E-01	
FYN	PHA-680632	1,2E-07	5,9E-08	5,3E-08	5,3E-08	5,6E+05	3,1E-02	
FYN	PHA-793887	≥ 2,0E-05		1,0E-05	1,0E-05	3,4E+02	3,4E-03	
FYN	PIK-75	7,0E-08	3,4E-08	6,5E-08	6,5E-08	≥ 5,4E+06	≥ 3,5E-01	
FYN	PLX-4720	6,3E-07	3,1E-07	1,7E-07	1,7E-07	≈ 7,2E+05	≈ 1,1E-01	
FYN	Ponatinib (AP24534)	4,9E-10	2,4E-10	2,5E-10	2,5E-10	1,1E+06	2,8E-04	
FYN	PP-121	3,1E-09	1,5E-09	4,7E-09	4,7E-09	1,5E+07	7,1E-02	
FYN	PP242	7,1E-07	3,5E-07	1,7E-07	1,7E-07	4,8E+05	8,2E-02	
FYN	Quercetin (Sophtoretin)	2,2E-06	1,1E-06	1,2E-06	1,2E-06	≈ 2,1E+05	≈ 2,6E-01	
FYN	Quizartinib (AC220)	≥ 2,0E-05		4,4E-06	4,4E-06	3,0E+02	1,3E-03	
FYN	R406	5,1E-08	2,5E-08	2,2E-08	2,2E-08	8,7E+06	2,0E-01	2
FYN	R788 (Fostamatinib) - prodrug	2,9E-06	1,4E-06	1,6E-06	1,6E-06	1,1E+05	9,9E-02	
FYN	Ruxolitinib (INCB018424)	≈ 3,7E-06	≈ 1,8E-06	2,9E-06	2,9E-06	≈ 7,8E+04	≈ 2,2E-01	
FYN	Saracatinib (AZD0530)	1,5E-08	7,5E-09	3,7E-09	3,7E-09	6,1E+06	2,1E-02	
FYN	SB 202190	6,4E-06	3,1E-06	2,1E-06	2,1E-06	3,4E+04	6,8E-02	
FYN	SB 203580	6,8E-06	3,3E-06	2,6E-06	2,6E-06	≈ 6,1E+04	≈ 1,7E-01	
FYN	SB590885	4,5E-06	2,2E-06	3,7E-06	3,7E-06	≥ 9,5E+04	≥ 3,5E-01	
FYN	Semaxanib (SU5416)	≥ 2,0E-05		1,4E-06	1,4E-06	2,5E+04	3,3E-02	
FYN	SNS-314	1,6E-05	7,7E-06	3,7E-06	3,7E-06	≈ 2,4E+03	≈ 8,9E-03	
FYN	Sotrastaurin (AEB071)	≥ 2,0E-05		7,4E-06	7,4E-06	1,5E+03	1,2E-02	
FYN	SP600125	1,2E-05	5,7E-06	3,8E-06	3,8E-06	≈ 2,2E+04	≈ 8,4E-02	
FYN	Staurosporine	4,8E-09	2,3E-09	1,2E-09	1,2E-09	3,5E+07	4,1E-02	
FYN	SU11274	6,7E-07	3,3E-07	9,4E-07	9,4E-07	9,0E+04	8,3E-02	
FYN	Sunitinib Malate (Sutent)	1,5E-07	7,4E-08	1,4E-07	1,4E-07	≈ 7,4E+05	≈ 1,2E-01	
FYN	TAE684 (NVP-TAE684)	1,0E-07	4,9E-08	1,4E-08	1,4E-08	1,0E+07	1,2E-01	
FYN	TAK-285	≥ 2,0E-05		6,3E-06	6,3E-06	2,3E+03	1,5E-02	
FYN	TAK-901	1,2E-09	5,9E-10	1,6E-09	1,6E-09	7,0E+06	1,1E-02	
FYN	TG101209	9,7E-08	4,7E-08	3,6E-08	3,6E-08	2,0E+06	7,1E-02	
FYN	TG101348 (SAR302503)	3,5E-07	1,7E-07	1,8E-07	1,8E-07	≈ 2,1E+06	≈ 3,3E-01	
FYN	Tie2 kinase inhibitor	≥ 2,0E-05		4,8E-06	4,8E-06	≈ 1,1E+03	≈ 4,6E-03	
FYN	Tivozanib (AV-951)	1,1E-07	5,5E-08	6,9E-08	6,9E-08	1,1E+06	7,1E-02	
FYN	Tofacitinib (CP-690550 - Tasocitinib)	2,6E-06	1,3E-06	8,8E-07	8,8E-07	1,3E+05	1,1E-01	
FYN	Torin 2	≥ 2,0E-05		5,1E-06	5,1E-06	2,8E+03	1,4E-02	
FYN	TPCA-1	8,5E-07	4,1E-07	4,8E-07	4,8E-07	≈ 1,7E+05	≈ 7,7E-02	
FYN	TSU-68 (SU6668)	3,8E-06	1,8E-06	1,8E-06	1,8E-06	7,7E+04	1,4E-01	
FYN	TWS119	2,8E-08	1,4E-08	5,9E-09	5,9E-09	1,2E+07	7,0E-02	
FYN	Vandetanib (Zactima)	5,7E-08	2,8E-08	1,1E-07	1,1E-07	≈ 2,1E+06	≈ 2,2E-01	
FYN	Vemurafenib (PLX4032)	≈ 4,0E-07	≈ 1,9E-07	2,2E-07	2,2E-07	1,9E+05	4,1E-02	1
FYN	VX-680 (MK-0457 - Tozasertib)	3,0E-07	1,5E-07	2,3E-07	2,3E-07	2,9E+05	6,6E-02	
FYN	WHI-P154	8,4E-07	4,1E-07	5,2E-07	5,2E-07	≈ 8,8E+04	≈ 3,6E-02	
FYN	WZ3146	1,4E-06	6,7E-07	7,4E-07	7,4E-07	≈ 1,0E+05	≈ 7,5E-02	
FYN	WZ8040	1,3E-06	6,1E-07	8,5E-07	8,5E-07	≈ 1,2E+05	≈ 9,7E-02	
FYN	XL-184 (Cabozantinib)	2,9E-07	1,4E-07	1,1E-07	1,1E-07	4,9E+05	5,3E-02	1
FYN	ZM-447439	5,5E-07	2,7E-07	7,0E-07	7,0E-07	1,2E+05	8,5E-02	
IGF1R	A-674563	8,4E-06	6,2E-06	9,2E-06	9,2E-06	n.e.	n.e.	
IGF1R	AT9283	1,3E-06	9,7E-07	5,7E-07	5,7E-07	2,1E+05	1,2E-01	
IGF1R	AZ 960	1,9E-06	1,4E-06	1,5E-06	1,5E-06	1,2E+05	1,8E-01	
IGF1R	AZD4547	3,3E-07	2,4E-07	8,9E-08	8,9E-08	1,1E+06	9,5E-02	
IGF1R	AZD7762	5,9E-07	4,4E-07	6,2E-07	6,2E-07	3,4E+05	2,0E-01	
IGF1R	BEZ235 (NVP-BEZ235)	≥ 2,0E-05		4,9E-06	4,9E-06	1,0E+04	4,9E-02	
IGF1R	BGJ398 (NVP-BGJ398)	≈ 3,7E-06	≈ 2,7E-06	≈ 2,2E-06	≈ 2,4E-06	≈ 1,4E+05	≈ 3,1E-01	
IGF1R	BI 2536	4,6E-06	3,4E-06	5,4E-06	5,4E-06	≥ 6,5E+04	≥ 3,5E-01	
IGF1R	BIBF1120 (Vargatef)	5,9E-07	4,3E-07	2,4E-07	2,4E-07	≈ 7,2E+05	≈ 1,5E-01	
IGF1R	Bosutinib (SKI-606)	5,2E-06	3,8E-06	3,0E-06	3,0E-06	≈ 2,8E+04	≈ 9,5E-02	
IGF1R	BX-795	2,8E-06	2,1E-06	4,1E-06	4,1E-06	≈ 2,3E+04	≈ 9,2E-02	
IGF1R	BX-912	9,5E-07	7,0E-07	1,1E-06	1,1E-06	7,5E+04	8,1E-02	
IGF1R	CCT137690	3,3E-06	2,4E-06	1,0E-05	1,0E-05	≥ 3,5E+04	≥ 3,5E-01	
IGF1R	CEP33779	3,6E-06	2,7E-06	4,2E-06	4,2E-06	1,6E+04	6,8E-02	
IGF1R	CH5424802	≥ 2,0E-05		2,4E-06	2,4E-06	≥ 1,5E+05	≥ 3,5E-01	
IGF1R	Crizotinib (PF-02341066)	5,0E-07	3,7E-07	3,9E-07	3,9E-07	≥ 9,0E+05	≥ 3,5E-01	
IGF1R	CYC116	≈ 5,2E-06	≈ 3,8E-06	1,5E-06	1,5E-06	4,5E+04	6,7E-02	
IGF1R	Dabrafenib (GSK2118436)	9,1E-06	6,7E-06	≈ 4,6E-06	6,7E-06	1,1E+04	5,1E-02	
IGF1R	Danuserib (PHA-739358)	1,1E-05	8,2E-06	≈ 1,3E-05	8,2E-06	n.e.	n.e.	
IGF1R	DCC-2036 (Rebastinib)	1,0E-05	7,5E-06	n.e.	7,5E-06	≈ 4,0E+03	1,6E-02	3
IGF1R	Dovitinib (TKI-258)	3,6E-06	2,6E-06	1,5E-06	1,5E-06	1,0E+05	1,5E-01	
IGF1R	ENMD-2076	6,0E-07	4,4E-07	8,1E-07	8,1E-07	9,7E+04	7,8E-02	
IGF1R	Foretinib (GSK1363089 - XL880)	2,5E-07	1,8E-07	4,1E-07	4,1E-07	≈ 4,7E+05	≈ 1,9E-01	
IGF1R	GDC-0941	≥ 2,0E-05		2,5E-06	2,5E-06	1,4E+03	3,2E-03	
IGF1R	GDC-0980 (RG7422)	1,6E-06	1,2E-06	1,6E-06	1,6E-06	3,4E+04	5,6E-02	
IGF1R	GSK1070916	≈ 1,7E-06	≈ 1,2E-06	9,2E-07	9,2E-07	2,0E+05	1,9E-01	
IGF1R	GSK1838705A	3,7E-09	2,7E-09	4,4E-09	4,4E-09	1,9E+06	8,4E-03	
IGF1R	GSK1904529A	≥ 2,0E-05		6,5E-06	6,5E-06	n.e.	n.e.	

kinase	Compound	IC ₅₀ [M] ePCA	K _D eq [M] ePCA *	K _D kin [M] kPCA	K _D [M] PCA **	k _{on} [M ⁻¹ s ⁻¹] kPCA	k _{off} [s ⁻¹] kPCA	comment
IGF1R	Hesperadin	1,3E-08	9,8E-09	5,1E-09	5,1E-09	1,3E+07	6,3E-02	
IGF1R	INK 128 (MLN0128)	1,6E-05	1,2E-05	4,1E-05	4,1E-05	2,4E+03	9,5E-02	
IGF1R	JNJ-7706621	1,3E-05	9,3E-06	2,9E-06	2,9E-06	≈ 3,0E+04	≈ 8,5E-02	
IGF1R	KW 2449	5,9E-07	4,3E-07	9,7E-07	9,7E-07	≈ 1,2E+05	≈ 1,3E-01	
IGF1R	Linifanib (ABT-869)	9,4E-06	6,9E-06	1,1E-05	1,1E-05	1,3E+04	1,4E-01	
IGF1R	Linsitinib (OSI-906)	8,4E-10	6,2E-10	n.e.	6,2E-10	2,1E+05	≤ 1,3E-04	4
IGF1R	LY2784544	4,5E-07	3,3E-07	5,2E-07	5,2E-07	1,1E+05	5,6E-02	
IGF1R	Milciclib (PHA-848125)	5,3E-06	3,9E-06	4,8E-06	4,8E-06	2,1E+04	9,1E-02	
IGF1R	MK-5108 (VX-689)	≈ 5,0E-07	≈ 3,7E-07	2,9E-07	2,9E-07	≈ 3,7E+05	≈ 1,1E-01	
IGF1R	MLN8054	1,3E-05	9,4E-06	7,1E-06	7,1E-06	2,1E+04	1,5E-01	
IGF1R	MLN8237 (Alisertib)	3,0E-06	2,2E-06	3,5E-06	3,5E-06	≈ 4,5E+04	≈ 1,7E-01	
IGF1R	Neratinib (HKI-272)	1,3E-05	9,8E-06	3,4E-06	3,4E-06	4,3E+04	1,4E-01	
IGF1R	NVP-ADW742	1,0E-09	7,4E-10	n.e.	7,4E-10	2,3E+07	≤ 1,7E-02	4
IGF1R	NVP-BSK805	6,0E-06	4,4E-06	3,8E-06	3,8E-06	1,4E+04	5,4E-02	
IGF1R	NVP-TAE226	3,9E-09	2,9E-09	3,6E-09	3,6E-09	9,3E+06	3,4E-02	
IGF1R	Pazopanib HCl	≥ 2,0E-05		2,7E-06	2,7E-06	3,7E+04	9,9E-02	
IGF1R	PF-00562271	1,4E-07	1,0E-07	1,1E-07	1,1E-07	6,9E+05	6,9E-02	
IGF1R	PF-03814735	2,6E-08	1,9E-08	2,1E-08	2,1E-08	≈ 1,6E+07	≈ 3,8E-01	
IGF1R	PHA-665752	≥ 2,0E-05		3,7E-06	3,7E-06	≈ 3,2E+04	≈ 1,2E-01	
IGF1R	PIK-75	≈ 6,4E-06	≈ 4,7E-06	2,8E-06	2,8E-06	2,7E+04	7,4E-02	
IGF1R	PLX-4720	1,6E-05	1,2E-05	8,2E-06	8,2E-06	1,7E+04	1,4E-01	
IGF1R	Ponatinib (AP24534)	2,0E-06	1,4E-06	3,2E-06	3,2E-06	≥ 1,1E+05	≥ 3,5E-01	
IGF1R	PP-121	5,4E-07	3,9E-07	8,6E-07	8,6E-07	1,1E+05	9,7E-02	
IGF1R	R406	1,3E-06	9,3E-07	2,0E-06	9,3E-07	1,2E+05	2,3E-01	2
IGF1R	R788 (Fostamatinib) - prodrug	1,6E-06	1,1E-06	1,4E-06	1,4E-06	8,8E+04	1,3E-01	
IGF1R	Semaxanib (SU5416)	≈ 5,5E-06	≈ 4,0E-06	2,2E-06	2,2E-06	3,3E+04	7,3E-02	
IGF1R	Stauroporine	4,5E-08	3,3E-08	4,0E-08	4,0E-08	≈ 6,2E+06	≈ 2,5E-01	
IGF1R	Sunitinib Malate (Sutent)	6,7E-07	4,9E-07	6,1E-07	6,1E-07	1,9E+05	1,2E-01	
IGF1R	TAE684 (NVP-TAE684)	≈ 2,3E-09	≈ 1,7E-09	8,7E-10	8,7E-10	2,7E+07	2,0E-02	
IGF1R	TAK-901	3,1E-08	2,3E-08	5,2E-08	5,2E-08	1,8E+06	9,2E-02	
IGF1R	TG101209	1,3E-07	9,5E-08	2,2E-07	2,2E-07	7,4E+05	1,6E-01	
IGF1R	TG101348 (SAR302503)	4,5E-07	3,3E-07	4,8E-07	4,8E-07	≈ 5,2E+05	≈ 2,4E-01	
IGF1R	TPCA-1	≈ 4,4E-06	≈ 3,3E-06	1,6E-06	1,6E-06	9,1E+04	1,5E-01	
IGF1R	TSU-68 (SU6668)	≈ 3,7E-06	≈ 2,7E-06	2,2E-06	2,2E-06	5,3E+04	1,1E-01	1
IGF1R	VX-680 (MK-0457 - Tozasertib)	1,3E-06	9,9E-07	2,0E-06	2,0E-06	≈ 1,3E+05	≈ 2,5E-01	
IGF1R	WZ3146	5,0E-07	3,6E-07	4,1E-07	4,1E-07	2,6E+05	1,1E-01	
IGF1R	WZ4002	4,7E-07	3,5E-07	4,3E-07	4,3E-07	2,2E+05	9,3E-02	1
IGF1R	WZ8040	2,7E-07	2,0E-07	6,1E-07	6,1E-07	9,3E+04	5,7E-02	
IGF1R	XL-184 (Cabozantinib)	≥ 2,0E-05		2,8E-06	2,8E-06	5,5E+04	1,6E-01	
IGF1R	ZM-447439	1,7E-06	1,2E-06	1,1E-05	1,2E-06	≈ 6,3E+03	6,6E-02	
IKK-alpha	A-674563	4,7E-07	2,7E-07	3,6E-07	3,6E-07	8,6E+04	3,0E-02	
IKK-alpha	AS-252424	6,8E-06	3,8E-06	2,9E-06	2,9E-06	5,3E+04	1,6E-01	
IKK-alpha	AS-605240	≈ 3,0E-06	≈ 1,7E-06	2,3E-06	2,3E-06	3,6E+04	7,6E-02	1
IKK-alpha	AT7867	1,0E-05	5,8E-06	9,0E-06	9,0E-06	2,3E+03	2,1E-02	
IKK-alpha	AT9283	2,8E-07	1,6E-07	1,1E-07	1,1E-07	3,3E+05	3,6E-02	
IKK-alpha	Aurora A Inhibitor I	≥ 2,0E-05		1,2E-05	1,2E-05	n.e.	n.e.	
IKK-alpha	AZD5438	4,2E-07	2,4E-07	3,6E-07	3,6E-07	≈ 2,8E+06	≈ 1,1E+00	
IKK-alpha	AZD7762	4,8E-07	2,7E-07	3,7E-07	3,7E-07	4,9E+05	≈ 2,0E-01	
IKK-alpha	Baricitinib (LY3009104 - incb28050)	1,0E-05	5,8E-06	4,5E-06	4,5E-06	n.e.	n.e.	
IKK-alpha	BIRB 796 (Doramapimod)	≥ 2,0E-05		8,8E-06	8,8E-06	2,4E+03	2,2E-02	
IKK-alpha	BIX 02188	≥ 2,0E-05		2,3E-05	2,3E-05	≥ 1,5E+04	≥ 3,5E-01	
IKK-alpha	BMS 777607	≥ 2,0E-05		1,2E-05	1,2E-05	3,8E+02	4,9E-03	
IKK-alpha	Bosutinib (SKI-606)	2,9E-06	1,7E-06	5,6E-07	5,6E-07	3,6E+04	1,9E-02	1
IKK-alpha	BX-795	1,6E-06	8,9E-07	1,2E-06	1,2E-06	≈ 3,2E+05	≈ 3,8E-01	
IKK-alpha	BX-912	1,9E-06	1,1E-06	1,4E-06	1,4E-06	1,6E+05	2,3E-01	
IKK-alpha	CCT128930	1,7E-05	9,4E-06	1,3E-05	1,3E-05	2,2E+03	2,7E-02	
IKK-alpha	CEP33779	1,0E-06	5,8E-07	6,4E-07	6,4E-07	≈ 5,6E+05	3,1E-01	
IKK-alpha	CHIR-124	7,1E-07	4,0E-07	8,2E-07	8,2E-07	5,3E+04	3,9E-02	
IKK-alpha	CP 673451	≥ 2,0E-05		1,1E-05	1,1E-05	n.e.	n.e.	
IKK-alpha	Crenolanib (CP-868596)	≥ 2,0E-05		7,5E-06	7,5E-06	3,1E+02	2,4E-03	
IKK-alpha	CX-4945 (Silmisertib)	≥ 2,0E-05		1,6E-05	1,6E-05	1,9E+02	≈ 3,3E-03	
IKK-alpha	CYC116	3,0E-08	1,7E-08	1,9E-08	1,9E-08	2,0E+06	3,7E-02	
IKK-alpha	Cyt387	2,7E-09	1,5E-09	≤ 4,5E-10	≤ 4,5E-10	4,7E+06	2,1E-03	
IKK-alpha	Dabrafenib (GSK2118436)	≥ 2,0E-05		8,8E-06	8,8E-06	≈ 3,8E+03	≈ 3,3E-02	
IKK-alpha	Desmethyl Erlotinib (CP-473420)	≥ 2,0E-05		9,3E-06	9,3E-06	1,5E+03	1,4E-02	
IKK-alpha	Dovitinib (TKI-258)	5,7E-06	3,2E-06	2,3E-06	2,3E-06	≥ 1,6E+05	≥ 3,5E-01	
IKK-alpha	ENMD-2076	3,8E-06	2,1E-06	1,9E-06	1,9E-06	8,2E+04	1,6E-01	
IKK-alpha	Foretinib (GSK1363089 - XL880)	≥ 2,0E-05		1,2E-05	1,2E-05	2,7E+03	3,2E-02	
IKK-alpha	GDC-0941	≥ 2,0E-05		1,7E-05	1,7E-05	≥ 2,1E+04	≥ 3,5E-01	
IKK-alpha	GDC-0980 (RG7422)	≥ 2,0E-05		1,7E-05	1,7E-05	3,3E+02	4,8E-03	
IKK-alpha	GSK1059615	≈ 3,9E-06	≈ 2,2E-06	7,3E-07	7,3E-07	≥ 4,8E+05	≥ 3,5E-01	1
IKK-alpha	GSK1070916	6,8E-06	3,8E-06	4,0E-06	4,0E-06	8,3E+03	3,2E-02	
IKK-alpha	GSK461364	1,6E-05	8,7E-06	6,2E-06	6,2E-06	≥ 5,7E+04	≥ 3,5E-01	
IKK-alpha	GSK690693	1,4E-05	7,6E-06	1,3E-05	1,3E-05	≈ 1,6E+03	≈ 2,5E-02	
IKK-alpha	JNJ-7706621	4,2E-06	2,4E-06	2,0E-06	2,0E-06	≥ 1,8E+05	≥ 3,5E-01	
IKK-alpha	KW 2449	3,2E-07	1,8E-07	5,2E-07	5,2E-07	≥ 6,8E+05	≥ 3,5E-01	
IKK-alpha	Milciclib (PHA-848125)	≥ 2,0E-05		1,2E-05	1,2E-05	≈ 3,8E+03	3,9E-02	
IKK-alpha	MK-5108 (VX-689)	1,8E-06	1,0E-06	1,3E-06	1,3E-06	≥ 2,7E+05	≥ 3,5E-01	
IKK-alpha	NVP-ADW742	≥ 2,0E-05		≈ 1,4E-05	≈ 1,4E-05	≥ 2,6E+04	≥ 3,5E-01	

kinase	Compound	IC ₅₀ [M] ePCA	K _D eq [M] ePCA *	K _D kin [M] kPCA	K _D [M] PCA **	k _{on} [M ⁻¹ s ⁻¹] kPCA	k _{off} [s ⁻¹] kPCA	comment
IKK-alpha	NVP-BGT226	≈ 2,0E-05	≈ 1,1E-05	9,6E-06	9,6E-06	≈ 5,9E+03	≈ 5,9E-02	
IKK-alpha	NVP-BSK805	9,4E-06	5,3E-06	4,3E-06	4,3E-06	1,1E+04	≈ 4,6E-02	
IKK-alpha	NVP-BVU972	≥ 2,0E-05		1,8E-05	1,8E-05	≥ 1,9E+04	≥ 3,5E-01	
IKK-alpha	NVP-TAE226	7,1E-06	4,0E-06	2,4E-06	2,4E-06	4,8E+04	1,1E-01	
IKK-alpha	PD153035 HCl	≥ 2,0E-05		1,7E-05	1,7E-05	≥ 2,1E+04	≥ 3,5E-01	
IKK-alpha	Pelitinib (EKB-569)	≥ 2,0E-05		1,2E-05	1,2E-05	6,8E+02	7,9E-03	
IKK-alpha	PF-00562271	1,2E-05	6,6E-06	5,6E-06	5,6E-06	1,0E+04	5,8E-02	
IKK-alpha	PF-03814735	1,9E-07	1,1E-07	1,4E-07	1,4E-07	6,1E+05	8,6E-02	
IKK-alpha	PHA-767491	8,9E-08	5,0E-08	4,9E-08	4,9E-08	1,3E+06	6,6E-02	
IKK-alpha	Piceatannol	9,2E-06	5,2E-06	5,8E-06	5,8E-06	≈ 6,1E+04	≈ 3,3E-01	
IKK-alpha	PIK-75	3,3E-06	1,9E-06	3,3E-06	3,3E-06	n.e.	n.e.	2
IKK-alpha	Ponatinib (AP24534)	1,0E-07	5,7E-08	8,9E-08	8,9E-08	1,8E+04	1,6E-03	
IKK-alpha	PP-121	1,4E-05	7,7E-06	8,7E-06	8,7E-06	1,8E+03	1,5E-02	
IKK-alpha	PP242	4,9E-06	2,7E-06	1,3E-06	1,3E-06	1,8E+04	2,2E-02	
IKK-alpha	Quercetin (Sophoretin)	3,4E-06	1,9E-06	3,1E-06	3,1E-06	6,1E+04	1,8E-01	
IKK-alpha	R406	3,1E-07	1,8E-07	3,7E-06	1,8E-07	3,5E+04	1,0E-01	12
IKK-alpha	R788 (Fostamatinib) - prodrug	1,2E-05	7,0E-06	1,4E-05	1,4E-05	6,0E+03	3,3E-02	
IKK-alpha	Ruxolitinib (INCB018424)	1,4E-05	7,9E-06	7,4E-06	7,4E-06	≈ 3,9E+03	≈ 2,6E-02	
IKK-alpha	SB 202190	2,8E-06	1,6E-06	1,4E-06	1,4E-06	≈ 1,4E+05	≈ 1,9E-01	
IKK-alpha	Semaxanib (SU5416)	1,7E-05	9,7E-06	8,6E-06	8,6E-06	≈ 2,1E+03	1,7E-02	
IKK-alpha	SNS-032 (BMS-387032)	≥ 2,0E-05		1,5E-05	1,5E-05	≈ 5,6E+04	≈ 7,8E-01	
IKK-alpha	SNS-314	6,3E-07	3,5E-07	3,4E-07	3,4E-07	2,0E+04	6,7E-03	
IKK-alpha	SP600125	4,5E-07	2,5E-07	2,3E-07	2,3E-07	6,0E+05	1,3E-01	
IKK-alpha	Staurosporine	1,9E-08	1,1E-08	5,2E-09	5,2E-09	1,8E+06	9,4E-03	
IKK-alpha	Sunitinib Malate (Sutent)	2,1E-06	1,2E-06	1,2E-06	1,2E-06	≥ 2,9E+05	≥ 3,5E-01	
IKK-alpha	TAE684 (NVP-TAE684)	≥ 2,0E-05		1,3E-05	1,3E-05	≥ 2,6E+04	≥ 3,5E-01	
IKK-alpha	TAK-901	1,4E-05	7,9E-06	7,3E-06	7,3E-06	9,9E+02	7,3E-03	
IKK-alpha	TG 100713	≥ 2,0E-05		≈ 5,3E-06	≈ 5,3E-06	≥ 6,6E+04	≥ 3,5E-01	
IKK-alpha	TG101209	5,7E-07	3,2E-07	3,6E-07	3,6E-07	1,8E+05	6,2E-02	
IKK-alpha	TG101348 (SAR302503)	2,0E-06	1,1E-06	1,2E-06	1,2E-06	5,3E+04	6,6E-02	
IKK-alpha	Thiazovivin	3,0E-06	1,7E-06	1,3E-06	1,3E-06	1,1E+05	1,4E-01	
IKK-alpha	Torin 2	≥ 2,0E-05		1,5E-05	1,5E-05	≥ 2,4E+04	≥ 3,5E-01	
IKK-alpha	TPCA-1	1,5E-07	8,3E-08	1,1E-07	1,1E-07	4,2E+05	4,2E-02	
IKK-alpha	TSU-68 (SU6668)	2,1E-06	1,2E-06	1,6E-06	1,6E-06	3,5E+04	5,5E-02	
IKK-alpha	TWS119	7,0E-06	4,0E-06	3,8E-06	3,8E-06	≈ 3,3E+04	1,1E-01	
IKK-alpha	U0126-EtOH	≥ 2,0E-05		2,6E-05	2,6E-05	≥ 1,3E+04	≥ 3,5E-01	
IKK-alpha	VX-680 (MK-0457 - Tozasertib)	1,5E-05	8,6E-06	1,1E-05	1,1E-05	≥ 3,2E+04	≥ 3,5E-01	
IKK-alpha	WAY-600	≈ 2,0E-05	≈ 1,1E-05	1,1E-05	1,1E-05	≈ 5,1E+02	≈ 5,0E-03	
IKK-alpha	WHI-P154	6,9E-06	3,9E-06	3,6E-06	3,6E-06	≈ 3,5E+04	≈ 1,2E-01	
IKK-alpha	WZ3146	1,5E-05	8,5E-06	7,9E-06	7,9E-06	≥ 4,4E+04	≥ 3,5E-01	
IKK-alpha	WZ8040	≥ 2,0E-05		1,9E-05	1,9E-05	≥ 6,7E+02	1,2E-02	
IKK-alpha	Y-27632 2HCl	3,1E-06	1,8E-06	2,2E-06	2,2E-06	≈ 2,5E+05	≈ 5,4E-01	
IKK-beta	A-674563	2,0E-06	1,2E-06	1,2E-06	1,2E-06	1,5E+04	1,8E-02	
IKK-beta	AS-605240	≈ 4,6E-06	≈ 2,8E-06	2,7E-06	2,7E-06	n.e.	n.e.	
IKK-beta	AT7867	1,6E-07	9,4E-08	n.e.	9,4E-08	2,3E+05	≤ 2,1E-02	4
IKK-beta	AT9283	6,2E-07	3,7E-07	2,1E-07	2,1E-07	8,3E+04	1,8E-02	
IKK-beta	Aurora A Inhibitor I	1,9E-07	1,1E-07	1,2E-07	1,2E-07	2,7E+05	3,0E-02	2
IKK-beta	AZ 960	1,6E-05	9,6E-06	4,4E-06	4,4E-06	≥ 8,0E+04	≥ 3,5E-01	
IKK-beta	AZD5438	1,2E-06	7,5E-07	1,3E-06	1,3E-06	n.e.	n.e.	
IKK-beta	AZD7762	4,7E-07	2,8E-07	4,6E-07	4,6E-07	4,6E+04	2,1E-02	
IKK-beta	Baricitinib (LY3009104 - incb28050)	1,5E-06	8,8E-07	4,0E-07	4,0E-07	4,5E+04	≈ 2,0E-02	
IKK-beta	BIX 02188	1,2E-06	7,2E-07	7,0E-07	7,0E-07	≈ 6,5E+04	≈ 4,0E-02	2
IKK-beta	BX-795	3,6E-06	2,2E-06	1,8E-06	1,8E-06	≥ 2,0E+05	≥ 3,5E-01	
IKK-beta	BX-912	2,8E-06	1,7E-06	3,2E-06	3,2E-06	≥ 1,1E+05	≥ 3,5E-01	
IKK-beta	CCT128930	≈ 4,9E-06	≈ 3,0E-06	3,8E-06	3,8E-06	1,1E+04	4,3E-02	
IKK-beta	CEP33779	3,1E-08	1,9E-08	5,9E-09	5,9E-09	3,8E+06	2,2E-02	
IKK-beta	CHIR-124	3,1E-06	1,9E-06	≈ 2,3E-06	1,9E-06	2,2E+04	4,5E-02	
IKK-beta	Crenolanib (CP-868596)	≥ 2,0E-05		2,7E-06	2,7E-06	≥ 1,3E+05	≥ 3,5E-01	
IKK-beta	CX-4945 (Siltitasertib)	≥ 2,0E-05		2,0E-06	2,0E-06	≥ 1,8E+05	≥ 3,5E-01	
IKK-beta	CYC116	8,5E-08	5,2E-08	5,9E-08	5,9E-08	5,1E+05	3,0E-02	
IKK-beta	Cyt387	1,0E-08	6,1E-09	2,3E-09	2,3E-09	4,9E+06	1,2E-02	
IKK-beta	Dabrafenib (GSK2118436)	3,9E-06	2,4E-06	7,3E-07	7,3E-07	4,0E+04	2,6E-02	
IKK-beta	Dovitinib (TKI-258)	1,4E-05	8,3E-06	5,3E-06	5,3E-06	2,5E+03	1,2E-02	
IKK-beta	E7080 (Lenvatinib)	≥ 2,0E-05		7,7E-06	7,7E-06	≥ 4,5E+04	≥ 3,5E-01	
IKK-beta	ENMD-2076	3,3E-07	2,0E-07	9,1E-08	9,1E-08	2,0E+05	1,9E-02	
IKK-beta	Enzastaurin (LY317615)	≥ 2,0E-05		7,3E-06	7,3E-06	4,9E+03	3,6E-02	
IKK-beta	GDC-0980 (RG7422)	≥ 2,0E-05		5,9E-06	5,9E-06	4,6E+03	2,5E-02	
IKK-beta	GSK1059615	1,0E-05	6,1E-06	≈ 3,0E-06	6,1E-06	≥ 1,1E+05	≥ 3,5E-01	
IKK-beta	INCB28060	≥ 2,0E-05		6,1E-06	6,1E-06	≥ 5,7E+04	≥ 3,5E-01	
IKK-beta	Indirubin	≥ 2,0E-05		6,6E-06	6,6E-06	3,7E+03	2,2E-02	
IKK-beta	JNJ-7706621	1,4E-06	8,6E-07	3,5E-07	3,5E-07	1,7E+05	6,0E-02	
IKK-beta	KW 2449	2,4E-06	1,4E-06	1,2E-06	1,2E-06	9,9E+04	1,2E-01	
IKK-beta	LY2784544	8,2E-06	5,0E-06	1,8E-06	1,8E-06	1,8E+04	3,4E-02	
IKK-beta	MK-5108 (VX-689)	7,8E-06	4,7E-06	4,1E-06	4,1E-06	≈ 1,4E+04	≈ 5,0E-02	
IKK-beta	NVP-BSK805	1,3E-07	8,1E-08	6,7E-08	6,7E-08	6,3E+05	4,3E-02	
IKK-beta	PD173074	1,5E-05	8,9E-06	4,7E-06	4,7E-06	3,3E+03	1,6E-02	
IKK-beta	PF-03814735	4,2E-07	2,5E-07	n.e.	2,5E-07	n.e.	n.e.	
IKK-beta	PHA-767491	4,7E-07	2,8E-07	1,8E-07	1,8E-07	2,9E+05	5,4E-02	
IKK-beta	PIK-75	7,3E-07	4,5E-07	1,2E-06	1,2E-06	3,4E+04	4,0E-02	

kinase	Compound	IC ₅₀ [M] ePCA	K _D eq [M] ePCA *	K _D kin [M] kPCA	K _D [M] PCA **	k _{on} [M ⁻¹ s ⁻¹] kPCA	k _{off} [s ⁻¹] kPCA	comment
IKK-beta	PIK-93	5,8E-06	3,5E-06	2,8E-06	2,8E-06	≈ 1,0E+04	2,3E-02	
IKK-beta	PLX-4720	1,1E-05	6,9E-06	4,3E-06	4,3E-06	≈ 1,9E+04	≈ 7,6E-02	
IKK-beta	Ponatinib (AP24534)	1,8E-07	1,1E-07	2,8E-07	2,8E-07	1,4E+04	4,0E-03	
IKK-beta	PP-121	1,2E-05	7,3E-06	≥ 2,0E-05	≥ 7,3E-06			
IKK-beta	PP242	≥ 2,0E-05		3,2E-06	3,2E-06	1,0E+04	3,3E-02	
IKK-beta	Quercetin (Sophoretin)	≥ 2,0E-05		3,3E-06	3,3E-06	n.e.	n.e.	
IKK-beta	R406	2,9E-08	1,7E-08	5,2E-08	5,2E-08	≈ 5,6E+05	1,1E-02	
IKK-beta	R788 (Fostamatinib) - prodrug	4,3E-06	2,6E-06	4,1E-06	3,0E-06	≈ 9,1E+03	1,8E-02	
IKK-beta	Ruxolitinib (INCB018424)	1,2E-06	7,2E-07	1,5E-06	1,5E-06	≈ 4,6E+04	≈ 8,0E-02	
IKK-beta	Semaxanib (SU5416)	≥ 2,0E-05		4,7E-06	4,7E-06	6,3E+03	3,1E-02	
IKK-beta	SNS-032 (BMS-387032)	5,3E-06	3,2E-06	3,2E-06	3,2E-06	5,7E+04	≈ 2,0E-01	
IKK-beta	SNS-314	6,3E-06	3,8E-06	8,3E-06	8,3E-06	n.e.	n.e.	
IKK-beta	Sotrastaurin (AEB071)	≥ 2,0E-05		7,4E-06	7,4E-06	1,2E+04	9,2E-02	
IKK-beta	SP600125	4,8E-07	2,9E-07	3,3E-07	3,3E-07	≈ 4,5E+05	≈ 1,6E-01	
IKK-beta	Staurosporine	3,3E-08	2,0E-08	1,4E-08	1,4E-08	1,2E+06	1,7E-02	
IKK-beta	Sunitinib Malate (Sutent)	8,9E-06	5,4E-06	3,8E-06	3,8E-06	≈ 4,5E+04	≈ 1,7E-01	
IKK-beta	TAK-901	3,6E-07	2,2E-07	n.e.	2,2E-07	n.e.	n.e.	
IKK-beta	TG101209	6,3E-08	3,8E-08	5,3E-08	5,3E-08	≈ 4,4E+05	2,1E-02	
IKK-beta	TG101348 (SAR302503)	8,9E-08	5,4E-08	1,6E-07	1,6E-07	≈ 1,3E+05	≈ 2,2E-02	
IKK-beta	Thiazovivin	2,1E-06	1,3E-06	1,6E-06	1,6E-06	≥ 2,2E+05	≥ 3,5E-01	1
IKK-beta	TPCA-1	2,7E-09	1,6E-09	7,4E-10	7,4E-10	3,1E+07	2,3E-02	
IKK-beta	WHI-P154	1,8E-05	1,1E-05	≈ 1,3E-05	1,1E-05	≥ 2,6E+04	≥ 3,5E-01	
IKK-beta	WZ3146	1,3E-05	7,9E-06	1,1E-05	1,1E-05	3,8E+03	4,4E-02	
IKK-beta	Y-27632 2HCl	2,2E-06	1,3E-06	4,2E-06	4,2E-06	≈ 4,6E+04	≈ 2,2E-01	
ITK	A-674563	≥ 2,0E-05		1,8E-05	1,8E-05	5,0E+03	8,6E-02	
ITK	AEE788 (NVP-AEE788)	1,4E-05	8,5E-06	3,3E-06	3,3E-06	5,8E+04	1,7E-01	
ITK	Afatinib (BIBW2992)	4,5E-07	2,7E-07	8,0E-06	2,7E-07	≈ 1,0E+03	≈ 1,1E-02	
ITK	AMG458	2,1E-07	1,3E-07	2,1E-07	2,1E-07	4,5E+04	8,8E-03	
ITK	AT9283	2,3E-08	1,4E-08	1,2E-08	1,2E-08	5,7E+06	6,4E-02	
ITK	Aurora A Inhibitor I	≈ 1,7E-06	≈ 1,0E-06	2,2E-06	2,2E-06	7,2E+04	≈ 1,7E-01	2
ITK	Axitinib	1,2E-05	7,0E-06	2,2E-06	2,2E-06	≈ 2,3E+05	≈ 5,5E-01	
ITK	AZ 960	2,6E-06	1,6E-06	1,2E-06	1,2E-06	≈ 1,5E+05	≈ 1,8E-01	
ITK	AZD4547	9,3E-07	5,6E-07	6,2E-07	6,2E-07	≈ 8,7E+04	≈ 6,5E-02	
ITK	AZD5438	6,8E-06	4,1E-06	5,1E-06	5,1E-06	≥ 6,8E+04	≥ 3,5E-01	
ITK	AZD7762	4,1E-08	2,5E-08	4,0E-08	4,0E-08	2,8E+06	1,1E-01	
ITK	Barasertib (AZD1152-HQPA)	5,5E-06	3,3E-06	2,4E-06	2,4E-06	≥ 1,4E+05	≥ 3,5E-01	
ITK	Baricitinib (LY3009104 - incb28050)	1,4E-05	8,4E-06	3,8E-06	3,8E-06	≈ 4,3E+04	≈ 1,7E-01	
ITK	BEZ235 (NVP-BEZ235)	≥ 2,0E-05		1,0E-05	1,0E-05	≈ 1,1E+04	≈ 8,6E-02	
ITK	BIBF1120 (Vargatef)	≈ 3,2E-07	≈ 1,9E-07	1,0E-07	1,0E-07	9,3E+05	9,6E-02	
ITK	BIRB 796 (Doramapimod)	≥ 2,0E-05		6,6E-06	6,6E-06	3,1E+04	2,0E-01	
ITK	BIX 02188	≥ 2,0E-05		5,9E-06	5,9E-06	≈ 9,8E+03	≈ 4,6E-02	
ITK	BKM120 (NVP-BKM120)	≥ 2,0E-05		1,0E-05	1,0E-05	9,6E+02	9,7E-03	
ITK	BMS 794833	5,4E-06	3,3E-06	n.e.	3,3E-06	2,9E+03	≤ 9,7E-03	4
ITK	Bosutinib (SKI-606)	7,8E-07	4,7E-07	4,2E-07	4,2E-07	5,6E+05	2,3E-01	
ITK	BX-795	3,3E-07	2,0E-07	2,0E-07	2,0E-07	5,0E+05	1,0E-01	
ITK	BX-912	1,4E-07	8,5E-08	1,2E-07	1,2E-07	≥ 2,9E+06	≥ 3,5E-01	
ITK	CCT129202	≥ 2,0E-05		4,5E-06	4,5E-06	2,8E+04	1,3E-01	
ITK	CCT137690	6,1E-07	3,7E-07	3,2E-06	3,7E-07	n.e.	n.e.	
ITK	CEP33779	≈ 7,7E-07	≈ 4,6E-07	4,0E-07	4,0E-07	3,1E+05	1,2E-01	
ITK	CH5424802	≈ 1,6E-06	≈ 1,0E-06	1,2E-06	1,2E-06	n.e.	n.e.	2
ITK	CHIR-124	3,6E-07	2,2E-07	3,8E-07	3,8E-07	2,0E+05	5,9E-02	
ITK	CI-1033 (Canertinib)	1,3E-07	8,1E-08	n.e.	8,1E-08	1,7E+03	≤ 1,3E-04	4
ITK	CP 673451	2,5E-07	1,5E-07	1,2E-07	1,2E-07	8,9E+05	1,1E-01	
ITK	Crenolanib (CP-868596)	1,6E-07	9,5E-08	1,5E-07	1,5E-07	9,4E+05	1,3E-01	
ITK	Crizotinib (PF-02341066)	8,5E-07	5,1E-07	1,0E-06	1,0E-06	≈ 2,2E+05	≈ 2,6E-01	2
ITK	CX-4945 (Silmatasertib)	≥ 2,0E-05		7,1E-06	7,1E-06	≈ 1,7E+04	≈ 1,3E-01	
ITK	CYC116	1,7E-06	1,0E-06	5,4E-07	5,4E-07	1,8E+05	9,3E-02	
ITK	Cyt387	1,2E-05	7,0E-06	2,8E-06	2,8E-06	2,7E+04	7,5E-02	
ITK	Dabrafenib (GSK2118436)	1,6E-06	9,6E-07	6,6E-07	6,6E-07	≥ 5,3E+05	≥ 3,5E-01	
ITK	Dacomitinib (PF299804 - PF-00299804)	4,6E-07	2,8E-07	≥ 2,0E-05	≥ 2,8E-07			
ITK	Danusertib (PHA-739358)	3,1E-06	1,9E-06	9,3E-07	9,3E-07	8,7E+04	8,1E-02	
ITK	Dasatinib (BMS-354825)	≥ 2,0E-05		8,7E-06	8,7E-06	≈ 1,1E+04	≈ 1,3E-01	
ITK	DCC-2036 (Rebastinib)	3,6E-07	2,2E-07	n.e.	2,2E-07	6,7E+03	≤ 1,5E-03	4
ITK	Desmethyl Erlotinib (CP-473420)	≥ 2,0E-05		7,9E-06	7,9E-06	1,8E+04	1,3E-01	
ITK	Dovitinib (TKI-258)	1,6E-07	9,5E-08	5,3E-08	5,3E-08	2,4E+06	1,1E-01	
ITK	E7080 (Lenvatinib)	≥ 2,0E-05		1,1E-05	1,1E-05	6,4E+03	6,5E-02	
ITK	ENMD-2076	1,1E-07	6,4E-08	8,6E-08	8,6E-08	≈ 4,1E+06	≈ 3,5E-01	
ITK	Erlotinib HCl	≥ 2,0E-05		1,7E-05	1,7E-05	1,9E+04	3,2E-01	
ITK	Flavopiridol HCl	5,5E-06	5,8E-06	5,0E-06	5,0E-06	1,8E+04	9,3E-02	
ITK	Foretinib (GSK1363089 - XL880)	1,6E-07	9,7E-08	2,5E-07	2,5E-07	1,5E+05	3,8E-02	
ITK	GDC-0980 (RG7422)	7,3E-07	4,4E-07	5,8E-07	5,8E-07	4,5E+05	2,6E-01	
ITK	Golitinib (E7050)	≥ 2,0E-05		1,6E-05	1,6E-05	7,8E+03	≈ 1,3E-01	
ITK	GSK1838705A	7,3E-06	4,4E-06	1,6E-06	1,6E-06	3,9E+04	6,1E-02	
ITK	GSK461364	≥ 2,0E-05		1,4E-05	1,4E-05	n.e.	n.e.	
ITK	Hesperadin	7,7E-09	4,7E-09	2,8E-09	2,8E-09	≈ 3,7E+07	≈ 1,1E-01	
ITK	JNJ-7706621	1,8E-06	1,1E-06	6,8E-07	6,8E-07	≈ 4,7E+05	≈ 2,0E-01	
ITK	Ki8751	≥ 2,0E-05		1,1E-05	1,1E-05	3,2E+02	3,6E-03	
ITK	KW 2449	1,3E-07	7,7E-08	3,9E-07	3,9E-07	≥ 9,1E+05	≥ 3,5E-01	
ITK	LDN193189	1,5E-05	8,8E-06	4,2E-06	4,2E-06	≈ 3,7E+04	≈ 1,4E-01	

kinase	Compound	IC ₅₀ [M] ePCA	K _D eq [M] ePCA *	K _D kin [M] kPCA	K _D [M] PCA **	k _{on} [M ⁻¹ s ⁻¹] kPCA	k _{off} [s ⁻¹] kPCA	comment
ITK	Linifanib (ABT-869)	≥ 2,0E-05		6,8E-06	6,8E-06	≈ 5,0E+03	≈ 2,4E-02	
ITK	Linsitinib (OSI-906)	≥ 2,0E-05		1,6E-05	1,6E-05	8,0E+03	1,3E-01	
ITK	LY2603618 (IC-83)	≈ 6,4E-06	≈ 3,9E-06	2,5E-05	2,5E-05	3,4E+03	8,7E-02	
ITK	LY2784544	2,8E-07	1,7E-07	1,0E-07	1,0E-07	≈ 1,9E+06	1,7E-01	
ITK	MGCD-265	7,5E-08	4,6E-08	2,3E-07	4,6E-08	2,4E+05	5,4E-02	2
ITK	Milciclib (PHA-848125)	1,2E-07	7,3E-08	3,9E-08	3,9E-08	2,0E+06	≈ 8,5E-02	
ITK	MK-2206 2HCl	1,5E-05	8,8E-06	7,2E-06	7,2E-06	4,2E+04	3,0E-01	
ITK	MK-2461	5,2E-07	3,1E-07	6,9E-07	6,9E-07	n.e.	n.e.	2
ITK	MK-5108 (VX-689)	9,9E-08	6,0E-08	7,1E-08	7,1E-08	6,8E+06	4,7E-01	
ITK	MLN8054	1,1E-05	6,5E-06	≈ 2,8E-06	6,5E-06	≥ 1,2E+05	≥ 3,5E-01	
ITK	Neratinib (HKI-272)	≥ 6,0E-07		≥ 2,0E-05	≥ 3,6E-07			
ITK	NVP-ADW742	1,8E-05	1,1E-05	≈ 7,1E-06	1,1E-05	≈ 3,9E+04	≈ 2,8E-01	
ITK	NVP-BGT226	1,3E-05	7,9E-06	4,9E-06	4,9E-06	7,4E+04	≈ 3,8E-01	
ITK	NVP-BSK805	8,3E-07	5,0E-07	8,0E-07	8,0E-07	≈ 6,9E+05	≈ 5,7E-01	
ITK	NVP-TAE226	1,6E-07	9,6E-08	1,2E-07	1,2E-07	≈ 1,2E+06	≈ 1,4E-01	
ITK	Pazopanib HCl	≥ 2,0E-05		3,9E-06	3,9E-06	≈ 2,0E+04	≈ 6,6E-02	
ITK	PCI-32765 (Ibrutinib)	≥ 2,5E-09	1,5E-09	n.e.	1,5E-09	2,4E+04	≤ 3,7E-05	4
ITK	PD 0332991 (Palbociclib) HCl	7,5E-06	4,5E-06	3,6E-06	3,6E-06	2,5E+04	8,9E-02	
ITK	PD173074	≈ 1,1E-05	≈ 6,4E-06	≈ 9,6E-06	≈ 8,0E-06	≈ 1,0E+04	≈ 9,6E-02	
ITK	Pelitinib (EKB-569)	2,0E-08	1,2E-08	3,1E-06	1,2E-08	≈ 5,6E+04	≈ 1,4E-01	
ITK	PF-00562271	2,3E-07	1,4E-07	1,0E-07	1,0E-07	≈ 1,3E+06	≈ 1,3E-01	
ITK	PF-03814735	6,3E-09	3,8E-09	4,5E-09	4,5E-09	8,1E+06	3,6E-02	
ITK	PHA-665752	≈ 3,0E-06	≈ 1,8E-06	1,4E-06	1,4E-06	7,5E+04	1,1E-01	
ITK	PHA-680632	≈ 1,0E-06	≈ 6,1E-07	7,0E-07	7,0E-07	8,3E+04	5,6E-02	
ITK	PIK-75	≈ 1,4E-06	≈ 8,3E-07	1,5E-06	1,5E-06	4,6E+04	6,6E-02	2
ITK	PLX-4720	≥ 2,0E-05		1,0E-05	1,0E-05	≈ 4,7E+03	≈ 5,0E-02	
ITK	Ponatinib (AP24534)	≈ 6,2E-07	≈ 3,7E-07	4,1E-07	4,1E-07	9,4E+04	4,0E-02	
ITK	PP-121	2,0E-06	1,2E-06	1,3E-06	1,3E-06	7,3E+04	9,0E-02	
ITK	PP242	1,2E-05	7,6E-06	2,2E-06	2,2E-06	2,0E+04	4,3E-02	
ITK	Quercetin (Sophoretin)	≈ 3,7E-06	≈ 2,3E-06	2,2E-06	2,2E-06	3,5E+04	7,8E-02	
ITK	R406	1,9E-07	1,1E-07	5,2E-07	1,9E-07	1,5E+05	1,1E-01	12
ITK	R788 (Fostamatinib) - prodrug	6,8E-06	4,1E-06	3,8E-06	3,8E-06	3,4E+04	8,7E-02	
ITK	Ruxolitinib (INCB018424)	3,5E-06	2,1E-06	5,3E-06	5,3E-06	2,6E+04	1,4E-01	
ITK	SAR131675	≈ 5,8E-06	≈ 3,5E-06	4,3E-06	4,3E-06	≈ 5,4E+04	≈ 2,3E-01	
ITK	Saracatinib (AZD0530)	≥ 2,0E-05		1,3E-05	1,3E-05	≈ 4,6E+03	≈ 5,3E-02	
ITK	Semaxanib (SU5416)	7,4E-07	4,5E-07	5,4E-07	5,4E-07	3,0E+05	1,6E-01	
ITK	SP600125	9,9E-07	6,0E-07	4,8E-07	4,8E-07	≈ 1,9E+05	≈ 9,9E-02	
ITK	Staurosporine	6,8E-09	4,1E-09	2,6E-09	2,6E-09	2,1E+07	5,2E-02	
ITK	SU11274	≈ 2,3E-07	≈ 1,4E-07	6,5E-07	6,5E-07	1,2E+05	8,0E-02	1
ITK	Sunitinib Malate (Sutent)	2,2E-08	1,3E-08	1,8E-08	1,8E-08	≈ 4,9E+06	≈ 8,3E-02	
ITK	TAE684 (NVP-TAE684)	6,2E-08	3,7E-08	2,2E-08	2,2E-08	3,9E+06	8,2E-02	
ITK	TAK-901	1,8E-09	1,1E-09	6,2E-09	1,1E-09	8,8E+06	5,5E-02	
ITK	Tandutinib (MLN518)	4,3E-06	2,6E-06	1,7E-06	1,7E-06	≥ 2,1E+05	≥ 3,5E-01	
ITK	TG101209	7,2E-08	4,3E-08	7,2E-08	7,2E-08	2,6E+06	1,8E-01	
ITK	TG101348 (SAR302503)	2,5E-07	1,5E-07	2,2E-07	2,2E-07	1,6E+06	2,4E-01	3
ITK	Tivozanib (AV-951)	≥ 2,0E-05		3,2E-06	3,2E-06	3,8E+04	1,2E-01	
ITK	Torin 2	≥ 2,0E-05		9,9E-06	9,9E-06	≈ 1,7E+04	≈ 1,2E-01	
ITK	TPCA-1	3,4E-07	2,1E-07	2,3E-07	2,3E-07	≈ 7,7E+05	≈ 1,9E-01	
ITK	Triciribine (Triciribine phosphate)	≥ 1,4E-05		≥ 2,0E-05	≥ 8,2E-06			
ITK	TSU-68 (SU6668)	3,0E-06	1,8E-06	1,4E-06	1,4E-06	≥ 2,5E+05	≥ 3,5E-01	
ITK	TWS119	≈ 5,0E-06	≈ 3,0E-06	2,5E-06	2,5E-06	2,8E+04	7,1E-02	
ITK	U0126-EtOH	≥ 2,0E-05		1,2E-05	1,2E-05	≥ 3,0E+04	≥ 3,5E-01	
ITK	Vandetanib (Zactima)	7,8E-06	4,7E-06	5,9E-06	5,9E-06	≈ 2,8E+04	≈ 9,1E-02	
ITK	VX-680 (MK-0457 - Tozasertib)	≈ 2,5E-07	≈ 1,5E-07	1,7E-07	1,7E-07	9,0E+05	1,6E-01	
ITK	WHI-P154	≥ 2,0E-05		5,5E-06	5,5E-06	3,3E+04	1,8E-01	
ITK	WZ3146	≤ 2,3E-10	≤ 1,4E-10	n.e.	≤ 1,4E-10	2,9E+06	≤ 4,1E-04	4
ITK	WZ4002	≈ 2,6E-09	≈ 1,6E-09	n.e.	≈ 1,6E-09	5,7E+04	≤ 8,9E-05	4
ITK	WZ8040	≤ 2,3E-10	≤ 1,4E-10	n.e.	≤ 1,4E-10	2,9E+06	≤ 4,0E-04	4
ITK	ZM-447439	8,2E-06	4,9E-06	5,8E-06	5,8E-06	≈ 1,9E+04	≈ 1,4E-01	
JAK2	A-674563	4,7E-06	2,1E-06	1,3E-06	1,3E-06	9,6E+03	1,2E-02	
JAK2	AEE788 (NVP-AEE788)	2,9E-06	1,3E-06	6,6E-07	6,6E-07	5,3E+04	3,5E-02	
JAK2	AG-1478 (Typhostin AG-1478)	≥ 2,0E-05		n.e.	≥ 8,8E-06	n.e.	n.e.	
JAK2	AMG 900	1,2E-06	5,1E-07	≥ 2,0E-05	≥ 5,1E-07			
JAK2	AS-252424	≥ 2,0E-05		6,6E-06	6,6E-06	7,2E+03	4,9E-02	
JAK2	AS-605240	≥ 2,0E-05		5,4E-06	5,4E-06	2,3E+03	1,2E-02	
JAK2	AT7867	1,5E-06	6,4E-07	3,5E-07	3,5E-07	≈ 4,7E+04	≈ 1,6E-02	
JAK2	AT9283	1,9E-09	8,3E-10	2,0E-10	2,0E-10	1,2E+07	2,4E-03	
JAK2	Aurora A Inhibitor I	6,1E-08	2,7E-08	1,3E-08	1,3E-08	2,6E+06	3,4E-02	
JAK2	Axitinib	6,1E-07	2,7E-07	9,9E-08	9,9E-08	1,2E+05	1,2E-02	
JAK2	AZ 960	3,0E-10	1,3E-10	n.e.	1,3E-10	1,0E+07	≤ 1,4E-03	4
JAK2	AZD4547	1,6E-06	7,1E-07	≈ 3,9E-07	7,1E-07	4,0E+04	2,8E-02	3
JAK2	AZD5438	2,8E-07	1,2E-07	8,4E-08	8,4E-08	≈ 4,0E+05	≈ 4,2E-02	
JAK2	AZD7762	1,1E-07	4,8E-08	2,6E-08	2,6E-08	5,7E+05	1,5E-02	
JAK2	AZD8931	≥ 2,0E-05		7,4E-06	7,4E-06	n.e.	n.e.	
JAK2	Baricitinib (LY3009104 - incb28050)	2,3E-10	1,0E-10	≤ 7,9E-11	≤ 7,9E-11	7,3E+07	5,9E-03	
JAK2	BEZ235 (NVP-BEZ235)	≈ 9,4E-08	≈ 4,1E-08	2,7E-08	2,7E-08	≈ 7,7E+05	≈ 2,1E-02	
JAK2	BI6727 (Volasertib)	≥ 2,0E-05		≈ 2,5E-06	≈ 2,5E-06	6,1E+02	1,3E-03	
JAK2	BIBF1120 (Vargatef)	7,6E-08	3,4E-08	1,2E-08	1,2E-08	2,2E+06	2,6E-02	
JAK2	BIX 02188	5,7E-06	2,5E-06	1,7E-06	1,7E-06	1,7E+04	3,0E-02	2

kinase	Compound	IC ₅₀ [M] ePCA	K _D eq [M] ePCA *	K _D kin [M] kPCA	K _D [M] PCA **	k _{on} [M ⁻¹ s ⁻¹] kPCA	k _{off} [s ⁻¹] kPCA	comment
JAK2	BIX 02189	4,9E-06	2,2E-06	≈ 1,5E-06	2,2E-06	≈ 8,8E+03	≈ 1,3E-02	
JAK2	BMS 777607	3,3E-06	1,4E-06	9,4E-07	9,4E-07	1,1E+04	9,7E-03	
JAK2	BMS 794833	≥ 2,0E-05		3,5E-06	3,5E-06	2,3E+03	8,3E-03	
JAK2	BMS-265246	≥ 2,0E-05		2,8E-06	2,8E-06	n.e.	n.e.	2
JAK2	Bosutinib (SKI-606)	4,3E-07	1,9E-07	1,4E-07	1,4E-07	≈ 3,9E+05	≈ 4,6E-02	
JAK2	BS-181 HCl	1,3E-05	5,7E-06	n.e.	5,7E-06	≈ 1,8E+03	≤ 1,0E-02	4
JAK2	BX-795	6,4E-09	2,8E-09	2,7E-09	2,7E-09	1,0E+07	2,8E-02	
JAK2	BX-912	1,2E-08	5,4E-09	9,3E-09	9,3E-09	3,2E+06	3,0E-02	
JAK2	CCT128930	1,3E-06	5,7E-07	2,5E-07	2,5E-07	≈ 4,9E+05	≈ 1,2E-01	
JAK2	CCT129202	1,9E-07	8,4E-08	4,7E-08	4,7E-08	≈ 1,5E+06	≈ 7,0E-02	2
JAK2	CCT137690	6,6E-08	2,9E-08	≈ 5,0E-08	2,9E-08	≈ 1,8E+06	≈ 8,8E-02	
JAK2	CEP33779	2,1E-09	9,4E-10	4,5E-10	4,5E-10	1,1E+07	4,6E-03	
JAK2	CH5424802	≥ 2,0E-05		2,4E-06	2,4E-06	≥ 1,4E+05	≥ 3,5E-01	
JAK2	CHIR-124	4,9E-07	2,2E-07	2,8E-07	2,8E-07	≈ 7,5E+04	≈ 1,9E-02	
JAK2	CI-1033 (Canertinib)	≥ 2,0E-05		4,0E-06	4,0E-06	≥ 8,7E+04	≥ 3,5E-01	
JAK2	CP 673451	4,3E-06	1,9E-06	9,2E-07	9,2E-07	≈ 1,7E+05	≈ 1,9E-01	
JAK2	Crenolanib (CP-868596)	4,4E-06	1,9E-06	6,6E-07	6,6E-07	≈ 4,2E+04	2,7E-02	
JAK2	Crizotinib (PF-02341066)	1,2E-08	5,2E-09	6,1E-09	6,1E-09	9,4E+06	5,6E-02	
JAK2	CX-4945 (Silmnitasertib)	7,2E-07	3,2E-07	≈ 3,5E-07	3,2E-07	≈ 6,8E+04	≈ 2,4E-02	
JAK2	CYC116	1,4E-08	6,3E-09	5,4E-09	5,4E-09	4,7E+06	2,5E-02	
JAK2	Cyt387	2,4E-09	1,1E-09	3,2E-10	3,2E-10	2,1E+07	6,7E-03	
JAK2	Dabrafenib (GSK2118436)	4,5E-07	2,0E-07	3,6E-08	2,0E-07	3,3E+05	1,2E-02	
JAK2	Danuseritib (PHA-739358)	3,1E-07	1,4E-07	1,2E-07	1,2E-07	7,2E+04	9,1E-03	
JAK2	Dasatinib (BMS-354825)	6,7E-07	2,9E-07	1,2E-07	1,2E-07	4,1E+05	4,9E-02	
JAK2	DCC-2036 (Rebastinib)	5,4E-07	2,4E-07	n.e.	2,4E-07	1,1E+03	≤ 2,7E-04	4
JAK2	Desmethyl Erlotinib (CP-473420)	1,2E-06	5,1E-07	3,1E-07	3,1E-07	1,6E+05	5,2E-02	
JAK2	Dovitinib (TKI-258)	5,6E-07	2,5E-07	1,2E-07	1,2E-07	7,9E+05	9,7E-02	
JAK2	ENMD-2076	1,3E-08	5,6E-09	3,5E-09	3,5E-09	3,4E+06	1,2E-02	
JAK2	Erlotinib HCl	1,3E-06	5,9E-07	4,9E-07	4,9E-07	≥ 7,2E+05	≥ 3,5E-01	
JAK2	Flavopiridol HCl	1,2E-05	5,3E-06	3,9E-06	3,9E-06	5,9E+03	2,3E-02	
JAK2	Foretinib (GSK1363089 - XL880)	7,9E-07	3,5E-07	5,2E-07	5,2E-07	≈ 8,1E+04	≈ 3,1E-02	
JAK2	GDC-0941	≥ 2,0E-05		1,6E-06	1,6E-06	7,0E+04	1,1E-01	
JAK2	GDC-0980 (RG7422)	2,3E-06	1,0E-06	1,0E-06	1,0E-06	n.e.	n.e.	
JAK2	Gefitinib (Iressa)	≥ 2,0E-05		8,0E-06	8,0E-06	≥ 4,4E+04	≥ 3,5E-01	
JAK2	Golvatinib (E7050)	9,2E-07	4,1E-07	2,0E-07	2,0E-07	5,2E+04	1,1E-02	
JAK2	GSK1059615	3,4E-07	1,5E-07	1,6E-07	1,6E-07	≥ 2,2E+06	≥ 3,5E-01	
JAK2	GSK1070916	1,6E-05	7,0E-06	3,0E-06	3,0E-06	≈ 7,3E+03	≈ 2,4E-02	
JAK2	GSK1838705A	≥ 2,0E-05		n.e.	≥ 8,8E-06	n.e.	n.e.	
JAK2	GSK690693	≥ 2,0E-05		6,7E-06	6,7E-06	n.e.	n.e.	
JAK2	Hesperadin	8,1E-09	3,6E-09	7,9E-10	7,9E-10	1,2E+07	9,3E-03	
JAK2	INK 128 (MLN0128)	≥ 2,0E-05		6,6E-06	6,6E-06	2,3E+03	1,5E-02	
JAK2	JNJ-7706621	2,4E-08	1,1E-08	4,4E-09	4,4E-09	≈ 2,4E+07	≈ 1,3E-01	
JAK2	KW 2449	1,3E-07	5,7E-08	1,1E-07	1,1E-07	≈ 1,3E+05	≈ 1,3E-02	
JAK2	Linifanib (ABT-869)	1,5E-05	6,5E-06	≈ 5,8E-06	6,5E-06	n.e.	n.e.	
JAK2	LY2784544	2,4E-10	1,1E-10	n.e.	1,1E-10	4,1E+06	≤ 4,4E-04	4
JAK2	Masitinib (AB1010)	≥ 2,0E-05		4,3E-06	4,3E-06	7,8E+02	3,6E-03	
JAK2	MGCD-265	≥ 2,0E-05		7,7E-06	7,7E-06	8,7E+02	6,5E-03	
JAK2	Milciclib (PHA-848125)	4,0E-06	1,8E-06	7,8E-07	7,8E-07	≈ 3,1E+04	≈ 2,5E-02	
JAK2	MK-2461	1,3E-07	5,7E-08	4,3E-08	4,3E-08	6,3E+06	2,8E-01	
JAK2	MK-5108 (VX-689)	1,9E-08	8,3E-09	8,3E-09	8,3E-09	≈ 1,8E+07	≈ 1,5E-01	
JAK2	MLN8237 (Alisertib)	6,6E-06	2,9E-06	≈ 3,0E-06	2,9E-06	≈ 1,1E+04	≈ 3,3E-02	
JAK2	Motesanib Diphosphate (AMG-706)	≥ 2,0E-05		7,0E-06	7,0E-06	n.e.	n.e.	
JAK2	Nilotinib (AMN-107)	≥ 2,0E-05		7,6E-06	7,6E-06	n.e.	n.e.	
JAK2	NVP-BGT226	1,6E-05	7,1E-06	≈ 7,5E-06	7,1E-06	n.e.	n.e.	
JAK2	NVP-BSK805	2,0E-10	8,9E-11	1,4E-10	1,4E-10	1,5E+07	2,1E-03	
JAK2	NVP-TAE226	2,9E-07	1,3E-07	5,5E-08	5,5E-08	≈ 6,0E+05	≈ 3,5E-02	
JAK2	Pazopanib HCl	≥ 2,0E-05		6,7E-07	6,7E-07	5,7E+04	4,0E-02	
JAK2	PD 0332991 (Palbociclib) HCl	1,3E-06	5,8E-07	7,3E-07	7,3E-07	4,2E+04	3,1E-02	1
JAK2	PD153035 HCl	6,0E-06	2,7E-06	1,2E-06	1,2E-06	1,2E+04	1,4E-02	
JAK2	Pelitinib (EKB-569)	1,5E-06	6,7E-07	2,9E-07	2,9E-07	8,0E+04	2,4E-02	
JAK2	PF-00562271	1,9E-08	8,5E-09	n.e.	8,5E-09	n.e.	n.e.	
JAK2	PF-03814735	1,2E-09	5,2E-10	n.e.	5,2E-10	n.e.	n.e.	
JAK2	PF-05212384 (PKI-587)	≥ 2,0E-05		n.e.	≥ 8,8E-06	n.e.	n.e.	
JAK2	PHA-665752	4,7E-07	2,1E-07	1,6E-07	1,6E-07	≈ 3,3E+05	≈ 5,3E-02	
JAK2	PHA-680632	3,5E-07	1,5E-07	1,0E-07	1,0E-07	4,1E+05	4,3E-02	
JAK2	PHA-767491	9,9E-07	4,4E-07	1,8E-07	1,8E-07	2,3E+05	4,1E-02	
JAK2	PIK-75	9,6E-09	4,3E-09	2,1E-09	2,1E-09	9,5E+06	2,0E-02	
JAK2	PLX-4720	9,3E-06	4,1E-06	2,6E-06	2,6E-06	≈ 3,7E+03	≈ 9,7E-03	
JAK2	Ponatinib (AP24534)	7,1E-08	3,1E-08	n.e.	3,1E-08	5,3E+03	≤ 1,7E-04	4
JAK2	PP-121	1,3E-07	5,8E-08	6,9E-08	6,9E-08	2,4E+05	1,6E-02	
JAK2	PP242	2,7E-08	1,2E-08	8,8E-09	8,8E-09	2,3E+06	2,0E-02	
JAK2	Quercetin (Sophoretin)	6,4E-06	2,8E-06	1,6E-06	1,6E-06	≈ 2,0E+04	≈ 3,6E-02	2
JAK2	R406	1,3E-09	5,7E-10	3,6E-10	3,6E-10	1,3E+07	4,2E-03	
JAK2	R788 (Fostamatnib) - prodrug	1,2E-07	5,4E-08	3,1E-08	3,1E-08	1,4E+05	3,4E-03	
JAK2	Ruxolitinib (INCB018424)	≤ 1,9E-10	≤ 8,4E-11	≤ 1,9E-11	≤ 1,9E-11	4,5E+07	8,3E-04	
JAK2	Saracatinib (AZD0530)	3,7E-06	1,6E-06	≈ 9,5E-07	1,6E-06	≈ 7,0E+04	≈ 6,6E-02	
JAK2	SB 415286	1,7E-05	7,5E-06	≈ 4,3E-06	7,5E-06	n.e.	n.e.	
JAK2	Semaxanib (SU5416)	4,6E-06	2,0E-06	9,9E-07	9,9E-07	3,0E+04	3,0E-02	
JAK2	SNS-314	≈ 1,3E-05	≈ 5,5E-06	5,3E-06	5,3E-06	≥ 6,7E+04	≥ 3,5E-01	

kinase	Compound	IC ₅₀ [M] ePCA	K _D eq [M] ePCA *	K _D kin [M] kPCA	K _D [M] PCA **	k _{on} [M ⁻¹ s ⁻¹] kPCA	k _{off} [s ⁻¹] kPCA	comment
JAK2	Sotrastaurin (AEB071)	1,5E-05	6,6E-06	1,3E-06	6,6E-06	4,9E+04	5,0E-02	
JAK2	SP600125	3,2E-07	1,4E-07	1,0E-07	1,0E-07	≈ 1,0E+06	≈ 1,1E-01	
JAK2	Staurosporine	2,0E-10	9,1E-11	n.e.	9,1E-11	2,2E+07	≤ 2,0E-03	4
JAK2	SU11274	1,5E-08	6,8E-09	1,3E-08	1,3E-08	1,9E+06	2,5E-02	
JAK2	Sunitinib Malate (Sutent)	2,1E-07	9,2E-08	9,8E-08	9,8E-08	≈ 5,5E+05	≈ 5,0E-02	
JAK2	TAE684 (NVP-TAE684)	9,5E-08	4,2E-08	1,1E-08	1,1E-08	1,9E+06	2,1E-02	
JAK2	TAK-901	5,0E-09	2,2E-09	2,5E-09	2,5E-09	≈ 3,0E+06	≈ 4,4E-03	
JAK2	Tandutinib (MLN518)	≥ 2,0E-05		5,2E-06	5,2E-06	1,8E+03	9,5E-03	
JAK2	TG100-115	8,0E-06	3,5E-06	1,5E-06	1,5E-06	4,1E+04	6,2E-02	
JAK2	TG101209	≤ 1,3E-10	≤ 5,8E-11	2,3E-10	2,3E-10	6,5E+06	1,5E-03	
JAK2	TG101348 (SAR302503)	8,5E-10	3,8E-10	≈ 4,2E-10	3,8E-10	≈ 1,6E+07	≈ 6,9E-03	
JAK2	Thiazovivin	1,3E-06	5,8E-07	4,9E-07	4,9E-07	7,6E+04	3,7E-02	
JAK2	Tivozanib (AV-951)	≥ 2,0E-05		3,2E-06	3,2E-06	1,2E+04	4,1E-02	
JAK2	Tofacitinib (CP-690550 - Tasocitinib)	3,0E-09	1,3E-09	4,6E-10	4,6E-10	1,5E+07	6,6E-03	
JAK2	Torin 1	≥ 2,0E-05		3,8E-06	3,8E-06	n.e.	n.e.	
JAK2	Torin 2	≥ 2,0E-05		1,1E-06	1,1E-06	4,7E+04	5,2E-02	
JAK2	TPCA-1	≈ 6,5E-09	≈ 2,9E-09	3,0E-09	3,0E-09	≈ 8,0E+06	2,2E-02	
JAK2	TSU-68 (SU6668)	7,9E-07	3,5E-07	3,0E-07	3,0E-07	9,6E+04	2,9E-02	
JAK2	TWS119	5,3E-07	2,4E-07	1,3E-07	1,3E-07	≈ 4,6E+05	≈ 6,4E-02	
JAK2	Vatalanib 2HCl (PTK787)	5,7E-06	2,5E-06	2,9E-06	2,9E-06	1,2E+03	3,5E-03	
JAK2	VX-680 (MK-0457 - Tozasertib)	5,8E-08	2,6E-08	3,4E-08	3,4E-08	1,4E+06	4,8E-02	
JAK2	WHI-P154	2,7E-06	1,2E-06	1,1E-06	1,1E-06	5,2E+04	5,8E-02	
JAK2	WZ3146	1,0E-07	4,5E-08	2,2E-08	2,2E-08	3,2E+06	6,8E-02	
JAK2	WZ4002	≥ 2,0E-05		2,0E-06	2,0E-06	≥ 1,7E+05	≥ 3,5E-01	
JAK2	WZ8040	1,0E-07	4,6E-08	4,0E-08	4,0E-08	6,6E+05	2,7E-02	
JAK2	XL-184 (Cabozantinib)	≥ 2,0E-05		1,9E-06	1,9E-06	n.e.	n.e.	2
JAK2	XL765	≈ 1,0E-05	≈ 4,6E-06	3,0E-06	3,0E-06	n.e.	n.e.	
KDR	A-769662	≥ 2,0E-05		2,5E-06	2,5E-06	5,2E+03	1,3E-02	
KDR	AEE788 (NVP-AEE788)	8,9E-08	3,4E-08	2,2E-08	2,2E-08	8,0E+05	1,7E-02	
KDR	AG-1478 (Tyrphostin AG-1478)	3,7E-06	1,4E-06	2,5E-06	2,5E-06	5,5E+03	1,4E-02	
KDR	AMG458	6,7E-06	2,6E-06	1,4E-06	1,4E-06	3,1E+03	4,0E-03	2
KDR	Apatinib (YN968D1)	1,3E-08	4,8E-09	n.e.	4,8E-09	1,9E+04	≤ 9,3E-05	4
KDR	ARQ 197 (Tivantinib)	6,7E-06	2,6E-06	≥ 2,0E-05	≥ 2,6E-06			
KDR	AS-252424	9,4E-06	3,6E-06	2,5E-06	2,5E-06	5,3E+03	1,3E-02	
KDR	AT9283	≥ 2,0E-05		3,4E-08	3,4E-08	2,7E+05	9,2E-03	
KDR	Aurora A Inhibitor I	3,3E-06	1,3E-06	2,2E-06	2,2E-06	8,7E+03	1,8E-02	2
KDR	Axitinib	3,5E-10	1,3E-10	5,6E-10	5,6E-10	1,5E+06	8,4E-04	2
KDR	AZ 960	9,0E-07	3,4E-07	3,0E-07	3,0E-07	6,4E+04	1,9E-02	
KDR	AZ628	≥ 2,0E-05		2,6E-09	2,6E-09	2,1E+04	5,4E-05	
KDR	AZD2014	1,1E-07	4,4E-08	≥ 2,0E-05	≥ 4,4E-08			
KDR	AZD4547	≥ 2,0E-05		1,4E-08	1,4E-08	6,6E+05	9,1E-03	
KDR	AZD5438	1,3E-05	5,1E-06	6,7E-06	6,7E-06	2,4E+03	1,7E-02	
KDR	AZD7762	4,4E-08	1,7E-08	2,3E-08	2,3E-08	5,1E+05	1,2E-02	
KDR	AZD8931	7,9E-07	3,0E-07	3,0E-07	3,0E-07	5,5E+04	1,7E-02	
KDR	Barasertib (AZD1152-HQPA)	≥ 2,0E-05		1,4E-07	1,4E-07	1,2E+05	1,8E-02	
KDR	BGJ398 (NVP-BGJ398)	5,5E-07	2,1E-07	1,9E-07	1,9E-07	6,8E+04	1,2E-02	
KDR	BIBF1120 (Vargatef)	2,8E-10	1,1E-10	n.e.	1,1E-10	6,6E+06	≤ 6,9E-04	4
KDR	BIRB 796 (Doramapimod)	5,1E-07	1,9E-07	n.e.	1,9E-07	8,1E+02	≤ 1,6E-04	4
KDR	BIX 02188	4,1E-07	1,6E-07	8,1E-08	8,1E-08	2,0E+05	1,6E-02	
KDR	BIX 02189	1,1E-05	4,1E-06	2,9E-06	2,9E-06	3,5E+03	9,8E-03	
KDR	BMS 777607	1,1E-07	4,1E-08	4,3E-08	4,3E-08	4,6E+04	2,0E-03	
KDR	BMS 794833	6,6E-09	2,5E-09	n.e.	2,5E-09	1,7E+04	≤ 4,2E-05	24
KDR	BMS-599626 (AC480)	≥ 2,0E-05		6,4E-06	6,4E-06	1,6E+03	9,9E-03	
KDR	Bosutinib (SKI-606)	≥ 2,0E-05		3,9E-06	3,9E-06	1,6E+03	6,1E-03	
KDR	Brivanib (BMS-540215)	6,0E-09	2,3E-09	3,1E-09	3,1E-09	8,2E+05	2,5E-03	
KDR	Brivanib alaninate (BMS-582664) - prodrug	≥ 2,0E-05		5,5E-09	5,5E-09	5,1E+05	2,8E-03	
KDR	BX-795	1,7E-06	6,5E-07	7,4E-07	7,4E-07	2,5E+04	1,9E-02	
KDR	BX-912	2,4E-07	9,2E-08	1,2E-07	1,2E-07	2,1E+05	2,4E-02	
KDR	CCT129202	6,6E-08	2,5E-08	5,6E-08	5,6E-08	2,1E+05	1,1E-02	2
KDR	CCT137690	2,2E-07	8,3E-08	5,6E-07	8,3E-08	n.e.	n.e.	2
KDR	Cediranib (AZD2171)	4,9E-09	1,9E-09	n.e.	1,9E-09	1,5E+06	≤ 2,9E-03	4
KDR	CEP33779	3,5E-07	1,4E-07	1,1E-06	1,4E-07	2,0E+04	2,1E-02	
KDR	CH5424802	≥ 2,0E-05		7,2E-06	7,2E-06	≥ 4,9E+04	≥ 3,5E-01	2
KDR	CHIR-124	2,6E-06	9,9E-07	2,7E-06	2,7E-06	n.e.	n.e.	
KDR	CHIR-98014	7,2E-06	2,7E-06	≥ 2,0E-05	≥ 2,7E-06			
KDR	CI-1033 (Canertinib)	1,4E-05	5,3E-06	2,5E-06	2,5E-06	1,2E+04	3,0E-02	
KDR	CP 673451	1,8E-06	6,8E-07	9,3E-07	9,3E-07	2,9E+04	2,7E-02	
KDR	Crenolanib (CP-868596)	1,3E-06	5,0E-07	4,2E-07	4,2E-07	2,0E+04	8,3E-03	2
KDR	Crizotinib (PF-02341066)	1,7E-05	6,3E-06	6,4E-06	6,4E-06	6,3E+02	4,0E-03	
KDR	CX-4945 (Silmnitasertib)	≥ 2,0E-05		4,9E-06	4,9E-06	7,0E+02	3,4E-03	
KDR	CYC116	2,3E-07	8,7E-08	1,1E-07	1,1E-07	2,0E+05	2,2E-02	
KDR	Cyt387	1,9E-06	7,3E-07	6,6E-07	6,6E-07	2,4E+04	1,6E-02	
KDR	Dabrafenib (GSK2118436)	≥ 2,0E-05		1,1E-06	1,1E-06	1,8E+04	2,0E-02	
KDR	Danuserib (PHA-739358)	3,7E-06	1,4E-06	1,7E-06	1,7E-06	8,1E+03	1,4E-02	
KDR	Dasatinib (BMS-354825)	6,7E-06	2,5E-06	2,0E-06	2,0E-06	1,6E+04	3,2E-02	
KDR	DCC-2036 (Rebastinib)	7,2E-08	2,8E-08	n.e.	2,8E-08	4,5E+03	≤ 1,3E-04	4
KDR	Deforolimus (Ridaforolimus)	2,5E-06	9,4E-07	n.e.	9,4E-07	1,7E+02	≤ 1,6E-04	4
KDR	Desmethyl Erlotinib (CP-473420)	3,3E-06	1,3E-06	1,3E-06	1,3E-06	1,3E+04	1,6E-02	
KDR	Dovitinib (TKI-258)	8,3E-09	3,2E-09	1,3E-09	1,3E-09	3,5E+06	4,3E-03	

kinase	Compound	IC ₅₀ [M] ePCA	K _D eq [M] ePCA *	K _D kin [M] kPCA	K _D [M] PCA **	k _{on} [M ⁻¹ s ⁻¹] kPCA	k _{off} [s ⁻¹] kPCA	comment
KDR	E7080 (Lenvatinib)	3,4E-10	1,3E-10	n.e.	1,3E-10	5,6E+05	≤ 7,3E-05	4
KDR	ENMD-2076	5,6E-09	2,1E-09	2,8E-09	2,8E-09	4,6E+05	1,3E-03	
KDR	Erlotinib HCl	4,8E-06	1,8E-06	2,3E-06	2,3E-06	1,1E+04	2,5E-02	
KDR	Foretinib (GSK1363089 - XL880)	2,1E-09	8,0E-10	n.e.	8,0E-10	5,6E+04	≤ 4,5E-05	4
KDR	GDC-0068	1,3E-07	4,8E-08	≥ 2,0E-05	≥ 4,8E-08			
KDR	GDC-0941	≥ 2,0E-05		5,1E-06	5,1E-06	2,9E+03	1,4E-02	
KDR	GDC-0980 (RG7422)	3,0E-06	1,1E-06	1,6E-06	1,6E-06	9,8E+03	1,6E-02	
KDR	Golitinib (E7050)	1,7E-08	6,3E-09	4,8E-09	4,8E-09	1,9E+05	9,0E-04	
KDR	GSK1070916	9,2E-07	3,5E-07	2,3E-07	2,3E-07	1,6E+04	3,8E-03	
KDR	Hesperadin	7,8E-07	3,0E-07	2,3E-07	2,3E-07	7,8E+04	1,8E-02	
KDR	Imatinib (Gleevec)	4,6E-06	1,8E-06	4,7E-06	2,4E-06	1,6E+03	7,8E-03	
KDR	Indirubin	≈ 1,0E-05	≈ 3,9E-06	≈ 3,9E-06	≈ 3,9E-06	≈ 4,3E+03	1,1E-02	2
KDR	INK 128 (MLN0128)	2,2E-06	8,5E-07	2,5E-06	2,5E-06	9,4E+03	2,3E-02	
KDR	JNJ-7706621	8,6E-07	3,3E-07	2,9E-07	2,9E-07	5,1E+04	1,5E-02	
KDR	Ki8751	5,0E-10	1,9E-10	n.e.	1,9E-10	2,5E+05	≤ 4,9E-05	24
KDR	KRN 633	4,2E-09	1,6E-09	n.e.	1,6E-09	3,5E+05	≤ 5,7E-04	4
KDR	KW 2449	5,4E-08	2,1E-08	4,8E-08	4,8E-08	5,3E+05	2,6E-02	
KDR	LDN193189	7,9E-06	3,0E-06	5,2E-06	5,2E-06	3,0E+03	1,4E-02	
KDR	Linifanib (ABT-869)	1,3E-09	5,0E-10	n.e.	5,0E-10	1,8E+05	≤ 9,2E-05	4
KDR	Linsitinib (OSI-906)	1,0E-05	3,8E-06	3,2E-06	3,2E-06	3,8E+03	1,2E-02	
KDR	LY2784544	8,0E-08	3,0E-08	2,2E-08	2,2E-08	5,3E+05	1,2E-02	
KDR	Masitinib (AB1010)	3,3E-06	1,2E-06	≥ 2,0E-05	≥ 1,2E-06			
KDR	MGCD-265	4,7E-09	1,8E-09	6,3E-09	6,3E-09	1,1E+05	7,0E-04	2
KDR	Milciclib (PHA-848125)	≥ 2,0E-05		2,9E-06	2,9E-06	7,7E+03	2,2E-02	
KDR	MK-2206 2HCl	≥ 2,0E-05		7,4E-06	7,4E-06	8,6E+02	6,4E-03	
KDR	MK-2461	2,7E-07	1,0E-07	9,0E-08	9,0E-08	2,9E+05	2,6E-02	
KDR	MK-5108 (VX-689)	5,5E-08	2,1E-08	2,3E-08	2,3E-08	1,1E+06	2,6E-02	
KDR	MLN8054	6,9E-06	2,6E-06	2,6E-06	2,6E-06	5,3E+03	1,4E-02	
KDR	MLN8237 (Alisertib)	5,0E-06	1,9E-06	2,5E-06	2,5E-06	9,6E+03	2,4E-02	
KDR	Motesanib Diphosphate (AMG-706)	6,1E-09	2,3E-09	n.e.	2,3E-09	1,5E+04	≤ 3,5E-05	24
KDR	Nilotinib (AMN-107)	≈ 2,0E-05	≈ 7,6E-06	≈ 2,1E-06	≈ 4,9E-06	n.e.	n.e.	
KDR	NVP-ADW742	7,2E-06	2,8E-06	3,3E-06	3,3E-06	3,7E+03	1,2E-02	
KDR	NVP-BGT226	≈ 2,0E-05	≈ 7,6E-06	≈ 5,0E-06	≈ 6,3E-06	n.e.	n.e.	
KDR	NVP-BSK805	1,8E-06	6,8E-07	8,7E-07	8,7E-07	2,2E+04	1,9E-02	
KDR	NVP-TAE226	≥ 2,0E-05		1,2E-06	1,2E-06	1,7E+04	2,0E-02	
KDR	OSI-930	5,8E-09	2,2E-09	n.e.	2,2E-09	3,7E+04	≤ 8,3E-05	4
KDR	OSU-03012	≥ 2,0E-05		1,3E-06	1,3E-06	≈ 1,9E+03	≈ 2,0E-03	
KDR	Pazopanib HCl	7,3E-10	2,8E-10	n.e.	2,8E-10	3,6E+05	≤ 1,0E-04	24
KDR	PCI-32765 (ibrutinib)	1,1E-06	4,1E-07	6,0E-07	6,0E-07	2,5E+04	1,5E-02	
KDR	PD 0332991 (Palbociclib) HCl	≥ 2,0E-05		4,5E-06	4,5E-06	3,9E+02	1,8E-03	
KDR	PD153035 HCl	4,8E-06	1,8E-06	2,5E-06	2,5E-06	1,1E+04	2,4E-02	
KDR	PD173074	5,3E-07	2,0E-07	2,4E-07	2,4E-07	4,7E+04	1,1E-02	
KDR	PD318088	1,5E-05	5,9E-06	n.e.	5,9E-06	3,8E+02	≤ 2,2E-03	4
KDR	Pelitinib (EKB-569)	≥ 2,0E-05		3,5E-06	3,5E-06	9,2E+02	3,3E-03	
KDR	PF-00562271	2,3E-06	8,9E-07	1,1E-06	1,1E-06	1,7E+04	1,9E-02	
KDR	PF-03814735	2,7E-08	1,0E-08	1,1E-08	1,1E-08	1,9E+06	2,0E-02	
KDR	PF-04217903	≈ 2,0E-05	≈ 7,6E-06	≈ 6,1E-06	≈ 6,9E-06	2,7E+02	≈ 1,8E-03	
KDR	PHA-665752	1,0E-06	4,0E-07	2,9E-07	2,9E-07	2,6E+04	7,6E-03	
KDR	PHA-680632	3,7E-06	1,4E-06	1,2E-06	1,2E-06	1,1E+04	1,3E-02	
KDR	PIK-75	3,5E-06	1,3E-06	1,7E-06	1,7E-06	1,3E+04	2,0E-02	
KDR	PLX-4720	≥ 2,0E-05		1,1E-06	1,1E-06	2,0E+04	2,1E-02	
KDR	Ponatinib (AP24534)	3,6E-09	1,4E-09	n.e.	1,4E-09	7,1E+04	≤ 9,7E-05	24
KDR	PP-121	1,6E-07	6,0E-08	1,4E-07	1,4E-07	1,4E+05	1,8E-02	
KDR	PP242	9,6E-07	3,7E-07	3,7E-07	3,7E-07	3,7E+04	1,3E-02	
KDR	Quercetin (Sophoretin)	8,8E-06	3,4E-06	4,3E-06	4,3E-06	2,2E+03	9,7E-03	
KDR	Quizartinib (AC220)	2,5E-08	9,6E-09	n.e.	9,6E-09	9,6E+02	≤ 9,2E-06	24
KDR	R406	7,4E-08	2,8E-08	5,8E-08	5,8E-08	2,8E+05	1,6E-02	2
KDR	R788 (Fostatinib) - prodrug	6,9E-06	2,6E-06	2,5E-06	2,5E-06	8,6E+03	1,3E-02	
KDR	Raf265 derivative	1,7E-06	6,4E-07	n.e.	6,4E-07	1,5E+03	≤ 9,3E-04	4
KDR	Roscovitine (Seliciclib - CYC202)	5,1E-08	2,0E-08	≥ 2,0E-05	≥ 2,0E-08			
KDR	Ruxolitinib (INCB018424)	1,6E-05	6,1E-06	≈ 3,9E-06	6,1E-06	n.e.	n.e.	
KDR	SAR131675	4,1E-07	1,6E-07	1,4E-07	1,4E-07	4,8E+04	6,5E-03	
KDR	Saracatinib (AZD0530)	≥ 2,0E-05		4,6E-06	4,6E-06	9,2E+02	4,4E-03	
KDR	SB 202190	≥ 2,0E-05		7,8E-06	7,8E-06	6,8E+02	5,4E-03	
KDR	SB 203580	≥ 2,0E-05		3,8E-06	3,8E-06	1,5E+03	5,5E-03	
KDR	SB 216763	≈ 2,0E-05	≈ 7,6E-06	n.e.	≈ 7,6E-06	1,0E+03	≤ 7,8E-03	4
KDR	SB590885	1,2E-05	4,6E-06	n.e.	4,6E-06	2,7E+02	≤ 1,3E-03	4
KDR	Semaxanib (SU5416)	1,0E-08	3,8E-09	8,6E-09	8,6E-09	1,2E+06	1,1E-02	
KDR	SNS-314	2,2E-06	8,2E-07	1,1E-07	8,2E-07	7,0E+04	7,4E-03	
KDR	Sotrastaurin (AEB071)	3,9E-07	1,5E-07	n.e.	1,5E-07	2,9E+03	≤ 4,2E-04	4
KDR	SP600125	1,2E-06	4,4E-07	3,1E-07	3,1E-07	6,4E+04	2,0E-02	
KDR	Staurosporine	4,1E-08	1,6E-08	1,7E-08	1,7E-08	7,0E+05	1,2E-02	
KDR	SU11274	1,5E-05	5,7E-06	2,2E-06	2,2E-06	7,2E+03	1,6E-02	
KDR	Sunitinib Malate (Sutent)	8,4E-10	3,2E-10	3,7E-10	3,7E-10	1,1E+07	4,2E-03	
KDR	TAE684 (NVP-TAE684)	2,5E-06	9,7E-07	3,6E-07	3,6E-07	5,1E+04	1,6E-02	
KDR	TAK-285	3,6E-08	1,4E-08	≥ 2,0E-05	≥ 1,4E-08			
KDR	TAK-901	1,9E-08	7,1E-09	1,4E-08	1,4E-08	8,6E+05	1,2E-02	
KDR	Tandutinib (MLN518)	6,8E-06	2,6E-06	3,3E-06	3,3E-06	9,2E+03	3,1E-02	
KDR	TG101209	1,2E-06	4,4E-07	7,7E-07	7,7E-07	2,2E+04	1,7E-02	

kinase	Compound	IC ₅₀ [M] ePCA	K _D eq [M] ePCA *	K _D kin [M] kPCA	K _D [M] PCA **	k _{on} [M ⁻¹ s ⁻¹] kPCA	k _{off} [s ⁻¹] kPCA	comment
KDR	TG101348 (SAR302503)	3,1E-06	1,2E-06	2,1E-06	2,1E-06	5,2E+03	1,1E-02	
KDR	Tie2 kinase inhibitor	1,6E-05	6,2E-06	4,7E-06	4,7E-06	2,5E+03	1,1E-02	
KDR	Tivozanib (AV-951)	4,3E-10	1,6E-10	n.e.	1,6E-10	5,0E+05	≤ 8,1E-05	24
KDR	Torin 1	≥ 2,0E-05		2,3E-06	2,3E-06	3,9E+02	9,1E-04	
KDR	Torin 2	≥ 2,0E-05		4,1E-06	4,1E-06	2,0E+03	8,2E-03	
KDR	TPCA-1	2,6E-06	1,0E-06	1,1E-06	1,1E-06	1,5E+04	1,7E-02	
KDR	TSU-68 (SU6668)	4,2E-09	1,6E-09	9,7E-10	9,7E-10	9,5E+06	9,3E-03	
KDR	TWS119	5,3E-08	2,0E-08	1,5E-08	1,5E-08	1,2E+06	1,8E-02	
KDR	Tyrphostin AG 879 (AG 879)	8,2E-06	3,1E-06	≥ 2,0E-05	≥ 3,1E-06			
KDR	Vandetanib (Zactima)	4,8E-08	1,8E-08	5,4E-08	5,4E-08	3,4E+05	1,8E-02	
KDR	Vatalanib 2HCl (PTK787)	9,4E-09	3,6E-09	n.e.	3,6E-09	4,3E+04	≤ 1,5E-04	4
KDR	VX-680 (MK-0457 - Tozasertib)	1,0E-06	3,8E-07	5,7E-07	5,7E-07	4,2E+04	2,4E-02	
KDR	WAY-600	≈ 2,0E-05	≈ 7,6E-06	≈ 4,0E-06	≈ 5,8E-06	n.e.	n.e.	
KDR	WHI-P154	1,8E-06	7,0E-07	1,0E-06	1,0E-06	2,1E+04	2,2E-02	
KDR	WP1066	3,9E-06	1,5E-06	≥ 2,0E-05	≥ 1,5E-06			
KDR	WZ3146	9,7E-07	3,7E-07	3,3E-07	3,3E-07	5,3E+04	1,8E-02	
KDR	WZ4002	≥ 2,0E-05		4,5E-06		≥ 7,8E+04	≥ 3,5E-01	
KDR	WZ8040	4,0E-07	1,5E-07	1,7E-07	1,7E-07	7,2E+04	1,2E-02	
KDR	XL-184 (Cabozantinib)	1,3E-09	5,0E-10	n.e.	5,0E-10	1,8E+05	≤ 9,0E-05	4
KDR	ZM-447439	1,0E-06	3,8E-07	7,7E-07	7,7E-07	3,0E+04	2,3E-02	
KIT	AEE788 (NVP-AEE788)	1,0E-06	4,0E-07	4,4E-07	4,4E-07	5,0E+05	2,1E-01	
KIT	AMG458	1,4E-05	5,8E-06	≈ 2,0E-06	5,8E-06	≈ 1,1E+03	≈ 6,6E-03	
KIT	Apatinib (YN968D1)	4,0E-08	1,6E-08	n.e.	1,6E-08	6,5E+03	≤ 1,0E-04	24
KIT	AT9283	6,0E-07	2,4E-07	1,1E-07	1,1E-07	3,7E+05	4,2E-02	
KIT	Aurora A Inhibitor I	2,5E-07	1,0E-07	n.e.	1,0E-07	6,5E+05	6,5E-02	123
KIT	Axitinib	3,5E-09	1,4E-09	n.e.	1,4E-09	3,5E+05	≤ 4,8E-04	24
KIT	AZ 960	6,0E-06	2,4E-06	1,9E-06	1,9E-06	6,0E+04	1,2E-01	
KIT	AZ628	7,0E-08	2,8E-08	n.e.	2,8E-08	5,8E+03	≤ 1,6E-04	4
KIT	AZD4547	9,5E-08	3,8E-08	3,1E-08	3,1E-08	1,4E+06	4,2E-02	
KIT	AZD5438	7,5E-06	3,0E-06	2,8E-06	2,8E-06	≈ 1,5E+05	≈ 4,1E-01	
KIT	AZD7762	6,0E-08	2,4E-08	1,3E-07	2,4E-08	7,7E+05	1,8E-02	23
KIT	AZD8931	≈ 2,0E-05	≈ 8,0E-06	≈ 6,0E-06	≈ 7,0E-06	1,7E+04	9,8E-02	
KIT	Barasertib (AZD1152-HQPA)	≈ 9,0E-07	≈ 3,6E-07	6,2E-07	6,2E-07	9,5E+04	5,5E-02	2
KIT	BGJ398 (NVP-BGJ398)	2,5E-07	1,0E-07	n.e.	1,0E-07	1,2E+05	1,2E-02	123
KIT	BIBF1120 (Vargatef)	2,5E-09	1,0E-09	7,4E-10	7,4E-10	9,7E+06	6,7E-03	
KIT	BIRB 796 (Doramapimod)	2,5E-06	1,0E-06	n.e.	1,0E-06	2,1E+02	≤ 2,1E-04	4
KIT	BIX 02188	3,0E-08	1,2E-08	9,5E-09	9,5E-09	2,3E+06	2,2E-02	
KIT	BIX 02189	5,0E-07	2,0E-07	4,3E-07	4,3E-07	9,1E+04	3,7E-02	2
KIT	BKM120 (NVP-BKM120)	2,0E-05	8,0E-06	5,1E-06	5,1E-06	≈ 1,2E+04	≈ 6,0E-02	
KIT	BMS 777607	3,0E-06	1,2E-06	1,4E-06	1,4E-06	7,1E+03	9,6E-03	
KIT	BMS 794833	3,5E-08	1,4E-08	n.e.	1,4E-08	2,5E+03	≤ 3,5E-05	24
KIT	Bosutinib (SKI-606)	4,0E-06	1,6E-06	1,4E-06	1,4E-06	3,5E+04	4,8E-02	
KIT	Brivanib (BMS-540215)	5,5E-07	2,2E-07	7,1E-07	7,1E-07	1,7E+05	1,2E-01	1
KIT	Brivanib alaninate (BMS-582664) - prodrug	3,0E-06	1,2E-06	6,2E-07	6,2E-07	≈ 2,1E+05	1,2E-01	
KIT	BX-795	2,0E-06	8,0E-07	1,1E-06	1,1E-06	8,5E+04	9,3E-02	
KIT	BX-912	6,5E-07	2,6E-07	5,6E-07	5,6E-07	2,5E+05	1,4E-01	
KIT	CCT137690	3,0E-06	1,2E-06	≈ 5,9E-06	1,2E-06	≥ 5,9E+04	≥ 3,5E-01	
KIT	Cediranib (AZD2171)	1,5E-07	6,0E-08	5,6E-09	6,0E-08	1,8E+06	1,0E-02	2
KIT	CEP33779	2,5E-06	1,0E-06	1,2E-06	1,2E-06	≈ 2,1E+05	≈ 2,3E-01	
KIT	CH5424802	≥ 2,0E-05		7,2E-06		≥ 4,9E+04	≥ 3,5E-01	
KIT	CHIR-124	2,5E-08	1,0E-08	n.e.	1,0E-08	2,8E+06	2,8E-02	23
KIT	CI-1033 (Canertinib)	≥ 2,0E-05		6,4E-06		≥ 5,5E+04	≥ 3,5E-01	
KIT	CP 673451	4,0E-06	1,6E-06	1,2E-06	1,2E-06	5,1E+04	5,8E-02	
KIT	Crenolanib (CP-868596)	1,5E-06	6,0E-07	8,5E-07	8,5E-07	3,7E+04	3,2E-02	
KIT	Crizotinib (PF-02341066)	≥ 2,0E-05		5,2E-06		1,2E+03	≈ 7,2E-03	
KIT	CYC116	2,0E-07	8,0E-08	9,3E-08	9,3E-08	7,6E+05	6,7E-02	
KIT	Cyt387	2,0E-05	8,0E-06	3,4E-06	3,4E-06	≈ 3,9E+04	≈ 1,9E-01	
KIT	Dabrafenib (GSK2118436)	1,0E-05	4,0E-06	3,9E-06	3,9E-06	≈ 1,3E+04	≈ 6,2E-02	
KIT	Danuserib (PHA-739358)	6,0E-06	2,4E-06	2,2E-06	2,2E-06	7,7E+03	1,6E-02	
KIT	Dasatinib (BMS-354825)	9,5E-10	3,8E-10	n.e.	3,8E-10	7,9E+05	≤ 3,0E-04	24
KIT	DCC-2036 (Rebastinib)	6,0E-07	2,4E-07	n.e.	2,4E-07	5,6E+02	≤ 1,3E-04	14
KIT	Deforolimus (Ridaforolimus)	2,0E-05	8,0E-06	≥ 2,0E-05	≥ 8,0E-06			
KIT	Desmethyl Erlotinib (CP-473420)	1,5E-05	6,0E-06	3,2E-06	3,2E-06	2,6E+04	8,2E-02	
KIT	Dovitinib (TKI-258)	1,2E-08	4,9E-09	2,2E-09	2,2E-09	8,5E+06	1,8E-02	
KIT	E7080 (Lenvatinib)	9,5E-09	3,8E-09	2,3E-08	3,8E-09	1,5E+05	3,4E-03	2
KIT	ENMD-2076	3,0E-08	1,2E-08	3,1E-08	3,1E-08	3,0E+05	9,1E-03	
KIT	Erlotinib HCl	≥ 2,0E-05		6,7E-06		≥ 5,3E+04	≥ 3,5E-01	
KIT	Foretinib (GSK1363089 - XL880)	6,0E-09	2,4E-09	n.e.	2,4E-09	2,9E+04	≤ 6,9E-05	24
KIT	GDC-0941	≥ 2,0E-05		1,0E-05		≥ 3,5E+04	≥ 3,5E-01	
KIT	GDC-0980 (RG7422)	3,0E-06	1,2E-06	2,0E-06	2,0E-06	5,2E+04	1,0E-01	
KIT	Gefitinib (Iressa)	≥ 2,0E-05		1,1E-05		≥ 3,2E+04	≥ 3,5E-01	
KIT	Golvatinib (E7050)	4,0E-08	1,6E-08	n.e.	1,6E-08	3,1E+04	≤ 4,9E-04	24
KIT	GSK1059615	≥ 2,0E-05		7,8E-06		≥ 4,5E+04	≥ 3,5E-01	
KIT	GSK1070916	≥ 2,5E-06	1,0E-06	1,2E-06		2,3E+04	2,7E-02	
KIT	Hesperadin	1,0E-06	4,0E-07	2,9E-07	2,9E-07	2,3E+05	6,7E-02	
KIT	Imatinib (Gleevec)	6,5E-08	2,6E-08	n.e.	2,6E-08	9,0E+03	≤ 2,3E-04	4
KIT	INK 128 (MLN0128)	2,5E-06	1,0E-06	9,4E-07	9,4E-07	1,9E+05	1,8E-01	
KIT	JNJ-7706621	4,0E-06	1,6E-06	1,0E-06	1,0E-06	≈ 3,6E+05	≈ 2,8E-01	
KIT	Ki8751	2,5E-09	1,0E-09	n.e.	1,0E-09	6,5E+04	≤ 6,5E-05	24

kinase	Compound	IC ₅₀ [M] ePCA	K _D eq [M] ePCA *	K _D kin [M] kPCA	K _D [M] PCA **	k _{on} [M ⁻¹ s ⁻¹] kPCA	k _{off} [s ⁻¹] kPCA	comment
KIT	KRN 633	1,0E-07	4,0E-08	4,9E-08	4,9E-08	1,1E+05	5,5E-03	2
KIT	KW 2449	2,5E-07	1,0E-07	3,7E-07	3,7E-07	6,4E+05	2,3E-01	2
KIT	LDN193189	2,0E-06	8,0E-07	1,9E-06	1,9E-06	5,1E+04	9,5E-02	1
KIT	Linifanib (ABT-869)	7,0E-09	2,8E-09	n.e.	2,8E-09	5,3E+03	≤ 1,5E-05	24
KIT	Linsitinib (OSI-906)	≥ 2,0E-05		6,9E-06	6,9E-06	8,3E+03	6,0E-02	
KIT	LY2603618 (IC-83)	4,5E-06	1,8E-06	3,9E-06	3,9E-06	2,5E+04	9,9E-02	
KIT	LY2784544	2,5E-07	1,0E-07	6,8E-08	6,8E-08	5,1E+05	3,4E-02	
KIT	Masitinib (AB1010)	4,5E-08	1,8E-08	n.e.	1,8E-08	1,3E+04	≤ 2,3E-04	24
KIT	MGCD-265	2,0E-08	8,0E-09	n.e.	8,0E-09	8,1E+04	≤ 6,4E-04	24
KIT	Miliciclib (PHA-848125)	≥ 2,0E-05		3,8E-06	3,8E-06	2,0E+04	7,1E-02	
KIT	MK-2206 2HCl	≥ 2,0E-05		9,1E-06	9,1E-06	≈ 1,1E+04	≈ 1,0E-01	
KIT	MK-2461	≥ 2,0E-05		5,0E-06	5,0E-06	≥ 7,1E+04	≥ 3,5E-01	
KIT	MK-5108 (VX-689)	2,0E-05	8,0E-06	1,0E-05	1,0E-05	≥ 3,4E+04	≥ 3,5E-01	
KIT	Motesanib Diphosphate (AMG-706)	4,0E-08	1,6E-08	n.e.	1,6E-08	7,8E+03	≤ 1,2E-04	4
KIT	Nilotinib (AMN-107)	3,5E-08	1,4E-08	n.e.	1,4E-08	n.e.	n.e.	1
KIT	NVP-ADW742	8,0E-07	3,2E-07	5,6E-07	5,6E-07	≈ 2,6E+05	≈ 1,2E-01	2
KIT	NVP-BGT226	≈ 2,0E-05	≈ 8,0E-06	9,4E-06	9,4E-06	≈ 1,1E+04	≈ 1,1E-01	
KIT	NVP-BHG712	2,0E-05	8,0E-06	≈ 6,3E-06	8,0E-06	5,8E+02	3,8E-03	
KIT	NVP-BSK805	1,5E-06	6,0E-07	9,2E-07	9,2E-07	5,9E+04	5,4E-02	
KIT	NVP-BVU972	≥ 2,0E-05		1,0E-05	1,0E-05	≥ 3,4E+04	≥ 3,5E-01	
KIT	NVP-TAE226	≥ 2,0E-05		3,0E-06	3,0E-06	2,7E+04	8,2E-02	
KIT	OSI-930	≥ 2,0E-08	8,0E-09	n.e.	8,0E-09	7,6E+03	≤ 6,1E-05	4
KIT	Pazopanib HCl	6,0E-09	2,4E-09	n.e.	2,4E-09	2,4E+05	≤ 5,8E-04	24
KIT	PCI-32765 (Ibrutinib)	2,0E-06	8,0E-07	8,1E-07	8,1E-07	7,6E+04	6,1E-02	
KIT	PD 0332991 (Palbociclib) HCl	≈ 2,0E-05	≈ 8,0E-06	4,5E-06	4,5E-06	≈ 4,0E+04	≈ 1,9E-01	
KIT	PD153035 HCl	≈ 2,0E-05	≈ 8,0E-06	6,6E-06	6,6E-06	≈ 7,4E+04	≈ 3,5E-01	
KIT	PD173074	≈ 2,0E-05	≈ 8,0E-06	3,6E-06	3,6E-06	≈ 2,2E+04	≈ 8,3E-02	
KIT	PF-00562271	4,0E-06	1,6E-06	1,5E-06	1,5E-06	6,1E+04	9,5E-02	
KIT	PF-03814735	8,5E-08	3,4E-08	5,9E-08	5,9E-08	8,9E+05	5,3E-02	
KIT	PHA-665752	7,5E-07	3,0E-07	2,9E-07	2,9E-07	4,7E+04	1,3E-02	
KIT	PHA-680632	5,0E-06	2,0E-06	1,7E-06	1,7E-06	1,9E+05	3,1E-02	
KIT	PIK-75	≥ 2,0E-05		3,1E-06	3,1E-06	≈ 8,0E+04	≈ 2,2E-01	2
KIT	PLX-4720	2,0E-06	8,0E-07	6,4E-07	6,4E-07	4,4E+04	2,8E-02	
KIT	Ponatinib (AP24534)	1,5E-08	6,0E-09	n.e.	6,0E-09	1,9E+04	≤ 1,2E-04	24
KIT	PP-121	3,0E-07	1,2E-07	2,2E-07	2,2E-07	2,9E+05	6,2E-02	
KIT	PP242	5,0E-06	2,0E-06	1,7E-06	1,7E-06	4,0E+04	6,8E-02	
KIT	Quercetin (Sophoretin)	4,5E-06	1,8E-06	2,7E-06	2,7E-06	6,2E+04	1,8E-01	
KIT	Quizartinib (AC220)	2,0E-08	8,0E-09	n.e.	8,0E-09	3,6E+03	≤ 2,9E-05	24
KIT	R406	8,5E-08	3,4E-08	n.e.	3,4E-08	1,6E+06	5,5E-02	123
KIT	R788 (Fostamatinib) - prodrug	≈ 1,1E-05	≈ 4,5E-06	4,4E-06	4,4E-06	1,9E+04	3,8E-02	
KIT	Raf265 derivative	4,0E-06	1,6E-06	≥ 2,0E-05	≥ 1,6E-06			
KIT	SAR131675	≈ 4,5E-06	≈ 1,8E-06	1,2E-06	1,2E-06	3,0E+04	3,5E-02	1
KIT	Saracatinib (AZD0530)	9,5E-07	3,8E-07	2,0E-07	2,0E-07	6,7E+04	1,4E-02	
KIT	Semaxanib (SU5416)	5,5E-08	2,2E-08	3,5E-08	3,5E-08	1,4E+06	4,9E-02	
KIT	SNS-314	≈ 5,5E-07	≈ 2,2E-07	1,2E-07	1,2E-07	≈ 1,1E+05	≈ 1,3E-02	2
KIT	SP600125	1,5E-06	6,0E-07	6,1E-07	6,1E-07	≈ 1,4E+05	8,3E-02	1
KIT	Staurosporine	5,5E-08	2,2E-08	3,0E-08	3,0E-08	9,6E+05	2,5E-02	2
KIT	SU11274	1,5E-07	6,0E-08	3,6E-07	6,0E-08	2,1E+05	7,6E-02	12
KIT	Sunitinib Malate (Sutent)	2,0E-09	8,0E-10	1,0E-09	1,0E-09	2,1E+07	2,1E-02	
KIT	TAE684 (NVP-TAE684)	2,0E-06	8,0E-07	1,9E-07	1,9E-07	5,9E+05	1,1E-01	
KIT	TAK-901	1,5E-08	6,0E-09	2,4E-08	2,4E-08	6,5E+05	1,5E-02	
KIT	Tandutinib (MLN518)	3,0E-07	1,2E-07	2,2E-07	2,2E-07	8,2E+04	1,8E-02	2
KIT	TG101209	5,0E-07	2,0E-07	2,9E-07	2,9E-07	2,8E+05	7,8E-02	
KIT	TG101348 (SAR302503)	7,0E-07	2,8E-07	4,0E-07	4,0E-07	1,4E+05	5,5E-02	
KIT	TGX-221	≥ 2,0E-05		1,3E-05	1,3E-05	2,2E+03	2,6E-02	
KIT	Tivozanib (AV-951)	2,5E-09	1,0E-09	n.e.	1,0E-09	1,0E+05	≤ 1,0E-04	24
KIT	Torin 2	1,0E-06	4,0E-07	1,3E-06	1,3E-06	≈ 6,4E+04	7,9E-02	1
KIT	TPCA-1	6,5E-07	2,6E-07	3,0E-07	3,0E-07	2,2E+05	6,5E-02	
KIT	TSU-68 (SU6668)	4,5E-08	1,8E-08	2,2E-08	2,2E-08	1,4E+06	3,0E-02	
KIT	TWS119	3,0E-07	1,2E-07	1,4E-07	1,4E-07	4,1E+05	5,4E-02	
KIT	Vandetanib (Zactima)	7,5E-07	3,0E-07	8,9E-07	8,9E-07	≈ 7,0E+04	≈ 6,7E-02	1
KIT	Vatalanib 2HCl (PTK787)	1,0E-07	4,0E-08	n.e.	4,0E-08	8,3E+03	≤ 3,3E-04	4
KIT	Vemurafenib (PLX4032)	≥ 2,0E-05		5,8E-06	5,8E-06	2,4E+03	1,4E-02	
KIT	VX-680 (MK-0457 - Tozasertib)	4,0E-06	1,6E-06	1,7E-06	1,7E-06	≈ 2,8E+05	≈ 4,5E-01	
KIT	WHI-P154	≈ 2,0E-05	≈ 8,0E-06	≈ 7,6E-06	≈ 7,8E-06	≈ 5,2E+02	≈ 4,0E-03	
KIT	WZ3146	1,0E-05	4,0E-06	3,2E-06	3,2E-06	≈ 1,7E+05	≈ 5,4E-01	
KIT	WZ4002	≥ 2,0E-05		8,4E-06	8,4E-06	≥ 4,2E+04	≥ 3,5E-01	
KIT	WZ8040	2,0E-06	8,0E-07	7,6E-07	7,6E-07	≈ 2,5E+05	≈ 1,8E-01	
KIT	XL-184 (Cabozantinib)	6,5E-09	2,6E-09	n.e.	2,6E-09	4,1E+04	≤ 1,1E-04	24
KIT	ZM 336372	2,0E-07	8,0E-08	n.e.	8,0E-08	5,2E+03	≤ 4,1E-04	4
KIT	ZM-447439	2,0E-07	8,0E-08	2,1E-07	2,1E-07	9,1E+05	1,8E-01	
LCK	AEE788 (NVP-AEE788)	2,5E-07	1,5E-07	2,1E-07	2,1E-07	≥ 1,7E+06	≥ 3,5E-01	
LCK	Afatinib (BIBW2992)	1,6E-06	9,4E-07	7,1E-07	7,1E-07	≥ 4,9E+05	≥ 3,5E-01	
LCK	AG-1478 (Typhostin AG-1478)	≈ 6,9E-07	≈ 4,2E-07	1,1E-06	1,1E-06	≈ 7,2E+05	≈ 7,0E-01	
LCK	AMG 900	5,7E-07	3,4E-07	1,3E-06	1,3E-06	≈ 1,1E+05	≈ 1,6E-01	1
LCK	AMG458	3,2E-07	1,9E-07	1,9E-07	1,9E-07	2,3E+05	4,0E-02	
LCK	Apatinib (YN968D1)	≥ 2,0E-05		9,5E-06	9,5E-06	≥ 3,7E+04	≥ 3,5E-01	
LCK	ARRY334543	≈ 2,6E-07	≈ 1,6E-07	1,8E-07	1,8E-07	≥ 1,9E+06	≥ 3,5E-01	
LCK	Arry-380	9,8E-06	5,9E-06	3,7E-06	3,7E-06	≥ 9,5E+04	≥ 3,5E-01	

kinase	Compound	IC ₅₀ [M] ePCA	K _D eq [M] ePCA *	K _D kin [M] kPCA	K _D [M] PCA **	k _{on} [M ⁻¹ s ⁻¹] kPCA	k _{off} [s ⁻¹] kPCA	comment
LCK	AT9283	8,6E-08	5,2E-08	3,6E-08	3,6E-08	≥ 9,8E+06	≥ 3,5E-01	
LCK	Aurora A Inhibitor I	≈ 1,9E-06	≈ 1,1E-06	2,9E-06	2,9E-06	n.e.	n.e.	2
LCK	Axitinib	2,3E-06	1,4E-06	1,9E-06	1,9E-06	≥ 1,9E+05	≥ 3,5E-01	
LCK	AZ 960	7,3E-07	4,5E-07	7,6E-07	7,6E-07	≥ 4,6E+05	≥ 3,5E-01	
LCK	AZ628	3,1E-07	1,9E-07	2,2E-07	2,2E-07	≈ 8,9E+05	≈ 1,7E-01	
LCK	AZD4547	8,7E-07	5,3E-07	3,5E-07	3,5E-07	≈ 2,8E+06	≈ 9,3E-01	
LCK	AZD5438	≈ 4,6E-06	≈ 2,8E-06	3,5E-06	3,5E-06	≥ 1,0E+05	≥ 3,5E-01	
LCK	AZD7762	1,6E-07	9,7E-08	1,6E-07	1,6E-07	≥ 2,2E+06	≥ 3,5E-01	
LCK	AZD8931	5,0E-07	3,1E-07	3,6E-07	3,6E-07	≥ 9,6E+05	≥ 3,5E-01	
LCK	Barasertib (AZD1152-HQPA)	5,9E-08	3,6E-08	5,1E-08	5,1E-08	≥ 6,9E+06	≥ 3,5E-01	
LCK	Baricitinib (LY3009104 - incb28050)	6,6E-06	4,0E-06	3,3E-06	3,3E-06	≥ 1,1E+05	≥ 3,5E-01	
LCK	BEZ235 (NVP-BEZ235)	7,0E-07	4,2E-07	1,3E-06	1,3E-06	≥ 7,0E+05	≈ 7,5E-01	1
LCK	BGJ398 (NVP-BGJ398)	1,1E-06	6,8E-07	1,1E-06	1,1E-06	≥ 3,1E+05	≥ 3,5E-01	
LCK	BIBF1120 (Vargatef)	4,0E-09	2,4E-09	1,4E-09	1,4E-09	≈ 4,3E+07	5,3E-02	
LCK	BIX 02188	9,3E-07	5,6E-07	4,1E-07	4,1E-07	≈ 8,0E+05	≈ 3,9E-01	
LCK	BIX 02189	4,4E-06	2,7E-06	2,5E-06	2,5E-06	≥ 1,4E+05	≥ 3,5E-01	
LCK	BMS 777607	5,8E-08	3,5E-08	8,3E-08	8,3E-08	5,8E+06	5,1E-01	1
LCK	BMS 794833	7,7E-08	4,7E-08	1,2E-07	1,2E-07	3,9E+05	4,6E-02	
LCK	BMS-265246	≈ 2,0E-05	≈ 1,2E-05	1,0E-05	1,0E-05	≥ 3,5E+04	≥ 3,5E-01	
LCK	BMS-599626 (AC480)	≈ 4,5E-06	≈ 2,7E-06	3,0E-06	3,0E-06	n.e.	n.e.	
LCK	Bosutinib (SKI-606)	1,4E-09	8,3E-10	1,5E-09	1,5E-09	5,0E+06	7,0E-03	
LCK	Brivanib (BMS-540215)	8,5E-07	5,2E-07	1,7E-06	1,7E-06	≈ 5,8E+04	≈ 1,0E-01	
LCK	Brivanib alaninate (BMS-582664) - prodrug	1,5E-06	9,0E-07	9,8E-07	9,8E-07	≥ 3,6E+05	≥ 3,5E-01	
LCK	BX-795	2,2E-06	1,3E-06	2,0E-06	2,0E-06	≥ 1,7E+05	≥ 3,5E-01	
LCK	BX-912	7,3E-07	4,4E-07	7,2E-07	7,2E-07	≈ 9,6E+05	≈ 6,1E-01	
LCK	CCT129202	1,5E-05	8,8E-06	≈ 9,9E-06	8,8E-06	≥ 3,5E+04	≥ 3,5E-01	
LCK	CCT137690	3,3E-06	2,0E-06	4,5E-06	4,5E-06	≥ 7,8E+04	≥ 3,5E-01	
LCK	Cediranib (AZD2171)	1,8E-06	1,1E-06	9,1E-08	1,1E-06	n.e.	n.e.	
LCK	CEP33779	6,4E-07	3,9E-07	4,9E-07	4,9E-07	≥ 7,2E+05	≥ 3,5E-01	
LCK	CH5424802	≥ 2,0E-05		4,7E-06	4,7E-06	≥ 7,4E+04	≥ 3,5E-01	
LCK	CHIR-124	4,2E-07	2,6E-07	4,2E-07	4,2E-07	≥ 8,3E+05	≥ 3,5E-01	
LCK	CI-1033 (Canertinib)	1,6E-07	9,7E-08	1,9E-07	1,9E-07	≥ 1,9E+06	≥ 3,5E-01	
LCK	CP 673451	1,6E-07	9,7E-08	9,7E-08	9,7E-08	≈ 9,7E+06	≈ 9,6E-01	
LCK	CP-724714	4,7E-06	2,8E-06	2,3E-06	2,3E-06	≥ 1,5E+05	≥ 3,5E-01	
LCK	Crenolanib (CP-868596)	2,9E-07	1,8E-07	2,5E-07	2,5E-07	≥ 1,4E+06	≥ 3,5E-01	
LCK	Crizotinib (PF-02341066)	6,1E-08	3,7E-08	1,1E-07	1,1E-07	n.e.	n.e.	2
LCK	CX-4945 (Silmnertinib)	≈ 1,3E-06	≈ 7,7E-07	1,1E-06	1,1E-06	≥ 3,3E+05	≥ 3,5E-01	
LCK	CYC116	4,9E-07	3,0E-07	3,1E-07	3,1E-07	≥ 1,1E+06	≥ 3,5E-01	
LCK	Cyt387	1,3E-06	8,0E-07	1,9E-06	1,9E-06	≥ 1,9E+05	≥ 3,5E-01	
LCK	Dabrafenib (GSK2118436)	3,5E-07	2,2E-07	3,7E-07	3,7E-07	≥ 9,5E+05	≥ 3,5E-01	
LCK	Dacomitinib (PF299804 - PF-00299804)	2,1E-07	1,3E-07	5,0E-07	5,0E-07	9,4E+05	≈ 4,9E-01	
LCK	Danuseritib (PHA-739358)	2,8E-07	1,7E-07	2,6E-07	2,6E-07	1,7E+05	4,6E-02	
LCK	Dasatinib (BMS-354825)	4,0E-10	2,4E-10	1,7E-10	1,7E-10	8,8E+06	1,5E-03	
LCK	DCC-2036 (Rebastinib)	≈ 1,6E-08	≈ 9,9E-09	5,2E-09	5,2E-09	1,6E+05	8,3E-04	
LCK	Desmethyl Erlotinib (CP-473420)	5,8E-07	3,5E-07	3,2E-07	3,2E-07	≥ 1,1E+06	≥ 3,5E-01	
LCK	Dovitinib (TKI-258)	4,3E-08	2,6E-08	1,6E-08	1,6E-08	≈ 1,8E+07	≈ 3,5E-01	
LCK	E7080 (Lenvatinib)	2,7E-07	1,6E-07	2,8E-07	2,8E-07	≈ 2,0E+06	≈ 5,5E-01	
LCK	ENMD-2076	3,8E-08	2,3E-08	3,0E-08	3,0E-08	≈ 3,4E+06	≈ 8,7E-02	
LCK	Erlotinib HCl	1,6E-06	9,7E-07	1,5E-06	1,5E-06	≈ 4,5E+05	≈ 6,3E-01	1
LCK	Flavopiridol HCl	7,2E-06	4,4E-06	6,6E-06	6,6E-06	≥ 5,3E+04	≥ 3,5E-01	
LCK	Foretinib (GSK1363089 - XL880)	2,3E-09	1,4E-09	2,2E-09	2,2E-09	1,1E+06	2,4E-03	
LCK	GDC-0980 (RG7422)	4,6E-07	2,8E-07	6,4E-07	6,4E-07	≥ 5,5E+05	≥ 3,5E-01	
LCK	Gefitinib (Iressa)	6,4E-07	3,9E-07	1,2E-06	1,2E-06	≥ 2,9E+05	≥ 3,5E-01	
LCK	Golvatinib (E7050)	5,0E-08	3,0E-08	2,5E-08	2,5E-08	5,5E+06	1,4E-01	
LCK	GSK1059615	≥ 2,0E-05		5,5E-06	5,5E-06	≥ 6,3E+04	≥ 3,5E-01	
LCK	GSK1070916	4,8E-07	2,9E-07	2,2E-07	2,2E-07	≈ 2,0E+06	≈ 4,3E-01	
LCK	GSK1838705A	≥ 2,0E-05		9,0E-06	9,0E-06	≥ 3,9E+04	≥ 3,5E-01	
LCK	GSK690693	≥ 2,0E-05		1,6E-05	1,6E-05	≥ 2,2E+04	≥ 3,5E-01	
LCK	Hesperadin	1,6E-09	9,8E-10	6,5E-10	6,5E-10	2,2E+07	1,4E-02	
LCK	Imatinib (Gleevec)	1,6E-06	9,9E-07	1,6E-06	1,6E-06	1,0E+05	1,7E-01	
LCK	INK 128 (MLN0128)	6,4E-07	3,9E-07	3,0E-07	3,0E-07	≈ 1,4E+06	≈ 4,3E-01	
LCK	JNJ-7706621	≈ 1,3E-06	≈ 7,9E-07	9,1E-07	9,1E-07	≥ 3,8E+05	≥ 3,5E-01	
LCK	Ki8751	8,0E-09	4,9E-09	1,0E-08	1,0E-08	2,6E+06	2,7E-02	
LCK	KRN 633	1,0E-06	6,3E-07	1,2E-06	1,2E-06	5,1E+05	5,9E-01	2
LCK	KW 2449	1,0E-06	6,2E-07	4,5E-06	6,2E-07	n.e.	n.e.	
LCK	Lapatinib Ditosylate (Tykerb)	≥ 2,0E-05		3,1E-06	3,1E-06	≥ 1,1E+05	≥ 3,5E-01	
LCK	LDN193189	5,7E-07	3,5E-07	5,6E-07	5,6E-07	≥ 6,2E+05	≥ 3,5E-01	
LCK	Linifanib (ABT-869)	1,4E-05	8,4E-06	8,2E-06	8,2E-06	≥ 4,3E+04	≥ 3,5E-01	
LCK	Linsitinib (OSI-906)	3,2E-06	1,9E-06	1,0E-06	1,0E-06	≈ 3,5E+05	≈ 3,2E-01	
LCK	LY2784544	7,3E-07	4,4E-07	4,3E-07	4,3E-07	≈ 4,5E+05	≈ 1,8E-01	
LCK	Masitinib (AB1010)	2,4E-07	1,4E-07	2,1E-07	2,1E-07	1,6E+05	3,6E-02	
LCK	MGCD-265	9,8E-10	5,9E-10	2,2E-09	2,2E-09	7,5E+05	1,6E-03	
LCK	Milciclib (PHA-848125)	1,7E-07	1,1E-07	7,7E-08	7,7E-08	≈ 4,3E+06	≈ 4,1E-01	
LCK	MK-2461	3,1E-06	1,9E-06	2,6E-06	2,6E-06	n.e.	n.e.	2
LCK	MK-5108 (VX-689)	1,9E-07	1,2E-07	3,3E-07	3,3E-07	≥ 1,1E+06	≥ 3,5E-01	
LCK	MLN8054	1,2E-06	7,6E-07	1,4E-06	1,4E-06	≈ 1,0E+05	≈ 1,3E-01	
LCK	MLN8237 (Alisertib)	4,0E-07	2,4E-07	3,1E-07	3,1E-07	≥ 1,1E+06	≥ 3,5E-01	
LCK	Motesanib Diphosphate (AMG-706)	1,3E-05	8,2E-06	7,5E-06	7,5E-06	≈ 1,3E+05	≈ 6,9E-01	
LCK	Neratinib (HKI-272)	5,9E-08	3,6E-08	8,2E-09	8,2E-09	5,5E+06	4,2E-02	

kinase	Compound	IC ₅₀ [M] ePCA	K _D eq [M] ePCA *	K _D kin [M] kPCA	K _D [M] PCA **	k _{on} [M ⁻¹ s ⁻¹] kPCA	k _{off} [s ⁻¹] kPCA	comment
LCK	Nilotinib (AMN-107)	1,4E-05	8,6E-06	4,8E-06	4,8E-06	2,4E+03	1,0E-02	2
LCK	NVP-ADW742	1,0E-07	6,3E-08	1,6E-07	1,6E-07	≥ 2,3E+06	≥ 3,5E-01	
LCK	NVP-BGT226	≈ 1,7E-06	≈ 1,0E-06	7,8E-07	7,8E-07	≥ 4,5E+05	≥ 3,5E-01	
LCK	NVP-BHG712	5,7E-07	3,5E-07	n.e.	3,5E-07	2,0E+03	≤ 7,1E-04	24
LCK	NVP-BSK805	8,5E-08	5,2E-08	8,2E-08	8,2E-08	≈ 4,9E+06	≈ 3,5E-01	
LCK	NVP-TAE226	9,1E-07	5,5E-07	5,1E-07	5,1E-07	≥ 6,9E+05	≥ 3,5E-01	
LCK	OSI-930	7,0E-07	4,3E-07	1,1E-06	1,1E-06	≈ 2,4E+05	≈ 3,0E-01	
LCK	Pazopanib HCl	≈ 2,3E-07	≈ 1,4E-07	3,8E-07	3,8E-07	≥ 9,3E+05	≥ 3,5E-01	
LCK	PCI-32765 (Ibrutinib)	9,5E-10	5,7E-10	n.e.	5,7E-10	1,2E+06	≤ 6,9E-04	4
LCK	PD 0332991 (Palbociclib) HCl	7,6E-06	4,6E-06	3,1E-06	3,1E-06	≥ 1,1E+05	≥ 3,5E-01	
LCK	PD153035 HCl	8,4E-07	5,1E-07	1,2E-06	1,2E-06	≥ 3,0E+05	≥ 3,5E-01	
LCK	PD173074	3,6E-06	2,2E-06	2,1E-06	2,1E-06	≈ 2,1E+05	≈ 4,4E-01	
LCK	Pelitinib (EKB-569)	8,7E-08	5,3E-08	8,9E-08	8,9E-08	≥ 3,9E+06	≥ 3,5E-01	
LCK	PF-00562271	2,3E-07	1,4E-07	3,6E-07	3,6E-07	≥ 9,7E+05	≥ 3,5E-01	
LCK	PF-03814735	5,2E-08	3,2E-08	8,9E-08	8,9E-08	≈ 3,1E+06	≈ 2,9E-01	
LCK	PHA-665752	3,1E-07	1,9E-07	2,5E-07	2,5E-07	≈ 2,6E+06	≈ 6,9E-01	
LCK	PHA-680632	5,1E-07	3,1E-07	3,9E-07	3,9E-07	≈ 1,2E+06	≈ 4,2E-01	
LCK	PIK-75	6,6E-07	4,0E-07	6,3E-07	6,3E-07	≈ 1,7E+06	≈ 7,7E-01	2
LCK	PLX-4720	1,4E-07	8,7E-08	5,2E-08	5,2E-08	≈ 5,6E+06	≈ 2,6E-01	
LCK	Ponatinib (AP24534)	5,1E-10	3,1E-10	n.e.	3,1E-10	1,9E+06	≤ 5,9E-04	4
LCK	PP-121	2,7E-08	1,6E-08	6,5E-08	6,5E-08	≈ 1,5E+07	≈ 8,2E-01	
LCK	PP242	3,3E-07	2,0E-07	3,4E-07	3,4E-07	≈ 2,7E+05	≈ 9,2E-02	
LCK	Quercetin (Sophoretin)	2,1E-06	1,3E-06	2,3E-06	2,3E-06	≥ 1,5E+05	≥ 3,5E-01	
LCK	Quizartinib (AC220)	1,4E-05	8,7E-06	1,4E-05	1,4E-05	≥ 2,4E+04	≥ 3,5E-01	
LCK	R406	6,1E-08	3,7E-08	1,4E-07	9,3E-08	5,0E+06	7,1E-01	12
LCK	R788 (Fostamatinib) - prodrug	5,3E-06	3,2E-06	3,1E-06	3,1E-06	≥ 1,8E+05	≥ 3,5E-01	
LCK	Ruxolitinib (INCB018424)	2,5E-06	1,5E-06	5,3E-06	5,3E-06	≥ 6,6E+04	≥ 3,5E-01	
LCK	Saracatinib (AZD0530)	3,1E-09	1,9E-09	8,3E-10	8,3E-10	8,2E+06	6,7E-03	
LCK	SB 202190	3,1E-06	1,9E-06	2,8E-06	2,8E-06	≈ 4,3E+04	≈ 1,2E-01	
LCK	SB 203580	3,2E-06	2,0E-06	2,6E-06	2,6E-06	≥ 1,3E+05	≥ 3,5E-01	
LCK	SB590885	4,7E-06	2,8E-06	3,8E-06	3,8E-06	≥ 9,1E+04	≥ 3,5E-01	
LCK	Semaxanib (SU5416)	1,4E-06	8,3E-07	1,7E-06	1,7E-06	≥ 2,1E+05	≥ 3,5E-01	
LCK	SNS-314	≈ 1,3E-06	≈ 7,8E-07	1,5E-06	1,5E-06	≥ 2,3E+05	≥ 3,5E-01	1
LCK	SP600125	≈ 1,3E-05	≈ 7,7E-06	3,2E-06	3,2E-06	≥ 1,1E+05	≥ 3,5E-01	
LCK	Staurosporine	4,3E-09	2,6E-09	2,3E-09	2,3E-09	1,6E+07	3,7E-02	
LCK	SU11274	6,0E-08	3,6E-08	1,8E-07	1,8E-07	n.e.	n.e.	2
LCK	Sunitinib Malate (Sutent)	2,6E-08	1,6E-08	2,7E-08	2,7E-08	≥ 1,3E+07	≥ 3,5E-01	
LCK	TAE684 (NVP-TAE684)	2,5E-07	1,5E-07	≈ 8,6E-08	1,5E-07	≈ 1,4E+07	≈ 3,8E-01	
LCK	TAK-285	4,3E-07	2,6E-07	3,1E-07	3,1E-07	≥ 1,1E+06	≥ 3,5E-01	
LCK	TAK-901	1,4E-09	8,7E-10	5,6E-09	8,7E-10	8,8E+06	4,9E-02	
LCK	Tandutinib (MLN518)	3,0E-06	1,8E-06	4,8E-06	4,8E-06	≥ 7,4E+04	≥ 3,5E-01	
LCK	TG100-115	1,9E-05	1,2E-05	6,2E-06	6,2E-06	≥ 5,7E+04	≥ 3,5E-01	
LCK	TG101209	6,1E-08	3,7E-08	4,4E-08	4,4E-08	≈ 1,2E+07	≈ 4,3E-01	
LCK	TG101348 (SAR302503)	1,9E-07	1,1E-07	9,9E-08	9,9E-08	≥ 3,5E+06	≥ 3,5E-01	
LCK	Tie2 kinase inhibitor	4,1E-06	2,5E-06	4,1E-06	4,1E-06	≥ 8,6E+04	≥ 3,5E-01	
LCK	Tivozanib (AV-951)	1,7E-08	1,0E-08	1,3E-08	1,3E-08	5,1E+06	6,6E-02	
LCK	Tofacitinib (CP-690550 - Tasocitinib)	≥ 2,0E-05		7,4E-06	7,4E-06	≈ 2,9E+04	≈ 1,5E-01	
LCK	Torin 2	≥ 2,0E-05		6,0E-06	6,0E-06	≥ 5,8E+04	≥ 3,5E-01	
LCK	TPCA-1	1,4E-06	8,7E-07	6,1E-07	6,1E-07	≥ 5,8E+05	≥ 3,5E-01	
LCK	TSU-68 (SU6668)	3,6E-06	2,2E-06	2,8E-06	2,8E-06	≥ 1,2E+05	≥ 3,5E-01	
LCK	TWS119	2,1E-07	1,3E-07	3,4E-07	3,4E-07	≥ 1,0E+06	≥ 3,5E-01	
LCK	Vandetanib (Zactima)	7,8E-09	4,7E-09	1,3E-08	1,3E-08	≈ 1,6E+07	≈ 1,9E-01	
LCK	Vemurafenib (PLX4032)	9,6E-08	5,8E-08	9,8E-08	9,8E-08	9,9E+05	9,7E-02	12
LCK	VX-680 (MK-0457 - Tozasertib)	4,9E-08	3,0E-08	1,2E-07	1,2E-07	≥ 3,0E+06	≥ 3,5E-01	
LCK	WHI-P154	1,5E-07	9,1E-08	2,2E-07	2,2E-07	≥ 1,6E+06	≥ 3,5E-01	
LCK	WZ3146	7,6E-07	4,6E-07	6,7E-07	6,7E-07	≈ 1,1E+06	≈ 6,7E-01	
LCK	WZ4002	≥ 2,0E-05		1,6E-05	1,6E-05	≥ 2,2E+04	≥ 3,5E-01	
LCK	WZ8040	9,7E-07	5,9E-07	1,5E-06	1,5E-06	≥ 2,4E+05	≥ 3,5E-01	
LCK	XL-184 (Cabozantinib)	2,9E-08	1,8E-08	1,6E-08	1,6E-08	2,5E+06	4,0E-02	
LCK	ZM-447439	1,3E-08	7,6E-09	1,9E-08	1,9E-08	≥ 1,8E+07	≥ 3,5E-01	
LYNa	A-674563	2,0E-05	1,2E-05	1,6E-05	1,6E-05	≥ 2,2E+04	≥ 3,5E-01	
LYNa	AEE788 (NVP-AEE788)	2,0E-07	1,2E-07	1,2E-07	1,2E-07	≥ 3,0E+06	≥ 3,5E-01	
LYNa	Afatinib (BIBW2992)	1,4E-06	8,5E-07	6,9E-07	6,9E-07	≈ 7,9E+05	≈ 5,4E-01	
LYNa	AG-1024	5,4E-06	3,3E-06	1,4E-06	1,4E-06	≥ 2,5E+05	≥ 3,5E-01	
LYNa	AG-1478 (Tyrosphostin AG-1478)	2,8E-07	1,7E-07	2,7E-07	2,7E-07	≥ 1,3E+06	≥ 3,5E-01	
LYNa	AMG 900	4,3E-06	2,6E-06	1,5E-06	1,5E-06	4,8E+05	7,2E-01	
LYNa	AMG458	9,0E-07	5,4E-07	7,1E-07	7,1E-07	2,5E+05	1,7E-01	
LYNa	Apatinib (YN968D1)	4,9E-07	2,9E-07	3,4E-07	3,4E-07	7,1E+04	2,4E-02	2
LYNa	ARRY334543	6,5E-07	3,9E-07	3,7E-07	3,7E-07	n.e.	n.e.	2
LYNa	Arry-380	≥ 2,0E-05		1,3E-05	1,3E-05	≥ 2,7E+04	≥ 3,5E-01	
LYNa	AT9283	1,4E-07	8,7E-08	5,9E-08	5,9E-08	≥ 5,9E+06	≥ 3,5E-01	
LYNa	Aurora A Inhibitor I	≥ 2,0E-05		2,2E-06	2,2E-06	≥ 1,6E+05	≥ 3,5E-01	
LYNa	Axitinib	6,9E-07	4,1E-07	4,2E-07	4,2E-07	≥ 8,4E+05	≥ 3,5E-01	
LYNa	AZ 960	1,8E-07	1,1E-07	1,2E-07	1,2E-07	≥ 2,9E+06	≥ 3,5E-01	
LYNa	AZ628	9,7E-08	5,8E-08	5,6E-08	5,6E-08	2,1E+05	1,2E-02	2
LYNa	AZD4547	1,1E-06	6,7E-07	3,0E-07	3,0E-07	≥ 1,2E+06	≥ 3,5E-01	
LYNa	AZD5438	1,0E-06	6,0E-07	1,2E-06	1,2E-06	≥ 2,9E+05	≥ 3,5E-01	
LYNa	AZD7762	1,7E-08	1,0E-08	9,6E-09	9,6E-09	≥ 3,7E+07	≥ 3,5E-01	
LYNa	AZD8931	3,7E-08	2,2E-08	2,1E-08	2,1E-08	n.e.	n.e.	2

kinase	Compound	IC ₅₀ [M] ePCA	K _D eq [M] ePCA *	K _D kin [M] kPCA	K _D [M] PCA **	k _{on} [M ⁻¹ s ⁻¹] kPCA	k _{off} [s ⁻¹] kPCA	comment
LYNa	Barasertib (AZD1152-HQPA)	9,2E-07	5,5E-07	5,3E-07	5,3E-07	≥ 6,6E+05	≥ 3,5E-01	
LYNa	Baricitinib (LY3009104 - incb28050)	7,3E-06	4,4E-06	2,6E-06	2,6E-06	≥ 1,4E+05	≥ 3,5E-01	
LYNa	BEZ235 (NVP-BEZ235)	≥ 2,0E-05		3,0E-06	3,0E-06	≈ 2,8E+05	≈ 8,6E-01	
LYNa	BGJ398 (NVP-BGJ398)	6,7E-07	4,0E-07	3,6E-07	3,6E-07	≈ 1,2E+06	≈ 5,6E-01	
LYNa	BIBF1120 (Vargatef)	8,7E-08	5,2E-08	3,4E-08	3,4E-08	2,2E+07	7,7E-01	2
LYNa	BIRB 796 (Doramapimod)	≈ 3,1E-06	≈ 1,8E-06	1,5E-06	1,5E-06	2,0E+03	3,0E-03	
LYNa	BIX 02188	1,2E-06	7,3E-07	5,9E-07	5,9E-07	≥ 5,9E+05	≥ 3,5E-01	
LYNa	BIX 02189	2,1E-06	1,3E-06	8,6E-07	8,6E-07	≥ 4,1E+05	≥ 3,5E-01	
LYNa	BMS 777607	6,9E-07	4,1E-07	3,3E-07	3,3E-07	≥ 1,1E+06	≥ 3,5E-01	
LYNa	BMS 794833	6,5E-07	3,9E-07	5,1E-07	5,1E-07	≈ 1,5E+05	≈ 7,1E-02	
LYNa	BMS-265246	≥ 2,0E-05		1,2E-05	1,2E-05	≥ 2,9E+04	≥ 3,5E-01	
LYNa	BMS-599626 (AC480)	7,0E-06	4,2E-06	1,9E-06	1,9E-06	≥ 1,9E+05	≥ 3,5E-01	
LYNa	Bosutinib (SKI-606)	7,4E-10	4,4E-10	6,2E-10	6,2E-10	4,7E+06	2,8E-03	
LYNa	Brivanib (BMS-540215)	2,6E-06	1,6E-06	1,3E-06	1,3E-06	≥ 2,7E+05	≥ 3,5E-01	
LYNa	Brivanib alaninate (BMS-582664) - prodrug	≥ 2,0E-05		1,2E-06	1,2E-06	≥ 2,9E+05	≥ 3,5E-01	
LYNa	BX-795	1,5E-06	9,0E-07	1,1E-06	1,1E-06	≥ 3,3E+05	≥ 3,5E-01	
LYNa	BX-912	5,1E-07	3,1E-07	5,9E-07	5,9E-07	≥ 5,9E+05	≥ 3,5E-01	
LYNa	CCT128930	≥ 2,0E-05		1,3E-05	1,3E-05	≥ 2,8E+04	≥ 3,5E-01	
LYNa	CCT129202	≥ 2,0E-05		1,2E-05	1,2E-05	n.e.	n.e.	
LYNa	CCT137690	1,1E-06	6,8E-07	4,3E-06	6,8E-07	n.e.	n.e.	12
LYNa	Cediranib (AZD2171)	9,3E-07	5,6E-07	1,1E-07	5,6E-07	n.e.	n.e.	
LYNa	CEP33779	6,6E-07	4,0E-07	7,1E-07	7,1E-07	≥ 4,9E+05	≥ 3,5E-01	
LYNa	CH5424802	4,6E-06	2,8E-06	1,5E-07	2,8E-06	n.e.	n.e.	2
LYNa	CHIR-124	1,1E-07	6,3E-08	2,2E-07	2,2E-07	≥ 1,6E+06	≥ 3,5E-01	
LYNa	CI-1033 (Canertinib)	1,1E-07	6,8E-08	9,6E-08	9,6E-08	≥ 3,6E+06	≥ 3,5E-01	
LYNa	CP 673451	2,3E-07	1,4E-07	1,2E-07	1,2E-07	≥ 3,0E+06	≥ 3,5E-01	
LYNa	CP-724714	1,6E-05	9,3E-06	5,9E-06	5,9E-06	≥ 5,9E+04	≥ 3,5E-01	
LYNa	Crenolanib (CP-868596)	3,5E-07	2,1E-07	1,8E-07	1,8E-07	1,3E+06	2,2E-01	
LYNa	Crizotinib (PF-02341066)	1,2E-06	7,1E-07	2,1E-06	2,1E-06	n.e.	n.e.	2
LYNa	CX-4945 (Silmisertib)	4,4E-06	2,6E-06	1,3E-06	1,3E-06	≥ 2,6E+05	≥ 3,5E-01	
LYNa	CYC116	3,0E-07	1,8E-07	2,5E-07	2,5E-07	≥ 1,4E+06	≥ 3,5E-01	
LYNa	Cyt387	1,8E-06	1,1E-06	8,0E-07	8,0E-07	≥ 4,4E+05	≥ 3,5E-01	
LYNa	Dabrafenib (GSK2118436)	6,4E-07	3,9E-07	1,1E-07	1,1E-07	1,1E+06	1,3E-01	
LYNa	Dacomitinib (PF299804 - PF-00299804)	2,6E-07	1,5E-07	3,0E-07	3,0E-07	≥ 1,2E+06	≥ 3,5E-01	
LYNa	Danuserib (PHA-739358)	2,6E-07	1,6E-07	3,6E-07	3,6E-07	5,9E+04	2,1E-02	
LYNa	Dasatinib (BMS-354825)	1,6E-10	9,6E-11	≤ 2,9E-11	≤ 2,9E-11	8,6E+06	2,5E-04	
LYNa	DCC-2036 (Rebastinib)	5,6E-09	3,4E-09	n.e.	3,4E-09	5,5E+04	≤ 1,9E-04	4
LYNa	Desmethyl Erlotinib (CP-473420)	1,8E-07	1,1E-07	1,0E-07	1,0E-07	≈ 3,7E+06	≈ 3,5E-01	
LYNa	Dovitinib (TKI-258)	9,0E-08	5,4E-08	2,5E-08	2,5E-08	≥ 1,5E+07	≥ 3,5E-01	
LYNa	E7080 (Lenvatinib)	3,1E-07	1,9E-07	2,5E-07	2,5E-07	≈ 1,0E+06	≈ 2,4E-01	
LYNa	ENMD-2076	2,0E-07	1,2E-07	9,3E-08	9,3E-08	≥ 3,8E+06	≥ 3,5E-01	
LYNa	Erlotinib HCl	8,3E-07	5,0E-07	4,3E-07	4,3E-07	≥ 8,1E+05	≥ 3,5E-01	
LYNa	Flavopiridol HCl	4,8E-06	2,9E-06	3,1E-06	3,1E-06	≥ 1,1E+05	≥ 3,5E-01	
LYNa	Foretinib (GSK1363089 - XL880)	3,0E-09	1,8E-09	4,7E-09	4,7E-09	1,1E+06	5,1E-03	
LYNa	GDC-0980 (RG7422)	1,0E-06	6,0E-07	8,3E-07	8,3E-07	≥ 4,2E+05	≥ 3,5E-01	
LYNa	Gefitinib (Iressa)	5,6E-07	3,4E-07	3,3E-07	3,3E-07	≥ 1,1E+06	≥ 3,5E-01	
LYNa	Golvatinib (E7050)	3,4E-07	2,0E-07	1,9E-07	1,9E-07	≈ 2,4E+06	≈ 4,2E-01	
LYNa	GSK1070916	1,5E-06	8,8E-07	8,2E-07	8,2E-07	≈ 5,4E+05	≈ 5,0E-01	
LYNa	Hesperadin	1,0E-08	6,0E-09	3,5E-09	3,5E-09	1,2E+07	4,1E-02	
LYNa	Imatinib (Gleevec)	4,3E-07	2,6E-07	7,3E-07	7,3E-07	8,9E+04	6,6E-02	
LYNa	INK 128 (MLN0128)	1,4E-06	8,4E-07	7,7E-07	7,7E-07	≥ 4,6E+05	≥ 3,5E-01	
LYNa	JNJ-7706621	1,0E-06	6,2E-07	4,6E-07	4,6E-07	≥ 7,6E+05	≥ 3,5E-01	
LYNa	Ki8751	3,7E-08	2,2E-08	2,9E-08	2,9E-08	8,7E+06	2,5E-01	2
LYNa	KRN 633	3,7E-06	2,2E-06	1,7E-06	1,7E-06	4,1E+05	6,9E-01	
LYNa	KW 2449	2,5E-06	1,5E-06	6,8E-06	6,8E-06	≥ 5,1E+04	≥ 3,5E-01	
LYNa	Lapatinib Ditosylate (Tykerb)	≥ 2,0E-05		4,9E-06	4,9E-06	≥ 7,2E+04	≥ 3,5E-01	
LYNa	LDN193189	5,4E-07	3,2E-07	5,7E-07	5,7E-07	≥ 6,1E+05	≥ 3,5E-01	
LYNa	Linifanib (ABT-869)	≥ 2,0E-05		2,0E-06	2,0E-06	≥ 1,7E+05	≥ 3,5E-01	
LYNa	Linsitinib (OSI-906)	≈ 7,2E-06	≈ 4,3E-06	2,4E-06	2,4E-06	≥ 1,5E+05	≥ 3,5E-01	
LYNa	LY2784544	2,3E-07	1,4E-07	6,3E-08	6,3E-08	3,2E+06	2,0E-01	
LYNa	Masitinib (AB1010)	1,6E-07	9,5E-08	7,7E-08	7,7E-08	1,9E+05	1,5E-02	
LYNa	MGCD-265	9,1E-09	5,5E-09	8,8E-09	8,8E-09	8,6E+05	7,3E-03	
LYNa	Milciclib (PHA-848125)	1,3E-07	8,1E-08	6,0E-08	6,0E-08	3,0E+06	1,8E-01	
LYNa	MK-2461	≈ 8,3E-06	≈ 5,0E-06	3,8E-06	3,8E-06	≥ 9,1E+04	≥ 3,5E-01	
LYNa	MK-5108 (VX-689)	4,2E-07	2,6E-07	4,3E-07	4,3E-07	≥ 8,2E+05	≥ 3,5E-01	
LYNa	MLN8054	1,1E-06	6,3E-07	6,6E-07	6,6E-07	≥ 5,3E+05	≥ 3,5E-01	1
LYNa	MLN8237 (Alisertib)	2,6E-07	1,5E-07	1,8E-07	1,8E-07	≈ 6,1E+06	≈ 1,1E+00	
LYNa	Motesanib Diphosphate (AMG-706)	2,7E-06	1,6E-06	7,8E-07	7,8E-07	≈ 1,1E+05	≈ 8,4E-02	
LYNa	Neratinib (HKI-272)	2,7E-07	1,6E-07	7,7E-08	7,7E-08	6,1E+06	3,9E-01	2
LYNa	Nilotinib (AMN-107)	8,3E-08	5,0E-08	2,5E-07	2,5E-07	1,5E+04	3,8E-03	2
LYNa	NVP-ADW742	2,0E-07	1,2E-07	1,3E-07	1,3E-07	≥ 2,6E+06	≥ 3,5E-01	
LYNa	NVP-BGT226	5,5E-06	3,3E-06	1,4E-06	1,4E-06	≥ 2,6E+05	≥ 3,5E-01	
LYNa	NVP-BHG712	≈ 1,9E-07	≈ 1,2E-07	1,6E-07	1,6E-07	1,3E+04	2,2E-03	2
LYNa	NVP-BSK805	6,4E-07	3,9E-07	3,5E-07	3,5E-07	≥ 1,0E+06	≥ 3,5E-01	
LYNa	NVP-TAE226	1,1E-06	6,7E-07	7,6E-07	7,6E-07	≥ 4,6E+05	≥ 3,5E-01	
LYNa	OSI-930	9,9E-08	6,0E-08	1,3E-07	1,3E-07	1,5E+05	2,0E-02	
LYNa	Pazopanib HCl	1,6E-07	9,6E-08	1,9E-07	1,9E-07	≥ 1,9E+06	≥ 3,5E-01	
LYNa	PCI-32765 (Ibrutinib)	4,8E-09	2,9E-09	7,1E-09	7,1E-09	2,1E+06	1,5E-02	
LYNa	PD 0332991 (Palbociclib) HCl	≥ 2,0E-05		1,5E-05	1,5E-05	≥ 2,3E+04	≥ 3,5E-01	

kinase	Compound	IC ₅₀ [M] ePCA	K _D eq [M] ePCA *	K _D kin [M] kPCA	K _D [M] PCA **	k _{on} [M ⁻¹ s ⁻¹] kPCA	k _{off} [s ⁻¹] kPCA	comment
LYNa	PD153035 HCl	2,5E-07	1,5E-07	1,7E-07	1,7E-07	≥ 2,1E+06	≥ 3,5E-01	
LYNa	PD173074	5,5E-06	3,3E-06	2,6E-06	2,6E-06	≥ 1,3E+05	≥ 3,5E-01	
LYNa	Pelitinib (EKB-569)	6,4E-08	3,8E-08	7,4E-08	7,4E-08	≥ 3,2E+06	≥ 2,4E-01	
LYNa	PF-00562271	4,4E-07	2,6E-07	3,8E-07	3,8E-07	≥ 9,1E+05	≥ 3,5E-01	
LYNa	PF-03814735	8,1E-08	4,9E-08	6,3E-08	6,3E-08	≥ 5,6E+06	≥ 3,5E-01	
LYNa	PHA-665752	2,1E-06	1,3E-06	7,1E-07	7,1E-07	≥ 4,9E+05	≥ 3,5E-01	
LYNa	PHA-680632	8,0E-07	4,8E-07	4,1E-07	4,1E-07	≥ 8,5E+05	≥ 3,5E-01	
LYNa	PIK-75	2,3E-07	1,4E-07	2,4E-07	2,4E-07	n.e.	n.e.	2
LYNa	PLX-4720	4,0E-07	2,4E-07	1,6E-07	1,6E-07	≥ 2,1E+06	≥ 3,5E-01	
LYNa	Ponatinib (AP24534)	3,0E-10	1,8E-10	n.e.	1,8E-10	≥ 2,4E+06	≥ 4,3E-04	4
LYNa	PP-121	6,9E-09	4,1E-09	1,1E-08	1,1E-08	≈ 1,9E+07	≈ 2,2E-01	
LYNa	PP242	5,3E-07	3,2E-07	1,7E-07	1,7E-07	≥ 2,0E+06	≥ 3,5E-01	
LYNa	Quercetin (Sophoretin)	3,0E-06	1,8E-06	1,8E-06	1,8E-06	≥ 2,0E+05	≥ 3,5E-01	
LYNa	Quizartinib (AC220)	≥ 2,0E-05		1,1E-05	1,1E-05	n.e.	n.e.	
LYNa	R406	3,3E-08	2,0E-08	2,3E-08	2,3E-08	≈ 2,7E+07	≈ 5,9E-01	
LYNa	R788 (Fostamatinib) - prodrug	3,8E-06	2,3E-06	1,8E-06	1,8E-06	≥ 3,0E+05	≥ 3,5E-01	
LYNa	Raf265 derivative	1,8E-05	1,1E-05	1,8E-05	1,8E-05	≥ 2,0E+04	≥ 3,5E-01	
LYNa	Ruxolitinib (INCB018424)	≈ 1,0E-05	≈ 6,0E-06	6,4E-06	6,4E-06	≥ 5,5E+04	≥ 3,5E-01	
LYNa	SAR131675	2,0E-05	1,2E-05	9,1E-06	9,1E-06	≥ 3,8E+04	≥ 3,5E-01	
LYNa	Saracatinib (AZD0530)	1,1E-08	6,7E-09	5,1E-09	5,1E-09	3,9E+06	2,0E-02	
LYNa	SB 202190	6,2E-06	3,7E-06	3,1E-06	3,1E-06	≥ 1,1E+05	≥ 3,5E-01	
LYNa	SB 203580	6,9E-06	4,1E-06	3,7E-06	3,7E-06	≥ 9,3E+04	≥ 3,5E-01	
LYNa	SB590885	1,2E-05	6,9E-06	7,3E-06	7,3E-06	≥ 4,8E+04	≥ 3,5E-01	
LYNa	Semaxanib (SU5416)	4,2E-06	2,5E-06	1,1E-06	1,1E-06	3,9E+05	4,2E-01	
LYNa	SNS-314	3,4E-06	2,0E-06	2,3E-06	2,3E-06	≥ 1,5E+05	≥ 3,5E-01	
LYNa	Sotrastaurin (AEB071)	≥ 2,0E-05		6,9E-06	6,9E-06	≥ 5,0E+04	≥ 3,5E-01	
LYNa	SP600125	6,0E-06	3,6E-06	2,9E-06	2,9E-06	≥ 1,2E+05	≥ 3,5E-01	
LYNa	Staurosporine	2,4E-09	1,5E-09	1,1E-09	1,1E-09	2,8E+07	2,9E-02	
LYNa	SU11274	1,8E-07	1,1E-07	2,3E-07	2,3E-07	≥ 1,5E+06	≥ 3,5E-01	
LYNa	Sunitinib Malate (Sutent)	6,4E-08	3,9E-08	4,7E-08	4,7E-08	≥ 7,5E+06	≥ 3,5E-01	
LYNa	TAE684 (NVP-TAE684)	5,6E-07	3,3E-07	6,3E-08	3,3E-07	≥ 1,1E+07	≥ 5,9E-01	2
LYNa	TAK-285	7,9E-06	4,7E-06	2,6E-06	2,6E-06	≥ 1,3E+05	≥ 3,5E-01	
LYNa	TAK-901	5,0E-09	3,0E-09	9,8E-09	9,8E-09	5,0E+06	4,8E-02	
LYNa	Tandutinib (MLN518)	1,1E-05	6,7E-06	1,9E-05	1,9E-05	≥ 1,8E+04	≥ 3,5E-01	
LYNa	TG100-115	≥ 2,0E-05		8,7E-06	8,7E-06	≥ 4,0E+04	≥ 3,5E-01	
LYNa	TG101209	1,6E-07	9,5E-08	8,2E-08	8,2E-08	≥ 4,3E+06	≥ 3,5E-01	
LYNa	TG101348 (SAR302503)	6,3E-07	3,8E-07	3,4E-07	3,4E-07	≥ 1,0E+06	≥ 3,5E-01	
LYNa	Tie2 kinase inhibitor	5,6E-06	3,4E-06	3,5E-06	3,5E-06	≥ 1,0E+05	≥ 3,5E-01	
LYNa	Tivozanib (AV-951)	6,4E-09	3,9E-09	5,0E-09	5,0E-09	5,9E+06	2,9E-02	
LYNa	Tofacitinib (CP-690550 - Tasocitinib)	9,2E-06	5,5E-06	4,4E-06	4,4E-06	≥ 7,9E+04	≥ 3,5E-01	
LYNa	Torin 2	≥ 2,0E-05		4,6E-06	4,6E-06	≥ 7,6E+04	≥ 3,5E-01	
LYNa	TPCA-1	5,9E-07	3,5E-07	6,0E-07	6,0E-07	≥ 5,8E+05	≥ 3,5E-01	
LYNa	TSU-68 (SU6668)	1,8E-06	1,1E-06	7,0E-07	7,0E-07	≥ 5,0E+05	≥ 3,5E-01	
LYNa	TWS119	8,3E-08	5,0E-08	2,2E-08	2,2E-08	4,2E+07	9,1E-01	
LYNa	Vandetanib (Zactima)	2,8E-08	1,7E-08	4,1E-08	4,1E-08	≥ 8,6E+06	≥ 3,5E-01	
LYNa	Vatalanib 2HCl (PTK787)	≥ 2,0E-05		5,0E-06	5,0E-06	≥ 7,1E+04	≥ 3,5E-01	
LYNa	Vemurafenib (PLX4032)	3,8E-07	2,3E-07	2,5E-07	2,5E-07	≈ 4,1E+05	≈ 1,0E-01	
LYNa	VX-680 (MK-0457 - Tozasertib)	4,9E-07	3,0E-07	5,8E-07	5,8E-07	≥ 6,1E+05	≥ 3,5E-01	
LYNa	WHI-P154	2,8E-07	1,7E-07	1,3E-07	1,3E-07	≥ 2,8E+06	≥ 3,5E-01	
LYNa	WZ3146	2,0E-06	1,2E-06	1,5E-06	1,5E-06	≥ 2,3E+05	≥ 3,5E-01	
LYNa	WZ8040	2,5E-06	1,5E-06	1,9E-06	1,9E-06	≥ 1,8E+05	≥ 3,5E-01	
LYNa	XL-184 (Cabozantinib)	4,4E-08	2,6E-08	3,3E-08	3,3E-08	≈ 5,9E+06	≈ 2,0E-01	
LYNa	ZM 336372	6,5E-06	3,9E-06	6,8E-06	6,8E-06	≥ 5,1E+04	≥ 3,5E-01	
LYNa	ZM-447439	4,0E-08	2,4E-08	9,2E-08	9,2E-08	≥ 3,8E+06	≥ 3,5E-01	
MAP2K1	A-674563	3,0E-06	1,4E-07	3,6E-07	3,6E-07	≈ 3,5E+04	≈ 1,5E-02	
MAP2K1	AEE788 (NVP-AEE788)	≥ 2,0E-05		6,9E-06	6,9E-06	1,7E+03	1,2E-02	
MAP2K1	AG-1478 (Typhostin AG-1478)	≥ 2,0E-05		≈ 4,8E-06	≈ 4,8E-06	≥ 7,4E+04	≥ 3,5E-01	
MAP2K1	AMG 900	3,2E-07	1,5E-08	1,1E-07	1,5E-08	≈ 4,5E+05	≈ 4,3E-02	1
MAP2K1	Apatinib (YN968D1)	≥ 2,0E-05		6,1E-06	6,1E-06	1,3E+03	8,3E-03	
MAP2K1	AS-252424	≥ 2,0E-05		2,6E-06	2,6E-06	≈ 6,4E+03	≈ 1,9E-02	
MAP2K1	AS-605240	≥ 2,0E-05		4,2E-06	4,2E-06	2,5E+03	1,1E-02	
MAP2K1	AS703026 (pimasertib)	≥ 2,0E-05		3,3E-06	3,3E-06	2,8E+03	9,4E-03	
MAP2K1	AT7867	≥ 2,0E-05		5,7E-06	5,7E-06	2,5E+03	1,5E-02	
MAP2K1	AT9283	6,6E-07	3,1E-08	1,1E-07	1,1E-07	3,2E+05	3,4E-02	
MAP2K1	Axitinib	≥ 2,0E-05		3,9E-06	3,9E-06	≥ 9,0E+04	≥ 3,5E-01	
MAP2K1	AZ 960	1,7E-05	8,2E-07	2,7E-06	2,7E-06	4,2E+03	≈ 1,2E-02	
MAP2K1	AZD4547	1,9E-05	9,1E-07	3,4E-06	3,4E-06	4,3E+03	1,5E-02	
MAP2K1	AZD5438	1,4E-06	6,6E-08	3,4E-07	6,6E-08	≈ 4,5E+04	≈ 1,6E-02	
MAP2K1	AZD7762	5,1E-08	2,4E-09	9,4E-09	9,4E-09	4,3E+06	4,1E-02	
MAP2K1	AZD8330	≥ 2,0E-05		2,7E-06	2,7E-06	2,2E+03	6,0E-03	
MAP2K1	Barasertib (AZD1152-HQPA)	≥ 2,0E-05		6,7E-06	6,7E-06	≥ 5,2E+04	≥ 3,5E-01	
MAP2K1	Baricitinib (LY3009104 - incb28050)	5,1E-06	2,4E-07	9,8E-07	9,8E-07	1,8E+04	1,8E-02	
MAP2K1	BEZ235 (NVP-BEZ235)	≥ 2,0E-05		2,4E-06	2,4E-06	≈ 1,0E+04	≈ 2,3E-02	
MAP2K1	BIBF1120 (Vargatef)	1,7E-06	7,9E-08	1,3E-07	1,3E-07	≈ 2,6E+05	≈ 3,1E-02	
MAP2K1	BIX 02188	≥ 2,0E-05		2,7E-06	2,7E-06	7,3E+03	1,9E-02	2
MAP2K1	BIX 02189	≈ 2,0E-05	≈ 9,4E-07	≈ 5,6E-06	≈ 3,3E-06	n.e.	n.e.	
MAP2K1	BMS 777607	1,8E-06	8,5E-08	2,4E-07	2,4E-07	6,4E+04	1,5E-02	
MAP2K1	BMS 794833	4,6E-06	2,1E-07	2,5E-07	2,5E-07	4,3E+04	1,0E-02	
MAP2K1	BMS-599626 (AC480)	≥ 2,0E-05		3,8E-06	3,8E-06	8,5E+03	3,0E-02	

kinase	Compound	IC ₅₀ [M] ePCA	K _D eq [M] ePCA *	K _D kin [M] kPCA	K _D [M] PCA **	k _{on} [M ⁻¹ s ⁻¹] kPCA	k _{off} [s ⁻¹] kPCA	comment
MAP2K1	Bosutinib (SKI-606)	3,3E-07	1,6E-08	2,2E-08	2,2E-08	≈ 6,4E+05	≈ 1,2E-02	
MAP2K1	BX-795	2,5E-07	1,2E-08	2,6E-08	2,6E-08	9,4E+05	2,5E-02	
MAP2K1	BX-912	5,4E-07	2,5E-08	8,6E-08	8,6E-08	3,7E+05	3,1E-02	
MAP2K1	CCT128930	2,7E-06	1,2E-07	2,5E-07	2,5E-07	≈ 5,9E+04	≈ 2,0E-02	
MAP2K1	CCT129202	≥ 2,0E-05		3,8E-06	3,8E-06	3,7E+03	1,4E-02	2
MAP2K1	CCT137690	1,3E-06	6,2E-08	9,1E-07	6,2E-08	n.e.	n.e.	
MAP2K1	Cediranib (AZD2171)	≥ 2,0E-05		3,7E-06	3,7E-06	1,5E+04	5,4E-02	
MAP2K1	CEP33779	3,7E-06	1,7E-07	6,6E-07	6,6E-07	≈ 4,5E+04	≈ 3,0E-02	
MAP2K1	CH5424802	≥ 2,0E-05		1,1E-05	1,1E-05	≈ 8,9E+03	≈ 1,0E-01	
MAP2K1	CHIR-124	≤ 1,2E-09	≤ 5,6E-11	n.e.	≤ 5,6E-11	2,1E+06	≤ 1,2E-04	4
MAP2K1	CI-1033 (Canertinib)	≥ 2,0E-05		4,0E-06	4,0E-06	≈ 2,5E+04	8,5E-02	
MAP2K1	CI-1040 (PD184352)	≥ 2,0E-05		8,9E-06	8,9E-06	≈ 2,1E+03	≈ 2,0E-02	
MAP2K1	CP 673451	2,3E-07	1,1E-08	n.e.	1,1E-08	5,3E+05	≤ 5,6E-03	4
MAP2K1	Crenolanib (CP-868596)	7,7E-07	3,6E-08	1,1E-07	1,1E-07	≈ 3,8E+05	≈ 4,6E-02	
MAP2K1	Crizotinib (PF-02341066)	≥ 2,0E-05		8,2E-06	8,2E-06	≈ 5,8E+03	≈ 4,7E-02	2
MAP2K1	CX-4945 (Silmisertib)	2,2E-06	1,0E-07	3,9E-07	3,9E-07	5,8E+04	2,2E-02	
MAP2K1	CYC116	3,1E-06	1,5E-07	4,9E-07	4,9E-07	1,8E+05	8,6E-02	
MAP2K1	Cyt387	≥ 2,0E-05		1,2E-06	1,2E-06	1,6E+04	1,8E-02	
MAP2K1	Dabrafenib (GSK2118436)	1,9E-05	9,1E-07	3,1E-06	3,1E-06	6,3E+03	1,9E-02	
MAP2K1	Dasatinib (BMS-354825)	7,5E-06	3,5E-07	7,4E-07	7,4E-07	4,9E+04	2,7E-02	
MAP2K1	DCC-2036 (Rebastinib)	3,7E-06	1,7E-07	n.e.	1,7E-07	1,3E+04	≤ 4,3E-03	4
MAP2K1	Desmethyl Erlotinib (CP-473420)	≥ 2,0E-05		4,2E-06	4,2E-06	3,8E+03	1,5E-02	
MAP2K1	Dovitinib (TKI-258)	6,1E-07	2,8E-08	7,7E-08	7,7E-08	7,9E+05	5,7E-02	
MAP2K1	E7080 (Lenvatinib)	≥ 2,0E-05		3,6E-06	3,6E-06	3,0E+03	9,6E-03	
MAP2K1	ENMD-2076	1,7E-06	7,9E-08	3,5E-07	3,5E-07	5,9E+04	2,1E-02	
MAP2K1	Enzastaurin (LY317615)	≥ 2,0E-05		4,8E-06	4,8E-06	n.e.	n.e.	
MAP2K1	Erlotinib HCl	≥ 2,0E-05		7,6E-06	7,6E-06	≈ 1,5E+03	≈ 1,2E-02	
MAP2K1	Flavopiridol HCl	≥ 2,0E-05		3,3E-06	3,3E-06	≈ 2,5E+03	≈ 1,0E-02	
MAP2K1	Foretinib (GSK1363089 - XL880)	9,2E-08	4,3E-09	1,1E-08	1,1E-08	1,5E+05	1,8E-03	
MAP2K1	GDC-0941	≥ 2,0E-05		4,5E-06	4,5E-06	5,8E+03	2,4E-02	
MAP2K1	GDC-0980 (RG7422)	≥ 2,0E-05		3,6E-06	3,6E-06	≥ 9,8E+04	≥ 3,5E-01	
MAP2K1	Gefitinib (Iressa)	≥ 2,0E-05		1,2E-05	1,2E-05	≈ 9,5E+02	≈ 1,1E-02	
MAP2K1	Golvatinib (E7050)	1,3E-05	6,3E-07	1,0E-06	1,0E-06	1,9E+04	2,0E-02	2
MAP2K1	GSK1059615	4,1E-07	1,9E-08	≈ 4,8E-08	1,9E-08	4,2E+06	8,0E-02	3
MAP2K1	GSK1070916	≥ 2,0E-05		5,5E-06	5,5E-06	≈ 2,5E+03	≈ 1,5E-02	
MAP2K1	GSK1120212 (Trametinib)	7,5E-06	3,5E-07	3,1E-07	3,1E-07	≥ 1,1E+06	≥ 3,5E-01	
MAP2K1	GSK1838705A	≥ 2,0E-05		5,2E-06	5,2E-06	≈ 1,4E+03	≈ 9,0E-03	
MAP2K1	GSK690693	≥ 2,0E-05		9,1E-06	9,1E-06	8,2E+02	7,5E-03	
MAP2K1	Hesperadin	3,8E-09	1,8E-10	9,6E-11	9,6E-11	5,4E+06	5,2E-04	
MAP2K1	INK 128 (MLN0128)	5,8E-06	2,7E-07	8,4E-07	8,4E-07	7,8E+04	6,6E-02	
MAP2K1	JNJ-7706621	n.e.	n.e.	3,5E-07	3,5E-07	≈ 9,4E+04	≈ 3,0E-02	
MAP2K1	Ki8751	≥ 2,0E-05		7,0E-06	7,0E-06	1,5E+03	1,0E-02	2
MAP2K1	KU-60019	6,2E-06	2,9E-07	n.e.	2,9E-07	6,6E+03	≤ 1,9E-03	4
MAP2K1	KW 2449	2,3E-06	1,1E-07	n.e.	1,1E-07	5,6E+04	≤ 5,9E-03	4
MAP2K1	LDN193189	≥ 2,0E-05		1,1E-05	1,1E-05	≈ 1,8E+03	≈ 2,0E-02	
MAP2K1	Linifanib (ABT-869)	1,8E-05	8,2E-07	2,4E-06	2,4E-06	n.e.	n.e.	
MAP2K1	Linsitinib (OSI-906)	≥ 2,0E-05		2,0E-06	2,0E-06	1,8E+04	3,5E-02	
MAP2K1	LY2603618 (IC-83)	≥ 2,0E-05		4,4E-06	4,4E-06	≈ 9,8E+02	≈ 5,9E-03	
MAP2K1	LY2784544	≥ 2,0E-05		4,3E-06	4,3E-06	2,6E+03	1,1E-02	
MAP2K1	MGCD-265	≥ 2,0E-05		9,3E-07	9,3E-07	3,2E+04	3,0E-02	
MAP2K1	Milciclib (PHA-848125)	≥ 2,0E-05		2,7E-06	2,7E-06	≈ 4,6E+04	≈ 1,3E-01	
MAP2K1	MK-2461	≥ 2,0E-05		8,2E-06	8,2E-06	≥ 4,3E+04	≥ 3,5E-01	
MAP2K1	MK-5108 (VX-689)	4,3E-06	2,0E-07	1,4E-06	2,0E-07	≈ 2,2E+04	≈ 2,9E-02	
MAP2K1	MLN8054	≥ 2,0E-05		1,1E-05	1,1E-05	1,3E+03	1,4E-02	
MAP2K1	Neratinib (HKI-272)	2,8E-06	1,3E-07	1,8E-07	1,8E-07	7,6E+04	1,1E-02	
MAP2K1	NVP-ADW742	1,5E-05	7,2E-07	2,5E-06	2,5E-06	≈ 1,1E+04	≈ 2,6E-02	
MAP2K1	NVP-BGT226	≥ 2,0E-05		4,0E-06	4,0E-06	≥ 8,8E+04	≥ 3,5E-01	
MAP2K1	NVP-BSK805	7,1E-06	3,4E-07	8,2E-07	8,2E-07	≈ 1,4E+04	≈ 1,2E-02	
MAP2K1	NVP-TAE226	≥ 2,0E-05		1,2E-06	1,2E-06	2,4E+04	2,9E-02	
MAP2K1	OSI-027	1,9E-05	9,1E-07	2,6E-06	2,6E-06	≈ 5,5E+03	≈ 1,7E-02	
MAP2K1	Pazopanib HCl	≥ 2,0E-05		8,1E-06	8,1E-06	1,9E+03	1,5E-02	
MAP2K1	PCI-32765 (Ibrutinib)	5,0E-06	2,3E-07	≈ 5,9E-07	2,3E-07	5,9E+04	1,4E-02	23
MAP2K1	PD 0332991 (Palbociclib) HCl	≥ 2,0E-05		3,1E-06	3,1E-06	1,3E+04	3,9E-02	
MAP2K1	PD0325901	≥ 2,0E-05		5,5E-06	5,5E-06	3,0E+03	1,6E-02	
MAP2K1	PD153035 HCl	≥ 2,0E-05		3,1E-06	3,1E-06	7,0E+03	2,0E-02	
MAP2K1	PD318088	≥ 2,0E-05		3,0E-06	3,0E-06	≈ 2,2E+03	≈ 8,5E-03	
MAP2K1	Pelitinib (EKB-569)	7,8E-06	3,6E-07	8,4E-07	8,4E-07	≈ 2,5E+04	≈ 2,1E-02	
MAP2K1	PF-00562271	4,2E-06	2,0E-07	4,5E-07	4,5E-07	≈ 4,2E+04	≈ 2,3E-02	2
MAP2K1	PF-03814735	1,4E-07	6,8E-09	2,6E-08	2,6E-08	≥ 1,3E+07	≥ 3,5E-01	
MAP2K1	PHA-665752	5,1E-06	2,4E-07	4,5E-07	4,5E-07	3,9E+05	1,7E-01	
MAP2K1	PHA-680632	≥ 2,0E-05		4,5E-06	4,5E-06	5,4E+03	2,5E-02	
MAP2K1	PHA-767491	1,1E-05	5,1E-07	1,6E-06	1,6E-06	≈ 9,2E+03	≈ 1,5E-02	
MAP2K1	Piceatannol	≥ 2,0E-05		6,5E-06	6,5E-06	≥ 5,4E+04	≥ 3,5E-01	
MAP2K1	PIK-75	2,8E-08	1,3E-09	4,9E-09	4,9E-09	2,2E+06	1,1E-02	
MAP2K1	PLX-4720	5,2E-06	2,5E-07	6,1E-07	6,1E-07	3,4E+04	2,1E-02	
MAP2K1	Ponatinib (AP24534)	5,9E-06	2,8E-07	1,1E-06	1,1E-06	2,4E+04	2,7E-02	
MAP2K1	PP-121	3,8E-06	1,8E-07	6,9E-07	6,9E-07	≈ 7,5E+04	≈ 5,9E-02	
MAP2K1	PP242	2,8E-06	1,3E-07	2,9E-07	2,9E-07	6,0E+04	1,8E-02	
MAP2K1	Quercetin (Sophoretin)	≥ 2,0E-05		1,7E-06	1,7E-06	1,8E+04	3,0E-02	

kinase	Compound	IC ₅₀ [M] ePCA	K _D eq [M] ePCA *	K _D kin [M] kPCA	K _D [M] PCA **	k _{on} [M ⁻¹ s ⁻¹] kPCA	k _{off} [s ⁻¹] kPCA	comment
MAP2K1	R406	1,2E-06	5,6E-08	3,4E-07	9,7E-08	6,5E+04	1,7E-02	2
MAP2K1	R788 (Fostamatinib) - prodrug	1,8E-05	8,4E-07	6,2E-06	6,2E-06	≈ 6,7E+03	2,8E-02	
MAP2K1	Ruxolitinib (INCB018424)	1,0E-05	4,9E-07	2,3E-06	2,3E-06	3,5E+04	8,1E-02	
MAP2K1	SAR131675	≥ 2,0E-05		3,4E-06	3,4E-06	1,5E+03	4,9E-03	
MAP2K1	Saracatinib (AZD0530)	1,7E-05	8,2E-07	2,4E-06	2,4E-06	≈ 5,5E+03	≈ 1,3E-02	
MAP2K1	SB 202190	≥ 2,0E-05		1,0E-05	1,0E-05	1,7E+03	1,8E-02	
MAP2K1	SB 415286	1,1E-05	5,2E-07	≈ 2,7E-06	5,2E-07	n.e.	n.e.	
MAP2K1	Semaxanib (SU5416)	1,0E-06	4,8E-08	2,5E-07	4,8E-08	≈ 1,4E+05	≈ 1,9E-02	
MAP2K1	SNS-314	7,9E-06	3,7E-07	1,1E-06	1,1E-06	2,6E+04	2,8E-02	
MAP2K1	Sotrastaurin (AEB071)	1,7E-05	8,1E-07	1,1E-06	1,1E-06	8,4E+04	8,9E-02	
MAP2K1	SP600125	5,9E-06	2,8E-07	5,9E-07	5,9E-07	3,9E+04	2,4E-02	
MAP2K1	Staurosporine	1,7E-09	8,2E-11	n.e.	8,2E-11	6,3E+06	≤ 5,2E-04	4
MAP2K1	SU11274	2,2E-07	1,0E-08	n.e.	1,0E-08	3,3E+05	≤ 3,3E-03	4
MAP2K1	Sunitinib Malate (Sutent)	1,0E-07	4,8E-09	2,5E-08	4,8E-09	2,9E+06	7,2E-02	
MAP2K1	TAE684 (NVP-TAE684)	2,1E-06	9,8E-08	1,2E-07	1,2E-07	2,0E+05	2,5E-02	
MAP2K1	TAK-285	8,3E-06	3,9E-07	1,2E-06	1,2E-06	1,1E+04	1,3E-02	
MAP2K1	TAK-733	1,6E-05	7,6E-07	2,3E-06	2,3E-06	≈ 1,9E+04	≈ 4,9E-02	
MAP2K1	TAK-901	5,5E-07	2,6E-08	1,7E-07	2,6E-08	≈ 8,0E+04	≈ 1,7E-02	
MAP2K1	TG101209	9,9E-06	4,6E-07	1,6E-06	1,6E-06	≈ 1,1E+04	≈ 2,1E-02	
MAP2K1	TG101348 (SAR302503)	≥ 2,0E-05		3,7E-06	3,7E-06	≈ 3,9E+03	≈ 1,5E-02	
MAP2K1	Thiazovivin	1,4E-06	6,3E-08	8,1E-08	8,1E-08	2,6E+05	2,1E-02	
MAP2K1	Tivozanib (AV-951)	8,1E-07	3,8E-08	2,0E-07	3,8E-08	≈ 3,6E+05	≈ 7,7E-02	
MAP2K1	Torin 1	≥ 2,0E-05		5,3E-06	5,3E-06	1,3E+03	7,1E-03	
MAP2K1	Torin 2	≥ 2,0E-05		3,5E-06	3,5E-06	9,8E+03	3,4E-02	
MAP2K1	TPCA-1	6,3E-07	3,0E-08	2,1E-07	3,0E-08	≈ 3,8E+05	≈ 8,4E-02	
MAP2K1	TSU-68 (SU6668)	4,5E-07	2,1E-08	7,4E-08	7,4E-08	3,3E+05	2,4E-02	
MAP2K1	TW5119	1,3E-05	5,9E-07	1,8E-06	1,8E-06	9,1E+03	1,1E-02	
MAP2K1	U0126-EtOH	≥ 2,0E-05		6,0E-06	6,0E-06	2,0E+03	1,2E-02	
MAP2K1	Vandetanib (Zactima)	1,2E-05	5,6E-07	n.e.	5,6E-07	4,8E+03	≤ 9,3E-03	4
MAP2K1	Vemurafenib (PLX4032)	≥ 2,0E-05		6,3E-06	6,3E-06	7,5E+02	5,0E-03	
MAP2K1	VX-680 (MK-0457 - Tozasertib)	7,5E-07	3,5E-08	1,6E-07	1,6E-07	2,1E+05	3,5E-02	
MAP2K1	WHI-P154	2,0E-05	9,3E-07	3,3E-06	3,3E-06	7,0E+03	2,3E-02	
MAP2K1	WZ3146	≥ 2,0E-05		4,8E-06	4,8E-06	≈ 1,1E+04	≈ 4,8E-02	
MAP2K1	WZ8040	1,9E-05	8,8E-07	1,7E-06	1,7E-06	1,0E+04	1,7E-02	
MAP2K1	XL-184 (Cabozantinib)	5,1E-07	2,4E-08	8,0E-08	8,0E-08	1,7E+05	1,3E-02	
MAP2K1	XL765	n.e.		≥ 2,0E-05	≥ 2,0E-05			
MAP2K1	ZM-447439	3,5E-06	1,6E-07	6,8E-07	6,8E-07	3,5E+04	5,7E-03	
Met	A-674563	≥ 2,0E-05		7,9E-06	7,9E-06	1,5E+03	1,2E-02	
Met	AEE788 (NVP-AEE788)	≈ 1,2E-05	≈ 8,2E-06	8,0E-06	8,0E-06	1,5E+03	1,3E-02	
Met	Afatinib (BIBW2992)	5,0E-07	3,4E-07	3,7E-07	3,7E-07	8,4E+04	3,1E-02	2
Met	AG-1024	≥ 2,0E-05		8,5E-06	8,5E-06	≈ 3,2E+03	2,0E-02	
Met	AG-1478 (Tyrphostin AG-1478)	6,4E-06	4,4E-06	7,2E-06	7,2E-06	2,1E+03	1,5E-02	
Met	AMG 900	≈ 1,0E-05	≈ 7,0E-06	3,0E-06	3,0E-06	n.e.	n.e.	2
Met	AMG-208	≈ 7,3E-10	≈ 5,0E-10	2,1E-09	2,1E-09	4,3E+06	8,2E-03	2
Met	AMG458	9,1E-09	6,3E-09	3,2E-09	3,2E-09	4,9E+05	1,6E-03	
Met	AT7867	1,4E-05	9,5E-06	7,3E-06	7,3E-06	3,1E+03	2,3E-02	
Met	AT9283	3,3E-07	2,3E-07	1,5E-07	1,5E-07	≈ 2,3E+05	2,8E-02	
Met	Aurora A Inhibitor I	1,6E-06	1,1E-06	5,4E-06	5,4E-06	4,3E+03	2,3E-02	2
Met	Axitinib	≈ 2,0E-06	≈ 1,4E-06	1,7E-06	1,7E-06	3,1E+04	5,3E-02	
Met	AZ 960	7,1E-06	4,9E-06	3,8E-06	3,8E-06	≈ 1,0E+04	3,4E-02	
Met	AZD4547	≈ 3,3E-06	≈ 2,3E-06	5,0E-06	5,0E-06	6,1E+03	3,0E-02	2
Met	AZD5438	2,8E-06	1,9E-06	5,1E-06	5,1E-06	4,4E+03	2,3E-02	
Met	AZD7762	1,7E-06	1,2E-06	1,5E-06	1,5E-06	1,0E+04	1,5E-02	
Met	Barasertib (AZD1152-HQPA)	3,5E-06	2,4E-06	6,3E-06	6,3E-06	4,1E+03	2,4E-02	
Met	Baricitinib (LY3009104 - incb28050)	3,9E-06	2,7E-06	≈ 1,2E-05	2,7E-06	n.e.	n.e.	
Met	BEZ235 (NVP-BEZ235)	≥ 2,0E-05		4,6E-06	4,6E-06	4,9E+03	2,2E-02	
Met	BI 2536	2,6E-06	1,8E-06	3,4E-06	3,4E-06	9,4E+03	2,9E-02	
Met	BIBF1120 (Vargatef)	4,2E-06	2,9E-06	1,0E-06	1,0E-06	≈ 1,3E+05	≈ 1,4E-01	
Met	BIX 02188	≥ 1,1E-05		≥ 2,0E-05	≥ 7,4E-06			
Met	BMS 777607	1,8E-09	1,3E-09	1,1E-09	1,1E-09	3,3E+06	3,6E-03	
Met	BMS 794833	1,1E-09	7,3E-10	1,0E-09	1,0E-09	1,1E+06	1,2E-03	2
Met	BMS-265246	≥ 1,0E-05		≥ 2,0E-05	≥ 7,0E-06			
Met	Bosutinib (SKI-606)	1,8E-06	1,2E-06	1,0E-06	1,0E-06	3,3E+04	4,0E-02	3
Met	Brivanib (BMS-540215)	4,5E-07	3,1E-07	2,0E-06	3,1E-07	7,5E+03	1,5E-02	2
Met	Brivanib alaninate (BMS-582664) - prodrug	8,5E-06	5,8E-06	4,4E-06	4,4E-06	3,4E+03	1,5E-02	
Met	BX-795	2,7E-06	1,8E-06	1,9E-06	1,9E-06	≈ 2,1E+04	≈ 3,7E-02	
Met	BX-912	≈ 6,3E-07	≈ 4,4E-07	1,6E-06	1,6E-06	1,6E+04	2,5E-02	
Met	CCT137690	4,9E-07	3,4E-07	2,3E-06	3,4E-07	n.e.	n.e.	
Met	Cediranib (AZD2171)	≈ 5,5E-06	≈ 3,8E-06	3,8E-07	3,8E-07	6,4E+04	2,4E-02	
Met	CEP33779	1,7E-06	1,1E-06	1,5E-06	1,5E-06	≈ 1,8E+04	≈ 3,0E-02	
Met	CI-1033 (Canertinib)	5,2E-07	3,6E-07	2,6E-07	2,6E-07	1,3E+05	3,2E-02	
Met	CP 673451	≥ 2,0E-05		6,1E-06	6,1E-06	6,4E+02	3,9E-03	
Met	Crenolanib (CP-868596)	7,0E-06	4,8E-06	3,2E-06	3,2E-06	7,7E+03	2,4E-02	
Met	Crizotinib (PF-02341066)	7,0E-10	4,9E-10	1,1E-09	1,1E-09	7,0E+06	7,5E-03	
Met	CX-4945 (Silmatasertib)	≥ 2,0E-05		4,9E-06	4,9E-06	5,1E+03	2,4E-02	
Met	CYC116	5,6E-07	3,9E-07	2,5E-07	2,5E-07	7,9E+04	2,0E-02	
Met	Cyt387	2,3E-06	1,6E-06	1,2E-06	1,2E-06	1,9E+04	2,3E-02	
Met	Dabrafenib (GSK2118436)	1,5E-06	1,1E-06	2,3E-06	2,3E-06	2,5E+04	5,4E-02	
Met	Dacomitinib (PF299804 - PF-00299804)	6,3E-07	4,4E-07	1,4E-06	1,4E-06	1,6E+04	2,3E-02	

kinase	Compound	IC ₅₀ [M] ePCA	K _D eq [M] ePCA *	K _D kin [M] kPCA	K _D [M] PCA **	k _{on} [M ⁻¹ s ⁻¹] kPCA	k _{off} [s ⁻¹] kPCA	comment
Met	Dasatinib (BMS-354825)	1,4E-05	9,5E-06	≈ 1,0E-05	9,5E-06	≈ 1,6E+03	≈ 2,1E-02	
Met	DCC-2036 (Rebastinib)	≈ 3,5E-08	≈ 2,4E-08	2,8E-08	2,8E-08	8,4E+04	2,4E-03	
Met	Desmethyl Erlotinib (CP-473420)	2,7E-06	1,9E-06	1,4E-06	1,4E-06	2,2E+04	2,9E-02	
Met	Dinaciclib (SCH727965)	≥ 2,0E-05		6,9E-06	6,9E-06	1,0E+03	6,8E-03	
Met	Dovitinib (TKI-258)	9,1E-06	6,3E-06	5,1E-06	5,1E-06	3,1E+03	1,6E-02	
Met	E7080 (Lenvatinib)	5,0E-07	3,5E-07	3,6E-07	3,6E-07	≈ 8,7E+04	≈ 3,0E-02	
Met	ENMD-2076	5,5E-07	3,8E-07	7,0E-07	7,0E-07	4,3E+04	≈ 3,1E-02	
Met	Enzastaurin (LY317615)	≥ 2,0E-05		8,3E-06	8,3E-06	1,9E+03	1,6E-02	
Met	Erlotinib HCl	≈ 8,4E-07	≈ 5,8E-07	3,4E-06	3,4E-06	5,1E+03	1,7E-02	
Met	Foretinib (GSK1363089 - XL880)	2,5E-10	1,7E-10	n.e.	1,7E-10	2,3E+05	≤ 4,0E-05	4
Met	GDC-0980 (RG7422)	≥ 2,0E-05		7,3E-06	7,3E-06	2,7E+03	2,0E-02	
Met	Gefitinib (Iressa)	4,5E-06	3,1E-06	2,0E-06	2,0E-06	1,8E+04	3,5E-02	
Met	Golvatinib (E7050)	3,1E-10	2,2E-10	n.e.	2,2E-10	2,0E+06	≤ 4,3E-04	4
Met	GSK1070916	1,7E-07	1,1E-07	2,4E-07	2,4E-07	7,4E+04	1,8E-02	
Met	GSK1838705A	≥ 2,0E-05		6,6E-06	6,6E-06	8,2E+02	≈ 6,0E-03	
Met	Hesperadin	7,9E-07	5,4E-07	2,0E-07	2,0E-07	1,4E+05	2,8E-02	
Met	INCB28060	3,4E-10	2,3E-10	n.e.	2,3E-10	1,4E+07	≤ 3,3E-03	4
Met	INK 128 (MLN0128)	≥ 2,0E-05		7,0E-06	7,0E-06	≈ 1,1E+03	≈ 7,4E-03	
Met	JNJ-38877605	2,8E-09	1,9E-09	1,4E-09	1,4E-09	1,0E+07	1,4E-02	
Met	JNJ-7706621	8,5E-07	5,9E-07	2,6E-07	2,6E-07	1,4E+05	3,7E-02	1
Met	Ki8751	6,0E-08	4,2E-08	7,1E-07	4,2E-08	2,9E+04	2,1E-02	2
Met	KRN 633	≥ 2,0E-05		4,8E-06	4,8E-06	6,0E+03	3,0E-02	
Met	KW 2449	5,5E-07	3,8E-07	1,1E-06	1,1E-06	2,8E+04	3,0E-02	
Met	Lapatinib Ditosylate (Tykerb)	≥ 2,0E-05		9,6E-06	9,6E-06	8,1E+02	8,0E-03	
Met	LDN193189	6,3E-06	4,3E-06	4,9E-06	4,9E-06	2,1E+03	1,0E-02	
Met	Linifanib (ABT-869)	9,7E-07	6,7E-07	1,1E-06	1,1E-06	2,1E+04	2,2E-02	
Met	Linsitinib (OSI-906)	≈ 8,9E-06	≈ 6,2E-06	2,7E-06	2,7E-06	≈ 1,1E+04	2,5E-02	
Met	LY2228820	≈ 1,3E-05	≈ 9,3E-06	≈ 1,3E-05	≈ 1,1E-05	n.e.	n.e.	
Met	LY2784544	2,2E-07	1,5E-07	1,7E-07	1,7E-07	9,0E+04	1,4E-02	
Met	MGCD-265	2,8E-10	1,9E-10	n.e.	1,9E-10	2,7E+05	≤ 5,2E-05	4
Met	Milciclib (PHA-848125)	≈ 5,2E-06	≈ 3,6E-06	1,2E-06	1,2E-06	3,0E+04	3,4E-02	
Met	MK-2461	≈ 1,9E-08	≈ 1,3E-08	1,0E-08	1,0E-08	1,9E+06	1,9E-02	2
Met	MK-5108 (VX-689)	1,3E-07	8,6E-08	1,6E-07	1,6E-07	1,9E+05	3,1E-02	
Met	MLN8054	≥ 2,0E-05		4,8E-06	4,8E-06	≈ 8,9E+03	≈ 3,6E-02	
Met	MLN8237 (Alisertib)	≈ 1,1E-05	≈ 7,4E-06	≈ 5,8E-06	≈ 6,6E-06	n.e.	n.e.	1
Met	Neratinib (HKI-272)	≈ 4,0E-06	≈ 2,8E-06	3,2E-06	3,2E-06	4,7E+03	1,5E-02	
Met	NVP-ADW742	2,0E-06	1,4E-06	3,6E-06	3,6E-06	1,0E+04	3,6E-02	
Met	NVP-BGT226	≥ 2,0E-05		3,7E-06	3,7E-06	6,4E+03	2,3E-02	
Met	NVP-BSK805	5,4E-07	3,7E-07	2,8E-07	2,8E-07	1,0E+05	2,8E-02	
Met	NVP-BVU972	2,0E-09	1,4E-09	1,3E-09	1,3E-09	4,5E+06	5,7E-03	
Met	NVP-TAE226	≈ 1,5E-07	≈ 1,0E-07	5,8E-08	5,8E-08	3,7E+05	1,9E-02	2
Met	Pazopanib HCl	≥ 2,0E-05		5,9E-07	5,9E-07	7,0E+04	4,2E-02	
Met	PCI-32765 (Ibrutinib)	2,3E-06	1,6E-06	4,2E-06	4,2E-06	5,2E+03	2,1E-02	
Met	PD153035 HCl	≥ 2,0E-05		5,0E-06	5,0E-06	7,3E+03	3,4E-02	
Met	Pellitinib (EKB-569)	≈ 3,3E-06	≈ 2,3E-06	1,3E-06	1,3E-06	2,1E+04	2,9E-02	
Met	PF-00562271	3,4E-07	2,3E-07	1,7E-07	1,7E-07	1,8E+05	3,0E-02	
Met	PF-03814735	1,5E-08	1,1E-08	1,2E-08	1,2E-08	1,7E+06	1,9E-02	
Met	PF-04217903	≈ 1,5E-10	≈ 1,0E-10	n.e.	≈ 1,0E-10	7,8E+06	≤ 8,1E-04	4
Met	PF-05212384 (PKI-587)	≥ 2,0E-05		7,3E-06	7,3E-06	1,1E+03	8,2E-03	
Met	PHA-665752	1,5E-10	1,0E-10	2,3E-10	2,3E-10	6,8E+06	1,4E-03	
Met	PHA-680632	7,5E-06	5,2E-06	2,8E-06	2,8E-06	8,1E+03	2,2E-02	
Met	PHA-767491	≥ 2,0E-05		2,0E-06	2,0E-06	5,5E+03	1,1E-02	2
Met	PIK-75	5,1E-09	3,5E-09	2,3E-09	2,3E-09	7,6E+06	1,7E-02	
Met	Ponatinib (AP24534)	≈ 1,2E-06	≈ 8,0E-07	2,2E-06	2,2E-06	7,6E+03	1,7E-02	
Met	PP-121	1,2E-05	8,6E-06	7,9E-06	7,9E-06	2,0E+03	1,6E-02	
Met	PP242	2,2E-06	1,6E-06	4,7E-06	4,7E-06	9,1E+02	4,3E-03	
Met	R406	1,0E-06	7,0E-07	1,4E-06	4,8E-07	4,0E+04	3,8E-02	12
Met	R788 (Fostatinib) - prodrug	6,6E-06	4,5E-06	4,8E-06	4,8E-06	8,1E+03	3,6E-02	
Met	Saracatinib (AZD0530)	6,1E-06	4,2E-06	1,9E-06	1,9E-06	1,3E+04	2,4E-02	
Met	SB 202190	1,8E-06	1,2E-06	3,4E-06	3,4E-06	7,3E+03	2,5E-02	
Met	SB 203580	1,1E-05	7,7E-06	2,6E-06	2,6E-06	6,2E+03	1,6E-02	
Met	SB590885	3,4E-06	2,3E-06	5,4E-06	5,4E-06	4,9E+03	2,5E-02	
Met	Semaxanib (SU5416)	≥ 2,0E-05		4,9E-06	4,9E-06	3,8E+03	1,8E-02	
Met	SGX-523	≈ 6,6E-10	≈ 4,6E-10	1,6E-09	1,6E-09	7,7E+06	1,2E-02	
Met	SNS-314	6,2E-07	4,3E-07	5,4E-07	5,4E-07	7,7E+04	4,3E-02	
Met	Sotrastaurin (AEB071)	9,0E-06	6,2E-06	2,1E-06	2,1E-06	1,1E+04	2,1E-02	
Met	SP600125	≈ 3,5E-06	≈ 2,4E-06	3,3E-06	3,3E-06	9,9E+03	3,2E-02	
Met	Staurosporine	2,8E-08	1,9E-08	2,4E-08	2,4E-08	1,4E+06	2,9E-02	
Met	SU11274	1,5E-09	1,0E-09	4,6E-09	4,6E-09	2,5E+06	6,1E-03	2
Met	Sunitinib Malate (Sutent)	≈ 1,9E-06	≈ 1,3E-06	1,5E-06	1,5E-06	3,1E+04	4,4E-02	
Met	TAE684 (NVP-TAE684)	5,4E-07	3,7E-07	1,5E-07	1,5E-07	2,8E+05	4,4E-02	
Met	TAK-285	≈ 3,5E-06	≈ 2,4E-06	4,7E-06	4,7E-06	1,6E+03	7,3E-03	
Met	TAK-901	3,7E-07	2,5E-07	7,8E-07	7,8E-07	≈ 7,4E+04	≈ 5,3E-02	
Met	TG100-115	≈ 4,2E-06	≈ 2,9E-06	1,6E-06	1,6E-06	2,8E+03	4,3E-03	
Met	TG101209	≈ 4,0E-06	≈ 2,7E-06	1,5E-06	1,5E-06	4,4E+04	6,2E-02	
Met	TG101348 (SAR302503)	4,7E-06	3,2E-06	3,8E-06	3,8E-06	5,3E+03	2,0E-02	
Met	Tie2 kinase inhibitor	≥ 2,0E-05		2,2E-06	2,2E-06	7,6E+03	1,7E-02	
Met	Tivozanib (AV-951)	≈ 5,1E-08	≈ 3,5E-08	6,3E-08	6,3E-08	5,1E+05	3,4E-02	
Met	Torin 1	≥ 2,0E-05		5,4E-06	5,4E-06	3,7E+03	2,0E-02	

kinase	Compound	IC ₅₀ [M] ePCA	K _D eq [M] ePCA *	K _D kin [M] kPCA	K _D [M] PCA **	k _{on} [M ⁻¹ s ⁻¹] kPCA	k _{off} [s ⁻¹] kPCA	comment
Met	Torin 2	≥ 2,0E-05		4,0E-06	4,0E-06	≈ 8,5E+03	≈ 3,4E-02	
Met	TSU-68 (SU6668)	≥ 2,0E-05		2,0E-06	2,0E-06	1,1E+04	2,2E-02	
Met	TWS119	≈ 3,0E-06	≈ 2,1E-06	3,4E-06	3,4E-06	9,0E+03	3,0E-02	2
Met	U0126-EtOH	9,1E-06	6,3E-06	≥ 2,0E-05	≥ 6,3E-06			
Met	Vandetanib (Zactima)	1,5E-06	1,0E-06	2,7E-06	2,7E-06	7,7E+03	2,0E-02	
Met	Vatalanib 2HCl (PTK787)	1,1E-06	7,3E-07	≥ 2,0E-05	≥ 7,3E-07			
Met	VX-680 (MK-0457 - Tozasertib)	8,2E-07	5,7E-07	9,1E-07	9,1E-07	4,6E+04	4,4E-02	
Met	WP1130	≥ 2,0E-05		6,3E-06	6,3E-06	7,4E+02	4,7E-03	
Met	WZ3146	4,5E-07	3,1E-07	4,0E-07	4,0E-07	≈ 1,6E+05	≈ 5,1E-02	
Met	WZ4002	≈ 2,4E-06	≈ 1,7E-06	2,6E-06	2,6E-06	≈ 1,1E+04	≈ 2,0E-02	
Met	WZ8040	2,8E-07	1,9E-07	2,9E-07	2,9E-07	6,3E+04	1,7E-02	
Met	XL-184 (Cabozantinib)	3,9E-10	2,7E-10	n.e.	2,7E-10	9,6E+05	≤ 2,6E-04	4
Met	XL765	≥ 2,0E-05		6,0E-06	6,0E-06	≥ 5,8E+04	≥ 3,5E-01	
Met	ZM-447439	3,5E-07	2,4E-07	4,8E-07	4,8E-07	1,7E+05	7,7E-02	
MPS1	Arry-380	1,6E-05	5,3E-06	≥ 2,0E-05	≥ 5,3E-06			1
MPS1	AST-1306	3,1E-05	1,1E-05	≥ 2,0E-05	≥ 1,1E-05			1
MPS1	AT9283	2,5E-06	8,4E-07	n.e.	8,4E-07	1,5E+05	≤ 1,2E-01	14
MPS1	Aurora A Inhibitor I	1,1E-05	3,8E-06	≥ 2,0E-05	≥ 3,8E-06			1
MPS1	AZD5438	8,3E-07	2,8E-07	8,2E-07	8,2E-07	≈ 1,6E+05	≈ 1,2E-01	1
MPS1	AZD7762	2,8E-05	9,7E-06	≈ 3,1E-06	9,7E-06	≈ 3,6E+03	≈ 1,1E-02	
MPS1	Barasertib (AZD1152-HQPA)	2,3E-05	7,9E-06	n.e.	7,9E-06	8,9E+02	≤ 7,0E-03	14
MPS1	Baricitinib (LY3009104 - incb28050)	9,6E-06	3,9E-06	2,0E-06	2,0E-06	≈ 3,0E+04	≈ 6,1E-02	1
MPS1	BEZ235 (NVP-BEZ235)	≥ 2,0E-05		1,8E-06	1,8E-06	8,0E+03	1,4E-02	
MPS1	BI 2536	1,3E-05	4,6E-06	≥ 2,0E-05	≥ 4,6E-06			1
MPS1	BI6727 (Volasertib)	1,7E-05	5,6E-06	≥ 2,0E-05	≥ 5,6E-06			1
MPS1	BIBF1120 (Vargatef)	1,5E-06	5,0E-07	6,2E-07	6,2E-07	≈ 2,8E+05	≈ 1,8E-01	1
MPS1	BIRB 796 (Doramapimod)	4,4E-06	1,5E-06	1,3E-06	1,3E-06	≈ 1,2E+05	≈ 1,9E-01	1
MPS1	Bosutinib (SKI-606)	≥ 2,0E-05		n.e.	≥ 6,8E-06	n.e.	n.e.	
MPS1	BS-181 HCl	1,3E-05	4,5E-06	≈ 3,0E-06	4,5E-06	≥ 1,2E+05	≥ 3,5E-01	1
MPS1	BX-795	2,6E-07	9,0E-08	1,3E-07	1,3E-07	≥ 2,8E+06	≥ 3,5E-01	1
MPS1	BX-912	2,2E-06	7,4E-07	1,4E-06	1,4E-06	2,6E+04	3,7E-02	
MPS1	CCT137690	1,6E-05	5,4E-06	≥ 2,0E-05	≥ 5,4E-06			1
MPS1	CEP33779	6,6E-06	2,2E-06	≈ 4,5E-06	2,2E-06	≈ 1,4E+05	≈ 2,2E-01	1
MPS1	CH5424802	9,4E-07	3,2E-07	n.e.	3,2E-07	n.e.	n.e.	1
MPS1	CHIR-124	1,4E-05	4,7E-06	2,3E-06	2,3E-06	≈ 3,9E+03	≈ 6,2E-03	1
MPS1	Crenolanib (CP-868596)	≥ 2,0E-05		4,1E-06	4,1E-06	≈ 4,3E+03	1,5E-02	
MPS1	CYC116	1,1E-07	3,7E-08	5,2E-08	5,2E-08	1,3E+06	6,5E-02	1
MPS1	Cyt387	7,2E-07	2,5E-07	1,8E-07	1,8E-07	≈ 3,3E+05	≈ 5,0E-02	1
MPS1	Dabrafenib (GSK2118436)	3,5E-05	1,2E-05	n.e.	1,2E-05	n.e.	n.e.	1
MPS1	DCC-2036 (Rebastinib)	7,4E-07	2,5E-07	4,2E-07	4,2E-07	3,5E+04	1,5E-02	1
MPS1	Dinaciclib (SCH727965)	3,8E-05	1,3E-05	≥ 2,0E-05	≥ 1,3E-05			1
MPS1	Dovitinib (TKI-258)	1,2E-05	4,2E-06	2,5E-06	3,6E-06	2,0E+03	4,9E-03	1
MPS1	Foretinib (GSK1363089 - XL880)	3,9E-06	1,3E-06	2,7E-06	2,7E-06	≈ 3,5E+05	≈ 5,8E-01	1
MPS1	Gefitinib (Iressa)	≥ 2,0E-05		7,1E-06	7,1E-06	≥ 4,9E+04	≥ 3,5E-01	
MPS1	GSK1070916	≈ 4,1E-05	≈ 1,4E-05	n.e.	≈ 1,4E-05	n.e.	n.e.	1
MPS1	GSK1838705A	8,0E-07	2,7E-07	3,7E-07	3,7E-07	7,1E+05	1,9E-01	1
MPS1	GSK2126458	5,5E-06	1,9E-06	1,6E-06	1,6E-06	4,5E+04	7,1E-02	1
MPS1	Hesperadin	5,3E-07	1,8E-07	1,2E-07	1,2E-07	2,1E+05	2,6E-02	1
MPS1	INK 128 (MLN0128)	7,7E-06	2,6E-06	≈ 1,8E-06	2,6E-06	≈ 9,1E+03	≈ 1,6E-02	1
MPS1	JNJ-7706621	6,2E-07	2,1E-07	1,7E-07	1,7E-07	1,4E+05	3,0E-02	13
MPS1	KW 2449	5,1E-06	1,7E-06	1,8E-06	1,8E-06	≥ 1,9E+05	≥ 3,5E-01	
MPS1	LDN193189	3,1E-05	1,1E-05	≥ 2,0E-05	≥ 1,1E-05			1
MPS1	Linifanib (ABT-869)	3,6E-05	1,2E-05	6,3E-06	6,3E-06	≥ 5,6E+04	≥ 3,5E-01	1
MPS1	Linsitinib (OSI-906)	3,2E-05	1,1E-05	≈ 1,2E-06	1,1E-05	≈ 3,4E+03	≈ 6,5E-03	1
MPS1	Milciclib (PHA-848125)	6,5E-07	2,2E-07	1,5E-07	1,5E-07	5,1E+05	7,6E-02	1
MPS1	MK-2461	1,2E-06	3,9E-07	8,6E-07	8,6E-07	≥ 4,1E+05	≥ 3,5E-01	1
MPS1	NVP-ADW742	2,0E-05	6,8E-06	≥ 2,0E-05	≥ 6,8E-06			1
MPS1	NVP-BGT226	7,8E-06	2,7E-06	1,5E-06	1,5E-06	≈ 1,7E+05	2,5E-01	1
MPS1	NVP-BSK805	1,9E-05	6,5E-06	1,6E-06	1,6E-06	2,0E+04	≈ 3,3E-02	1
MPS1	NVP-TAE226	2,9E-08	9,8E-09	1,1E-08	1,1E-08	6,1E+06	6,1E-02	1
MPS1	Pazopanib HCl	3,2E-07	1,1E-07	7,8E-08	7,8E-08	≈ 1,2E+05	≈ 1,1E-02	1
MPS1	PCI-32765 (Ibrutinib)	9,7E-06	3,3E-06	3,6E-06	3,6E-06	1,9E+05	6,6E-01	1
MPS1	PD 0332991 (Palbociclib) HCl	3,7E-07	1,2E-07	2,0E-07	2,0E-07	4,3E+05	5,4E-02	13
MPS1	PF-00562271	1,3E-08	4,3E-09	≈ 6,8E-09	4,3E-09	≥ 5,1E+07	≥ 3,5E-01	1
MPS1	PF-03814735	8,5E-08	2,9E-08	5,9E-08	5,9E-08	≥ 5,9E+06	≥ 3,5E-01	1
MPS1	PHA-680632	9,8E-06	3,3E-06	1,7E-06	1,7E-06	3,3E+04	5,4E-02	1
MPS1	PIK-75	1,3E-06	4,5E-07	9,3E-07	9,3E-07	1,4E+05	1,3E-01	1
MPS1	PP-121	4,9E-06	1,7E-06	1,5E-06	1,5E-06	1,6E+04	2,6E-02	1
MPS1	PP242	8,4E-06	2,8E-06	2,0E-06	2,0E-06	≥ 1,8E+05	≥ 3,5E-01	1
MPS1	Quercetin (Sophoretin)	9,2E-06	3,1E-06	3,9E-06	3,9E-06	≥ 8,9E+04	≥ 3,5E-01	1
MPS1	Raf265 derivative	2,3E-05	7,8E-06	n.e.	7,8E-06	n.e.	n.e.	1
MPS1	Roscovitine (Seliciclib - CYC202)	8,0E-06	2,7E-06	3,0E-06	3,0E-06	≥ 1,2E+05	≥ 3,5E-01	1
MPS1	Ruxolitinib (INCB018424)	3,2E-06	1,1E-06	1,8E-06	1,8E-06	≥ 2,0E+05	≥ 3,5E-01	1
MPS1	SB 203580	2,7E-05	9,1E-06	≈ 6,1E-06	9,1E-06	≈ 6,8E+04	≈ 4,2E-01	1
MPS1	SB 431542	3,4E-05	1,1E-05	≈ 3,1E-06	1,1E-05	≈ 6,3E+02	≈ 2,0E-03	1
MPS1	SB590885	2,9E-05	1,0E-05	≥ 2,0E-05	≥ 1,0E-05			1
MPS1	Semaxanib (SU5416)	1,0E-05	3,5E-06	1,9E-06	1,9E-06	≥ 1,9E+05	≥ 3,5E-01	1
MPS1	SNS-314	1,3E-05	4,5E-06	1,4E-06	1,4E-06	2,0E+04	3,0E-02	1
MPS1	SP600125	8,5E-07	2,9E-07	2,3E-07	2,3E-07	1,3E+06	3,0E-01	1

kinase	Compound	IC ₅₀ [M] ePCA	K _D eq [M] ePCA *	K _D kin [M] kPCA	K _D [M] PCA **	k _{on} [M ⁻¹ s ⁻¹] kPCA	k _{off} [s ⁻¹] kPCA	comment
MPS1	Staurosporine	1,0E-07	3,4E-08	1,9E-08	1,9E-08	≈ 7,1E+06	≈ 8,0E-02	1
MPS1	Sunitinib Malate (Sutent)	3,3E-07	1,1E-07	1,4E-07	1,4E-07	1,2E+05	1,5E-02	1
MPS1	TAE684 (NVP-TAE684)	5,6E-07	1,9E-07	1,2E-07	1,2E-07	≈ 3,6E+06	≈ 4,4E-01	1
MPS1	TAK-901	4,9E-06	1,7E-06	2,1E-06	2,1E-06	1,9E+03	3,2E-03	1
MPS1	TG 100713	2,3E-05	7,6E-06	n.e.	7,6E-06	n.e.	n.e.	1
MPS1	TG101209	4,5E-07	1,5E-07	2,0E-07	2,0E-07	1,1E+06	1,7E-01	1
MPS1	TG101348 (SAR302503)	1,4E-06	4,6E-07	n.e.	4,6E-07	1,8E+05	≤ 8,3E-02	14
MPS1	Thiazovivin	3,7E-05	1,2E-05	≥ 2,0E-05	≥ 2,0E-05			1
MPS1	Tofacitinib (CP-690550 - Tasocitinib)	4,0E-05	1,4E-05	≥ 2,0E-05	≥ 1,4E-05			
MPS1	Torin 1	≥ 2,0E-05		3,6E-06	3,6E-06	≈ 4,6E+04	≈ 1,6E-01	
MPS1	Torin 2	2,5E-06	8,6E-07	1,1E-06	1,1E-06	≥ 3,3E+05	≥ 3,5E-01	1
MPS1	TPCA-1	2,3E-05	7,9E-06	3,8E-06	3,8E-06	≥ 9,2E+04	≥ 3,5E-01	1
MPS1	TSU-68 (SU6668)	1,3E-06	4,3E-07	5,1E-07	5,1E-07	≥ 6,8E+05	≥ 3,5E-01	1
MPS1	WHI-P154	1,8E-05	6,1E-06	≈ 2,0E-06	6,1E-06	≈ 2,3E+03	≈ 4,4E-03	1
MPS1	WZ3146	1,2E-06	4,1E-07	7,8E-07	7,8E-07	≈ 2,3E+05	≈ 1,1E-01	1
MPS1	WZ4002	3,4E-07	1,1E-07	1,9E-07	1,9E-07	4,1E+05	7,0E-02	1
MPS1	WZ8040	9,7E-07	3,3E-07	4,5E-07	4,5E-07	≈ 4,7E+05	≈ 1,9E-01	
MPS1	XL-184 (Cabozantinib)	9,1E-06	3,1E-06	2,1E-06	2,1E-06	≥ 1,7E+05	≥ 3,5E-01	1
MPS1	ZM-447439	1,6E-06	5,3E-07	2,0E-06	2,0E-06	≥ 1,7E+05	≥ 3,5E-01	1
p38alpha	AEE788 (NVP-AEE788)	5,0E-06	2,3E-06	1,7E-06	1,7E-06	5,9E+04	9,6E-02	
p38alpha	Afatinib (BIBW2992)	1,0E-06	4,5E-07	5,1E-07	5,1E-07	2,9E+05	1,5E-01	
p38alpha	AG-1478 (Typhostin AG-1478)	5,0E-06	2,3E-06	2,7E-06	2,7E-06	3,8E+04	1,0E-01	
p38alpha	AMG 900	1,5E-07	6,8E-08	1,3E-07	1,3E-07	3,9E+04	4,8E-03	1
p38alpha	Apatinib (YN968D1)	≥ 2,0E-05		3,2E-06	3,2E-06	≈ 4,5E+04	1,2E-01	
p38alpha	Axitinib	≥ 2,0E-05		1,1E-05	1,1E-05	1,0E+04	1,0E-01	
p38alpha	AZ628	2,5E-08	1,1E-08	9,1E-09	9,1E-09	1,3E+06	1,1E-02	
p38alpha	AZD8931	≈ 2,0E-06	≈ 9,1E-07	6,3E-07	6,3E-07	1,8E+05	1,1E-01	
p38alpha	BEZ235 (NVP-BEZ235)	≥ 2,0E-05		≈ 3,5E-05	≈ 3,5E-05	≈ 5,5E+03	≈ 1,0E-01	
p38alpha	BIBF1120 (Vargatef)	≥ 2,0E-05		3,5E-06	3,5E-06	4,4E+04	1,5E-01	
p38alpha	BIRB 796 (Doramapimod)	≈ 1,0E-08	≈ 4,5E-09	4,5E-09	4,5E-09	9,2E+04	4,0E-04	
p38alpha	BIX 02189	6,5E-06	2,9E-06	2,7E-06	2,7E-06	7,2E+04	2,0E-01	
p38alpha	BMS 777607	9,5E-06	4,3E-06	4,4E-06	4,4E-06	2,1E+04	9,0E-02	
p38alpha	BMS 794833	≈ 1,8E-06	≈ 8,2E-07	3,4E-07	3,4E-07	1,4E+05	4,2E-02	
p38alpha	Bosutinib (SKI-606)	3,0E-06	1,4E-06	1,9E-06	1,9E-06	4,2E+04	7,9E-02	
p38alpha	Brivanib alaninate (BMS-582664) - prodrug	≥ 2,0E-05		8,7E-06	8,7E-06	≈ 1,5E+04	≈ 1,5E-01	
p38alpha	Cediranib (AZD2171)	≥ 2,0E-05		9,2E-06	9,2E-06	1,2E+04	1,1E-01	
p38alpha	CI-1033 (Canertinib)	≈ 5,0E-06	≈ 2,3E-06	1,4E-06	1,4E-06	8,6E+04	1,2E-01	1
p38alpha	CX-4945 (Silmatasertib)	3,0E-06	1,4E-06	1,5E-06	1,5E-06	7,4E+04	1,1E-01	
p38alpha	CYC116	≥ 2,0E-05		2,3E-05	2,3E-05	≈ 1,0E+04	≈ 2,5E-01	
p38alpha	Dacomitinib (PF299804 - PF-00299804)	8,0E-07	3,6E-07	1,4E-06	1,4E-06	8,2E+04	1,1E-01	1
p38alpha	Dasatinib (BMS-354825)	2,0E-07	9,1E-08	8,8E-08	8,8E-08	1,9E+06	1,7E-01	
p38alpha	DCC-2036 (Rebastinib)	3,5E-08	1,6E-08	n.e.	1,6E-08	3,1E+04	≤ 4,9E-04	4
p38alpha	Desmethyl Erlotinib (CP-473420)	≥ 2,0E-05		1,2E-05	1,2E-05	7,0E+03	9,4E-02	
p38alpha	E7080 (Lenvatinib)	9,5E-08	4,3E-08	4,9E-08	4,9E-08	2,3E+06	1,1E-01	
p38alpha	Foretinib (GSK1363089 - XL880)	5,0E-07	2,3E-07	4,3E-07	4,3E-07	2,1E+05	9,1E-02	
p38alpha	Gefitinib (Iressa)	7,0E-06	3,2E-06	1,9E-06	1,9E-06	6,5E+04	1,2E-01	
p38alpha	Golvatinib (E7050)	8,0E-07	3,6E-07	3,6E-07	3,6E-07	3,4E+05	1,2E-01	
p38alpha	GSK1070916	3,0E-06	1,4E-06	3,4E-06	3,4E-06	8,8E+04	1,2E-01	3
p38alpha	Imatinib (Gleevec)	≥ 2,0E-05		2,4E-05	2,4E-05	6,3E+03	1,3E-01	
p38alpha	Ki8751	≥ 2,0E-05		9,7E-06	9,7E-06	1,1E+04	≈ 1,1E-01	
p38alpha	Linifanib (ABT-869)	1,0E-05	4,5E-06	≈ 4,0E-06	4,5E-06	2,6E+04	1,2E-01	3
p38alpha	LY2228820	6,5E-09	2,9E-09	n.e.	2,9E-09	2,4E+06	7,0E-03	3
p38alpha	LY2603618 (IC-83)	6,0E-06	2,7E-06	6,8E-06	6,8E-06	2,1E+04	1,4E-01	
p38alpha	MGCD-265	≥ 2,0E-05		≈ 4,4E-05	≈ 4,4E-05	≈ 1,1E+04	1,7E-01	
p38alpha	Milciclib (PHA-848125)	1,5E-05	6,8E-06	6,3E-06	6,3E-06	1,6E+04	1,0E-01	
p38alpha	Motesanib Diphosphate (AMG-706)	≈ 2,0E-05	≈ 9,1E-06	6,3E-06	6,3E-06	1,2E+04	7,3E-02	
p38alpha	Nilotinib (AMN-107)	3,0E-08	1,4E-08	6,3E-08	6,3E-08	1,4E+05	9,0E-03	1
p38alpha	NVP-ADW742	≥ 2,0E-05		7,4E-06	7,4E-06	≈ 2,1E+04	≈ 1,7E-01	
p38alpha	NVP-BHG712	≥ 2,0E-05		1,1E-05	1,1E-05	3,1E+03	3,2E-02	
p38alpha	NVP-BVU972	≥ 2,0E-05		1,9E-05	1,9E-05	6,4E+02	1,3E-02	
p38alpha	NVP-TAE226	≥ 2,0E-05		4,9E-06	4,9E-06	2,3E+04	1,1E-01	
p38alpha	OSI-027	2,0E-05	9,1E-06	≈ 8,1E-06	9,1E-06	1,3E+04	1,2E-01	3
p38alpha	OSI-930	1,0E-05	4,5E-06	≈ 4,4E-06	4,5E-06	2,3E+04	1,0E-01	3
p38alpha	Pazopanib HCl	≥ 2,0E-05		1,4E-05	1,4E-05	≈ 1,2E+04	1,1E-01	
p38alpha	PD153035 HCl	5,5E-06	2,5E-06	2,1E-06	2,1E-06	5,9E+04	1,2E-01	
p38alpha	PD173074	3,0E-06	1,4E-06	1,2E-06	1,2E-06	8,4E+04	1,0E-01	
p38alpha	Pelitinib (EKB-569)	≈ 2,0E-05	≈ 9,1E-06	6,9E-06	6,9E-06	1,3E+04	9,0E-02	
p38alpha	PF-04217903	≥ 2,0E-05		1,5E-05	1,5E-05	1,2E+04	1,8E-01	
p38alpha	PH-797804	3,0E-09	1,4E-09	2,7E-09	2,7E-09	1,3E+07	3,5E-02	
p38alpha	PHA-665752	≥ 2,0E-05		≥ 2,0E-05	≥ 9,1E-06			
p38alpha	PLX-4720	≥ 2,0E-05		5,7E-06	5,7E-06	3,4E+04	1,9E-01	
p38alpha	Ponatinib (AP24534)	2,0E-08	9,1E-09	5,6E-09	5,6E-09	8,5E+05	4,8E-03	
p38alpha	PP-121	7,5E-06	3,4E-06	3,6E-06	3,6E-06	3,1E+04	1,1E-01	
p38alpha	Quizartinib (AC220)	≥ 2,0E-05		7,1E-06	7,1E-06	8,5E+03	5,2E-02	
p38alpha	Saracatinib (AZD0530)	9,0E-07	4,1E-07	4,7E-07	4,7E-07	2,8E+05	1,3E-01	
p38alpha	SB 202190	2,0E-08	9,1E-09	9,1E-09	9,1E-09	1,3E+07	1,2E-01	
p38alpha	SB 203580	3,5E-08	1,6E-08	2,0E-08	2,0E-08	5,2E+06	1,1E-01	
p38alpha	SB 431542	2,0E-05	9,1E-06	6,2E-06	6,2E-06	3,0E+04	1,8E-01	
p38alpha	SB 525334	9,5E-06	4,3E-06	3,1E-06	3,1E-06	4,3E+04	1,3E-01	

kinase	Compound	IC ₅₀ [M] ePCA	K _D eq [M] ePCA *	K _D kin [M] kPCA	K _D [M] PCA **	k _{on} [M ⁻¹ s ⁻¹] kPCA	k _{off} [s ⁻¹] kPCA	comment
p38alpha	SB590885	3,5E-06	1,6E-06	2,1E-06	2,1E-06	5,8E+04	1,1E-01	
p38alpha	SNS-314	2,0E-05	9,1E-06	5,6E-06	5,6E-06	1,9E+04	1,1E-01	
p38alpha	TAE684 (NVP-TAE684)	≥ 2,0E-05		6,0E-06	6,0E-06	1,7E+04	9,3E-02	
p38alpha	TG100-115	≥ 2,0E-05		1,5E-05	1,5E-05	9,0E+02	1,3E-02	
p38alpha	TG101209	9,5E-06	4,3E-06	3,8E-06	3,8E-06	≈ 5,9E+04	≈ 1,9E-01	
p38alpha	TG101348 (SAR302503)	≥ 2,0E-05		1,7E-05	1,7E-05	6,1E+03	1,1E-01	
p38alpha	Tie2 kinase inhibitor	≈ 2,0E-05	≈ 9,1E-06	4,7E-06	4,7E-06	2,7E+04	1,2E-01	
p38alpha	Tivozanib (AV-951)	7,0E-07	3,2E-07	3,9E-07	3,9E-07	2,5E+05	9,7E-02	
p38alpha	TPCA-1	≥ 2,0E-05		2,0E-05	2,0E-05	9,4E+03	1,8E-01	
p38alpha	TWS119	≈ 5,0E-06	≈ 2,3E-06	1,6E-06	1,6E-06	5,4E+04	8,4E-02	
p38alpha	Vandetanib (Zactima)	7,0E-06	3,2E-06	4,1E-06	4,1E-06	2,8E+04	1,2E-01	
p38alpha	VX-702	3,5E-08	1,6E-08	7,3E-09	7,3E-09	9,3E+06	6,6E-02	
p38alpha	WHI-P154	9,0E-06	4,1E-06	3,7E-06	3,7E-06	1,5E+04	5,3E-02	
p38alpha	WYE-687	≥ 2,0E-05		1,1E-05	1,1E-05	1,4E+04	1,4E-01	
p38alpha	WZ4002	≥ 2,0E-05		6,8E-06	6,8E-06	2,1E+04	1,4E-01	
p38alpha	ZM 336372	4,0E-07	1,8E-07	2,0E-07	2,0E-07	4,6E+05	8,6E-02	
PIK3CA	A66	6,1E-08	6,3E-09	3,2E-09	3,2E-09	≈ 4,4E+07	≈ 1,5E-01	
PIK3CA	AG-490	n.e.	n.e.	≥ 2,0E-05	≥ 2,0E-05			
PIK3CA	Arry-380	≥ 2,0E-05		1,3E-06	1,3E-06	1,4E+05	1,8E-01	
PIK3CA	AS-252424	8,1E-07	8,4E-08	8,9E-08	8,9E-08	1,0E+06	9,1E-02	1
PIK3CA	AS-604850	≈ 1,9E-05	≈ 1,9E-06	3,2E-06	3,2E-06	≥ 1,1E+05	≥ 3,5E-01	
PIK3CA	AS-605240	≈ 3,9E-07	≈ 4,0E-08	2,0E-08	2,0E-08	≈ 8,0E+06	≈ 1,1E-01	
PIK3CA	AZD2014	3,2E-07	3,3E-08	2,5E-08	2,5E-08	≈ 1,0E+07	≈ 2,4E-01	
PIK3CA	AZD5438	8,1E-06	8,4E-07	7,8E-07	7,8E-07	≥ 4,5E+05	≥ 3,5E-01	
PIK3CA	AZD8055	1,3E-07	1,4E-08	4,5E-09	4,5E-09	5,5E+07	2,5E-01	
PIK3CA	AZD8931	≥ 2,0E-05		5,6E-06	5,6E-06	≥ 6,3E+04	≥ 3,5E-01	
PIK3CA	Baricitinib (LY3009104 - incb28050)	≈ 2,0E-05	≈ 2,1E-06	3,0E-06	3,0E-06	≥ 1,2E+05	≥ 3,5E-01	
PIK3CA	BEZ235 (NVP-BEZ235)	8,5E-08	8,8E-09	2,6E-09	2,6E-09	1,4E+07	3,7E-02	
PIK3CA	BI 2536	≥ 2,0E-05		2,6E-06	2,6E-06	≥ 1,4E+05	≥ 3,5E-01	
PIK3CA	BKM120 (NVP-BKM120)	8,3E-08	8,6E-09	6,9E-09	6,9E-09	2,7E+07	1,8E-01	
PIK3CA	BMS 777607	≈ 1,3E-05	≈ 1,3E-06	2,7E-06	2,7E-06	≥ 1,3E+05	≥ 3,5E-01	
PIK3CA	BYL719	1,6E-08	1,7E-09	7,1E-10	7,1E-10	3,1E+07	2,2E-02	
PIK3CA	CAL-101 (GS-1101)	1,8E-06	1,9E-07	1,6E-07	1,6E-07	≈ 3,6E+06	≈ 5,7E-01	1
PIK3CA	CX-4945 (Silmatasertib)	5,5E-07	5,8E-08	9,4E-08	9,4E-08	≈ 5,9E+06	≈ 4,8E-01	1
PIK3CA	CYC116	1,7E-06	1,7E-07	3,0E-07	3,0E-07	4,4E+05	1,3E-01	1
PIK3CA	Cyt387	≈ 2,0E-05	≈ 2,0E-06	2,9E-06	2,9E-06	≥ 1,2E+05	≥ 3,5E-01	
PIK3CA	Dabrafenib (GSK2118436)	≥ 2,0E-05		1,3E-06	1,3E-06	≈ 1,2E+05	≈ 1,5E-01	
PIK3CA	E7080 (Lenvatinib)	≥ 2,0E-05		3,3E-06	3,3E-06	≈ 1,8E+04	≈ 6,5E-02	
PIK3CA	GDC-0941	1,1E-08	1,2E-09	4,6E-10	4,6E-10	3,6E+07	1,6E-02	
PIK3CA	GDC-0980 (RG7422)	4,1E-09	4,2E-10	6,6E-10	6,6E-10	2,4E+07	1,6E-02	
PIK3CA	GSK1059615	1,5E-08	1,5E-09	4,8E-10	4,8E-10	≈ 3,1E+08	1,3E-01	
PIK3CA	GSK2126458	≤ 2,3E-10	≤ 2,4E-11	n.e.	≤ 2,4E-11	4,7E+07	≤ 1,1E-03	4
PIK3CA	GSK461364	≥ 2,0E-05		2,0E-06	2,0E-06	≥ 1,8E+05	≥ 3,5E-01	
PIK3CA	Hesperadin	≥ 2,0E-05		1,8E-06	1,8E-06	≥ 2,0E+05	≥ 3,5E-01	
PIK3CA	INK 128 (MLN0128)	1,3E-07	1,4E-08	9,6E-09	9,6E-09	4,2E+07	4,0E-01	
PIK3CA	JNJ-38877605	≥ 2,0E-05		4,5E-06	4,5E-06	≥ 7,8E+04	≥ 3,5E-01	
PIK3CA	JNJ-7706621	≥ 2,0E-05		1,5E-06	1,5E-06	n.e.	n.e.	
PIK3CA	Ku-0063794	1,6E-07	1,7E-08	1,9E-08	1,9E-08	≈ 3,9E+06	≈ 6,7E-02	
PIK3CA	KU-55933	5,4E-06	5,6E-07	3,0E-07	3,0E-07	1,4E+06	4,2E-01	
PIK3CA	KU-60019	3,1E-06	3,2E-07	1,2E-07	1,2E-07	1,2E+06	1,4E-01	1
PIK3CA	LY2784544	1,3E-05	1,4E-06	6,0E-07	6,0E-07	≥ 5,9E+05	≥ 3,5E-01	
PIK3CA	LY294002	2,2E-06	2,2E-07	2,3E-07	2,3E-07	≥ 1,5E+06	≥ 3,5E-01	
PIK3CA	MK-2461	≥ 2,0E-05		1,3E-06	1,3E-06	≥ 2,7E+05	≥ 3,5E-01	
PIK3CA	NU7441 (KU-57788)	8,9E-07	9,2E-08	9,6E-08	9,6E-08	2,1E+06	2,0E-01	1
PIK3CA	NVP-ADW742	≈ 1,7E-05	≈ 1,7E-06	1,3E-06	1,3E-06	≈ 4,6E+04	≈ 6,4E-02	
PIK3CA	NVP-BGT226	1,4E-08	1,4E-09	5,0E-10	5,0E-10	1,0E+07	5,0E-03	
PIK3CA	NVP-BSK805	9,1E-06	9,5E-07	1,1E-06	1,1E-06	≥ 3,3E+05	≥ 3,5E-01	
PIK3CA	OSI-027	5,6E-06	5,8E-07	3,4E-07	3,4E-07	≈ 6,4E+05	≈ 2,3E-01	
PIK3CA	Pazopanib HCl	≥ 2,0E-05		6,7E-07	6,7E-07	≈ 1,0E+05	≈ 6,2E-02	
PIK3CA	PCI-32765 (Ibrutinib)	≈ 9,4E-06	≈ 9,8E-07	8,3E-06	8,3E-06	n.e.	n.e.	
PIK3CA	PD 0332991 (Palbociclib) HCl	≈ 1,6E-05	≈ 1,7E-06	2,3E-06	2,3E-06	≥ 1,5E+05	≥ 3,5E-01	
PIK3CA	PF-04691502	5,0E-09	5,2E-10	2,7E-10	2,7E-10	3,2E+07	8,2E-03	
PIK3CA	PF-05212384 (PKI-587)	3,1E-07	3,2E-08	1,9E-08	1,9E-08	3,8E+06	7,2E-02	
PIK3CA	PI-103	5,0E-09	5,2E-10	4,3E-10	4,3E-10	4,1E+07	1,8E-02	
PIK3CA	PIK-294	≥ 2,0E-05		2,6E-06	2,6E-06	≥ 1,3E+05	≥ 3,5E-01	
PIK3CA	PIK-75	1,1E-08	1,1E-09	5,2E-10	5,2E-10	4,8E+07	2,5E-02	1
PIK3CA	PIK-90	6,5E-09	6,8E-10	≈ 2,2E-11	6,8E-10	≈ 1,3E+09	≈ 4,9E-02	
PIK3CA	PIK-93	4,4E-07	4,5E-08	1,5E-08	1,5E-08	≈ 7,2E+06	≈ 1,1E-01	
PIK3CA	PKI-402	1,5E-07	1,5E-08	4,7E-09	4,7E-09	6,6E+06	3,1E-02	
PIK3CA	Ponatinib (AP24534)	≥ 2,0E-05		2,0E-06	2,0E-06	≥ 1,7E+05	≥ 3,5E-01	
PIK3CA	PP-121	4,0E-07	4,1E-08	5,5E-08	5,5E-08	3,5E+06	1,9E-01	
PIK3CA	PP242	1,0E-06	1,1E-07	8,6E-08	8,6E-08	2,7E+06	2,3E-01	
PIK3CA	Quercetin (Sophoretin)	≈ 1,5E-05	≈ 1,5E-06	2,2E-06	2,2E-06	≥ 1,6E+05	≥ 3,5E-01	
PIK3CA	SAR131675	6,9E-06	7,2E-07	7,3E-07	7,3E-07	≈ 2,7E+05	≈ 2,1E-01	
PIK3CA	SP600125	≥ 2,0E-05		1,1E-06	1,1E-06	≥ 3,2E+05	≥ 3,5E-01	
PIK3CA	Staurosporine	1,4E-05	1,5E-06	6,6E-07	6,6E-07	≈ 2,3E+05	≈ 1,4E-01	
PIK3CA	Sunitinib Malate (Sutent)	≥ 2,0E-05		3,3E-06	3,3E-06	≥ 1,1E+05	≥ 3,5E-01	
PIK3CA	TAK-901	2,2E-06	2,3E-07	3,7E-07	3,7E-07	≈ 3,3E+05	≈ 1,2E-01	
PIK3CA	TG 100713	≈ 4,1E-07	≈ 4,3E-08	1,0E-08	1,0E-08	5,9E+07	6,1E-01	

kinase	Compound	IC ₅₀ [M] ePCA	K _D eq [M] ePCA *	K _D kin [M] kPCA	K _D [M] PCA **	k _{on} [M ⁻¹ s ⁻¹] kPCA	k _{off} [s ⁻¹] kPCA	comment
PIK3CA	TG100-115	2,9E-07	3,0E-08	3,4E-08	3,4E-08	≈ 1,5E+07	≈ 5,3E-01	
PIK3CA	TGX-221	2,9E-06	3,0E-07	2,7E-07	2,7E-07	≈ 1,5E+06	≈ 3,9E-01	
PIK3CA	Torin 1	1,4E-07	1,5E-08	8,8E-09	8,8E-09	3,3E+06	2,8E-02	
PIK3CA	Torin 2	1,1E-08	1,1E-09	4,6E-10	4,6E-10	3,2E+07	1,4E-02	
PIK3CA	TPCA-1	≥ 2,0E-05		5,5E-06	5,5E-06	≥ 6,4E+04	≥ 3,5E-01	
PIK3CA	WAY-600	1,0E-06	1,1E-07	7,5E-08	7,5E-08	1,5E+06	1,1E-01	1
PIK3CA	Wortmannin	8,9E-09	9,2E-10	3,8E-09	3,8E-09	1,8E+05	3,9E-04	
PIK3CA	WYE-125132	4,0E-06	4,1E-07	1,5E-07	1,5E-07	≈ 2,5E+06	≈ 3,5E-01	
PIK3CA	WYE-354	6,0E-07	6,3E-08	3,6E-08	3,6E-08	6,0E+06	2,2E-01	
PIK3CA	WYE-687	1,5E-06	1,5E-07	2,4E-08	1,5E-07	2,0E+07	4,8E-01	1
PIK3CA	XL765	≈ 2,0E-05	≈ 2,0E-06	3,3E-07	3,3E-07	2,5E+05	7,8E-02	
PIK3CA	YM201636	5,4E-07	5,6E-08	4,7E-08	4,7E-08	4,1E+06	1,9E-01	1
PIK3CA	ZSTK474	1,1E-08	1,2E-09	1,0E-09	1,0E-09	5,4E+07	4,9E-02	
PKCeta	A-674563	1,2E-08	4,9E-09	5,6E-09	5,6E-09	3,6E+05	2,0E-03	
PKCeta	Afatinib (BIBW2992)	≥ 2,0E-05		1,7E-05	1,7E-05	5,7E+01	9,9E-04	
PKCeta	AT7867	1,2E-06	4,7E-07	1,1E-06	1,1E-06	8,0E+03	9,1E-03	
PKCeta	AT9283	≥ 2,0E-05		9,0E-06	9,0E-06	1,7E+02	1,5E-03	
PKCeta	Axitinib	≥ 2,0E-05		7,7E-06	7,7E-06	7,3E+01	5,1E-04	
PKCeta	AZ 960	4,2E-06	1,7E-06	1,6E-06	1,6E-06	≥ 1,9E+04	≥ 3,0E-02	
PKCeta	AZD2014	≥ 2,0E-05		1,6E-05	1,6E-05	3,9E+01	6,4E-04	
PKCeta	AZD6244 (Selumetinib)	≥ 2,0E-05		1,4E-05	1,4E-05	5,6E+01	7,6E-04	
PKCeta	AZD7762	4,7E-06	1,9E-06	4,2E-06	4,2E-06	3,4E+02	1,4E-03	
PKCeta	AZD8330	≥ 2,0E-05		2,6E-05	2,6E-05	8,7E+01	2,2E-03	
PKCeta	Baricitinib (LY3009104 - incb28050)	7,8E-07	3,1E-07	3,5E-07	3,5E-07	5,2E+03	1,8E-03	
PKCeta	BEZ235 (NVP-BEZ235)	≥ 2,0E-05		1,5E-05	1,5E-05	7,6E+01	1,1E-03	
PKCeta	BI6727 (Volasertib)	≥ 2,0E-05		1,1E-05	1,1E-05	7,4E+01	7,9E-04	
PKCeta	BIBF1120 (Vargatef)	≥ 2,0E-05		1,7E-05	1,7E-05	5,2E+01	8,3E-04	
PKCeta	BIX 02188	≥ 2,0E-05		1,4E-05	1,4E-05	9,6E+01	1,4E-03	
PKCeta	BIX 02189	≥ 2,0E-05		1,8E-05	1,8E-05	8,1E+01	1,5E-03	
PKCeta	BMS-265246	≥ 2,0E-05		1,8E-06	1,8E-06	6,6E+02	1,2E-03	2
PKCeta	Bosutinib (SKI-606)	≥ 2,0E-05		6,2E-06	6,2E-06	2,6E+02	1,6E-03	
PKCeta	BX-795	≥ 2,0E-05		7,5E-06	7,5E-06	4,1E+02	2,6E-03	
PKCeta	CCT128930	7,4E-06	2,9E-06	1,7E-06	1,7E-06	1,4E+03	2,4E-03	
PKCeta	CEP33779	≥ 2,0E-05		1,4E-05	1,4E-05	1,6E+02	2,2E-03	
PKCeta	CHIR-124	9,3E-07	3,7E-07	7,0E-07	7,0E-07	≈ 5,3E+03	3,3E-03	
PKCeta	CP 673451	3,4E-06	1,3E-06	1,4E-06	1,4E-06	3,0E+03	4,3E-03	
PKCeta	Crenolanib (CP-868596)	6,6E-06	2,6E-06	2,1E-06	2,1E-06	1,7E+03	3,7E-03	
PKCeta	CX-4945 (Silmatasertib)	≥ 2,0E-05		1,7E-05	1,7E-05	7,0E+01	1,2E-03	
PKCeta	CYC116	≥ 2,0E-05		1,2E-05	1,2E-05	1,6E+02	1,9E-03	
PKCeta	Cyt387	≈ 1,6E-05	≈ 6,3E-06	3,6E-06	3,6E-06	3,9E+02	1,4E-03	
PKCeta	Desmethyl Erlotinib (CP-473420)	≥ 2,0E-05		1,5E-05	1,5E-05	7,6E+01	1,0E-03	
PKCeta	Enzastaurin (LY317615)	≥ 2,0E-05		5,9E-06	5,9E-06	6,7E+02	≈ 4,1E-03	2
PKCeta	Flavopiridol HCl	1,2E-06	4,6E-07	7,0E-07	7,0E-07	7,5E+03	5,4E-03	2
PKCeta	GDC-0068	≥ 2,0E-05		1,2E-05	1,2E-05	2,5E+02	2,7E-03	
PKCeta	GDC-0980 (RG7422)	≥ 2,0E-05		2,0E-05	2,0E-05	5,4E+01	1,1E-03	
PKCeta	GSK1838705A	≥ 2,0E-05		1,1E-05	1,1E-05	1,2E+02	1,4E-03	
PKCeta	GSK690693	4,0E-08	1,6E-08	2,2E-08	2,2E-08	3,0E+04	6,6E-04	2
PKCeta	Hesperadin	≥ 2,0E-05		9,4E-06	9,4E-06	4,0E+02	3,7E-03	
PKCeta	Imatinib (Gleevec)	≥ 2,0E-05		1,8E-05	1,8E-05	1,2E+02	2,3E-03	
PKCeta	IMD 0354	≥ 2,0E-05		2,3E-05	2,3E-05	7,4E+01	1,7E-03	
PKCeta	Indirubin	≥ 2,0E-05		2,6E-05	2,6E-05	2,8E+01	7,3E-04	
PKCeta	JNJ-7706621	7,4E-06	2,9E-06	2,5E-06	2,5E-06	5,8E+02	1,3E-03	
PKCeta	Lapatinib Ditosylate (Tykerb)	≥ 2,0E-05		1,6E-05	1,6E-05	1,7E+02	2,5E-03	
PKCeta	Linsitinib (OSI-906)	≥ 2,0E-05		1,6E-05	1,6E-05	4,9E+01	7,5E-04	
PKCeta	LY2228820	≥ 2,0E-05		1,1E-05	1,1E-05	6,9E+01	7,6E-04	
PKCeta	MK-2206 2HCl	≥ 2,0E-05		1,8E-05	1,8E-05	6,7E+01	9,5E-04	
PKCeta	NVP-BGT226	≥ 2,0E-05		1,3E-05	1,3E-05	5,3E+01	6,5E-04	
PKCeta	NVP-BSK805	≥ 2,0E-05		7,1E-06	7,1E-06	8,9E+01	6,3E-04	2
PKCeta	PD318088	≥ 2,0E-05		1,6E-05	1,6E-05	2,4E+01	4,0E-04	
PKCeta	PF-00562271	≥ 2,0E-05		1,2E-05	1,2E-05	3,7E+01	4,3E-04	
PKCeta	PF-04217903	≥ 2,0E-05		1,8E-05	1,8E-05	3,7E+01	6,8E-04	
PKCeta	PHA-767491	6,7E-08	2,7E-08	3,6E-08	3,6E-08	7,8E+04	2,7E-03	2
PKCeta	PIK-75	1,5E-08	5,8E-09	5,8E-09	5,8E-09	3,6E+05	2,0E-03	
PKCeta	PP-121	8,5E-07	3,4E-07	9,5E-07	9,5E-07	9,6E+03	9,2E-03	
PKCeta	PP242	1,7E-06	6,8E-07	6,7E-07	6,7E-07	4,5E+03	3,1E-03	
PKCeta	Quercetin (Sophoretin)	≥ 2,0E-05		1,1E-05	1,1E-05	2,2E+02	2,4E-03	
PKCeta	Ruxolitinib (INCB018424)	2,7E-06	1,1E-06	2,2E-06	2,2E-06	9,8E+02	2,1E-03	
PKCeta	SAR131675	≥ 2,0E-05		1,0E-05	1,0E-05	8,7E+01	7,1E-04	
PKCeta	SB 202190	≥ 2,0E-05		6,5E-06	6,5E-06	1,4E+02	9,3E-04	
PKCeta	SB590885	≥ 2,0E-05		1,8E-05	1,8E-05	4,8E+01	8,5E-04	
PKCeta	Sotrastaurin (AEB071)	1,4E-07	5,3E-08	9,4E-07	5,3E-08	1,2E+03	1,0E-03	
PKCeta	Staurosporine	7,6E-09	3,0E-09	1,6E-09	1,6E-09	4,2E+05	6,2E-04	2
PKCeta	TG101209	≥ 2,0E-05		1,4E-05	1,4E-05	5,1E+01	7,6E-04	
PKCeta	Thiazovivin	4,3E-07	1,7E-07	1,6E-07	1,6E-07	1,8E+04	2,8E-03	
PKCeta	Tofacitinib (CP-690550 - Tasocitinib)	2,0E-06	8,0E-07	1,3E-06	1,3E-06	1,2E+03	1,4E-03	
PKCeta	Torin 1	≥ 2,0E-05		8,1E-06	8,1E-06	4,5E+01	3,7E-04	
PKCeta	TPCA-1	≥ 2,0E-05		6,4E-06	6,4E-06	2,0E+02	1,3E-03	
PKCeta	WP1066	≥ 2,0E-05		2,3E-05	2,3E-05	2,9E+01	6,6E-04	
PKCeta	WZ3146	≥ 2,0E-05		2,0E-05	2,0E-05	3,5E+01	7,4E-04	

kinase	Compound	IC ₅₀ [M] ePCA	K _D eq [M] ePCA *	K _D kin [M] kPCA	K _D [M] PCA **	k _{on} [M ⁻¹ s ⁻¹] kPCA	k _{off} [s ⁻¹] kPCA	comment
PKCeta	Y-27632 2HCl	1,9E-07	7,5E-08	2,7E-07	2,7E-07	8,2E+03	2,2E-03	
PLK1	A-769662	1,7E-05	2,0E-06	≥ 2,0E-05	≥ 2,0E-06			
PLK1	AG-1024	3,2E-06	3,7E-07	6,6E-07	6,6E-07	4,3E+04	1,6E-02	3
PLK1	Arry-380	n.e.	n.e.	≥ 2,0E-05	≥ 2,0E-05			
PLK1	AS-605240	1,0E-05	1,2E-06	1,5E-06	1,5E-06	3,2E+03	4,7E-03	
PLK1	AT9283	6,2E-06	7,1E-07	3,6E-07	3,6E-07	3,5E+04	1,3E-02	
PLK1	AZD7762	1,1E-05	1,2E-06	6,6E-07	6,6E-07	2,2E+04	1,4E-02	
PLK1	Baricitinib (LY3009104 - incb28050)	2,8E-06	3,2E-07	3,1E-07	3,1E-07	4,1E+04	1,3E-02	
PLK1	BEZ235 (NVP-BEZ235)	≥ 2,0E-05		1,7E-06	1,7E-06	8,4E+03	1,3E-02	
PLK1	BI 2536	≤ 6,6E-10	≤ 7,5E-11	≤ 1,0E-10	≤ 1,0E-10	1,6E+07	1,5E-03	2
PLK1	BI6727 (Volasertib)	≤ 6,3E-10	≤ 7,2E-11	n.e.	≤ 7,2E-11	n.e.	n.e.	
PLK1	BIX 02188	≥ 2,0E-05		1,2E-06	1,2E-06	5,8E+03	6,6E-03	
PLK1	BMS-265246	6,6E-08	7,5E-09	n.e.	7,5E-09	2,7E+06	2,0E-02	123
PLK1	Bosutinib (SKI-606)	1,9E-06	2,2E-07	5,6E-07	5,6E-07	2,6E+04	1,5E-02	
PLK1	BX-795	1,2E-05	1,3E-06	6,0E-07	6,0E-07	1,9E+04	1,1E-02	
PLK1	BX-912	6,8E-06	7,7E-07	5,3E-07	5,3E-07	2,4E+04	1,2E-02	
PLK1	CEP33779	8,1E-06	9,2E-07	5,3E-07	5,3E-07	2,6E+04	1,4E-02	
PLK1	CH5424802	≥ 2,0E-05		2,8E-07	2,8E-07	6,2E+04	1,5E-02	2
PLK1	Crizotinib (PF-02341066)	≥ 2,0E-05		≈ 3,8E-06	≈ 3,8E-06	≈ 6,8E+03	1,4E-02	
PLK1	CX-4945 (Silmisertib)	6,0E-08	6,8E-09	n.e.	6,8E-09	2,7E+06	1,8E-02	23
PLK1	CYC116	1,2E-05	1,4E-06	5,2E-07	5,2E-07	2,4E+04	1,2E-02	
PLK1	Dabrafenib (GSK2118436)	≥ 2,0E-05		5,6E-07	5,6E-07	1,1E+04	5,8E-03	
PLK1	Danuseritib (PHA-739358)	2,8E-06	3,2E-07	2,4E-07	2,4E-07	4,9E+04	1,2E-02	
PLK1	Dovitinib (TKI-258)	≥ 2,0E-05		1,2E-06	1,2E-06	5,4E+03	6,8E-03	
PLK1	GDC-0068	≥ 2,0E-05		1,2E-06	1,2E-06	2,9E+03	3,6E-03	
PLK1	GDC-0980 (RG7422)	≥ 2,0E-05		1,5E-06	1,5E-06	1,2E+04	1,7E-02	
PLK1	GSK1059615	7,3E-07	8,3E-08	9,0E-08	9,0E-08	3,2E+05	2,4E-02	2
PLK1	GSK1838705A	7,8E-08	8,9E-09	4,4E-07	8,9E-09	3,1E+04	1,4E-02	2
PLK1	GSK2126458	5,6E-06	6,4E-07	≈ 1,1E-06	6,4E-07	1,2E+04	1,2E-02	
PLK1	GSK461364	3,2E-09	3,7E-10	n.e.	3,7E-10	3,7E+07	1,4E-02	23
PLK1	Hesperadin	1,2E-06	1,4E-07	1,8E-07	1,8E-07	8,3E+04	1,5E-02	
PLK1	JNJ-7706621	5,6E-06	6,4E-07	3,5E-07	3,5E-07	4,3E+04	1,4E-02	
PLK1	KU-55933	1,2E-05	1,4E-06	4,3E-07	4,3E-07	2,0E+04	8,7E-03	
PLK1	KU-60019	8,9E-06	1,0E-06	5,3E-07	5,3E-07	2,2E+04	1,1E-02	
PLK1	Lapatinib Ditosylate (Tykerb)	≥ 2,0E-05		1,7E-06	1,7E-06	4,7E+03	6,8E-03	
PLK1	LY294002	1,9E-06	2,1E-07	1,2E-07	1,2E-07	9,9E+04	1,2E-02	
PLK1	Milciclib (PHA-848125)	6,0E-06	6,8E-07	9,0E-07	9,0E-07	6,2E+03	5,6E-03	
PLK1	MK-2461	≥ 2,0E-05		≈ 2,8E-06	≈ 2,8E-06	≈ 3,4E+03	6,2E-03	
PLK1	MK-5108 (VX-689)	5,4E-06	6,2E-07	8,2E-07	8,2E-07	1,7E+04	1,4E-02	
PLK1	MLN8054	1,0E-05	1,2E-06	6,1E-07	6,1E-07	1,7E+04	1,0E-02	
PLK1	MLN8237 (Alisertib)	1,2E-05	1,3E-06	6,5E-07	6,5E-07	2,3E+04	1,5E-02	
PLK1	Neratinib (HKI-272)	≥ 2,0E-05		1,1E-06	1,1E-06	1,6E+04	1,5E-02	
PLK1	NVP-TAE226	4,7E-08	5,3E-09	5,7E-09	5,7E-09	2,6E+06	1,5E-02	2
PLK1	Pazopanib HCl	≥ 2,0E-05		9,4E-07	9,4E-07	9,0E+03	8,5E-03	
PLK1	PD 0332991 (Palbociclib) HCl	7,8E-07	8,9E-08	4,8E-08	4,8E-08	2,8E+05	1,3E-02	2
PLK1	PD153035 HCl	≥ 2,0E-05		6,6E-07	6,6E-07	≈ 4,1E+03	≈ 3,3E-03	
PLK1	Pelitinib (EKB-569)	1,2E-05	1,4E-06	8,5E-07	8,5E-07	9,0E+03	7,5E-03	
PLK1	PF-00562271	1,9E-06	2,2E-07	6,1E-07	6,1E-07	2,4E+04	1,4E-02	
PLK1	PF-03814735	1,6E-06	1,8E-07	7,8E-07	7,8E-07	1,6E+04	1,3E-02	
PLK1	PHA-665752	≥ 2,0E-05		7,5E-07	7,5E-07	7,9E+03	6,0E-03	
PLK1	PHA-680632	1,1E-07	1,3E-08	4,2E-08	4,2E-08	3,6E+05	1,4E-02	2
PLK1	PHA-767491	9,4E-07	1,1E-07	6,5E-07	1,1E-07	1,6E+04	1,1E-02	
PLK1	Phenformin HCl	1,4E-05	1,6E-06	≥ 2,0E-05	≥ 1,6E-06			
PLK1	PHT-427	7,4E-06	8,4E-07	≥ 2,0E-05	≥ 8,4E-07			
PLK1	PIK-75	2,2E-07	2,6E-08	3,7E-08	3,7E-08	4,5E+05	1,6E-02	2
PLK1	PLX-4720	1,7E-05	1,9E-06	n.e.	1,9E-06	6,4E+03	≤ 7,1E-03	4
PLK1	PP-121	1,3E-06	1,5E-07	7,9E-07	1,5E-07	1,9E+04	1,5E-02	
PLK1	PP242	1,0E-05	1,1E-06	≈ 2,0E-06	1,1E-06	5,3E+03	1,1E-02	
PLK1	Quercetin (Sophoretin)	≥ 2,0E-05		1,3E-06	1,3E-06	6,2E+03	7,7E-03	
PLK1	R406	2,3E-06	2,6E-07	4,3E-07	4,3E-07	3,7E+04	1,6E-02	2
PLK1	R788 (Fostamatinib) - prodrug	4,9E-06	5,5E-07	≈ 1,2E-06	5,5E-07	3,0E+05	3,5E-01	
PLK1	Roscovitine (Seliciclib - CYC202)	1,3E-05	1,5E-06	4,5E-07	4,5E-07	2,9E+04	1,3E-02	
PLK1	Ruxolitinib (INCB018424)	2,9E-07	3,3E-08	4,7E-08	4,7E-08	3,2E+05	1,4E-02	2
PLK1	Semaxanib (SU5416)	≥ 2,0E-05		6,8E-07	6,8E-07	≥ 5,2E+05	≥ 3,5E-01	
PLK1	SNS-314	≥ 2,0E-05		8,0E-07	8,0E-07	1,2E+04	9,4E-03	
PLK1	SP600125	≥ 2,0E-05		8,7E-07	8,7E-07	7,2E+03	6,3E-03	
PLK1	Staurosporine	1,7E-07	2,0E-08	3,9E-08	3,9E-08	3,3E+05	1,3E-02	2
PLK1	SU11274	≥ 2,0E-05		7,7E-07	7,7E-07	1,1E+04	8,4E-03	
PLK1	Sunitinib Malate (Sutent)	1,7E-05	1,9E-06	1,0E-06	1,0E-06	7,8E+03	7,9E-03	
PLK1	TAE684 (NVP-TAE684)	9,9E-08	1,1E-08	2,5E-09	2,5E-09	5,6E+06	1,3E-02	2
PLK1	TAK-901	1,8E-06	2,1E-07	8,8E-07	8,8E-07	1,8E+04	1,5E-02	
PLK1	TG101209	3,8E-07	4,3E-08	3,7E-07	4,3E-08	4,3E+04	1,6E-02	2
PLK1	TG101348 (SAR302503)	6,9E-07	7,9E-08	5,8E-07	7,9E-08	1,7E+04	9,6E-03	2
PLK1	TGX-221	≥ 2,0E-05		7,5E-07	7,5E-07	5,6E+03	4,1E-03	
PLK1	TPCA-1	≈ 4,7E-06	≈ 5,4E-07	3,3E-07	3,3E-07	3,1E+04	9,8E-03	
PLK1	Tyrphostin AG 879 (AG 879)	≥ 2,0E-05		3,7E-07	3,7E-07	1,5E+04	5,6E-03	
PLK1	WHI-P154	≥ 2,0E-05		1,7E-06	1,7E-06	4,9E+03	8,5E-03	
PLK1	Wortmannin	6,6E-06	7,6E-07	5,3E-08	7,6E-07	≈ 4,6E+04	2,0E-03	
PLK1	WZ3146	7,0E-06	8,0E-07	4,4E-07	4,4E-07	2,9E+04	1,3E-02	

kinase	Compound	IC ₅₀ [M] ePCA	K _D eq [M] ePCA *	K _D kin [M] kPCA	K _D [M] PCA **	k _{on} [M ⁻¹ s ⁻¹] kPCA	k _{off} [s ⁻¹] kPCA	comment
PLK1	WZ4002	3,8E-06	4,4E-07	2,2E-07	2,2E-07	6,8E+04	1,4E-02	
PLK1	WZ8040	1,0E-05	1,2E-06	4,8E-07	4,8E-07	3,0E+04	1,4E-02	
PLK1	XL-184 (Cabozantinib)	7,6E-06	8,7E-07	≥ 2,0E-05	≥ 8,7E-07			
PLK1	ZSTK474	≥ 2,0E-05		4,5E-07	4,5E-07	2,8E+04	1,3E-02	2
Ret	A-674563	3,5E-06	8,1E-07	1,0E-06	1,0E-06	3,9E+04	4,0E-02	
Ret	AEE788 (NVP-AEE788)	7,8E-07	1,8E-07	1,8E-07	1,8E-07	1,9E+06	3,5E-01	
Ret	Afatinib (BIBW2992)	5,0E-06	1,2E-06	1,6E-06	1,6E-06	8,2E+04	1,3E-01	2
Ret	AG-1478 (Tyrphostin AG-1478)	1,8E-07	4,2E-08	9,6E-08	9,6E-08	2,3E+06	2,2E-01	
Ret	AMG 900	1,6E-07	3,8E-08	1,9E-07	1,9E-07	1,0E+05	1,8E-02	2
Ret	AMG458	≈ 1,0E-05	≈ 2,4E-06	6,0E-06	6,0E-06	n.e.	n.e.	
Ret	Apatinib (YN968D1)	3,5E-08	8,1E-09	n.e.	8,1E-09	9,5E+04	≤ 7,7E-04	4
Ret	ARQ 197 (Tivantinib)	n.e.	n.e.	≥ 2,0E-05	≥ 2,0E-05			
Ret	AS-252424	1,3E-05	3,0E-06	2,4E-06	2,4E-06	≈ 8,3E+04	≈ 2,0E-01	
Ret	AT7867	4,0E-06	9,4E-07	1,1E-06	1,1E-06	3,8E+05	4,0E-01	
Ret	AT9283	≈ 1,5E-08	≈ 3,4E-09	1,5E-09	1,5E-09	6,7E+06	1,0E-02	
Ret	Aurora A Inhibitor I	2,6E-07	6,0E-08	5,7E-08	5,7E-08	2,2E+06	1,3E-01	12
Ret	Axitinib	1,1E-07	2,5E-08	≈ 3,2E-08	2,5E-08	≈ 3,2E+06	≈ 1,0E-01	
Ret	AZ 960	4,0E-08	9,3E-09	6,6E-09	6,6E-09	5,8E+06	3,8E-02	
Ret	AZ628	≈ 6,3E-09	≈ 1,5E-09	n.e.	≈ 1,5E-09	2,1E+05	≤ 3,1E-04	4
Ret	AZD2014	n.e.	n.e.	≥ 2,0E-05	≥ 2,0E-05			
Ret	AZD4547	≈ 6,4E-08	≈ 1,5E-08	9,4E-09	9,4E-09	1,0E+07	9,9E-02	
Ret	AZD5438	3,0E-06	6,9E-07	1,2E-06	1,2E-06	≈ 4,4E+05	≈ 5,4E-01	
Ret	AZD7762	4,4E-09	1,0E-09	6,5E-10	6,5E-10	3,4E+07	2,1E-02	
Ret	AZD8931	5,0E-08	1,2E-08	1,2E-08	1,2E-08	≈ 1,2E+07	≈ 1,3E-01	
Ret	Barasertib (AZD1152-HQPA)	≈ 2,7E-07	≈ 6,3E-08	3,3E-08	3,3E-08	2,9E+06	8,5E-02	
Ret	Baricitinib (LY3009104 - incb28050)	2,9E-07	6,7E-08	7,3E-08	7,3E-08	6,4E+05	4,7E-02	
Ret	BEZ235 (NVP-BEZ235)	≥ 2,0E-05		2,6E-06	2,6E-06	8,9E+03	2,3E-02	
Ret	BGJ398 (NVP-BGJ398)	≈ 1,3E-06	≈ 3,0E-07	2,1E-07	2,1E-07	3,9E+05	7,4E-02	
Ret	BIBF1120 (Vargatef)	1,9E-09	4,4E-10	1,4E-10	1,4E-10	1,5E+07	2,1E-03	
Ret	BIRB 796 (Doramapimod)	8,5E-08	2,0E-08	n.e.	2,0E-08	3,1E+03	≤ 6,1E-05	4
Ret	BIX 02188	2,3E-07	5,2E-08	3,1E-08	3,1E-08	1,2E+06	3,9E-02	2
Ret	BIX 02189	7,0E-07	1,6E-07	1,5E-07	1,5E-07	≈ 1,1E+06	≈ 1,5E-01	
Ret	BMS 777607	≈ 4,8E-07	≈ 1,1E-07	4,7E-07	4,7E-07	≈ 1,8E+06	≈ 7,5E-01	
Ret	BMS 794833	2,3E-08	5,4E-09	4,7E-09	4,7E-09	2,5E+05	1,1E-03	
Ret	BMS-599626 (AC480)	4,3E-06	1,0E-06	8,6E-07	8,6E-07	4,3E+05	≈ 4,1E-01	
Ret	Bosutinib (SKI-606)	1,4E-06	3,3E-07	2,8E-07	2,8E-07	8,7E+04	2,4E-02	2
Ret	Brivanib (BMS-540215)	3,0E-07	6,9E-08	6,0E-08	6,0E-08	7,8E+06	4,5E-01	
Ret	Brivanib alaninate (BMS-582664) - prodrug	≈ 6,7E-07	≈ 1,5E-07	1,4E-07	1,4E-07	7,7E+05	1,1E-01	
Ret	BX-795	2,9E-08	6,7E-09	6,3E-09	6,3E-09	4,1E+06	2,5E-02	
Ret	BX-912	5,2E-08	1,2E-08	1,9E-08	1,9E-08	1,0E+07	1,8E-01	
Ret	CCT128930	1,3E-06	3,1E-07	4,0E-07	4,0E-07	3,7E+05	1,5E-01	
Ret	CCT129202	5,8E-08	1,3E-08	2,6E-08	2,6E-08	1,9E+06	4,9E-02	2
Ret	CCT137690	1,3E-08	3,1E-09	1,4E-08	1,4E-08	7,1E+06	9,2E-02	
Ret	Cediranib (AZD2171)	8,8E-08	2,1E-08	2,0E-09	2,1E-08	1,4E+07	2,7E-02	
Ret	CEP33779	4,2E-07	9,7E-08	9,5E-08	9,5E-08	≈ 3,6E+06	≈ 3,3E-01	
Ret	CH5424802	2,5E-08	5,8E-09	9,9E-10	5,8E-09	7,1E+06	6,4E-03	
Ret	CHIR-124	2,2E-08	5,2E-09	1,8E-08	1,8E-08	2,3E+06	3,4E-02	
Ret	CHIR-98014	n.e.	n.e.	≥ 2,0E-05	≥ 2,0E-05			
Ret	CI-1033 (Canertinib)	4,0E-07	9,4E-08	9,8E-08	9,8E-08	≥ 3,6E+06	≥ 3,5E-01	
Ret	CP 673451	2,4E-07	5,6E-08	7,0E-08	7,0E-08	≈ 2,3E+06	≈ 1,6E-01	
Ret	CP-724714	6,9E-06	1,6E-06	1,2E-06	1,2E-06	6,1E+04	7,3E-02	
Ret	Crenolanib (CP-868596)	1,5E-07	3,6E-08	5,8E-08	5,8E-08	4,1E+05	2,4E-02	
Ret	Crizotinib (PF-02341066)	1,8E-06	4,3E-07	5,3E-07	5,3E-07	≈ 8,2E+05	≈ 4,3E-01	
Ret	CX-4945 (Silmatasertib)	1,8E-06	4,1E-07	3,8E-07	3,8E-07	2,0E+05	7,5E-02	
Ret	CYC116	1,3E-07	3,0E-08	3,8E-08	3,8E-08	4,0E+06	1,4E-01	
Ret	Cyt387	6,2E-07	1,4E-07	1,2E-07	1,2E-07	≈ 1,6E+06	≈ 2,0E-01	
Ret	Dabrafenib (GSK2118436)	≈ 8,8E-07	≈ 2,0E-07	1,7E-07	1,7E-07	4,4E+05	7,5E-02	
Ret	Dacomitinib (PF299804 - PF-00299804)	1,4E-06	3,2E-07	6,3E-07	6,3E-07	1,9E+05	1,2E-01	
Ret	Danuserib (PHA-739358)	3,0E-08	6,9E-09	1,0E-08	1,0E-08	1,6E+05	1,6E-03	
Ret	Dasatinib (BMS-354825)	2,7E-07	6,2E-08	5,6E-08	5,6E-08	≥ 6,3E+06	≥ 3,5E-01	
Ret	DCC-2036 (Rebastinib)	1,2E-08	2,8E-09	n.e.	2,8E-09	2,8E+04	≤ 7,9E-05	4
Ret	Desmethyl Erlotinib (CP-473420)	3,1E-07	7,2E-08	9,9E-08	9,9E-08	5,7E+05	5,6E-02	
Ret	Dovitinib (TKI-258)	1,1E-08	2,4E-09	1,3E-09	1,3E-09	3,1E+07	3,6E-02	
Ret	E7080 (Lenvatinib)	1,4E-09	3,2E-10	3,4E-10	3,4E-10	1,7E+07	5,9E-03	
Ret	ENMD-2076	1,4E-08	3,3E-09	5,4E-09	5,4E-09	3,5E+06	1,9E-02	
Ret	Erlotinib HCl	3,7E-07	8,6E-08	≈ 7,3E-08	8,6E-08	≥ 4,8E+06	≥ 3,5E-01	
Ret	Everolimus (RAD001)	5,9E-06	1,4E-06	≥ 2,0E-05	≥ 1,4E-06			
Ret	Flavopiridol HCl	3,7E-06	8,5E-07	1,2E-06	1,2E-06	1,6E+05	1,9E-01	
Ret	Foretinib (GSK1363089 - XL880)	≤ 1,9E-10	≤ 4,4E-11	n.e.	≤ 4,4E-11	1,7E+06	≤ 7,6E-05	4
Ret	GDC-0068	n.e.	n.e.	≥ 2,0E-05	≥ 2,0E-05			
Ret	GDC-0941	≥ 2,0E-05		3,8E-06	3,8E-06	≥ 9,3E+04	≥ 3,5E-01	
Ret	GDC-0980 (RG7422)	4,3E-06	1,0E-06	1,7E-06	1,7E-06	5,2E+04	8,9E-02	
Ret	Gefitinib (Iressa)	1,5E-06	3,5E-07	3,9E-07	3,9E-07	≥ 8,9E+05	≥ 3,5E-01	
Ret	Golvatinib (E7050)	4,1E-08	9,6E-09	1,1E-08	1,1E-08	1,0E+06	1,2E-02	2
Ret	GSK1059615	≥ 2,0E-05		7,5E-06	7,5E-06	≥ 4,7E+04	≥ 3,5E-01	
Ret	GSK1070916	2,1E-06	4,8E-07	5,2E-07	5,2E-07	1,6E+05	8,1E-02	
Ret	GSK461364	4,4E-06	1,0E-06	4,9E-06	4,9E-06	≈ 3,4E+03	≈ 1,3E-02	
Ret	GSK690693	5,3E-06	1,2E-06	1,5E-06	1,5E-06	7,1E+04	1,0E-01	
Ret	Hesperadin	3,4E-09	7,9E-10	3,8E-10	3,8E-10	1,4E+07	5,2E-03	

kinase	Compound	IC ₅₀ [M] ePCA	K _D eq [M] ePCA *	K _D kin [M] kPCA	K _D [M] PCA **	k _{on} [M ⁻¹ s ⁻¹] kPCA	k _{off} [s ⁻¹] kPCA	comment
Ret	INK 128 (MLN0128)	≈ 6,0E-07	≈ 1,4E-07	1,4E-07	1,4E-07	≥ 2,5E+06	≥ 3,5E-01	
Ret	JNJ-7706621	4,9E-07	1,1E-07	1,2E-07	1,2E-07	≈ 5,1E+06	≈ 6,6E-01	
Ret	KI8751	2,2E-09	5,1E-10	9,5E-10	9,5E-10	4,6E+06	4,4E-03	
Ret	KRN 633	2,3E-08	5,4E-09	4,1E-09	4,1E-09	6,8E+06	2,8E-02	
Ret	KW 2449	6,6E-08	1,5E-08	4,6E-08	4,6E-08	≈ 4,8E+06	≈ 2,1E-01	
Ret	LDN193189	≈ 1,3E-05	≈ 3,0E-06	1,5E-06	1,5E-06	≥ 2,4E+05	≥ 3,5E-01	
Ret	Linifanib (ABT-869)	9,6E-08	2,2E-08	4,3E-08	4,3E-08	3,5E+05	1,5E-02	2
Ret	Linsitinib (OSI-906)	1,9E-06	4,5E-07	5,1E-07	5,1E-07	5,1E+05	2,5E-01	
Ret	LY2603618 (IC-83)	2,5E-07	5,8E-08	1,7E-07	1,7E-07	≈ 7,9E+05	≈ 1,1E-01	
Ret	LY2784544	1,8E-08	4,3E-09	2,9E-09	2,9E-09	3,0E+06	8,5E-03	
Ret	Masitinib (AB1010)	≥ 2,0E-05		8,7E-06	8,7E-06	≥ 4,0E+04	≥ 3,5E-01	
Ret	MGCD-265	4,6E-08	1,1E-08	3,6E-08	3,6E-08	6,1E+05	2,2E-02	
Ret	Milciclib (PHA-848125)	≈ 5,6E-07	≈ 1,3E-07	6,4E-08	6,4E-08	1,2E+06	7,6E-02	
Ret	MK-2461	2,5E-07	5,8E-08	8,4E-08	8,4E-08	≥ 4,2E+06	≥ 3,5E-01	
Ret	MK-5108 (VX-689)	1,3E-08	3,0E-09	4,8E-09	4,8E-09	≈ 9,9E+07	≈ 4,9E-01	
Ret	MLN8054	2,7E-06	6,3E-07	5,5E-07	5,5E-07	≥ 6,4E+05	≥ 3,5E-01	
Ret	MLN8237 (Alisertib)	4,4E-07	1,0E-07	9,5E-08	9,5E-08	2,7E+06	2,5E-01	
Ret	Motesanib Diphosphate (AMG-706)	2,3E-08	5,3E-09	1,6E-08	1,6E-08	2,6E+05	4,1E-03	
Ret	Neratinib (HKI-272)	2,1E-06	4,8E-07	3,3E-06	4,8E-07	7,4E+03	≈ 2,7E-02	
Ret	Nilotinib (AMN-107)	4,5E-07	1,0E-07	3,0E-07	3,0E-07	3,4E+04	9,7E-03	
Ret	NVP-ADW742	4,3E-07	9,9E-08	1,1E-07	1,1E-07	≈ 4,1E+06	≈ 4,6E-01	
Ret	NVP-BGT226	1,4E-05	3,3E-06	1,2E-06	1,2E-06	≈ 2,2E+05	≈ 2,8E-01	
Ret	NVP-BSK805	1,6E-07	3,8E-08	6,1E-08	6,1E-08	8,9E+05	≈ 5,7E-02	
Ret	NVP-TAE226	≈ 4,1E-07	≈ 9,5E-08	1,2E-07	1,2E-07	2,0E+06	2,4E-01	
Ret	OSI-027	9,1E-08	2,1E-08	4,8E-08	4,8E-08	3,3E+06	≈ 1,6E-01	
Ret	OSI-930	2,1E-08	5,0E-09	9,7E-09	9,7E-09	5,6E+05	5,4E-03	
Ret	Pazopanib HCl	4,3E-08	9,9E-09	2,6E-08	2,6E-08	≈ 8,2E+06	≈ 1,9E-01	
Ret	PCI-32765 (Ibrutinib)	4,1E-08	9,5E-09	3,2E-08	3,2E-08	1,6E+06	4,8E-02	
Ret	PD 0332991 (Palbociclib) HCl	6,0E-06	1,4E-06	1,6E-06	1,6E-06	≥ 2,2E+05	≥ 3,5E-01	
Ret	PD153035 HCl	2,9E-07	6,7E-08	9,4E-08	9,4E-08	3,0E+06	2,9E-01	
Ret	PD173074	5,0E-07	1,2E-07	1,3E-07	1,3E-07	≈ 2,3E+06	≈ 3,2E-01	
Ret	Pelitinib (EKB-569)	4,2E-06	9,7E-07	1,7E-06	1,7E-06	8,9E+03	1,4E-02	
Ret	PF-00562271	1,5E-07	3,5E-08	5,7E-08	5,7E-08	1,6E+06	9,8E-02	
Ret	PF-03814735	2,8E-09	6,4E-10	9,3E-10	9,3E-10	4,4E+06	4,1E-03	
Ret	PF-05212384 (PKI-587)	≥ 2,0E-05		2,3E-06	2,3E-06	1,3E+03	3,1E-03	
Ret	PHA-665752	5,1E-07	1,2E-07	8,9E-08	8,9E-08	≥ 3,9E+06	≥ 3,5E-01	
Ret	PHA-680632	3,7E-08	8,5E-09	6,8E-09	6,8E-09	1,1E+06	7,3E-03	
Ret	PHT-427	1,4E-05	3,2E-06	≥ 2,0E-05	≥ 3,2E-06			
Ret	PIK-75	6,0E-08	1,4E-08	1,1E-08	1,1E-08	8,5E+06	8,9E-02	2
Ret	PLX-4720	6,3E-06	1,5E-06	1,3E-06	1,3E-06	≥ 2,8E+05	≥ 3,5E-01	
Ret	Ponatinib (AP24534)	≤ 2,3E-10	≤ 5,3E-11	n.e.	≤ 5,3E-11	3,7E+06	≤ 1,9E-04	4
Ret	PP-121	1,1E-09	2,6E-10	7,7E-10	7,7E-10	2,3E+07	1,7E-02	
Ret	PP242	7,2E-09	1,7E-09	1,2E-09	1,2E-09	1,8E+07	2,2E-02	
Ret	Quercetin (Sophoretin)	6,9E-07	1,6E-07	1,1E-07	1,1E-07	4,1E+05	4,4E-02	2
Ret	Quizartinib (AC220)	9,0E-09	2,1E-09	n.e.	2,1E-09	1,9E+05	≤ 4,1E-04	24
Ret	R406	4,7E-09	1,1E-09	7,6E-10	7,6E-10	7,6E+06	5,4E-03	
Ret	R788 (Fostatinib) - prodrug	2,9E-07	6,7E-08	6,7E-08	6,7E-08	1,4E+05	8,3E-03	
Ret	Raf265 derivative	1,1E-06	2,6E-07	4,4E-07	4,4E-07	2,3E+04	9,0E-03	
Ret	Roscovitine (Seliciclib - CYC202)	n.e.	n.e.	≥ 2,0E-05	≥ 2,0E-05			
Ret	Ruxolitinib (INCB018424)	2,3E-07	5,3E-08	9,7E-08	9,7E-08	≈ 1,5E+07	≈ 1,4E+00	
Ret	SAR131675	2,1E-07	5,0E-08	6,8E-08	6,8E-08	≈ 1,4E+06	≈ 9,1E-02	
Ret	Saracatinib (AZD0530)	2,2E-06	5,2E-07	4,3E-07	4,3E-07	3,4E+05	≈ 1,5E-01	
Ret	SB 202190	2,2E-06	5,0E-07	7,1E-07	7,1E-07	≈ 6,6E+05	≈ 4,5E-01	
Ret	SB 203580	2,6E-06	6,0E-07	5,9E-07	5,9E-07	≈ 2,4E+06	≈ 1,6E+00	
Ret	SB 216763	≥ 2,0E-05		5,8E-06	5,8E-06	≈ 1,5E+04	≈ 1,2E-01	
Ret	SB 415286	1,2E-05	2,7E-06	1,8E-06	1,8E-06	≈ 7,7E+03	1,1E-02	
Ret	SB590885	≥ 2,0E-05		6,8E-06	6,8E-06	4,7E+02	3,2E-03	
Ret	Semaxanib (SU5416)	9,2E-08	2,1E-08	6,3E-08	6,3E-08	8,7E+05	5,4E-02	
Ret	SNS-314	3,6E-07	8,4E-08	6,4E-08	6,4E-08	2,8E+06	1,7E-01	
Ret	Sotrastaurin (AEB071)	≈ 1,0E-05	≈ 2,3E-06	3,7E-06	3,7E-06	5,6E+04	2,0E-01	
Ret	SP600125	5,2E-07	1,2E-07	1,0E-07	1,0E-07	≈ 2,1E+06	≈ 1,9E-01	
Ret	Staurosporine	1,2E-09	2,7E-10	2,4E-10	2,4E-10	1,4E+07	3,5E-03	
Ret	SU11274	6,9E-08	1,6E-08	4,7E-08	4,7E-08	2,3E+06	1,0E-01	
Ret	Sunitinib Malate (Sutent)	5,2E-09	1,2E-09	2,1E-09	2,1E-09	7,1E+07	1,5E-01	
Ret	TAE684 (NVP-TAE684)	4,4E-07	1,0E-07	≈ 7,5E-08	1,0E-07	2,0E+06	1,3E-01	2
Ret	TAK-285	n.e.	n.e.	≥ 2,0E-05	≥ 2,0E-05			
Ret	TAK-901	5,2E-09	1,2E-09	3,3E-09	3,3E-09	4,2E+06	1,4E-02	
Ret	Tandutinib (MLN518)	5,2E-06	1,2E-06	1,9E-06	1,9E-06	≥ 1,9E+05	≥ 3,5E-01	
Ret	TG101209	1,4E-08	3,3E-09	1,1E-08	1,1E-08	3,4E+06	3,7E-02	
Ret	TG101348 (SAR302503)	1,1E-07	2,6E-08	3,7E-08	3,7E-08	1,3E+06	4,9E-02	
Ret	Tie2 kinase inhibitor	≥ 2,0E-05		3,6E-06	3,6E-06	≈ 1,8E+04	≈ 5,4E-02	
Ret	Tivozanib (AV-951)	3,6E-10	8,4E-11	n.e.	8,4E-11	9,5E+06	≤ 8,0E-04	4
Ret	Tofacitinib (CP-690550 - Tasocitinib)	7,1E-06	1,7E-06	1,6E-06	1,6E-06	≥ 2,3E+05	≥ 3,5E-01	
Ret	Torin 1	≥ 2,0E-05		1,4E-06	1,4E-06	2,6E+04	3,7E-02	
Ret	Torin 2	≈ 2,3E-06	≈ 5,4E-07	5,0E-07	5,0E-07	1,4E+06	6,9E-01	
Ret	TPCA-1	1,9E-07	4,5E-08	9,0E-08	9,0E-08	7,2E+05	6,6E-02	
Ret	TSU-68 (SU6668)	4,5E-08	1,0E-08	9,4E-09	9,4E-09	6,8E+06	6,3E-02	
Ret	TWS119	1,3E-08	3,1E-09	3,6E-09	3,6E-09	1,5E+07	5,5E-02	
Ret	Tyrphostin AG 879 (AG 879)	n.e.	n.e.	≥ 2,0E-05	≥ 2,0E-05			

kinase	Compound	IC ₅₀ [M] ePCA	K _D eq [M] ePCA *	K _D kin [M] kPCA	K _D [M] PCA **	k _{on} [M ⁻¹ s ⁻¹] kPCA	k _{off} [s ⁻¹] kPCA	comment
Ret	Vandetanib (Zactima)	5,0E-09	1,2E-09	5,1E-09	5,1E-09	4,8E+07	2,5E-01	
Ret	Vatalanib 2HCl (PTK787)	2,4E-06	5,6E-07	7,7E-07	7,7E-07	2,8E+05	2,2E-01	
Ret	VX-680 (MK-0457 - Tozasertib)	2,8E-08	6,5E-09	1,4E-08	1,4E-08	9,2E+06	1,3E-01	
Ret	WHI-P154	2,3E-07	5,3E-08	5,3E-08	5,3E-08	3,2E+06	1,7E-01	
Ret	WZ3146	8,2E-08	1,9E-08	2,6E-08	2,6E-08	6,4E+06	1,6E-01	
Ret	WZ4002	5,6E-06	1,3E-06	7,9E-07	7,9E-07	2,4E+05	1,6E-01	
Ret	WZ8040	6,7E-08	1,5E-08	8,0E-08	1,5E-08	5,4E+05	4,3E-02	
Ret	XL-184 (Cabozantinib)	1,6E-09	3,6E-10	5,3E-10	5,3E-10	4,1E+06	2,2E-03	
Ret	ZM-447439	2,5E-08	5,9E-09	1,0E-08	1,0E-08	1,2E+07	1,2E-01	
ROCK1	A-674563	≈ 1,9E-05	≈ 1,2E-05	3,6E-06	3,6E-06	1,3E+03	5,0E-03	
ROCK1	A-769662	n.e.	n.e.	≥ 2,0E-05	≥ 2,0E-05			
ROCK1	AEE788 (NVP-AEE788)	1,4E-05	8,8E-06	6,9E-06	6,9E-06	9,2E+03	6,4E-02	
ROCK1	Afatinib (BIBW2992)	≥ 2,0E-05		6,3E-06	6,3E-06	3,3E+03	2,1E-02	
ROCK1	AMG458	≈ 1,6E-05	≈ 1,0E-05	3,7E-06	3,7E-06	1,5E+04	5,8E-02	
ROCK1	AT7867	4,1E-07	2,6E-07	n.e.	2,6E-07	3,7E+03	≤ 9,7E-04	14
ROCK1	AT9283	≥ 2,0E-05		1,1E-05	1,1E-05	n.e.	n.e.	
ROCK1	Axitinib	≥ 2,0E-05		7,7E-06	7,7E-06	n.e.	n.e.	
ROCK1	AZ628	≥ 2,0E-05		1,2E-05	1,2E-05	n.e.	n.e.	
ROCK1	AZD2014	≥ 2,0E-05		8,7E-06	8,7E-06	1,0E+03	8,4E-03	
ROCK1	AZD4547	≥ 2,0E-05		1,1E-05	1,1E-05	1,5E+03	1,9E-02	
ROCK1	Baricitinib (LY3009104 - incb28050)	1,3E-05	8,4E-06	1,0E-05	1,0E-05	9,8E+02	9,9E-03	
ROCK1	BIBF1120 (Vargatef)	≥ 2,0E-05		4,4E-06	4,4E-06	5,6E+03	2,4E-02	
ROCK1	BMS 777607	7,2E-07	4,6E-07	1,2E-06	1,2E-06	4,6E+04	5,7E-02	1
ROCK1	BMS 794833	≥ 2,0E-05		7,4E-06	7,4E-06	4,0E+03	2,9E-02	
ROCK1	Bosutinib (SKI-606)	1,0E-05	6,5E-06	1,5E-06	1,5E-06	1,7E+04	2,5E-02	
ROCK1	BS-181 HCl	≥ 2,0E-05		1,1E-05	1,1E-05	2,0E+03	2,2E-02	
ROCK1	BX-795	≈ 8,2E-06	≈ 5,2E-06	2,4E-06	2,4E-06	1,6E+04	4,0E-02	2
ROCK1	BX-912	≥ 2,0E-05		1,2E-05	1,2E-05	7,1E+03	8,5E-02	
ROCK1	CCT128930	≥ 2,0E-05		9,6E-06	9,6E-06	1,0E+03	9,8E-03	
ROCK1	CCT129202	≥ 2,0E-05		1,1E-05	1,1E-05	9,1E+02	9,5E-03	
ROCK1	CEP33779	≈ 1,4E-05	≈ 8,9E-06	4,8E-06	4,8E-06	9,4E+03	4,6E-02	
ROCK1	CHIR-124	≥ 2,0E-05		5,7E-06	5,7E-06	5,7E+03	3,3E-02	
ROCK1	CI-1033 (Canertinib)	≥ 2,0E-05		1,6E-05	1,6E-05	≈ 2,5E+04	≈ 4,0E-01	
ROCK1	CP 673451	≥ 2,0E-05		7,8E-06	7,8E-06	≈ 1,0E+04	≈ 8,3E-02	
ROCK1	Crenolanib (CP-868596)	≥ 2,0E-05		4,3E-06	4,3E-06	2,8E+03	1,2E-02	
ROCK1	CX-4945 (Siltitasertib)	≥ 2,0E-05		1,5E-05	1,5E-05	n.e.	n.e.	
ROCK1	CYC116	≥ 2,0E-05		3,3E-06	3,3E-06	1,1E+04	3,5E-02	
ROCK1	Cyt387	≈ 8,2E-06	≈ 5,2E-06	3,3E-06	3,3E-06	6,9E+03	2,2E-02	12
ROCK1	Dasatinib (BMS-354825)	≥ 2,0E-05		9,6E-06	9,6E-06	1,6E+03	1,5E-02	
ROCK1	Desmethyl Erlotinib (CP-473420)	≥ 2,0E-05		7,4E-06	7,4E-06	2,7E+03	1,9E-02	
ROCK1	Dovitinib (TKI-258)	2,4E-06	1,6E-06	1,3E-06	1,3E-06	3,8E+04	4,9E-02	
ROCK1	ENMD-2076	7,7E-06	4,9E-06	2,9E-06	2,9E-06	≈ 1,7E+04	≈ 5,0E-02	
ROCK1	Erlotinib HCl	≥ 2,0E-05		1,8E-05	1,8E-05	6,4E+03	1,1E-01	
ROCK1	Foretinib (GSK1363089 - XL880)	≈ 8,4E-07	≈ 5,4E-07	5,5E-07	5,5E-07	7,5E+04	4,0E-02	12
ROCK1	GDC-0980 (RG7422)	≥ 2,0E-05		7,2E-06	7,2E-06	1,7E+03	1,2E-02	
ROCK1	Gefitinib (Iressa)	≥ 2,0E-05		1,4E-05	1,4E-05	5,1E+02	7,3E-03	
ROCK1	Golvatinib (E7050)	≥ 2,0E-05		1,3E-05	1,3E-05	n.e.	n.e.	
ROCK1	GSK1070916	1,3E-07	8,2E-08	1,8E-06	8,2E-08	1,2E+04	2,2E-02	12
ROCK1	GSK1838705A	≥ 2,0E-05		8,6E-06	8,6E-06	≈ 1,0E+04	≈ 7,9E-02	
ROCK1	Hesperadin	≈ 1,8E-05	≈ 1,1E-05	4,3E-06	4,3E-06	1,1E+04	4,8E-02	
ROCK1	JNJ-7706621	1,5E-05	9,5E-06	2,6E-06	2,6E-06	1,3E+04	3,3E-02	
ROCK1	KW 2449	2,4E-06	1,5E-06	2,9E-06	2,9E-06	2,1E+04	6,1E-02	
ROCK1	LDN193189	1,3E-05	8,6E-06	2,2E-05	2,2E-05	1,2E+04	2,4E-01	
ROCK1	Linifanib (ABT-869)	≥ 2,0E-05		3,5E-06	3,5E-06	7,3E+03	2,4E-02	
ROCK1	Linsitinib (OSI-906)	≥ 2,4E-06	1,5E-06	1,3E-06	1,3E-06	4,7E+04	6,1E-02	
ROCK1	LY2228820	≥ 2,0E-05		1,4E-05	1,4E-05	7,9E+02	1,1E-02	
ROCK1	NVP-ADW742	≈ 5,0E-06	≈ 3,2E-06	2,2E-06	2,2E-06	2,7E+04	6,0E-02	2
ROCK1	NVP-BSK805	≥ 2,0E-05		1,1E-05	1,1E-05	n.e.	n.e.	
ROCK1	NVP-TAE226	≥ 2,0E-05		5,6E-06	5,6E-06	≈ 7,9E+03	≈ 4,5E-02	
ROCK1	PCI-32765 (Ibrutinib)	≈ 1,4E-05	≈ 8,7E-06	5,1E-06	5,1E-06	4,7E+03	2,4E-02	
ROCK1	PD153035 HCl	≥ 2,0E-05		8,1E-06	8,1E-06	≈ 2,1E+03	≈ 1,7E-02	
ROCK1	Pelitinib (EKB-569)	≥ 2,0E-05		5,3E-06	5,3E-06	3,5E+03	1,9E-02	
ROCK1	PF-00562271	≥ 2,0E-05		9,6E-06	9,6E-06	1,4E+03	1,4E-02	
ROCK1	PF-03814735	≥ 5,1E-07	3,2E-07	1,5E-06	1,5E-06	2,3E+04	3,4E-02	12
ROCK1	PIK-75	≥ 2,0E-05		4,9E-06	4,9E-06	2,0E+03	9,8E-03	
ROCK1	PLX-4720	≥ 2,0E-05		6,6E-06	6,6E-06	4,5E+03	≈ 3,0E-02	
ROCK1	PP-121	≈ 9,6E-06	≈ 6,2E-06	7,2E-06	7,2E-06	1,6E+03	1,2E-02	
ROCK1	Quercetin (Sophoretin)	≥ 2,0E-05		1,4E-05	1,4E-05	≥ 2,5E+04	≥ 3,5E-01	
ROCK1	Quizartinib (AC220)	≥ 2,0E-05		8,5E-06	8,5E-06	5,4E+02	4,7E-03	
ROCK1	Roscovitine (Seliciclib - CYC202)	≥ 2,0E-05		8,9E-06	8,9E-06	5,8E+03	5,0E-02	
ROCK1	Saracatinib (AZD0530)	≥ 2,0E-05		1,2E-05	1,2E-05	n.e.	n.e.	
ROCK1	SB590885	≥ 1,6E-05		≥ 2,0E-05	≥ 1,1E-05			
ROCK1	Semaxanib (SU5416)	3,1E-06	2,0E-06	2,6E-06	2,6E-06	2,8E+04	7,2E-02	2
ROCK1	SNS-314	≥ 2,0E-05		≈ 1,6E-05	≈ 1,6E-05	4,4E+03	≈ 7,9E-02	
ROCK1	Sotrastaurin (AEB071)	≥ 2,0E-05		1,8E-05	1,8E-05	2,2E+02	4,0E-03	
ROCK1	SP600125	≥ 2,0E-05		7,0E-06	7,0E-06	4,7E+03	3,4E-02	
ROCK1	Staurosporine	1,9E-07	1,2E-07	9,8E-08	9,8E-08	2,1E+05	2,1E-02	2
ROCK1	SU11274	≥ 2,0E-05		6,2E-06	6,2E-06	1,1E+04	7,1E-02	
ROCK1	Sunitinib Malate (Sutent)	2,5E-06	1,6E-06	1,7E-06	1,7E-06	4,5E+04	7,5E-02	1

kinase	Compound	IC ₅₀ [M] ePCA	K _D eq [M] ePCA *	K _D kin [M] kPCA	K _D [M] PCA **	k _{on} [M ⁻¹ s ⁻¹] kPCA	k _{off} [s ⁻¹] kPCA	comment
ROCK1	TAE684 (NVP-TAE684)	≈ 1,9E-05	≈ 1,2E-05	1,5E-06	1,5E-06	3,0E+04	4,1E-02	2
ROCK1	Thiazovivin	≈ 2,0E-05		≈ 5,8E-06	≈ 5,8E-06	5,1E+02	≈ 3,9E-03	
ROCK1	Tivozanib (AV-951)	≈ 2,0E-05		3,1E-06	3,1E-06	8,2E+03	2,6E-02	
ROCK1	TPCA-1	≈ 2,0E-05		1,3E-05	1,3E-05	8,6E+02	1,1E-02	
ROCK1	TSU-68 (SU6668)	1,2E-06	7,7E-07	1,5E-06	1,5E-06	2,7E+04	4,0E-02	1
ROCK1	Vandetanib (Zactima)	≈ 2,0E-05	≈ 1,3E-05	6,7E-06	6,7E-06	2,0E+03	≈ 1,4E-02	
ROCK1	Vemurafenib (PLX4032)	≈ 2,0E-05		4,3E-06	4,3E-06	5,9E+03	2,4E-02	
ROCK1	VX-680 (MK-0457 - Tozasertib)	≈ 2,0E-05		8,2E-06	8,2E-06	≈ 1,5E+04	≈ 1,2E-01	
ROCK1	WZ3146	≈ 4,4E-06	≈ 2,8E-06	3,7E-06	3,7E-06	1,7E+04	6,1E-02	1
ROCK1	WZ4002	≈ 2,0E-05		5,2E-06	5,2E-06	1,8E+04	9,4E-02	
ROCK1	WZ8040	8,2E-06	5,2E-06	2,0E-06	2,0E-06	1,4E+04	2,7E-02	
ROCK1	XL-184 (Cabozantinib)	≈ 2,0E-05		2,9E-06	2,9E-06	2,1E+04	6,0E-02	
ROCK1	ZM-447439	6,1E-06	3,9E-06	2,9E-06	2,9E-06	4,6E+04	1,3E-01	
SRC	A-674563	1,8E-05	9,6E-06	5,5E-06	5,5E-06	≈ 5,1E+03	≈ 2,6E-02	
SRC	AEE788 (NVP-AEE788)	4,8E-08	2,5E-08	2,5E-08	2,5E-08	≥ 1,4E+07	≥ 3,5E-01	
SRC	Afatinib (BIBW2992)	2,5E-06	1,3E-06	8,7E-07	8,7E-07	9,4E+04	8,0E-02	
SRC	AG-1024	9,7E-06	5,1E-06	2,7E-06	2,7E-06	5,1E+04	1,3E-01	
SRC	AG-1478 (Tyrphostin AG-1478)	6,4E-07	3,4E-07	5,4E-07	5,4E-07	≥ 6,5E+05	≥ 3,5E-01	
SRC	AMG458	1,5E-06	7,9E-07	6,6E-07	6,6E-07	2,3E+04	1,5E-02	
SRC	Apatinib (YN968D1)	5,6E-06	2,9E-06	1,0E-06	1,0E-06	2,6E+04	2,7E-02	
SRC	ARRY334543	6,9E-06	3,6E-06	2,1E-06	2,1E-06	≈ 1,8E+05	≈ 3,7E-01	
SRC	AT9283	6,8E-08	3,6E-08	1,9E-08	1,9E-08	5,4E+06	1,0E-01	
SRC	Aurora A Inhibitor I	≥ 2,0E-05		≈ 2,6E-06	≈ 2,6E-06	≈ 2,5E+05	4,1E-01	2
SRC	Axitinib	≈ 4,4E-06	≈ 2,3E-06	1,7E-06	1,7E-06	≈ 5,3E+04	≈ 9,5E-02	
SRC	AZ 960	1,2E-07	6,2E-08	6,5E-08	6,5E-08	≈ 6,7E+06	≈ 3,6E-01	
SRC	AZ628	6,8E-07	3,6E-07	3,9E-07	3,9E-07	5,6E+04	2,2E-02	
SRC	AZD4547	1,2E-06	6,4E-07	3,2E-07	3,2E-07	≈ 5,9E+05	≈ 1,9E-01	
SRC	AZD5438	2,1E-06	1,1E-06	1,2E-06	1,2E-06	≈ 1,4E+05	≈ 1,7E-01	
SRC	AZD7762	4,8E-09	2,6E-09	3,4E-09	3,4E-09	1,1E+08	3,5E-01	
SRC	AZD8931	1,8E-07	9,4E-08	1,0E-07	1,0E-07	≈ 2,0E+06	≈ 2,0E-01	
SRC	Barasertib (AZD1152-HQPA)	3,6E-06	1,9E-06	1,4E-06	1,4E-06	≈ 1,1E+05	≈ 1,5E-01	
SRC	Baricitinib (LY3009104 - incb28050)	2,9E-06	1,5E-06	1,4E-06	1,4E-06	≈ 2,5E+05	≈ 3,6E-01	
SRC	BEZ235 (NVP-BEZ235)	≥ 2,0E-05		3,8E-06	3,8E-06	4,6E+03	1,8E-02	
SRC	BGJ398 (NVP-BGJ398)	4,9E-06	2,6E-06	2,0E-06	2,0E-06	4,6E+04	9,3E-02	
SRC	BI6727 (Volasertib)	≥ 2,0E-05		7,3E-06	7,3E-06	5,1E+02	3,6E-03	
SRC	BIBF1120 (Vargatef)	6,6E-08	3,5E-08	1,1E-08	1,1E-08	≈ 1,0E+07	≈ 9,8E-02	
SRC	BIX 02188	2,4E-06	1,3E-06	7,1E-07	7,1E-07	≥ 5,0E+05	≥ 3,5E-01	
SRC	BIX 02189	7,1E-06	3,8E-06	2,3E-06	2,3E-06	2,8E+04	6,3E-02	
SRC	BMS 777607	5,8E-07	3,0E-07	3,5E-07	3,5E-07	1,6E+05	5,7E-02	
SRC	BMS 794833	8,7E-07	4,6E-07	4,1E-07	4,1E-07	7,7E+04	3,1E-02	
SRC	BMS-265246	≥ 2,0E-05		4,4E-06	4,4E-06	3,0E+02	1,4E-03	
SRC	BMS-599626 (AC480)	1,7E-05	9,2E-06	5,1E-06	5,1E-06	≈ 3,2E+04	≈ 1,7E-01	
SRC	Bosutinib (SKI-606)	4,0E-10	2,1E-10	4,2E-10	4,2E-10	1,7E+07	6,8E-03	
SRC	Brivanib (BMS-540215)	2,4E-06	1,3E-06	1,0E-06	1,0E-06	≥ 3,3E+05	≥ 3,5E-01	
SRC	Brivanib alaninate (BMS-582664) - prodrug	≈ 5,4E-06	≈ 2,9E-06	7,7E-07	7,7E-07	≈ 8,4E+05	≈ 6,1E-01	
SRC	BX-795	1,6E-06	8,5E-07	1,0E-06	1,0E-06	≥ 3,4E+05	≥ 3,5E-01	
SRC	BX-912	8,1E-07	4,3E-07	4,9E-07	4,9E-07	≥ 7,2E+05	≥ 3,5E-01	
SRC	CCT129202	≥ 2,0E-05		6,0E-06	6,0E-06	2,9E+03	1,8E-02	2
SRC	CCT137690	3,3E-07	1,7E-07	1,4E-06	1,7E-07	n.e.	n.e.	2
SRC	Cediranib (AZD2171)	7,2E-07	3,8E-07	6,8E-08	3,8E-07	3,5E+06	2,4E-01	
SRC	CEP33779	7,6E-07	4,0E-07	6,3E-07	6,3E-07	≥ 5,6E+05	≥ 3,5E-01	
SRC	CH5424802	≥ 2,0E-05		1,8E-06	1,8E-06	3,5E+05	5,0E-01	
SRC	CHIR-124	3,3E-07	1,7E-07	4,1E-07	4,1E-07	1,9E+05	6,7E-02	
SRC	CI-1033 (Canertinib)	1,3E-07	7,1E-08	1,2E-07	1,2E-07	≈ 1,2E+06	≈ 1,7E-01	
SRC	CP 673451	8,8E-07	4,7E-07	3,2E-07	3,2E-07	≈ 9,5E+05	≈ 3,0E-01	
SRC	Crenolanib (CP-868596)	1,7E-06	9,0E-07	6,3E-07	6,3E-07	1,4E+05	8,8E-02	
SRC	Crizotinib (PF-02341066)	3,1E-07	1,6E-07	5,9E-07	5,9E-07	n.e.	n.e.	2
SRC	CX-4945 (Silmintasertib)	4,9E-06	2,6E-06	1,8E-06	1,8E-06	4,8E+04	8,6E-02	
SRC	CYC116	2,1E-07	1,1E-07	1,3E-07	1,3E-07	≥ 2,7E+06	≥ 3,5E-01	
SRC	Cyt387	1,4E-06	7,6E-07	6,1E-07	6,1E-07	2,1E+05	1,3E-01	1
SRC	Dabrafenib (GSK2118436)	1,1E-06	5,6E-07	2,1E-07	2,1E-07	3,6E+05	7,2E-02	
SRC	Dacomitinib (PF299804 - PF-00299804)	4,8E-07	2,5E-07	5,9E-07	5,9E-07	≈ 1,8E+05	≈ 1,0E-01	
SRC	Danuseritib (PHA-739358)	1,5E-08	7,9E-09	1,2E-08	1,2E-08	2,1E+05	2,4E-03	
SRC	Dasatinib (BMS-354825)	≤ 1,1E-10	≤ 5,7E-11	≤ 1,2E-11	≤ 1,2E-11	3,5E+07	4,1E-04	
SRC	DCC-2036 (Rebastinib)	1,6E-08	8,4E-09	n.e.	8,4E-09	2,8E+04	≤ 2,3E-04	4
SRC	Desmethyl Erlotinib (CP-473420)	3,7E-07	2,0E-07	1,9E-07	1,9E-07	1,1E+06	2,0E-01	
SRC	Dovitinib (TKI-258)	1,2E-07	6,5E-08	5,1E-08	5,1E-08	1,3E+07	5,9E-01	
SRC	E7080 (Lenvatinib)	9,2E-06	4,9E-06	2,9E-06	2,9E-06	3,5E+04	1,0E-01	
SRC	ENMD-2076	1,6E-08	8,6E-09	8,8E-09	8,8E-09	6,7E+06	6,0E-02	
SRC	Erlotinib HCl	6,2E-07	3,3E-07	5,3E-07	5,3E-07	≥ 6,6E+05	≥ 3,5E-01	
SRC	Flavopiridol HCl	5,9E-06	3,1E-06	4,1E-06	4,1E-06	2,2E+04	9,0E-02	
SRC	Foretinib (GSK1363089 - XL880)	9,5E-09	5,0E-09	7,2E-09	7,2E-09	1,6E+06	1,2E-02	
SRC	GDC-0941	≥ 2,0E-05		7,3E-06	7,3E-06	7,9E+04	5,5E-01	
SRC	GDC-0980 (RG7422)	3,5E-07	1,8E-07	3,5E-07	3,5E-07	≈ 2,1E+05	≈ 7,0E-02	
SRC	Gefitinib (Iressa)	6,5E-07	3,4E-07	8,5E-07	8,5E-07	≈ 6,3E+05	≈ 5,0E-01	
SRC	Golvatinib (E7050)	4,2E-07	2,2E-07	2,1E-07	2,1E-07	3,7E+05	7,9E-02	
SRC	GSK1070916	7,2E-07	3,8E-07	4,9E-07	4,9E-07	2,8E+05	1,3E-01	
SRC	GSK1838705A	≥ 2,0E-05		6,7E-06	6,7E-06	1,3E+03	8,4E-03	
SRC	Hesperadin	1,1E-08	5,7E-09	1,6E-09	1,6E-09	7,1E+07	1,0E-01	

kinase	Compound	IC ₅₀ [M] ePCA	K _D eq [M] ePCA *	K _D kin [M] kPCA	K _D [M] PCA **	k _{on} [M ⁻¹ s ⁻¹] kPCA	k _{off} [s ⁻¹] kPCA	comment
SRC	Imatinib (Gleevec)	1,7E-05	9,1E-06	n.e.	9,1E-06	2,8E+02	≤ 2,5E-03	4
SRC	INK 128 (MLN0128)	4,2E-06	2,2E-06	1,4E-06	1,4E-06	≥ 2,4E+05	≥ 3,5E-01	
SRC	JNJ-7706621	1,6E-06	8,6E-07	8,4E-07	8,4E-07	≈ 3,4E+05	≈ 3,1E-01	
SRC	Ki8751	≈ 4,3E-07	≈ 2,3E-07	9,6E-07	9,6E-07	2,5E+05	2,4E-01	2
SRC	KRN 633	≥ 2,0E-05		6,3E-06	6,3E-06	n.e.	n.e.	
SRC	KW 2449	1,7E-06	9,2E-07	5,4E-06	9,2E-07	1,4E+05	7,1E-01	
SRC	Lapatinib Ditosylate (Tykerb)	≥ 2,0E-05		5,4E-06	5,4E-06	7,6E+02	4,2E-03	
SRC	LDN193189	1,7E-06	9,0E-07	9,0E-07	9,0E-07	≈ 4,6E+05	≈ 4,8E-01	
SRC	Linifanib (ABT-869)	≥ 2,0E-05		2,9E-06	2,9E-06	8,3E+03	2,4E-02	
SRC	Linsitinib (OSI-906)	1,9E-05	9,8E-06	4,0E-06	4,0E-06	≈ 2,1E+04	≈ 8,1E-02	
SRC	LY2784544	5,4E-08	2,8E-08	2,3E-08	2,3E-08	≈ 2,1E+07	≈ 4,9E-01	2
SRC	Masitinib (AB1010)	1,4E-06	7,6E-07	6,5E-07	6,5E-07	2,3E+04	1,5E-02	
SRC	MGCD-265	1,4E-08	7,5E-09	6,4E-09	6,4E-09	1,4E+06	9,0E-03	
SRC	Milciclib (PHA-848125)	≈ 7,4E-08	≈ 3,9E-08	2,2E-08	2,2E-08	≈ 7,1E+06	≈ 1,6E-01	
SRC	MK-2461	7,1E-06	3,8E-06	3,6E-06	3,6E-06	≥ 9,6E+04	≥ 3,5E-01	
SRC	MK-5108 (VX-689)	8,5E-08	4,5E-08	3,1E-08	3,1E-08	1,5E+07	4,7E-01	
SRC	MLN8054	7,8E-07	4,1E-07	2,9E-07	2,9E-07	3,0E+05	9,0E-02	
SRC	MLN8237 (Alisertib)	1,9E-07	9,8E-08	1,1E-07	1,1E-07	≈ 1,7E+06	≈ 2,0E-01	
SRC	Motesanib Diphosphate (AMG-706)	1,4E-05	7,6E-06	6,8E-06	6,8E-06	9,4E+02	6,7E-03	
SRC	Neratinib (HKI-272)	1,4E-06	7,5E-07	6,0E-07	6,0E-07	1,9E+05	1,2E-01	
SRC	Nilotinib (AMN-107)	≥ 2,0E-05		3,4E-06	3,4E-06	1,4E+03	4,7E-03	
SRC	NVP-ADW742	1,6E-06	8,7E-07	8,4E-07	8,4E-07	1,6E+05	1,4E-01	
SRC	NVP-BGT226	≥ 2,0E-05		2,0E-06	2,0E-06	≥ 1,7E+05	≥ 3,5E-01	
SRC	NVP-BHG712	9,4E-06	5,0E-06	3,3E-06	3,3E-06	2,1E+03	6,7E-03	
SRC	NVP-BSK805	2,1E-07	1,1E-07	1,3E-07	1,3E-07	≈ 9,3E+05	≈ 1,3E-01	
SRC	NVP-TAE226	1,4E-06	7,6E-07	4,3E-07	4,3E-07	1,3E+06	5,5E-01	
SRC	OSI-930	9,3E-07	4,9E-07	6,9E-07	6,9E-07	1,4E+05	9,7E-02	
SRC	Pazopanib HCl	2,2E-07	1,2E-07	3,2E-07	3,2E-07	≈ 3,2E+05	≈ 1,1E-01	
SRC	PCI-32765 (ibrutinib)	2,6E-08	1,4E-08	2,2E-08	2,2E-08	2,3E+06	4,5E-02	
SRC	PD153035 HCl	6,2E-07	3,3E-07	6,1E-07	6,1E-07	≈ 1,9E+05	≈ 1,1E-01	
SRC	PD173074	1,4E-05	7,3E-06	6,0E-06	6,0E-06	≥ 5,8E+04	≥ 3,5E-01	
SRC	Pelitinib (EKB-569)	1,6E-07	8,4E-08	6,8E-08	6,8E-08	≈ 4,1E+06	≈ 2,7E-01	
SRC	PF-00562271	2,6E-07	1,4E-07	1,6E-07	1,6E-07	≈ 5,5E+06	≈ 1,0E+00	
SRC	PF-03814735	≈ 7,9E-08	≈ 4,2E-08	4,7E-08	4,7E-08	≥ 7,4E+06	≥ 3,5E-01	
SRC	PHA-665752	3,4E-06	1,8E-06	9,4E-07	9,4E-07	≈ 4,0E+05	≈ 3,5E-01	
SRC	PHA-680632	5,6E-08	2,9E-08	2,0E-08	2,0E-08	1,7E+06	3,4E-02	
SRC	PIK-75	1,1E-07	5,6E-08	6,4E-08	6,4E-08	≈ 4,5E+06	≈ 3,0E-01	2
SRC	PLX-4720	1,1E-06	6,0E-07	3,0E-07	3,0E-07	≈ 7,6E+05	≈ 2,1E-01	
SRC	Ponatinib (AP24534)	1,8E-09	9,4E-10	n.e.	9,4E-10	3,4E+05	≤ 3,1E-04	4
SRC	PP-121	4,8E-09	2,6E-09	8,7E-09	8,7E-09	4,0E+07	3,4E-01	
SRC	PP242	6,5E-07	3,4E-07	1,7E-07	1,7E-07	≈ 3,1E+06	≈ 4,6E-01	
SRC	Quercetin (Sophoretin)	5,0E-06	2,6E-06	2,5E-06	2,5E-06	≈ 5,7E+04	≈ 1,3E-01	
SRC	R406	1,3E-08	7,1E-09	6,1E-09	6,1E-09	3,7E+07	2,1E-01	
SRC	R788 (Fostamatinib) - prodrug	8,9E-07	4,7E-07	3,9E-07	3,9E-07	1,0E+06	2,3E-01	
SRC	Ruxolitinib (INCB018424)	3,3E-06	1,7E-06	2,6E-06	2,6E-06	≥ 1,3E+05	≥ 3,5E-01	
SRC	Saracatinib (AZD0530)	3,0E-09	1,6E-09	1,0E-09	1,0E-09	2,4E+07	2,4E-02	
SRC	SB 202190	2,8E-06	1,5E-06	1,6E-06	1,6E-06	≈ 2,1E+05	≈ 3,5E-01	
SRC	SB 203580	3,0E-06	1,6E-06	2,3E-06	2,3E-06	≥ 1,5E+05	≥ 3,5E-01	
SRC	Semaxanib (SU5416)	≥ 2,0E-05		2,9E-06	2,9E-06	3,2E+04	9,5E-02	
SRC	SNS-314	1,4E-05	7,5E-06	5,8E-06	5,8E-06	≈ 1,3E+04	≈ 8,3E-02	
SRC	SP600125	1,7E-05	8,8E-06	4,5E-06	4,5E-06	≥ 7,7E+04	≥ 3,5E-01	
SRC	Staurosporine	4,9E-09	2,6E-09	1,3E-09	1,3E-09	6,5E+07	8,4E-02	
SRC	SU11274	1,7E-07	9,2E-08	3,4E-07	3,4E-07	≈ 8,1E+05	≈ 2,7E-01	
SRC	Sunitinib Malate (Sutent)	2,0E-07	1,0E-07	1,5E-07	1,5E-07	≥ 2,3E+06	≥ 3,5E-01	
SRC	TAE684 (NVP-TAE684)	3,5E-07	1,9E-07	5,0E-08	5,0E-08	6,8E+06	3,3E-01	2
SRC	TAK-285	1,3E-05	7,0E-06	3,4E-06	3,4E-06	≈ 1,1E+04	≈ 3,3E-02	
SRC	TAK-901	≈ 5,7E-10	≈ 3,0E-10	1,0E-09	1,0E-09	1,8E+07	1,8E-02	
SRC	TG100-115	≥ 2,0E-05		4,7E-06	4,7E-06	3,2E+02	1,5E-03	
SRC	TG101209	2,6E-08	1,4E-08	1,9E-08	1,9E-08	≈ 9,6E+06	≈ 1,8E-01	
SRC	TG101348 (SAR302503)	9,8E-08	5,2E-08	5,2E-08	5,2E-08	≈ 5,4E+06	≈ 3,0E-01	
SRC	Tie2 kinase inhibitor	≥ 2,0E-05		8,1E-06	8,1E-06	≈ 1,3E+03	≈ 1,0E-02	
SRC	Tivozanib (AV-951)	9,2E-08	4,8E-08	5,0E-08	5,0E-08	1,3E+06	6,7E-02	
SRC	Torin 2	1,8E-05	9,4E-06	4,4E-06	4,4E-06	≈ 4,4E+04	≈ 1,9E-01	
SRC	TPCA-1	2,1E-07	1,1E-07	2,4E-07	2,4E-07	≥ 1,5E+06	≥ 3,5E-01	
SRC	TSU-68 (SU6668)	6,5E-06	3,4E-06	2,4E-06	2,4E-06	≥ 1,5E+05	≥ 3,5E-01	
SRC	TWS119	3,3E-08	1,8E-08	5,0E-09	5,0E-09	5,6E+07	2,7E-01	
SRC	Vandetanib (Zactima)	1,5E-08	7,9E-09	4,0E-08	7,9E-09	≈ 6,5E+06	≈ 1,9E-01	
SRC	Vemurafenib (PLX4032)	1,7E-06	9,1E-07	3,9E-07	3,9E-07	4,9E+05	1,9E-01	
SRC	VX-680 (MK-0457 - Tozasertib)	2,2E-07	1,2E-07	1,7E-07	1,7E-07	2,3E+06	3,9E-01	
SRC	WHI-P154	7,7E-07	4,1E-07	4,0E-07	4,0E-07	1,9E+05	7,5E-02	
SRC	WZ3146	2,0E-07	1,0E-07	3,9E-07	3,9E-07	≈ 1,0E+06	≈ 3,8E-01	
SRC	WZ4002	≈ 6,2E-06	≈ 3,3E-06	6,6E-06	6,6E-06	n.e.	n.e.	
SRC	WZ8040	5,6E-07	2,9E-07	5,7E-07	5,7E-07	1,2E+05	7,0E-02	
SRC	XL-184 (Cabozantinib)	1,6E-07	8,2E-08	8,6E-08	8,6E-08	7,0E+05	6,0E-02	1
SRC	ZM-447439	1,9E-07	9,8E-08	3,6E-07	3,6E-07	≈ 7,9E+05	≈ 3,0E-01	
SYK	AEE788 (NVP-AEE788)	≥ 2,0E-05		5,7E-06	5,7E-06	≥ 6,1E+04	≥ 3,5E-01	
SYK	AMG458	≥ 2,0E-05		3,2E-06	3,2E-06	≥ 1,1E+05	≥ 3,5E-01	
SYK	AT9283	1,5E-06	3,2E-07	n.e.	3,2E-07	n.e.	n.e.	
SYK	Axitinib	≥ 2,0E-05		2,7E-06	2,7E-06	≥ 1,3E+05	≥ 3,5E-01	

kinase	Compound	IC ₅₀ [M] ePCA	K _D eq [M] ePCA *	K _D kin [M] kPCA	K _D [M] PCA **	k _{on} [M ⁻¹ s ⁻¹] kPCA	k _{off} [s ⁻¹] kPCA	comment
SYK	AZ 960	9,7E-06	2,1E-06	4,9E-07	4,9E-07	≥ 7,2E+05	≥ 3,5E-01	
SYK	AZD4547	6,6E-06	1,4E-06	n.e.	1,4E-06	n.e.	n.e.	
SYK	AZD5438	≥ 2,0E-05		1,7E-06	1,7E-06	≈ 1,1E+05	≈ 2,0E-01	
SYK	AZD7762	1,4E-06	3,1E-07	1,1E-07	1,1E-07	≥ 3,2E+06	≥ 3,5E-01	
SYK	BMS 794833	≥ 2,0E-05		2,7E-06	2,7E-06	≥ 1,3E+05	≥ 3,5E-01	
SYK	Bosutinib (SKI-606)	1,2E-05	2,6E-06	6,5E-07	6,5E-07	≥ 5,4E+05	≥ 3,5E-01	
SYK	BX-795	n.e.	n.e.	5,4E-07	5,4E-07	≥ 6,5E+05	≥ 3,5E-01	
SYK	BX-912	5,0E-06	1,1E-06	3,3E-07	3,3E-07	≈ 1,1E+06	≈ 4,1E-01	
SYK	CCT137690	≥ 2,0E-05		3,1E-06	3,1E-06	≥ 1,1E+05	≥ 3,5E-01	
SYK	CP 673451	1,6E-05	3,5E-06	7,7E-06	7,7E-06	≥ 4,6E+04	≥ 3,5E-01	
SYK	Crenolanib (CP-868596)	≥ 2,0E-05		5,3E-06	5,3E-06	≈ 9,3E+03	≈ 5,5E-02	
SYK	CX-4945 (Silmatasertib)	≥ 2,0E-05		4,4E-06	4,4E-06	≥ 8,0E+04	≥ 3,5E-01	
SYK	CYC116	1,3E-05	2,8E-06	4,8E-07	2,8E-06	n.e.	n.e.	
SYK	Cyt387	≥ 2,0E-05		1,2E-06	1,2E-06	≈ 4,8E+04	≈ 6,7E-02	
SYK	Dabrafenib (GSK2118436)	≈ 2,0E-05	≈ 4,4E-06	≈ 3,5E-06	≈ 3,9E-06	≥ 1,0E+05	≥ 3,5E-01	
SYK	Danuseritib (PHA-739358)	≥ 2,0E-05		6,4E-06	6,4E-06	≥ 5,5E+04	≥ 3,5E-01	
SYK	Dasatinib (BMS-354825)	1,7E-05	3,7E-06	6,3E-07	3,7E-06	n.e.	n.e.	
SYK	DCC-2036 (Rebastinib)	8,1E-06	1,8E-06	5,6E-07	5,6E-07	1,1E+04	6,1E-03	
SYK	Dovitinib (TKI-258)	≥ 2,0E-05		2,4E-06	2,4E-06	≈ 1,4E+05	≈ 3,5E-01	
SYK	E7080 (Lenvatinib)	≥ 2,0E-05		n.e.	≥ 4,4E-06	n.e.	n.e.	
SYK	ENMD-2076	3,2E-06	7,1E-07	≈ 3,2E-07	7,1E-07	≥ 1,1E+06	≥ 3,5E-01	
SYK	Foretinib (GSK1363089 - XL880)	1,4E-05	3,1E-06	≈ 1,7E-06	3,1E-06	≥ 2,1E+05	≥ 3,5E-01	
SYK	GDC-0879	≥ 2,0E-05		n.e.	≥ 4,4E-06	n.e.	n.e.	
SYK	GDC-0980 (RG7422)	1,4E-05	3,1E-06	1,6E-06	1,6E-06	≥ 2,2E+05	≥ 3,5E-01	
SYK	Hesperadin	1,6E-05	3,5E-06	4,2E-07	3,5E-06	n.e.	n.e.	
SYK	INCB28060	≥ 2,0E-05		n.e.	≥ 4,4E-06	n.e.	n.e.	
SYK	INK 128 (MLN0128)	≥ 2,0E-05		n.e.	≥ 4,4E-06	n.e.	n.e.	
SYK	JNJ-38877605	≥ 2,0E-05		n.e.	≥ 4,4E-06	n.e.	n.e.	
SYK	JNJ-7706621	1,0E-05	2,3E-06	n.e.	2,3E-06	n.e.	n.e.	
SYK	KW 2449	1,2E-05	2,7E-06	2,0E-06	2,0E-06	≥ 1,8E+05	≥ 3,5E-01	
SYK	LDN193189	≥ 2,0E-05		3,5E-06	3,5E-06	≥ 1,0E+05	≥ 3,5E-01	
SYK	LY2784544	≥ 2,0E-05		9,1E-07	9,1E-07	≈ 3,6E+04	≈ 3,1E-02	
SYK	MGCD-265	4,9E-07	1,1E-07	6,7E-08	6,7E-08	2,3E+06	1,5E-01	
SYK	Milciclib (PHA-848125)	≥ 2,0E-05		3,7E-06	3,7E-06	≈ 1,2E+04	≈ 5,2E-02	
SYK	MK-5108 (VX-689)	9,8E-06	2,1E-06	6,7E-07	6,7E-07	≥ 5,3E+05	≥ 3,5E-01	
SYK	Motesanib Diphosphate (AMG-706)	≥ 2,0E-05		4,5E-06	4,5E-06	≥ 7,9E+04	≥ 3,5E-01	
SYK	NVP-BSK805	≥ 2,0E-05		6,4E-06	6,4E-06	≈ 3,4E+04	≈ 1,9E-01	
SYK	NVP-TAE226	≥ 2,0E-05		n.e.	≥ 4,4E-06	n.e.	n.e.	
SYK	OSI-930	≥ 2,0E-05		n.e.	≥ 4,4E-06	n.e.	n.e.	
SYK	OSU-03012	≥ 2,0E-05		n.e.	≥ 4,4E-06	n.e.	n.e.	
SYK	Pazopanib HCl	≥ 2,0E-05		3,2E-07	3,2E-07	≥ 1,1E+06	≥ 3,5E-01	
SYK	PD173074	≥ 2,0E-05		n.e.	≥ 4,4E-06	n.e.	n.e.	
SYK	Pellitinib (EKB-569)	≥ 2,0E-05		3,9E-06	3,9E-06	≈ 3,8E+04	≈ 1,3E-01	
SYK	PF-00562271	1,5E-05	3,2E-06	7,9E-07	7,9E-07	≥ 4,4E+05	≥ 3,5E-01	
SYK	PF-03814735	2,0E-07	4,3E-08	1,5E-08	1,5E-08	≈ 1,7E+07	≈ 2,1E-01	
SYK	PHA-680632	≥ 2,0E-05		4,1E-06	4,1E-06	≥ 8,6E+04	≥ 3,5E-01	
SYK	Ponatinib (AP24534)	≥ 2,0E-05		5,1E-06	5,1E-06	≈ 9,7E+03	≈ 5,7E-02	
SYK	PP-121	≥ 2,0E-05		5,4E-06	5,4E-06	≥ 6,5E+04	≥ 3,5E-01	
SYK	Quercetin (Sophostein)	≥ 2,0E-05		4,5E-06	4,5E-06	≥ 7,8E+04	≥ 3,5E-01	
SYK	R406	≥ 2,0E-05		3,9E-08	3,9E-08	n.e.	n.e.	2
SYK	R788 (Fostatinib) - prodrug	7,5E-06	1,7E-06	3,5E-06	3,5E-06	≈ 1,5E+05	2,4E-01	
SYK	Sotrastaurin (AEB071)	≥ 2,0E-05		n.e.	≥ 4,4E-06	n.e.	n.e.	
SYK	SP600125	1,8E-05	4,0E-06	1,4E-06	1,4E-06	≥ 2,4E+05	≥ 3,5E-01	
SYK	Staurosporine	7,8E-09	1,7E-09	3,5E-10	3,5E-10	1,7E+07	6,0E-03	
SYK	TAE684 (NVP-TAE684)	≥ 2,0E-05		n.e.	≥ 4,4E-06	n.e.	n.e.	
SYK	TAK-901	2,4E-06	5,3E-07	2,9E-07	2,9E-07	≥ 1,2E+06	≥ 3,5E-01	
SYK	TG101209	1,7E-05	3,7E-06	1,4E-06	1,4E-06	≈ 7,8E+04	≈ 1,3E-01	
SYK	TG101348 (SAR302503)	≥ 2,0E-05		4,8E-06	4,8E-06	≥ 7,3E+04	≥ 3,5E-01	
SYK	Tideglusib	≥ 2,0E-05		n.e.	≥ 4,4E-06	n.e.	n.e.	
SYK	Tivozanib (AV-951)	≥ 2,0E-05		n.e.	≥ 4,4E-06	n.e.	n.e.	
SYK	TPCA-1	≥ 2,0E-05		2,9E-06	2,9E-06	≥ 1,2E+05	≥ 3,5E-01	
SYK	TSU-68 (SU6668)	≥ 2,0E-05		4,6E-06	4,6E-06	≈ 1,5E+04	≈ 6,7E-02	
SYK	TWS119	2,8E-06	6,1E-07	1,3E-07	1,3E-07	1,1E+06	≈ 1,5E-01	1
SYK	Tyrphostin AG 879 (AG 879)	≥ 2,0E-05		n.e.	≥ 4,4E-06	n.e.	n.e.	
SYK	VX-680 (MK-0457 - Tozasertib)	1,1E-05	2,4E-06	6,0E-07	6,0E-07	≥ 5,8E+05	≥ 3,5E-01	
SYK	WZ3146	≥ 2,0E-05		n.e.	≥ 4,4E-06	n.e.	n.e.	
SYK	WZ4002	≥ 2,0E-05		n.e.	≥ 4,4E-06	n.e.	n.e.	
SYK	WZ8040	4,1E-06	9,0E-07	≈ 4,7E-07	9,0E-07	≥ 7,5E+05	≥ 3,5E-01	
SYK	XL147	≥ 2,0E-05		n.e.	≥ 4,4E-06	n.e.	n.e.	
SYK	XL-184 (Cabozantinib)	≥ 2,0E-05		n.e.	≥ 4,4E-06	n.e.	n.e.	
SYK	XL765	≥ 2,0E-05		6,1E-06	6,1E-06	≥ 5,7E+04	≥ 3,5E-01	
SYK	ZM-447439	n.e.	n.e.	≥ 2,0E-05	≥ 2,0E-05			
TGFBR1	A66	1,9E-05	1,1E-05	9,3E-06	9,3E-06	≥ 3,8E+04	≥ 3,5E-01	
TGFBR1	A-674563	3,3E-06	2,0E-06	3,7E-06	3,7E-06	≈ 2,4E+04	≈ 1,2E-01	
TGFBR1	AEE788 (NVP-AEE788)	7,1E-07	4,4E-07	6,7E-07	6,7E-07	≥ 5,2E+05	≥ 3,5E-01	
TGFBR1	Afatinib (BIBW2992)	1,3E-05	7,9E-06	≈ 5,9E-06	7,9E-06	≥ 5,9E+04	≥ 3,5E-01	
TGFBR1	AG-1024	1,2E-06	7,1E-07	≈ 7,4E-07	7,1E-07	≥ 4,7E+05	≥ 3,5E-01	
TGFBR1	AG-1478 (Tyrphostin AG-1478)	1,7E-06	1,0E-06	2,9E-06	2,9E-06	6,6E+04	1,9E-01	
TGFBR1	ARRY334543	≥ 2,0E-05		5,4E-06	5,4E-06	≥ 6,5E+04	≥ 3,5E-01	

kinase	Compound	IC ₅₀ [M] ePCA	K _D eq [M] ePCA *	K _D kin [M] kPCA	K _D [M] PCA **	k _{on} [M ⁻¹ s ⁻¹] kPCA	k _{off} [s ⁻¹] kPCA	comment
TGFBR1	Arry-380	≥ 2,0E-05		n.e.	≥ 1,2E-05	n.e.	n.e.	
TGFBR1	AS-252424	3,9E-07	2,4E-07	6,6E-07	6,6E-07	≥ 5,3E+05	≥ 3,5E-01	
TGFBR1	AS-605240	≈ 6,1E-06	≈ 3,7E-06	3,8E-06	3,8E-06	≥ 9,2E+04	≥ 3,5E-01	
TGFBR1	AT7867	1,9E-05	1,2E-05	1,4E-05	1,4E-05	≥ 2,5E+04	≥ 3,5E-01	
TGFBR1	AT9283	2,1E-08	1,3E-08	9,4E-09	9,4E-09	1,4E+06	1,3E-02	
TGFBR1	Aurora A Inhibitor I	7,2E-07	4,5E-07	3,3E-06	4,5E-07	n.e.	n.e.	2
TGFBR1	Axitinib	2,6E-07	1,6E-07	3,4E-07	3,4E-07	≥ 1,0E+06	≥ 3,5E-01	
TGFBR1	AZ 960	1,5E-07	9,3E-08	1,1E-07	1,1E-07	≥ 3,2E+06	≥ 3,5E-01	
TGFBR1	AZD4547	2,2E-06	1,4E-06	9,1E-07	9,1E-07	≥ 3,9E+05	≥ 3,5E-01	
TGFBR1	AZD5438	9,8E-08	6,1E-08	≈ 8,1E-08	6,1E-08	≈ 2,8E+06	≈ 3,9E-01	
TGFBR1	AZD7762	1,2E-06	7,7E-07	7,2E-07	7,2E-07	≥ 4,8E+05	≥ 3,5E-01	
TGFBR1	AZD8931	4,2E-07	2,6E-07	2,8E-07	2,8E-07	≈ 5,3E+05	≈ 1,5E-01	
TGFBR1	Barasertib (AZD1152-HQPA)	1,3E-06	8,3E-07	9,0E-07	9,0E-07	≥ 3,9E+05	≥ 3,5E-01	
TGFBR1	Baricitinib (LY3009104 - incb28050)	4,1E-06	2,5E-06	2,0E-06	2,0E-06	≥ 1,7E+05	≥ 3,5E-01	
TGFBR1	BEZ235 (NVP-BEZ235)	≈ 9,3E-06	≈ 5,7E-06	1,8E-06	1,8E-06	2,8E+05	4,9E-01	
TGFBR1	BGJ398 (NVP-BGJ398)	7,9E-06	4,9E-06	5,7E-06	5,7E-06	≥ 6,2E+04	≥ 3,5E-01	
TGFBR1	BIBF1120 (Vargatef)	3,0E-08	1,9E-08	≈ 1,6E-08	1,9E-08	≈ 2,9E+06	≈ 4,5E-02	
TGFBR1	BIX 02188	8,0E-07	5,0E-07	4,0E-07	4,0E-07	≥ 8,7E+05	≥ 3,5E-01	
TGFBR1	BIX 02189	1,1E-07	7,0E-08	7,5E-08	7,5E-08	≈ 1,9E+06	1,2E-01	
TGFBR1	BMS-265246	≥ 2,0E-05		1,0E-05	1,0E-05	≥ 3,4E+04	≥ 3,5E-01	
TGFBR1	BMS-599626 (AC480)	7,0E-06	4,3E-06	3,6E-06	3,6E-06	≥ 9,9E+04	≥ 3,5E-01	
TGFBR1	Bosutinib (SKI-606)	5,1E-06	3,2E-06	1,2E-06	1,2E-06	≥ 2,9E+05	≥ 3,5E-01	
TGFBR1	Brivanib (BMS-540215)	1,7E-06	1,1E-06	2,4E-06	2,4E-06	≈ 1,1E+05	≈ 2,6E-01	
TGFBR1	Brivanib alaninate (BMS-582664) - prodrug	3,7E-06	2,3E-06	2,3E-06	2,3E-06	≥ 1,5E+05	≥ 3,5E-01	
TGFBR1	BX-795	5,8E-07	3,6E-07	6,0E-07	6,0E-07	≥ 5,9E+05	≥ 3,5E-01	
TGFBR1	BX-912	1,5E-06	9,5E-07	1,3E-06	1,3E-06	≥ 2,6E+05	≥ 3,5E-01	
TGFBR1	BYL719	8,0E-06	5,0E-06	5,5E-06	5,5E-06	≥ 6,4E+04	≥ 3,5E-01	
TGFBR1	CCT128930	1,3E-05	7,8E-06	8,7E-06	8,7E-06	≥ 4,0E+04	≥ 3,5E-01	
TGFBR1	CCT129202	≥ 2,0E-05		6,4E-06	6,4E-06	n.e.	n.e.	
TGFBR1	CCT137690	2,4E-06	1,5E-06	3,0E-06	3,0E-06	≥ 1,2E+05	≥ 3,5E-01	
TGFBR1	Cediranib (AZD2171)	7,7E-07	4,8E-07	7,6E-08	4,8E-07	n.e.	n.e.	
TGFBR1	CEP33779	6,1E-06	3,8E-06	3,7E-06	3,7E-06	≥ 9,5E+04	≥ 3,5E-01	
TGFBR1	CHIR-124	≥ 2,0E-05		7,4E-06	7,4E-06	≥ 4,7E+04	≥ 3,5E-01	
TGFBR1	CI-1033 (Canertinib)	4,6E-07	2,9E-07	3,8E-07	3,8E-07	1,5E+06	5,4E-01	
TGFBR1	CI-1040 (PD184352)	≥ 2,0E-05		5,5E-06	5,5E-06	≥ 6,3E+04	≥ 3,5E-01	
TGFBR1	CP 673451	2,3E-07	3,9E-07	4,5E-07	4,5E-07	≈ 1,3E+05	≈ 6,3E-02	
TGFBR1	Crenolanib (CP-868596)	2,1E-07	1,3E-07	9,3E-08	9,3E-08	≈ 2,1E+06	≈ 1,4E-01	
TGFBR1	Crizotinib (PF-02341066)	5,0E-08	3,1E-08	1,4E-07	1,4E-07	n.e.	n.e.	2
TGFBR1	CX-4945 (Silmintasertib)	2,8E-07	1,7E-07	2,8E-07	2,8E-07	≥ 1,3E+06	≥ 3,5E-01	
TGFBR1	CYC116	4,3E-08	2,7E-08	2,9E-08	2,9E-08	≈ 2,9E+06	≈ 8,7E-02	
TGFBR1	Cyt387	6,5E-08	4,0E-08	4,1E-08	4,1E-08	≥ 8,6E+06	≥ 3,5E-01	
TGFBR1	Dabrafenib (GSK2118436)	1,7E-09	1,1E-09	n.e.	1,1E-09	≈ 1,2E+04	≤ 1,2E-05	4
TGFBR1	Dacomitinib (PF299804 - PF-00299804)	2,7E-06	1,6E-06	2,6E-06	2,6E-06	≈ 2,0E+04	≈ 3,1E-02	
TGFBR1	Danuseritib (PHA-739358)	3,8E-07	2,4E-07	2,6E-07	2,6E-07	1,0E+05	2,2E-02	
TGFBR1	Dasatinib (BMS-354825)	1,5E-08	9,5E-09	9,2E-09	9,2E-09	4,0E+06	3,7E-02	
TGFBR1	Desmethyl Erlotinib (CP-473420)	2,2E-06	1,3E-06	1,5E-06	1,5E-06	≈ 7,3E+04	≈ 1,4E-01	
TGFBR1	Dovitinib (TKI-258)	2,2E-06	1,4E-06	1,4E-06	1,4E-06	≥ 2,6E+05	≥ 3,5E-01	
TGFBR1	E7080 (Lenvatinib)	7,7E-07	4,7E-07	5,1E-07	5,1E-07	≈ 2,6E+05	≈ 1,3E-01	
TGFBR1	ENMD-2076	1,3E-07	7,9E-08	9,5E-08	9,5E-08	≈ 9,0E+05	≈ 7,7E-02	
TGFBR1	Enzastaurin (LY317615)	≥ 2,0E-05		9,2E-06	9,2E-06	1,1E+04	1,1E-01	
TGFBR1	Erlotinib HCl	1,1E-05	6,7E-06	5,4E-06	5,4E-06	≥ 6,5E+04	≥ 3,5E-01	
TGFBR1	Flavopiridol HCl	7,0E-07	4,3E-07	9,7E-07	9,7E-07	≈ 3,5E+05	≈ 3,4E-01	
TGFBR1	Foretinib (GSK1363089 - XL880)	3,1E-06	1,9E-06	3,5E-06	3,5E-06	≈ 2,7E+04	≈ 9,1E-02	
TGFBR1	GDC-0879	4,1E-07	2,6E-07	5,3E-07	5,3E-07	≥ 6,6E+05	≥ 3,5E-01	
TGFBR1	GDC-0941	≈ 4,8E-06	≈ 3,0E-06	4,2E-06	4,2E-06	≥ 8,3E+04	≥ 3,5E-01	
TGFBR1	Gefitinib (Iressa)	4,9E-06	3,0E-06	3,5E-06	3,5E-06	≥ 1,0E+05	≥ 3,5E-01	
TGFBR1	Golvatinib (E7050)	2,0E-05	1,2E-05	9,0E-06	9,0E-06	≥ 3,9E+04	≥ 3,5E-01	
TGFBR1	GSK1059615	2,9E-07	1,8E-07	1,8E-07	1,8E-07	≥ 1,9E+06	≥ 3,5E-01	
TGFBR1	GSK1070916	1,5E-08	9,4E-09	5,3E-08	9,4E-09	3,0E+05	1,4E-02	
TGFBR1	GSK2126458	9,8E-06	6,0E-06	4,8E-06	4,8E-06	≥ 7,2E+04	≥ 3,5E-01	
TGFBR1	Hesperadin	1,6E-08	9,8E-09	6,0E-09	6,0E-09	5,6E+06	3,2E-02	
TGFBR1	INK 128 (MLN0128)	4,2E-08	2,6E-08	2,9E-08	2,9E-08	≥ 1,2E+07	≥ 3,5E-01	
TGFBR1	JNJ-38877605	1,3E-05	7,8E-06	≥ 2,0E-05	≥ 7,8E-06			
TGFBR1	JNJ-7706621	2,6E-07	1,6E-07	1,8E-07	1,8E-07	≥ 1,9E+06	≥ 3,5E-01	
TGFBR1	Ki8751	≥ 2,0E-05		6,0E-06	6,0E-06	≈ 4,3E+04	≈ 2,4E-01	
TGFBR1	KW 2449	8,5E-07	5,3E-07	2,9E-06	5,3E-07	n.e.	n.e.	
TGFBR1	LDN193189	1,9E-09	1,2E-09	2,7E-09	2,7E-09	9,6E+06	2,4E-02	
TGFBR1	Linifanib (ABT-869)	1,7E-06	1,1E-06	6,2E-07	6,2E-07	n.e.	n.e.	
TGFBR1	Linsitinib (OSI-906)	5,3E-06	3,3E-06	3,0E-06	3,0E-06	≥ 1,2E+05	≥ 3,5E-01	
TGFBR1	LY2228820	7,5E-07	4,7E-07	3,1E-07	3,1E-07	1,5E+05	4,6E-02	
TGFBR1	LY2784544	4,9E-08	3,0E-08	3,7E-08	3,7E-08	6,4E+05	2,3E-02	
TGFBR1	MGCD-265	≥ 2,0E-05		9,9E-06	9,9E-06	n.e.	n.e.	
TGFBR1	Milciclib (PHA-848125)	6,5E-07	4,0E-07	4,2E-07	4,2E-07	≈ 7,9E+05	≈ 4,0E-01	
TGFBR1	MK-2461	≥ 2,0E-05		1,2E-05	1,2E-05	≥ 2,9E+04	≥ 3,5E-01	
TGFBR1	MK-5108 (VX-689)	5,1E-09	3,2E-09	8,7E-09	8,7E-09	3,2E+06	2,9E-02	
TGFBR1	Nilotinib (AMN-107)	≥ 2,0E-05		3,8E-06	3,8E-06	≥ 9,3E+04	≥ 3,5E-01	
TGFBR1	NVP-ADW742	2,3E-07	1,4E-07	3,3E-07	3,3E-07	≥ 1,1E+06	≥ 3,5E-01	
TGFBR1	NVP-BGT226	≥ 2,0E-05		2,2E-06	2,2E-06	≈ 2,6E+05	≈ 3,1E-01	
TGFBR1	NVP-BSK805	2,3E-07	1,4E-07	1,5E-07	1,5E-07	≥ 2,4E+06	≥ 3,5E-01	

kinase	Compound	IC ₅₀ [M] ePCA	K _D eq [M] ePCA *	K _D kin [M] kPCA	K _D [M] PCA **	k _{on} [M ⁻¹ s ⁻¹] kPCA	k _{off} [s ⁻¹] kPCA	comment
TGFBR1	NVP-BVU972	3,0E-06	1,9E-06	2,4E-06	2,4E-06	≥ 1,5E+05	≥ 3,5E-01	
TGFBR1	NVP-TAE226	5,8E-07	3,6E-07	6,5E-07	6,5E-07	≈ 1,5E+05	≈ 9,6E-02	
TGFBR1	OSI-027	7,5E-06	4,6E-06	1,0E-05	1,0E-05	≥ 3,5E+04	≥ 3,5E-01	
TGFBR1	Pazopanib HCl	≈ 9,3E-07	≈ 5,7E-07	1,2E-06	1,2E-06	≈ 3,6E+05	≈ 4,5E-01	
TGFBR1	PCI-32765 (Ibrutinib)	8,7E-07	5,4E-07	7,9E-07	7,9E-07	≈ 2,2E+05	≈ 2,0E-01	
TGFBR1	PD 0332991 (Palbociclib) HCl	≥ 2,0E-05		8,4E-06	8,4E-06	≥ 4,1E+04	≥ 3,5E-01	
TGFBR1	PD0325901	9,1E-07	5,6E-07	1,3E-06	1,3E-06	≥ 2,7E+05	≥ 3,5E-01	
TGFBR1	PD153035 HCl	1,1E-06	7,0E-07	1,5E-06	1,5E-06	≥ 2,3E+05	≥ 3,5E-01	
TGFBR1	PD173074	9,8E-07	6,1E-07	2,6E-07	2,6E-07	≈ 1,5E+06	≈ 5,5E-01	
TGFBR1	PD318088	3,8E-07	2,3E-07	5,2E-07	5,2E-07	≥ 6,8E+05	≥ 3,5E-01	
TGFBR1	PF-00562271	1,6E-06	1,0E-06	1,4E-06	1,4E-06	≈ 3,1E+05	≈ 4,2E-01	
TGFBR1	PF-03814735	1,2E-07	7,5E-08	n.e.	7,5E-08	6,3E+05	≈ 4,7E-02	4
TGFBR1	PHA-665752	1,4E-06	8,5E-07	1,3E-06	1,3E-06	≥ 2,7E+05	≥ 3,5E-01	
TGFBR1	PHA-680632	9,4E-08	5,8E-08	7,2E-08	7,2E-08	3,3E+05	2,4E-02	
TGFBR1	PHA-767491	1,2E-07	7,6E-08	1,4E-07	1,4E-07	≈ 1,6E+06	≈ 1,7E-01	
TGFBR1	Phenformin HCl	1,4E-05	8,8E-06	≥ 2,0E-05	≥ 8,8E-06			
TGFBR1	Piceatannol	5,3E-06	3,3E-06	4,9E-06	4,9E-06	≥ 7,1E+04	≥ 3,5E-01	
TGFBR1	PIK-294	1,3E-05	8,3E-06	8,8E-06	8,8E-06	≥ 4,0E+04	≥ 3,5E-01	
TGFBR1	PIK-75	2,7E-08	1,6E-08	2,2E-08	2,2E-08	≈ 2,7E+06	≈ 6,0E-02	
TGFBR1	PLX-4720	1,6E-07	1,0E-07	7,0E-08	7,0E-08	3,3E+06	2,3E-01	
TGFBR1	Ponatinib (AP24534)	1,6E-05	9,8E-06	≈ 1,4E-05	9,8E-06	n.e.	n.e.	
TGFBR1	PP-121	≤ 1,2E-10	≤ 7,4E-11	n.e.	≤ 7,4E-11	7,5E+06	≤ 5,5E-04	4
TGFBR1	PP242	9,1E-09	5,7E-09	2,7E-09	2,7E-09	1,6E+07	4,3E-02	
TGFBR1	Quercetin (Sophoretin)	1,2E-06	7,6E-07	2,2E-06	2,2E-06	≥ 1,6E+05	≥ 3,5E-01	
TGFBR1	R406	1,2E-07	7,3E-08	1,9E-07	1,9E-07	1,4E+06	2,9E-01	12
TGFBR1	R788 (Fostamatinib) - prodrug	2,6E-06	1,6E-06	3,2E-06	3,2E-06	≈ 3,3E+04	≈ 1,2E-01	
TGFBR1	Ruxolitinib (INC018424)	1,3E-06	8,0E-07	1,4E-06	1,4E-06	≥ 2,5E+05	≥ 3,5E-01	
TGFBR1	Saracatinib (AZD0530)	5,6E-09	3,5E-09	≈ 1,7E-09	3,5E-09	≈ 1,1E+06	≈ 1,9E-03	
TGFBR1	SB 202190	5,1E-08	3,2E-08	7,4E-08	7,4E-08	≥ 4,8E+06	≥ 3,5E-01	
TGFBR1	SB 203580	2,1E-07	1,3E-07	≈ 2,0E-07	1,3E-07	≥ 1,7E+06	≥ 3,5E-01	
TGFBR1	SB 216763	≥ 2,0E-05		≈ 1,6E-05	≈ 1,6E-05	≥ 2,2E+04	≥ 3,5E-01	
TGFBR1	SB 431542	9,7E-09	6,0E-09	9,5E-09	9,5E-09	6,2E+06	5,9E-02	
TGFBR1	SB 525334	1,6E-09	9,9E-10	1,1E-09	1,1E-09	1,7E+06	1,9E-03	
TGFBR1	SB590885	6,8E-08	4,2E-08	6,3E-08	6,3E-08	≈ 7,5E+06	≈ 4,5E-01	
TGFBR1	SP600125	1,5E-06	9,4E-07	≈ 8,5E-07	9,4E-07	≥ 4,1E+05	≥ 3,5E-01	
TGFBR1	Staurosporine	1,6E-08	9,7E-09	9,0E-09	9,0E-09	2,1E+06	1,9E-02	
TGFBR1	SU11274	2,3E-07	1,4E-07	8,9E-07	1,4E-07	n.e.	n.e.	
TGFBR1	Sunitinib Malate (Sutent)	1,2E-06	7,4E-07	1,0E-06	1,0E-06	≥ 3,5E+05	≥ 3,5E-01	
TGFBR1	TAE684 (NVP-TAE684)	1,4E-08	8,9E-09	7,3E-09	7,3E-09	8,4E+05	5,9E-03	
TGFBR1	TAK-901	2,8E-09	1,7E-09	6,9E-09	6,9E-09	1,7E+06	1,2E-02	
TGFBR1	Tandutinib (MLN518)	1,5E-05	9,0E-06	≈ 1,5E-05	9,0E-06	≥ 2,3E+04	≥ 3,5E-01	
TGFBR1	TG 100713	4,0E-06	2,5E-06	3,0E-06	3,0E-06	≥ 1,2E+05	≥ 3,5E-01	
TGFBR1	TG100-115	5,6E-06	3,5E-06	5,6E-06	5,6E-06	≥ 6,3E+04	≥ 3,5E-01	
TGFBR1	TG101209	1,9E-07	1,2E-07	1,5E-07	1,5E-07	≥ 2,3E+06	≥ 3,5E-01	
TGFBR1	TG101348 (SAR302503)	5,1E-07	3,1E-07	≈ 3,1E-07	3,1E-07	≥ 1,1E+06	≥ 3,5E-01	
TGFBR1	Thiazovivin	9,1E-07	5,6E-07	7,1E-07	7,1E-07	≈ 6,4E+05	≈ 4,7E-01	
TGFBR1	Tie2 kinase inhibitor	7,7E-09	4,8E-09	1,9E-08	1,9E-08	1,5E+06	2,7E-02	
TGFBR1	Tivozanib (AV-951)	8,8E-07	5,5E-07	1,1E-06	1,1E-06	≥ 3,1E+05	≥ 3,5E-01	
TGFBR1	Torin 2	1,4E-06	8,4E-07	9,7E-07	9,7E-07	≥ 3,6E+05	≥ 3,5E-01	
TGFBR1	TPCA-1	8,1E-07	5,0E-07	7,0E-07	7,0E-07	≥ 5,0E+05	≥ 3,5E-01	
TGFBR1	TWS119	1,8E-07	1,1E-07	1,4E-07	1,4E-07	≈ 2,1E+06	≈ 3,2E-01	
TGFBR1	Vandetanib (Zactima)	1,9E-07	1,2E-07	4,6E-07	4,6E-07	≈ 3,2E+05	≈ 1,3E-01	
TGFBR1	Vemurafenib (PLX4032)	1,0E-07	6,2E-08	2,0E-07	2,0E-07	1,4E+05	2,7E-02	2
TGFBR1	VX-680 (MK-0457 - Tozasertib)	5,6E-07	3,5E-07	8,5E-07	8,5E-07	≥ 4,1E+05	≥ 3,5E-01	
TGFBR1	VX-702	8,9E-06	5,5E-06	9,6E-06	9,6E-06	≈ 1,9E+04	≈ 1,4E-01	
TGFBR1	WHI-P154	8,4E-07	5,2E-07	9,6E-07	9,6E-07	≈ 2,6E+05	≈ 2,8E-01	
TGFBR1	WZ3146	1,6E-06	1,0E-06	8,4E-07	8,4E-07	≥ 4,2E+05	≥ 3,5E-01	
TGFBR1	WZ8040	3,3E-06	2,1E-06	4,4E-06	4,4E-06	≥ 7,9E+04	≥ 3,5E-01	
TGFBR1	Y-27632 2HCl	1,8E-05	1,1E-05	1,3E-05	1,3E-05	≥ 2,7E+04	≥ 3,5E-01	
TGFBR1	YM201636	≥ 2,0E-05		1,0E-05	1,0E-05	≥ 3,4E+04	≥ 3,5E-01	
Tie2	A-674563	1,2E-05	8,1E-06	≈ 7,4E-06	8,1E-06	≈ 2,4E+04	≈ 1,4E-01	
Tie2	AEE788 (NVP-AEE788)	6,6E-07	4,6E-07	1,3E-06	1,3E-06	≥ 2,6E+05	≥ 3,5E-01	
Tie2	Afatinib (BIBW2992)	3,6E-06	2,5E-06	2,7E-06	2,7E-06	≥ 1,3E+05	≥ 3,5E-01	
Tie2	AG-1478 (Typhostin AG-1478)	8,7E-06	6,0E-06	1,6E-05	1,6E-05	≥ 2,2E+04	≥ 3,5E-01	
Tie2	AMG 900	6,1E-08	4,2E-08	1,6E-07	1,6E-07	≥ 2,1E+06	≥ 3,5E-01	
Tie2	AMG458	1,2E-07	8,2E-08	1,2E-07	1,2E-07	≈ 2,8E+06	≈ 3,7E-01	
Tie2	AS-252424	3,5E-07	2,4E-07	8,7E-07	8,7E-07	5,0E+05	4,4E-01	
Tie2	AT9283	1,1E-07	7,3E-08	4,1E-08	4,1E-08	≈ 2,3E+06	≈ 1,1E-01	
Tie2	Axitinib	1,8E-07	1,2E-07	1,9E-07	1,9E-07	≈ 1,9E+06	≈ 3,5E-01	
Tie2	AZ 960	1,3E-06	9,3E-07	2,2E-06	2,2E-06	≈ 7,2E+04	≈ 1,1E-01	
Tie2	AZ628	4,2E-06	2,9E-06	2,9E-06	2,9E-06	1,1E+05	3,0E-01	
Tie2	AZD4547	1,7E-07	1,2E-07	7,4E-08	7,4E-08	9,8E+05	7,2E-02	
Tie2	AZD5438	3,6E-06	2,5E-06	4,0E-06	4,0E-06	≈ 3,3E+03	≈ 1,4E-02	
Tie2	AZD7762	1,5E-06	1,0E-06	1,8E-06	1,8E-06	≈ 2,4E+04	≈ 5,1E-02	
Tie2	AZD8931	6,2E-06	4,3E-06	4,7E-06	4,7E-06	2,5E+04	≈ 1,2E-01	
Tie2	Barasertib (AZD1152-HQPA)	3,4E-07	2,3E-07	3,4E-07	3,4E-07	≈ 1,5E+06	≈ 4,3E-01	
Tie2	Baricitinib (LY3009104 - incb28050)	1,4E-05	9,4E-06	5,8E-06	5,8E-06	≥ 6,0E+04	≥ 3,5E-01	
Tie2	BGJ398 (NVP-BGJ398)	1,1E-07	7,8E-08	9,6E-08	9,6E-08	1,8E+06	1,7E-01	
Tie2	BIBF1120 (Vargatef)	2,6E-07	1,8E-07	9,7E-08	9,7E-08	≈ 3,0E+05	≈ 2,9E-02	

kinase	Compound	IC ₅₀ [M] ePCA	K _D eq [M] ePCA *	K _D kin [M] kPCA	K _D [M] PCA **	k _{on} [M ⁻¹ s ⁻¹] kPCA	k _{off} [s ⁻¹] kPCA	comment
Tie2	BIRB 796 (Doramapimod)	2,7E-09	1,9E-09	2,7E-09	2,7E-09	2,2E+06	6,0E-03	
Tie2	BMS 777607	2,9E-08	2,0E-08	1,7E-08	1,7E-08	≥ 2,0E+07	≥ 3,5E-01	
Tie2	BMS 794833	9,4E-09	6,5E-09	1,2E-08	1,2E-08	4,1E+06	5,1E-02	
Tie2	BMS-599626 (AC480)	4,6E-06	3,2E-06	4,7E-06	4,7E-06	≈ 9,6E+04	≈ 3,9E-01	
Tie2	Bosutinib (SKI-606)	9,7E-07	6,7E-07	7,4E-07	7,4E-07	1,4E+05	1,1E-01	
Tie2	Brivanib (BMS-540215)	1,2E-07	8,2E-08	4,0E-07	4,0E-07	1,4E+05	5,5E-02	
Tie2	Brivanib alaninate (BMS-582664) - prodrug	4,0E-07	2,8E-07	≈ 4,0E-07	2,8E-07	≈ 4,8E+04	≈ 9,4E-02	
Tie2	BX-795	7,0E-07	4,8E-07	9,1E-07	9,1E-07	≈ 6,4E+04	≈ 5,7E-02	
Tie2	BX-912	6,5E-07	4,5E-07	1,9E-06	1,9E-06	≈ 7,5E+04	≈ 1,0E-01	
Tie2	CCT129202	≥ 2,0E-05		4,4E-06	4,4E-06	≥ 8,0E+04	≥ 3,5E-01	
Tie2	CCT137690	6,5E-07	4,5E-07	1,6E-06	1,6E-06	≥ 2,2E+05	≥ 3,5E-01	
Tie2	Cediranib (AZD2171)	4,1E-07	2,8E-07	5,6E-08	2,8E-07	≈ 4,6E+05	≈ 3,4E-02	
Tie2	CEP33779	1,4E-06	9,7E-07	1,2E-06	1,2E-06	≈ 4,3E+04	≈ 5,7E-02	
Tie2	CHIR-98014	1,5E-05	1,0E-05	≥ 2,0E-05	≥ 1,0E-05			
Tie2	CI-1033 (Canertinib)	9,2E-07	6,3E-07	1,6E-06	1,6E-06	≈ 4,6E+04	≈ 7,9E-02	
Tie2	CP 673451	3,3E-06	2,3E-06	3,3E-06	3,3E-06	≈ 4,0E+04	≈ 1,1E-01	
Tie2	CP-724714	1,2E-05	8,0E-06	≈ 8,5E-06	8,0E-06	≥ 4,1E+04	≥ 3,5E-01	
Tie2	Crenolanib (CP-868596)	2,7E-06	1,9E-06	1,8E-06	1,8E-06	2,8E+04	4,8E-02	
Tie2	Crizotinib (PF-02341066)	1,1E-07	7,6E-08	3,3E-07	3,3E-07	n.e.	n.e.	2
Tie2	CYC116	1,9E-07	1,3E-07	1,3E-07	1,3E-07	≥ 2,7E+06	≥ 3,5E-01	
Tie2	Cyt387	2,2E-06	1,5E-06	2,1E-06	2,1E-06	2,6E+04	5,4E-02	
Tie2	Dabrafenib (GSK2118436)	5,4E-08	3,7E-08	4,9E-07	3,7E-08	n.e.	n.e.	
Tie2	Dacomitinib (PF299804 - PF-00299804)	2,7E-06	1,9E-06	5,4E-06	5,4E-06	≈ 1,1E+04	≈ 6,0E-02	
Tie2	Danuserib (PHA-739358)	6,3E-08	4,3E-08	1,2E-07	1,2E-07	1,2E+05	1,3E-02	
Tie2	Dasatinib (BMS-354825)	1,4E-06	9,9E-07	1,2E-06	1,2E-06	≈ 1,7E+05	≈ 2,0E-01	
Tie2	DCC-2036 (Rebastinib)	2,8E-10	2,0E-10	1,5E-10	1,5E-10	2,7E+06	4,0E-04	
Tie2	Desmethyl Erlotinib (CP-473420)	1,1E-06	7,3E-07	9,1E-07	9,1E-07	9,0E+04	7,5E-02	
Tie2	Dovitinib (TKI-258)	1,3E-06	9,2E-07	9,5E-07	9,5E-07	≈ 5,5E+04	≈ 5,1E-02	
Tie2	E7080 (Lenvatinib)	6,1E-07	4,2E-07	6,3E-07	6,3E-07	1,1E+05	6,9E-02	
Tie2	ENMD-2076	7,8E-07	5,4E-07	8,5E-07	8,5E-07	≈ 5,1E+04	≈ 4,6E-02	
Tie2	Erlotinib HCl	2,3E-06	1,6E-06	2,3E-06	2,3E-06	≥ 1,5E+05	≥ 3,5E-01	
Tie2	Foretinib (GSK1363089 - XL880)	8,7E-10	6,0E-10	2,1E-09	2,1E-09	3,7E+06	7,9E-03	
Tie2	Golitinib (E7050)	5,4E-09	3,7E-09	4,0E-09	4,0E-09	1,6E+07	6,3E-02	
Tie2	GSK1070916	5,2E-09	3,6E-09	5,4E-09	5,4E-09	6,3E+06	3,2E-02	
Tie2	GSK461364	1,5E-05	1,1E-05	6,5E-06	6,5E-06	≈ 8,8E+03	≈ 5,6E-02	
Tie2	Hesperadin	3,6E-07	2,5E-07	1,2E-07	1,2E-07	≈ 2,5E+05	≈ 3,5E-02	
Tie2	INK 128 (MLN0128)	9,3E-07	6,5E-07	1,1E-06	1,1E-06	≥ 3,2E+05	≥ 3,5E-01	
Tie2	JNJ-7706621	2,3E-07	1,6E-07	1,0E-07	1,0E-07	≥ 3,4E+06	≥ 3,5E-01	
Tie2	Ki8751	3,9E-08	2,7E-08	2,4E-07	2,7E-08	n.e.	n.e.	2
Tie2	KRN 633	≈ 5,0E-06	≈ 3,4E-06	2,6E-06	2,6E-06	1,7E+04	4,2E-02	
Tie2	KW 2449	9,9E-07	6,8E-07	3,4E-06	6,8E-07	n.e.	n.e.	
Tie2	LDN193189	2,2E-06	1,5E-06	1,7E-06	1,7E-06	≈ 7,0E+04	≈ 1,3E-01	
Tie2	Linifanib (ABT-869)	9,1E-08	6,3E-08	9,1E-08	9,1E-08	2,5E+06	1,7E-01	
Tie2	Linsitinib (OSI-906)	4,3E-07	3,0E-07	6,0E-07	6,0E-07	≈ 1,4E+05	≈ 6,5E-02	
Tie2	LY2228820	7,1E-06	4,9E-06	6,7E-06	6,7E-06	≈ 2,6E+04	≈ 1,2E-01	
Tie2	LY2784544	1,7E-07	1,2E-07	3,4E-07	3,4E-07	≈ 1,1E+06	≈ 3,9E-01	
Tie2	MGCD-265	1,3E-08	9,2E-09	4,7E-08	9,2E-09	2,0E+06	9,4E-02	2
Tie2	Milciclib (PHA-848125)	4,6E-07	3,2E-07	2,5E-07	2,5E-07	≈ 5,2E+05	≈ 8,4E-02	
Tie2	MK-2461	1,7E-07	1,2E-07	2,2E-07	2,2E-07	≥ 1,6E+06	≥ 3,5E-01	
Tie2	MK-5108 (VX-689)	1,6E-08	1,1E-08	2,0E-08	2,0E-08	≈ 2,0E+07	≈ 4,0E-01	
Tie2	MLN8054	6,4E-08	4,4E-08	9,0E-08	9,0E-08	≥ 3,9E+06	≥ 3,5E-01	
Tie2	MLN8237 (Alisertib)	5,4E-08	3,7E-08	5,2E-08	5,2E-08	≥ 6,7E+06	≥ 3,5E-01	
Tie2	Neratinib (HKI-272)	≈ 2,3E-06	≈ 1,6E-06	3,0E-07	3,0E-07	≈ 8,5E+05	≈ 1,9E-01	2
Tie2	Nilotinib (AMN-107)	6,5E-08	4,5E-08	2,3E-07	4,5E-08	n.e.	n.e.	12
Tie2	NVP-ADW742	4,1E-07	2,8E-07	7,0E-07	7,0E-07	≥ 5,0E+05	≥ 3,5E-01	
Tie2	NVP-BGT226	≥ 2,0E-05		7,2E-06	7,2E-06	≥ 4,9E+04	≥ 3,5E-01	
Tie2	NVP-BHG712	7,4E-06	5,1E-06	5,5E-06	5,5E-06	≥ 6,4E+04	≥ 3,5E-01	
Tie2	NVP-BSK805	1,7E-06	1,1E-06	1,1E-06	1,1E-06	5,1E+04	5,7E-02	
Tie2	NVP-TAE226	4,2E-07	2,9E-07	6,1E-07	6,1E-07	≥ 5,7E+05	≥ 3,5E-01	
Tie2	OSI-027	1,4E-05	1,0E-05	≥ 2,0E-05	≥ 1,0E-05			
Tie2	Pazopanib HCl	1,7E-07	1,2E-07	3,3E-07	3,3E-07	3,4E+05	1,1E-01	1
Tie2	PCI-32765 (ibrutinib)	4,1E-07	2,9E-07	3,1E-07	3,1E-07	3,5E+05	8,8E-02	
Tie2	PD153035 HCl	5,0E-06	3,4E-06	4,8E-06	4,8E-06	≈ 9,7E+03	3,2E-02	
Tie2	PD173074	5,0E-07	3,5E-07	3,8E-07	3,8E-07	≈ 4,2E+05	≈ 1,4E-01	
Tie2	Pelitinib (EKB-569)	1,0E-06	6,9E-07	1,0E-06	1,0E-06	≈ 1,3E+05	≈ 1,3E-01	
Tie2	PF-00562271	2,1E-07	1,5E-07	2,3E-07	2,3E-07	≥ 1,5E+06	≥ 3,5E-01	
Tie2	PF-03814735	5,7E-08	3,9E-08	1,1E-07	1,1E-07	≥ 3,3E+06	≥ 3,5E-01	
Tie2	PHA-665752	1,6E-06	1,1E-06	1,3E-06	1,3E-06	≈ 9,4E+04	≈ 1,1E-01	
Tie2	PHA-680632	5,7E-08	4,0E-08	3,4E-08	3,4E-08	3,4E+06	1,2E-01	
Tie2	PIK-294	8,6E-06	6,0E-06	7,8E-06	7,8E-06	≥ 4,5E+04	≥ 3,5E-01	
Tie2	PIK-75	1,8E-06	1,2E-06	≈ 4,5E-06	1,2E-06	≥ 7,7E+04	≥ 3,5E-01	
Tie2	PLX-4720	2,2E-06	1,5E-06	1,6E-06	1,6E-06	≈ 4,2E+04	≈ 6,6E-02	
Tie2	Ponatinib (AP24534)	7,0E-10	4,8E-10	4,6E-10	4,6E-10	1,3E+07	6,1E-03	
Tie2	PP-121	1,3E-07	9,1E-08	5,3E-07	9,1E-08	≈ 6,5E+04	≈ 4,3E-02	
Tie2	PP242	1,2E-06	8,5E-07	1,5E-06	1,5E-06	≈ 5,3E+04	≈ 1,2E-01	
Tie2	Quercetin (Sphoretin)	9,7E-06	6,7E-06	≈ 7,6E-06	6,7E-06	≥ 4,6E+04	≥ 3,5E-01	
Tie2	Quizartinib (AC220)	≈ 2,0E-05	≈ 1,4E-05	8,9E-06	8,9E-06	1,3E+04	1,2E-01	
Tie2	R406	6,1E-08	4,2E-08	1,3E-07	1,3E-07	≥ 2,8E+06	≥ 3,5E-01	2
Tie2	R788 (Fostatinib) - prodrug	9,9E-07	6,8E-07	1,3E-06	1,3E-06	≈ 3,0E+05	≈ 3,5E-01	

kinase	Compound	IC ₅₀ [M] ePCA	K _D eq [M] ePCA *	K _D kin [M] kPCA	K _D [M] PCA **	k _{on} [M ⁻¹ s ⁻¹] kPCA	k _{off} [s ⁻¹] kPCA	comment
Tie2	Raf265 derivative	6,3E-06	4,3E-06	≥ 2,0E-05	≥ 4,3E-06			
Tie2	Ruxolitinib (INCB018424)	3,4E-06	2,3E-06	5,5E-06	5,5E-06	≈ 3,5E+04	≈ 2,4E-01	
Tie2	Saracatinib (AZD0530)	4,5E-06	3,1E-06	4,8E-06	4,8E-06	≈ 1,2E+05	≈ 3,9E-01	
Tie2	SB 202190	1,6E-05	1,1E-05	7,7E-06	7,7E-06	≈ 2,6E+04	≈ 1,7E-01	
Tie2	SB 203580	7,9E-06	5,5E-06	5,7E-06	5,7E-06	≥ 6,2E+04	≥ 3,5E-01	
Tie2	SB590885	5,2E-07	3,6E-07	6,7E-07	6,7E-07	1,3E+05	8,6E-02	
Tie2	SNS-314	2,7E-08	1,9E-08	2,8E-08	2,8E-08	≈ 4,8E+06	≈ 1,1E-01	
Tie2	SP600125	5,1E-06	3,5E-06	4,6E-06	4,6E-06	≈ 7,7E+03	≈ 3,5E-02	
Tie2	Staurosporine	1,0E-08	7,1E-09	8,8E-09	8,8E-09	≈ 6,4E+06	≈ 6,0E-02	
Tie2	SU11274	2,4E-07	1,7E-07	1,2E-06	1,7E-07	4,9E+04	5,8E-02	
Tie2	Sunitinib Malate (Sutent)	2,0E-06	1,4E-06	3,3E-06	3,3E-06	≥ 1,0E+05	≥ 3,5E-01	
Tie2	TAE684 (NVP-TAE684)	4,0E-08	2,8E-08	9,1E-09	9,1E-09	≥ 3,8E+07	≥ 3,5E-01	
Tie2	TAK-285	9,5E-06	6,6E-06	9,2E-06	9,2E-06	n.e.	n.e.	
Tie2	TAK-901	5,2E-08	3,6E-08	1,3E-07	1,3E-07	≈ 4,2E+05	≈ 4,8E-02	
Tie2	Tandutinib (MLN518)	1,2E-05	8,2E-06	≥ 2,0E-05	≥ 8,2E-06			
Tie2	TG100-115	1,2E-05	8,3E-06	6,7E-06	6,7E-06	≈ 5,5E+03	≈ 3,9E-02	
Tie2	TG101209	2,0E-07	1,4E-07	1,4E-07	1,4E-07	≈ 7,6E+05	≈ 1,1E-01	
Tie2	TG101348 (SAR302503)	6,2E-07	4,3E-07	8,1E-07	8,1E-07	≈ 1,0E+05	≈ 1,1E-01	
Tie2	Tie2 kinase inhibitor	6,2E-08	4,3E-08	2,0E-07	2,0E-07	≥ 1,7E+06	≥ 3,5E-01	
Tie2	Tivozanib (AV-951)	1,8E-08	1,2E-08	2,0E-08	2,0E-08	≈ 4,7E+06	≈ 8,2E-02	
Tie2	Torin 2	9,2E-06	6,3E-06	6,3E-06	6,3E-06	≈ 9,1E+03	≈ 6,0E-02	
Tie2	TPCA-1	1,3E-06	8,7E-07	1,2E-06	1,2E-06	≥ 2,9E+05	≥ 3,5E-01	
Tie2	TWS119	5,4E-07	3,7E-07	5,0E-07	5,0E-07	6,7E+04	≈ 3,7E-02	
Tie2	Vandetanib (Zactima)	8,0E-08	5,5E-08	1,7E-07	1,7E-07	≈ 2,2E+06	≈ 3,5E-01	
Tie2	Vemurafenib (PLX4032)	≈ 2,0E-05	≈ 1,4E-05	6,7E-06	6,7E-06	5,2E+03	3,3E-02	
Tie2	VX-680 (MK-0457 - Tozasertib)	9,7E-08	6,7E-08	≈ 2,4E-07	6,7E-08	≈ 3,4E+05	≈ 8,6E-02	
Tie2	WHI-P154	3,3E-06	2,3E-06	4,0E-06	4,0E-06	n.e.	n.e.	
Tie2	WZ3146	6,8E-07	4,7E-07	8,6E-07	8,6E-07	≥ 4,1E+05	≥ 3,5E-01	
Tie2	WZ4002	5,4E-06	3,8E-06	≈ 5,3E-06	3,8E-06	≈ 1,8E+04	≈ 9,0E-02	
Tie2	WZ8040	1,0E-06	7,1E-07	1,6E-06	1,6E-06	≈ 2,5E+05	≈ 3,7E-01	
Tie2	XL-184 (Cabozantinib)	2,0E-08	1,3E-08	3,0E-08	3,0E-08	≈ 1,2E+07	≈ 3,5E-01	
Tie2	ZM-447439	3,8E-07	2,7E-07	5,8E-07	5,8E-07	≈ 6,5E+05	≈ 4,0E-01	
TRKB	A-674563	≥ 2,0E-05		1,7E-06	1,7E-06	≈ 3,7E+04	≈ 5,3E-02	
TRKB	AEE788 (NVP-AEE788)	7,1E-06	4,1E-07	4,9E-07	4,9E-07	≈ 4,6E+05	≈ 2,8E-01	
TRKB	AMG458	4,6E-06	2,6E-07	3,2E-07	3,2E-07	5,6E+04	1,8E-02	
TRKB	AT7867	≥ 2,0E-05		3,6E-06	3,6E-06	≥ 9,8E+04	≥ 3,5E-01	
TRKB	AT9283	1,0E-06	5,7E-08	2,1E-08	2,1E-08	≈ 5,7E+06	≈ 1,3E-01	
TRKB	Aurora A Inhibitor I	≥ 2,0E-05		2,2E-06	2,2E-06	≥ 1,6E+05	≥ 3,5E-01	2
TRKB	Axitinib	≥ 2,0E-05		2,2E-07	2,2E-07	≈ 1,0E+05	≈ 3,3E-02	2
TRKB	AZ 960	1,3E-08	7,4E-10	7,7E-10	7,7E-10	6,9E+06	5,1E-03	
TRKB	AZD4547	1,5E-07	8,7E-09	6,1E-09	6,1E-09	≈ 7,0E+06	≈ 5,0E-02	
TRKB	AZD5438	1,5E-05	8,4E-07	5,5E-07	5,5E-07	≈ 2,5E+04	≈ 1,9E-02	
TRKB	AZD7762	1,2E-07	6,9E-09	3,4E-09	3,4E-09	≈ 4,4E+06	3,1E-02	3
TRKB	Barasertib (AZD1152-HQPA)	1,4E-05	8,0E-07	6,9E-07	6,9E-07	≈ 2,1E+05	≈ 1,3E-01	
TRKB	Baricitinib (LY3009104 - incb28050)	1,3E-05	7,2E-07	4,2E-07	4,2E-07	≈ 3,8E+05	≈ 2,0E-01	
TRKB	BEZ235 (NVP-BEZ235)	≥ 2,0E-05		6,9E-07	6,9E-07	≈ 1,8E+05	9,6E-02	2
TRKB	BIBF1120 (Vargatef)	6,3E-07	3,6E-08	2,1E-08	2,1E-08	4,1E+06	8,3E-02	
TRKB	BIRB 796 (Doramapimod)	5,6E-06	3,2E-07	n.e.	3,2E-07	1,2E+04	≤ 4,0E-03	4
TRKB	BIX 02188	≥ 2,0E-05		8,9E-07	8,9E-07	≈ 1,5E+05	≈ 1,2E-01	
TRKB	BIX 02189	1,5E-05	8,4E-07	5,9E-07	5,9E-07	1,6E+05	9,5E-02	
TRKB	BMS 777607	4,9E-07	2,8E-08	3,7E-08	3,7E-08	≈ 1,1E+06	≈ 4,3E-02	
TRKB	BMS 794833	2,0E-08	1,2E-09	2,9E-09	2,9E-09	4,4E+05	1,3E-03	
TRKB	BMS-265246	≥ 2,0E-05		4,4E-06	4,4E-06	≥ 7,9E+04	≥ 3,5E-01	
TRKB	Bosutinib (SKI-606)	3,1E-07	1,8E-08	1,2E-07	1,8E-08	≈ 1,7E+06	≈ 1,9E-01	2
TRKB	BX-795	5,7E-07	3,3E-08	5,4E-08	5,4E-08	≥ 6,5E+06	≥ 3,5E-01	
TRKB	BX-912	3,9E-07	2,3E-08	2,3E-08	2,3E-08	≈ 5,0E+06	≈ 1,2E-01	
TRKB	CCT128930	≥ 2,0E-05		2,8E-06	2,8E-06	≈ 7,4E+03	≈ 2,4E-02	
TRKB	CCT129202	≥ 2,0E-05		3,8E-06	3,8E-06	≥ 9,3E+04	≥ 3,5E-01	
TRKB	CCT137690	3,6E-06	2,1E-07	8,3E-07	8,3E-07	≈ 4,2E+05	≈ 3,5E-01	
TRKB	CEP33779	4,4E-06	2,5E-07	2,2E-07	2,2E-07	≈ 1,1E+06	≈ 2,7E-01	
TRKB	CH5424802	≥ 2,0E-05		8,4E-07	8,4E-07	≈ 2,9E+05	≈ 1,6E-01	2
TRKB	CHIR-124	1,9E-08	1,1E-09	n.e.	1,1E-09	6,6E+06	≤ 7,1E-03	4
TRKB	CP 673451	2,6E-07	1,5E-08	1,1E-08	1,1E-08	3,8E+06	3,9E-02	
TRKB	Crenolanib (CP-868596)	3,8E-07	2,2E-08	1,7E-08	1,7E-08	1,5E+06	2,6E-02	
TRKB	Crizotinib (PF-02341066)	6,5E-08	3,7E-09	5,9E-09	5,9E-09	≈ 2,4E+07	≈ 1,1E-01	2
TRKB	CX-4945 (Silmisertib)	≥ 2,0E-05		1,6E-06	1,6E-06	1,3E+05	2,0E-01	
TRKB	CYC116	4,6E-06	2,6E-07	1,7E-07	1,7E-07	≈ 3,2E+05	≈ 5,6E-02	
TRKB	Cyt387	≥ 2,0E-05		1,7E-06	1,7E-06	≈ 1,7E+05	≈ 2,6E-01	
TRKB	Dabrafenib (GSK2118436)	1,1E-06	6,0E-08	4,3E-08	4,3E-08	≈ 4,5E+06	2,0E-01	
TRKB	Danuserib (PHA-739358)	1,2E-06	6,8E-08	9,0E-08	9,0E-08	1,2E+05	1,1E-02	
TRKB	Dasatinib (BMS-354825)	≥ 2,0E-05		1,2E-06	1,2E-06	≈ 3,6E+05	≈ 4,0E-01	
TRKB	DCC-2036 (Rebastinib)	8,6E-09	4,9E-10	n.e.	4,9E-10	5,2E+04	≤ 2,5E-05	4
TRKB	Desmethyl Erlotinib (CP-473420)	≥ 2,0E-05		3,3E-06	3,3E-06	≈ 3,9E+04	≈ 1,4E-01	
TRKB	Dovitinib (TKI-258)	1,8E-07	1,0E-08	6,0E-09	6,0E-09	7,9E+06	4,8E-02	
TRKB	E7080 (Lenvatinib)	≥ 2,0E-05		2,4E-06	2,4E-06	≈ 1,7E+04	≈ 3,5E-02	
TRKB	ENMD-2076	2,5E-07	1,4E-08	1,9E-08	1,9E-08	1,2E+06	2,3E-02	
TRKB	Enzastaurin (LY317615)	≥ 2,0E-05		1,3E-06	1,3E-06	n.e.	n.e.	
TRKB	Flavopiridol HCl	≥ 2,0E-05		9,0E-07	9,0E-07	5,0E+04	4,5E-02	
TRKB	Foretinib (GSK1363089 - XL880)	1,6E-08	9,2E-10	n.e.	9,2E-10	≈ 4,5E+05	≤ 4,2E-04	24

kinase	Compound	IC ₅₀ [M] ePCA	K _D eq [M] ePCA *	K _D kin [M] kPCA	K _D [M] PCA **	k _{on} [M ⁻¹ s ⁻¹] kPCA	k _{off} [s ⁻¹] kPCA	comment
TRKB	GDC-0941	≥ 2,0E-05		1,8E-06	1,8E-06	≈ 2,6E+05	≈ 3,7E-01	
TRKB	GDC-0980 (RG7422)	≥ 2,0E-05		1,3E-06	1,3E-06	≈ 7,2E+04	≈ 1,1E-01	
TRKB	Golitinib (E7050)	7,9E-07	4,5E-08	2,3E-08	2,3E-08	≈ 7,8E+05	≈ 1,8E-02	
TRKB	GSK1059615	≥ 2,0E-05		1,4E-06	1,4E-06	≈ 5,0E+05	≈ 5,7E-01	
TRKB	GSK1070916	≥ 2,0E-05		4,7E-07	4,7E-07	≈ 5,2E+05	≈ 2,5E-01	
TRKB	GSK1838705A	≥ 2,0E-05		3,7E-06	3,7E-06	≈ 3,3E+04	≈ 1,3E-01	
TRKB	GSK2126458	≥ 2,0E-05		4,8E-06	4,8E-06	≥ 7,4E+04	≥ 3,5E-01	
TRKB	Hesperadin	3,3E-09	1,9E-10	7,0E-11	7,0E-11	≈ 8,6E+06	≈ 5,6E-04	
TRKB	INCB28060	≥ 2,0E-05		2,6E-06	2,6E-06	≥ 1,3E+05	≥ 3,5E-01	
TRKB	Indirubin	≥ 2,0E-05		n.e.	≥ 1,1E-06	n.e.	n.e.	
TRKB	INK 128 (MLN0128)	≥ 2,0E-05		5,5E-07	5,5E-07	≈ 4,7E+05	≈ 2,5E-01	
TRKB	JNJ-38877605	≥ 2,0E-05		4,6E-06	4,6E-06	≈ 1,7E+04	≈ 5,6E-02	
TRKB	JNJ-7706621	4,9E-06	2,8E-07	1,2E-07	1,2E-07	≈ 1,5E+06	≈ 1,9E-01	2
TRKB	Ki8751	≈ 1,8E-06	≈ 1,0E-07	6,0E-08	6,0E-08	≈ 5,4E+05	≈ 3,3E-02	2
TRKB	KW 2449	4,7E-07	2,7E-08	7,7E-08	7,7E-08	≈ 1,3E+06	≈ 8,5E-02	2
TRKB	Linifanib (ABT-869)	≈ 2,6E-06	≈ 1,5E-07	2,5E-07	2,5E-07	≈ 3,3E+05	≈ 8,2E-02	
TRKB	Linsitinib (OSI-906)	≥ 2,0E-05		6,3E-06	6,3E-06	≥ 5,6E+04	≥ 3,5E-01	
TRKB	LY2784544	3,5E-08	2,0E-09	2,2E-09	2,2E-09	≈ 2,6E+06	≈ 5,2E-03	2
TRKB	MGCD-265	4,5E-07	2,6E-08	1,1E-07	1,1E-07	≈ 3,2E+05	≈ 2,9E-02	2
TRKB	Milciclib (PHA-848125)	1,0E-06	5,7E-08	3,6E-08	3,6E-08	≈ 9,1E+05	≈ 3,8E-02	
TRKB	MK-2461	1,9E-06	1,1E-07	9,7E-08	9,7E-08	≥ 3,6E+06	≥ 3,5E-01	2
TRKB	MK-5108 (VX-689)	≤ 9,9E-10	≤ 5,7E-11	8,7E-11	8,7E-11	≈ 1,0E+07	≈ 9,0E-04	
TRKB	MLN8054	6,1E-06	3,5E-07	3,4E-07	3,4E-07	≈ 7,8E+04	≈ 2,9E-02	
TRKB	MLN8237 (Alisertib)	3,0E-06	1,7E-07	1,3E-07	1,3E-07	≈ 4,7E+05	≈ 5,7E-02	
TRKB	Neratinib (HKI-272)	≥ 2,0E-05		n.e.	≥ 1,1E-06	n.e.	n.e.	
TRKB	Nilotinib (AMN-107)	≥ 2,0E-05	≈ 1,9E-06	≈ 1,9E-06	≈ 1,9E-06	≈ 1,9E+05	≈ 3,4E-01	
TRKB	NVP-ADW742	≥ 2,0E-05		1,2E-06	1,2E-06	≈ 5,1E+04	≈ 6,1E-02	
TRKB	NVP-BGT226	≥ 2,0E-05		3,0E-07	3,0E-07	≈ 4,1E+05	≈ 1,6E-01	
TRKB	NVP-BSK805	3,7E-06	2,1E-07	1,3E-07	1,3E-07	≈ 2,8E+06	≈ 5,1E-01	
TRKB	NVP-BVU972	≥ 2,0E-05		6,4E-07	6,4E-07	≈ 1,4E+05	≈ 1,1E-01	
TRKB	NVP-TAE226	3,6E-06	2,1E-07	2,9E-07	2,9E-07	≈ 2,2E+05	≈ 6,8E-02	
TRKB	OSI-930	≥ 2,0E-05		5,7E-06	5,7E-06	≈ 1,3E+04	≈ 4,7E-02	
TRKB	Pazopanib HCl	≥ 2,0E-05		1,6E-06	1,6E-06	≈ 6,7E+03	≈ 1,0E-02	
TRKB	PCI-32765 (Ibrutinib)	≥ 2,0E-05		1,9E-06	1,9E-06	≈ 8,0E+04	≈ 1,5E-01	
TRKB	PD 0332991 (Palbociclib) HCl	≥ 2,0E-05		1,3E-06	1,3E-06	≈ 9,0E+04	≈ 1,1E-01	
TRKB	PF-00562271	8,0E-08	4,6E-09	3,8E-09	3,8E-09	≈ 7,4E+06	≈ 2,4E-02	
TRKB	PF-03814735	1,9E-08	1,1E-09	1,9E-09	1,9E-09	≈ 8,0E+06	≈ 1,5E-02	
TRKB	PHA-665752	2,3E-06	1,3E-07	1,1E-07	1,1E-07	≈ 7,2E+05	≈ 7,5E-02	
TRKB	PHA-680632	4,7E-06	2,7E-07	1,4E-07	1,4E-07	≈ 9,0E+05	≈ 1,2E-01	
TRKB	PIK-75	1,8E-07	1,0E-08	1,9E-08	1,9E-08	≈ 3,5E+06	≈ 5,5E-02	2
TRKB	PLX-4720	≥ 2,0E-05		5,2E-06	5,2E-06	≈ 1,3E+05	≈ 7,2E-01	
TRKB	Ponatinib (AP24534)	3,0E-08	1,7E-09	7,1E-10	7,1E-10	≈ 2,4E+06	≈ 1,7E-03	
TRKB	PP-121	≥ 2,0E-05		1,2E-06	1,2E-06	≈ 4,4E+04	≈ 5,3E-02	
TRKB	PP242	1,5E-05	8,8E-07	5,3E-07	5,3E-07	≈ 4,8E+04	≈ 2,4E-02	
TRKB	Quercetin (Sophoretin)	4,1E-06	2,3E-07	2,7E-07	2,7E-07	≈ 1,6E+05	≈ 4,2E-02	2
TRKB	Quizartinib (AC220)	≈ 2,2E-06	≈ 1,3E-07	1,0E-07	1,0E-07	≈ 4,1E+05	≈ 4,0E-02	
TRKB	R406	≥ 2,0E-05		2,9E-07	2,9E-07	≈ 1,6E+05	≈ 2,8E-02	2
TRKB	R788 (Fostatinib) - prodrug	≥ 2,0E-05		1,8E-06	1,8E-06	≈ 6,7E+04	≈ 7,0E-02	
TRKB	Ruxolitinib (INCB018424)	2,6E-06	1,5E-07	1,5E-07	1,5E-07	≈ 7,9E+05	≈ 1,0E-01	
TRKB	Saracatinib (AZD0530)	6,7E-06	3,8E-07	2,7E-07	2,7E-07	≈ 1,1E+05	≈ 4,0E-02	
TRKB	Semaxanib (SU5416)	3,8E-07	2,2E-08	5,3E-08	5,3E-08	≈ 1,2E+07	≈ 6,0E-01	
TRKB	SNS-314	8,2E-08	4,7E-09	5,7E-09	5,7E-09	≈ 3,2E+06	≈ 1,9E-02	
TRKB	Sotrastaurin (AEB071)	≥ 2,0E-05		7,1E-07	7,1E-07	≈ 8,5E+04	≈ 8,1E-02	
TRKB	SP600125	3,0E-06	1,7E-07	9,8E-08	9,8E-08	≈ 3,4E+06	≈ 3,6E-01	
TRKB	Staurosporine	≤ 8,3E-10	≤ 4,8E-11	n.e.	≤ 4,8E-11	≈ 1,1E+07	≈ 5,0E-04	4
TRKB	SU11274	1,5E-07	8,5E-09	2,7E-08	2,7E-08	≈ 8,1E+06	≈ 1,9E-01	
TRKB	Sunitinib Malate (Sutent)	2,2E-07	1,2E-08	2,6E-08	2,6E-08	≈ 7,2E+06	≈ 9,0E-02	3
TRKB	TAE684 (NVP-TAE684)	2,8E-06	1,6E-07	7,4E-08	7,4E-08	≈ 6,6E+05	≈ 4,9E-02	
TRKB	TAK-901	1,4E-08	8,2E-10	≈ 1,4E-09	8,2E-10	≈ 9,5E+06	≈ 7,8E-03	3
TRKB	Tandutinib (MLN518)	2,8E-06	1,6E-07	2,3E-07	2,3E-07	≈ 8,5E+04	≈ 1,9E-02	
TRKB	TG101209	7,1E-07	4,1E-08	5,3E-08	5,3E-08	≈ 4,4E+06	≈ 2,3E-01	
TRKB	TG101348 (SAR302503)	1,9E-06	1,1E-07	1,2E-07	1,2E-07	≈ 6,2E+05	≈ 6,4E-02	
TRKB	Tivozanib (AV-951)	2,0E-07	1,2E-08	1,6E-08	1,6E-08	≈ 1,1E+06	≈ 1,8E-02	
TRKB	Torin 2	≥ 2,0E-05		9,1E-07	9,1E-07	≈ 1,6E+05	≈ 1,5E-01	
TRKB	TPCA-1	2,3E-06	1,3E-07	1,2E-07	1,2E-07	≥ 2,9E+06	≥ 3,5E-01	
TRKB	TSU-68 (SU6668)	2,8E-07	1,6E-08	1,4E-08	1,4E-08	≈ 1,0E+07	≈ 1,3E-01	
TRKB	TWS119	1,6E-05	8,9E-07	1,4E-06	1,4E-06	≈ 9,7E+04	≈ 1,4E-01	
TRKB	Vandetanib (Zactima)	≥ 2,0E-05		1,7E-06	1,7E-06	≈ 3,4E+04	≈ 6,0E-02	
TRKB	VX-680 (MK-0457 - Tozasertib)	4,2E-07	2,4E-08	4,0E-08	4,0E-08	≈ 1,2E+07	≈ 5,4E-01	
TRKB	WZ3146	2,0E-06	1,2E-07	9,5E-08	9,5E-08	≈ 4,9E+06	≈ 4,4E-01	
TRKB	WZ8040	2,2E-06	1,2E-07	1,9E-07	1,9E-07	≈ 4,6E+05	≈ 7,7E-02	
TRKB	XL-184 (Cabozantinib)	1,9E-07	1,1E-08	1,8E-08	1,8E-08	≈ 1,1E+06	≈ 1,8E-02	
TRKB	ZM-447439	≥ 2,0E-05		5,3E-07	5,3E-07	≥ 6,7E+05	≥ 3,5E-01	



■ Personal Details

E-mail: Victoria.Georgi@gmx.de
Date, Place of Birth: 17.05.1989, Berlin

■ Education

since 10 / 2015: **PhD student, Pharmacy, Johann Wolfgang Goethe-University Frankfurt**
10 / 2007 - 08 / 2013: **Study of Biotechnology, Technische Universität Berlin, Berlin**
Diplom-Ingenieur Degree; **Overall Grade: 1.0; VDI Prize for excellent graduation**
09 / 1999 - 07 / 2007: **Rudolf-Hildebrand-Gymnasium, Markkleeberg; Abitur; Overall Grade: 1.4**
09 / 1995 - 07 / 1999: **Grundschule Markkleeberg West, Markkleeberg**

■ Professional Experience & Studies

since 08 / 2017: **Laboratory Head at Bayer AG in Berlin, department "Screening Biochemistry"**

- Project work on immuno-oncology & tumor signaling; direct supervisor: Jörg Fanghänel
- employee responsibility; development of uHTS assays for lead identification

01 / 2015 - 08 / 2017: **PhD student at Bayer (Pharma) AG in Berlin, department "Screening Biochemistry"**

- direct supervisor: Amaury Ernesto Fernández-Montalván
- work on IMI K4DD (Kinetics for Drug Discovery) project
- title of thesis: "Large-scale analysis of kinase inhibitors' target binding kinetics. Implications for drug discovery?"; supervisors: Prof. Dr. Stefan Knapp, Prof. Dr. Michael Brands; several publications accepted and in progress

since 08 / 2015: **side job as research associate at Fraunhofer IZM in Berlin,**

- work group "Assembly & Encapsulation Technologies"; direct supervisors: Karl Friedrich Becker, Tanja Braun
- member of advisory board for PoC-ID (Platform for ultra-sensitive Point-of-Care diagnostics for Infectious Diseases) project

06 / 2011 - 12 / 2014: **Student assistant (until 09 / 13) and research associate at Fraunhofer IZM in Berlin**

- work group "Medical Microsystems"; direct supervisor: Erik Jung
- work on Fraunhofer Lighthouse Project "Cell-Free Bioproduction"; Successful acquisition of H2020 EU project, PHC-10-2014; Commissioning of cell culture laboratory

08 / 2012 - 08 / 2013: **Diploma thesis at the TU Berlin in cooperation with Fraunhofer-Institutes IZM in Berlin & IBMT in Potsdam**

- work groups "Medical Microsystems" and "Cell-free Protein Synthesis"; direct supervisors: Erik Jung, Dr. Stefan Kubick
- title: "Immobilization of mRNA and magnetic force actuated particle transfer for on-chip automation of cell-free protein synthesis"; supervisors: Prof. Dr. Roland Lauster, Prof. Dr. Frank Bier; **grade: 1.0; awarded with "Clara von Simson-Preis" (1st prize)**
- results laid foundation for a patent, a model reactor of the Fraunhofer Lighthouse Project and were published in Lab on a Chip

04 / 2010 - 06 / 2011: **Student project "Assay development" at AptRes AG in Berlin**

- development of a homogenous laboratory medical assay for the quantification of influenza nucleoproteins using aptamers; Supervisor: Dr. Andreas Kage
- presentation of results at the "International student congress of (bio-)medical sciences" ISCOMS 2011 in Groningen, the Netherlands

10 / 2010 - 02 / 2011: **Internship and Student Research Project at the Charité in Berlin;**

- work group "Biochemical Human Genetics"; direct supervisor: Prof. Dr. Joachim Klose
- title: "Analysis of carbonylated proteins in a mouse model for Alzheimer's disease"; supervisors: Dr. Daniela Hartl; Prof. Dr. Roland Lauster
- **grade: 1.0; results published in Journal of Proteome Research**

08 - 09 / 2010: **Internship at Fraunhofer IBMT in Potsdam; work group "Cell-Assay Development"**

- development of a method for the preparation of a calibration standard for single-cell quantitative PCR; direct supervisor: Dr. Andreas Lankenau
